

The synthesis of advanced " special pair " models for the photosynthetic reaction centre

Author:

Mecker, Christoph J

Publication Date:

2000

DOI:

<https://doi.org/10.26190/unsworks/19899>

License:

<https://creativecommons.org/licenses/by-nc-nd/3.0/au/>

Link to license to see what you are allowed to do with this resource.

Downloaded from <http://hdl.handle.net/1959.4/17835> in <https://unsworks.unsw.edu.au> on 2024-04-27

THE SYNTHESIS OF ADVANCED 'SPECIAL PAIR' MODELS FOR THE PHOTOSYNTHETIC REACTION CENTRE

by Christoph J. Mecker

A thesis submitted in fulfilment of the requirements for the degree of Doctor of Philosophy

Supervisor: Prof. Michael N. Paddon-Row

March 2000

School of Chemistry, University of New South Wales
Sydney, Australia

CERTIFICATE OF ORIGINALITY



I hereby declare that this submission is my own work and to the best of my knowledge it contains no materials previously published or written by another person, nor material which to a substantial extent has been accepted for the award of any other degree or diploma at UNSW or any other educational institution, except where due acknowledgement is made in the thesis. Any contribution made to the research by others, with whom I have worked at UNSW or elsewhere, is explicitly acknowledged in the thesis.

I also declare that the intellectual content of this thesis is the product of my own work, except to the extent that assistance from others in the project's design and conception or style, presentation and linguistic expression is acknowledged.

(Signed)

ABSTRACT

Multi-step photoinduced electron transfer takes place over a large distance in the photosynthetic reaction centres (PRCs). Electron donor in this life-spending event is the photo-excited 'special pair', a unit of two electronically coupled porphyrinoid chromophores. Bacteriopheophytin and two quinone molecules function as electron acceptors and contribute to the charge separation with almost unit quantum efficiency.

The natural photosynthetic reaction centre is the most sophisticated molecular electronic device to date and interest is high in increasing our understanding of the basic quantum mechanical principles behind efficient electron transfer and ultimately copying Nature and construct similar efficient devices.

Two main approaches towards a better understanding of the mechanisms involved have been taken. The more biological disciplines isolate, cultivate and alternate reaction centres whereas synthetic chemists prefer to construct well-defined models that mimic certain aspects of the reaction centres. Such a synthetic approach is described in the 'Synthesis of Advanced 'Special Pair' Models for the Photosynthetic Reaction Centre'.

The aspect to be mimicked is the 'special pair'. One or two porphyrins in a well-defined spatial disposition (kinked or non-kinked in respect to each other) were to act as electron donor in rigid bichromophoric and trichromophoric systems. A tetracyanonaphthoquinodimethane (TCNQ) unit was employed as the electron acceptor in the series of dyads synthesised. The TCNQ acceptor was replaced by a naphthoquinone (NQ) primary acceptor covalently linked to a TCNQ secondary electron acceptor in the series of triads. Rigid norbornylogous bridges held the chromophores in place and Diels-Alder methodology as well as condensation reactions were applied to link donor, bridge and acceptor components.

Despite larger interchromophoric separation than in the natural 'special pair', the two porphyrin chromophores of the series of 'special pair' dyads show some interaction and thereby prove the success of our approach towards 'special pair' mimics. Strong fluorescence quenching in the porphyrin-TCNQ dyads indicates the sought after electron transfer process.

A number of synthetic problems experienced and overcome in the synthesis of the series of triads led to discovery of a one-step 'bis-ketonisation' from an olefin under Sharpless bis-hydroxylation conditions with N-methylmorpholine-N-oxide. High pressure was applied to circumvent a lack of reactivity in the condensation reaction used to attach the porphyrin moieties (one or two) to the donor backbone. For the linkage of donor, bridge and acceptor component, a procedure was developed and successfully applied to give the giant mono-porphyrin-NQ-TCNQ trichromophore. In a similar manner 'special pair' trichromophoric systems should be available as part of future work.

ACKNOWLEDGEMENTS

A PhD project is seldom done by one person alone. So in this case, where thanks are due to a number of colleagues, collaborators and friends...

...and my supervisor, Professor Michael N. Paddon-Row, who provided me with this challenging PhD project, his generously shared advice, sufficient funds and some quite inspirational moments.

His group provided the essential support network that I couldn't have done without. Group members Stephen R. Davies (**10, 12, 16, 17, 19, 28**), Paul Harvey (**85**), and Nigel Lokan (**87, 155**) contributed the compounds given in brackets; Garth Jones and Michael Shephard carried out all AM1 calculations mentioned in this Thesis. Peter Bickers, Peter Gulyas †₁₉₉₉, Nick Head, Kate Joliffe, Steven Langford, Kai Look, Hania Oliver, Millagahamada G. Ranasinghe, and Danny Rothenfluh made my time in the Paddon-Row group an enjoyable experience.

I would like to thank Hilda Stender, James Hook, and Graham Ball for their help with the high field NMR work; Joe Brophy for high resolution mass spectra; Anne Poltjak, Martin Bucknall, Mark Leuwin for MALDI mass spectra, and Don Craig for the X-ray structures.

David Young and Annette Neuendorf, later Sov Atkinson of Griffith University, Queensland, came to my rescue when high-pressure equipment was desperately needed. Without their contribution the project would have stalled halfway.

David Black is gratefully acknowledged for triggering my move from Hamburg to Sydney, which was later enabled by the award of an Overseas Postgraduate Research Scholarship.

My partner Christiane is very much loved for initially sharing my life, since making it our life in Australia. Next to her I deeply thank my parents Gertraude and Joerg Mecker for their amazing confidence in me and my actions.

I dedicate this thesis to my friend Dr. Peter Thomas Gulyas †

TABLE OF CONTENTS

A Introduction.....	1
A.1 Preamble.....	1
A.2 Electron Transfer.....	2
A.3 Basic Electron Transfer Theory.....	4
A.3.1 Expressions for Rate Constants.....	5
A.3.2 Electron Transfer Variables	9
A.4 Molecular Devices	20
A.4.1 Requirements	21
A.4.2 Multichromophoric Concept.....	22
A.5 Photosynthesis.....	23
A.5.1 The Photosynthetic Reaction Centre.....	24
A.6 Photosynthetic Mimics.....	28
A.6.1 Porphyrin - Quinone Dyads	28
A.6.2 Porphyrin - Quinone Triads, Tetrads, Pentads.....	32
A.6.3 Multi Porphyrin Arrays.....	38
A.6.4 Conclusion	41
A.7 Aim of Thesis.....	42
 B Syntheses	 48
B.1 General	48
B.2 Synthesis of the Series of Dyads.....	49
B.2.1 Building the Carbon Backbones	51
B.2.2 Synthesis of Diones and Tetraones.....	53
B.2.3 Condensations	60
B.2.4 From Energy Transfer to Electron Transfer.....	69
B.3 Synthesis of the Series of Triads.....	77
B.3.1 Synthesis of the Donors	80
B.3.2 Synthesis of the Bridge	116
B.3.3 Synthesis of the Acceptor Precursor.....	120
B.3.4 Assembling the Triads	121
B.4 Synthesis of an all- <i>trans</i> ring-expanded Dyad.....	127
B.5 Synthesis of the 'Diaminoporphyrin'.....	135

C Summary & Conclusion.....	139
C.1 The Series of Dyads.....	139
C.2 The Series of Triads.....	141
C.3 The all- <i>trans</i> ring-expanded Dyad.....	148
 D Experimental Part.....	 152
D.1 Synthesis of the Dyads.....	153
D.1.1 Synthesis of the 6B-Porphyrin-Dyads.....	158
D.1.2 Synthesis of the 2B-Porphyrin-Dyads.....	163
D.1.3 Synthesis of the Bis-Porphyrin-Dyads.....	168
D.1.4 Synthesis of the Kinked Bis-Porphyrin-Dyads.....	173
D.2 Synthesis of the Triads.....	182
D.2.1 Synthesis of the 2B-Porphyrin Donor.....	182
D.2.2 Model Reactions.....	191
D.2.3 Synthesis of the Bis-Porphyrin Donor.....	207
D.2.4 Synthesis of the Kinked Bis-Porphyrin Donor.....	213
D.2.5 Synthesis of the Bridge.....	217
D.2.6 Synthesis of the Acceptor Precursor.....	224
D.2.7 Assembling the Triads.....	226
D.3 Synthesis of the all- <i>trans</i> ring-expanded Dyad.....	231
D.4 Synthesis of the 'Diaminoporphyrin'.....	237
 E Appendix.....	 242
E.1 Abbreviations.....	242
E.2 Compounds in Numerical Order.....	245
E.2.1 Compounds 1 to 30.....	245
E.2.2 Compounds 31 to 47.....	246
E.2.3 Compounds 48 to 88.....	247
E.2.4 Compounds 89 to 109.....	248
E.2.5 Compounds 110 to 133.....	249
E.2.6 Compounds 134 to 147.....	250
E.2.7 Compounds 148 to 155.....	251

E.3 Chemicals in Alphabetical Order	252
E.4 X-Ray Data	260
E.4.1 2B-dione-trans-diacetate 79	260
E.4.2 Mono-ring closed Mesylate 69	268
E.5 Representative Proton NMR Data	280
E.6 Captions	285
E.6.1 List of Equations	285
E.6.2 List of Examples	285
E.6.3 List of Figures	286
E.6.4 List of Schemes	291
E.6.5 List of Tables	296
E.7 Literature	297

A 'INTRODUCTION'



A INTRODUCTION

A.1 PREAMBLE

Popeye the sailor already knew where to get the energy. Now Elias Greenbaum and his colleagues at Oak Ridge National Laboratory in Tennessee believe that the tiny generators found in the leaves of spinach could soon be used as batteries or components in nanoscale electronic devices.¹⁻⁴ The 'generators' are the photosynthetic reaction centres (PRCs), which undergo electron transfer (ET) when hit by light. After excitation an electron is transferred within picoseconds from the donor moiety (D, the so-called 'special pair') to the acceptor (A, a quinone) of the reaction centre, resulting in a charge-separated state. According to Greenbaum the potential energy stored in this charge-separated state could be used to power tiny devices.

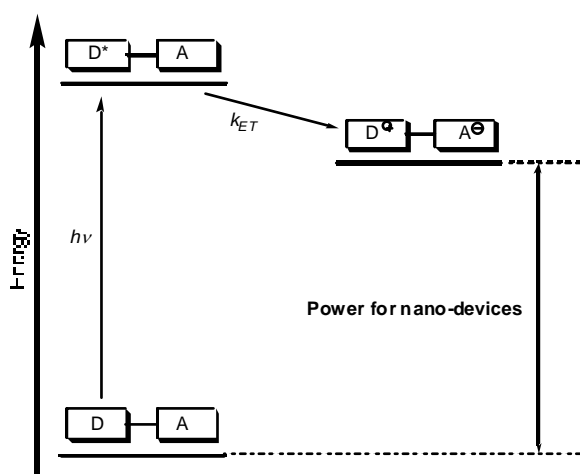


Figure 1: Photo-excitation followed by an electron-transfer step resulting in a high-energy charge-separated species

What sounds like a science-fiction fantasy is part of the efforts to utilise electron transfer phenomena in the emerging field of molecular electronics.⁵

Electron transfer processes have been under intense investigation since the late 1940s and the Nobel Prize awarded to R.A. Marcus in 1992⁶ underscored the recognition of the wide-ranging importance of ET phenomena in both chemistry and life. Interestingly the solution of the most important fundamental questions in intramolecular electron transfer was possible thanks to unprecedented collaboration between theorists, experimentalists and synthetic chemists. As a result of the success, a new and increasingly dominant style of physical

chemistry research, in which the synthesis of the most appropriate model compound is an intrinsic part of a well designed experiment, has emerged. The Nature of electron transfer studies is truly multidisciplinary and the continuing development in this field will increasingly depend on the involvement of skillful synthetic chemists. This Introduction gives a brief insight into the fundamentals of electron transfer, in particular photoinduced electron transfer. It describes electron transfer within the most fascinating natural converter of solar energy into chemical potential, the photosynthetic reaction centre, and thereafter focuses on synthetic efforts, directed towards a versatile set of mimics, to probe this behaviour. Those synthetic efforts will be taken a step further, when the 'Synthesis of Advanced 'Special Pair' Models for the Photosynthetic Reaction Centre', the objective of this thesis, is described in the following chapter **B** 'Syntheses'.

A.2 ELECTRON TRANSFER

Electron transfer (ET) describes the most fundamental reaction in chemistry. No chemical bonds are necessarily broken or formed, but an electron is transferred from an electron donor (D) to an electron acceptor (A). This can occur as an intermolecular process or an intramolecular process. If donor and acceptor are not in direct contact with each other (namely within the sum of their van der Waals radii), the coupling of the donor and acceptor wave functions needs to be mediated. Media that may mediate long-range electron transfer processes include solvents, non-covalent or covalent bonds. These media provide 'orbitals' (π , π^* , σ , σ^*) the migrating electron can use to tunnel between donor and acceptor. The electron in an ET reaction moves coherently between the chromophores, and not as a defect (i.e. polaron) such as in electron transport. In an electron transport process the electron becomes thermally injected into the conduction band of the bridge and it actually becomes localised within the bridge. In this case the medium is regarded as a molecular wire and the distance dependence of the electron transport rate is determined by Ohmic scattering and therefore varies inversely with interchromophoric separation.^{7,8} In contrast, the electron in an electron transfer process can not be thermally injected into the bridge virtual states (**Figure 2**) since the energy gap (ΔE) between the HOMO of the donor and the LUMO of the medium is too high (several eV). The distance dependence of the electron transfer rate is exponential decay (**Equation 13**, page 14).

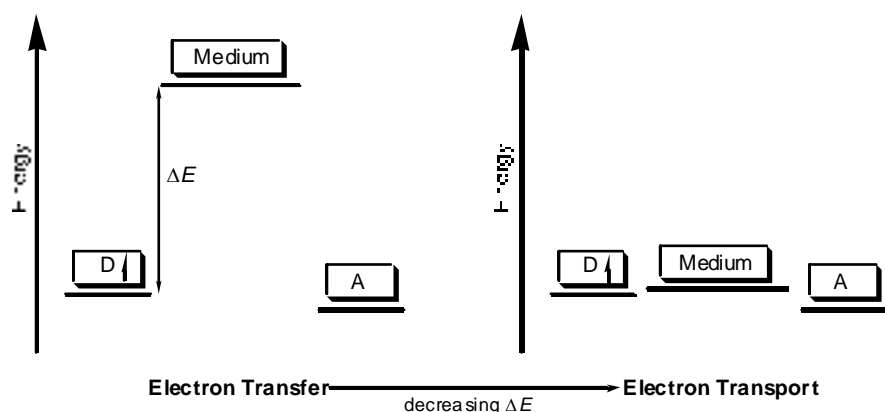


Figure 2: Electron transfer vs. electron transport

Whereas electron transport is fairly well understood, electron transfer is not and therefore it remains the subject of intense research, to illuminate its role in Nature.

Basically electron transfer reactions can be divided into three distinct categories: thermal, optical and photoinduced ET (**Figure 3**). Each may involve either charge shift ($D^+ + A \rightarrow D + A^-$) or complete charge separation ($D + A \rightarrow D^+ + A^-$).

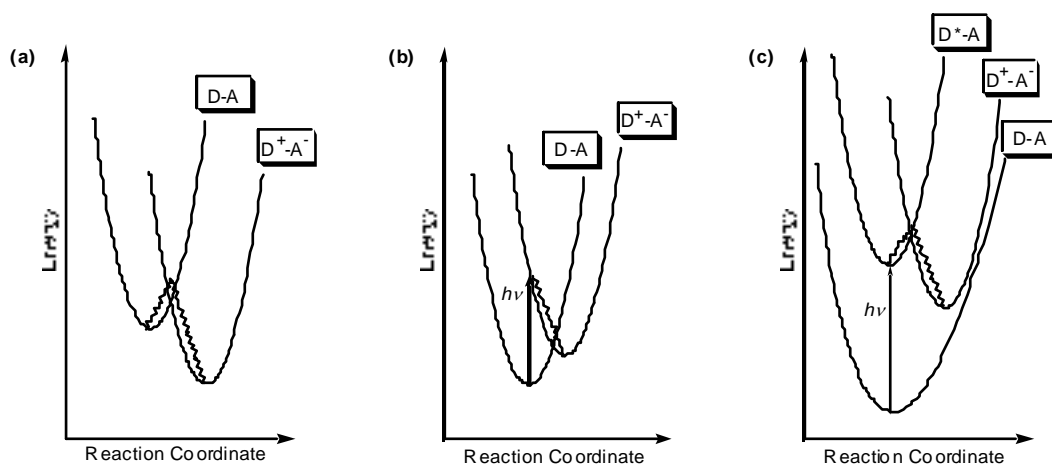


Figure 3: Schematic representations showing (a) thermal ET, (b) optical ET, and (c) photoinduced ET

In thermal electron transfer (**Figure 3 (a)**), the free energy of the products is lower than the free energy of the reactants. It is the exergonic nature that enables ET to occur.

In optical electron transfer (**Figure 3 (b)**), photoexcitation results in direct electronic excitation into the charge-separated state and is represented as a vertical transition from the

reactant to the product surface. Following the optical electron transfer the charge-separated species relaxes into its most stable geometry.

In photoinduced electron transfer (**Figure 3 (c)**), either the donor or acceptor is locally excited by light of an appropriate wavelength. Subsequent thermal electron transfer occurs from this excited state to give the charge-separated product. Photoinduced ET is the most useful form of electron transfer as it converts the energy of light into chemical potential, which can be utilised to carry out work. In order to rationally design such photovoltaic devices a sound knowledge of the parameters that effect electron transfer is essential.

A.3 BASIC ELECTRON TRANSFER THEORY

A system which is to undergo long-range photoinduced intramolecular electron transfer must consist of a light absorbing species (chromophore) which either acts as an electron donor or electron acceptor in its first electronically excited state. As mentioned above, electron donor and electron acceptor need to be connected by a medium that enables the coupling of the wavefunctions of the reactant state (first excited state) and the product state (the charge-separated state). The magnitude of the electronic coupling element (H_{rp}) distinguishes between two types of electron transfer. It is defined by **Equation 1** where Ψ_R^o and Ψ_P^o are the diabatic electronic wave functions of the reactant (e.g. $[D^*-A]$) and the product (e.g. $[D^+-A^-]$), respectively. H_{el} is the Born-Oppenheimer Hamiltonian for the system.⁹

$$H_{rp} = \langle \Psi_R^o | H_{el} | \Psi_P^o \rangle$$

Equation 1: Definition of the electronic coupling element H_{rp}

If H_{rp} is moderately large ($\geq 200 \text{ cm}^{-1}$), the term adiabatic ET is used. The potential energy surfaces of the reactant and the product do not intersect but rather strongly 'avoid' one another and the ET reaction remains on the lower energy surface as it proceeds through the transition state (**Figure 4 (1)**). Adiabatic intramolecular electron transfer is generally found when donor and acceptor are strongly coupled. The splitting of the adiabatic surfaces is equal to $2H_{rp}$.^{10,11}

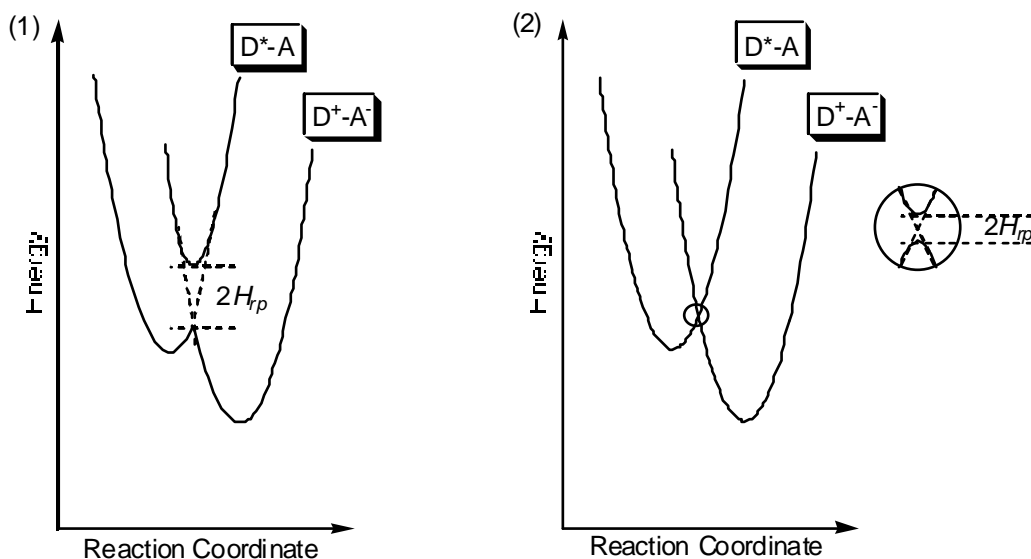


Figure 4: (1) adiabatic and (2) nonadiabatic Gibbs free energy surfaces

If H_{rp} is small ($< 200 \text{ cm}^{-1}$), the energy surfaces of the reactant and the product no longer interact significantly at their formal point of intersection. In this case the system normally remains on the reactant surface as it passes through the intersection point. Only occasionally does it cross over to the product energy surface and so-called nonadiabatic electron transfer occurs (**Figure 4 (2)**). Most long-range electron transfer processes, including those described in this thesis, occur nonadiabatically.¹² In order to describe the phenomenon a quantum mechanical approach is needed.

A.3.1 Expressions for Rate Constants

Quantum mechanical treatments of electron transfer begin with Fermi's golden rule formulation¹³ for the probability of a radiationless transition between two states (**Equation 2**). The rate of electron transfer (k_{ET}) is expressed as a function of the electronic coupling element (H_{rp}) between the reactant and the product,

$$k_{ET} = \frac{2\pi}{\hbar} |H_{rp}|^2 FCWD$$

Equation 2: Fermi's golden rule

where $FCWD$ is the Franck-Condon weighted density-of-states, or more precisely, the squared overlap integral of the vibrational wave functions weighted by the Boltzmann distribution. Despite the fact that one can relate $FCWD$ to experimental data, such an expression remains

complex and not very practical for chemists, as it does not contain easily accessible (measurable) and accurate parameters.

On the basis of a classical approximation, Marcus provided a more 'practical' (and Nobel Prize winning) expression.^{6,13} He treated the solvent as a dielectric continuum and considered the Franck-Condon principle, which states that during the instantaneous electron transfer the nuclei do not have time to change either their positions or their momenta. To satisfy these two conditions simultaneously the transfer has to occur at or near nuclear configurations for which the total potential energy of the reactants and the surrounding solvent is equal to that of the products and the surrounding solvent. This is the case at the formal point of intersection for the two parabolic potential energy surfaces in **Figure 5**.

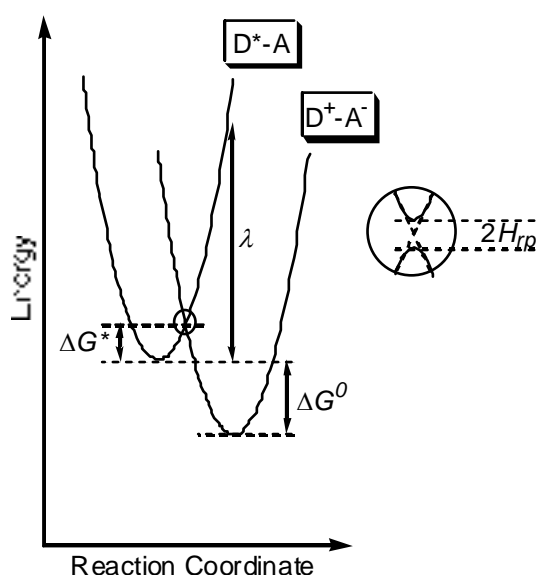


Figure 5: Representation of the Gibbs free energy surfaces according to Marcus theory.

In Marcus theory¹³ the curvature of the reactant and product surface is assumed to be the same. The position of the two parabolas relative to each other is completely described by the Gibbs free energy of the reaction ΔG^0 and the reorganisation energy, λ . Since allowed transitions can only occur where the parabolas cross, the free energy of activation ΔG^* for the electron transfer reaction can be calculated from ΔG^0 and λ .

$$\Delta G^* = \frac{(\lambda + \Delta G^0)^2}{4\lambda}$$

Equation 3: Gibbs free energy of activation

According to classical transition-state theory, the first-order rate constant k_{ET} is given by

$$k_{ET} = \kappa_{el} \nu_n \exp\left(\frac{-\Delta G^*}{k_B T}\right)$$

Equation 4: First order rate constant in classical transition-state theory

where κ_{el} is the electronic transmission coefficient, ν_n is the frequency of passage (nuclear motion) through the transition state ($\nu_n \cong 10^{13} \text{ s}^{-1}$), k_B is the Boltzmann constant, and T is the absolute temperature. ΔG^* is the Gibbs energy of activation for the ET process. Application of **Equation 3** leads to the classical Marcus equation¹³

$$k_{ET} = \kappa_{el} \nu_n \exp\left(\frac{-(\lambda + \Delta G^0)^2}{4\lambda k_B T}\right)$$

Equation 5: Classical Marcus equation

where λ is the total reorganisation energy, which is usually divided into contributions of an outer (λ_o) and an inner (λ_i) component, with $\lambda = \lambda_o + \lambda_i$. The value of λ_i may be calculated from the force constants for all the molecular vibrations in both the reactant and the product, while the outer reorganisational energy λ_o can be determined by application of the dielectric continuum model of a solvent. The simplest application of this model assumes that the donor and acceptor are spherical with radii r_D and r_A , respectively, lying at a centre-to-centre distance, r_{DA} , apart. The charge transferred from one reactant to the other is Δe . If ϵ_{op} and ϵ_s are the optical and static dielectric constants of the solvent, Marcus⁶ has shown that

$$\lambda_o = (\Delta e)^2 \left(\frac{1}{2r_D} + \frac{1}{2r_A} - \frac{1}{r_{DA}} \right) \left(\frac{1}{\epsilon_{op}} - \frac{1}{\epsilon_s} \right)$$

Equation 6: Outer component of the total reorganisation energy

In experiments λ_o varies from near zero for non-polar solvents to 1.0 - 1.5 eV for polar solvents,¹² whereas for several organic donor-acceptor systems λ_i was found to be between

0.3 and 0.6 eV.¹⁴⁻¹⁶ Therefore in polar solvents the outer reorganisation energy is the dominant contribution to λ and interchromophoric separation has a greater effect.

A key feature of **Equation 5** is that it predicts that the rate of electron transfer will slow down, when the standard free energy of the reaction becomes very large. In contrast to the so-called "normal region" this is called the "inverted region". At $-\Delta G^0 = \lambda$ ("nearly optimal region") the rate of electron transfer reaches its maximum and enters the "inverted region" with k_{ET} decreasing for further increasing ΔG^0 (**Figure 6**) It took about 20 years to verify this prediction by experiment.¹⁷

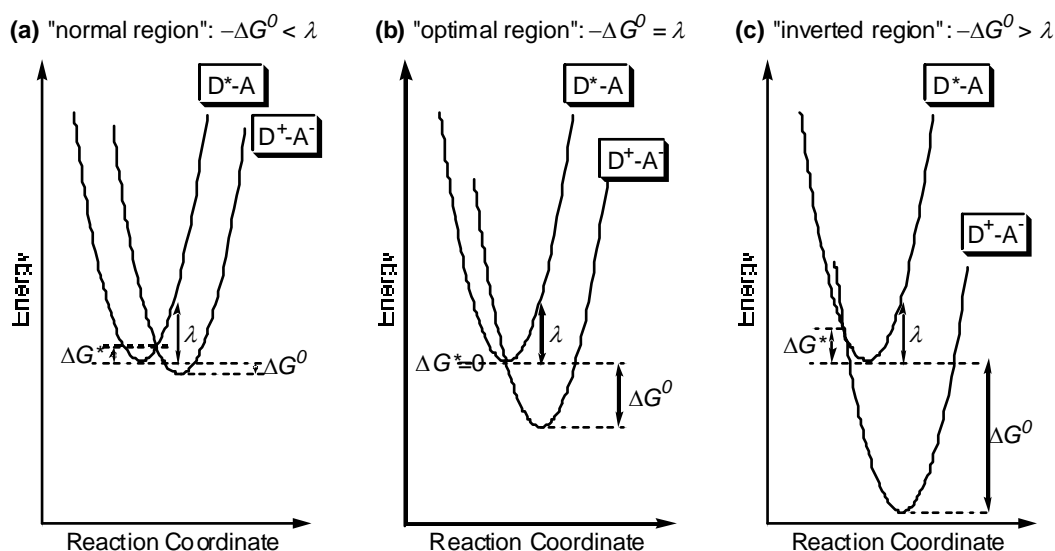


Figure 6: Marcus "normal", "optimal" and "inverted" region

The classical Marcus theory generally works well for electron transfer reactions where $\kappa_{el} = 1$, corresponding to a unit probability of electron transfer at the transition state. However, for most nonadiabatic ET reactions the probability of electron transfer is $\ll 1$, resulting in the above mentioned quantum mechanical approach (**Equation 2**). If in this approach the low energetic solvent vibrations are treated classically and only the high-frequency internal modes are treated quantum mechanically as an average mode, a semiclassical expression for the high-temperature limit can be derived.^{13,18}

$$k_{ET} = \frac{2\pi}{\hbar} |H_{rp}|^2 \frac{1}{\sqrt{4\pi\lambda k_B T}} \exp\left(\frac{-(\lambda + \Delta G^0)^2}{4\lambda k_B T}\right)$$

Equation 7: High-temperature limit of the semiclassical Marcus expressions

Equation 7 works very well for the normal region, and thus is often used even though the conditions do not justify the high-temperature limit. **Equation 7** is equivalent to **Equation 5** with

$$\kappa_{el} \nu_n = \frac{2\pi}{\hbar} |H_{rp}|^2 \left(\frac{1}{\sqrt{4\pi\lambda k_B T}} \right)$$

Equation 8: Classic equivalent

Thus, the classical Gibbs energy diagrams can be retained for nonadiabatic electron transfer, provided that $\kappa_{el} \nu_n$ is reinterpreted according to **Equation 8**.

A.3.2 Electron Transfer Variables

The semiclassical Marcus theory predicts in which way the electronic coupling element (H_{rp}), the free energy of reaction (ΔG^0), the total nuclear reorganisation energy (λ), and the temperature (T) influence the rate of electron transfer. Variables of electron transfer systems such as the type of chromophores involved, the distance between the chromophores, their orientation in respect to each other, as well as the type of bridge connecting the chromophores affect these parameters and subsequently the rate of their intramolecular electron transfer. These dependencies have been investigated through synthesis of suitable models and the investigation of their photophysical properties. In many cases the results confirm the predictions made by the theory.

A.3.2.1 Chromophore dependence

Different electron donors or electron acceptors vary in their electron donating or accepting ability. Those abilities are reflected in their redox potentials. The change in free energy (ΔG^0) for a photoinduced charge separation process can be expressed with those redox potentials as shown schematically in **Figure 7**.

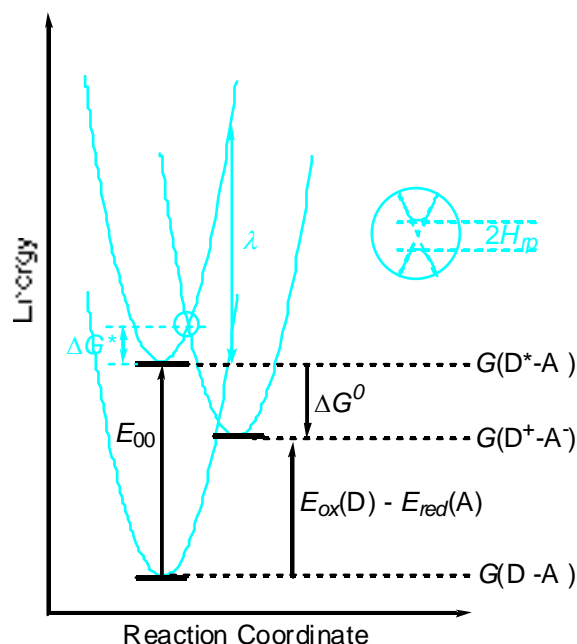


Figure 7: Schematic representation of the change in free energy (ΔG^0) for a photoinduced electron transfer reaction. E_{00} is the zero-zero electronic excitation energy to the first excited singlet state (D^*); $E_{ox}(D)$ and $E_{red}(A)$ are the oxidation and reduction potentials of D and A, respectively.

From **Figure 7** it can be observed that the free energy change for the ET reaction may be given by the Rehm–Weller equation^{19,20}

$$\Delta G^0(\infty) = E_{ox}(D) - E_{red}(A) - E_{00}$$

Equation 9: Rehm-Weller equation for infinite $[D^+]$ - $[A^-]$ separation

for donor and acceptor at infinite separation. If the donor and the acceptor are at finite distances, **Equation 9** must be modified to account for the Coulombic attraction energy (ΔG_{ip}) between the positive charged donor and the negative charged acceptor:²¹

$$\Delta G^0 = E_{ox}(D) - E_{red}(A) - E_{00} + \Delta G_{ip}$$

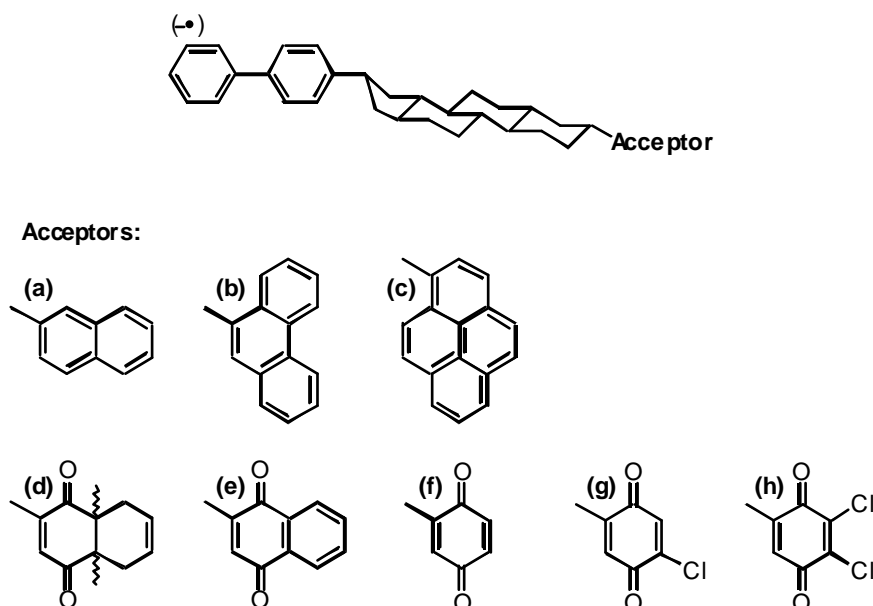
Equation 10: Rehm-Weller equation for finite $[\text{D}^+]$ - $[\text{A}^-]$ separation

The Coulombic attraction energy (ΔG_{ip}) is defined as

$$\Delta G_{ip} = \frac{-e^2}{4\pi\epsilon_0\epsilon_s r_{DA}}$$

Equation 11: Coulombic attraction energy

As shown above (**Equation 7**) the rate of electron transfer depends on the Gibbs free energy change of the electron transfer reaction, which in turn depends on the oxidation potential of the donor and the reduction potential of the acceptor. This dependence was confirmed in many experiments. The first experiment to confirm the existence of the Marcus inverted region was the one carried out by Miller *et al.*^{14,17} on a series of compounds (**Example 1**) - bearing a biphenyl donor - which undergo thermal electron transfer.



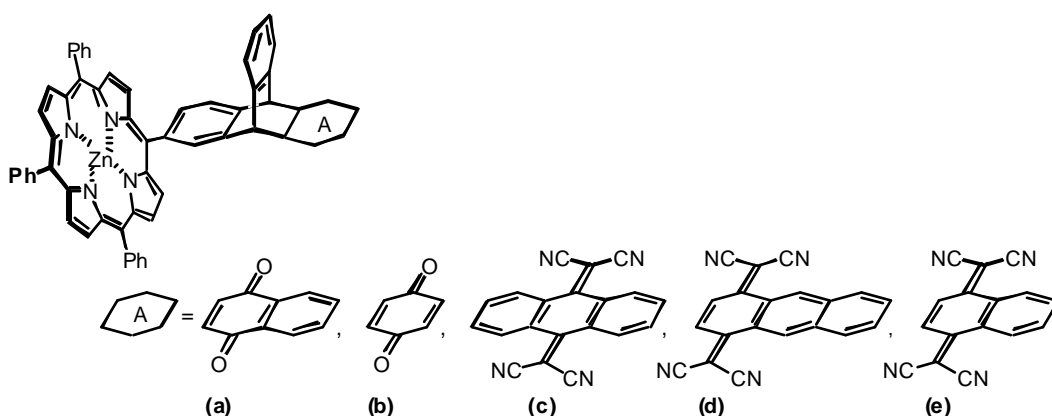
Example 1: First intramolecular ET models by Miller *et al.* to establish experimentally the existence of the Marcus inverted region

A 4-biphenyl donor is covalently attached to the 3- β position of a rigid, steroidal 5 α -androstane skeleton. A variety of eight acceptors were attached to the 16- β position of the androstane skeleton, separating donor and acceptor by 10 Å. With increasing exergonicity (**Table 1**) the rate of electron transfer raised from $1.5 \pm 0.5 \times 10^6 \text{ s}^{-1}$ (for a 2-naphthyl acceptor) to $>2 \times 10^9 \text{ s}^{-1}$ (for a hexahydronaphthoquinon-2-yl acceptor), and then decreased to $7 \pm 3 \times 10^7 \text{ s}^{-1}$ (for a 5,6-dichlorobenzoquinon-2-yl acceptor).

Table 1: First experimental proof for the Marcus inverted region by Miller *et al.* (1984)

Acceptor Group for Example 1	$-\Delta G^0$	k_{ET} in MTHF
2-naphthyl (a)	0.05 eV	$1.5 \pm 0.5 \times 10^6 \text{ s}^{-1}$
9-phenanthryl (b)	0.16 eV	$1.25 \pm 0.2 \times 10^7 \text{ s}^{-1}$
1-pyrenyl (c)	0.52 eV	$1.5 \pm 0.5 \times 10^9 \text{ s}^{-1}$
hexahydronaphthoquinon-2-yl (d)	1.23 eV	$>2 \times 10^9 \text{ s}^{-1}$
2-naphthoquinoyl (e)	1.93 eV	$3.8 \pm 1 \times 10^8 \text{ s}^{-1}$
2-benzoquinoyl (f)	2.10 eV	$2.5 \pm 0.3 \times 10^8 \text{ s}^{-1}$
5-chlorobenzoquinon-5-yl (g)	2.29 eV	$1.7 \pm 0.2 \times 10^8 \text{ s}^{-1}$
5,6-dichlorobenzoquinon-2-yl (h)	2.40 eV	$7 \pm 3 \times 10^7 \text{ s}^{-1}$

An example for photoinduced electron transfer entering the inverted region is given by the Wasielewski group²²⁻²⁶ His group studied a series of 32 molecules where 8 different acceptors were covalently attached to 4 different donors - all of them porphyrins, metallated or non-metallated with phenyl- or pentyl-groups in the *meso*-positions. Seventeen of those molecules underwent rapid photoinduced charge separation and five of them are pictured in **Example 2**.



Example 2: Intramolecular photoinduced ET models by Wasielewski *et al.*
Proof for the existence of the Marcus inverted region

With increasing driving force ((a) to (e)) the rate of electron transfer rises and reaches a maximum before entering the Marcus inverted region (**Figure 8**). The fit to the data was obtained by using an electronic coupling of 33 cm^{-1} , an average vibrational frequency of 500 cm^{-1} , a total reorganisation energy $\lambda = 0.6 \text{ eV}$, and $\Delta G^0 = 0.8 \text{ eV}$.

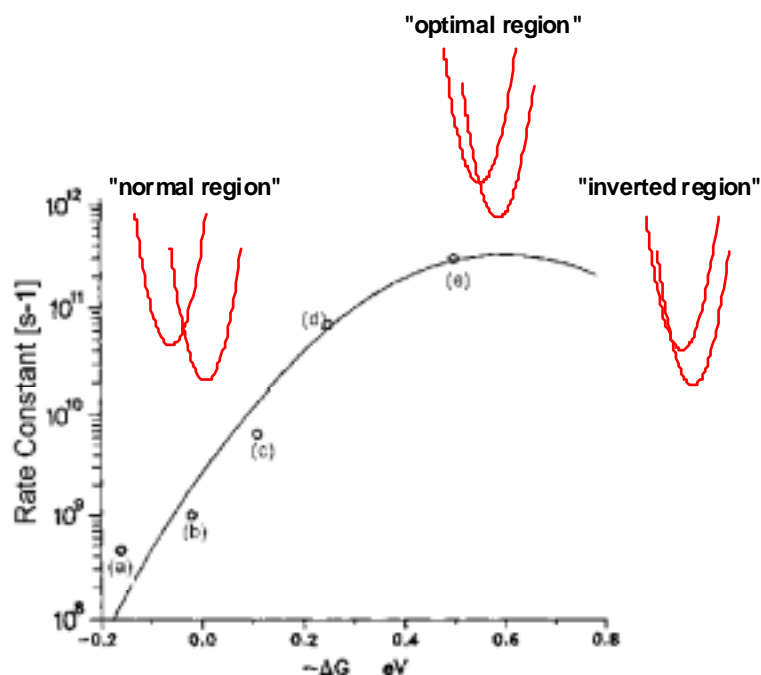


Figure 8: Rate constant for the Wasielowski series Example 2 (a) - (e) vs. driving force $-\Delta G$

Both examples, Miller and Wasielowski, nicely demonstrate the dependence of electron-transfer rates on the nature of the chromophores.

A.3.2.2 Distance Dependence

The electronic coupling element (H_{rp}) and the reorganisation energy (λ) are the only factors that depend significantly on the interchromophoric separation (r_{DA}). λ Depends weakly on r_{DA} , so H_{rp} should be the major factor in the dependence of the rate of electron transfer on distance. Electron-transfer rates have been measured as a function of distance in rigid glasses,^{18,27-31} in dyads in which a preferably rigid spacer group holds the donor and acceptor apart (see examples in this thesis), in monolayer assemblies,³²⁻³⁴ in proteins,³⁵⁻³⁸ and DNA.^{39,40} Where it has been possible to accurately measure dependence on distance, it has always been found that electron-transfer rates decayed exponentially because of the exponential decrease of electronic coupling with distance

$$H_{rp}^2(r_{DA}) = H_{rp}^2(r_0) \exp(-\beta(r_{DA} - r_0))$$

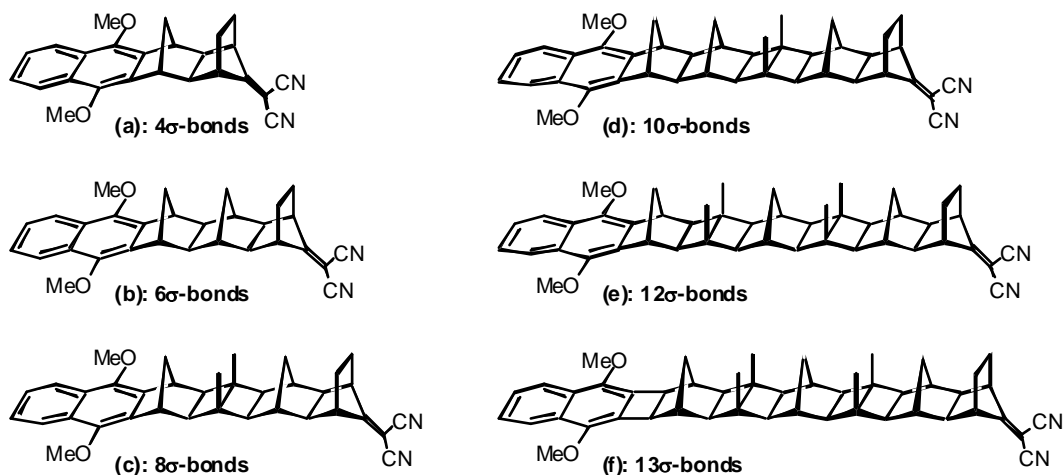
Equation 12: Exponential dependence of H_{rp} on distance

where r_0 is a reference distance at which the largest rate of ET ($k_{ET}(r_0)$) occurs (normally at the van der Waals contact between the chromophores) and β is an attenuation constant, which depends on both the absolute and relative donor, acceptor and bridge energetics. In a series of dyads with the same values for ΔG^0 and λ but differing r_{DA} , the rate constants should follow the relation

$$k_{ET}(r_{DA}) = k_{ET}(r_0) \exp(-\beta(r_{DA} - r_0))$$

Equation 13: Rate constant - distance relation

Perhaps the most conclusive study on distance dependence of photoinduced intramolecular electron transfer rates has been performed by the Paddon-Row and Verhoeven groups on a series of rigid donor-bridge-acceptor molecules.^{15,41-47} Electron transfer occurs from the locally excited state of a dimethoxynaphthalene (DMN) donor to a dicyanovinyl (DCV) acceptor *via* polynorbornane-bicyclo[2.2.0]-hexane ('norbornylogous') bridges with an effective length of 4 to 13 σ -bonds (**Example 3**). The norbornylogous bridges hold the donor and acceptor at well-defined distances and orientations.



Example 3: Series of DMN-DCV dyads by the Paddon-Row group

With increasing edge-to-edge interchromophoric separation (r_{DA}) from 7.1 Å (4 σ -bonds) to 15.6 Å (13 σ -bonds) the rate of electron transfer dropped by three orders of magnitude, but was still as high as $1.5 \times 10^8 \text{ s}^{-1}$ for the DMN - 13 σ -bonds - DCV dyad. The efficiency of charge separation was near unity for the 4 to 10 σ -bond systems and fell off to 89 % for **Example 3(e)** and 45 % for **Example 3(f)**. With increasing charge-separation the lifetime of the charge-separated state increased significantly and predictably (see **Table 2**). Unusually

large for a simple dyad was the lifetime of 1.5 μ s for **Example 3 (f)**. That charge separation had indeed occurred was demonstrated using time-resolved microwave conductivity, which gives an estimate of the dipole moment of the charge-separated species. The measurements were consistent with the [DMN⁺-bridge-DCV] formation.⁴⁸

Table 2: Electron transfer rates and lifetimes of the charge-separated state for DMN-DCV dyads by the Paddon-Row group

Compound	r_{DA}	k_{ET} , THF, 20 °C	t_{CR} , dioxane
Example 3 (a)	7.1 Å	$> 3300 \times 10^8 \text{ s}^{-1}$	$< 0.5 \text{ ns}$
Example 3 (b)	9.0 Å	$\geq 3300 \times 10^8 \text{ s}^{-1}$	0.5 ns
Example 3 (c)	11.8 Å	$670 \times 10^8 \text{ s}^{-1}$	2.5 ns
Example 3 (d)	13.3 Å	$120 \times 10^8 \text{ s}^{-1}$	43 ns
Example 3 (e)	14.9 Å	$13 \times 10^8 \text{ s}^{-1}$	297 ns
Example 3 (f)	15.6 Å	$1.5 \times 10^8 \text{ s}^{-1}$	1500 ns

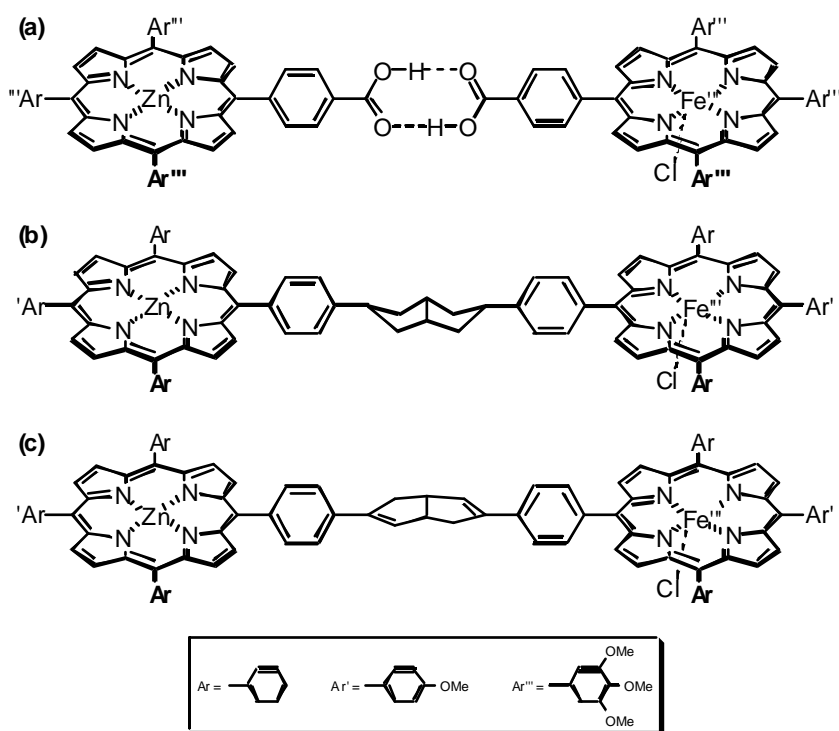
The upper value of β for the norbornylogous bridge was determined to be 0.46 Å⁻¹ in THF, 0.50 Å⁻¹ in ethyl acetate, and 0.61 Å⁻¹ in acetonitrile. Similar studies on distance dependence of electron transfer rates for other types of media between donor and acceptor lead to the β -values (per bond) shown in **Table 3**.

Table 3: β -values for different media, $k_{ET} \propto \exp(-\beta r)$

Medium	β -value
Through space (vacuum)	6.0
Through saturated C-C bonds ⁴⁹	0.9 - 1.2
Through helical oligoproline ³⁷	0.2 - 0.3
Through proteins ⁵⁰	
β -sheets	0.8 - 1.2
α -helix	1.2 - 1.6
Through DNA ^{39,40,51-54}	0.64 - 1.4
Ru ²⁺ (phen') ₂ dppz-{DNA Helix}-Rh ³⁺ (phi) ₂ phen' ⁵⁵	< 0.2

A.3.2.3 Bridge dependence

In a sense the dependence of electron transfer rates on the type of bridge is reflected in the different β -values for different media derived from distance dependence studies. This is proof that long-range electron transfer is mediated by the bridge (through bond (TB) mechanism) and does not occur through space (TS). Bridges can consist of saturated, unsaturated, conjugated, or aromatic spacers. Proteins in different secondary structures^{56,57} have been utilised as electron transfer mediators as well as DNA^{55,58-60}, metal complexes⁶¹ and hydrogen bonds.⁶²⁻⁶⁴ A very elegant comparison of electron transfer mediated by single bonds, double bonds or hydrogen bonds has been published by Therien *et al.*⁶⁵ The supramolecular complexes feature (porphyrinato)zinc donors and (porphyrinato)iron(III)chloride acceptors separated by a virtually constant distance, thus establishing uniform driving force and reorganisation energy for the ET reaction. The bridges that connect donors to acceptors are rigid and 14 bonds long and their central 4 bonds contain hydrogen, single, or double bonds (**Example 4(a)-(c)**).



Example 4: Bis-porphyrin dyads by Therien *et al.* (1995)

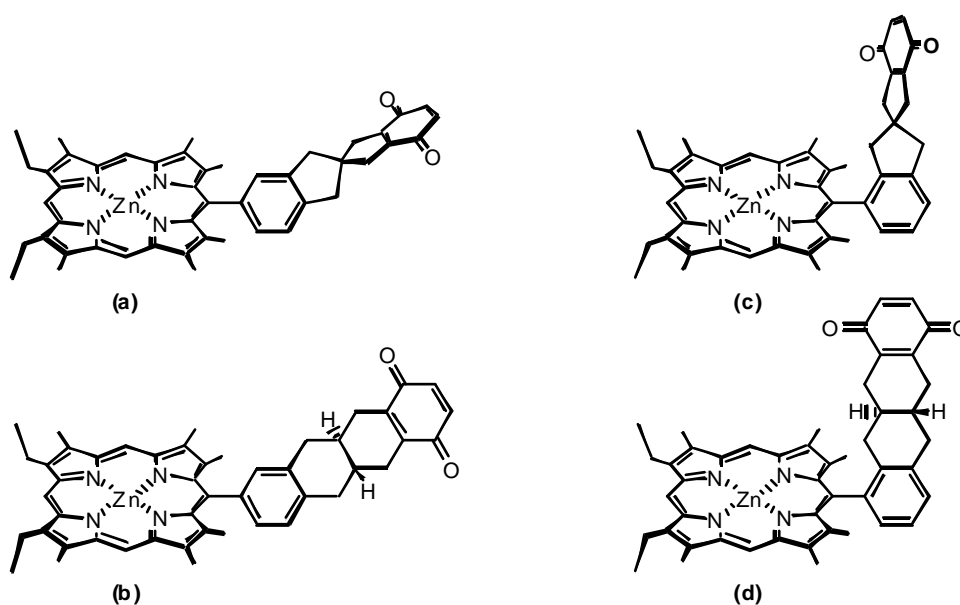
The main purpose of this work was to prove that hydrogen bonds are good mediators of electron transfer and therefore should play an important role in biological electron transfer processes. The measured electron-transfer rates of these systems confirm that point of view (**Table 4**).

Table 4: Distance, driving force, and electron-transfer rates for bis-porphyrin dyads by Therien *et al.*

Compound	Distance (TB)	$-\Delta G^0$	k_{ET} in DCM
Example 4 (a)	22.4 Å	0.70 eV	$8.1 \times 10^9 \text{ s}^{-1}$
Example 4 (b)	23.7 Å	0.87 eV	$4.3 \times 10^9 \text{ s}^{-1}$
Example 4 (c)	23.1 Å	0.87 eV	$8.8 \times 10^9 \text{ s}^{-1}$

A.3.2.4 Geometry dependence

Theoretical studies indicate that the electronic coupling element (H_{rp}) is sensitive to the relative orientations of the donor and acceptor, as well as the overlap of the π -systems of the chromophores with the bridge linking them.^{66,67} For many ET reactions H_{rp} can either be positive or negative, depending on angles, and in principle, there may be angles at which the coupling can be zero. In experiments with a series of bichromophoric systems where the chromophores, their distance from each other, as well as the number and type of bonds connecting them were kept unchanged, the dependence on the chromophore's orientation has been investigated.^{17,57,67,68} One recent example is that of Sakata *et al.*⁶⁹ shown in **Example 5**.



Example 5: Porphyrin-quinone dyads by Sakata *et al.* (1994)

In these four systems ((a)/(b), (c)/(d)) the edge-to-edge distance varies by 0.4 Å or 0.1 Å only, the relative orientation of porphyrin and quinone, however, by 90°. This results in a

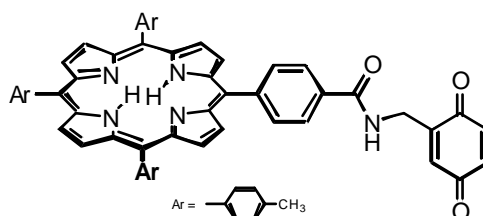
reduction of the rate for photoinduced electron transfer and charge recombination (**Table 5**). It was shown that the decrease in the rate constants was due to the different orientations affecting the electronic coupling element (H_{rp}). A similar result was obtained for the free-base analogues.^{70,71}

Table 5: Edge-to-edge distance, driving force, ET-, and charge recombination (CR) rates for porphyrin-quinone dyads by Sakata *et al.* (1994)

Compound	r_{DA}	$-\Delta G^0$	k_{ET} in THF	k_{CR} in THF
Example 5 (a)	8.2 Å	0.83 eV	$2.6 \times 10^{11} \text{ s}^{-1}$	$4.6 \times 10^{10} \text{ s}^{-1}$
Example 5 (b)	8.6 Å	0.82 eV	$3.2 \times 10^{10} \text{ s}^{-1}$	$3.6 \times 10^{10} \text{ s}^{-1}$
Example 5 (c)	6.4 Å	0.76 eV	$1.7 \times 10^{10} \text{ s}^{-1}$	$1.6 \times 10^{10} \text{ s}^{-1}$
Example 5 (d)	6.3 Å	0.76 eV	$5.0 \times 10^9 \text{ s}^{-1}$	$7.9 \times 10^9 \text{ s}^{-1}$

A.3.2.5 Solvent dependence

The surrounding solvent changes two parameters that can markedly alter electron transfer rates. First, the exergonicity (ΔG^0) can be affected through different solvation of the product ion pair $[D^+ - A^-]$. Second, the external contribution to the reorganisation energy (λ_o) is altered through changes in ϵ_{op} and ϵ_s , the optical and dielectrical constants. Schmidt *et al.*⁷² have shown that changing the solvent can change λ by as much as 1.2 eV. Exergonicity (ΔG^0) can vary by 0.3 eV with different solvents.^{72,73} For **Example 6** by Schmidt *et al.*^{72,74,75} the rates of electron transfer were measured in 22 different solvents and found to vary from $1.4 \times 10^7 \text{ s}^{-1}$ to $2.3 \times 10^9 \text{ s}^{-1}$.

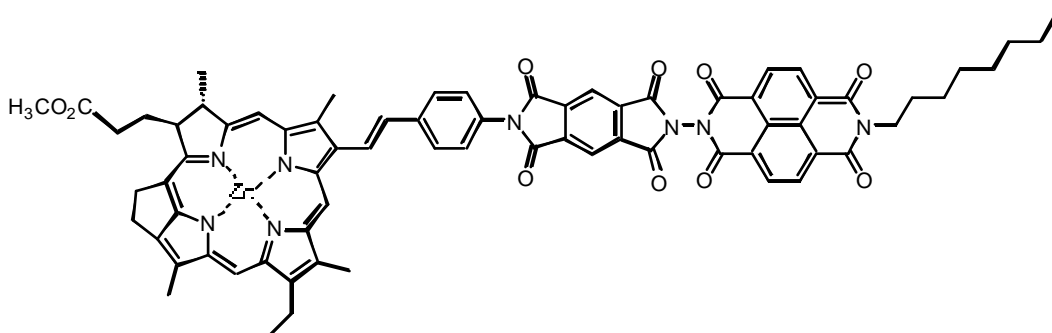


Example 6: Porphyrin-quinone dyad by Schmidt *et al.* (1985)

The results were analysed according to the high temperature limit of the semiclassical Marcus equation (**Equation 7**) and were found to conform reasonably well to the Marcus predicted

behaviour. Scatter in the data was explained with a solvent dependence of the electronic coupling element (H_{rp}). This solvent sensitivity of H_{rp} was suggested to arise from different average conformations of the porphyrin-quinone dyad. In solvents with high dielectric constants the molecule might adopt a more folded conformation, which would bring donor and acceptor closer together and thus enhance H_{rp} . In some conformations through-solvent (rather than through-bond) electron transfer could play an important role, too. Size and shape of solvents were also considered to have a possible impact on k_{ET} .

For very large electron transfer rates (k_{ET}), the motion of solvent molecules can limit the electron transfer rate. This is known as the dynamic solvent effect.⁷⁶ The re-orientation of the solvent molecules around $[D^+ - A^-]$ becomes sluggish compared to the time-scale of the ET process. This essentially limits the rate of electron transfer to the timescale for solvent motions.⁹ For a trichromophore Wiederrecht *et al.*⁷⁷ have found large differences in the rate of photoinduced electron transfer in similar low-polarity solvents. The triad comprises a zinc methyl 13¹-desoxypyropheophorbide *a* (Chl) as a donor, a pyromellitimide (PI) as a primary electron acceptor, and 1,8:4,5-naphthalenediimide (NI) as a secondary acceptor (**Example 7**).



Example 7: Chlorophyll-pyromellitimide-naphthalenediimide (Chl-PI-NI) triad by Wiederrecht *et al.* (1996)

These differences in electron-transfer rates were attributed to dynamic solvent effects. A better insight into the solvent reorientation - electron transfer rate relation is provided by studies of rigid molecules in low temperature solid solutions.^{24,78} Below the freezing point solvent reorientation is strongly hindered, which has a considerable impact on the driving force. In some cases electron transfer becomes even endothermic.

A.3.2.6 Temperature dependence

As with any rate constant for an activated process, electron transfer rate constants normally exhibit an Arrhenius temperature dependence (see **Equation 7**). "Normally" appears to be the key word in this sentence as experimental results^{73,79-82} and further theoretical considerations⁹ indicate that this simple description may be adequate in the "normal" region, but tends to fail in the "inverted" region. The interpretation of temperature-dependent electron-transfer kinetics is complicated by the relatively large influence of the temperature dependence of the solvent dielectric properties. This problem becomes especially evident if the barrier is small, when it may lead to an overall nullification or even inversion of the temperature effect on the experimental rate. Upon correction for the temperature dependence of the solvent properties, the rate of electron transfer is found to be independent of temperature in the inverted region, where nuclear tunnelling involving high frequency modes becomes dominant. This contradicts expectations based on Marcus theory.

This last example is only one of many where experimental results do not match predictions made by theory and even though much progress has been made in respect of how certain parameters influence electron transfer behaviour, there remain puzzles to be solved.⁸³ Solving puzzles on one hand and using the knowledge gained on the other are two fields of research in the electron transfer context. The latter finds its application in the rational design of molecular devices, which exhibit high quantum efficiency, fast electron transfer and a long-lived charge-separated state.

A.4 MOLECULAR DEVICES

One of the most sought after goals in electron transfer is the rational design and successful construction of molecular photovoltaic devices,^{5,84} i.e., those molecular systems that are capable of transducing photon energy into chemical potential through creation of a charge-separated state. The basic scheme for a bichromophoric donor-acceptor [D-A] molecular photovoltaic device is given in **Figure 9**.

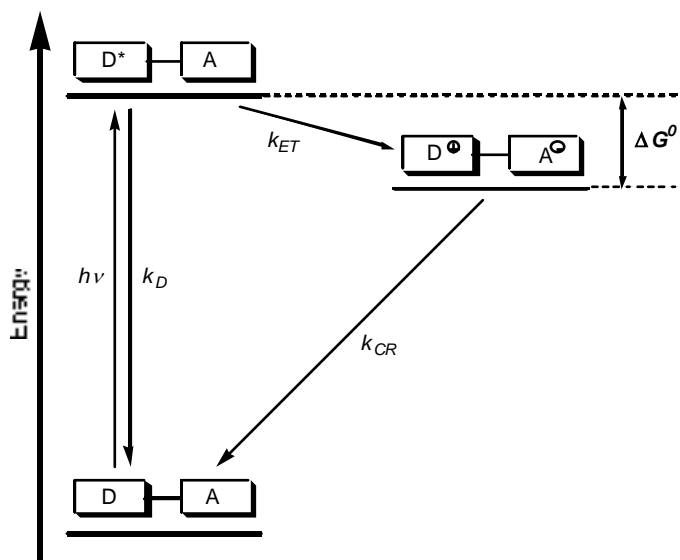


Figure 9: Energy diagram illustrating pathways available in a photoinduced electron-transfer event within a dyad [D-A].

Absorption of light by the dyad leads to the (eventual) formation of the first excited state whose excitation energy is localised on either the donor or acceptor moiety. The locally excited state can then either decay non-productively back to the ground state (with a rate k_D) or it may undergo desired electron transfer (ET) to give the charge-separated (CS) state $[D^{\bullet+}-A^{\bullet-}]$ (with a rate k_{ET}). The amount of chemical potential stored during this process is given by the quantity $(h\nu + \Delta G^0)$. Left to itself, the CS state eventually undergoes charge recombination (with a rate k_{CR}).

A.4.1 Requirements

The following criteria should be met when designing a molecular photovoltaic device:

- (1) The quantum yield for the charge separation process should be as high as possible, that is, $k_{ET} \gg k_D$.
- (2) The lifetime, τ_{CR} , of the charge-separated state must be long enough that it is able to carry out 'useful' chemical work. In practice, τ_{CR} should be greater than 1 μ s.
- (3) The energy content of the CS state should be as high as possible, thereby ensuring maximum conversion of photonic energy into chemical potential. Thus, $|\Delta G^0|$ should be small.

To meet requirement (1), the magnitude of k_{ET} should be greater than 10^{10} s^{-1} . This number follows from the observation that the lifetimes of the excited states of the majority of potentially useful chromophores are about 10^{-9} s . Thus, simultaneous satisfaction of requirements (1) and (2) means that the ratio of the rates of charge separation to charge recombination (k_{ET} / k_{CR}) should be greater than 10^4 . This dual requirement of high efficiency of charge separation and longevity of the charge-separated state cannot be easily met by bichromophoric systems. Generally, the lifetime of the charge-separated state in dyads increases with increasing separation between the two chromophores, whereas the efficiency for its formation decreases with bridge length.

A.4.2 Multichromophoric Concept

Increasing the lifetime of the charge-separated state can be achieved by increasing the interchromophoric separation. However, this can not be easily done in bichromophoric systems without severely compromising the efficiency of formation of the charge-separated state. This problem can be circumvented by using multichromophoric systems, i.e., triads, tetrads, pentads etc.,⁸⁵ that constitute a gradient of redox centres arranged within a spatially well-defined array. The principle behind this concept is illustrated in **Figure 10** for the case of a covalently linked triad [D-A₁-A₂], in which D is initially locally excited.

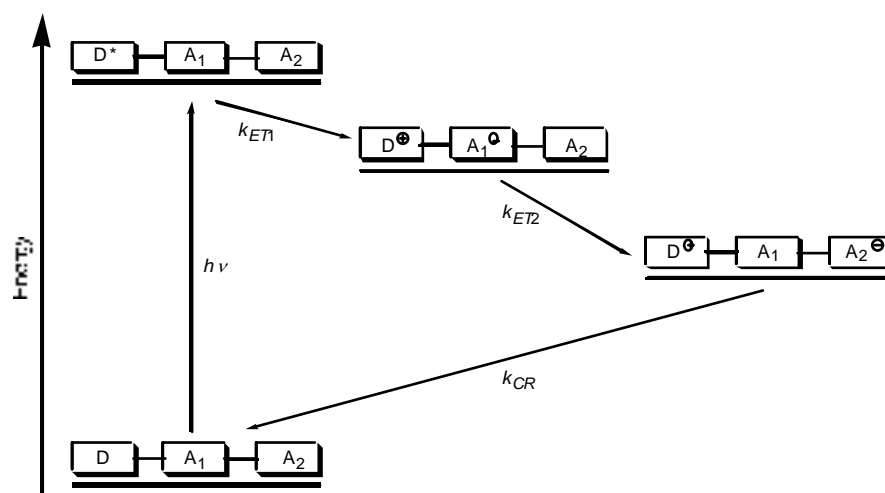


Figure 10: Energy diagram for multichromophoric concept

In this system, the electron transfer takes place in a sequence of rapid 'hops' between adjacent chromophores that are separated by a bridge short enough to guarantee that each hop occurs

with near unit efficiency. The final result is charge separation over a sufficiently large distance that the unwanted charge-recombination step becomes acceptably slow.

In the process of evolution, Nature has been able to develop such systems. Photoinduced electron transfer occurs with almost 100 % efficiency over a large distance in the photosynthetic reaction centres (PRCs) of bacteria and green plants. The resulting charge-separated state lives long enough to provide the electrochemical potential that drives all subsequent biochemical reactions and, indirectly, almost all living things.

A.5 PHOTOSYNTHESIS

Photosynthesis literally means assembling by light. Commonly used, photosynthesis describes the process by which plants synthesise organic compounds from inorganic materials in the presence of sunlight. The appearance of photosynthesising bacteria about 3.5 billion years ago represented an enormous step in the process of evolution.^{86,87} Purple bacteria and green sulfur bacteria developed slightly different photosystems (PSI- and PSII-types). Genomic fusion between a bacterium possessing a purple bacterial PSII-type reaction centre and a bacterium having a bacterial PSI-type reaction centre has been suggested for the development of the cyanobacteria that contain two photosystems (**Figure 11**). How and when water oxidising capacity was incorporated into this gene-fusion product to enable oxygenic photosynthesis is not yet known.⁸⁸

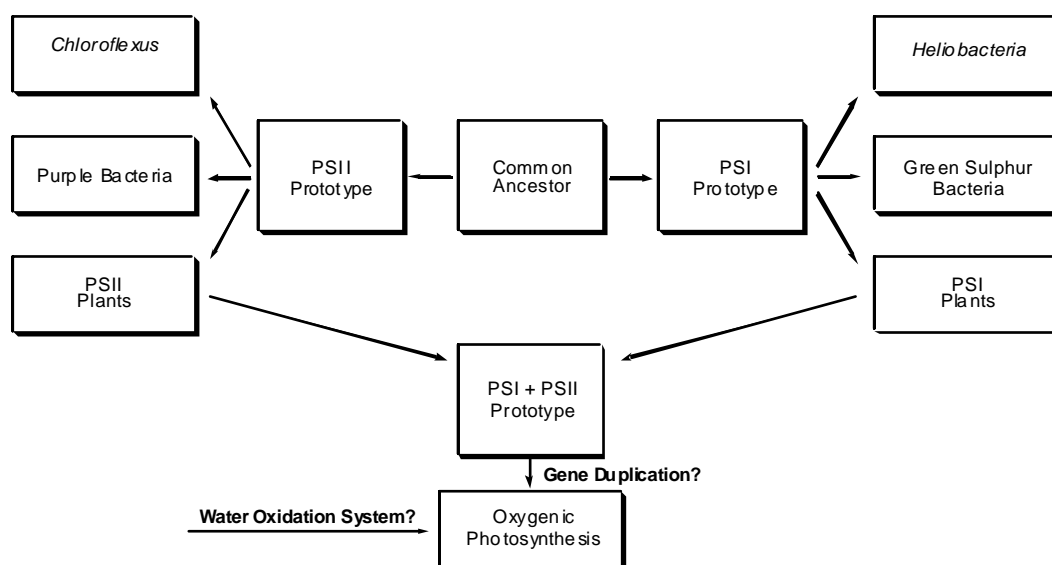


Figure 11: Proposed scheme for the evolution of photosynthetic reaction centres (after Nitschke and Rutherford, 1991, and Blankenship, 1992)

What is well known is that oxygenic photosynthesis, or green plant photosynthesis with the two photosystems I and II provides the means by which a large part of the biosphere was created. Green plants are able to reduce carbon dioxide with the weak reducing agent water and form carbohydrates and oxygen. Photosynthesis is essential for maintaining all forms of life. The conversion of solar energy into chemical potential occurs in the photosynthetic reaction centres (PRCs).

A.5.1 The Photosynthetic Reaction Centre

The photosynthetic reaction centres in both bacteria and green plants, are membrane-bound chromophore–protein complexes. The structures of two purple non-sulfur bacterial reaction centres (*Rb. sphaeroides*⁸⁹ and *Rps. viridis*⁹⁰) were the first to be determined by X–ray diffraction. Only minor differences were found.⁹¹ The reaction centres in green plants are similar too, although more complex in Nature.

The bacterial reaction centre from *Rhodobacter sphaeroides* is an internal membrane protein composed of three subunits (L (*for light*), M (*for medium*) and H (*for heavy*)) and 9 cofactors (chromophores): four bacteriochlorophylls (BChl), two bacteriopheophytins (BPh), two coenzyme quinone molecules (Q_A and Q_B), and a non-heme iron atom. Two of the three subunits (L and M) provide the necessary scaffolding to hold the cofactors in place. The third

polypeptide (H) is not required for charge separation, but is essential for the correct assembly of the PRC and its interaction with the light-harvesting complex which funnels excitations to the primary donor, the 'special pair'. The chromophores are tightly bound within this protein matrix and arranged along what are known as the L and M branches. The arrangement of the chromophores within the reaction centre of *Rhodospseudomonas viridis* is shown in **Figure 12**.

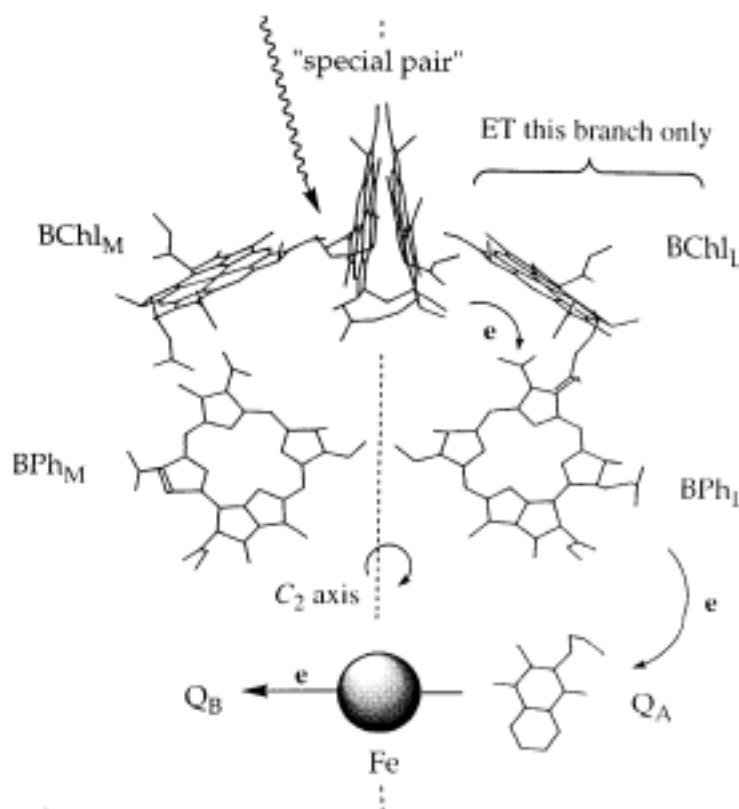


Figure 12: Chromophores in the photosynthetic reaction centre (PRC) (this one of *Rhodospseudomonas viridis*)

Two of the BChl molecules form the primary electron donor or 'special pair' (BChl₂). The distance between the magnesium ions of the two BChl molecules is approximately 6.6 Å and the angle between the planes of the two ring systems is 15°. In edge-to-edge positions, relative to the special pair, lie the other two 'accessory' BChl molecules. The centre-to-centre distance from the special pair to the adjacent BChl monomer has been determined to be 11.0 Å for the L Branch and 11.4 Å for the M Branch. Each BChl monomer is adjacent to a BPh molecule (10.5 Å (L Branch), 10.5 Å (M Branch)), which in turn is adjacent to a quinone species (Q_A or Q_B). Midway between the two quinone units lies a non-heme iron species.⁹¹

Electron transfer proceeds only along the L branch of an almost C_2 - symmetrically twinned set of reagents.^{92,93} The M branch is apparently excluded, since the effective dielectric constant of the surrounding medium differs.⁹⁴ A slightly higher polarity around the L branch favours electron transfer along this direction,⁹⁵ although the reaction can be made to proceed along the M branch in mutagenically modified PRC complexes.⁹⁶

Within the L branch photoinduced electron transfer proceeds from the 'special pair' ($BChl_2$) along the monomeric bacteriochlorophyll ($BChl$) and the bacteriopheophytin (BPh_L) to the primary quinone (Q_A). Excitation of the 'special pair' either by direct light or by energy transfer from nearby antennae⁹⁷ (e.g., carotenoid polyenes, chlorophylls or polypyrroles) results in the transfer of an electron over a distance of approximately 17 Å to bacteriopheophytin (BPh_L) with unity quantum yield in 2.8 ps.⁹⁸⁻¹⁰² Recent studies suggest that the extra bacteriochlorophyll ($BChl_L$) serves as an intermediate in this electron transfer.¹⁰³ Investigation of the PRC of *Rhodobacter sphaeroides* with polarised light using sub-picosecond absorption spectroscopy revealed the existence of the extra bacteriochlorophyll radical anion with a half-life of 0.9 ps. This short-lived intermediate $[(BChl_L)_2^{\bullet+}-BChl_L^{\bullet-}-BPh_L-Q_A]$ quickly undergoes subsequent ET to form the $[(BChl_L)_2^{\bullet+}-BChl_L-BPh_L^{\bullet-}-Q_A]$ intermediate. The electron transfer from BPh_L to Q_A occurs in about 200 ps over a distance of 14 Å to yield the $[(BChl_L)_2^{\bullet+}-BChl_L-BPh_L-Q_A^{\bullet-}]$ giant charge-separated state which has a lifetime of about 100 ms with Q_B absent (**Figure 13**).¹⁰⁴ Thus, in only three sequential electron-transfer events the reaction centre protein has separated charge across 35 Å with high quantum yield to give a long-lived intermediate.

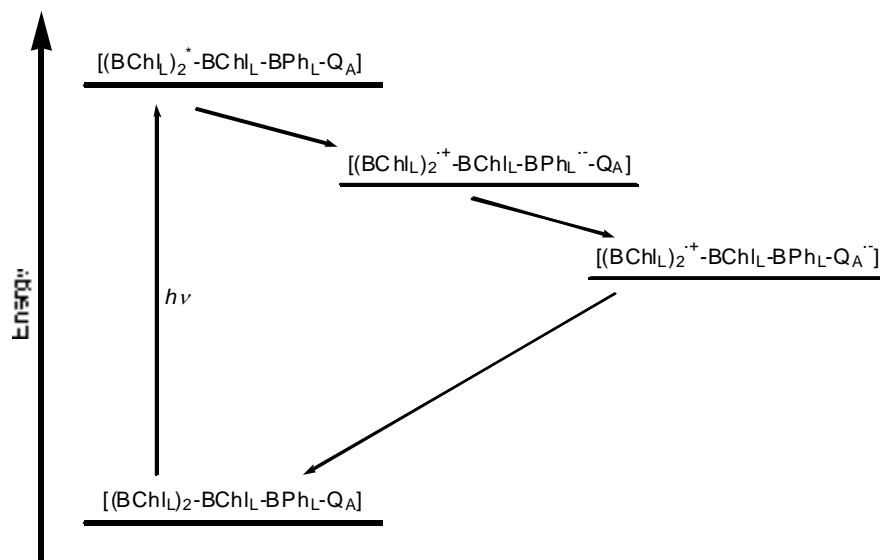


Figure 13: Downhill ET in PRC from a photo-excited 'special pair'

If Q_B is present, the reduced Q_A^- transfers an electron donor to the secondary Q_B in about 0.1 ms.¹⁰⁵ The oxidised $(BChl)_2^+$ is reduced by an electron from the exogenous electron donor cytochrome- c_2 . Another light induced electron transfer step leads to the second electron transfer to Q_B and the uptake of two protons from the solution. The dihydroquinone is subsequently oxidised, releasing protons that contribute to an electrochemical potential across the membrane that is used to drive the subsequent biochemical reactions.

There are two approaches towards a better understanding of the mechanisms involved in the separation of charge in the photosynthetic reaction centre. The more biological disciplines prefer to cultivate and isolate reaction centres¹⁰⁶ and not just investigate those complex systems but also substitute chromophores within those systems.¹⁰⁷ Synthetic chemists, however, choose to prepare models that mimic the reaction centre in their most important characteristics. The possibility to systematically vary the structure of those models as well as the environment in which they operate has helped to define the numerous factors that control ET from a donor to an acceptor.

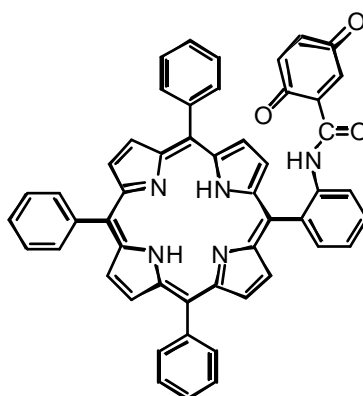
A.6 PHOTOSYNTHETIC MIMICS

The chromophores involved in ET processes within photosynthetic reaction centres are derivatives of porphyrins and quinones. Both types of chromophores are well suited for their task. Porphyrins absorb light over a wide spectral range of wavelengths and have a high molar absorption coefficient. Their redox potentials in the electronically excited and ground states differ drastically from the ground state, meeting the electrochemical requirements for subsequent electron transfer. Quinones appear to be predestined to be electron acceptors in Nature for a variety of reasons. They possess suitable redox potentials and can be converted stepwise *via* semiquinones into hydroquinones, the stable reduction products. They form hydrogen bonds and can undergo protonation and deprotonation with ease. Finally, they are small molecules that can shuttle redox equivalents to the quinone pool.

Research into photosynthetic mimics has focused on using these chromophores. Porphyrins and quinones have been linked through various bridges and with an increasing number of additional chromophores, modelling the multi-step nature of ET in photosynthetic reaction centres, and form the basis of this thesis.

A.6.1 Porphyrin - Quinone Dyads

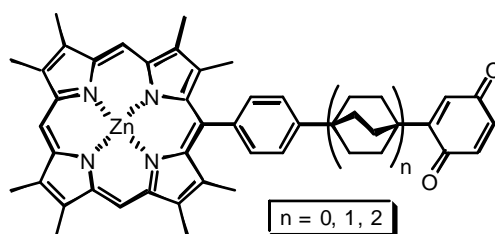
One of the earliest porphyrin - quinone systems synthesised was the dyad by Tabushi *et al.* shown in **Example 8**.¹⁰⁸



Example 8: Porphyrin-quinone dyad by Tabushi *et al.* (1979)

The porphyrin donor is attached to the quinone acceptor *via* an amide group. Fluorescence of the free-base porphyrin was found to be strongly quenched relatively to the acceptor-free porphyrin, indicating that electron transfer or energy transfer had taken place.

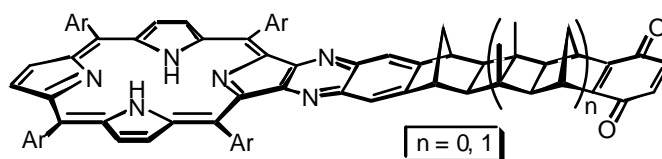
Joran *et al.*¹⁰⁹⁻¹¹¹ as well as Bolton *et al.*¹¹² synthesised a series of porphyrin-quinone dyads like the one shown in **Example 9**. The chromophores are connected by a bridge containing a variable number of bicyclooctane spacers that prevent translational displacement and only allow rotational freedom. The edge-to-edge distances of the chromophores are fixed at 6 Å ($n = 0$), 10 Å ($n = 1$) or 14 Å ($n = 2$).



Example 9: Porphyrin-quinone dyads by Joran *et al.* (1985)

Joran *et al.* found that with increasing separation the rates of photoinduced electron transfer dropped in benzene by the factor 10,000 from $2.2 \times 10^{11} \text{ s}^{-1}$ ($n = 0$), $1.25 \times 10^{10} \text{ s}^{-1}$ ($n = 1$) to smaller than $9 \times 10^6 \text{ s}^{-1}$ ($n = 2$). The lifetime of the charge-separated state increased from 64 ps ($n = 0$) *via* 76 ps ($n = 1$) to 1.45 ns ($n = 2$) with increasing length of the bridge. Bolton *et al.* find a less efficient electron transfer in their series with a *meso*-tris-*p*-tolylporphyrin donor. They explain the contradicting results with the different substitution pattern on the porphyrin rings and their effect upon the conformation of the phenyl-linking group relative to the plane of the porphyrin ring.

Such an effect would be excluded in the rigid porphyrin-quinone dyads (**Example 10**) studied by Antolovich *et al.*¹¹³ In these examples both the separation and the relative orientation of the chromophores are well defined.

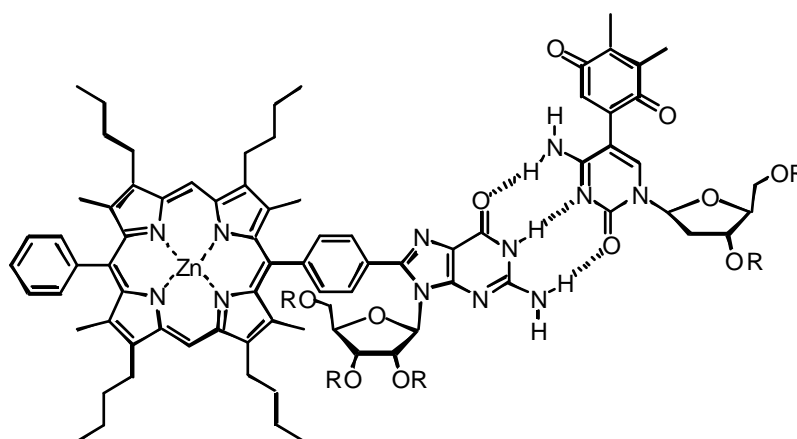


Example 10: Rigid porphyrin-quinone dyad by Antolovich *et al.* (1991)

The chromophores are connected by rigid norbornylogous hydrocarbon bridges of two ($n = 0$) or six ($n = 1$) σ -bonds in length resulting in a centre-to-centre separation of 11.6 Å or 16.2 Å respectively. In solvents of moderate to high polarity the rate constant for photoinduced electron transfer was observed to be $2.5 \times 10^{10} \text{ s}^{-1}$ to $3.3 \times 10^{10} \text{ s}^{-1}$ for $n = 0$ or smaller than $6 \times 10^8 \text{ s}^{-1}$ for $n = 1$. Incorporating zinc into the porphyrin donor of the six-bond dyad increases the rate constant for photoinduced electron transfer up to $1.45 \times 10^{10} \text{ s}^{-1}$. This result enhances those of Joran *et al.* and provides evidence that charge separation between a porphyrin and a quinone moiety separated by a large array of saturated bonds can be achieved. The norbornyl spacer proved to be an extremely efficient mediator of through-bond coupling, as previously demonstrated by numerous photoelectron spectroscopic^{10,114-118} and electron transmission spectroscopic studies^{10,115,118,119} together with Koopman's theorem calculations.^{10,120}

In contrast to this behaviour hydrogen bonds were often suspected of providing a weaker electronic coupling than the more widely studied covalent linkages. This suspicion was based on purely speculative grounds (hydrogen bonds are much weaker, and therefore should result in weak donor-acceptor interactions). Therien *et al.* have settled that controversy by the synthesis and investigation of a set of homologous bis-porphyrin compounds, which allow a direct comparison of electron transfer proceeding through C-C single bonds, C=C double bonds, and hydrogen bonds (**Example 4**, page 11).⁶⁵ It turned out that hydrogen bonds are in fact good mediators for electron transfer and their results predict that the hydrogen-bond interface in protein could mediate ET as efficiently as a covalent bridge.

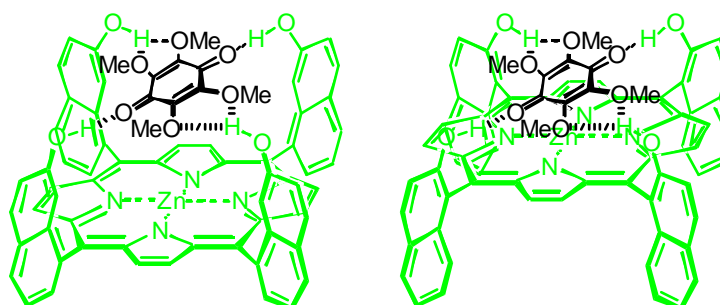
Harriman and Sessler were among the first to study porphyrin-quinone dyads linked by hydrogen bonds.^{64,121} Their 'improved' 1993 model is pictured in **Example 11**.



Example 11: Non-covalent porphyrin-quinone dyad by Sessler *et al.* (1993)

Porphyrin and quinone have guanine and cytidine substituents, respectively, as recognition sites to form Watson-Crick hydrogen-bonding interaction. The edge-to-edge separation is about 14 Å. Upon addition of the quinone to a dichloromethane solution of the porphyrin, the quenching of the zinc porphyrin fluorescence was observed and the fluorescence decay profile became biphasic with two exponential components of lifetimes $\tau_1 = 1.8$ ns and $\tau_2 = 0.74$ ns. Their results indicate that singlet ET from the photo-excited porphyrin to the quinone takes place with a rate constant of ca. $8 \times 10^8 \text{ s}^{-1}$ through an exothermic process by 0.50 eV.

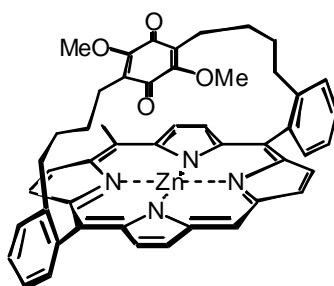
Capped hydrogen-bonded porphyrin-quinone dyads have been investigated by Hayashi and co-workers.¹²² The distances between the porphyrin plane and quinone for the two models shown in **Example 12** are estimated to be 3.5 Å and 6.0 Å, respectively.



Example 12: Capped porphyrin-ubiquinone dyads linked *via* multiple hydrogen bonds by Hayashi and Ogoshi (1994)

Time-resolved fluorescence measurements in toluene reveal monoexponential decay with a lifetime of 2.0 ± 0.1 ns and 2.2 ± 0.1 ns. The electron transfer rate constants for both compounds were estimated to be $\leq 4 \times 10^{11} \text{ s}^{-1}$ (limited by the pulse width and signal-to-noise

ratio).¹²³ Charge recombination occurs rapidly as well with a rate constant of $1.1 \pm 0.4 \times 10^{11} \text{ s}^{-1}$ and $6.8 \pm 0.3 \times 10^{10} \text{ s}^{-1}$, respectively. Comparison with covalently bridged porphyrin-quinone systems like the quinone-capped porphyrin by Staab *et al.*^{80,124,125} (**Example 13**) reveal that hydrogen bonds can compete with covalent bonds as conduits for electronic coupling.

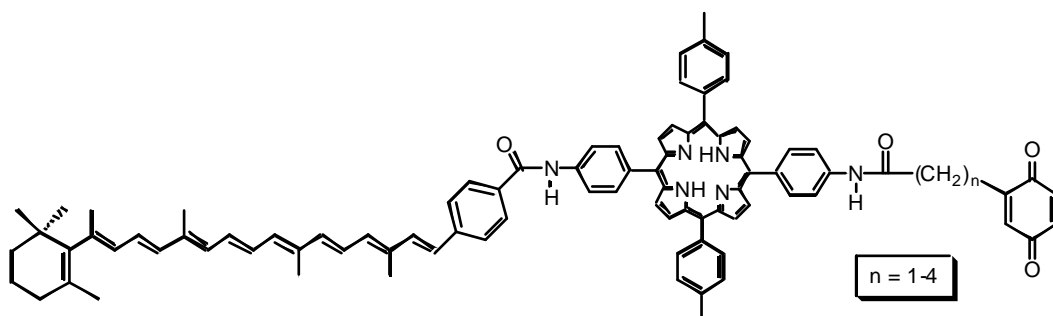


Example 13: Capped porphyrin-quinone dyad linked covalently by Staab *et al.* (1984)

Above examples show that electron transfer does occur rapidly in dyads with small interchromophoric separation and so does charge-recombination. Larger spacers between donor and acceptor were found to increase the lifetime of the charge-separated state but the initial charge separation was less effective. At this stage multichromophoric systems (**A.4.2**, page 22) were introduced, showing a series of short and therefore quick downhill electron-hops from chromophore to chromophore, finally resulting in a huge charge separation and an enhanced lifetime of the charge separated state.

A.6.2 Porphyrin - Quinone Triads, Tetrads, Pentads

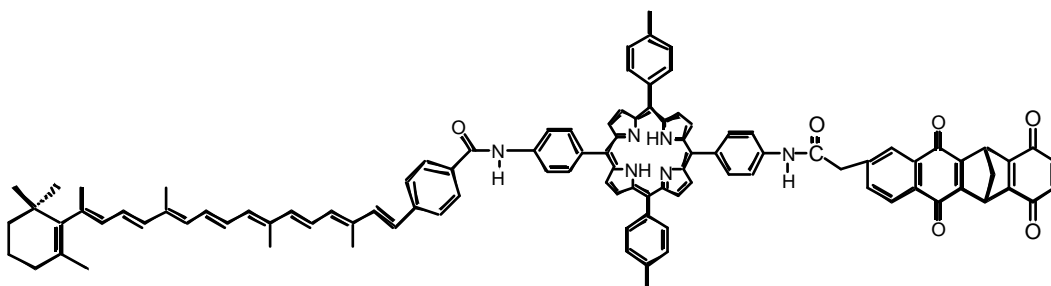
Over the last decade an impressive series of carotenoid-porphyrin-quinone (C-P-Q) triads has been synthesised and studied by Moore, Gust and Moore.¹²⁶⁻¹²⁹ Shown in **Example 14** is a series of their first successful photosynthetic models of that type,¹³⁰ which since then have been improved for ET efficiency and lifetimes of the charge-separated state.¹³¹



Example 14: Carotenoid-porphyrin-quinone [C-P-Q] triad by Moore, Gust and Moore (1987)

In these systems, local excitation of the porphyrin results in rapid intramolecular electron transfer to form the initial $[C-P^{\bullet+}-Q^{\bullet-}]$ charge-separated state with rate constants between $9.7 \times 10^9 \text{ s}^{-1}$ ($n = 0$) and $0.15 \times 10^9 \text{ s}^{-1}$ ($n = 4$), and near 100 % quantum efficiency for $n = 0$, decreasing with increasing interchromophoric separation. Rapid thermal hole transfer from the porphyrin cation radical to the carotenoid group leads to the formation of the giant charge-separated state $[C^{\bullet+}-P-Q^{\bullet-}]$ with a lifetime of about 300 ns. Thus, the lifetime of the final charge-separated state is at least three orders of magnitude longer than in the above mentioned porphyrin-quinone dyads. The final state is also a high-energy species, preserving about 1.1 eV of the 1.9 eV stored in the porphyrin excited state. A downside of this assembly is a low quantum yield of about 4-6 % for the second electron-transfer process.

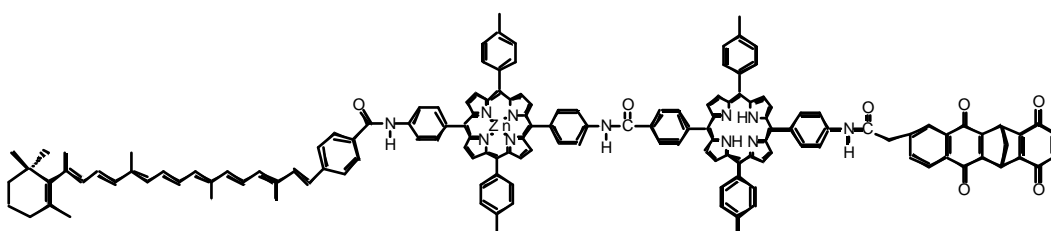
A year later the molecular tetrad **Example 15** was published by Moore, Gust and Moore.¹³²⁻¹³⁴ It consists of four covalently linked chromophores: a carotene, a porphyrin, a naphthoquinone and a benzoquinone. The naphthoquinone with the more negative redox potential was attached directly to the porphyrin, while the benzoquinone with the less negative redox potential was at the terminus. This arrangement is designed to promote sequential electron transfer from the naphthoquinone to the benzoquinone.



Example 15: Carotenoid-porphyrin-naphthoquinone-benzoquinone tetrad by Moore, Gust and Moore (1988)

The initial charge-separated species $[C-P^{\bullet+}-NQ^{\bullet-}-BQ]$ is formed with a rate constant of $\geq 2 \times 10^{10} \text{ s}^{-1}$ and lies about 1.6 eV above the ground state. The final giant charge-separated species $[C^{\bullet+}-P-NQ-BQ^{\bullet-}]$ is formed with a quantum yield of 23 % and has a lifetime of 460 ns in dichloromethane (4 μs in acetonitrile). About 1.1 eV is preserved in this state. The rates and yields of the intermediate electron transfer processes are not known to date.

In 1990 the Gust and Moore team¹³⁵ extended their multistep electron transfer models to include a carotene-zincporphyrin-porphyrin-naphthoquinone-benzoquinone pentad (**Example 16**). The strategic aim was again to maximise the quantum yield of the ion pair formation and the lifetime of the charge-separated state.⁸⁵



Example 16: Carotenoid - porphyrin_{Zn} - porphyrin - naphthoquinone - benzoquinone pentad by Moore, Gust and Moore (1990)

This pentad is designed so that photoinduced electron transfer from the free-base porphyrin to the attached naphthoquinone can be followed by a cascade of electron-transfer pathways which converge upon a final $[C^{\bullet+}-P_{Zn}-P-NQ-BQ^{\bullet-}]$ charge-separated state (**Figure 14**).

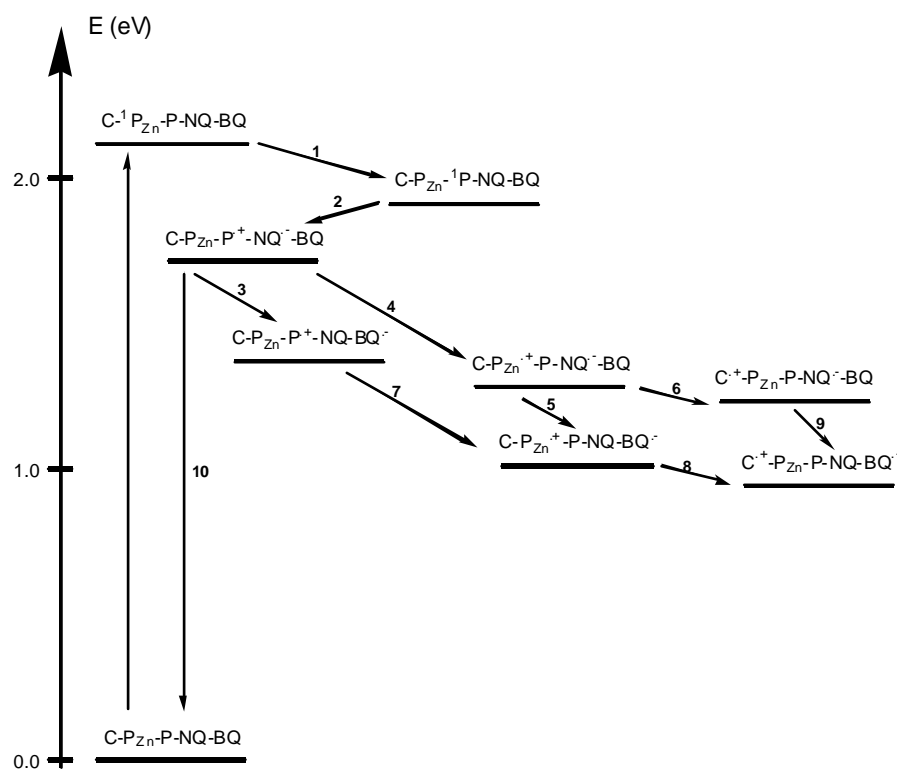


Figure 14: Transient states for Example 16 by Moore, Gust and Moore

The process begins with excitation of the free base porphyrin moiety. This can occur *via* direct absorption of light, or by singlet-singlet energy transfer from the attached zinc porphyrin (**step 1**). The rate constant for the energy transfer process is $2.3 \times 10^{10} \text{ s}^{-1}$ and it occurs with a quantum efficiency of 90 %. The free base porphyrin first excited state decays in part to the attached naphthoquinone (**step 2**) to produce the $[\text{C-P}_{\text{Zn}}\text{-P}^{\bullet+}\text{-NQ}^{\bullet-}\text{-BQ}]$ species with a rate constant of $7.1 \times 10^8 \text{ s}^{-1}$ and a quantum yield of 85 %. A number of electron transfer steps along two parallel pathways (**steps 3-8**) result in the giant charge-separated state $[\text{C}^{\bullet+}\text{-P}_{\text{Zn}}\text{-P-NQ-BQ}^{\bullet-}]$ which is generated in about 83 % efficiency and has a lifetime of 55 μs (in chloroform; 60 % and 200 μs in dichloromethane). As the yield (in chloroform) is essentially the same as that of the initially formed $[\text{C-P}_{\text{Zn}}\text{-P}^{\bullet+}\text{-NQ}^{\bullet-}\text{-BQ}]$ species, the parallel electron-transfer pathways compete very efficiently with **step 10**. Once again little is known about the rates of the multitude of intermediate electron transfer reactions within pathways that lead to the final carotene cation - benzoquinone anion ion pair.

It was mentioned that the triad structures led to charge-separation lifetimes at least 1000 times longer than those found for simple porphyrin-quinone dyads. The pentad systems extend this lifetime by another three orders of magnitude.

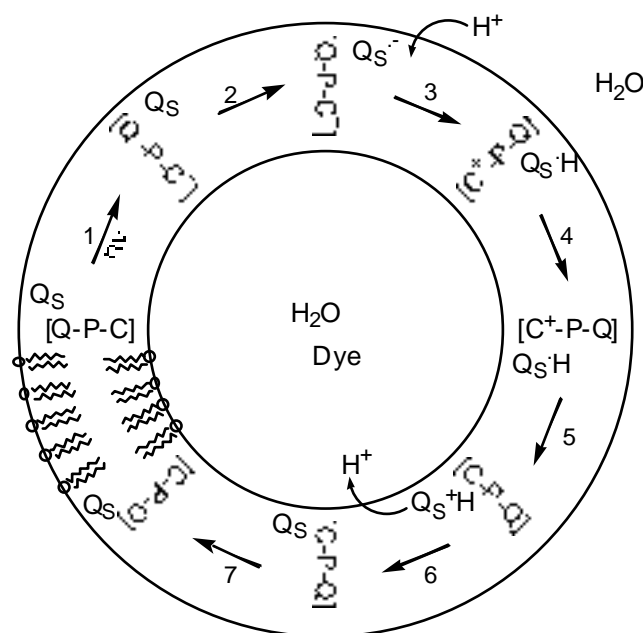


Figure 15: Photoelectrochemical cycle of the 'proton pump' generating a pH gradient across a liposome bilayer

Following the above-mentioned mechanism, photoexcitation of the porphyrin moiety results in the formation of the giant $[C^{\bullet+}-P-Q^{\bullet-}]$ charge-separated state, which was observed by monitoring the transient absorbance of the carotenoid radical cation (**Figure 15, Step 1**). In a second step electron transfer from $[-Q^{\bullet-}]$ to the lipid soluble 2,5-diphenylquinone (Q_s) results in the formation of the radical anion $Q_s^{\bullet-}$ (**Figure 15, Step 2**), which accepts a proton from the external aqueous solution (**Figure 15, Step 3**). The uncharged semiquinone (Q_sH^{\bullet}) diffuses through the membrane, performing the crucial step of a proton shuttle (**Figure 15, Step 4**). Upon reaching the interior layer of the membrane Q_sH^{\bullet} encounters the carotenoid radical cation, undergoes oxidation to Q_s^+H (**Figure 15, Step 5**) and releases the proton into the aqueous medium (**Figure 15, Step 6**). Random diffusion of the regenerated Q_s closes the cycle (**Figure 15, Step 7**).

The pH dependent fluorescence excitation spectrum of a water-soluble dye was used to monitor changes in the proton concentration inside the liposomes. The pH gradient, which has been established across the bilayer membrane, gives rise to a proton motive force that potentially could be utilised to perform work. This task was recently accomplished by Moore, Gust and Moore.¹³⁷ They reconstituted proteoliposomes with ATP synthase built into the lipid

bilayer and harnessed the pH gradient set up by the 'proton pump' to perform ATP synthesis (**Figure 16**).

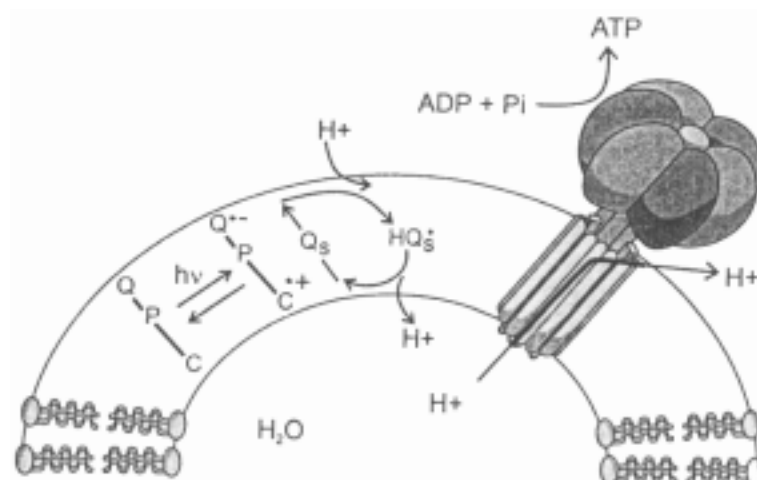


Figure 16: Diagram of a liposome-based artificial photosynthetic membrane by Moore, Gust and Moore (1998)

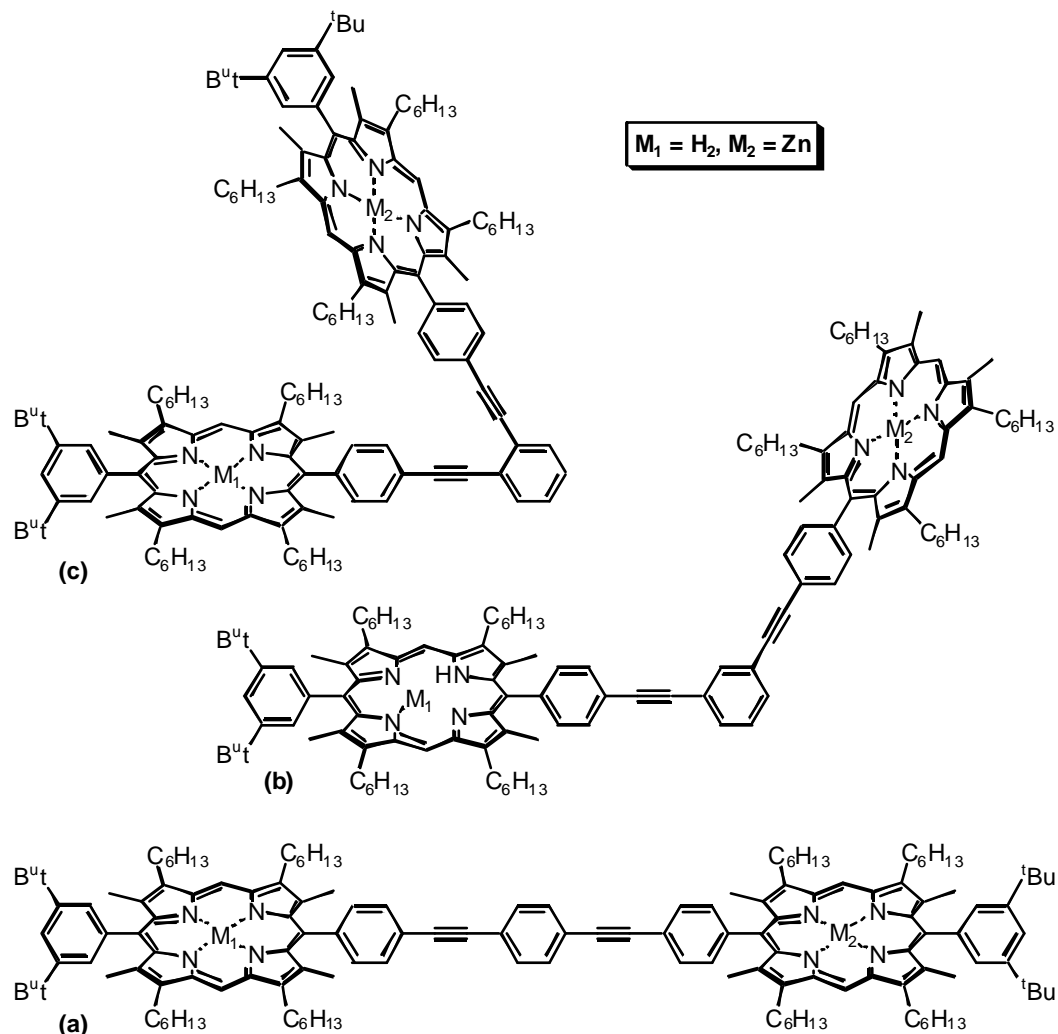
It has been estimated that one molecule of ATP is synthesised per 14 absorbed photons of 633 nm light, and that up to 4 % of the absorbed light energy is conserved in this system, which operates efficiently over a timescale of hours.

Examples like the above mentioned are quite remarkable. They provide insight into important aspects of the photosynthetic reaction centre. However, they do not mimic the 'special pair' itself. The 'special pair' issue was addressed through oligoporphyrin models such as those described in the following section **A.6.3 'Multi Porphyrin Arrays'**.

A.6.3 Multi Porphyrin Arrays

Porphyrins are a widely used ingredient in organic synthesis and several porphyrins have been linked to each other in various ways. Only a small fraction of these multi-porphyrin arrays were synthesised to probe energy- or electron-transfer properties of porphyrins linked by different bridges.

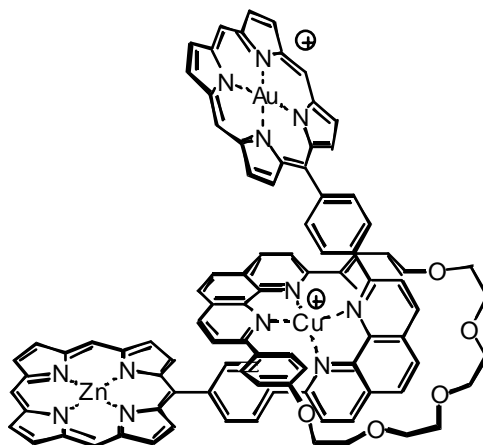
A bis(phenylethyl)phenylene bridge was recently used by Osuka *et al.*¹³⁸ to link a zinc and a free-base porphyrin and investigate their singlet energy transfer characteristics. The central phenyl group was substituted in the *para*-, *meta*- or *ortho*-position (**Example 18 (a) - (c)**).



Example 18: Bis-porphyrin arrays by Osuka *et al.* (1997)

It was found that **Example 18 (a)** and **(b)** display almost the same rate constant for energy transfer ($k_{EnT} = 5.7 \times 10^8 \text{ s}^{-1}$) indicating a through-bond electronic interaction. In **Example 18 (c)** the energy transfer rate constant was found to be one order of magnitude larger ($k_{EnT} = 4.4 \times 10^9 \text{ s}^{-1}$) suggesting through-space interaction.

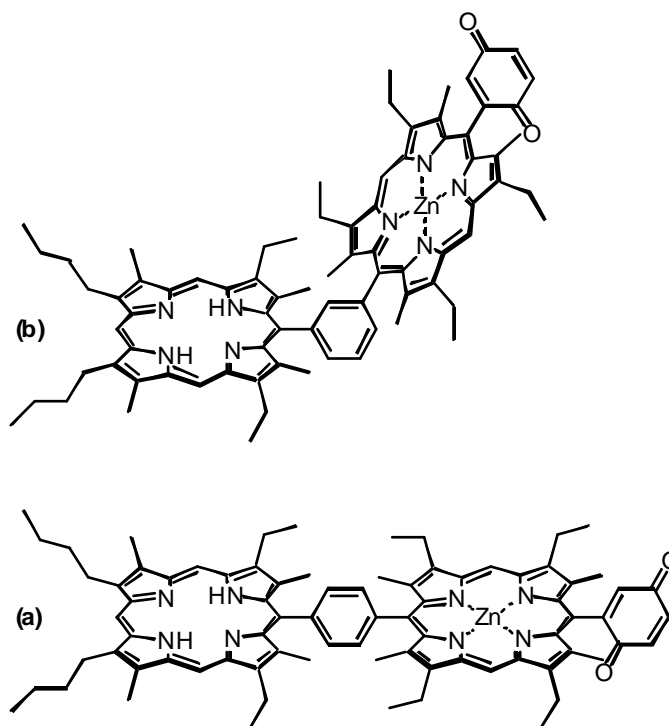
Electron rather than energy transfer was studied on a bis-porphyrin rotaxane by Harriman and Sauvage.⁶¹ The zinc (II) and gold (III) porphyrins were separated by a 2,9-diphenyl-1,10-phenanthroline bridge. The dyad was used as a stopper in the below-pictured [2]-rotaxane (**Example 19**), which can contain or not contain a metal centre.



Example 19: Bis-porphyrin rotaxane by Harriman and Sauvage (1996)

Following selective excitation of the zinc porphyrin, through-bond electron transfer to the gold porphyrin occurred within 1 ps. In competition with charge recombination, the zinc porphyrin π -radical cation oxidised the central Cu(I) complex (20 ps) before the initial ground state was restored (2.5 ns). The bis-porphyrin dyad itself (not the rotaxane) showed slower charge separation (55 ps) and faster charge recombination (600 ps). Thus, the transition metal cation can tune the electronic properties of the bridge and enhance electron transfer. In 1997 Sauvage published similar results on tris-porphyrin rotaxanes.¹³⁹

More closely related to the photosynthetic reaction centre was an early example by Sessler *et al.*,¹⁴⁰ which contained two porphyrins and a quinone as acceptor moiety (**Example 20**). The two porphyrins, one of them metallated, were linked by a phenyl group in the para- (**a**) or meta-position (**b**).



Example 20: Mono metallated bis-porphyrin quinone triads by Sessler *et al.* (1989)

The electron-transfer rates for both compounds were found to be high: $1.1 \times 10^{10} \text{ s}^{-1}$ (**Example 20, a**) and $5.4 \times 10^{10} \text{ s}^{-1}$ (**Example 20, b**), respectively. It was suggested that through-bond electron transfer occurs from the free-base porphyrin to the quinone, with the second porphyrin acting as medium for electron transfer.

A.6.4 Conclusion

Much progress has been made in the field of long-range intramolecular photoinduced electron transfer and numerous models for the photosynthetic reaction centre have been designed. The last three examples (**A.6.3**, page 38) model the 'special pair' of the photosynthetic reaction centres to a certain extent. But by no means do they represent a systematic approach towards the 'special pair' issue. The flexibility of the molecules affects a number of parameters that then affect the rate of electron transfer and charge recombination. By keeping the majority of ET-affecting parameters constant (e.g. distance, geometry, and type of acceptor) conclusions on how changes to the 'special pair' effect electron transfer can be derived.

Schematically such a rigid 'special pair' mimic could look like the one depicted in **Figure 17**.

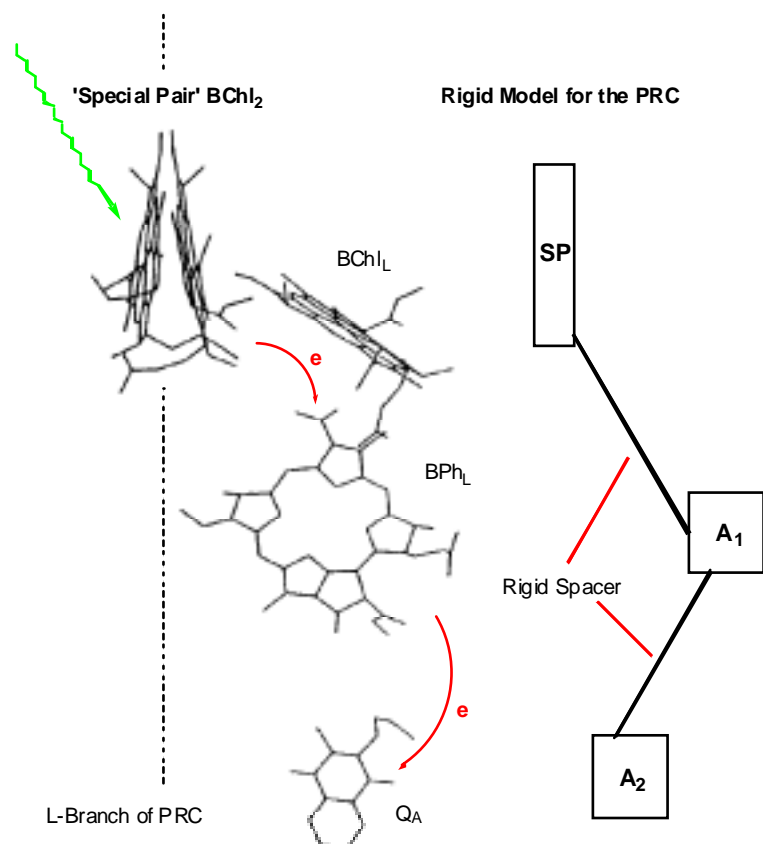


Figure 17: Sought after rigid model of the photosynthetic reaction centre (PRC). SP: 'special pair', A1: primary acceptor, A2: secondary acceptor

A rigid spacer keeps the chromophores at a well-defined distance and spatial disposition. Destined for a systematic approach are the well-established rigid norbornylogous bridges that hold chromophores in place. They are easily accessible and are brilliant mediators of through-bond electron transfer processes.^{11,46,118} Chromophores should include a 'special pair' and one or two quinone-related species. The vision of such an 'advanced model for the photosynthetic reaction centre' was the driving force behind this PhD project.

A.7 AIM OF THESIS

The synthesis of a series of advanced models for the photosynthetic reaction centre (PCR), incorporating 'special pairs' and one or two other quinone-related chromophores is the synthetic challenge of this thesis. The interchromophoric separation is to be kept constant and similar to that found in the natural PCR, whereas the 'special pair', acting as a primary

electron donor in these models is to be altered systematically. Such alterations can include different, but well-defined spatial dispositions of the two porphyrins or the removal of one porphyrin unit. After the successful synthesis, photophysical experiments can evaluate the influence of the 'special pair' changes on the electron transfer behaviour and will allow further insight into the fascinating world of electron transfer, and subsequently the photosynthetic reaction centre.

With the chromophores, the type of bridge and the interchromophoric separation being roughly set, a comparison with the natural photosynthetic reaction centre determined the ultimate synthetic goal (**Figure 18**).

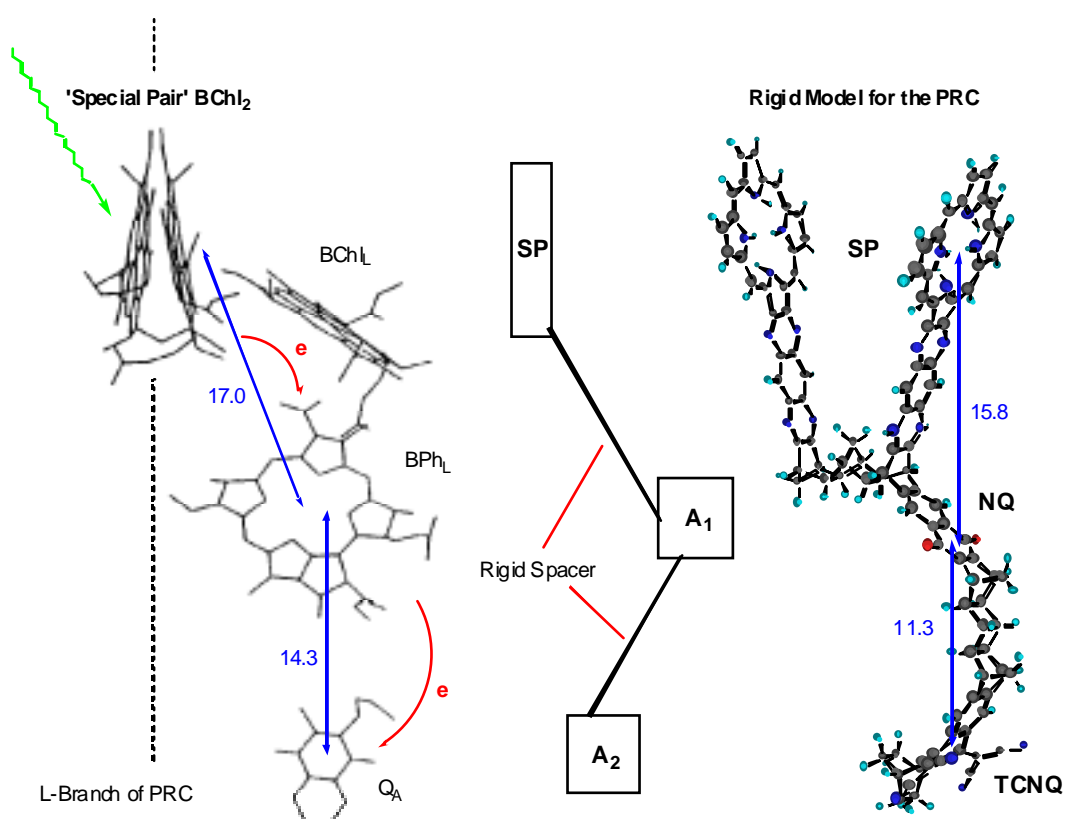


Figure 18: Comparison with the L-branch of the photosynthetic reaction centre of *Rhodospseudomonas viridis* determined the synthetic goal. Interchromophoric separations are given in Å

AM1 calculations on the proposed target molecule reveal interchromophoric distances very similar to the natural blueprint. The two porphyrins of the 'special pair' are connected to a rigid norbornylogous framework, defining their spatial disposition. Naphthoquinone (NQ) and tetracyanonaphthoquinodimethane (TCNQ) are chosen as quinone-related electron acceptors.

The two porphyrin units of the natural 'special pair' are kinked in respect to each other with just two pyrrole rings being staggered above each other. This aspect can be mimicked nicely by an expansion of the bicycloheptane backbone that is holding one of the two porphyrins (Figure 19).

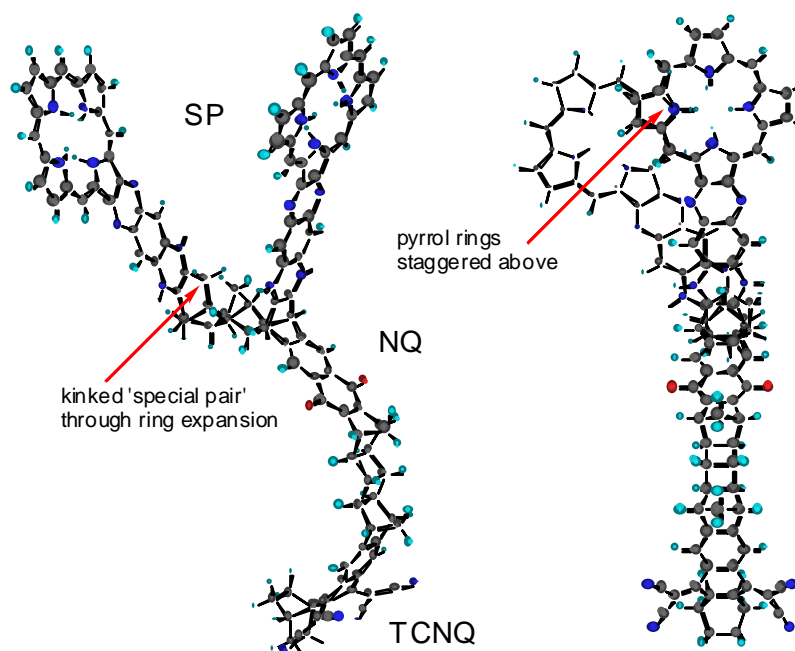


Figure 19: The kinked model of the photosynthetic reaction centre. Only two pyrrole rings are staggered above each other

To evaluate the effect of the two kinked and non-kinked 'special pairs' in comparison to just one porphyrin, a mono-porphyrin triad was added to the target pool (Figure 20).

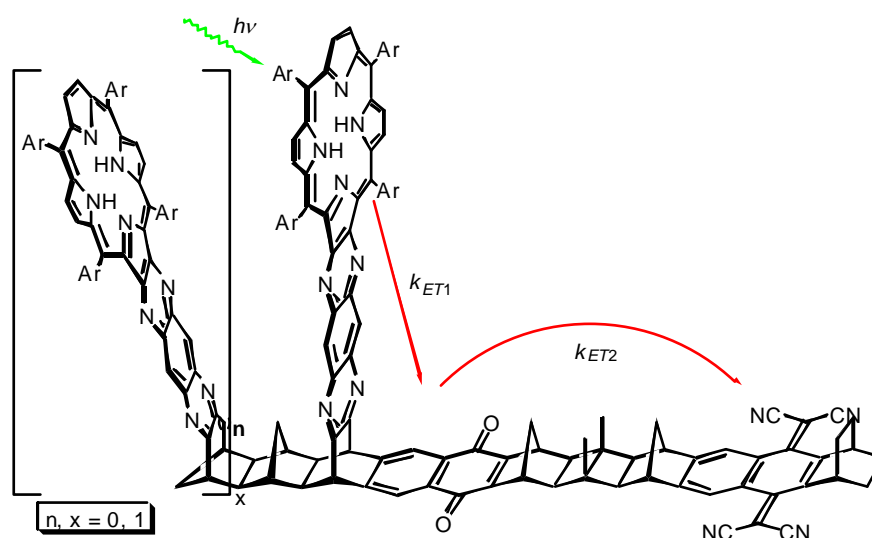


Figure 20: Series of targets derived from comparison with PRC's

In summary the 'special pair' consists of two porphyrins (kinked ($n, x = 1$) or non-kinked ($n = 0, x = 1$)), or just one porphyrin ($n, x = 0$) acts as electron donor. The norbornylogous bridge connecting the naphthoquinone (NQ) with the tetracyanonaphthoquinodimethane (TCNQ) can either be *syn*- (shown above) or *anti*- to the methano bridge of the 'special pair', thereby doubling the number of targets. The *syn*-series, ring-expanded or non-ring-expanded, will be y-shaped as shown above, the *anti*-series will be w-shaped, or s-shaped and u-shaped for the mono-porphyrin targets (**Figure 21**).

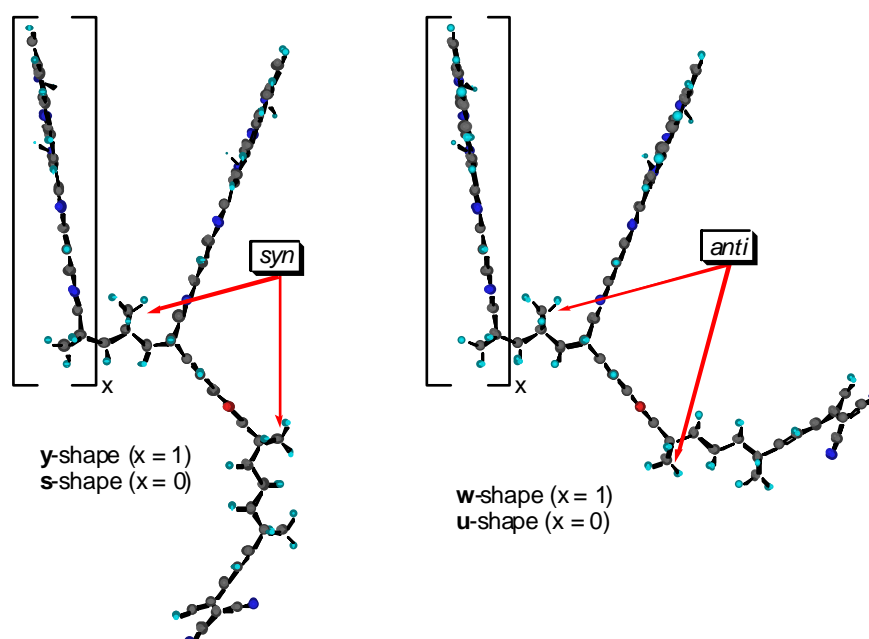


Figure 21: *Syn*- and *anti*-isomers result in four different shapes: y, w, s, and u

This pool of six advanced 'special pair' models for the photosynthetic reaction centre was classified as a series of triads. In relation to the PRC the two porphyrins of the 'special pairs' were counted as one chromophore (SP). Therefore the aimed at set of targets comprised four [SP-NQ-TCNQ] triads (kinked, non-kinked, *syn*, and *anti*) and two [P-NQ-TCNQ] trichromophores (*syn* and *anti*).

Prior to the attempted synthesis of these giant trichromophores the construction of a series of closely related bichromophoric systems was envisaged, in which the 'NQ-bridge-TCNQ' unit of the trichromophores is replaced by a single dimethoxynaphthalene (DMN) or tetracyanonaphthoquinodimethane (TCNQ) acceptor group (**Figure 22**).

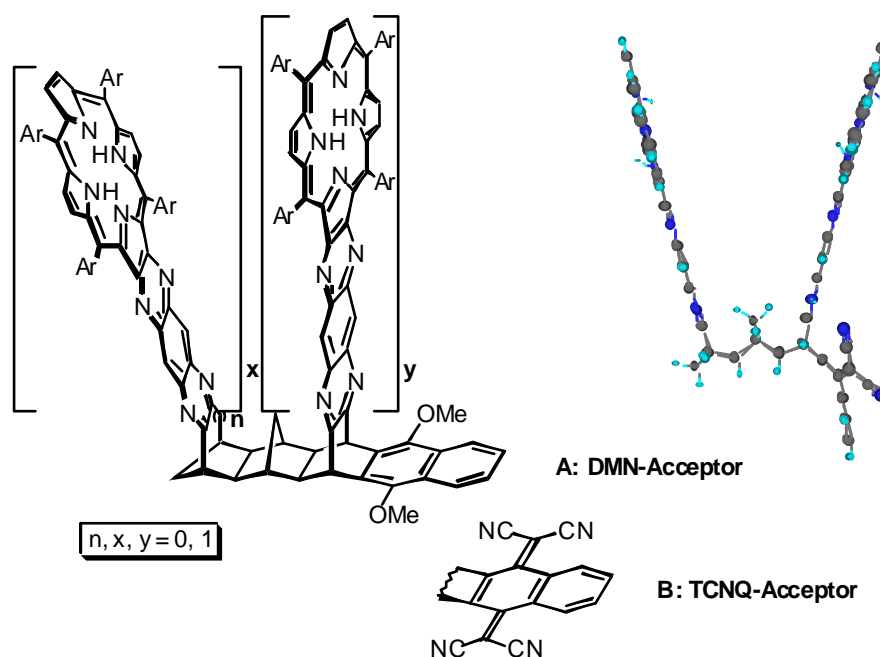
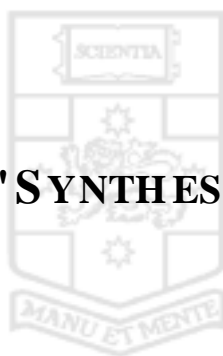


Figure 22: Series of bichromophoric targets closely related to triads

The TCNQ unit is a much stronger electron acceptor than the DMN (by ca. 1V), and so the latter might only facilitate energy transfer rather than electron transfer. In relation to the series of triads the two porphyrins of the 'special pair' donor are either kinked or non-kinked in respect to each other, thereby resulting in two [SP-DMN] and two [SP-TCNQ] bichromophoric systems. Four mono-porphyrin systems complete the series of dyads. The porphyrin donor is either separated by six σ -bonds from the acceptor group ([6B-P-DMN] and [6B-P-TCNQ]) or by just two σ -bonds ([2B-P-DMN] and [2B-P-TCNQ]).

The synthesis of these two-times four bichromophoric systems alone comprised a considerable synthetic challenge. The approach to this challenge is described first in the following chapter **B** 'Syntheses'. The description of the synthetic efforts towards a successful synthesis of the projected series of triads and more follows thereafter.

B 'SYNTHESES'



B SYNTHESSES

B.1 GENERAL

One important characteristic in the development of synthetic procedures towards the dyads and triads is versatility. Facile alterations to the chromophores attached or bridges used would allow the extension of this work beyond the scope of a single PhD project. One way to achieve such versatility is to employ a component-wise construction of the multichromophoric systems. Donors, bridge, and acceptor could be synthesised separately, then fused by Diels-Alder methodology. In the future one component, e.g. the acceptor, could be easily changed, giving access to a range of new, but comparable multichromophoric ET systems.

The following chapters describe the synthesis of the different components and their linkage. The synthesis of the series of dyads is described first (**B.2**, page 49). The chapter on the triad synthesis is conveniently split into four sections that separately outline the synthesis of the donors (**B.3.1**, page 80), the bridge (**B.3.2**, page 116), the acceptor precursor (**B.3.3**, page 120), and the assembly of those components (**B.3.4**, page 121). The chapter on syntheses concludes with a short summary on the synthetic efforts towards an all-*trans* ring-expanded 6B-porphyrin-TCNQ dyad (**B.4**, page 127) and the synthesis of known 'diaminoporphyrin' (**B.5**, page 135).

The most important tool in the characterisation of compounds is high-field nuclear magnetic resonance (NMR) spectroscopy. In this chapter chemical shifts in ppm, relative to TMS, are occasionally given or spectra depicted. The general way chemical shifts are represented is shown in **Figure 23(A)**. The assignment of resonances was usually assisted by COSY, DEPT135, and DEPT90 experiments.

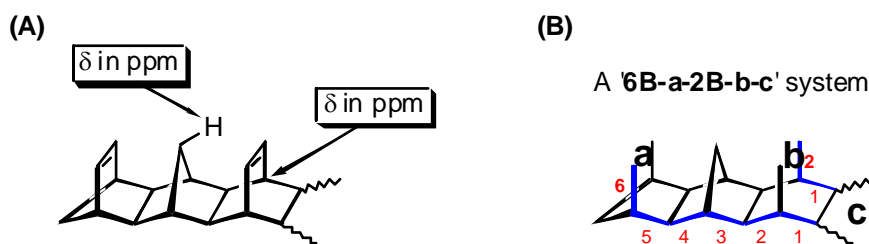


Figure 23: (A) Representation of selected chemical shifts (proton and carbon); (B) The '2B' and '6B' numbering concept used throughout this thesis

The terms '2B' or '6B' are used throughout this thesis to describe the distance of a functionality or donor (**a** and **b**) relative to another functionality or acceptor (**c**). '2B' thereby means a separation of two σ -bonds and '6B' of six σ -bonds (**Figure 23(B)**).

B.2 SYNTHESIS OF THE SERIES OF DYADS

Eight target compounds were envisaged in the synthesis of a series of closely related dyads. The acceptor moiety was to consist of a dimethoxynaphthalene (DMN) or a tetracyanonaphthoquinodimethane (TCNQ). A porphyrin, separated by two (2B: $n, x = 0, y = 1$) or six σ -bonds (6B: $n, y = 0, x = 1$) apart from the acceptor, was to function as a donor, as well as a kinked ($n, x, y = 1$) and non-kinked ($n = 0, x, y = 1$) 'special pair', consisting of two porphyrin molecules (**Figure 24**).

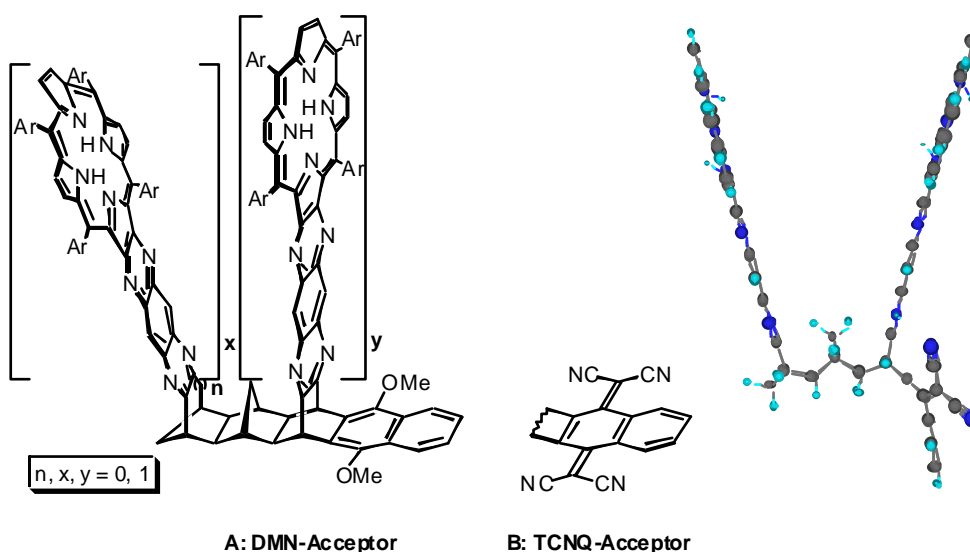


Figure 24: Four target molecules per acceptor group (DMN or TCNQ)

In relation to the photosynthetic reaction centre the two porphyrin chromophores of the 'special pair' were treated as one. In Nature the strong electronic coupling between the two 'special pair' porphyrins justifies that point of view.⁹² For this series, a similar strong interaction is desired, but not guaranteed. The centre-to-centre separation in the 'special pair' models ($x, y = 1$) was calculated (AM1) to be 12.0 Å ($n = 0$) or 13.3 Å ($n = 1$), respectively, compared to 6.6 Å in the PRC of *Rhodospseudomonas viridis*. Nevertheless throughout this thesis the two kinked or non-kinked porphyrins are considered as one chromophore, resulting in distinct series of dyads (this chapter) and triads (chapter **B.3**, page 77). NMR spectroscopic results will later show that there is an interaction between the two porphyrins (section **B.2.4**, page 69), making this assumption reasonable.

The retrosynthetic approach suggests three building blocks: porphyrindione, benzenetetramine and four different diones/tetraones connected to a dimethoxynaphthalene (DMN) moiety (**Figure 25**), a strategy pioneered by Crossley *et al.*¹⁴¹⁻¹⁴⁴

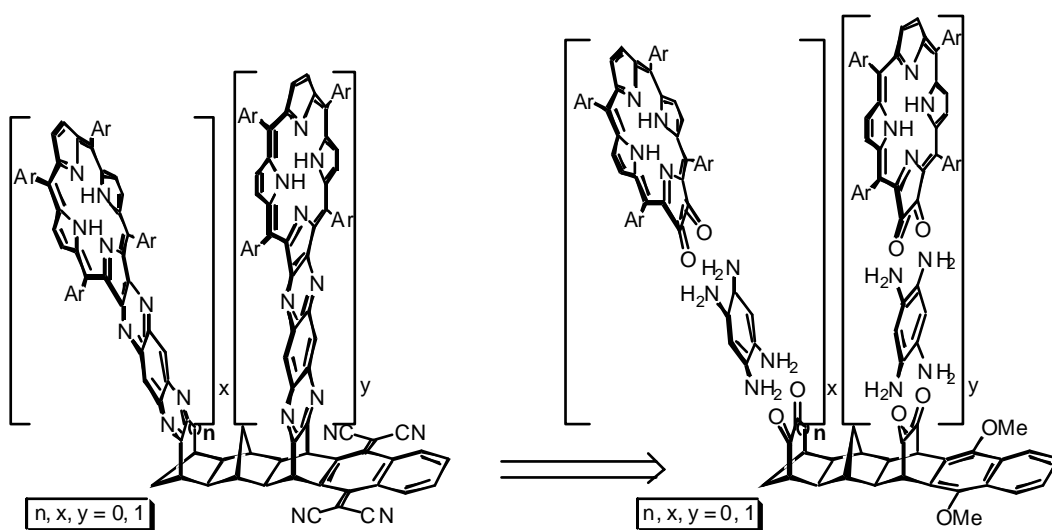


Figure 25: Retrosynthetic approach for chromophore attachment

The 'porphyrindione' is available through synthesis as outlined in chapter **B.5** (page 135), benzenetetramine is commercially available as its tetrahydrochloric salt, and the diones/tetraones should be accessible *via* Diels-Alder methodology followed by hydroxylation and oxidation as outlined in **Figure 26**.

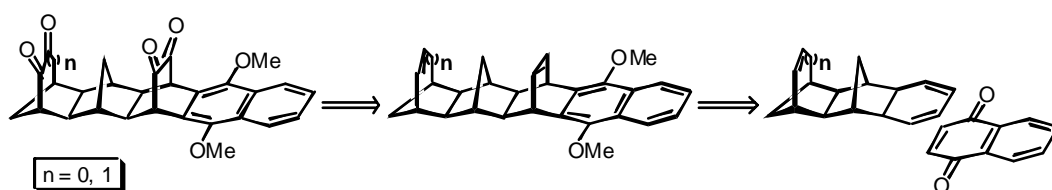
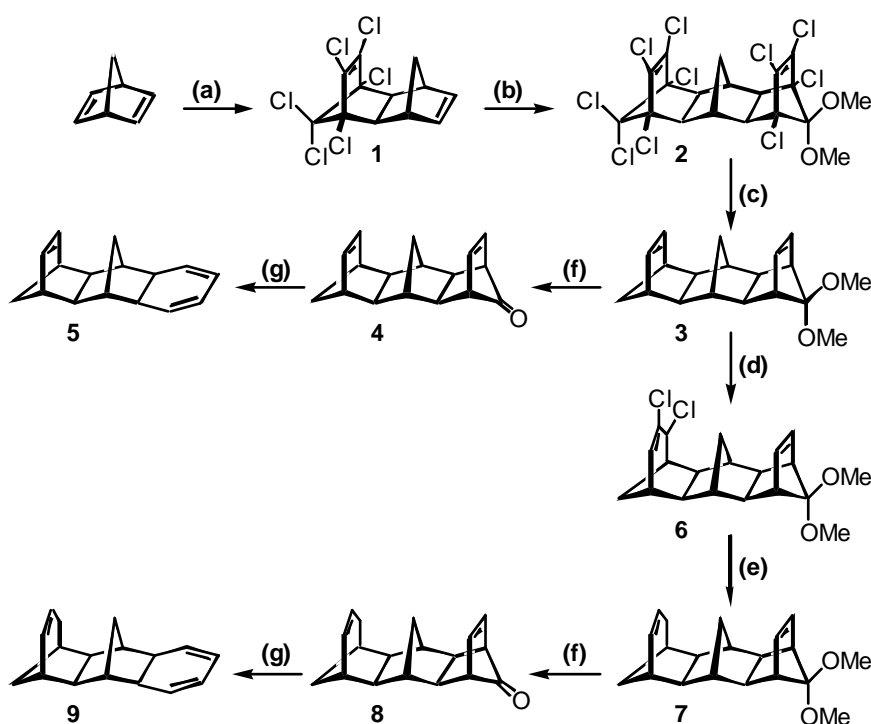


Figure 26: Retrosynthetic approach for dione/tetraone synthesis

1,4-Naphthoquinone is commercially available and the (non-) ring-expanded carbon backbones were synthesised as described in the next section **B.2.1**.

B.2.1 Building the Carbon Backbones

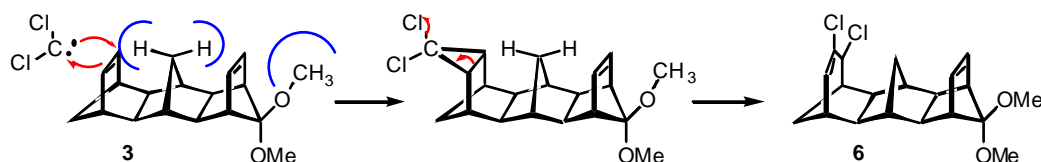
The synthesis of the carbon backbones began with the Diels-Alder addition of hexachlorocyclopentadiene to norbornadiene (slight excess) to give the mono-adduct Aldrin **1**¹⁴⁵⁻¹⁴⁸ in 70 % yield (**Scheme 1 (a)**).



Scheme 1: Building the dyad carbon backbone. (a) 1,2,3,4,5,5-Hexachlorocyclopentadiene, reflux, 6h, 70 % ; (b) 5,5-dimethoxy-1,2,3,4-tetrachlorocyclopentadiene, toluene, reflux, 46 h, 72 % ; (c) Na, THF/*i*-PrOH, reflux, 4 d, 54 % ; (d) NaOMe, CCl₃CO₂C₂H₅, light petroleum, RT, 22 h, 52 % ; (e) Na, THF/*i*-PrOH, reflux, 21 h, 99 % ; (f) HCOOH, THF, RT, 92 % ; (g) toluene, reflux, 2 h

A second Diels-Alder reaction with 5,5-dimethoxy-1,2,3,4-tetrachlorocyclopentadiene (**Scheme 1 (b)**), which was synthesised from hexachlorocyclopentadiene in methanol under basic conditions in 75 % yield,¹⁴⁹ afforded the decachloro-adduct **2** in 72 % yield. Reductive dechlorination of **2** with sodium (**Scheme 1 (c)**) yielded the dimethyl acetal **3** in 54 %.¹¹⁸ Other products (about 18 %) were identified as partly dechlorinated compounds, which were recovered and fully dechlorinated in a second attempt.

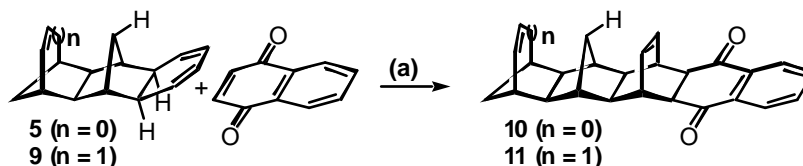
With the right-hand double bond depicted in **3** (**Scheme 2**) sterically protected by the methano bridge on one side and the methoxy group on the other, the less sterically congested double bond was selectively attacked by *in-situ* generated dichlorocarbene to give the ring-expanded dimethyl acetal **6** after two repetitions in 52 % yield (**Scheme 1 (d)**, **Scheme 2**).



Scheme 2: Formation of two enantiomeric dimethyl acetals 6 after ring-expansion with *in-situ* generated dichlorocarbene

Reductive dechlorination of the ring-expanded dimethyl acetal **6** afforded the ring-expanded diene **7** in quantitative yield (**Scheme 1 (e)**).

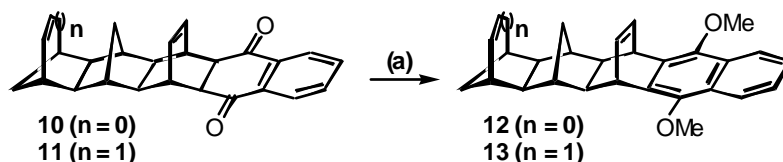
Acidic hydrolysis of the non-ring-expanded diene **3** and the ring-expanded diene **7** gave the corresponding ketones **4** and **8** (**Scheme 1 (f)**), which then underwent facile cheletropic loss of carbon monoxide under thermal conditions (**Scheme 1 (g)**) to give the enophiles **5** and **9** for the subsequent Diels-Alder reaction with 1,4-naphthoquinone (**Scheme 3**).



Scheme 3: Diels-Alder reaction with 1,4-naphthoquinone. (a) Ethanol, reflux, 4 h, 74 % (10), 84 % (11)

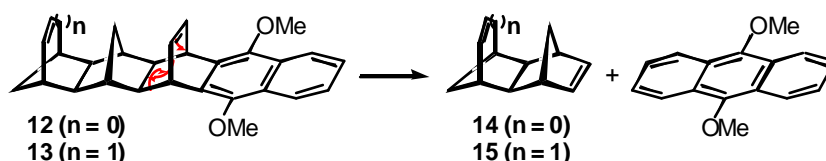
The only diastereoisomer observed was the *endo* adduct as depicted, where naphthoquinone approaches the diene *anti* to the methano group of the inner [2.2.1] bicyclic ring. The *endo* attack results in the newly formed etheno bridge being *syn* to the central methano bridge. The

methylene bridge proton confirms the endo attack by its proton resonance found at 1.48 ppm (**10**) and 1.52 ppm (**11**), respectively. Yields obtained were 74 % (**10**, non-ring-expanded) and 84 % (**11**, ring-expanded), respectively. Aromatisation and subsequent methylation yielded the dimethoxynaphthalenes **12** and **13** in 43 % only (**Scheme 4**).



Scheme 4: Aromatisation / methylation. (a) HMPA, THF, $\text{KN}(\text{SiMe}_3)_2$, toluene, 0 °C, followed by MeI, RT, 18 h, 43 %

The moderate yields were attributed to the competing retro-Diels-Alder reaction (**Scheme 5**). For the ring-expanded system, the retro-Diels-Alder products 9,10-dimethoxyanthracene and **15** were isolated and fully characterised, while for the non-ring-expanded compound the strong fluorescence attributable to dimethoxyanthracene was taken as evidence for the occurrence of the retro-Diels-Alder pathway.



Scheme 5: Retro-Diels-Alder reaction

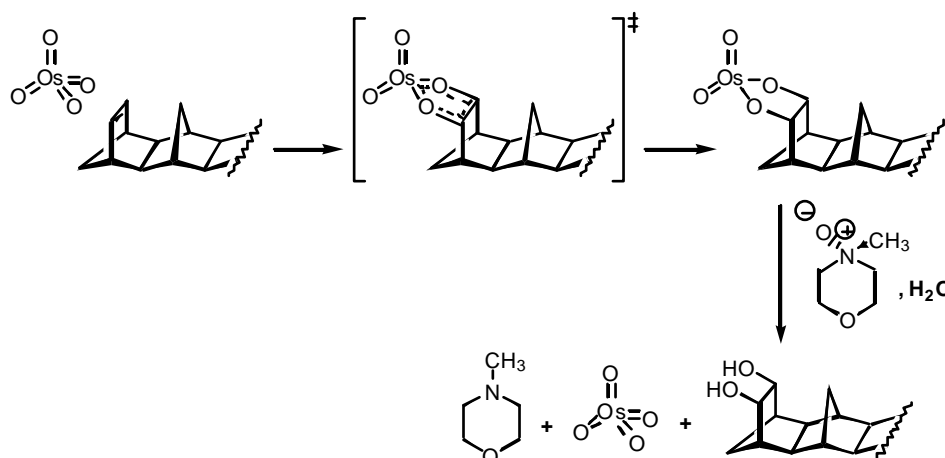
Despite the moderate yields enough of the dienes **12** and **13** was synthesised to proceed with the introduction of the keto-functionalities. The keto groups were then to be used for the attachment of the porphyrin chromophores (section B.2.3, page 60).

B.2.2 Synthesis of Diones and Tetraones

B.2.2.1 The *Sharpless* Bis-hydroxylation

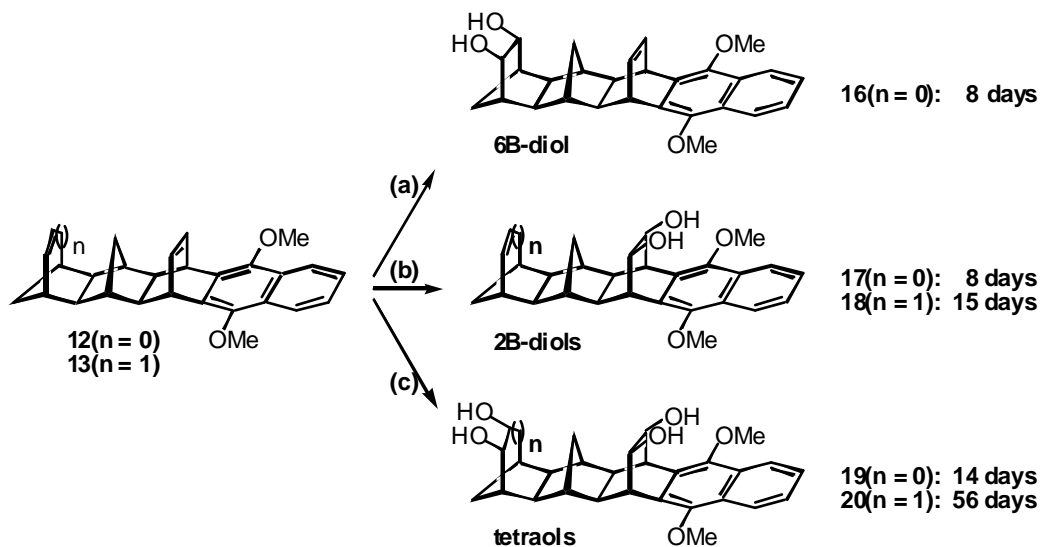
As an initial step towards the introduction of keto-functionalities (diones or tetraones) the dienes were hydroxylated using the *Sharpless* bis-hydroxylation method.¹⁵⁰ Osmium tetroxide, earlier used in stoichiometric amounts,¹⁵¹⁻¹⁵³ was used in catalytic amounts (1-2 %)¹⁵⁴ and was re-oxidised by *N*-methylmorpholine-*N*-oxide (NMO) in 1,4-dioxane as the solvent of choice.¹⁵⁵ The mechanism of the (enantioselective) *Sharpless* bis-hydroxylation

reaction is still under intense discussion.¹⁵⁶⁻¹⁶⁰ Both, [3+2] and a [2+2] mechanisms have their supporters.¹⁶¹ A concerted [3+2] mechanism is shown in **Scheme 6**.



Scheme 6: *Sharpless* bis-hydroxylation with catalytic amounts of OsO_4 and NMO as oxidant, shown is a concerted [3+2] mechanism

The amount of *N*-methylmorpholine-*N*-oxide as well as the time given for the reactants to react, controlled the ratio of diols to tetraols (**Scheme 7**).



Scheme 7: *Sharpless* bis-hydroxylation. (a) OsO_4 , 1 eq. NMO, 45 °C, 8 d, 31 % ; (b, n = 0) OsO_4 , 1 eq. NMO, 45 °C, 8 d, 9 % ; (b, n = 1) OsO_4 , 2.5 eq. NMO, RT, 15 d, 20 % ; (c, n = 0) OsO_4 , 2 eq. NMO, 40 °C, 14 d, 56 % ; (c, n = 1) OsO_4 , 2.5 eq. NMO, RT, 56 d, 70 %

The non-ring-expanded 6B-ene-2B-ene-DMN **12** gave the 6B-diol-DMN **16** and the 2B-diol-DMN **17** in a ratio of 3:1 after 8 days at 45 °C. For an extended reaction time (14 days) at 45 °C the tetraol **19** was obtained in 56 % yield.

The bis-hydroxylation of the ring-expanded double bond appeared to be somewhat more difficult. Only the 2B-diol-DMN **18** was isolated in 20 % yield after 15 days. In order to enable the hydroxylation of the ring-expanded olefin in good yields the reaction time had to be prolonged drastically. After 56 days the ring-expanded tetraol-DMN **20** was isolated in an extraordinarily high yield of 70 %. This was extraordinary in the sense that longer reaction times usually did not significantly increase yields in other OsO₄ experiments. **Figure 27** shows selected ¹³C chemical shifts for (the enantiomeric mixtures of) the ring-expanded 6B-ene-2B-ene-DMN **13**, 6B-ene-2B-diol-DMN **18**, and the ring-expanded 6B-diol-2B-diol-DMN **20**.

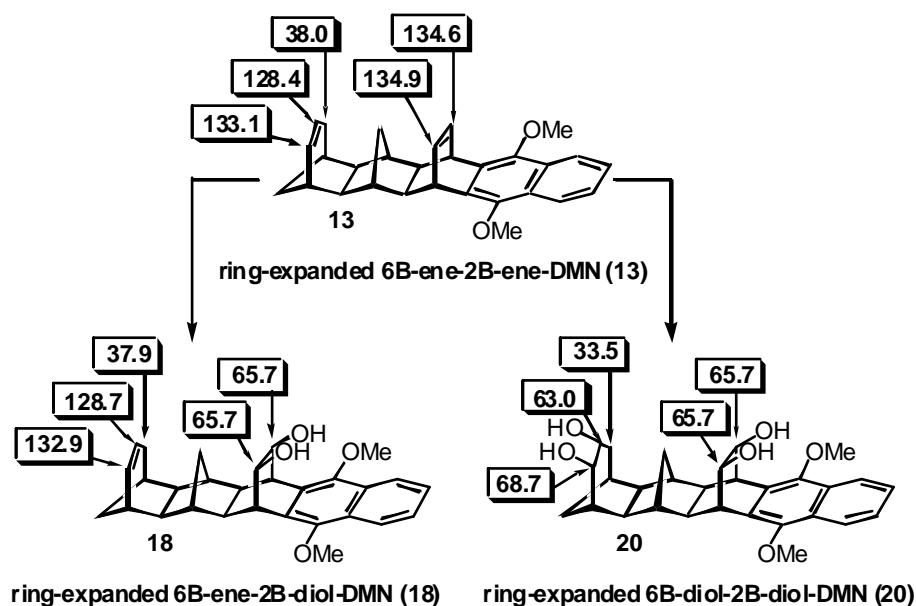
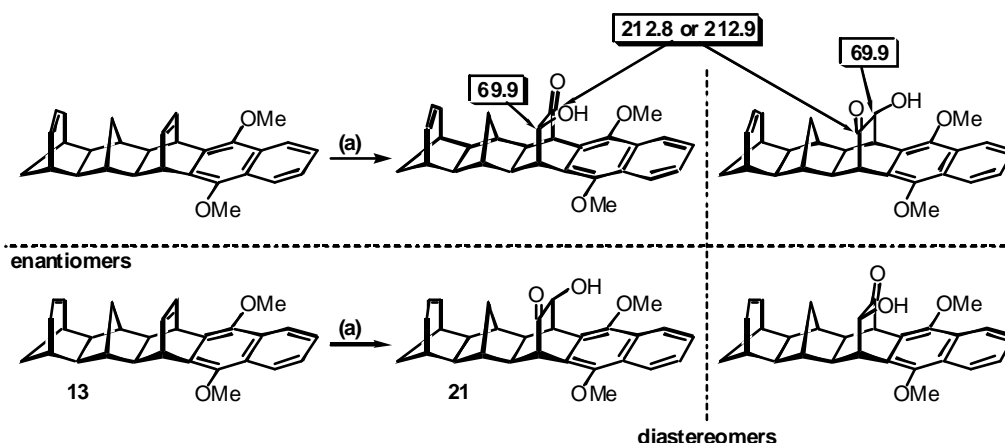


Figure 27: Selected ¹³C-NMR chemical shifts (75.5 MHz) for the isolated ring-expanded systems 6B-ene-2B-ene-DMN (**13**), 6B-ene-2B-diol-DMN (**18**), and 6B-diol-2B-diol-DMN (**20**)

The assignment of the chemical shifts is straightforward for the ring-expanded system. Its knowledge is helpful when assigning the chemical shifts for the non-ring-expanded systems (2B or 6B). As a side product of the *Sharpless* bis-hydroxylation a diastereomeric mixture of two enantiomeric ring-expanded 2B-ketols **21** was isolated in 5 % yield (**Scheme 8**).

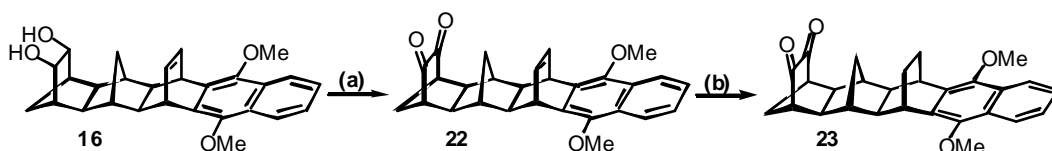


Scheme 8: Oxidation to α -ketols 21 under *Sharpless* bis-hydroxylation conditions. (a) OsO_4 , 2.5 eq. NMO, RT, 15 d, 5 %

In comparison with the ring-expanded 2B-diol-DMN **18** (**Figure 27**) the $^{13}\text{CHOH}$ signal was shifted downfield by 4.2 ppm to $\delta = 69.9$ ppm. This, together with the appearance of carbonyl carbon signals at 212.8 and 212.9 ppm for each diastereomer confirmed the formation of an α -ketol. The oxidation to α -ketols under bis-hydroxylation conditions had been reported by Van Rheenen *et al.*¹⁵⁵ with NaClO_3 or $\text{NMO} - \text{H}_2\text{O}_2$ 1:1, but was not found when NMO was used without H_2O_2 . For a discussion of the oxidation to ketones under *Sharpless* bis-hydroxylation conditions with NMO see section **B.3.1.2** 'Modified *Sharpless* Bis-hydroxylation' on page 90.

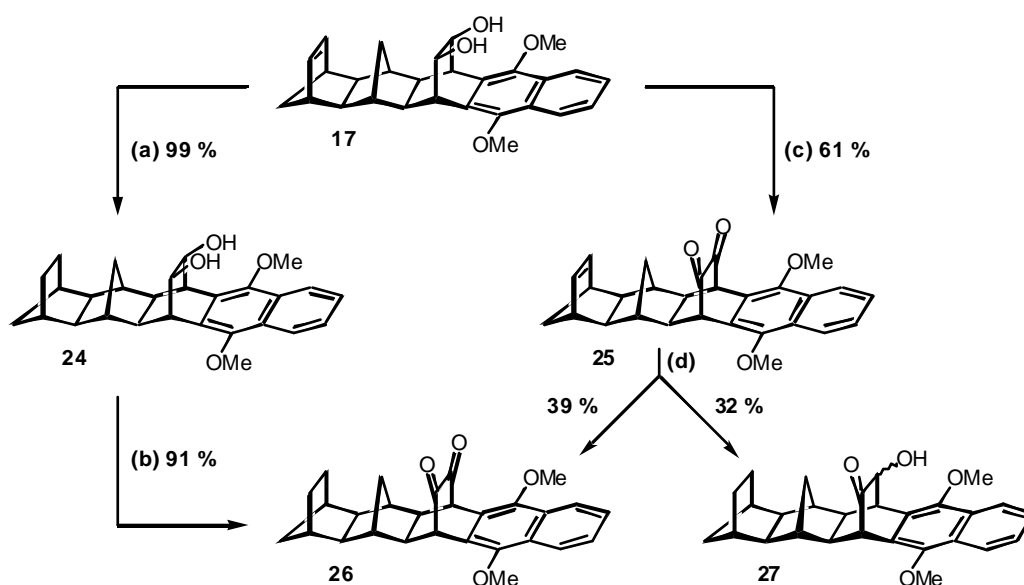
B.2.2.2 TEMPO Reaction

The non-ring-expanded 6B-diol-2B-ene-DMN **16** was the first diol to be converted into the saturated dione system. A sequence TEMPO reaction^{162,163} followed by Pd/C-H_2 was chosen (**Scheme 9**) and the oxidation of the diols and the subsequent hydrogenation yielded the desired saturated 6B-dione-DMN **23** in 59 % overall yield.



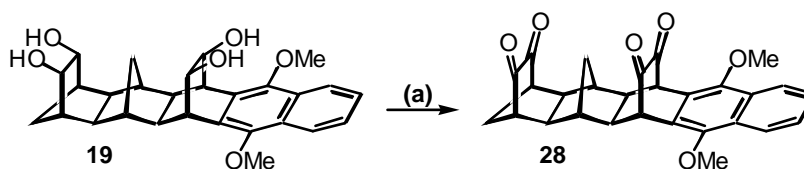
Scheme 9: TEMPO reaction followed by hydrogenation. (a) TEMPO reagent, *p*-toluenesulfonic acid, DCM, 0 °C/RT, 6 d, 63 % ; (b) Pd/C-H_2 , ethyl acetate, RT, 24 h, 93 %

The same reaction sequence was initially attempted for the 6B-ene-2B-diol-DMN **17** (**Scheme 10 (c) and (d)**). The hydrogenation of the TEMPO product 6B-ene-2B-dione-DMN **25**, however, yielded the desired saturated 2B-dione-DMN **26** in just 39 % yield. As a second product the 2B-ketol-DMN **27** (δ_{CHOH} : 74.3, $\delta_{\text{C=O}}$: 213.0 ppm) was isolated in 32 %. To avoid the reduction of one keto-functionality, the reaction sequence was altered with outstanding yields for both the initial Pd/C hydrogenation as well as the subsequent TEMPO reaction (**Scheme 10 (a) and (b)**).



Scheme 10: Hydrogenation then TEMPO or TEMPO then Hydrogenation?
(a) and (d) Pd/C-H₂, ethyl acetate, RT, 24 h; (b) and (c) TEMPO reagent, *p*-toluenesulfonic acid, DCM, 0 °C/RT, 5 d

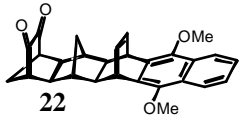
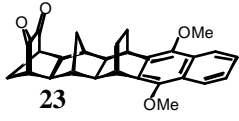
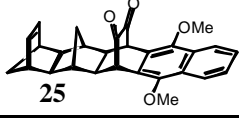

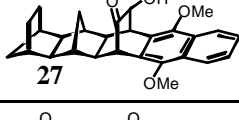
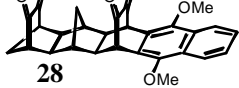
For the oxidation of the non-ring-expanded 6B-diol-2B-diol-DMN **19** the same procedure was applied with the equivalents of TEMPO reagent and *p*-toluenesulfonic acid being doubled (10-fold excess). The corresponding tetraone **28** was obtained in 56 % yield (**Scheme 11**).



Scheme 11: TEMPO reaction of the non-ring-expanded tetraol. (a) TEMPO reagent, *p*-toluenesulfonic acid, DCM, 0 °C/RT, 26 h, 56 %

Table 6 gives an overview of the ^{13}C -NMR chemical shifts in ppm relative to TMS found for the non-ring-expanded saturated and unsaturated diones (**22-26**), the 2B-ketol-DMN **27** and the tetraone **28**.

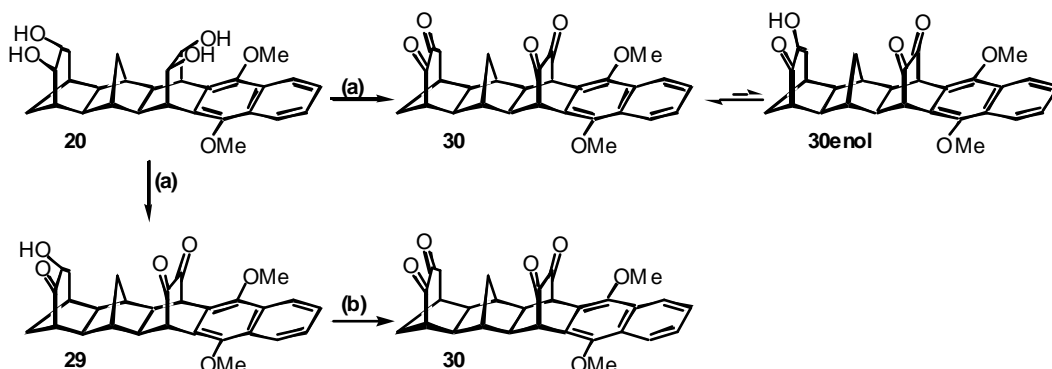
Table 6: ^{13}C -NMR shifts for non-ring-expanded TEMPO-reaction products in ppm relative to TMS

Compound	6B _{C=C}	6B _{C-C}	6B _{C=O}	2B _{C=C}	2B _{C-C}	2B _{C=O}	2B _{COH}	2B _{C=O}
 22			202.9	134.6				
 23			203.3		21.3			
 25	135.4					191.8		
 26		24.3				192.2		
 27		~24.6					74.3	213.0
 28			202.1			191.1		

The ^{13}C -chemical shifts for the carbonyl groups close to the aromatic system (2B-dione) are shifted up field by about 11 ppm (~192 ppm) compared to the 6B-carbonyl signals (203 ppm). The chemical shifts (δ_{CHOH} , $\delta_{\text{C=O}}$) observed for the enantiomeric α -ketols **27** are similar to the ones observed previously for the ring-expanded 2B-ketols **21** (**Scheme 8**, page 56). The chemical shifts for the saturated ethano-bridge (6B_{C-C}) are 24.3 ppm and 24.6 ppm, respectively.

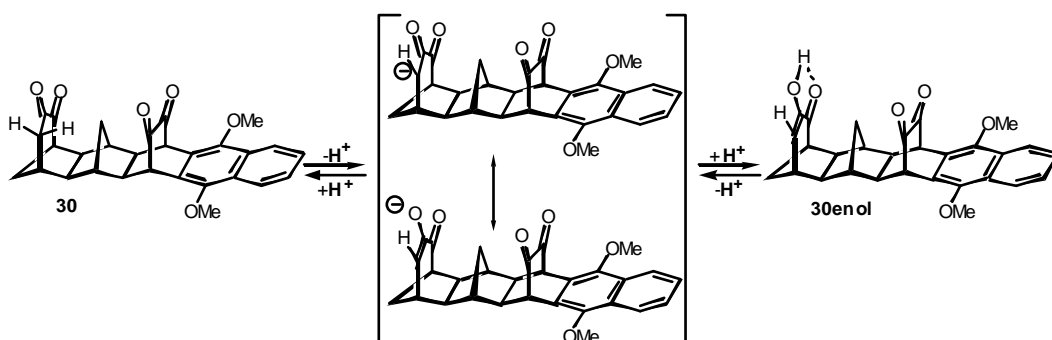
The TEMPO reaction for the ring-expanded 6B-diol-2B-diol-DMN **20** appeared to be more complex. The desired ring-expanded tetraone **30** was found to be the minor product (29 %) only, which tautomerised in deuterated chloroform into a trione-enol system **30enol**. The

major product (54 %) in this reaction was identified as the incompletely oxidised 6B-ketol-2B-dione-DMN **29** (**Scheme 12 (a)**).



Scheme 12: TEMPO reaction on ring-expanded tetraol. (a) TEMPO reagent, p-toluenesulfonic acid, DCM, 0 °C/RT, 5 d, 29 % (tetraone) / 54 % (trione-enol); (b) TEMPO reagent, p-toluenesulfonic acid, DCM, 0 °C/RT, 20 d, 57 %

The 6B-ketol-2B-dione-DMN **29** was then converted by another TEMPO reaction (20 days) into the desired 6B-dione-2B-dione-DMN **30** in 57 % yield (**Scheme 12 (b)**). Interestingly, four distinct carbonyl signals were found when characterised by ^{13}C -NMR spectroscopy in deuterated chloroform. There was no evidence for the presence of olefinic $=\text{CH}$ or $=\text{COH}$ and, therefore, keto-enol tautomerism was not observed. This could be due to a different batch of chloroform- d_1 that might have been more acidic than the one used previously. An acidic environment shifts the equilibrium between the dione **30** and the ambident anion towards the dione (**Scheme 13**).

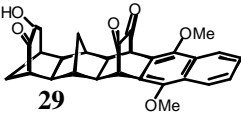
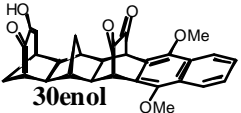
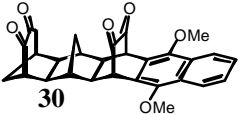


Scheme 13: Mechanism of keto-enol tautomerism for a ring-expanded dione

Once the enol is formed it is stabilised through the formation of the conjugated enone and hydrogen bonding between the hydroxy group and the vicinal carbonyl functionality. Selected ^{13}C chemical shifts in ppm relative to TMS for the ring-expanded TEMPO-reaction products are given in **Table 7**. ^1H -NMR resonances observed are in accordance with the three proposed

structures. The olefinic proton of the tautomerised tetraone **30enol** showed as a doublet at 6.11 ppm.

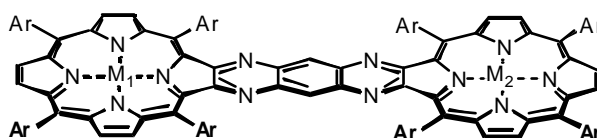
Table 7: ^{13}C -NMR shifts for ring-expanded TEMPO-reaction products in ppm relative to TMS

Compound	$6\text{B}_{\text{C}=\text{C}}$	$6\text{B}_{\text{C}=\text{O}}$	6B_{COH}	$6\text{B}_{=\text{COH}}$	$6\text{B}_{=\text{CH}}$	$2\text{B}_{\text{C}=\text{O}}$	$2\text{B}_{\text{C}=\text{O}}$
 29		210.1	72.3			191.6	192.0
 30enol	196.4			149.9	119.5	191.5	191.5
 30	196.4	190.9				191.4	191.9

Now, with the diones and tetraones in hand, the stage was set for the attachment of the porphyrin moieties. The attachment *via* two subsequent condensation reactions is described in the following section **B.2.3**.

B.2.3 Condensations

As mentioned above (chapter **B.2**, page 49) the strategy behind the condensation of 'porphyrindione' and benzenetetramine was pioneered by Crossley *et al.*^{142,143} In fact, his group's bis-porphyrins (**Example 21**) were the first examples of two porphyrins covalently linked through the β -pyrrolic positions.¹⁴²



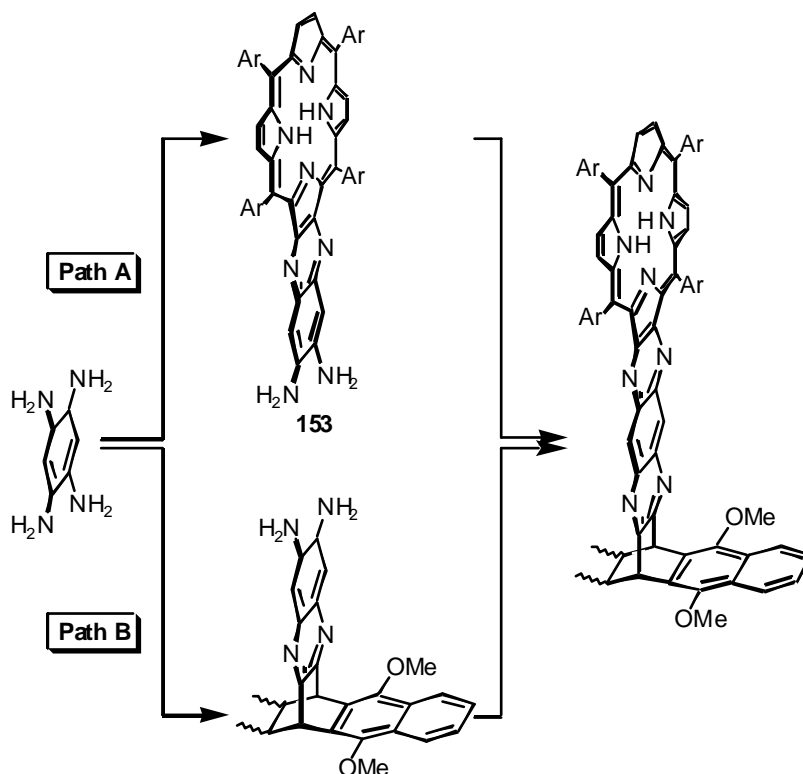
Ar = phenyl or 3,5-di-*tert*-butylphenyl; $\text{M}_1, \text{M}_2 = 2\text{H}, \text{Ni}, \text{Pd}, \text{Zn}, \text{Cu}, \text{Fe}(\text{Cl})$

Example 21: First bis-porphyrins covalently linked through the β -pyrrolic positions by Crossley *et al.* (1987)

Motive behind Crossley's work was the development of molecular wires and his group successfully extended the 'benzenetetramine strategy' to construct oligo-porphyrin systems.^{141,144}

In this thesis two different α -diketones were to be linked by benzenetetramine. As benzenetetramine is commercially distributed as its tetrahydrochloric salt, all condensation reactions with benzenetetramine were carried out in pyridine to generate the free base that then undergoes the condensation with the α -diketone. As benzenetetramine is the reacting species I refrain from explicitly mentioning on each occasion that the tetrahydrochloric salt was the chemical actually used.

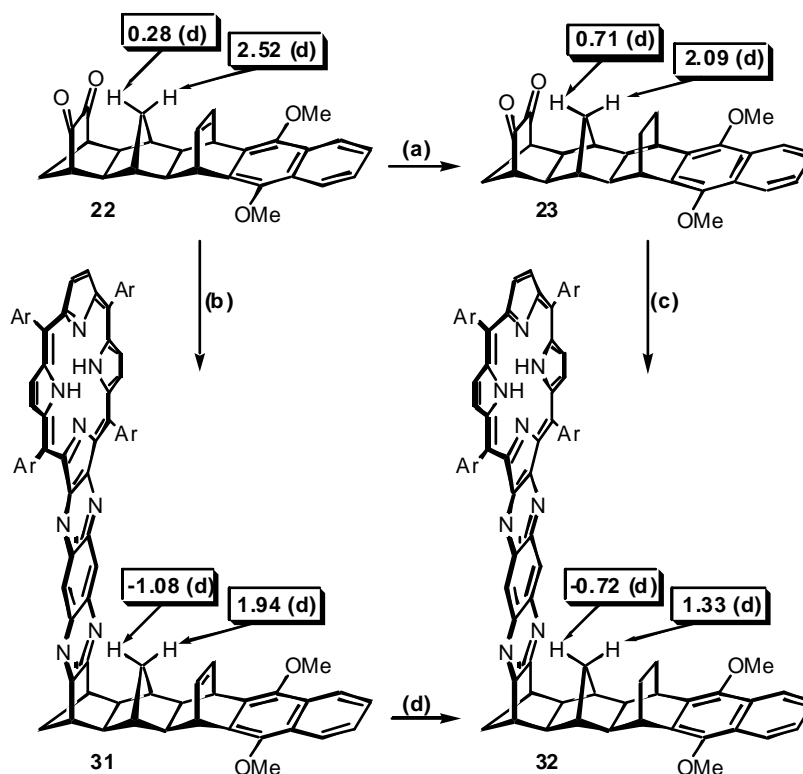
In principle two different pathways (**Scheme 14**) exist to successfully link the benzenetetramine with one equivalent of 'porphyrindione' and one equivalent of the diones/tetraones described above. One could either condense benzenetetramine and 'porphyrindione' first and then condense the adduct with the diones/tetraones (**Scheme 14 (Path A)**) or vice versa (**Scheme 14 (Path B)**).



Scheme 14: Two condensation sequences. Path A: 'porphyrindione' followed by diones/tetraones; Path B: diones/tetraones followed by porphyrindione

Both pathways were tested with pathway 'A' being chosen after the condensation of benzenetetramine and 'porphyrindione' was optimised. Carried out in pyridine with a 1.5 excess of benzenetetramine, the yields obtained were quantitative and the product 5,10,15,20-tetrakis-(3,5-di-*tert*-butylphenyl)-2³-2⁴-diaminoquinoxalino[2,3-*b*]porphyrin, for the remainder of the thesis referred to as 'diaminoporphyrin', was easily purified by column chromatography. The formation of the bis-porphyrin adduct, previously synthesised by Crossley *et al.*¹⁴² was negligible.

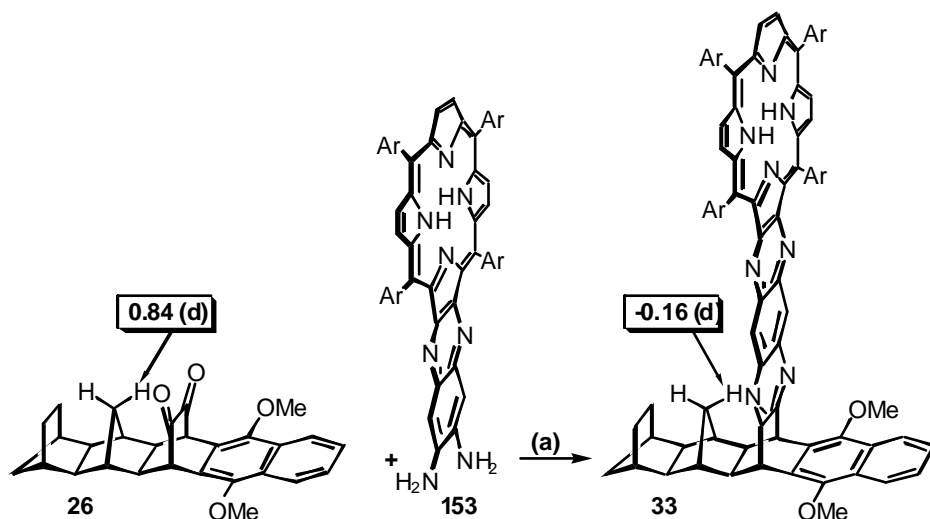
The condensation of the unsaturated 6B-dione-2B-ene-DMN **22** with 'diaminoporphyrin' in de-oxygenated pyridine at 125 °C in a dark pressure tube (**Scheme 15 (b)**) gave moderate yields only (27-29 %). In contrast the saturated 6B-dione-DMN **23** gave the desired adduct in high yields (54 %) under similar conditions, but in de-oxygenated dichloromethane instead (**Scheme 15 (c)**).



Scheme 15: Synthesis of 6B-porphyrin-DMN. (a) Pd/C-H₂, ethyl acetate, RT, 24 h, 93 % ; (b) 'diaminoporphyrin', pyridine, 125 °C, pressure tube, 3d, 29 % ; (c) 'diaminoporphyrin', DCM, 125 °C, pressure tube, 3d, 54 % ; (d) Pd/C, H₂, ethyl acetate, RT, 24 h, 79 %

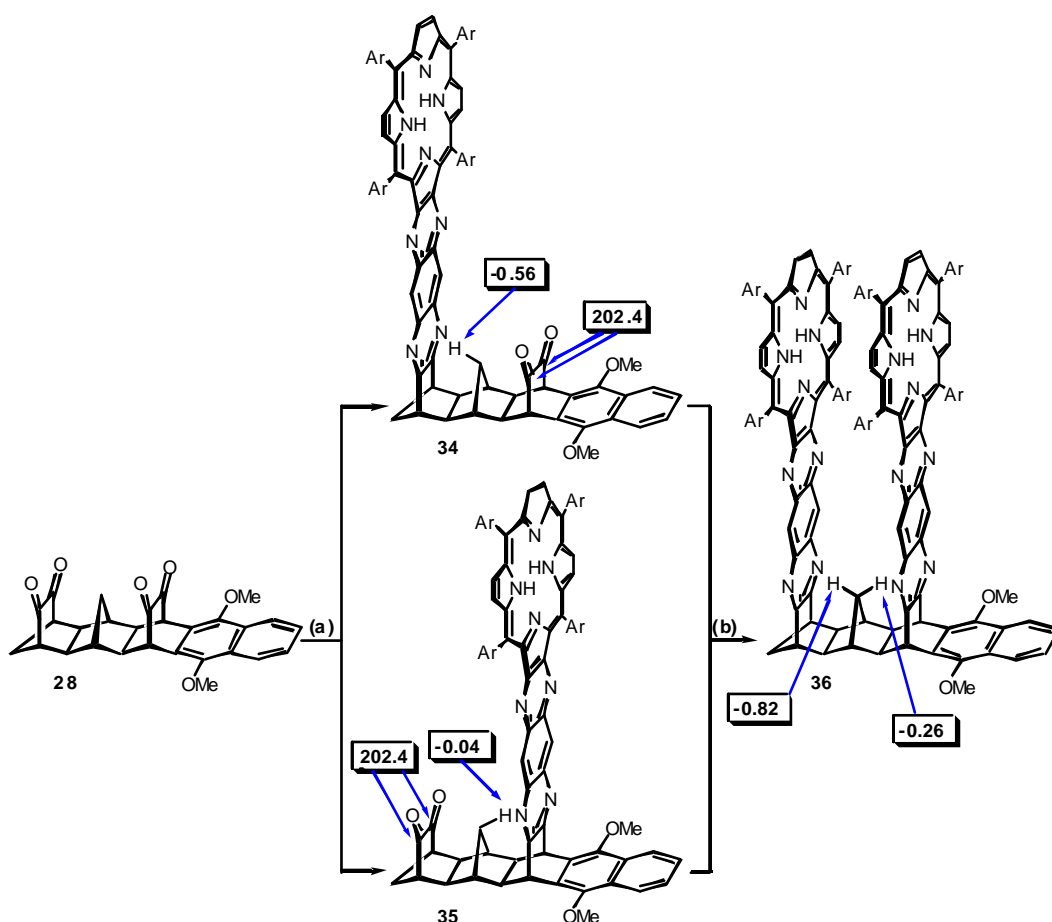
Most striking evidence for a successful condensation are the chemical shifts of the methylene-bridge protons. Upon successful condensation, the signals for the methylene protons directed towards the newly condensed aromatic system shifted upfield by 1.36 ppm and 1.43 ppm, respectively (**Scheme 15**). Both protons showed as a doublet with typical coupling constants between 12.2 and 12.7 Hz. The upfield shift of the methylene protons was used to monitor the progress of the condensations, which were carried out under the above-mentioned optimised conditions in de-oxygenated dichloromethane. Upon completion of the reaction, dichloromethane was blown off under an argon stream, and the crude product was purified by column chromatography.

The 2B-dione-DMN **26** and 'diaminoporphyrin' yielded under these conditions the desired 2B-porphyrin-DMN **33** in 73 % (**Scheme 16**) with the methylene proton facing the aromatic system undergoing an upfield shift by 1 ppm.



Scheme 16: Synthesis of 2B-porphyrin-DMN 33. (a) DCM, 125 °C, pressure tube, 4 d, 73 %

The attempt to condense two 'diaminoporphyrins' and one non-ring-expanded tetraone resulted initially in the 6B- (**34**) and 2B-mono-adducts (**35**) only (**Scheme 17**). Both products were easily identified by the proton signal for the methano bridge ($\delta = -0.04$ ppm (2B); $\delta = -0.56$ ppm (6B)) and the carbon signal of the carbonyl groups ($\delta_{\text{C=O}}$: 202.4 ppm (2B), 191.4 ppm (6B)). The ratio 2B/6B was found to be ~3:1. Under the same conditions a mixture of these mono-adducts was reacted with further 'diaminoporphyrin' to yield the bis-porphyrin-DMN **36** in 38 % yield (**Scheme 17**).



Scheme 17: Condensation of the non-ring-expanded tetraone. (a)
'diaminoporphyrin', DCM, 125 °C, pressure tube, 3 d, 12 % (34), 31 % (35);
(b) 'diaminoporphyrin', DCM, 120 °C, pressure tube, 4 d, 38 %

Mass spectrometry (MALDI) confirmed the successful synthesis of bis-porphyrin-DMN **36** ($MH^+ = 2777$). The 1H -NMR spectrum of the bis-adduct is given in **Figure 28**. All proton signals were assigned with the support of a COSY experiment. The 144 *tert*-butyl protons gave 6 distinct signals that integrated to 18, 18, 36, 36, 18, and 18 protons, respectively. The two methylene protons were significantly shifted upfield for the bis-porphyrin-DMN system **36**. Their chemical shifts could be found at -0.82 (facing the 6B-porphyrin) and -0.26 ppm (facing the 2B-porphyrin), respectively.

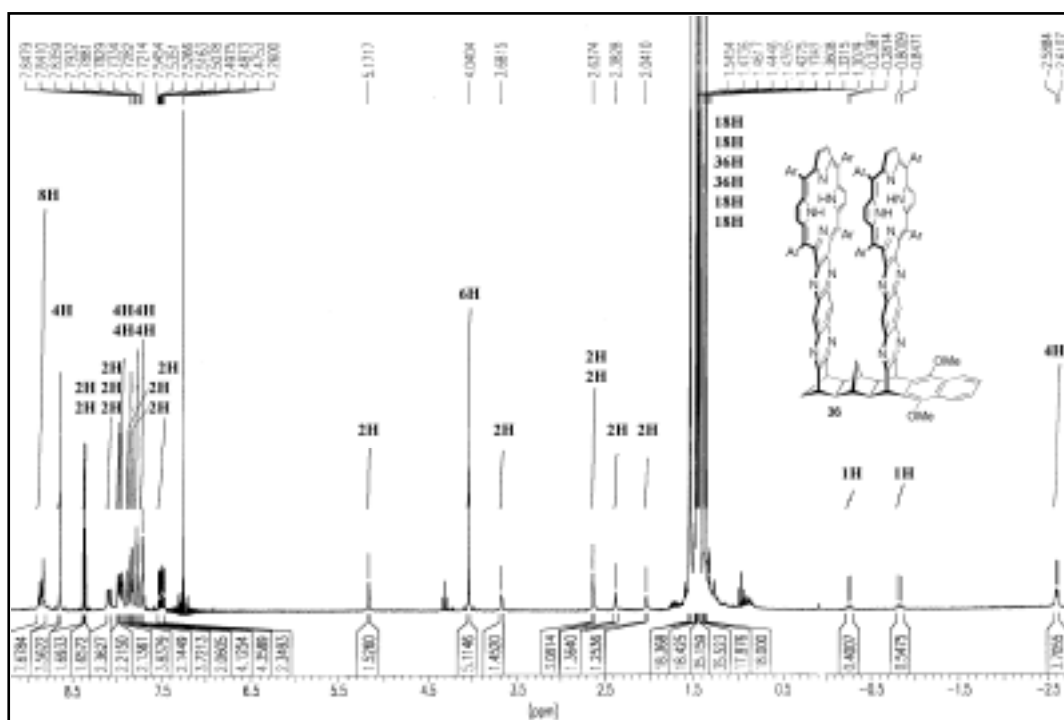


Figure 28: ^1H -NMR spectrum (300 MHz) of bis-porphyrin-DMN 36

Both methylene protons coupled with the vicinal bridge-head protons ($\delta = 2.63$ ppm) and each of the protons showed W-type coupling with the respective protons next to the bridge head at $\delta = 2.64$ and 2.38 ppm, respectively (**Figure 29**).

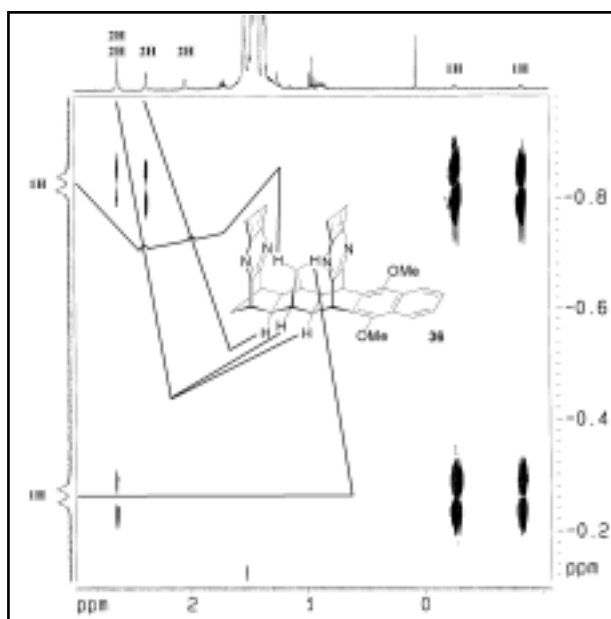


Figure 29: Detail of COSY spectrum (500 MHz) of bis-porphyrin-DMN 36

The inner protons of the two porphyrin rings showed at -2.59 and -2.62 ppm, respectively. Comparison with the chemical shifts for the inner protons of the 6B-porphyrin-DMN 32

($\delta = -2.39$ ppm) and the 2B-porphyrin-DMN **33** ($\delta: -2.30$ ppm) suggests that an interaction between the two porphyrin rings exists, causing the upfield shift of 0.2 and 0.3 ppm, respectively. Treatment of the two porphyrin chromophores as one 'special pair' seems to be therefore justified.

The UV-Vis spectrum of the bis-porphyrin-DMN **36** showed the maximum of the Soret band at 423 nm and for the Q-bands at 536 nm, 609.5 nm, and 658 nm. The spectrum of the 6B-porphyrin-DMN **32** is almost identical in respect to observed maxima, the extinction coefficient ϵ , however, is smaller (**Figure 30**).

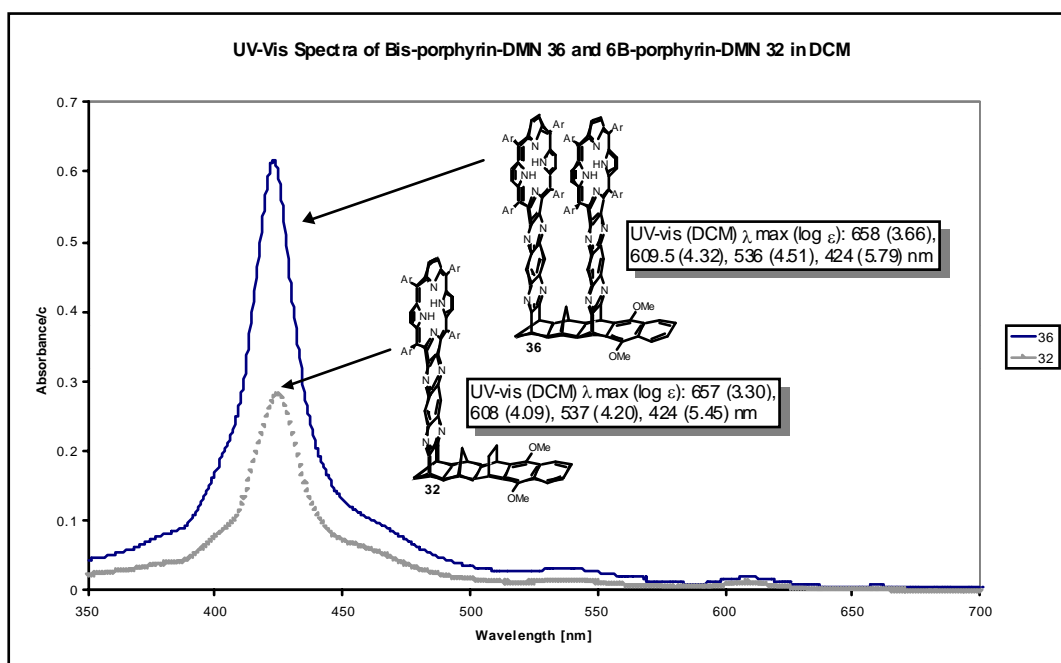


Figure 30: UV-Vis spectra of bis-porphyrin-DMN 36 and 6B-porphyrin-DMN 32 in dichloromethane

A concentration 2×10^{-6} mol/l for UV-Vis absorption and steady state fluorescence spectroscopy was found to be adequate for the bis-porphyrin compounds; solutions of the mono-porphyrin adducts were used roughly four times more concentrated ($8-9 \times 10^{-6}$ mol/l). Excited at a wavelength of 400 nm the bis-porphyrin-DMN **36** showed a fluorescence band with two maxima at 660.5 nm and 664.5 nm (**Figure 31**). The fluorescence spectrum of the mono-adduct, the 6B-porphyrin-DMN **32**, showed only one emission maximum at 662.5 nm. Conclusions on the cause of the two maxima must be derived carefully as the level of background noise was high.

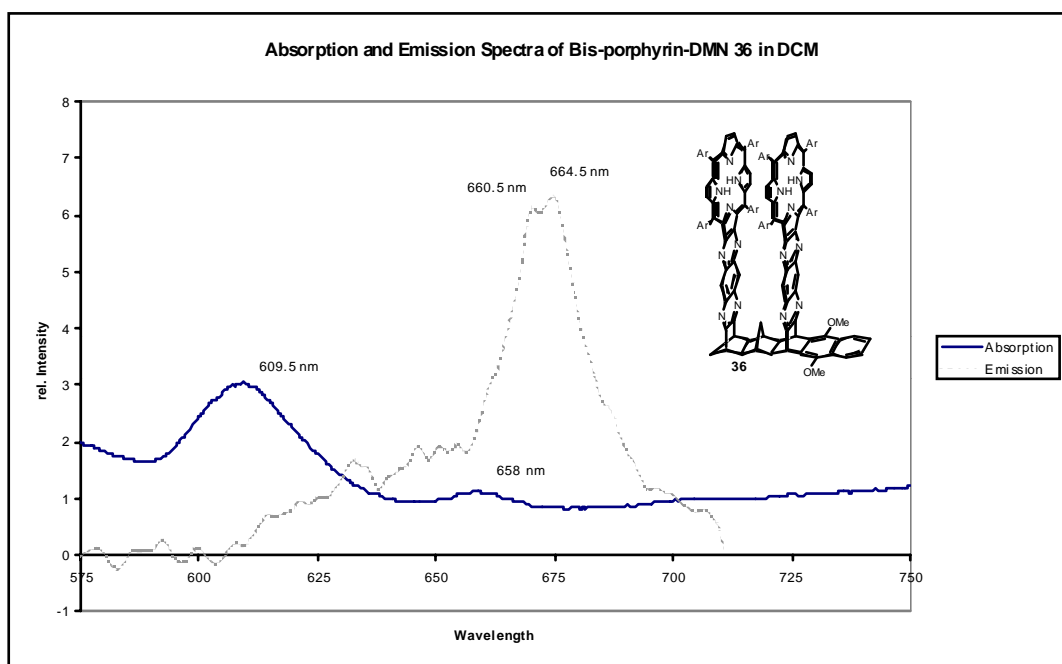
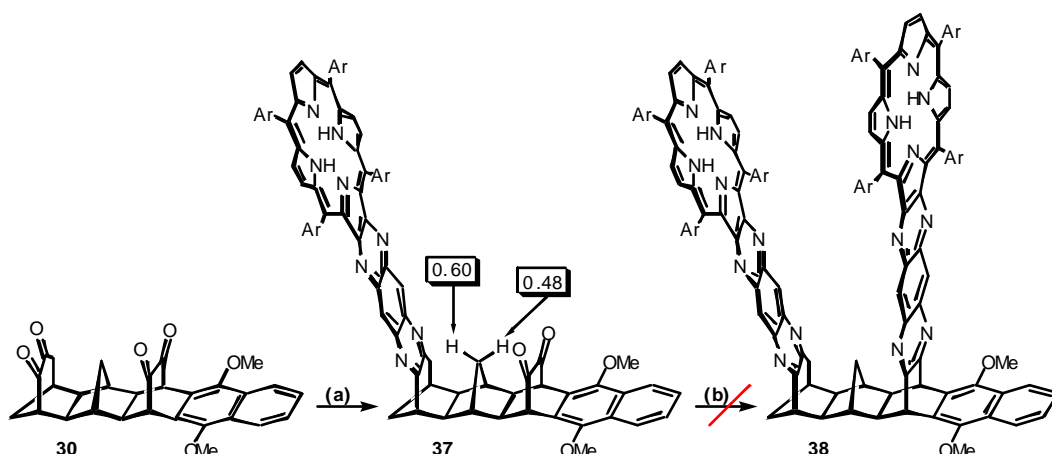


Figure 31: Absorption and emission spectrum of bis-porphyrin-DMN 36

Quenching of the fluorescence band for the corresponding TCNQ bichromophoric systems would count as evidence for a non-radiative decay of the excited state. A pathway for such a non-radiative decay could be provided by an ET transfer process from the porphyrin donor to the TCNQ acceptor.

For the ring-expanded system, only the 6B-porphyrin-2B-dione-DMN **37** (the mono-adduct) was found in low yield when the corresponding ring-expanded tetraone **30** was reacted with two equivalents of 'diaminoporphyrin' (**Scheme 18**).



Scheme 18: Condensation of the ring-expanded tetraone 30. (a) 2 eq. 'diaminoporphyrin', DCM, 120 °C, pressure tube, 5 d, 15 % (b) not successful to date.

Unlike the non-ring-expanded 6B-porphyrin-2B-dione-DMN **34**, the methylene protons of the 6B-mono-adduct **37** were not significantly shifted upfield (0.60 ppm, 0.48 ppm). Due to the kinked nature of the porphyrin attachment, the methylene proton is no longer shielded by the newly formed aromatic system. Together with the carbonyl signals for the 2B-dione (191.6 ppm, 191.7 ppm) they confirmed the synthesis of the 6B-mono-adduct **37** (not the 2B-mono-adduct). Mass spectrometry (MALDI) provided further evidence for the mono-addition ($MH^+ = 1631$).

The synthesis of the kinked bis-porphyrin-DMN **38** was not successful under the chosen conditions. Nevertheless, the successful synthesis of 6B-porphyrin-DMN **32**, 2B-porphyrin-DMN **33**, and bis-porphyrin-DMN **36** remains a major achievement in the synthesis of the initially envisaged series of target compounds. This series of dyads is not expected to exhibit electron transfer from a locally excited porphyrin(s) to the dimethoxynaphthalene acceptor. In order to achieve electron transfer the acceptor strength had to be increased.

B.2.4 From Energy Transfer to Electron Transfer

A conversion of the dimethoxynaphthalene (DMN) into the strong electron acceptor tetracyanonaphthoquinodimethane (TCNQ)^{24,164} increases the driving force for electron transfer. The Rehm-Weller equation^{19,20} (**Equation 10**, page 10) provides the relationship between the driving force for ET (ΔG^0) and the redox potentials (E_{ox} and E_{red}) of the chromophores. In a polar solvent and at a relatively large donor-acceptor separation the driving force can be calculated according to **Equation 14**.

$$\Delta G^0 = E_{ox}(D) - E_{red}(A) - E_{00}$$

Equation 14: Rehm-Weller equation for large donor-acceptor separation. E_{00} is the zero-zero electronic excitation energy to the first excited singlet state (D^*); $E_{ox}(D)$ and $E_{red}(A)$ are the oxidation and reduction potentials of donor and acceptor, respectively

If only the acceptor is changed, the zero-zero electronic excitation energy (E_{00}) and the oxidation potential of the porphyrin donor ($E_{ox}(D)$) remain the same. The change in driving force is then directly reflected in the change of the reduction potential of the acceptor ($E_{red}(A)$). The known redox potentials of 4B-DMN **39** and 2B-TCNQ **40** are -1.10 eV and -0.10 eV, respectively (**Figure 32**).^{164,165}

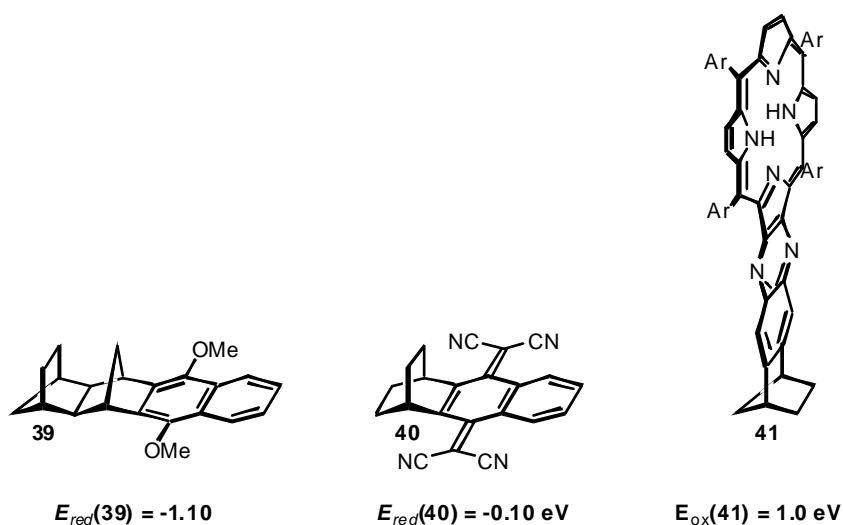
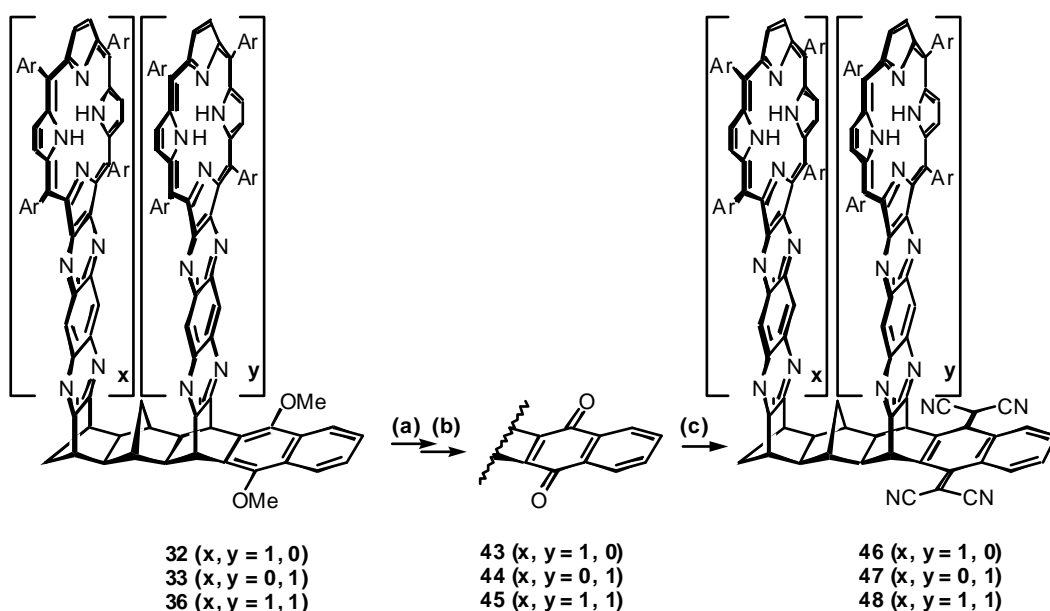


Figure 32: Redox potentials of related acceptor and donor chromophores

The E_{00} value evaluated from the absorption spectrum of the bis-porphyrin-DMN **36** (**Figure 30**, page 66) is roughly 1.9 eV, which corresponds well to the value reported for the known 2B-porphyrin **41** (1.91 eV).¹¹³ The oxidation potential of the latter compound is 1.00 eV.

Assuming solvent independence, the driving forces for electron transfer (ΔG°) are estimated using the Rehm-Weller equation (**Equation 14**) to be +0.2 eV for the porphyrin-DMN species and -0.8 eV for the porphyrin-TCNQ dyads, which confirms that a change of the acceptor from DMN to TCNQ makes the electron transfer process thermodynamically accessible.

The conversion of dimethoxynaphthalene (DMN) to tetracyanonaphthoquinodimethane (TCNQ) was achieved *via* the corresponding hydroquinone and naphthoquinone. Demethylation of the dimethyl ethers (of DMN) was achieved using boron tribromide^{43,113,166,167} The resulting hydroquinones (only the 6B-porphyrin-HNQ **42** (not depicted) was isolated) oxidised readily with lead dioxide^{113,168} to the corresponding naphthoquinones shown in **Scheme 19**. The yields for these first two steps were found to be high.



Scheme 19: From DMN to TCNQ. (a) BBr_3 , DCM, -45°C / RT, over night; (b) PbO_2 , DCM, RT, 30 min; (c) malononitrile, TiCl_4 , DCM, β -alanine, pyridine

The procedure for the subsequent TiCl_4 -reaction was first developed by Wasielewski *et al.*²⁴ and gave variable yields between 29 % and 58 % (**Table 8**).

Table 8: Yields from DMN to TCNQ

Reactant	n, x, y	Yield (a) x (b)	Yield (c)
6B-porphyrin-DMN 32	0, 1, 0	93 %	58 %
2B-porphyrin-DMN 33	0, 0, 1	95 %	31 %
bis-porphyrin-DMN 36	0, 1, 1	83 %	29 %

The highest yield for the TiCl_4 -reaction was obtained for 6B-porphyrin-NQ **43**. Significantly lower yields were found for systems with the porphyrin moiety only 2 σ -bonds away from the reacting naphthoquinone (**44**, **45**). Steric or electronic influences on yields could not be excluded, but due to the small number of experiments they also couldn't be confirmed.

For all three TCNQ systems **46**, **47**, and **48** ^1H -NMR, COSY, and ^{13}C -NMR (including DEPT90 and DEPT135) spectra were obtained and signals assigned where possible. Their mass spectra (MALDI) matched their calculated molecular weight, melting points were above 300 °C. As an example the proton and carbon NMR spectra of the bis-porphyrin-TCNQ target **48** are given (**Figure 33** and **Figure 34**). A more detailed discussion of the ^1H -NMR spectrum including a number of expansions is given in **Error! Reference source not found.** 'Error! Reference source not found.' in the Appendix of this thesis on page **Error! Book mark not defined.**

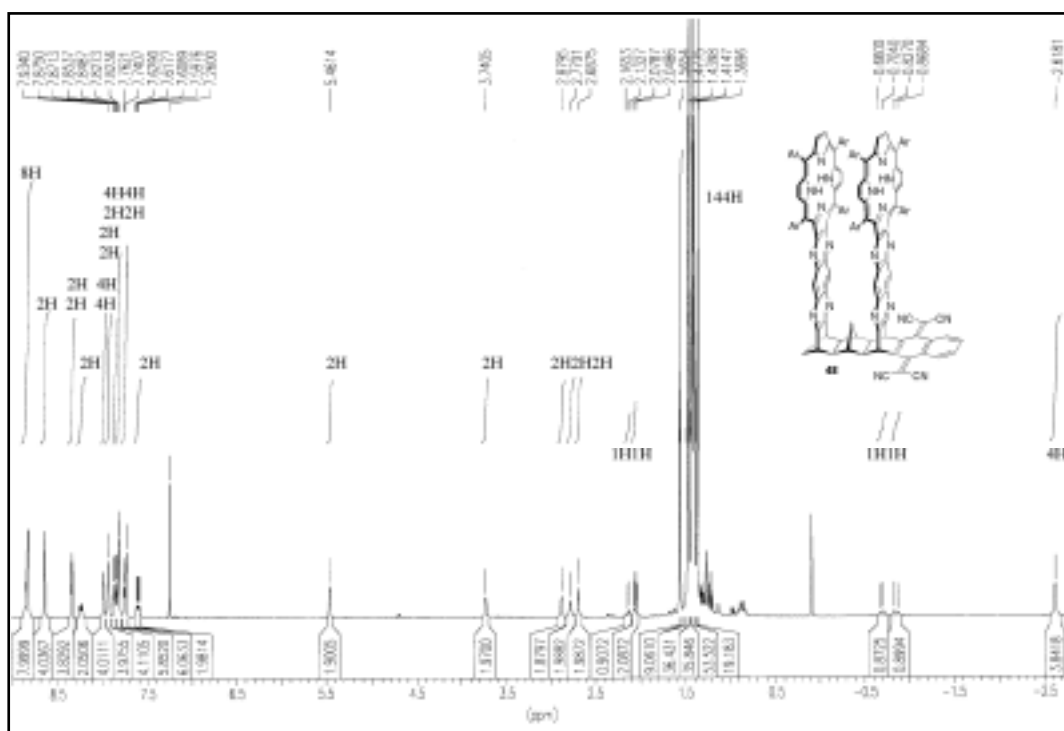


Figure 33: ^1H -NMR spectrum (300 MHz) of bis-porphyrin-TCNQ 48

The signals for the four inner protons of the two porphyrins show as far upfield as -2.61 and -2.62 ppm, respectively. The two methylene bridge protons show as doublets at -0.84 and -0.68 ppm with a coupling constant of 12.1 Hz. Very significant is the chemical shift for the two bridge head protons next to the TCNQ acceptor. Their singlet is found at 5.46 ppm (5.17 for DMN, 5.21 for NQ). Stronger evidence for the successful TiCl_4 reaction is found in the ^{13}C -NMR spectrum (**Figure 34**).

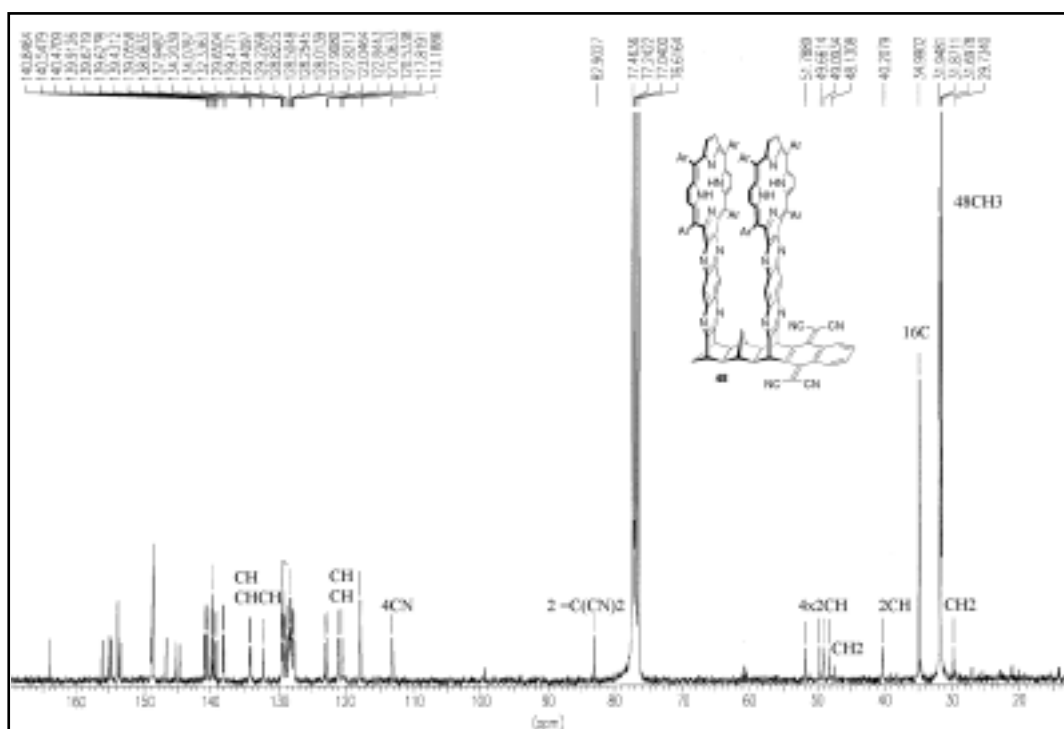


Figure 34: ^{13}C -NMR spectrum (75.5 MHz) of bis-porphyrin-TCNQ 48

The carbonyl signal at $\delta_{\text{C=O}}$: 180.8 ppm of the starting material (bis-porphyrin-NQ) is absent and a peak for the four CN resonances is present, appearing at 113.2 ppm. The two =C(CN)₂ resonances showed at 82.9 ppm.

The above-described interaction between the two porphyrin units (**B.2.3**, page 60), evident in the upfield shift of the inner porphyrin-protons, was found in the naphthoquinone (NQ) and tetracyanonaphthoquinodimethane (TCNQ) systems as well. Compared to the mono-porphyrin systems peaks shift upfield by 0.2 to 0.3 ppm (**Figure 35**).

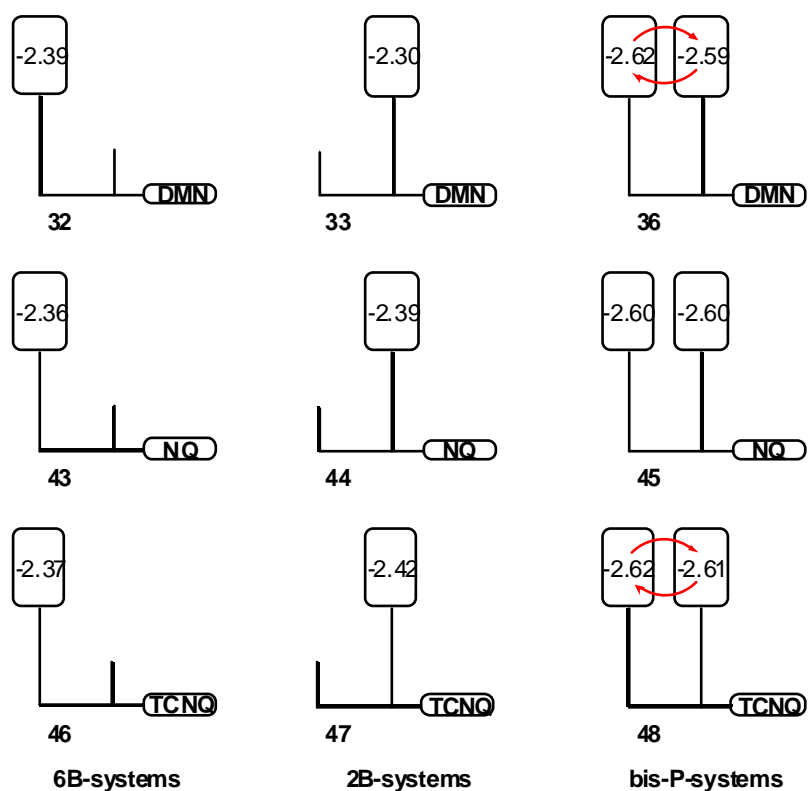
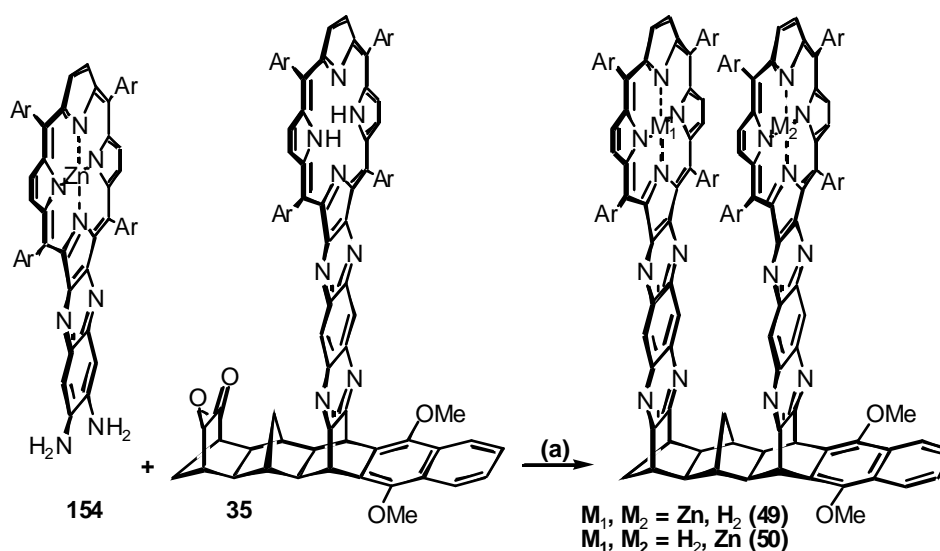


Figure 35: Upfield shift of inner-proton resonance in bis-porphyrin systems compared to the 6B- and 2B-mono-porphyrin dyads

Throughout the series of bis-porphyrin-adducts (DMN, NQ, TCNQ) the two porphyrins seem indeed 'special'. Despite the large inter-porphyrin separation (12 Å, AM1) they exhibit some interaction, as is characteristic of the two porphyrins of the 'special pair' in photosynthetic reaction centres, which are only separated by ~ 6.6 Å.

The metallation of one 'special pair'-porphyrin or the introduction of different metals into the porphyrin moiety would give access to a study of inter-porphyrin (energy) transfer processes in conjunction with the projected electron transfer to the TCNQ acceptor. A statistical metallation of the bis-adducts is believed to result in a challenging separation problem. However, isolation of the mono-porphyrin-mono-dione intermediates **34** and **35** in the bis-condensation reaction and a subsequent condensation with a metallated 'diaminoporphyrin' should result in one well-defined bis-adduct with different porphyrin moieties. This concept was applied to the earlier isolated (page 64) 6B-dione-2B-porphyrin-DMN **35** (**Scheme 20**).



Scheme 20: Attempted synthesis of a 6B-[porphyrinato]zinc(II)-2B-porphyrin-DMN 49. (a) de-oxygenated DCM, dark pressure tube, 120 °C, 21 d

Unfortunately the reaction conditions (DCM, pressure tube, 120 °C, 21 days) proved to be too harsh to keep the zinc(II) in place and a mixture of 6B-[porphyrinato]zinc(II)-2B-porphyrin-DMN **49** and 6B-porphyrin-2B-[porphyrinato]zinc(II)-DMN **50** was isolated from the reaction mixture. In principle stronger bound metal-ions should stand those reaction conditions and give controlled access to mono-metallated bis-adducts. In order to go ahead with this concept, more mono-porphyrin adduct is required.

With the successful synthesis of the three donor-DMN and three donor-TCNQ systems the synthesis of the non-ring-expanded dyads had been completed. For the TCNQ dyads a driving force for electron transfer (ΔG^0) had been calculated to be roughly -0.8 eV (**Equation 14**). Assuming a typical reorganisation energy of 1 eV,^{22,111,113} the barrier for charge separation in polar solvents (ΔG^*) can be estimated according to **Equation 15** to be 0.01 eV.

$$\Delta G^* = \frac{(\lambda + \Delta G^0)^2}{4\lambda}$$

Equation 15: Gibbs free energy of activation (Equation 3, page 7)

Experimental evidence for non-radiative decay (such as electron transfer) was found in the emission spectra of the porphyrin-TCNQ dyads. Comparison with the corresponding DMN

bichromophores revealed strong fluorescence quenching, in fact >94 %. **Figure 36** compares the emission spectra of 6B-porphyrin-DMN **32** and 6B-porphyrin-TCNQ **48**.

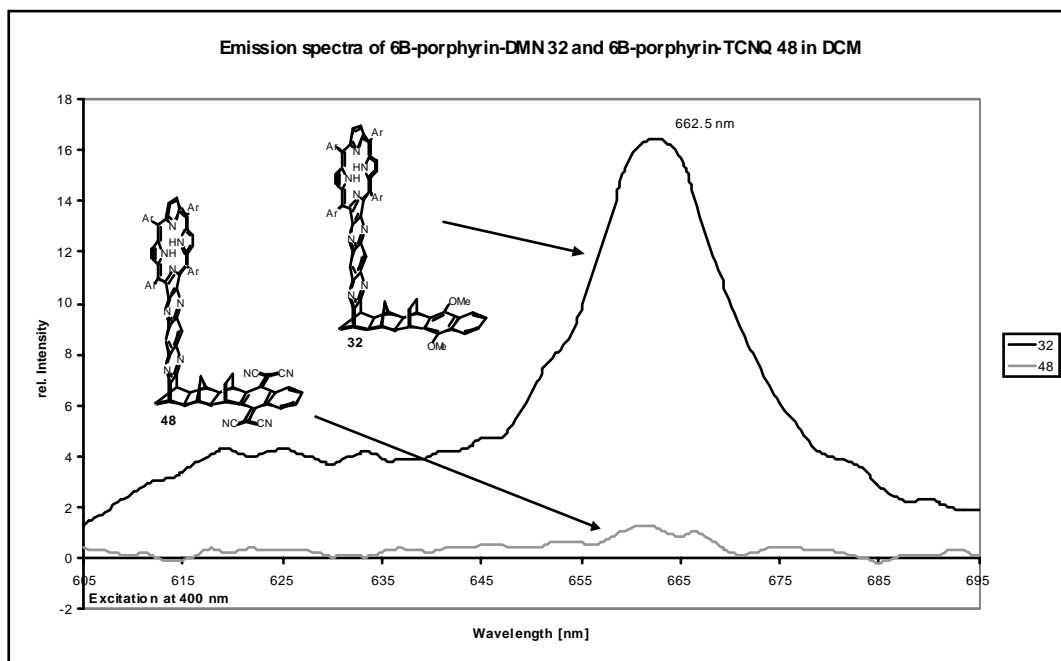


Figure 36: Fluorescence spectra of 6B-porphyrin-DMN **32 and 6B-porphyrin-TCNQ **48**; 94 % quenching**

The assumption that electron transfer takes place seems reasonable considering the above mentioned results. But time-resolved photophysical experiments will have to confirm the existence of a charge-separated state and establish electron transfer characteristics, such as electron transfer rates (k_{ET}) and the lifetime of the charge-separated state (τ_{CR}).

The lifetime of the charge-separated species is expected to be short (**A.4.2** 'Multichromophoric Concept', page 22) but should be significantly prolonged by attachment of a third chromophore another six σ -bonds away. The synthesis of such triads and the problems that accompanied their construction are described in the following chapter **B.3**.

B.3 SYNTHESIS OF THE SERIES OF TRIADS

The synthesis of the series of triads is an extension to the above-described work on the dyads. The TCNQ acceptor of the dyads is replaced by a naphthoquinone primary acceptor linked *via* a norbornylogous bridge, 6 σ -bonds in length, to the TCNQ secondary electron acceptor. The donor component consist either of one single porphyrin ($x = 0$) or one 'special pair', with two porphyrins kinked ($n, x = 1$) or non-kinked ($n = 0, x = 1$) in respect to each other (**Figure 37**). Each of these three target molecules comes in two stereoisomeric forms: a w-shaped form where the methano bridges of donor component and bridge are *syn* to each other or a y-shaped form where they are *anti*. The mono-porphyrin trichromophores ($x = 0$) are either u-shaped (*anti*) or s-shaped (*syn*).

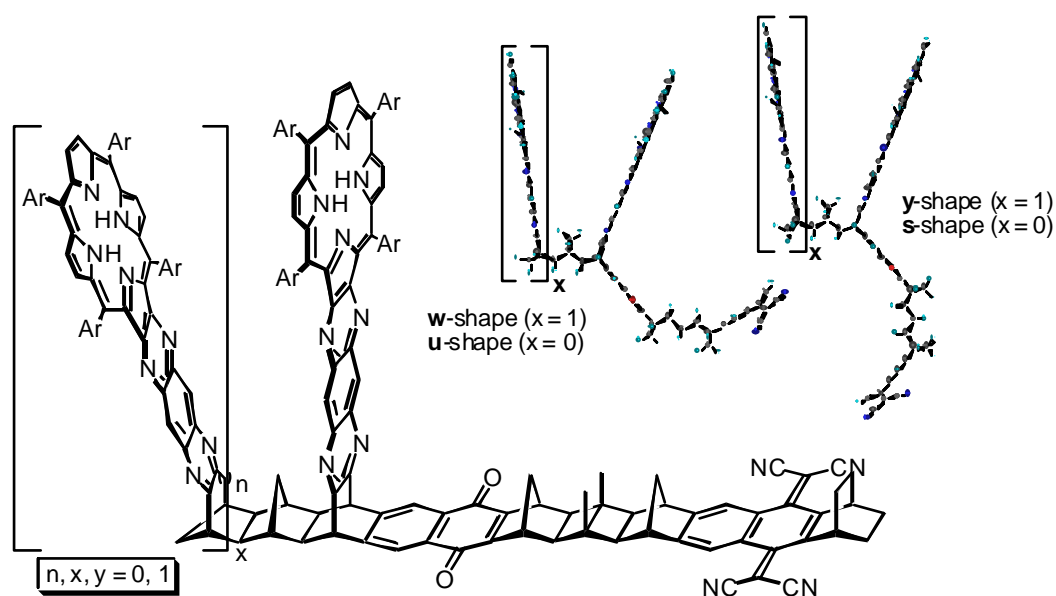


Figure 37: Two-times three targets in the triad synthesis (w/u- and y/s-shaped) and the AM1 calculated structures of *anti* and *syn* bis-porphyrin-NQ-TCNQ

After excitation of the porphyrin chromophore two subsequent electron transfer "hops" are envisaged. The first electron transfer is to occur from the excited porphyrin moiety to the naphthoquinone followed by a second electron transfer process from the naphthoquinone to the strong electron acceptor TCNQ (**Figure 38**).

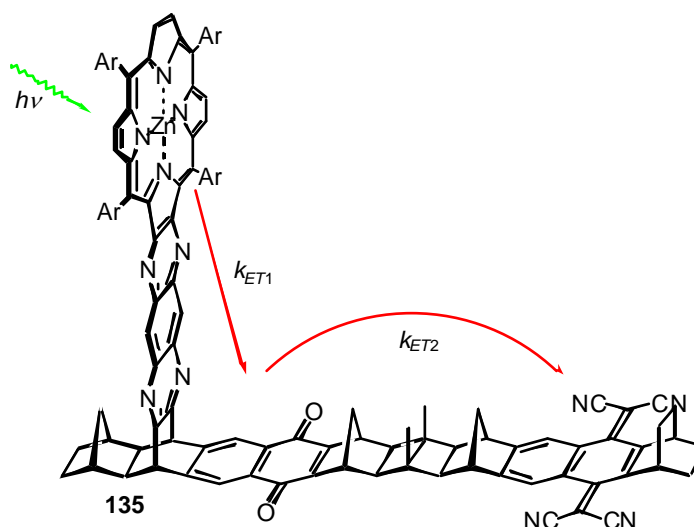


Figure 38: Envisaged sequence of ET processes for the series of triads

Application of the Rehm-Weller equation (**Equation 14**) for polar solvents and large interchromophoric separation allows an estimation of the thermodynamic accessibility of the electron transfer pathways. Insertion of the redox potentials given below (**Figure 39**) into the Rehm-Weller equation gave a driving force (ΔG^0) of roughly -0.4 eV for the first electron transfer and -0.7 eV for the consecutive electron transfer step.

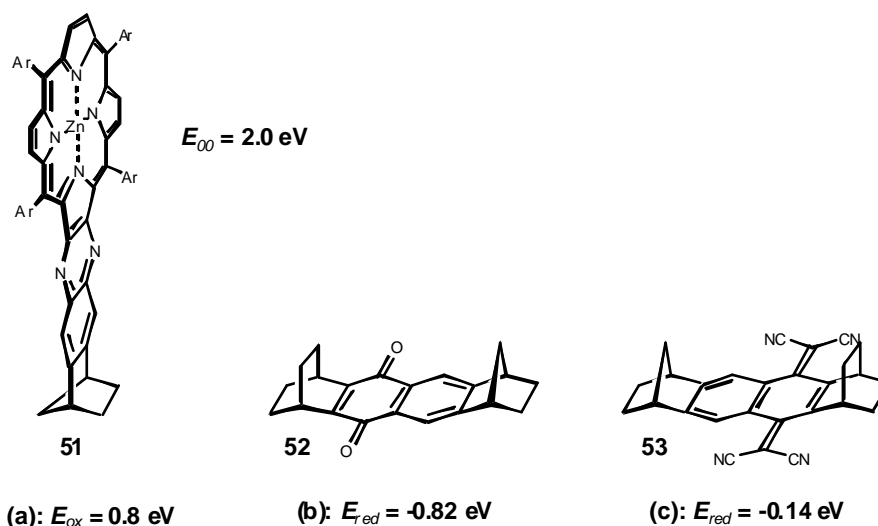


Figure 39: Redox potentials of relevant donor and acceptor chromophores^{113,164,169}

These calculations predict that electron transfer is thermodynamically accessible. The estimated Gibbs free energy of activation (ΔG^* , **Equation 3**, page 7) is small (0.09 eV for ET₁, 0.02 eV for ET₂) that electron transfer should not be inhibited for kinetic reasons.

The synthesis of the triads follows the same methodology as applied in the dyad synthesis. A retrosynthetic approach sees the naphthoquinone unit segmented into an exocyclic 1,3-diene and a benzoquinone. The benzoquinone-bridge-TCNQ segment can be split into a bridge component and the acceptor precursor. The synthesis of these components is described in **B.3.2** (page 116) and **B.3.3** (page 120), respectively. The donor component can be split into porphyrindione, benzenetetramine and a dione or (non-) ring-expanded tetraones (**Figure 40**).

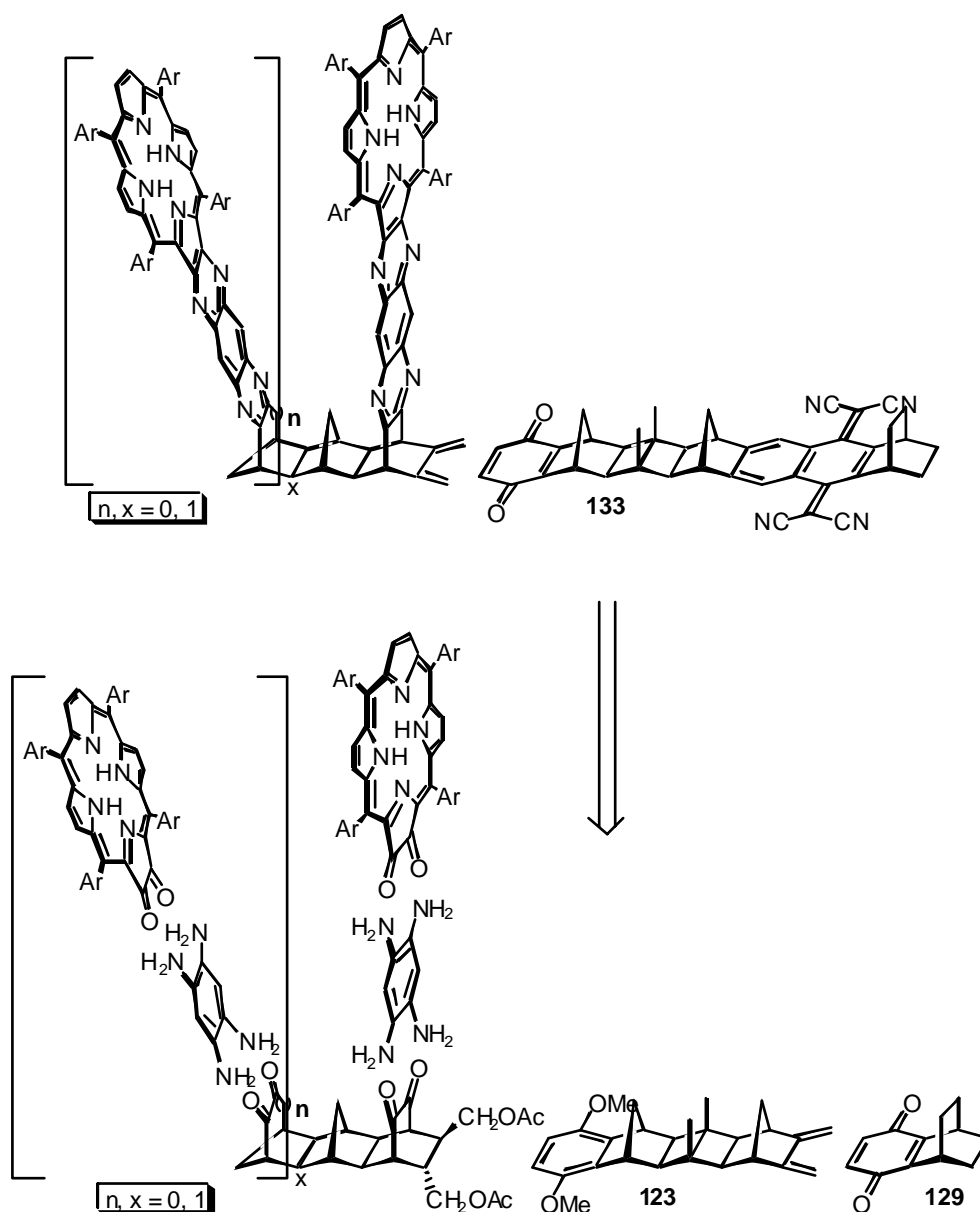
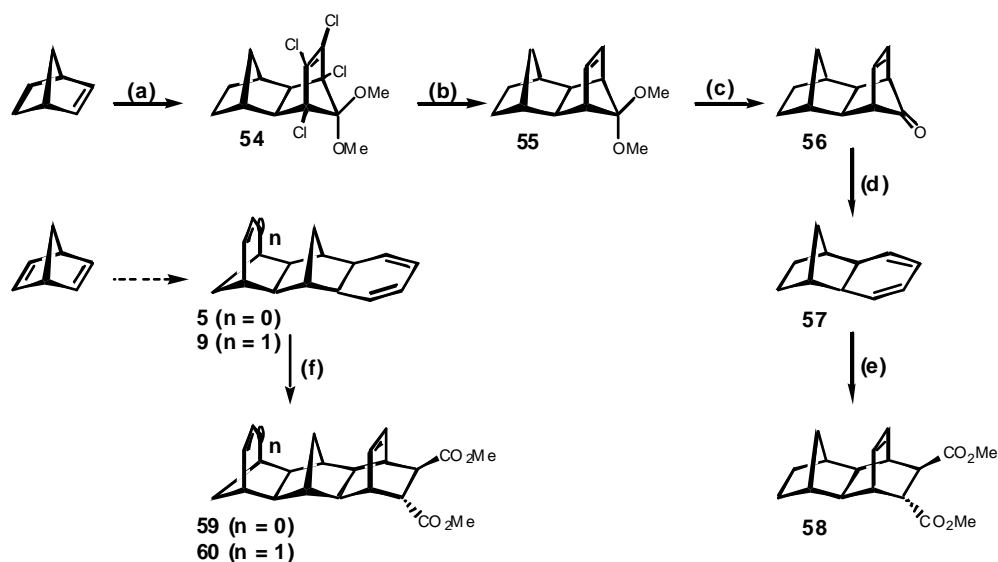


Figure 40: Retrosynthetic approach for the triad synthesis

The synthesis of 'diaminoporphyrin' is described in **B.5** (page 135), benzenetetramine (as its tetrahydrochloric salt) is a commercial product, and the synthesis of the dione and the tetraones is described below (**B.3.1**).

B.3.1 Synthesis of the Donors

The donor component of the triads is based on the same carbon backbone used for the synthesis of the dyads. The synthesis of the mono-porphyrin donor started with norbornene (instead of norbornadiene, **Scheme 21**) then followed well-established methods within our group.^{148,170,171} A Diels-Alder cycloaddition with 1,2,3,4-tetrachloro-5,5-dimethoxycyclopentadiene¹⁴⁹ gave the tetrachloro-adduct **54**^{172,173} in 52 % yield. Reductive dechlorination gave **55**, deketalisation and thermal loss of carbon monoxide yielded the known 1,3-cyclohexadiene derivative **57**¹⁷⁴, which underwent another Diels-Alder reaction with dimethyl fumarate (in contrast to the cycloaddition of 1,4-naphthoquinone in the dyad synthesis) to give **58**.¹⁷⁵ The overall yield of steps **Scheme 21** (b) to (e) was 58 %.



Scheme 21: Synthesis of the triad carbon backbones. (a) 0, toluene, reflux, 40 h, 52 % ; (b) Na, THF / *i*-PrOH, reflux, 16 h; (c) HCOOH, THF, RT, 16 h; (d) toluene, reflux, 2 h; (e) dimethyl fumarate, toluene, reflux, 18 h; (f) dimethyl fumarate, toluene, reflux, 87 h, 82 % ($n = 0$); 18 h, 61 % ($n = 1$)

The Diels-Alder reaction of dimethyl fumarate with the cyclohexadienes **5** and **9** known from the dyad synthesis gave the (non-) ring-expanded *trans*-diesters in 82 % (**59**) and 61 % (**60**), respectively. For the 2B-ene-*trans*-diester **58** and for the non-ring-expanded compound **59** the cyclo-addition resulted in a mixture of two enantiomers. The ring-expanded system **60** yielded the four stereoisomers shown in **Figure 41**.

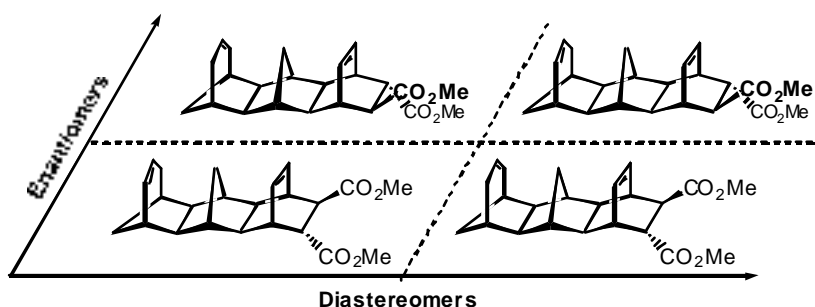
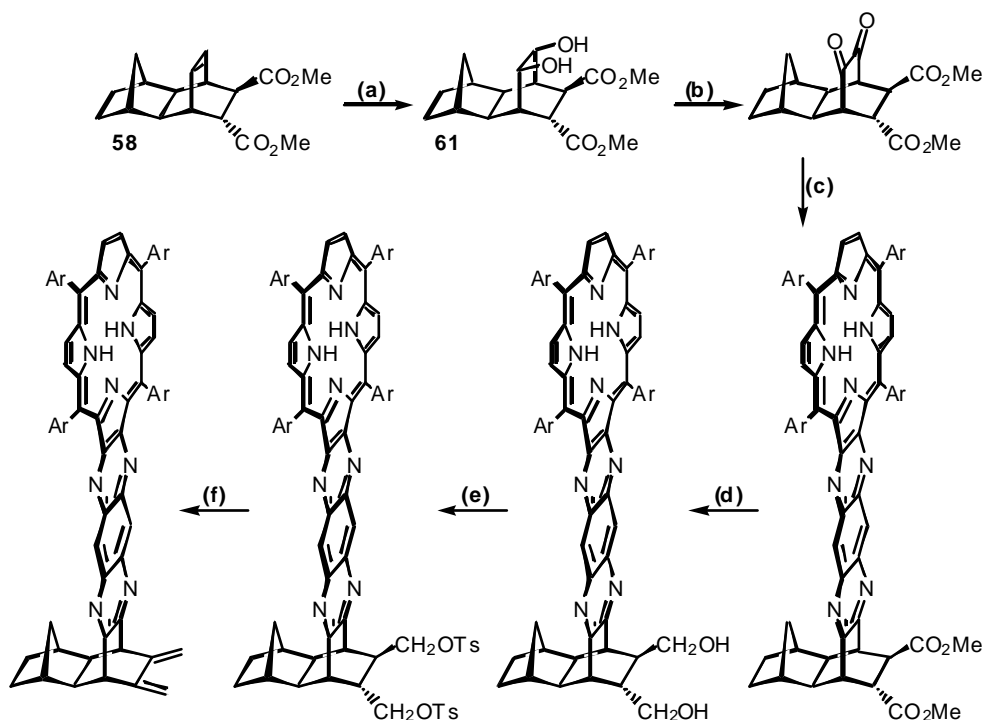


Figure 41: Stereoisomeric forms of the ring-expanded *trans*-diester 60

Whereas enantiomers possess the same spectra, diastereomers do not. ^1H -NMR and ^{13}C -NMR spectra of the diastereomeric mixtures of the ring-expanded series were therefore found to be complex. Signals were assigned with the support of COSY, DEPT90, and DEPT135 experiments.

The proposed pathway for the introduction of a α -diketone, the porphyrin moiety, and an exocyclic 1,3-diene was as outlined in **Scheme 22**, with the conversion of the *trans*-diester into the exocyclic 1,3-diene being a well established procedure within our group.^{148,170}

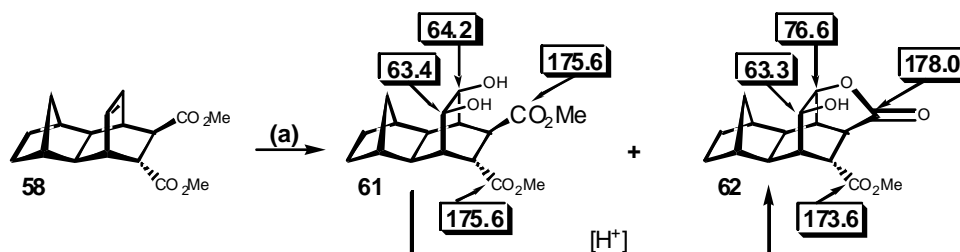


Scheme 22: Proposed synthetic pathway for mono-dione. (a) Sharpless bis-hydroxylation; (b) TEMPO reaction; (c) condensations; (d) reduction; (e) tosylation; (f) dehydrotosylation

The 'dyad methodology': a *Sharpless* bis-hydroxylation (**Scheme 22 (a)**) followed by a TEMPO reaction (**Scheme 22 (b)**) was suggested for the introduction of the α -diketo-functionality. Two subsequent condensations were planned to introduce the porphyrin chromophore (**Scheme 22 (c)**). For the conversion of the *trans*-diester into an exocyclic diene, a reduction to the bis-alcohol (**Scheme 22 (d)**), tosylation (**Scheme 22 (e)**), and dehydrotosylation (**Scheme 22 (f)**) were envisaged. This sequence was to be tested for the 2B-ene-*trans*-diester **58** and then to be applied to the (non-) ring-expanded special pair precursors.

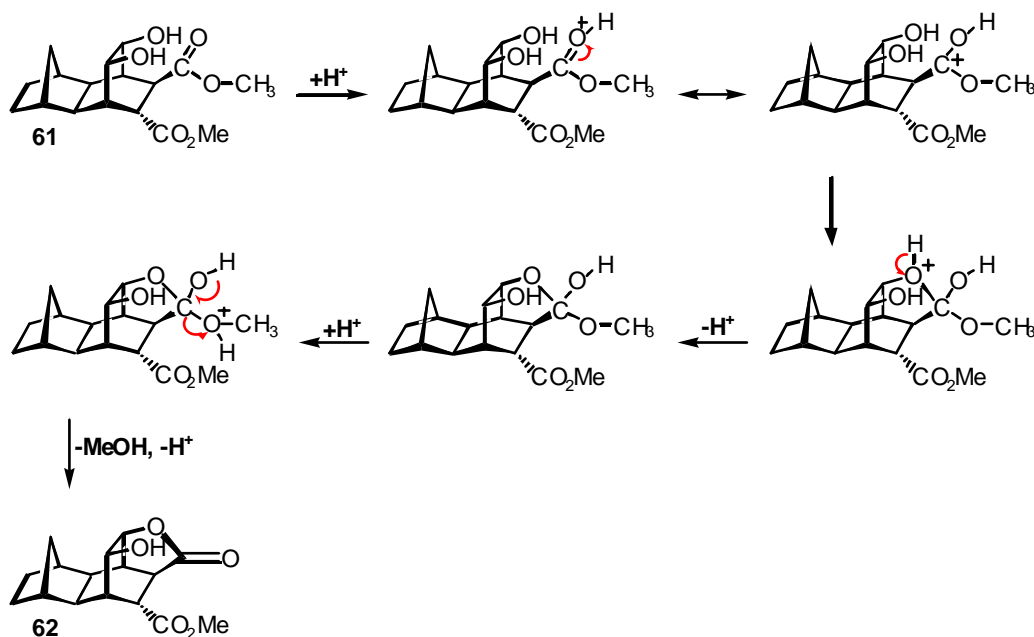
B.3.1.1 *Sharpless* Bis-hydroxylation Reaction

The initial step of the above-outlined reaction sequence (**Scheme 22 (a)**) is an OsO_4 -catalysed *Sharpless* bis-hydroxylation reaction with *N*-methylmorpholine-*N*-oxide (NMO) as the oxidant to recover OsO_4 .¹⁵⁵ Applied to the 2B-ene-*trans*-diester **58** two major products were isolated: the desired 2B-diol-*trans*-diester **61** and the mono-ring-closed lactone **62** with only one hydroxyl and one ester group present (**Scheme 23**).



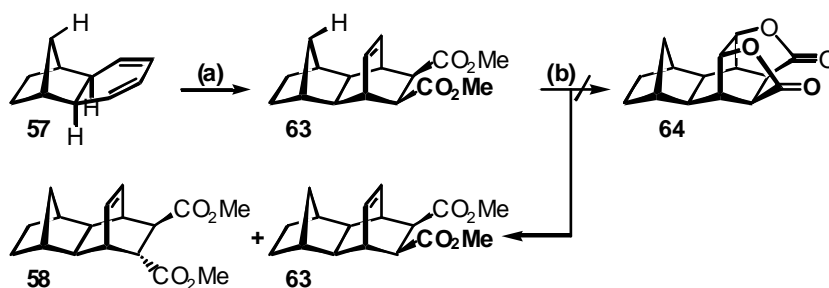
Scheme 23: Products of the *Sharpless* bis-hydroxylation and selected ^{13}C chemical shifts. (a) OsO_4 (2 %), NMO (3 eq.), H_2O , 1,4-dioxane, RT, 16 h, 50 %

The overall yield for both products was about 50 %, with the diol being the major one. The diol, however, easily converted into the lactone when exposed to mild acidic conditions as found in tap water or on silica gel used for chromatography. To confirm the conversion in an acidic medium, D_2O and acidic chloroform- d_1 were added to a NMR sample containing the diol. The ring-closure proceeded immediately and in quantitative yield. The proposed mechanism for the acid-catalysed internal ring closure is shown in (**Scheme 24**).



Scheme 24: Proposed mechanism of the acid-catalysed lactone formation

Spurred by curiosity, a double ring-closure was attempted for the 2B-ene-*cis*-diester **63** under Sharpless bis-hydroxylation conditions. The *endo-cis*-diester was accessible *via* Diels-Alder reaction between **57** and dimethyl maleate (**Scheme 25 (a)**). The methylene proton facing the new etheno bridge ($\delta = 2.13$ ppm) confirmed the *endo* attack. The subsequent OsO_4 conditions, however, did not result in the formation of the dicarbollactone **64**. Instead a mixture of starting material and the *trans*-diester **58** was found when reacted at 80 °C (**Scheme 25 (b)**).



Scheme 25: Attempted synthesis of a double lactone. (a) Dimethyl maleate, toluene, reflux, 4 d, 41 % ; (b) OsO_4 , NMO, 1,4-dioxane, 80 °C, 10 d

Possibly steric hindrance is responsible for the reaction not proceeding in the desired way. On one side the double bond is protected by a methano bridge and the two ester groups *syn* to the double bond seem to protect it from the other side and thereby preventing the formation of the

osmate ester and the subsequent hydrolysis to the diol. **Figure 42** shows the different accessibilities of the double bond in the *trans*- and *cis*-diester.

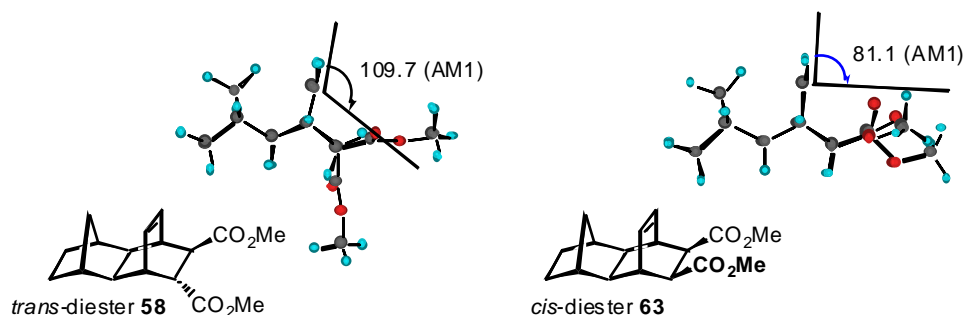


Figure 42: AM1-optimised structures for the 2B-ene-*trans*-diester **58 and 2B-ene-*cis*-diester **63****

Higher temperature (80 °C) did not change the accessibility of the double bond, but led to an epimerisation of the carbon centres bonded to the ester groups. Such an isomerisation had been observed before¹⁷⁶ and proceeded most likely *via* deprotonation and re-protonation at the carbon atom next to the ester group. The *cis*- to *trans*-diester ratio determined by ^1H -NMR spectroscopy was found to be 2:3 after chromatography. The ^1H -NMR spectrum is given below (**Figure 43**) and compares well with the spectra for the 2B-ene-*cis*-diester **63** and the 2B-ene-*trans*-diester **58**.

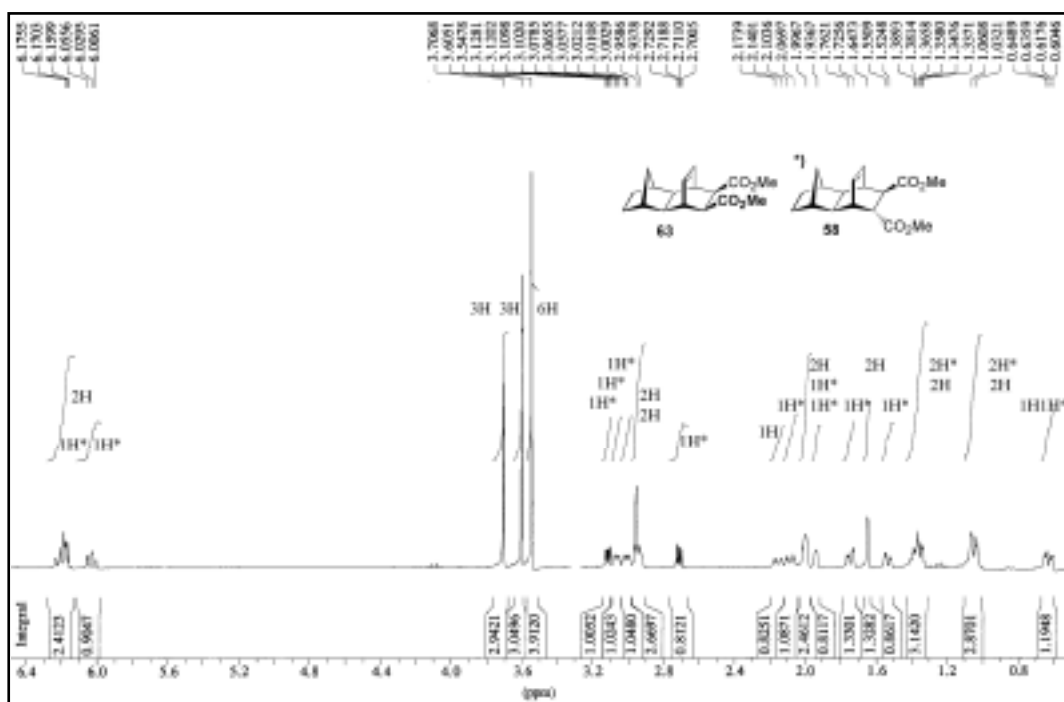
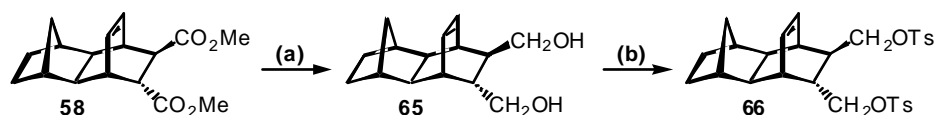


Figure 43: ^1H -NMR spectrum (300 MHz) of a mixture (2:3) of 2B-ene-*cis*-diester **63** and 2B-ene-*trans*-diester **58** as found after attempted OsO_4 -reaction at 80 °C

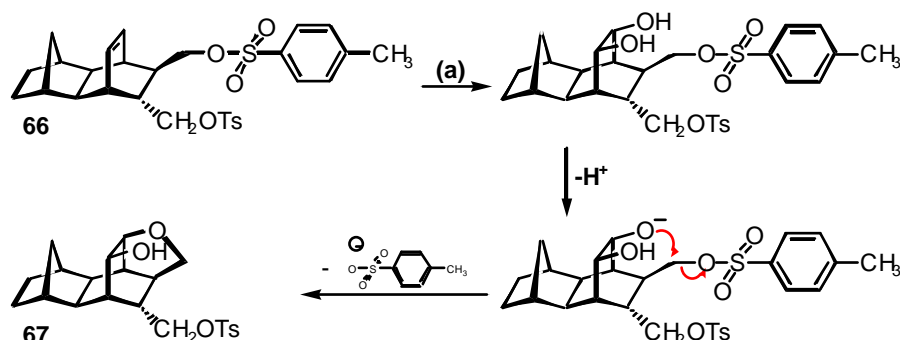
One possibility to overcome (and avoid rather than reverse) the unwanted acid-catalysed lactonisation is to use functional groups that are stable to acids and do not undergo this type of internal transesterification. As the ester groups were to be converted into tosylates at a later stage of the reaction sequence (**Scheme 22 (d)**, page 81), the 2B-ene-*trans*-ditosylate **66** was exposed to *Sharpless* bis-hydroxylation conditions next. The conversion of esters into tosylates followed standard procedures as outlined in **Scheme 26**.¹⁷⁷



Scheme 26: Conversion of ester groups into tosylates. (a) LiAlH_4 , THF, reflux, 20 h, 99 % ; (b) TsCl , pyridine, -23 °C, 8 d, 94 %

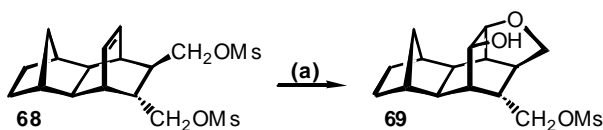
The OsO_4 reaction, however, gave exclusively the ring-closed product **67**. Under the basic reaction conditions the formed diol was possibly deprotonated and with one positive polarised carbon atom within its reach, the alkoxy group underwent an intramolecular nucleophilic

attack to form the cyclic ether **67**. The tosyl-group acted as a leaving group in this process (**Scheme 27**).



Scheme 27: Proposed mechanism of the base-catalysed cyclic ether formation. (a) OsO_4 (2 %), NMO (3 eq.), 1,4-dioxane, RT, 23 h, 71 %

The same result was found when the tosyl groups were replaced by mesyl groups as shown in **Scheme 28**.



Scheme 28: Cyclic ether formation with a mesyl functionality acting as leaving group. (a) OsO_4 (2 %), NMO (3 eq.), 1,4-dioxane, RT, 23 h, 77 %

From the mono-ring-closed product **69** an x-ray structure was obtained (**Figure 44**), which suggests intramolecular hydrogen bonding between the vicinal hydroxy group and the ether oxygen. Its crystallographic data can be found in **E 'Appendix'**, page 268.

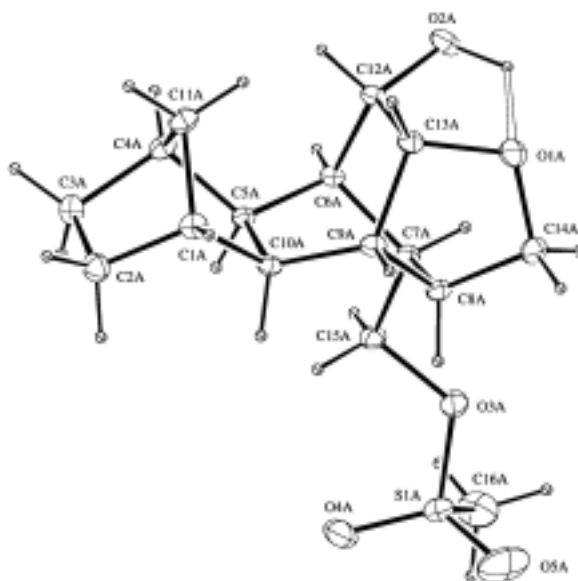
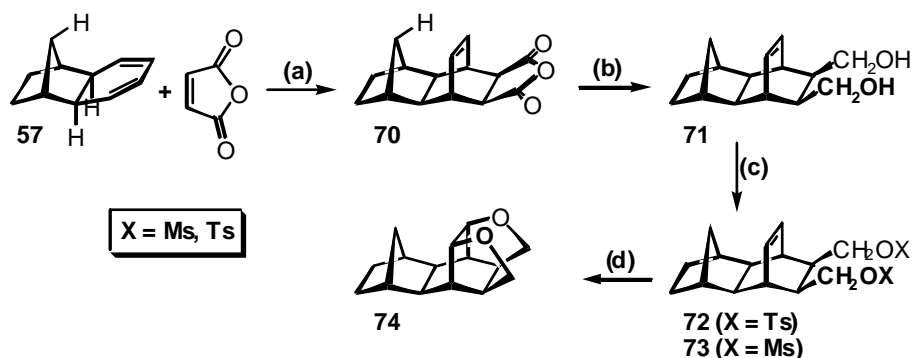


Figure 44: X-ray structure of mono-ring-closed mesyl derivative 69

A double ring-closure was achieved when the 2B-ene-*cis*-ditosylate **72** and the 2B-ene-*cis*-dimesylate **73** were exposed to the OsO₄-conditions. The *cis*-derivatives were accessible *via* the *cis*-diol **71**, which was derived from the cyclic anhydride **70** by reduction with LiAlH₄ (Scheme 29).



Scheme 29: (a) Toluene, reflux, 15 h, 53 % ; (b) LiAlH₄, THF, RT, 3 h, 94 % ;
 (c) TsCl (X = Ts) or MsCl (X = Ms), pyridine, -18 °C, 6 d, 85 % (X = Ts) or
 67 % (X = Ms); (d) OsO₄, NMO, RT, 6 d, 21 % (X = Ts) or 24 % (X = Ms)

The Diels-Alder cycloaddition between **57** and maleic anhydride gave the *endo*-product **70**, evident in the chemical shift (2.00 ppm) of the methylene proton facing the etheno bridge (Scheme 29 (a)). Tosylation and mesylation of the 2B-ene-*cis*-diol **71** gave good yields (Scheme 29 (c)) and the low yields given for the final OsO₄-reaction (Scheme 29 (d)) are not

corrected on recovered starting material (37 - 50 %). Relevant ^{13}C -NMR data for the mono and double ring-closed products are given in **Figure 45**.

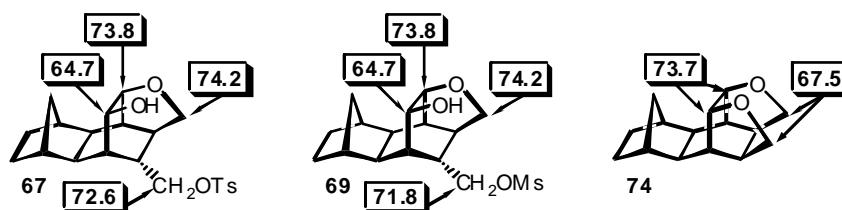
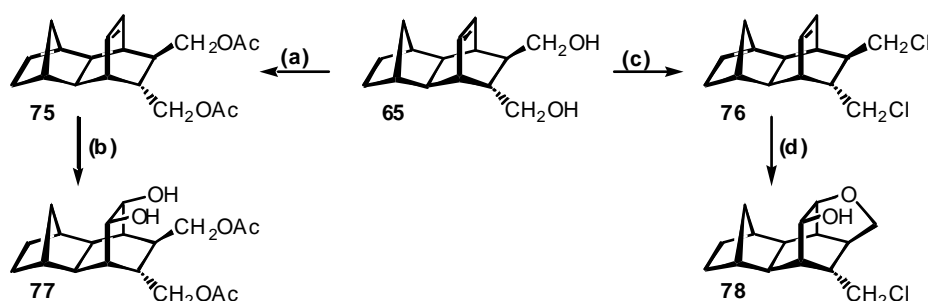


Figure 45: Carbon chemical shifts for the mono and double cyclic ethers

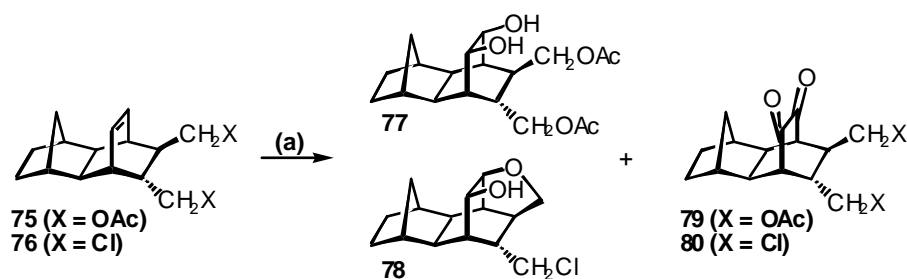
Both tosylates and mesylates are such good leaving groups that unwanted ring-closure follows the OsO_4 reaction in the basic medium. Employing weaker leaving groups would result in two extra steps in the synthesis, but was most likely the easiest way to overcome the ring-closure problems. Two functionalities chosen were the chloro and acetoxy groups.

Reaction of the 2B-ene-*trans*-diol **65** with acetic anhydride (**Scheme 30 (a)**) gave the diacetoxy system **75** in 75 % yield; reaction with freshly distilled thionyl chloride (**Scheme 30 (c)**) yielded the 2B-ene-*trans*-bis(chloromethyl) compound **76** in 50 %.



Scheme 30: (a) Acetic anhydride, pyridine, RT, 18 h, 75 % ; (b) OsO_4 , NMO, 1,4-dioxane, RT, 3 d, 45 % (c) thionyl chloride, pyridine, 70 °C, 2 h, 50 % ; (d) OsO_4 , NMO, 1,4-dioxane, RT, 3 d, 57 %

The subsequent OsO_4 reactions carried out on these compounds gave the desired 2B-diol-*trans*-diacetate **77** in 45 % (**Scheme 30 (b)**) and the less-desirable ring-closed product **78** in 57 % yield (**Scheme 30 (d)**). One thing both reactions had in common was the formation of a substantial amount of a bright yellow side product. These side products were identified as the related diones and were obtained in 28 % (**79**, X = OAc) and 12 % (**80**, X = Cl) yield, respectively (**Scheme 31**).



Scheme 31: Formation of diones **79 and **80** under *Sharpless* bis-hydroxylation conditions**

The strongest evidence for the dione formation was the presence of carbonyl signals and the absence of CHOH signals in the ^{13}C -NMR spectra of **79** and **80**. The ^1H -NMR spectra showed 18 (**80**) and 24 (**79**) protons only. Characteristic chemical shifts are given in **Figure 46**.

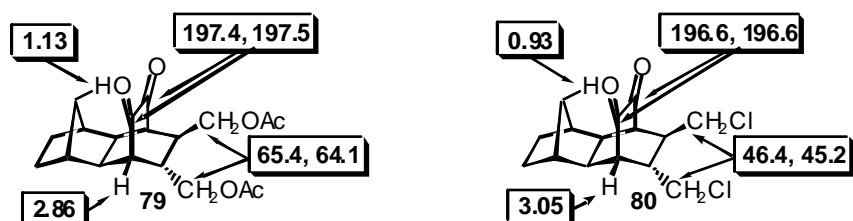


Figure 46: Selected ^1H -NMR and ^{13}C -NMR chemical shifts of the 2B-diones **79 and **80** formed under *Sharpless* bis-hydroxylation conditions**

Beside the characterisation by NMR spectroscopy and mass spectrometry an x-ray structure was obtained for the 2B-dione-*trans*-diacetate **79**. It is shown in **Figure 47** and parameters are given in **E 'Appendix'**, page 260.

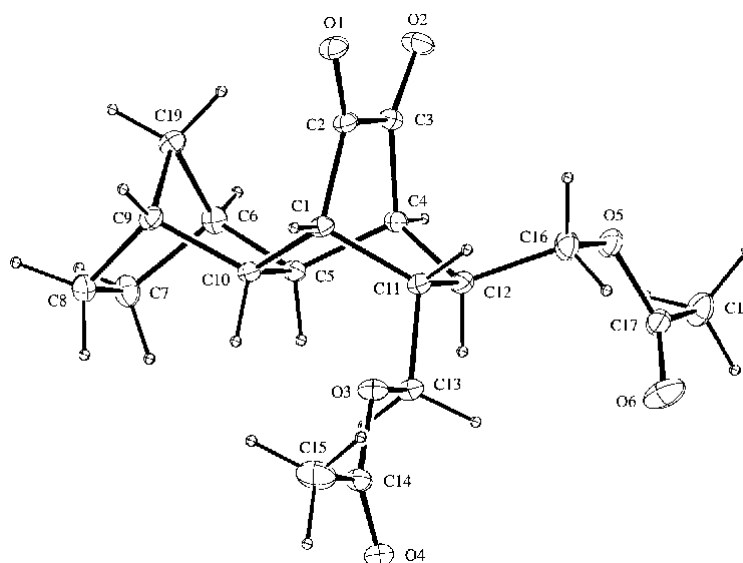


Figure 47: X-ray structure for the 2B-dione-*trans*-diacetate 79

The one-step oxidation from olefins to diones was observed when stoichiometric amounts of OsO_4 and hydrogen peroxide as oxidant were used.^{178,179} Under *Sharpless* bis-hydroxylation conditions the one-step 'bis-ketonisation' appears not to have a literature precedent. However, there are examples of ketol formation under similar conditions,^{180,181} and yellow 'impurities' have been observed before.¹⁸² Nevertheless, the yields observed in this work go far beyond those normally attributed to 'impurities' and a further investigation was warranted.

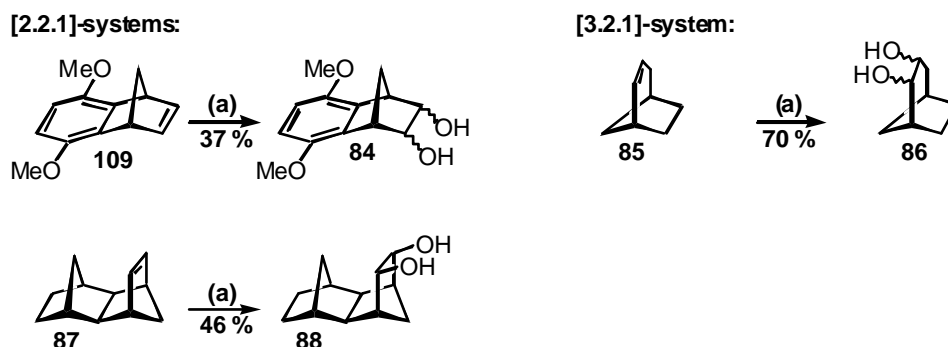
B.3.1.2 Modified *Sharpless* Bis-hydroxylation

One reason for the investigation of the one-step oxidation of olefins to diones under *Sharpless* bis-hydroxylation conditions (apart from scientific interest) was the possible avoidance of expected solubility problems with the formation of the ring-expanded and non-ring-expanded tetraols. In addition to that, one synthetic step could be saved, if conditions were possibly altered in a way that the dione/tetraones become the major products. In order to achieve this goal a variety of reaction conditions were tested for the 'bis-ketonisation' of the 2B-ene-*trans*-diacetate **75**. A minimum amount of 1,4-dioxane, 2 % OsO_4 , about 6 eq. of *N*-methylmorpholine-*N*-oxide and no water additional to that contained in 1,4-dioxane increased the yield of 2B-dione-*trans*-diacetate **79** to 79 % after three days, with only 8 % of the corresponding diol **77** found. Application of these optimised conditions to other systems gave similar results (**Table 9**):

Table 9: OsO₄-reaction under optimised 'bis-ketonisation' conditions

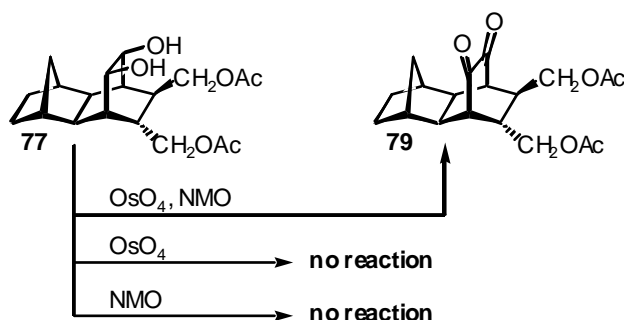
Olefin	Lactone	Furan	Diol	Dione
58 (X = CO ₂ Me)	50 % (62)			
76 (X = CH ₂ Cl)		57 % (78)		12 % (80)
75 (X = CH ₂ OAc)			8 % (77)	79 % (79)
81 X = H			12 % (82)	52 % (83)

The results shown in **Table 9** indicate that the one-step conversion of olefins to diketones under modified *Sharpless* bis-hydroxylation conditions could be common to [2.2.2]-ring systems of the above type. To investigate its application to other systems, such as [2.2.1]- and [3.2.1]-ring systems (as they are part of the (non-) ring-expanded special pair precursors), a few model systems were tested (**Scheme 32**). However, none of the tested models showed any evidence for the formation of a keto-functionality but gave the according *cis*-diols **84**, **86**, **88** only.



Scheme 32: Application of the optimised 'bis-ketonisation' conditions to [2.2.1] and [3.2.1] ring systems. (a) OsO₄ (2 %), NMO (6 eq.), 1,4-dioxane (minimum amount), RT, 3d

To evaluate the role of the catalyst and the oxidant *N*-methylmorpholine-*N*-oxide a simple experiment was carried out. The 2B-diol-*trans*-diacetate **77** was exposed to the optimised 'bis-ketonisation' conditions, but in which either *N*-methylmorpholine-*N*-oxide or OsO₄ was omitted from the reaction mixture (**Scheme 33**). In both experiments no conversion to the dione occurred. Only upon addition of the missing ingredient, oxidation proceeded.



Scheme 33: What is the oxidising species in the 'bis-ketonisation'?

From these experiments *N*-methylmorpholine-*N*-oxide can be excluded as the single oxidising species, which is hardly surprising. More importantly, it is necessary to have the *N*-methylmorpholine-*N*-oxide present. A complex formed between OsO_4 , the diol and possibly NMO must facilitate the oxidation. Such a complex could also explain the 'discriminating' behaviour. Different ring systems ([2.2.1], [2.2.2], [3.2.1]) would result in slightly different geometries of the intermediate osmate ester, which then could possibly promote or not promote the oxidation to the diones.

The observed differentiation between [2.2.2] systems on one side and the [3.2.1] and [2.2.1] systems on the other could lead to a selective 'bis-ketonisation' in the synthesis of the (non-) ring-expanded 'special pair' donors. The non-ring-expanded system contains one '[2.2.1] double bond' and one '[2.2.2] double bond', which could be oxidised in one step to the '[2.2.1] diol' and '[2.2.2] dione', respectively, under 'bis-ketonisation' conditions. The same discrimination would apply to the ring-expanded donor precursor. In principle this enables the controlled attachment of one (metallated) porphyrin, before the other diol is oxidised to a dione and a different porphyrin could be attached (**Figure 48**).

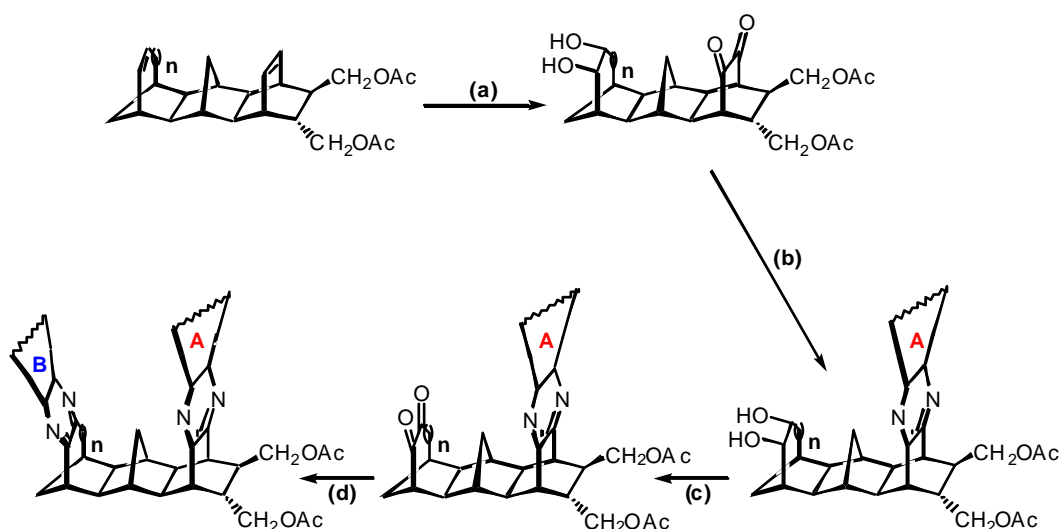
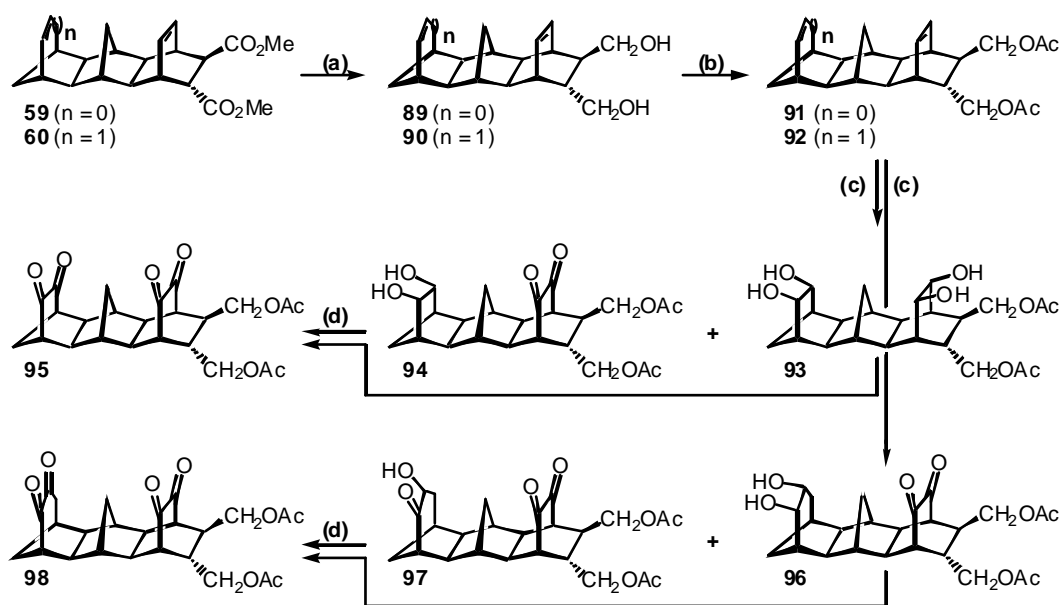


Figure 48: Controlled attachment of two different porphyrin moieties (A and B) through (a) selective 'bis-ketonisation' followed by (b) condensation, (c) TEMPO reaction, and (d) condensation of second porphyrin

The controlled attachment of different porphyrins would open doors to the study of energy transfer processes between porphyrins in addition to the electron transfer processes aimed at between the 'special pair' and NQ or TCNQ, respectively. This idea had been mentioned before (**B.2.4**, page 69), but the concept behind the attachment of two different porphyrins is not the same, as the 'discriminating bis-ketonisation' hadn't been discovered during the dyad synthesis.

B.3.1.3 Synthesis of the Tetraones

The synthetic strategy for the above-mentioned 2B-dione-*trans*-diacetate **79** was applied to the synthesis of the ring-expanded and non-ring-expanded tetraones. The synthesis of the backbone, including the Diels-Alder reaction with dimethyl fumarate (**Scheme 21**, page 80), followed the reaction sequence outlined in **Scheme 34**.



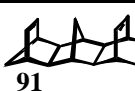

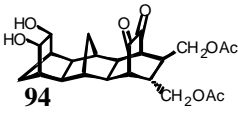
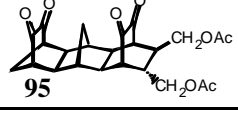
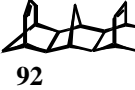
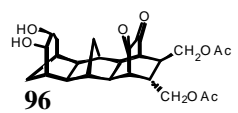
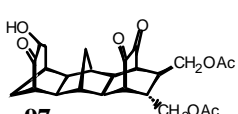
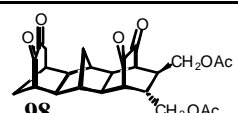
Scheme 34: Synthesis of tetraones (a) LiAlH_4 , THF, reflux, 20 / 24 h, 84 % ($n = 0$) / 99 % ($n = 1$); (b) acetic anhydride, RT, 23 / 17 h, 93 % ($n = 0$) / 89 % ($n = 1$); (c) OsO_4 , NMO, RT, 18 h - 6 d ($n = 0$) / 50 d ($n = 1$); (d) TEMPO reagent, *p*-toluenesulfonic acid, DCM, RT, 4 d, 74 % ($n = 0$) / 57 % ($n = 1$)

The ratio of the two products isolated from the OsO_4 -reaction (**Scheme 34 (c)**) can be varied by altering the amount of *N*-methylmorpholine-*N*-oxide as well as by permitting more or less time for the reaction to proceed. A "short" reaction time of 18 hours yielded the tetraol **93** in 32 % and the 6B-diol-2B-dione-*trans*-diacetate **94** in 26 %. A prolonged reaction time of 6 days resulted in the exclusive formation of the 6B-diol-2B-dione-*trans*-diacetate **94** in 59 % yield.

As solubility problems of the tetraol were observed, the reaction time for the ring-expanded system **92** was extended dramatically, which resulted in the formation of the kinked 6B-diol-2B-dione-*trans*-diacetate **96** and the further oxidised kinked 6B-ketol-2B-dione **97** in 20 % and 18 %, respectively. This result contradicted that obtained earlier for the OsO_4 -reaction with a [3.2.1]-model ring system (**B.3.1.2**) but is in accordance with the observations made during the synthesis of the ring-expanded dyads. Both compounds, the kinked 6B-diol-2B-dione-*trans*-diacetate **96** as well as the corresponding 6B-ketol-2B-dione-system **97** were converted into the sought after ring-expanded tetraone **98** under TEMPO conditions (**Scheme 34 (d)**).

A few characteristic ^{13}C -NMR chemical shifts are given in **Table 10**. The diastereomeric ring-expanded systems were not separated and therefore resulted in fairly complex NMR spectra throughout the synthesis of the tetraones (and beyond).

Table 10: ^{13}C -NMR shifts for OsO_4 and TEMPO reaction products in ppm relative to TMS

Compound	$6\text{B}_{\text{C}=\text{C}}$	$6\text{B}_{\text{C}-\text{OH}}$	$6\text{B}_{\text{C}=\text{O}}$	$2\text{B}_{\text{C}=\text{C}}$	$2\text{B}_{\text{C}-\text{OH}}$	$2\text{B}_{\text{C}=\text{O}}$
 91	135.4 135.5			135.2 131.6		
 93		69.5 69.5			64.4 63.3	
 94		70.0 70.0				197.1 196.9
 95			202.2 202.2			196.2 196.1
 92	133.1 128.4			131.2 131.6 134.9 135.1		
 96		58.4 68.1				196.7 196.9
 97		70.0	212.46 212.50			196.6 196.7 196.8 197.0
 98			196.7 203.3			196.3 196.1

The NMR data are consistent with the previously obtained NMR spectra of the series of dyads (**B.2.2**, page 53). Characteristic for the successful oxidation of the secondary alcohol groups to ketones is the downfield shift of the relevant bridgehead protons. In the case of the tetraone **95** their corresponding signals were found at 3.12 ppm ([2.2.1]) and 2.89 ppm ([2.2.2]),

respectively. The ^1H -NMR and ^{13}C -NMR spectra of the 6B-dione-2B-dione-*trans*-diacetate **95** are depicted in **Figure 49** and **Figure 50**, respectively.

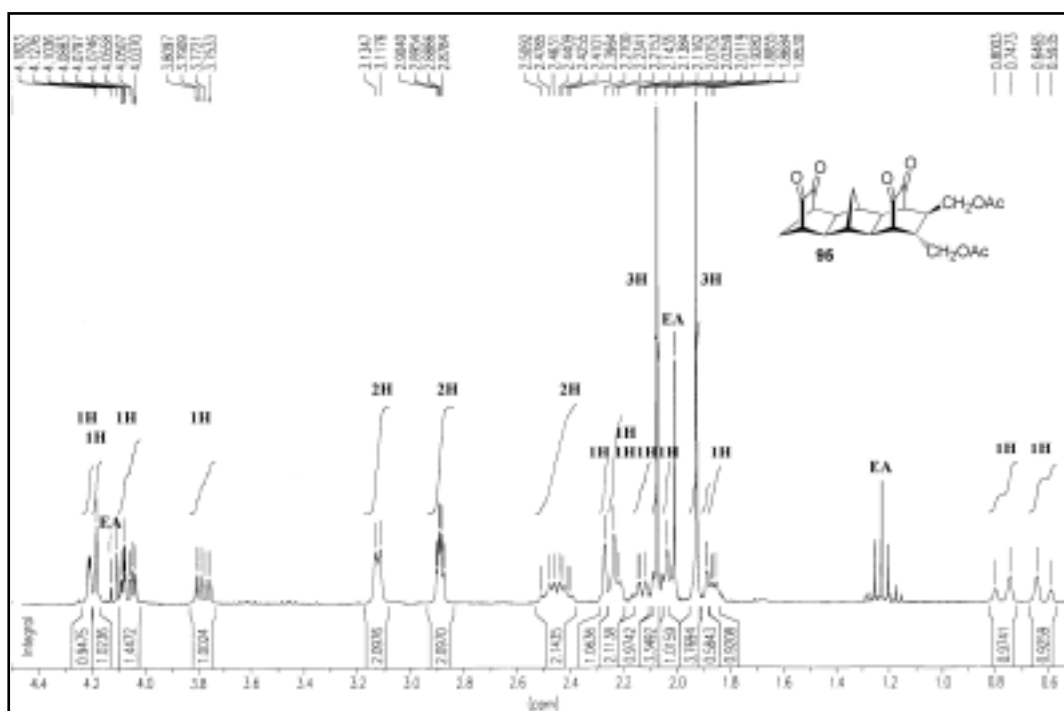


Figure 49: ^1H -NMR spectrum (300 MHz) of **95**

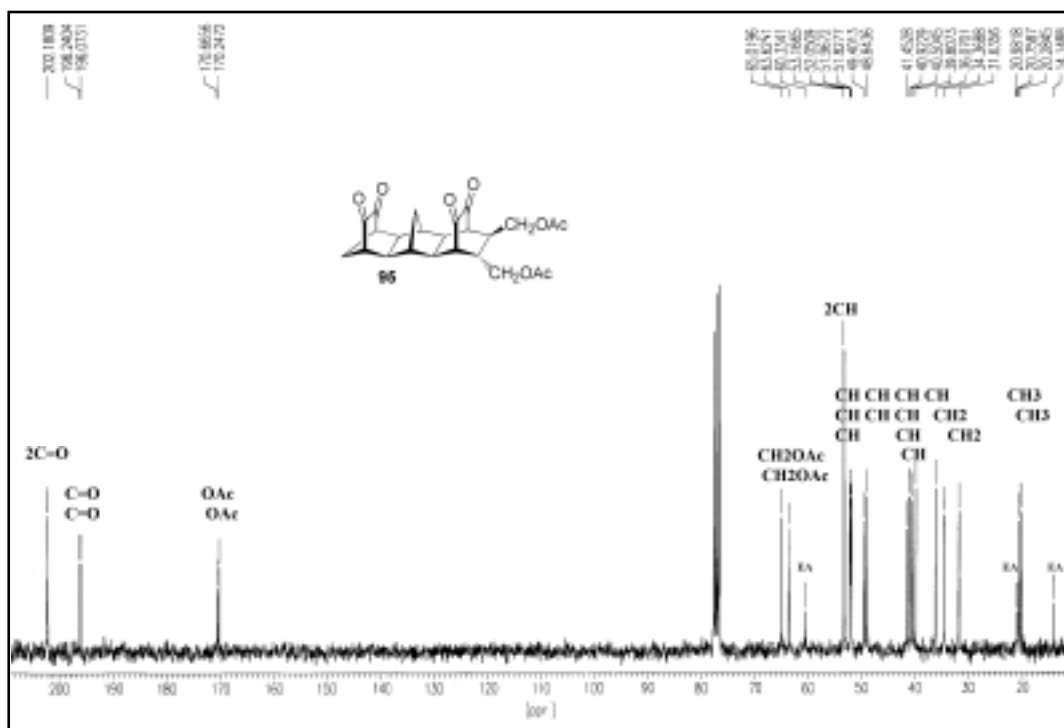


Figure 50: ^{13}C -NMR spectrum (75.5 MHz) of 6B-dione-2B-dione-*trans*-diacetate **95**

B.3.1.4 Condensations

After the synthesis of the dione **79** and the tetraones **95** and **98** had been achieved, the supposedly straightforward condensations with 'diaminoporphyrin' were amongst the penultimate steps towards the synthesis of the triad donors. It turned out, however, that very harsh conditions are required to make the condensations work.

Initial attempts to react the 2B-dione-*trans*-diacetate **79** with 'diaminoporphyrin' at atmospheric pressure failed completely over a range of temperatures (25 - 115 °C), reaction times (1 - 28 d), concentrations and solvents. Steric hindrance is responsible for this stubborn lack of reactivity. The bulky acetoxy group in the *exo* position reduced the accessibility of the carbonyl group in comparison with the dyad systems synthesised previously (**Figure 51**).

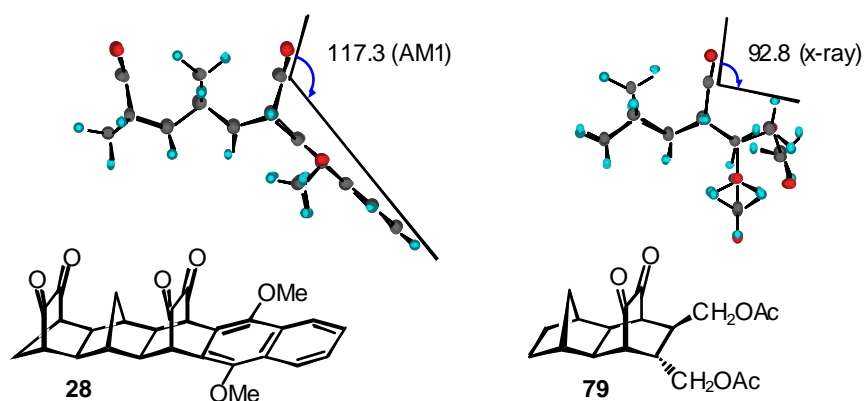
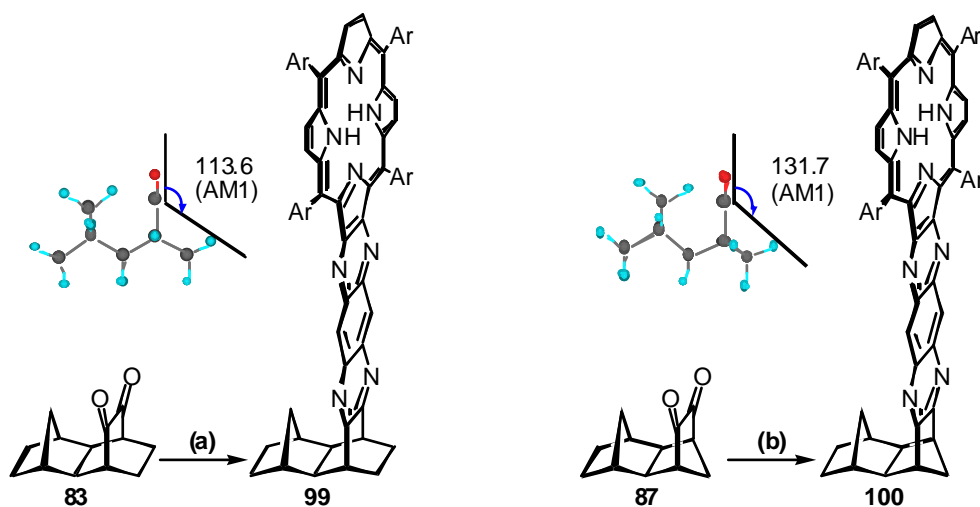


Figure 51: Comparison of carbonyl group accessibility in dyad **28 (left) and triad donor systems **79** (right)**

The oxygen-carbon-hydrogen angle for the tetraone was calculated to be 117.3° (AM1 optimised). X-Ray analysis of the dione-*trans*-diacetate **79** gave an oxygen-carbon-hydrogen angle of 92.8° for the acetate *syn* to the carbonyl group and 116.1° for the acetate *anti* to the carbonyl group. As the nucleophilic attack of the amine on the carbonyl group can occur from this side only (the other side is obstructed by the methano bridge), the different accessibilities are a reasonable explanation for the unsuccessful condensation under 'normal' conditions. This point of view was supported by the successful condensation of 'neighbour group-free' model diones and 'diaminoporphyrin' under comparably mild conditions (**Scheme 35**).



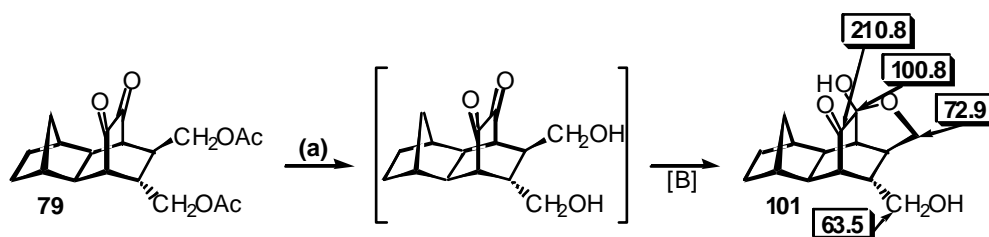
Scheme 35: 'Neighbour group-free' condensation reactions. (a)

'diaminoporphyrin', pyridine, 110 °C, pressure tube, 11 d, 42 % ; (b)

'diaminoporphyrin', pyridine, 125 °C, pressure tube, 12 d, 10 %

AM1 calculations give O, C, H - angles of 113.6 ° for the [2.2.2]-dione **83** and 131.7 ° for the [2.2.1]-dione **87**, a compound which was kindly provided by Nigel Lokan. Despite the better accessibility of the carbonyl groups in **87**, the yield was found to be lower than for the dione **83**. Not surprisingly though, as similar differences in yields were observed for the condensations of 'diaminoporphyrin' with the 2B-dione-DMN **26** (a [2.2.2]-system) and the 6B-dione-DMN **23** (a [2.2.1]-system), as well as the according tetraone **28** (**B.2.3**, page 60). Such differences were attributed to the slightly different geometries of [2.2.2] and [2.2.1] systems. [2.2.2] systems were found to be more suitable for the condensation with 'diaminoporphyrin' than [2.2.1]-systems. At least as long as the accessibility of the dione wasn't significantly limited by bulky neighbour groups like the ones faced in this triad donor synthesis.

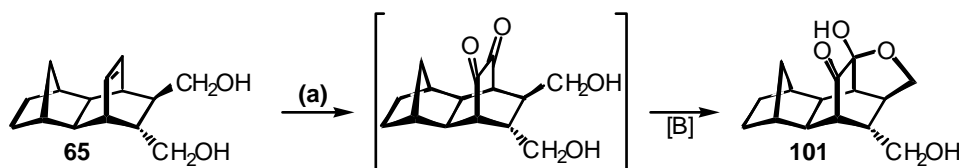
A little less spacious than an acetoxy group would be a hydroxy group. Mild conditions (K_2CO_3 , MeOH, H_2O) converted the acetoxy functionality back into the alcohols but once formed, the hydroxy group *syn* to the ketone underwent an intramolecular nucleophilic attack on the carbonyl carbon to give the hemi-acetal **101** in the basic reaction medium (**Scheme 36**). Carbon NMR-spectroscopy proved to be very useful for the characterisation of the product.



Scheme 36: Mild transesterification and subsequent hemi-acetal formation.

(a) K_2CO_3 , MeOH, H_2O , 18 h, RT, 32 %

The same product was found previously in an attempt to streamline the overall synthesis of the donor component. After the discovery of the 'bis-ketonisation' the one-step oxidation of the 2B-ene-*trans*-diol **65** to the according dione was attempted (**Scheme 37**). If successful, the two step acetoxy detour could have been avoided, but, as mentioned before, the hemi-acetal **101** was formed under the basic modified *Sharpless* 'bis-ketonisation' reaction conditions as well.

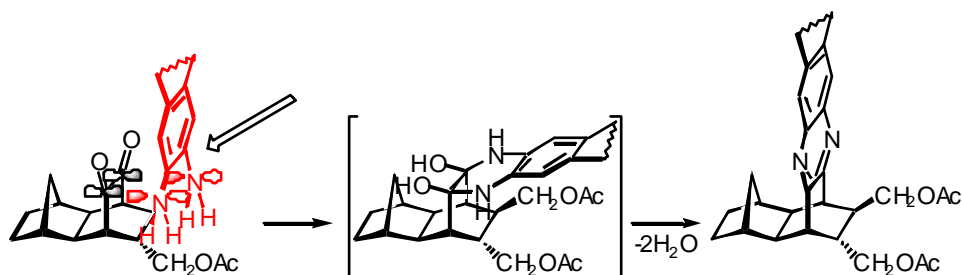


Scheme 37: 'Bis-ketonisation' and subsequent hemi-acetal formation. (a)

OsO_4 (2 %), NMO (5 eq.), 1,4-dioxane, RT, 5d, 55 %

An acidic environment should ring open the hemi-acetal, but the basic reaction conditions of the following condensation reaction would reverse this process. Therefore focus moved back to the search for reaction conditions that would allow a successful condensation despite the bulky acetoxy groups in close proximity to the reacting carbonyl group.

The application of high pressure was the next approach taken. The initial step of the condensation is the formation of one tetrahedral adduct between dione and diamine, subsequently followed by the loss of two water molecules (**Scheme 38**).



Scheme 38: Formation of the initial tetrahedral adduct and subsequent loss of two water molecules

The formation of the tetrahedral adduct is most likely the rate determining step. As the molar volume of this tetrahedral adduct is smaller than the sum of the partial molar volumes of the two reactants, the activation volume ΔV^* becomes negative according to **Equation 16**.

$$\Delta V^* = V^* - \Sigma V$$

Equation 16: ΔV^* : activation volume; V^* : molar volume of transition state;
 ΣV : sum of partial molar volumes of reactants

If the activation volume ΔV^* of a liquid phase reaction is negative, the application of pressure is expected to accelerate (or enable) this reaction. The effect of pressure on the rate constant of a liquid phase reaction (k) is defined by the **Equation 17**.

$$\Delta V^* = -RT \, d(\ln k) / dp$$

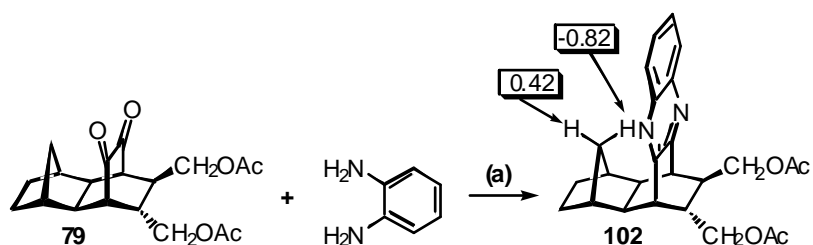
Equation 17: Reaction volume - pressure - rate constant

The required high-pressure equipment was made available by Prof. David Young and operated by Annette Neuendorf at Griffith University, Queensland. His group's machine features a maximum working volume of 77 mL, pressures up to 20 kbar, and temperatures up to 150 °C (**Figure 52**).



Figure 52: High pressure apparatus at Griffith University, Queensland

Amongst the first model reactions carried out was the condensation of the 2B-dione-*trans*-diacetate **79** and phenylenediamine in pyridine at 40 °C and 15 kbar. This reaction was previously attempted twice for a period of 6 days at atmospheric pressure in refluxing ethanol and pyridine. Both reactions gave mostly starting material and only a small amount of the desired adduct. At high pressure, however, the desired product **102** was obtained in high yields after three days in a pyridine solution (**Table 11 (1-3)**). The formation of the desired adduct was evident in the significant ¹H-NMR up field shift of the methylene proton facing the aromatic system (**Scheme 39**).

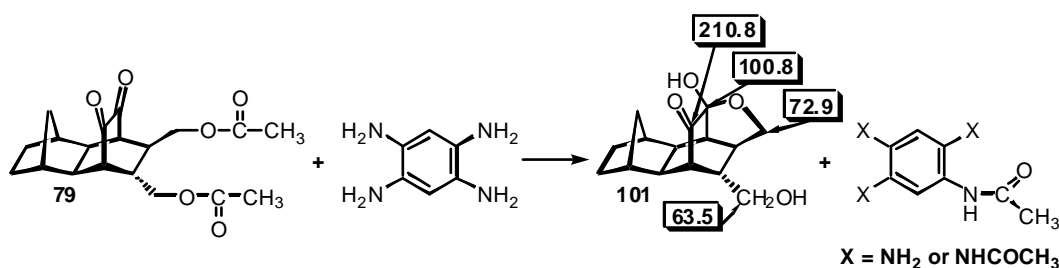


Scheme 39: Condensation successful under high pressure. (a)
phenylenediamine, pyridine, 40 °C, 15 kbar, 3 d, 72 %

Encouraged by this result the condensation with benzenetetramine (its tetrahydrochloric salt) was attempted in pyridine. At atmospheric pressure and 75 °C no product was isolated after 5 days. An equally disappointing result was obtained after 3 days at 25 °C and 15 kbar.

Increasing temperatures, however, led to a conversion of the 2B-dione-*trans*-diacetate **79**. Unfortunately, the product formed was not the desired one.

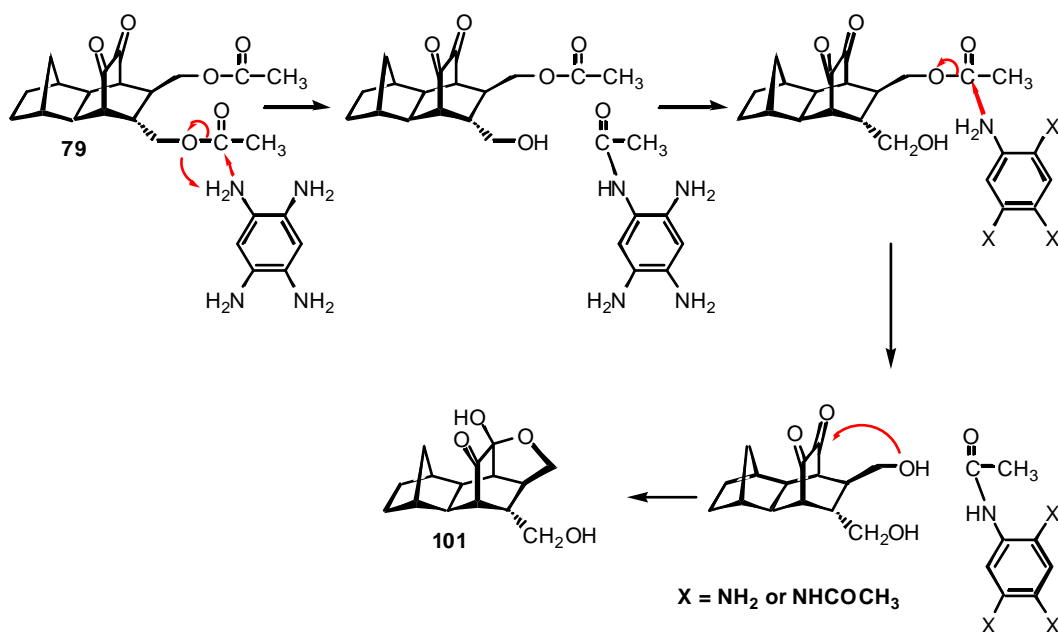
Under the chosen conditions (pyridine, 50-100 °C, 15 kbar, 2-3 d), the reaction proceeded at the carboxyl functionality of the acetoxy group rather than at the carbonyl functionality. The resulting product was the hemi-acetal **101** (**Scheme 40**) that was formed previously under different reaction conditions (**Scheme 36**, **Scheme 37**).



Scheme 40: Nucleophilic attack on acetoxy, not ketone group in pyridine at 15 kbar and high temperatures

Throughout the condensation experiments it was taken great care that the pyridine used as solvent was anhydrous. This fact excludes the possibility that a classic hydrolysis took place in the basic reaction medium. The condensation has to proceed first before water becomes available. As no condensation adduct was observed the involvement of the strong base benzenetetramine was proposed as indicated above in **Scheme 40**.

A mechanism for this unwanted ring-closure in anhydrous pyridine is proposed in **Scheme 41**. Whereas for the hydroxy group *anti* to the dione the keto functionality is out of reach, the hydroxy group *syn* to the dione can perform an intramolecular nucleophilic attack on the carbonyl carbon and form the observed ring-closed hemi-acetal **101**.



Scheme 41: Proposed mechanism for loss of acetoxy groups under high pressure in anhydrous pyridine

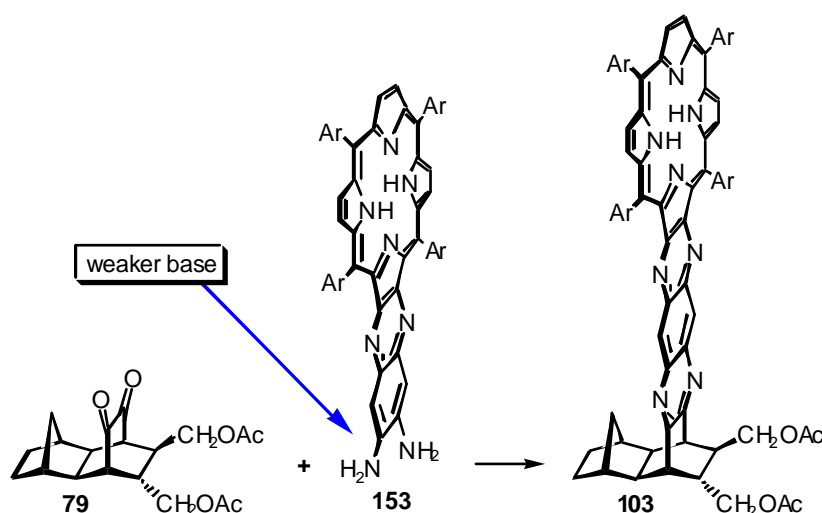
Table 11 summarises the results obtained from the condensation between the 2B-dione-*trans*-diacetate **79** and phenylenediamine (**1-3**) or benzenetetramine (**4-8**).

Table 11: Summary for condensations between the 2B-dione-*trans*-diacetate **79 and phenylenediamine (X = H) or benzenetetramine (X = NH₂)**

No.	X	Time	Solvent	T [°C]	p [k bar]	Result
1	H	6 d	ethanol	78	0.001	s.m., some 102
2	H	3 d	pyridine	115	0.001	s.m., some 102
3	H	3 d	pyridine	40	15	Yield: 72 % (102)
4	NH ₂	5 d	pyridine	80	0.001	s.m., no product
5	NH ₂	3 d	pyridine	80	5	s.m., no product
6	NH ₂	3 d	pyridine	25	15	s.m., no product
7	NH ₂	3 d	pyridine	50	15	s.m., some 101
8	NH ₂	2 d	pyridine	100	15	mostly 101

Whereas the reaction with benzenetetramine did not proceed in the desired way, the condensation with the weaker base phenylenediamine did under comparable reaction

conditions. This fact gave rise to the prediction that the reaction with 'diaminoporphyrin' **153**, a weaker base too, would proceed at the carbonyl groups (**Scheme 42**) and give the condensation product **103**.



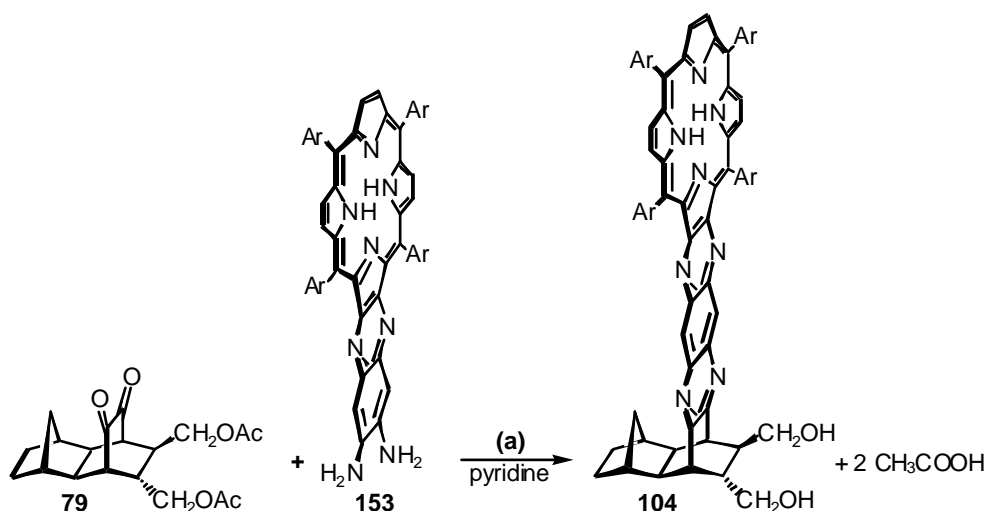
Scheme 42: Envisaged reaction of the 2B-dione-*trans*-diacetate **79** with the weaker base 'diaminoporphyrin' **153**

Numerous experiments were carried out and **Table 12** summarises the results obtained for condensations at 80 °C, variable pressure and two different solvents.

Table 12: Summary for condensations between 2B-dione-*trans*-diacetate **79** and 'diaminoporphyrin'

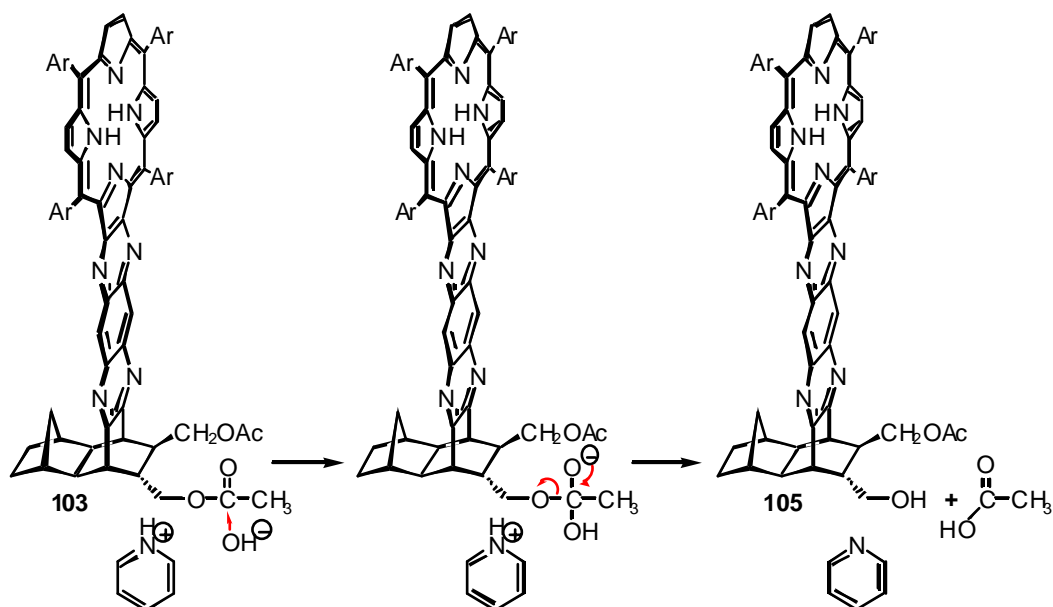
No.	Time	Solvent	T [°C]	p [kbar]	Result
1	21 d	pyridine	80	0.001	s.m., no product
2	3 d	pyridine	80	5	s.m., no product
3	3 d	pyridine	80	15	Yield: 49.6 % (104)
4	3 d	DCM	80	15	Yield: 63.0 % (103)

Neither at atmospheric pressure nor at 5 kbar products were formed. After increasing the pressure to 15 kbar, the 2B-porphyrin-*trans*-diol **104**, not the sought after diacetate **103**, was isolated in 50 % yield (**Scheme 43**).



Scheme 43: Loss of acetoxy groups in pyridine. (a) 'Diaminoporphyrin', pyridine, 15 kbar, 80 °C, 3d, 50 %

With the condensation being successful the solvent ceased to be anhydrous and the hydrolysis of the diacetate proceeded with the base pyridine present. The mechanism is given in **Scheme 44**. The depicted mono-hydrolysed 2B-porphyrin-*trans*-ol-acetate **105** was isolated as a side-product in this reaction.



Scheme 44: Hydrolysis of 2B-porphyrin-*trans*-diacetate 95 in pyridine. Double hydrolysis results in the formation of the main product 2B-porphyrin-*trans*-diol 96

The isolation of the mono-hydroxy derivative **105** excludes the presence of excess water and may be seen as evidence for the anhydrous nature of the pyridine used for the condensation reactions. The NMR spectra revealed the presence of one acetoxy group only and the MALDI mass spectrum confirmed the findings. Only one peak at $M^+ = 1466$ was observed which is in accordance with the calculated molecular weight (MW = 1466) of the 2B-porphyrin-*trans*-ol-acetate **105**. Its ^{13}C -NMR spectrum is depicted in **Figure 53**.

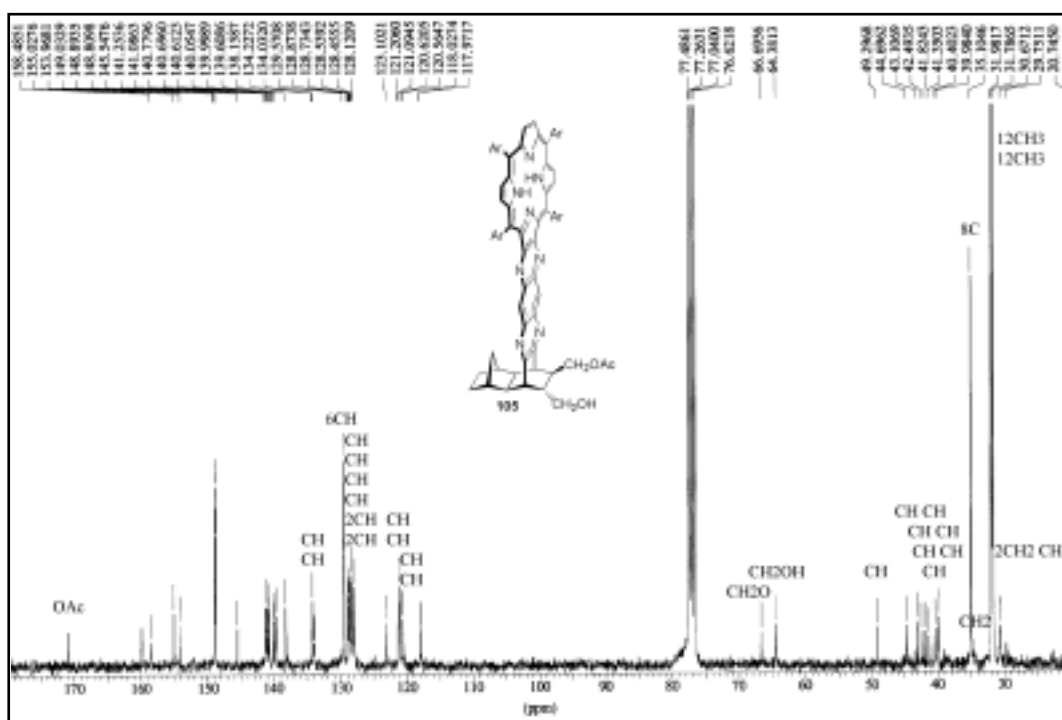


Figure 53: ^{13}C -NMR spectrum (75.5 MHz) of the mono-hydrolysed 2B-porphyrin-*trans*-ol-acetate **105**

The key signals of the ^{13}C -NMR spectrum are the ones for the carboxyl carbon of the acetoxy group at 170.8 ppm, the CH_2 adjacent to the acetoxy group at 66.7 ppm, and the carbon signal for the primary alcohol at 64.4 ppm.

The loss of one or both acetoxy groups at this stage was certainly not intended, but it didn't comprise a problem either as it consequently saved the removal of the acetoxy groups in the next synthetic step. The use of molecular sieves might have circumvented the hydrolysis in pyridine but was not attempted. Instead the solvent was changed.

Whereas pyridine is required as a solvent for the condensations with benzenetetramine (to generate the free base from its tetrahydrochloric salt, **B.2.3**), it is not essential for the reaction with 'diaminoporphyrin'. And indeed, a change of the solvent to dichloromethane kept the acetoxy groups intact, simplified the work-up procedure and yielded the 2B-porphyrin-*trans*-diacetate **103** in 63 %.

The successful condensation with 'diaminoporphyrin' is easily proven by the strong upfield shift of the methylene proton resonance. The chemical shifts for the protons facing the aromatic system were found at -0.51 ppm (**103**) and -0.43 ppm (**104**), respectively (**Figure 54**).

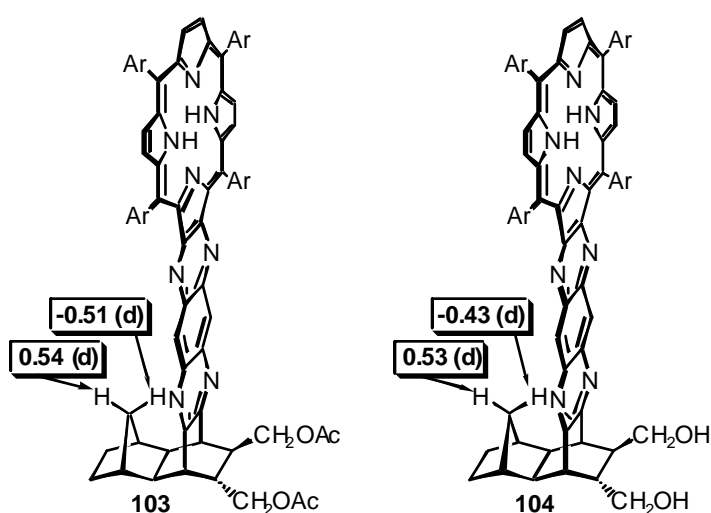
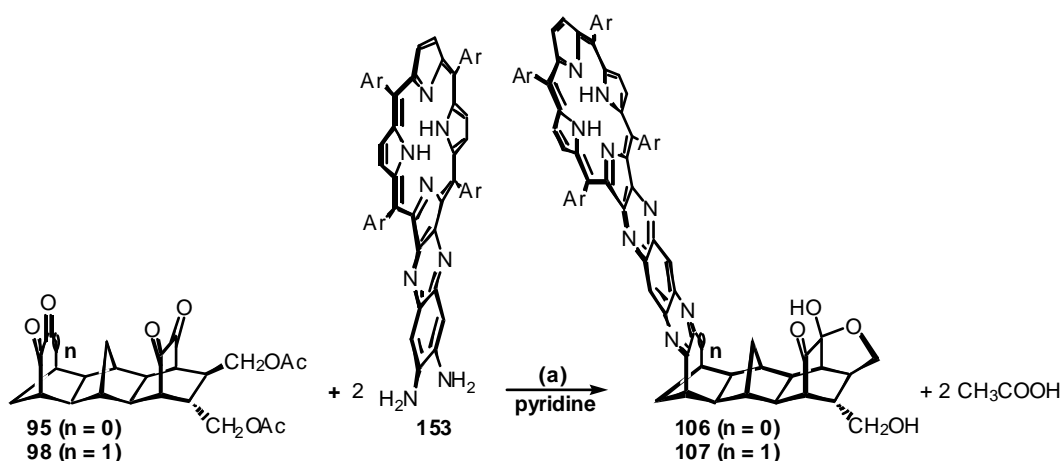


Figure 54: ¹H-NMR chemical shifts of the methylene-bridge protons for the 2B-porphyrin-*trans*-diacetate **103** and the 2B-porphyrin-*trans*-diol **104**

The application of high pressure was obviously a good approach to circumvent the lack of reactivity. The optimised high-pressure conditions (80 °C, 15 kbar, 3 days, and high concentrations in either pyridine or dichloromethane) were then applied to the tetraones **95** (non-ring-expanded) and **98** (ring-expanded), respectively.

The condensation proceeded at the more accessible 6B-dione first. The water released by this reaction led expectedly to the hydrolysis of the acetoxy groups in pyridine (see mechanism above, **Scheme 44**). Unfortunately the hydroxy group *syn* to the 2B-dione attacked the carbonyl group internally to form the corresponding hemi-acetal before a second 'diaminoporphyrin' could undergo condensation. As a consequence in pyridine, only the 6B-mono-adducts **106** (non-ring-expanded) and **107** (ring-expanded) were isolated (**Scheme 45**).



Scheme 45: 6B-mono-condensations only between 'diaminoporphyrin' **153 and tetraones **95** and **98** in pyridine. (a) $80\text{ }^{\circ}\text{C}$, 15 kbar, 3 d, 22 % (**106**), 25 % (**107**)**

The hemi-acetals **106** and **107** were identified by NMR spectroscopy. The loss of the acetoxy groups was obvious from the ^1H -NMR spectra. Integration confirmed the attachment of one porphyrin only. Evidence for the ketone, hemi-acetal and alcohol was easily derived from the ^{13}C -NMR spectra. Relevant chemical shifts are given in **Figure 55**.

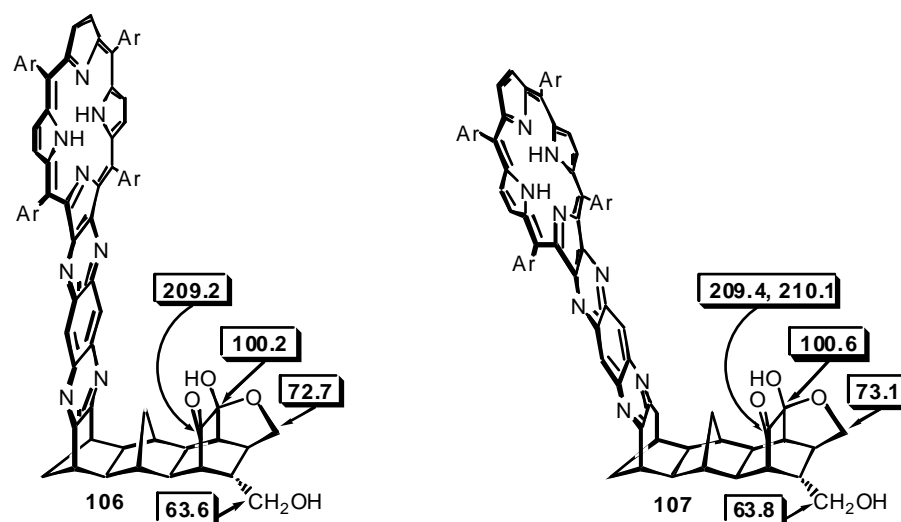
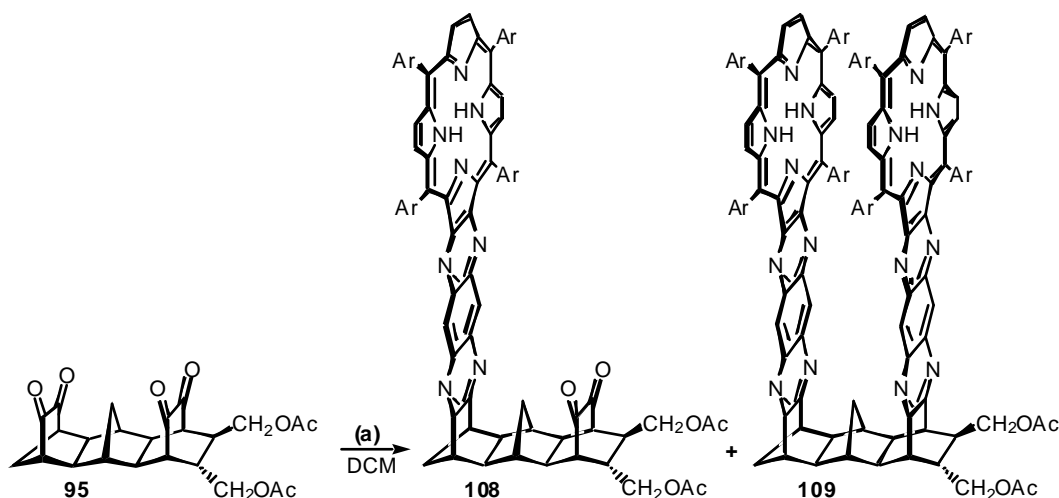


Figure 55: Selected ^{13}C -NMR chemical shifts for the 6B-porphyrin-hemi-acetals **106 and **107** formed in pyridine**

Under the same conditions, but in dichloromethane, the non-ring-expanded tetraone **95** yielded the 6B-porphyrin-2B-dione-*trans*-diacetate **108** as well as the bis-porphyrin-*trans*-diacetate **109** (**Scheme 46**). The fact that no 6B-dione-2B-porphyrin-*trans*-diacetate was detected supported the earlier expressed view that the 6B-dione is more accessible and the

condensation therefore proceeds at this end of the molecule first. Again, a change of solvent kept the acetoxy groups intact and enabled the attachment of a second porphyrin moiety.



Scheme 46: Condensation between the non-ring-expanded tetraone **89 and 'diaminoporphyrin' in dichloromethane. (a) 'Diaminoporphyrin', 80 °C, 15 kbar, 3 d, 35 % (**108**), 9 % (**109**)**

The ¹H-NMR spectrum for the 6B-porphyrin-2B-dione-*trans*-diacetate **108** showed a doublet for each methylene-bridge proton at -0.76 ppm and 0.16 ppm ($J = 14.4$ Hz). The methylene-bridge protons of the bis-porphyrin adduct **109** were observed at -0.96 ppm and -0.69 ppm ($J = 13.2$ Hz), respectively. The inner protons of the porphyrin moieties gave a singlet at -2.60 ppm. Compared to the 6B-porphyrin-2B-dione-*trans*-diacetate **108** (-2.34 ppm) and the 2B-porphyrin-*trans*-diacetate **103** (-2.38 ppm) the signals were significantly shifted upfield, proving some degree of interaction and therefore the desired 'special pair' character of the bis-adduct **109**. Its ¹H-NMR spectrum is given in the following **Figure 56**.

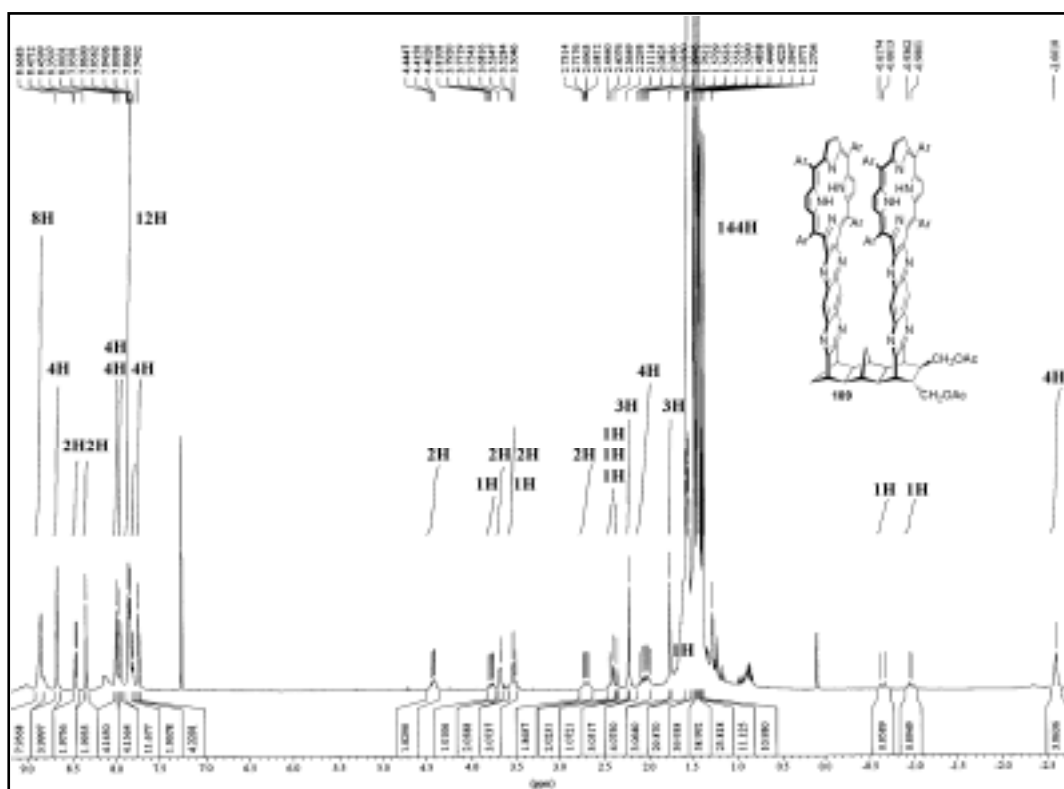


Figure 56: ^1H -NMR spectrum (300 MHz) of bis-porphyrin-*trans*-diacetate **109**

In agreement with the calculated molecular weights, the molecular peaks in the MALDI mass spectra for both compounds were observed at $\text{MH}^+ = 1602$ (**108**) and $\text{MH}^+ = 2763$ (**109**), respectively. **Figure 57** shows both spectra combined.

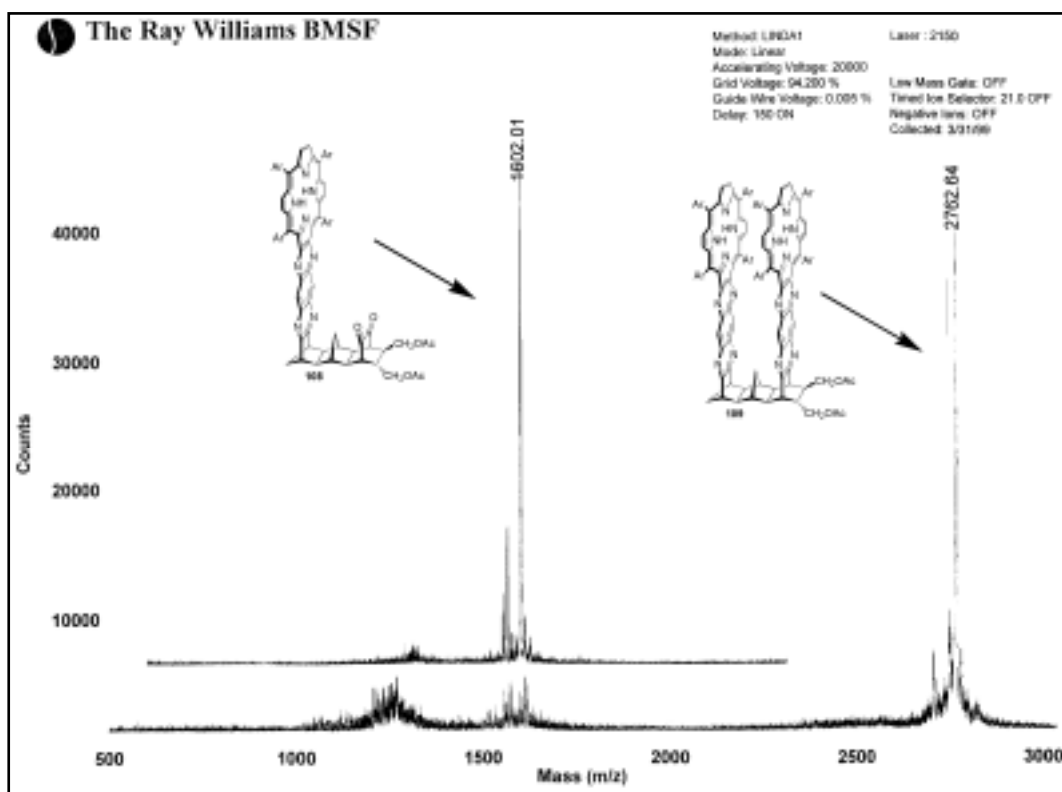
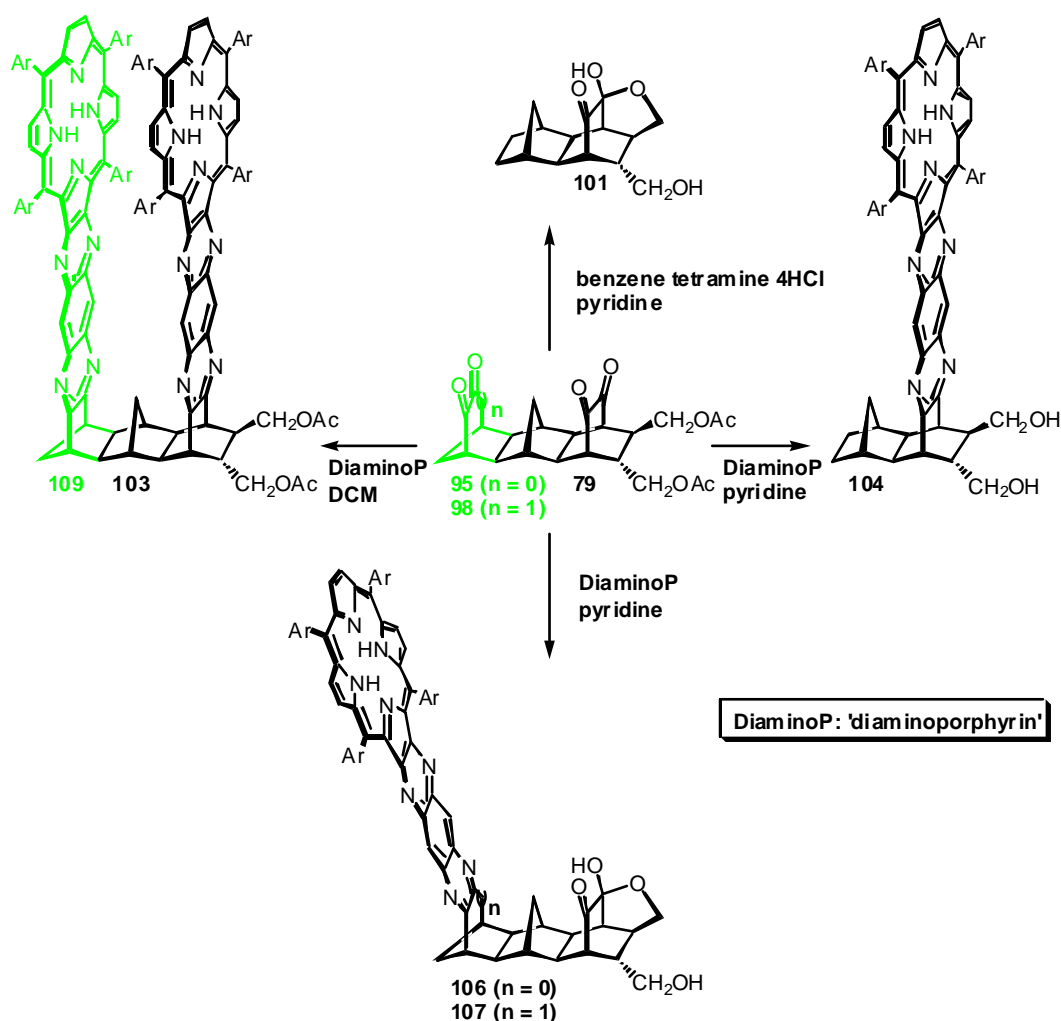


Figure 57: MALDI mass spectra of 6B-porphyrin-2B-dione-*trans*-diacetate 108 and bis-porphyrin-*trans*-diacetate 109

With the successful synthesis of these giant systems it has been shown that the application of high pressure and the optimisation of other parameters such as temperature, reaction time, concentration, and solvent finally results in the desired condensation products in reasonable yields.

The condensation of the ring-expanded tetraone **98** with 'diaminoporphyrin' has not been repeated in dichloromethane yet. However, the concept successfully applied to the non-ring-expanded tetraone **95** is expected to give the kinked bis-porphyrin-*trans*-diacetate with equally good results.

A summary of the findings obtained from the high-pressure work included in this thesis is given in **Scheme 47**.



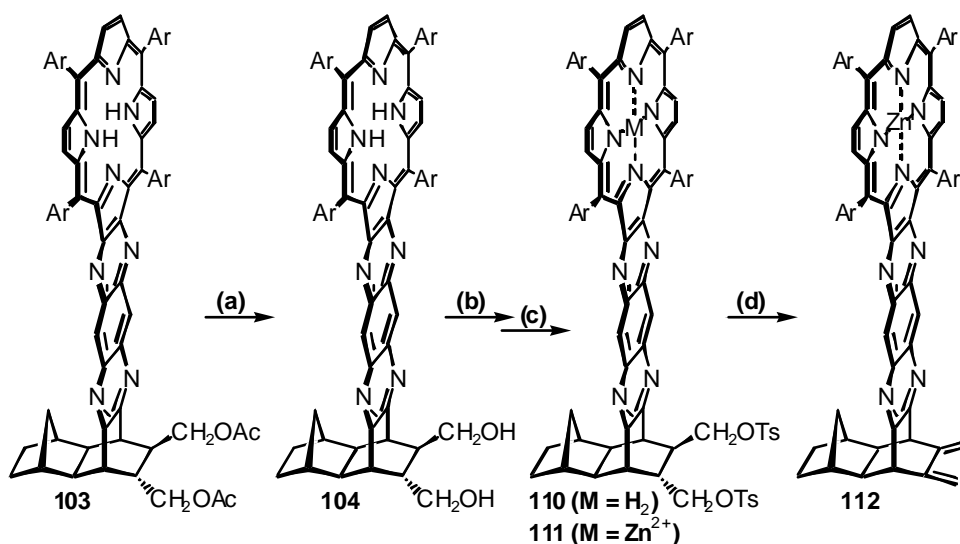
Scheme 47: Summary of high-pressure findings

To enable attachment of the bridge-acceptor component *via* Diels-Alder methodology the acetoxy groups had to be converted into 1,3-exocyclic dienes. They can then act as an enophile in a Diels-Alder reaction. The applied procedure for the conversion, first developed by Butler and Snow¹⁷⁷ is described in the following section **B.3.1.5** 'From Acetates to Exocyclic Dienes'.

B.3.1.5 From Acetates to Exocyclic Dienes

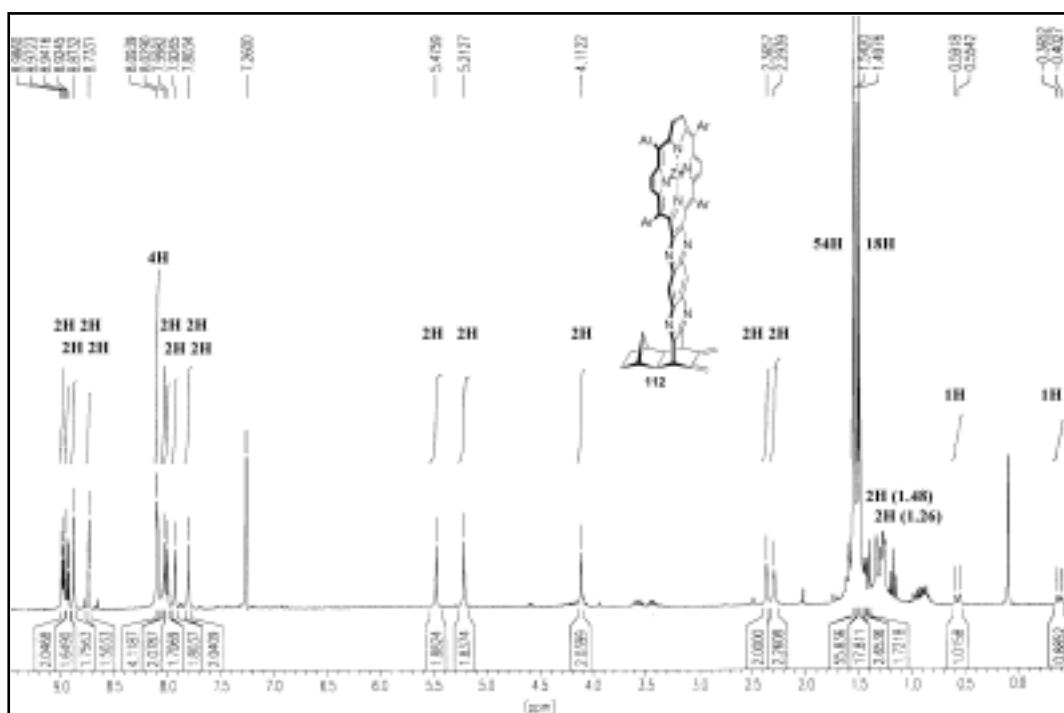
The condensation of the 2B-dione-*trans*-diacetate **79** and 'diaminoporphyrin' **153** in dichloromethane left the acetoxy groups intact. Mild conditions were applied (K_2CO_3 , MeOH) to convert the acetoxy groups into the primary alcohols (**Scheme 48 (a)**). The conversion of the alcohols into tosylates proceeded in pyridine with tosyl chloride at $-18^\circ C$ over a period of 7 days (**Scheme 48 (b)**). Before the de-tosylation with potassium *tert*-butoxide in

dimethylformamide (DMF) (**Scheme 48 (d)**) was carried out, the free-base porphyrin **103** was metallated with zinc(II) acetate in methanol and dichloromethane (**Scheme 48 (c)**). All synthetic steps gave high to very high yields.



Scheme 48: From acetate to diene. (a) K_2CO_3 , MeOH, THF, H_2O , RT, 18 h, 60 % ; (b) TsCl, pyridine, DCM, freezer, 7 d, 99 % ; (c) ZnOAc, MeOH, DCM, RT, 18h, 93 % ; (d) KO^tBu , DMF, RT, 3 h, 93 %

With the removal of the *trans*-tosyl groups (**Scheme 48 (d)**) C_5 -symmetry returned and obtained NMR spectra were significantly simplified. The ^1H -NMR spectrum of **112** is given in **Figure 58**.



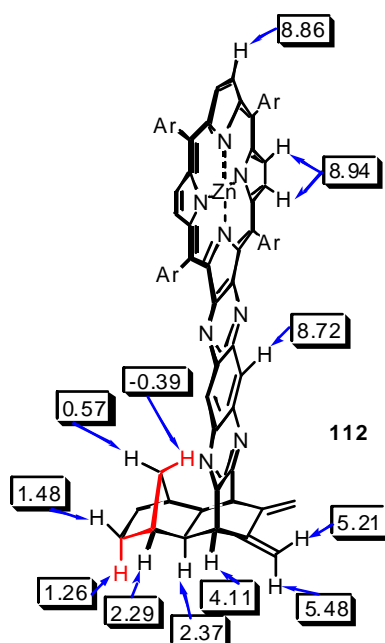


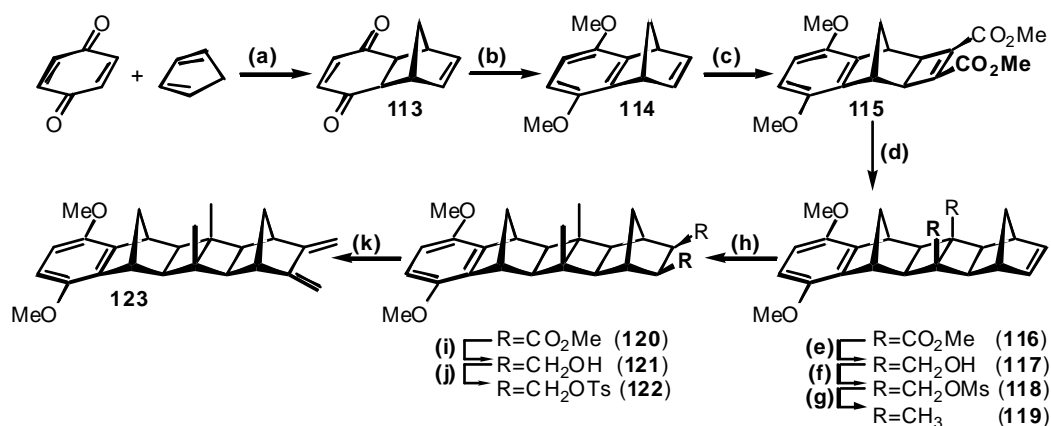
Figure 59: Vicinal and long-range (W-type) couplings to assist assignment of signals hidden under the giant *tert*-butyl signals of 2B-porphyrin-dimethylidene **112**

The assignment of signals in the ¹³C-NMR spectrum of **112** was assisted by DEPT135 and DEPT90 experiments. The olefinic ¹³C signals, further evidence for the successful synthesis of the exocyclic dienes were found at 143.2 ppm (2C=CH₂) and 107.8 ppm (2=CH₂), respectively. The spectrum is given in **Figure 60**. The MALDI mass spectrum showed a peak at MH⁺ = 1452, which corresponds to the molecular weight of **112** (MW = 1451.4).



Figure 61: Norbornylogous bridge designed for the attachment of donor and acceptor moieties via Diels-Alder methodology

The synthesis of this bridge is outlined in **Scheme 49**. Steps (a) to (g) followed a procedure developed by Antolovich *et al.*^{165,183} The reaction of benzoquinone with cyclopentadiene gave the Diels-Alder adduct **113**^{184,185}, which was converted into the known 5,8-dimethoxy-benzonornornadiene **114**^{186,187} by treatment with sodium hydride and methyl iodide (**Scheme 49** (b)). The norbornane framework was extended using tandem Mitsunobu-Smith methodology.¹⁸⁸⁻¹⁹⁰ The $\text{RuH}_2\text{CO}(\text{PPh}_3)_3$ ¹⁹¹ - catalysed $[\pi_2\text{s} + \pi_2\text{s}]$ thermal cycloaddition of DMAD and **114** (**Scheme 49** (c)) yielded the diester **115**, which underwent a thermal $[\pi_2\text{s} + \sigma_2\text{s} + \sigma_2\text{s}]$ cycloaddition reaction with quadricyclane (**Scheme 49** (d)). This methodology is well established within our group.^{43,118,148,170,183,192,193}



Scheme 49: Synthesis of the bridge component. (a) EtOH, 0 °C, 2 h, 61 % ; (b) 1) NaH, 2) MeI, THF, RT, 18 h, 52 % ; (c) DMAD, $\text{RuH}_2\text{CO}(\text{PPh}_3)_3$ ¹⁹¹, toluene, reflux, 24 h, 45 % ; (d) quadricyclane, toluene, reflux, 6 d, 75 % ; (e) LiAlH_4 , THF, reflux, 20 h, 87 % ; (f) Mesyl chloride, pyridine, freezer, 70 h; (g) LiAlH_4 , THF, reflux, 3 d, 52 % ; (h) - (k) see Scheme 50, page 118

A LiAlH_4 reduction (**Scheme 49** (e)), bismesylation (**Scheme 49** (f)) and another LiAlH_4 reduction (**Scheme 49** (g)) converted the ester into methyl groups in 45 % yield. An incomplete bismesylation reaction followed by the LiAlH_4 reduction led to the mono-hydroxymethyl-mono-methyl derivative **124** (**Figure 62**).

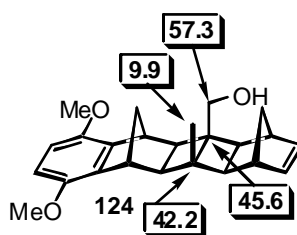
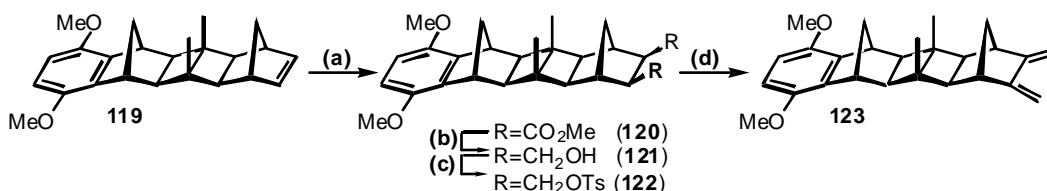


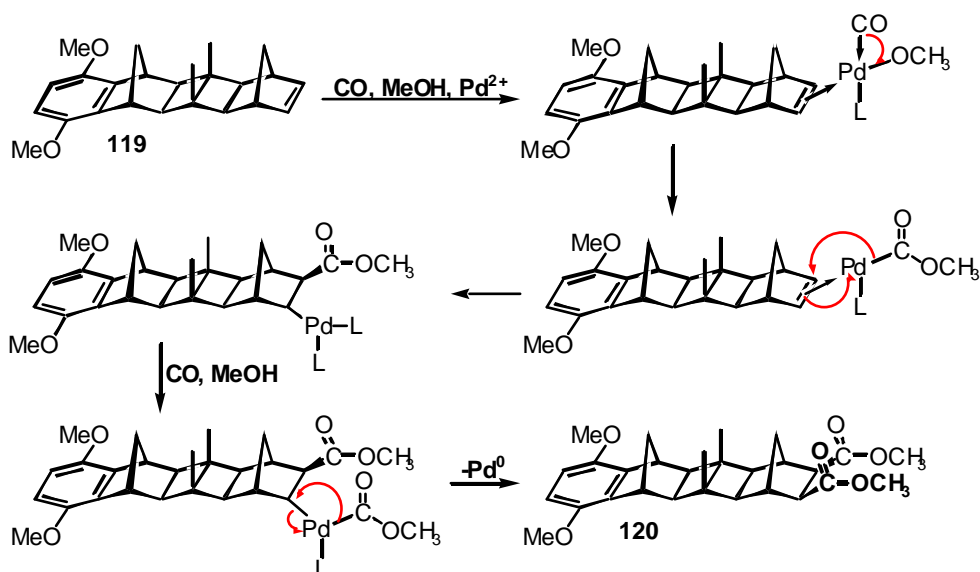
Figure 62: ^{13}C chemical shifts of the mono-hydroxymethyl-mono-methyl side product **124**

For the conversion of the norbornene-system into the exocyclic 1,3-diene **123**, methods developed by Stille *et al.*^{194,195} as well as Butler and Snow¹⁷⁷ were applied. The application of their methodologies to norbornylogous systems such as **119** is well established within our group (**Scheme 50**).^{193,196,197}



Scheme 50: Synthesis of the bridge component, part 2. (a) CuCl_2 , NaOAc , CO , Pd/C , MeOH , THF , RT , 97 h, 63 % ; (b) LiAlH_4 , THF , reflux, 15 h, 98 % ; (c) tosyl chloride, pyridine, freezer, 6 d, 66 % ; (d) KO^tBu , DMF , RT , 18 h, 91 %

First synthetic step of the conversion is the palladium-catalysed bismethoxycarbonylation with carbon monoxide and methanol (**Scheme 50 (a)**), that Stille and coworkers have reported for a number of olefins¹⁹⁴, including norbornene¹⁹⁵. Originally catalytic amounts of palladium(II) chloride and a stoichiometric amount of copper(II) chloride at 2-3 atm were employed. Later increased amounts of copper(II) chloride were found to improve yields. Further improvements to the reaction were achieved by replacing palladium(II) chloride with 10 % Pd/C , as suggested by Vogel *et al.*¹⁹⁸ Yamada *et al.*¹⁹⁹ reported the bismethoxycarbonylation of the *endo*-anhydride of norbornene in high yields and at atmospheric pressure. These improved reaction conditions were applied by Kate Joliffe¹⁹⁷ to the bismethoxycarbonylation of the DMB-6B-ene **119**. Due to poor solubility in methanol, THF was used as a co-solvent. The mechanism proposed by Kate Joliffe^{195,197} for this reaction is shown in **Scheme 51**.



Scheme 51: Proposed mechanism for Pd-catalysed bismethoxycarbonylation

In an initial step a palladium(II) species forms a π -complex with the double bond. As a result of electronic and torsional factors the complexation occurs on the *exo*-face only. Carbon monoxide and a methoxy group then complex to the palladium. Insertion of this CO-ligand into the Pd-methoxy bond gives the acetoxy-substituted complex. This acetoxy ligand then inserts into the dative olefin-palladium bond to give the σ -bonded palladium complex. A second complexation of carbon monoxide and a methoxy group followed by insertions result in the formation of the *cis*-diester **120** as well as Pd^0 , which is re-oxidised by copper(II) chloride. The preserved C_S -symmetry was evident in the simplicity of the ^1H -NMR spectrum. The doublet with a coupling constant of 2.1 Hz observed for the methylene bridge protons is typical of long-range W-type coupling and proved the *exo*-nature of the bismethoxycarbonylation (**Figure 63**).

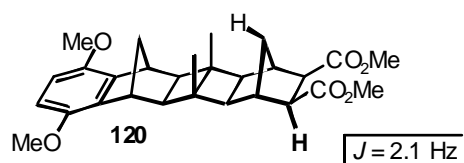
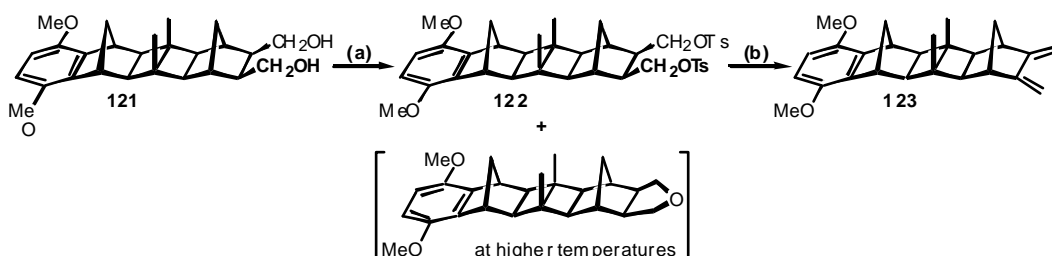


Figure 63: W-type coupling of *endo*-protons with one methylene bridge proton in **120**

The conversion of the *cis*-diester **120** into the exocyclic 1,3-diene **123** followed the Butler and Snow methodology¹⁷⁷ as applied in the triad donor synthesis (**B.3.1.3**, page 93). Reduction of the diester **120** with lithium aluminium hydride in THF yielded the diol **121** in 98 %. *Cis*-

diols are known to form furan derivatives in reactions with tosyl chloride under basic conditions. By using five equivalents of tosyl chloride at -23 °C this side reaction was avoided and the known *cis*-ditosylate **122**¹⁹³ was obtained (**Scheme 52**).

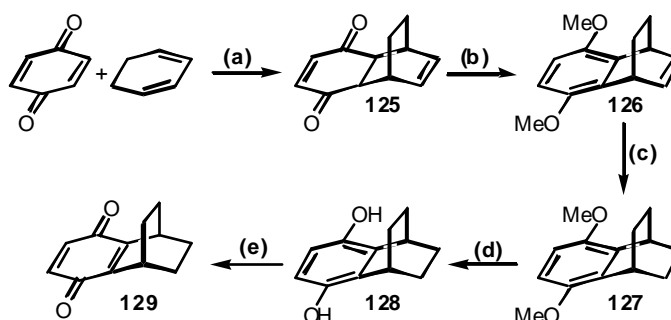


Scheme 52: (a) Tosyl chloride, pyridine, freezer, 6 d, 66 % ; (b) KO^tBu, DMF, RT, 18 h, 91 %

Detosylation with potassium *tert*-butoxide in DMF gave the desired DMB-6B-exocyclic-1,3-diene **123** in 91 % yield. In principle a whole variety of dienophiles can be attached to this diene, making the component-wise synthesis of the trichromophores the sought-after versatile method. In this thesis the following precursor of an electron acceptor was the only dienophile attached.

B.3.3 Synthesis of the Acceptor Precursor

The synthesis of known *p*-benzoquinonenorbornane **129**²⁰⁰ as the acceptor precursor was carried out using well-established literature procedures.

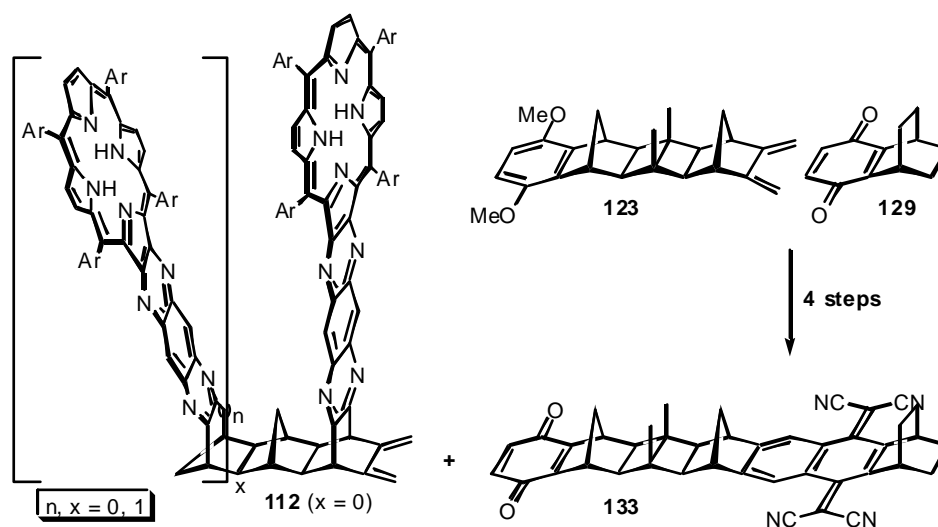


Scheme 53: Synthesis of acceptor precursor. (a) benzoquinone, 1,3-cyclohexadiene, EtOH, 60 °C, 2.5 h, 57 % ; (b) NaH, THF, MeI, RT, 64 h, 64 % ; (c) Pd/C, H₂, EA, RT, 10 h, 95 % ; (d) BBr₃, DCM, 0 °C / RT, 20 h, 88 % ; (e) Ag₂O, MgSO₄, Et₂O, RT, 3.5 h, 79 %

The Diels-Alder cycloaddition of 1,3-cyclohexadiene to *p*-benzoquinone¹⁸⁴ (**Scheme 53 (a)**) gave the adduct **125**, which was converted into the dimethoxybenzene derivative **126** using sodium hydride followed by methyl iodide in anhydrous THF (**Scheme 53 (b)**). Catalytic hydrogenation (Pd/C) (**Scheme 53 (c)**) gave the saturated adduct **127**, which was treated with boron tribromide in anhydrous dichloromethane (**Scheme 53 (d)**) to give the hydroquinone **128**.^{43,113,166,167,201} The desired acceptor precursor **129** was obtained in high yield through silver(I) oxide oxidation^{200,202-205} under anhydrous and inert atmospheric conditions (**Scheme 53 (e)**).

B.3.4 Assembling the Triads

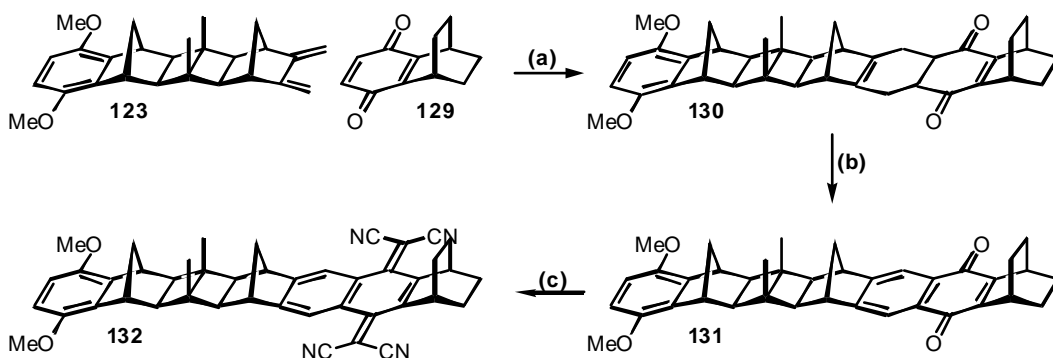
With the acceptor precursor **129**, the bridge **123**, and at least the 2B-porphyrin-dimethylidene **112** as donor component in hand, the ingredients were synthesised to assemble the first giant trichromophoric target molecule. Diels-Alder methodology was to be used to fuse the different components together. Donor and bridge feature exocyclic 1,3-dienes. The acceptor precursor consists of a 1,4-benzoquinone as a suitable dienophile. The dimethoxybenzene end of the bridge can be seen as a protected benzoquinone, which can undergo a cycloaddition after deprotection (**Scheme 54**).



Scheme 54: Assembling the triads using Diels-Alder methodology

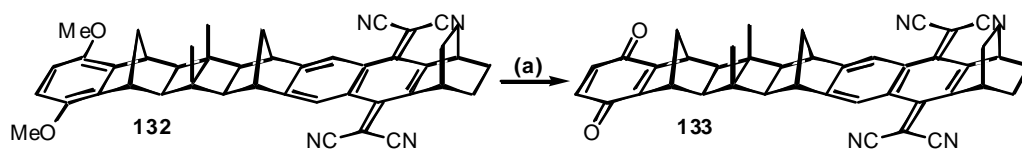
Initial steps included the Diels-Alder cycloaddition of the bridge **123** and the acceptor precursor **129** in 5M lithium perchlorate-diethyl ether^{193,206}, the aromatisation of the Diels-Alder adduct **130** with 2,3-dichloro-5,6-dicyano-1,4-benzoquinone (DDQ) and the subsequent

conversion of the naphthoquinone (NQ) derivative **131** into the tetracyanonaphthoquinodimethane (TCNQ) system **132** (Scheme 55).



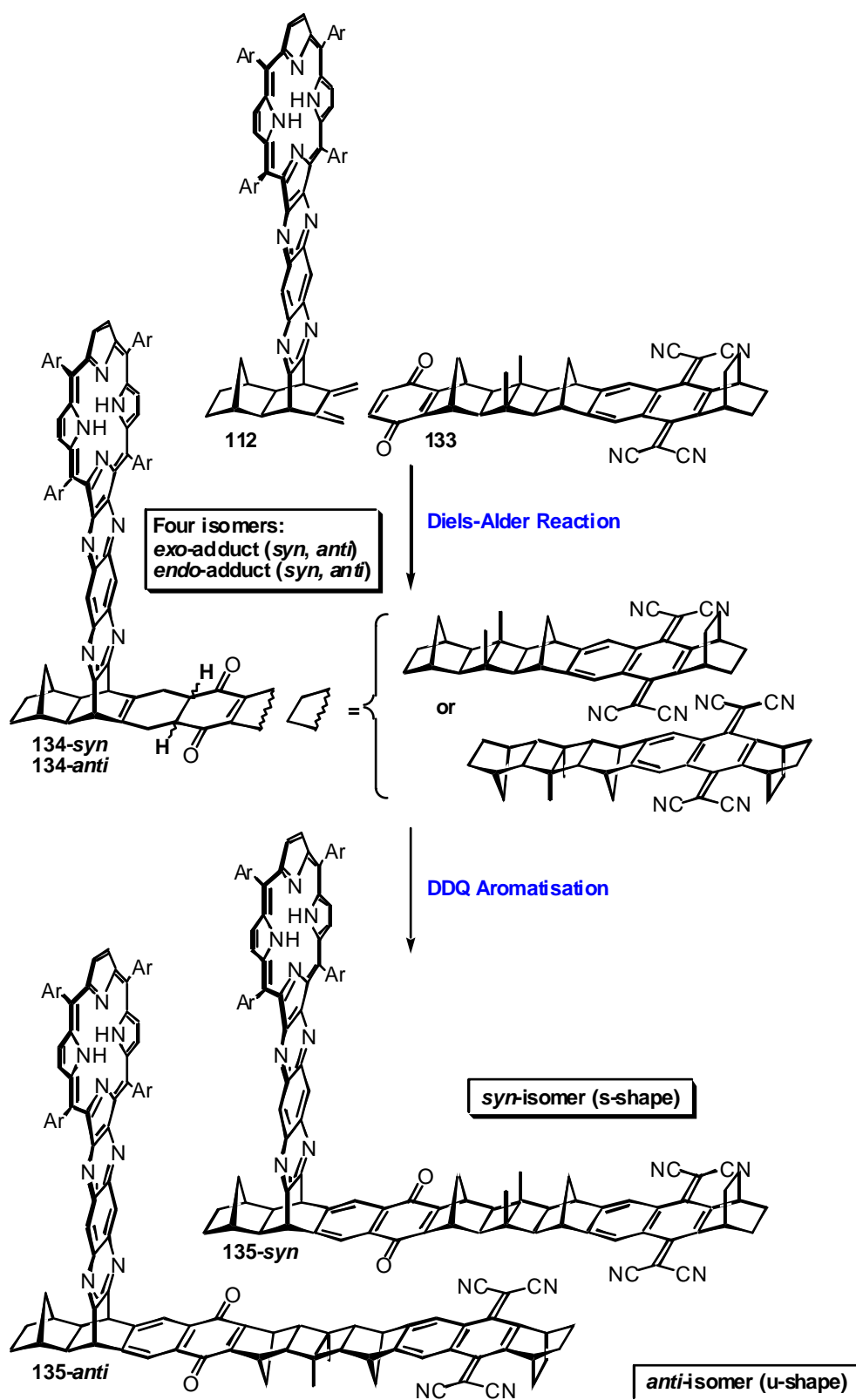
Scheme 55: Fusing bridge and acceptor. (a) 5M ethereal LiClO_4 , RT, 3 d, 98 % ; (b) DDQ, 1,4-dioxane, reflux, 48 h, 66 % ; (c) malononitrile, pyridine, TiCl_4 , DCM, reflux, 15 minutes, 88 %

The yields obtained for all three steps were satisfying and in accordance with those reported previously by Daniel Rothenfluh¹⁶⁹. The high yields repeatedly achieved for the TiCl_4 -catalysed Knoevenagel reaction^{164,207,208} were particularly pleasing. Oxidative cleavage of the methyl ethers with silver(II) oxide gave the according 1,4-benzoquinone **133**^{169,209} (Scheme 56).



Scheme 56: Deprotection of dimethoxybenzene. (a) AgO , 6M HNO_3 , THF, RT, 15 min, 69 %

With the completed synthesis of both the 2B-porphyrin-dimethylidene **112** as the first donor component and the bridge-acceptor block **133**, the stage was set for the final two steps, a Diels-Alder cycloaddition and a subsequent aromatisation, in the 48-step synthesis of the 2B-porphyrin-NQ-TCNQ triad **135** (Scheme 57).



Scheme 57: Final two steps of 2B-porphyrin-NQ-TCNQ triad 135

^1H -NMR, ^{13}C -NMR, and MALDI mass spectra indicate a successful linkage of the two giant components and their subsequent aromatisation. However, the purity of the isolated

compounds did not meet standards. Repeated column chromatography and size-exclusion chromatography to separate the s-shaped *syn*-isomer from the u-shaped *anti*-isomer or their mixture from other impurities failed to lead to satisfying results. If the observed NMR spectra would be complex due to the mixture of the two isomers only, the MALDI mass spectrum of the same sample would have shown just one signal but did not (**Figure 64**). However, a peak at $MH^+ = 2075$ was assigned.

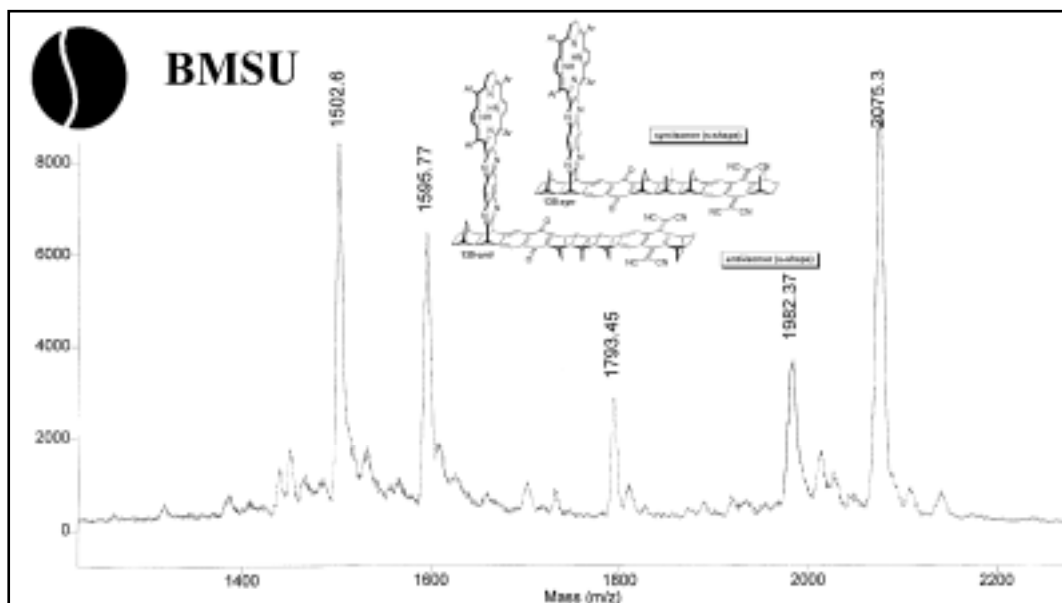


Figure 64: MALDI mass spectra obtained for the proposed 2B-porphyrin-NQ-TCNQ triad **135**

This peak is in reasonable accordance with the calculated molecular weight of the giant trichromophore **135** (MW = 2072.1 g/mol). Its spiky nature allows for discussion of accuracy (± 1) in the peak assignment and the detected species could well be $(\mathbf{135}+H)^+$ or even $(\mathbf{135}+2H)^+$. An incomplete aromatisation with 2,3-dichloro-5,6-dicyano-1,4-benzoquinone (DDQ) would lead to a compound with a molecular weight of 2074.1 g/mol for a perfect match. However, I do not consider this likely with the excess DDQ used for the aromatisation.

Further evidence for a successful linkage can be found in the NMR spectra. They showed neither the methylenide protons or the olefinic carbons of the 2B-porphyrin donor component nor the aromatic protons of the benzoquinone unit of the bridge-acceptor block, but displayed proton signals at chemical shifts as anticipated for the 2B-porphyrin-NQ-TCNQ triad **135** (**Figure 65**).

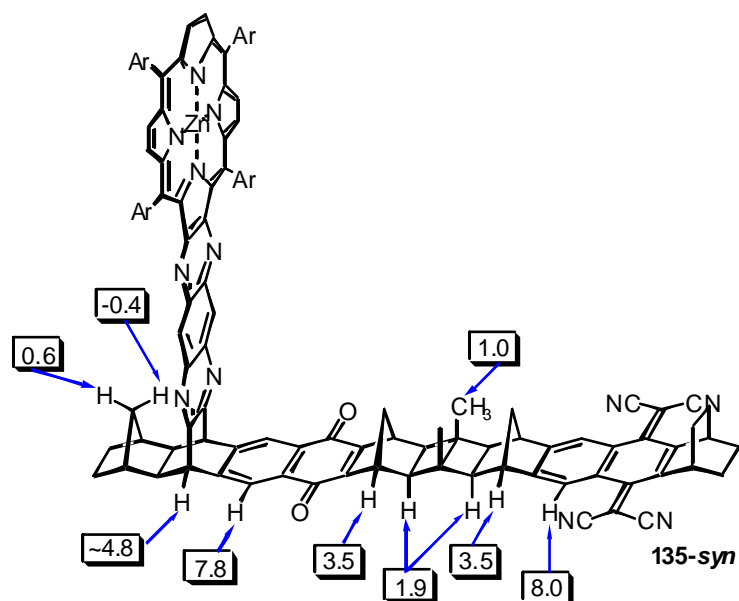


Figure 65: Anticipated ¹H-NMR shifts of the proposed 2B-porphyrin-NQ-TCNQ triad **135** (pictured: **135-syn**)

The proton signal of the central naphthoquinone unit, expected at ~7.8 ppm, was not clearly identified due to the proton resonances of the aromatic porphyrin substituents exhibiting a similar chemical shift. All other anticipated chemical shifts given in **Figure 65** were found in the average spectrum. More convincing evidence was derived from the ¹³C-NMR spectrum, which is shown in **Figure 66**.

Unfortunately the carbon resonance of the C=O group of the naphthoquinone was not observed, despite 40,000 scans. Selected ¹³C-NMR shifts extracted from the above-pictured spectrum are given in **Figure 67**. Further purification/separation attempts to obtain a better ¹H-NMR spectrum led to even smaller amounts of triad **135**, making the acquisition of good quality ¹³C-NMR spectra an even more difficult task.

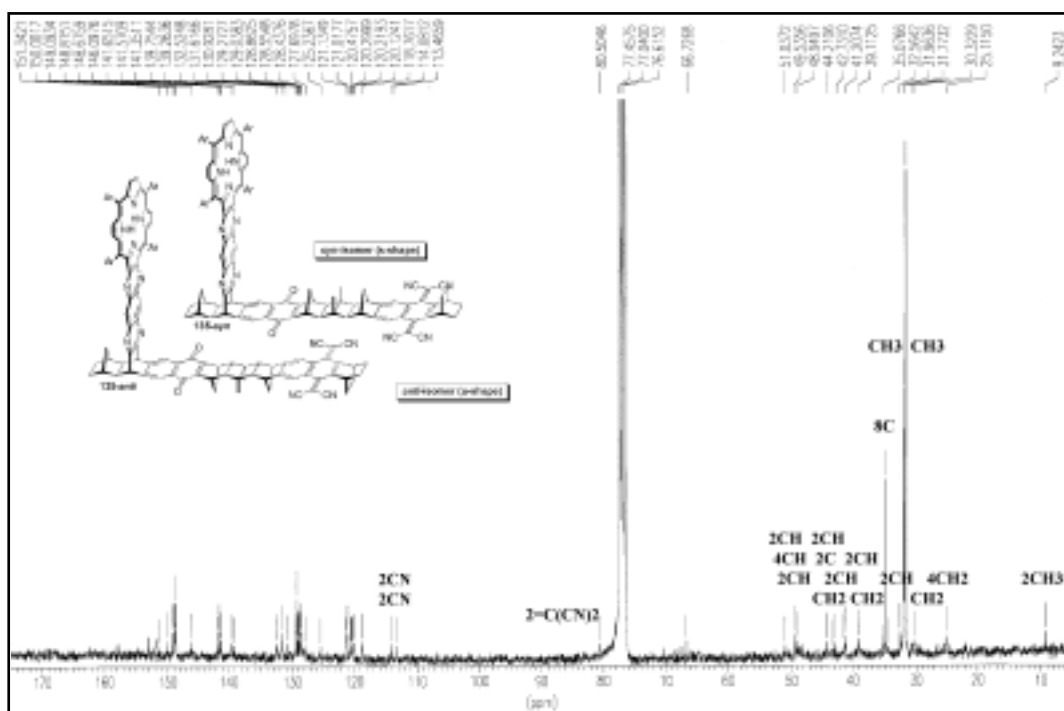


Figure 66: ^{13}C -NMR spectrum (75.5 MHz) of the proposed 2B-porphyrin-NQ-TCNQ triad 135

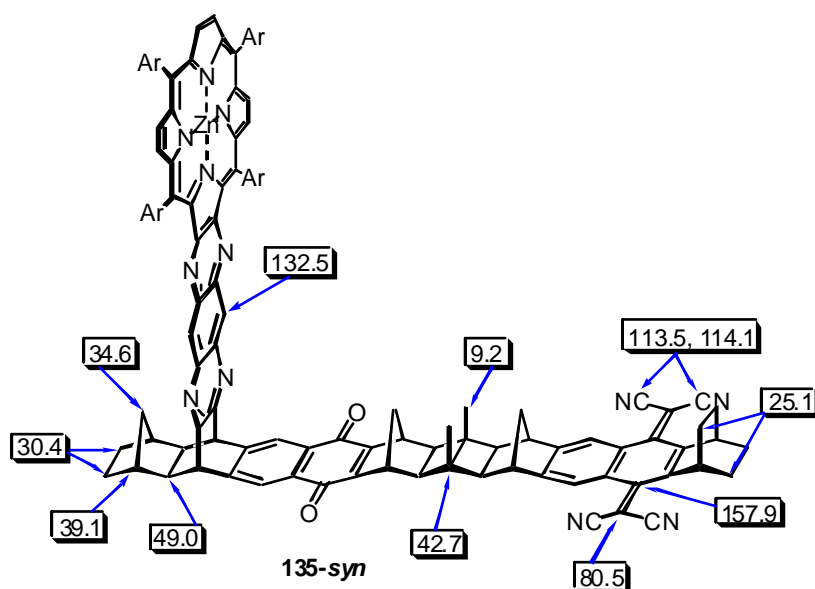


Figure 67: Selected ^{13}C -NMR chemical shifts of the proposed 2B-porphyrin-NQ-TCNQ triad 135 (pictured: 135-syn)

The observations described above are the results of two experiments each performed under equal Diels-Alder and aromatisation conditions. The conditions chosen were similar to the ones successfully applied to related systems.^{169,210} In order to investigate the difficulties experienced, more 2B-porphyrin-dimethylidene **112** is required. Access to the high-pressure equipment in Queensland will give more 2B-porphyrin-*trans*-diacetate **103** and subsequently the starting material **112**. As an alternative to the usage of 2,3-dichloro-5,6-dicyano-1,4-benzoquinone (DDQ) as the aromatising agent, an excess of the quinone²¹⁰ or lead dioxide¹⁹⁶ should be attempted. A change of the reaction procedure might reduce the amount of impurities and subsequently minimise purification problems.

In summary, the characterisation of the 2B-porphyrin-NQ-TCNQ target **135** was not satisfactory despite considerable purification/separation efforts. However, data have been presented that strongly indicate the successful synthesis of the first giant trichromophore. A methodology for the synthesis of the series of trichromophoric systems has been developed with only the last step requiring optimisation.

For a more comprehensive summary of the achievements on the synthesis of a series of dyads and triads see chapter C 'Summary & Conclusion', starting page 139. The following section **B.4** describes the scope of a small side project that outlines the synthetic efforts towards an all-*trans* ring-expanded dyad.

B.4 SYNTHESIS OF AN ALL-TRANS RING-EXPANDED DYAD

The dyad described in this section was initially not part of the overall concept of the series of bichromophoric and trichromophoric targets. Nevertheless it comprises another systematic addition to target pool. Instead of a *cisoid* linkage of the porphyrin chromophores to the bridge, the porphyrin in this additional target is connected in an all-*trans* arrangement (**Figure 68**). A norbornylogous bridge, six σ -bonds in length, separates the porphyrin donor from the electron acceptor TCNQ.

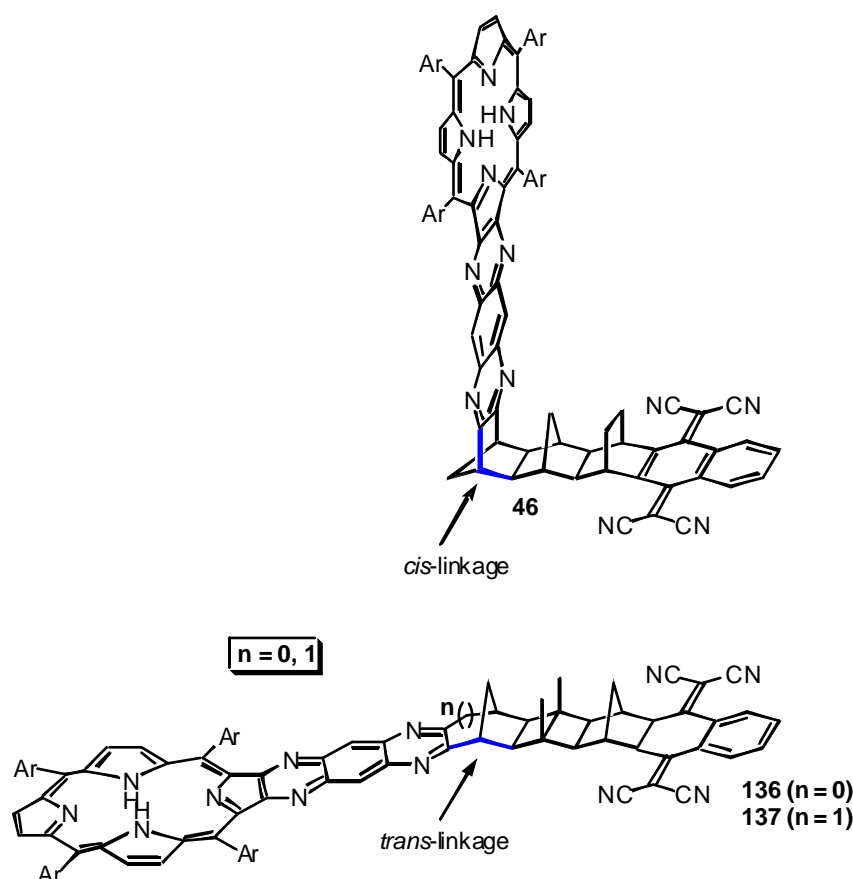


Figure 68: 6B-porphyrin-TCNQ **46 and the comparable all-*trans*-analogues**

In an all-*trans*-arrangement through-bond (TB) coupling is maximised^{115,211} and electron-transfer rates are expected to be higher than in equivalent systems possessing *cis*-linkages. The prediction has received experimental verification^{44,212} and according results are expected for the comparison of the 6B-porphyrin-TCNQ **46** and the all-*trans* 6B-porphyrin-TCNQ **136**, which has been synthesised previously within the Paddon-Row group.

More interesting could be the comparison of this previously synthesised dyad with the new all-*trans* ring-expanded 6B-porphyrin-TCNQ target **137**. Experimental verification of the (relative) parity rule^{10,211,213,214} and, in this context, further insight into the influence of constructive and destructive interference on the ET process is sought after.

For the electron transfer process through a norbornylogous bridge, six σ -bonds in length, a range of different pathways exist. Each of them is weighted differently regarding its contribution to the overall coupling between the donor (porphyrin) and the acceptor (TCNQ).

Figure 69 shows the most important pathways through such a bridge. Pathways of the same

parity thereby lead to constructive interference, different parity results in destructive effects on the overall coupling and consequently the electron-transfer rate.

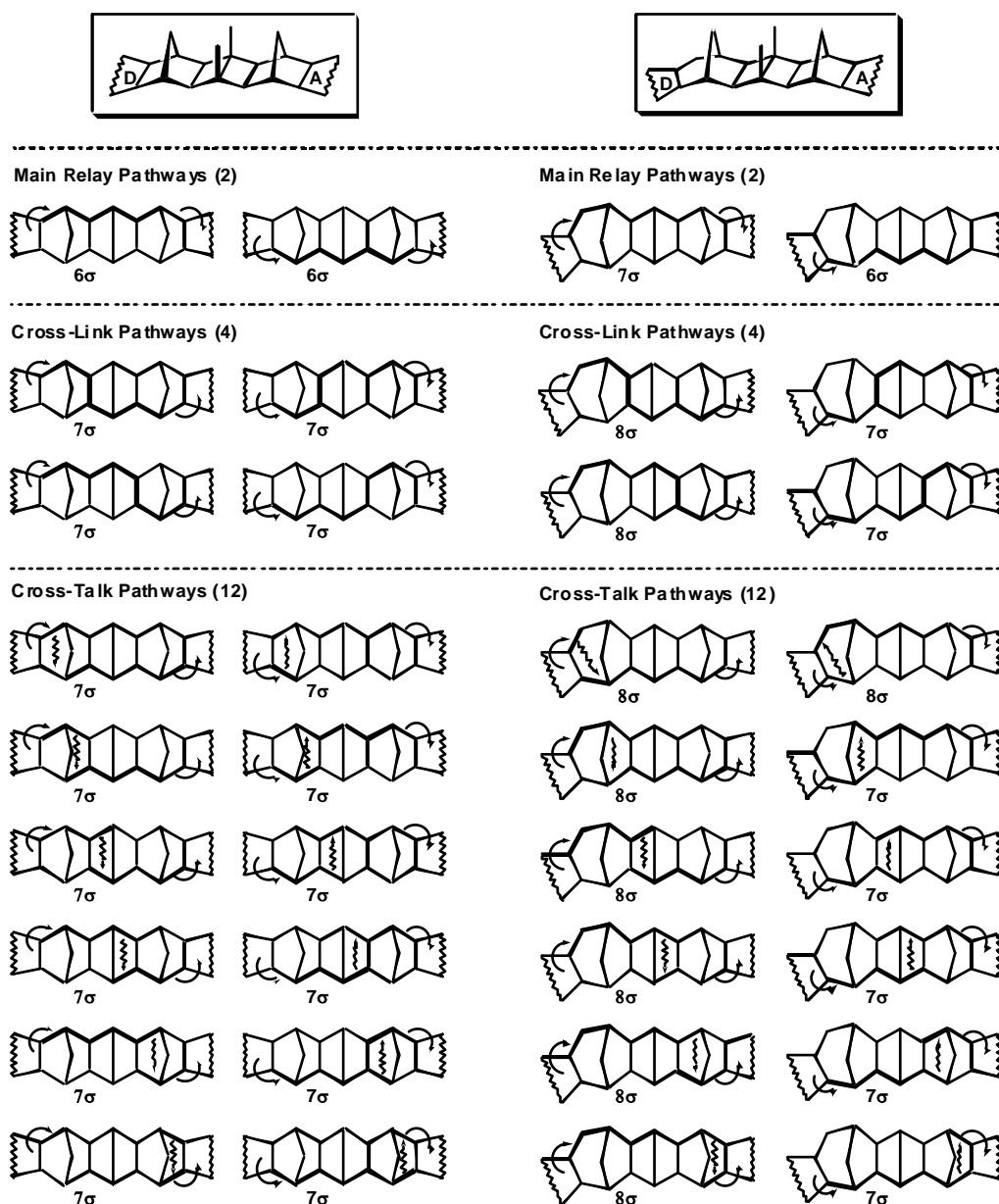


Figure 69: Electron transfer pathways for the non-ring-expanded (left) and ring-expanded norbornylogous bridge

For the non-ring-expanded bridge (**Figure 69 left**) the two main relays work constructively but all other cross-link and cross-talk pathways contribute destructively towards the overall coupling. The main relays of the ring-expanded bridge (six or seven σ -bonds in length) interfere destructively but nine cross-link and cross-talk pathways shown (**Figure 69 right**) contribute constructively towards the six bond main relay.

To experimentally probe the influence of constructive and destructive interference is the motive behind the synthesis of the ring-expanded target. The addition of a double ring-expanded species, incorporating a so-called 'superbridge',²¹⁴ would nicely complete the series in the future (**Figure 70**). In a superbridge the main relays are of the same parity (here six or eight σ -bonds in length) and so are all cross-link and cross-talk pathways of the type shown in **Figure 69**.

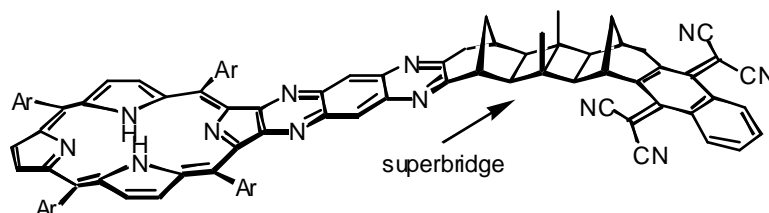
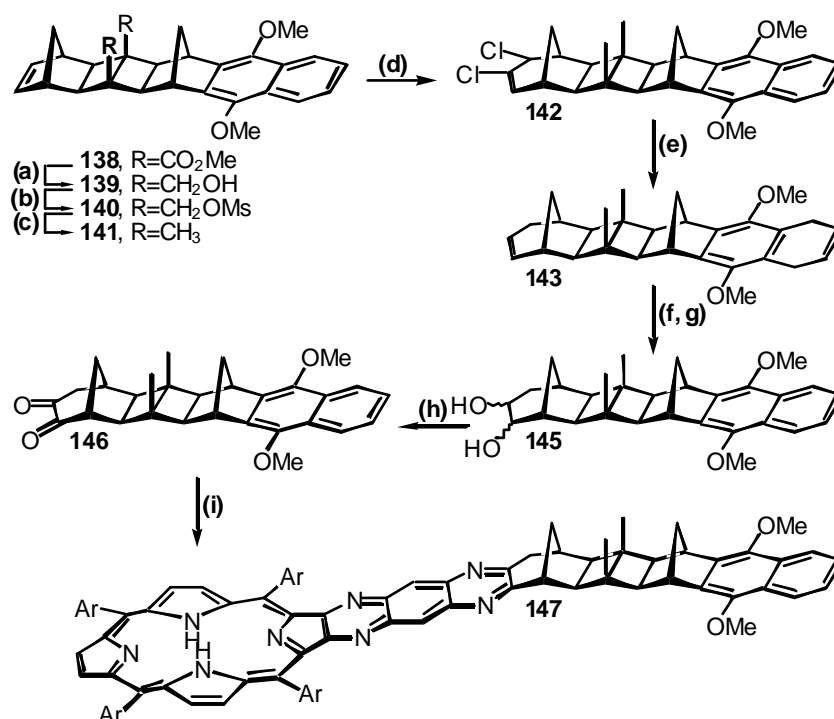


Figure 70: Constructive interference to a large extent: a 'superbridge'!

The attempted synthesis of the all-*trans* mono-ring-expanded 6B-porphyrin-TCNQ dyad **137** started with the known diester-DMN system **138**.^{165,183} Following our standard procedures, the ester groups were converted into methyl groups *via* the respective hydroxymethyl and mesyloxymethyl groups (**Scheme 58 (a) - (c)**).^{43,118,148,170,183,192,193}

The ring-expansion of **141** with *in-situ* generated dichlorocarbene (**Scheme 58 (d)**) gave similar yields to those found for the ring-expansion of the dyad and triad carbon backbone (**Section B.2.1**, page 51).

The reductive dechlorination of **142** with sodium (**Scheme 58 (e)**) led to de-aromatisation of the dimethoxynaphthalene unit in **143**, which was subsequently re-aromatised with DDQ (**Scheme 58 (f)**).



Scheme 58: Synthesis of the all-*trans* ring-expanded 6B-porphyrin-DMN **147**.

(a) LiAlH₄, THF, reflux, 18 h, 98 % ; (b) MsCl, pyridine, -18 °C, 3 d, 76 % ;
 (c) LiAlH₄, THF, reflux, 2 d, 51 % ; (d) Cl₃CCO₂Et, NaOMe, PE, RT, 3 d, 33 % ;
 (e) Na, *i*-PrOH, THF, reflux, 1 day, 54 % ; (f) DDQ, DCM, RT, 22 h, 82 % ;
 (g) OsO₄, NMO, 1,4-dioxane, RT, 2 d, 55 % ; (h) TEMPO reagent, *p*-toluenesulfonic acid, DCM, RT, 3 d, 42 % ; (i) 'diaminoporphyrin', pyridine, 80 °C, 5 kbar, 1 day, 12 %

The successful ring expansion, reductive dechlorination and aromatisation are evident in the NMR spectra of the all-*trans* ring-expanded 6B-ene-DMN **144**. The ¹H-NMR spectrum showed two distinct singlets for the methyl groups at 0.89 ppm and 0.91 ppm as well as two singlets for the methoxy groups at 3.98 ppm and 3.99 ppm, respectively. The olefinic protons show as a doublet of triplets at 5.31 ppm (next to CH₂ ring-expansion) and a doublet of doublets at 5.87 ppm. Selected ¹H-NMR chemical shifts are given in **Figure 71**.

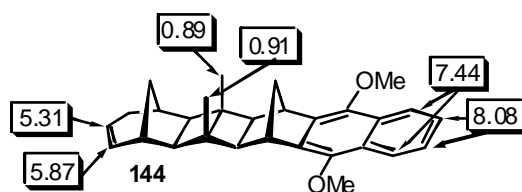


Figure 71: Selected ^1H -NMR data of the all-*trans* ring-expanded 6B-ene-DMN **144**

The ^{13}C -NMR spectrum (**Figure 72**) displayed the olefinic carbon signals at 134.8 ppm and 124.6 ppm (next to CH_2 ring-expansion), respectively. The quaternary carbon atoms of the bridge showed at 44.0 ppm and 43.3 ppm, allowing no doubt in the success of the reaction sequence.

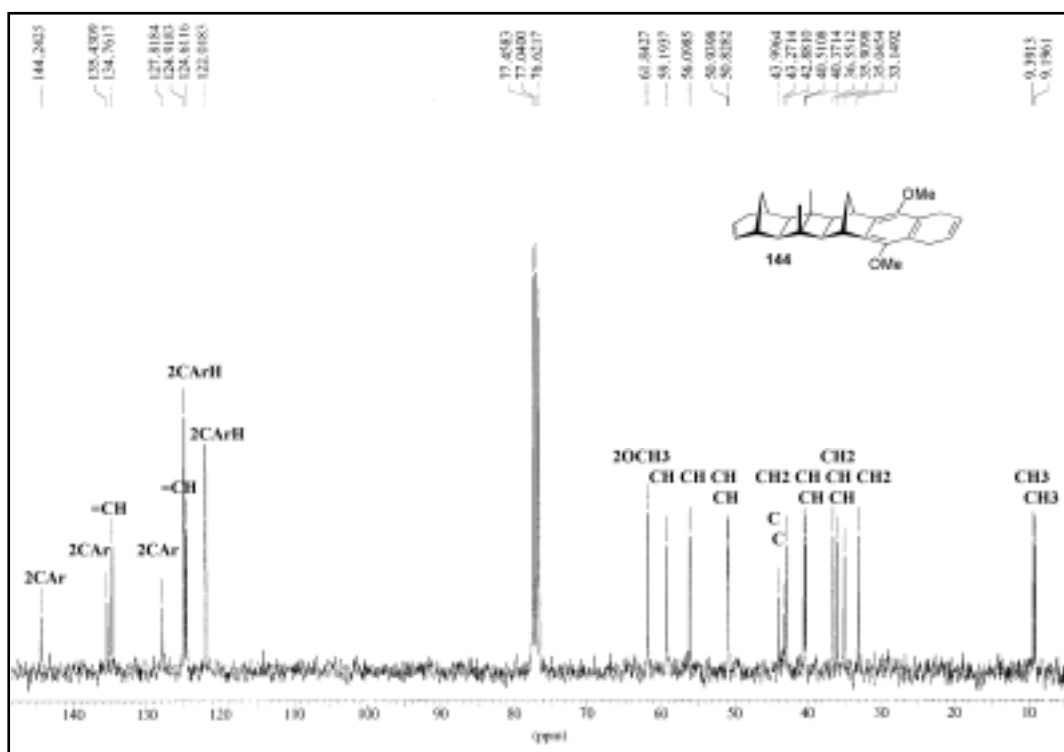


Figure 72: ^{13}C -NMR spectrum (75.5 MHz) of the all-*trans* ring-expanded 6B-ene-DMN **144**

The *Sharpless* bis-hydroxylation on the all-*trans* ring-expanded 6B-ene-DMN **144** (**Scheme 58** (g)) gave the corresponding diol **145** and subsequent TEMPO reaction (**Scheme 58** (h)) afforded the all-*trans* ring-expanded 6B-dione-DMN system **146**.

The condensation with 'diaminoporphyrin' was carried out in pyridine at 80 °C and 5 kbar (**Scheme 58 (i)**). After 1 day the sought after all-*trans* ring-expanded 6B-porphyrin-DMN **147** was isolated in 12 % yield and characterised by ^1H -NMR spectroscopy (**Figure 73**).

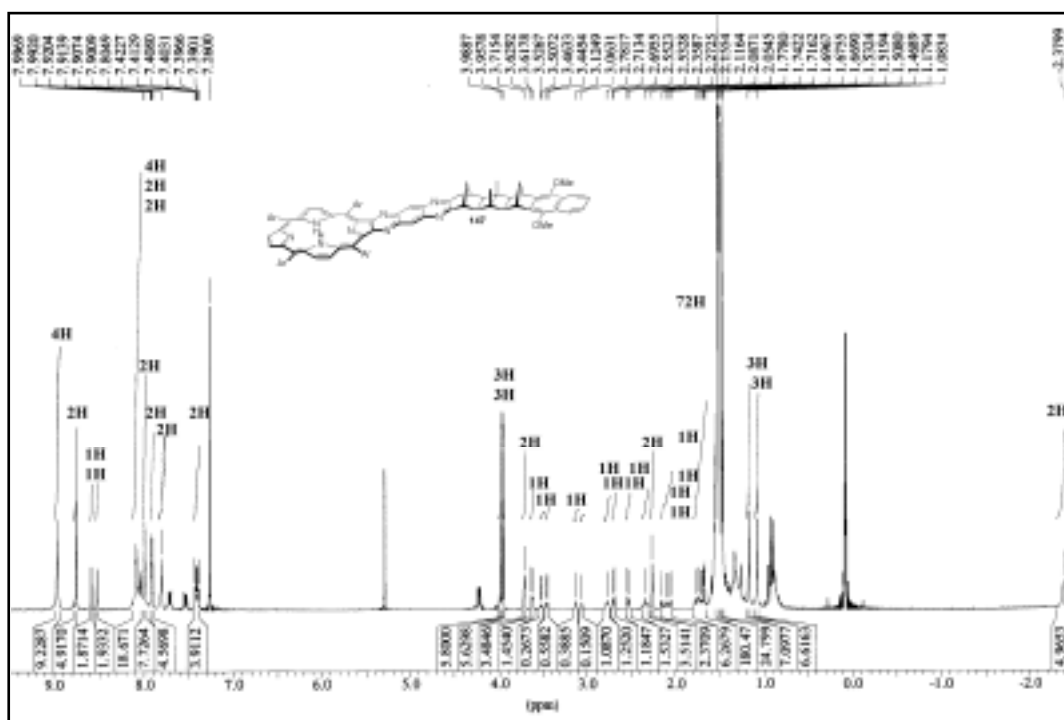


Figure 73: ^1H -NMR spectrum (300 MHz) of the ring-expanded all-*trans*-6B-porphyrin-DMN **147**

Due to the kinked nature of the condensation adduct the two quinoxaline protons showed as two singlets at 8.58 ppm and 8.52 ppm, respectively. Two distinct singlets were also found for the methoxy (3.98 ppm and 3.95 ppm) and methyl signals (1.18 ppm and 1.08 ppm). As the condensation was carried out on a small scale, only 3 mg of the all-*trans* dyad **147** were obtained, not enough to run a ^{13}C -NMR experiment within a reasonable time, but enough to obtain a MALDI mass spectrum (**Figure 74**). It is in good agreement with the calculated molecular weight of **147** (MW = 1602.3 g/mol).

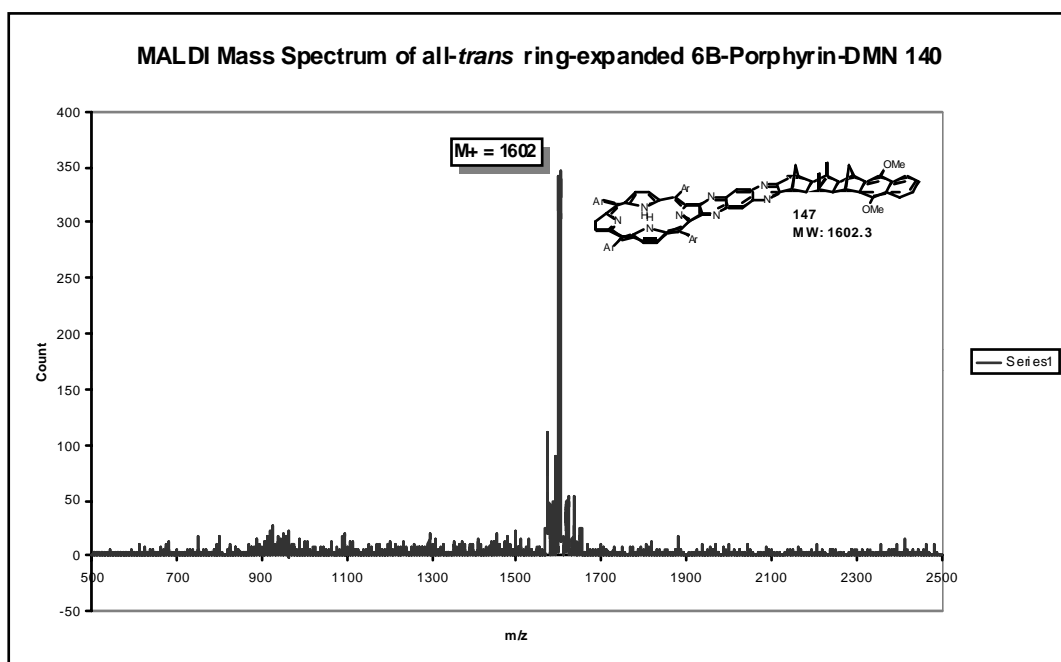
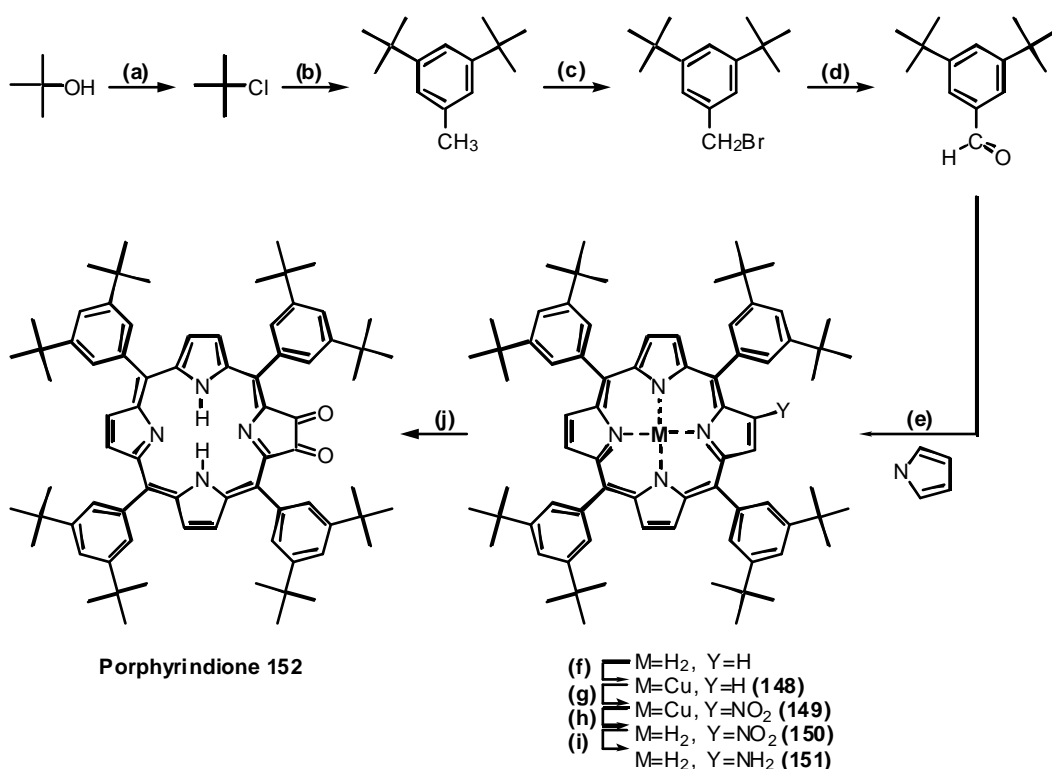


Figure 74: MALDI mass spectrum of the all-*trans* ring-expanded 6B-porphyrin-DMN 147

Due to the small amount of **147** the conversion of the DMN unit into the strong electron acceptor TCNQ was not pursued any further. It is expected that the procedure successfully applied to the series of dyads (**B.2.4**, page 69) will be equally applicable to the all-*trans*-system.

B.5 SYNTHESIS OF THE 'DIAMINOPORPHYRIN'

The synthesis of known 5,10,15,20-tetrakis-(3,5-di-*tert*-butylphenyl)-2³-2⁴-diamino-quinoxalino[2,3-*b*]porphyrin ('diaminoporphyrin') **153** followed the methodology partly developed by Crossley *et al.*²¹⁵⁻²¹⁸ Outlined in **Scheme 59** is the synthesis of the precursor 5,10,15,20-tetrakis-(3,5-di-*tert*-butylphenyl)porphyrin-2,3-dione ('porphyrindione') **152**, which undergoes a condensation reaction with benzenetetramine to give the sought after 'diaminoporphyrin' **153**.

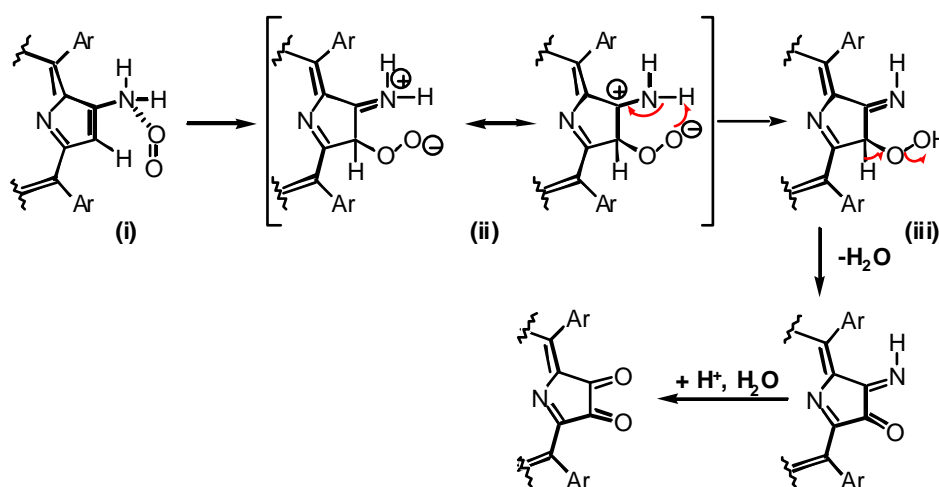


Scheme 59: Synthesis of porphyrindione. (g) NO_2 , light petroleum, RT; (h) H_2SO_4 , RT, 78 % ; (i) SnCl_2 , HCl, DCM, RT, 2d, 76 % ; (j) O_2 , hv, RT, 6d, H_2SO_4 (3M), 2 hr, 86 %

Steps (**Scheme 59 (a)**) to (**Scheme 59 (f)**) were carried out by Stephen R. Davies. The yields he obtained were in accordance with the above mentioned references. The nitration of **148 (g)** followed by de-metallation (**Scheme 59 (h)**) with concentrated sulfuric acid yielded the 2-nitro-porphyrin **150** in 78 % yield. The reduction (**Scheme 59 (i)**) to the 2-amino-derivative **151** occurred with Tin(II)chloride in 76 % yield. The photo-oxidation (**Scheme 59 (j)**) was carried out in dichloromethane, using the sun as the source of light and atmospheric oxygen as the oxidant. After six days sulfuric acid (3 M) was added to hydrolyse the intermediate imino-

oxo-porphyrin (**Scheme 60**) to give the 'porphyrindione' **152**. Yields for the two-step reaction were improved to 86 %.

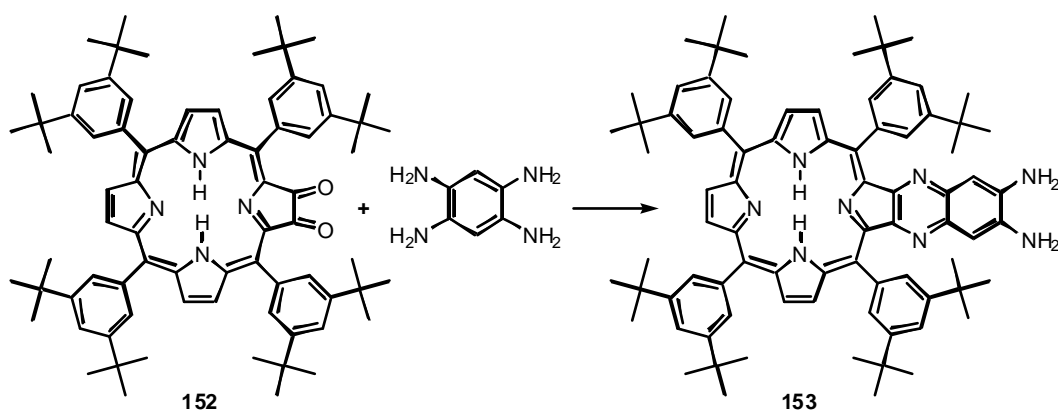
The photo-oxidation reaction proceeds *via* the formation of singlet oxygen. Singlet oxygen is produced by energy transfer from an excited sensitizer to ground state oxygen.²¹⁹ Porphyrins, especially free-base porphyrins, are such singlet-oxygen sensitizers.²²⁰ The overall mechanism can be described as in **Scheme 60**.



Scheme 60: Mechanism of photo-oxidation followed by hydrolysis

The rate determining step is the charge transfer step.^{221,222} The charge-transfer complex (i) can rearrange to the zwitterion (ii) which has a number of canonical forms. The zwitterion converts to the hydroperoxide (iii) through protolysis involving an amine proton. Loss of water gives the corresponding keto-imine, which then hydrolyses readily in weak acid to give the 'porphyrindione' **152**.

The condensation with a 50 % excess of benzenetetramine in pyridine gave the 'diaminoporphyrin' **153** in quantitative yield (**Scheme 61**).



Scheme 61: Synthesis of 5,10,15,20-tetrakis-(3,5-di-*tert*-butylphenyl)-2³-2⁴-diaminoquinoxalino[2,3-*b*]porphyrin 153 ('diaminoporphyrin')

The eight *tert*-butyl groups (72 protons) of 'diaminoporphyrin' were certainly inconvenient when it came to ¹H-NMR spectroscopy but aided solubility. In comparison 5,10,15,20-tetrakis-(3,5-di-*tert*-butylphenyl)porphyrin is 390 times more soluble in hexane than 5,10,15,20-tetraphenylporphyrin.²²³ Where applicable proton signals hidden under the giant *tert*-butyl signal were detected with the aid of a COSY experiment.

With the description of the synthesis of 'diaminoporphyrin' **153** chapter **B** on 'Syntheses' concludes. Most of the work undertaken during the PhD period has been outlined. Experimental details of the reactions above can be found in **D** 'Experimental Part'. A summary of the achievements is given in the following chapter **C** 'Summary and Conclusion'.

C 'SUMMARY & CONCLUSION'

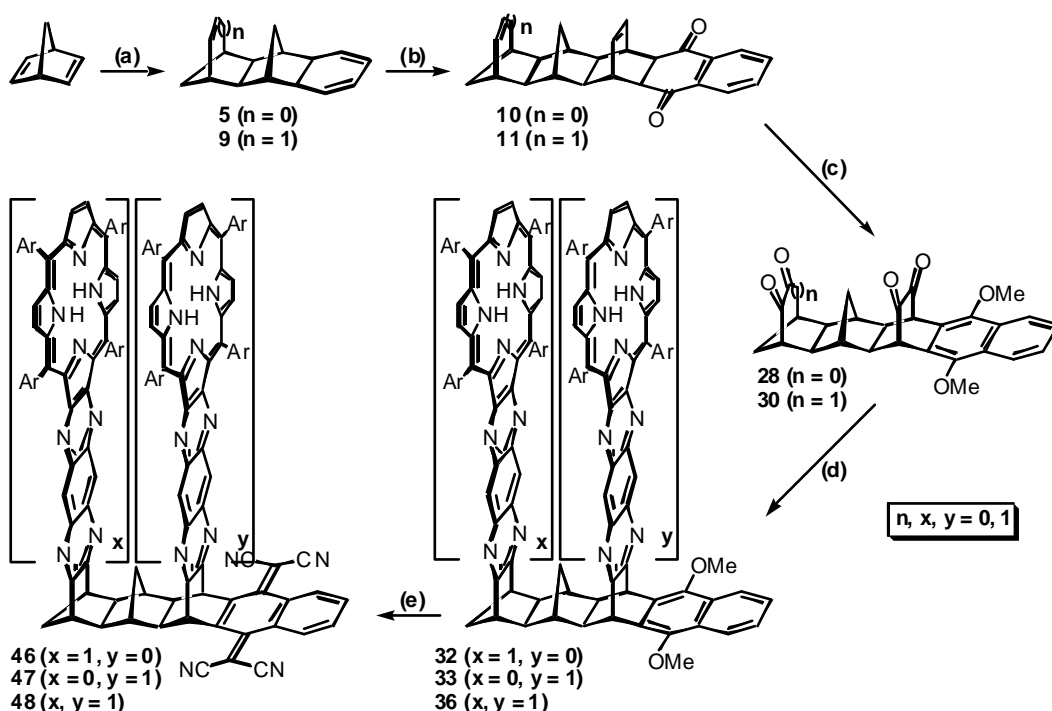


C SUMMARY & CONCLUSION

Eleven ambitious targets were chosen for the 'Synthesis of Advanced 'Special Pair' Models for the Photosynthetic Reaction Centre' (chapter A.7) with seven being achieved to date. Where the synthesis of the target was not successful, pathways have been established that will enable their synthesis as part of future work.

C.1 THE SERIES OF DYADS

Results obtained from the synthesis of the dyads confirmed the elegance of the strategic concept: building the carbon backbones, Diels-Alder reaction with naphthoquinone, introduction of keto functionalities, subsequent attachment of the porphyrin moieties and increase of the acceptor strength (DMN to TCNQ) worked well (**Scheme 62**).



Scheme 62: The dyad strategy. (a) building the backbone; (b) Diels-Alder reaction with naphthoquinone; (c) introduction of keto functionalities; (d) attachment of porphyrin moieties; (e) increase of the acceptor strength

Calculations on the free energy change (ΔG^0) for a photoinduced electron-transfer reaction (**Equation 14**) have shown that electron transfer is thermodynamically not accessible for the porphyrin-DMN dyads but is accessible for the three synthesised porphyrin-TCNQ

bichromophores. Evidence for a non-radiative decay, such as electron transfer, was found in the steady state fluorescence spectra of the TCNQ systems. Comparison of the fluorescence spectra with the ones obtained from their DMN analogues revealed a >94 % fluorescence quenching (**Figure 36**, page 76) indicating a high efficiency of a non-radiative pathway. Time-resolved spectroscopic techniques are able to detect the presence of a charge-separated state, such as $[P^{\bullet+}-TCNQ^{\bullet-}]$, and will have to confirm that the non-radiative decay observed is the desired electron-transfer process.

^1H -NMR techniques revealed an interaction between the two porphyrins of the 'special pair' dyads (**36**, **45**, and **48**) synthesised. The interaction is evident in an upfield shift of 0.2 - 0.3 ppm by the inner protons (NH) of the porphyrin moieties (**Figure 35**). Fears that the interporphyrinic separation would be too large to achieve the 'special pair' character desired were therefore not necessarily justified (**Figure 75**).

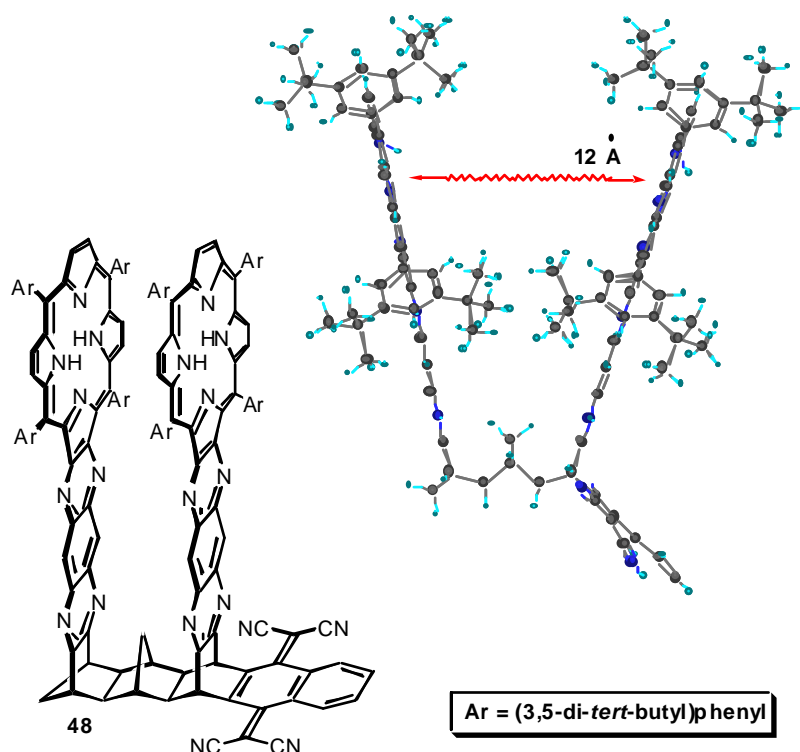
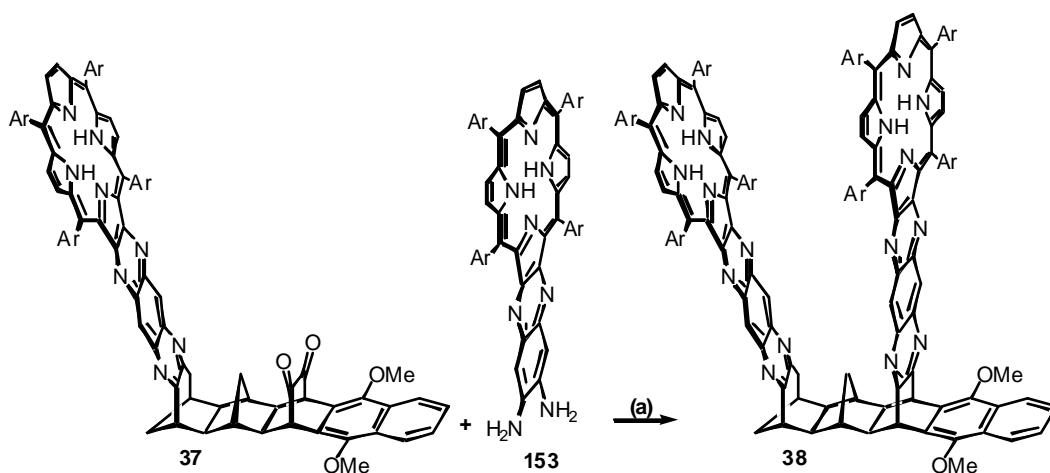


Figure 75: Interaction despite 12 Å separation (AM1)

The interaction between the two porphyrins proves the success of our systematic approach towards the synthesis of 'special pair' photosynthetic mimics. Concepts to introduce differently metallated porphyrins into the 'special pair' have been outlined (**Scheme 20** and **Figure 48**). On the basis of these systems, selective excitation of one porphyrin moiety would

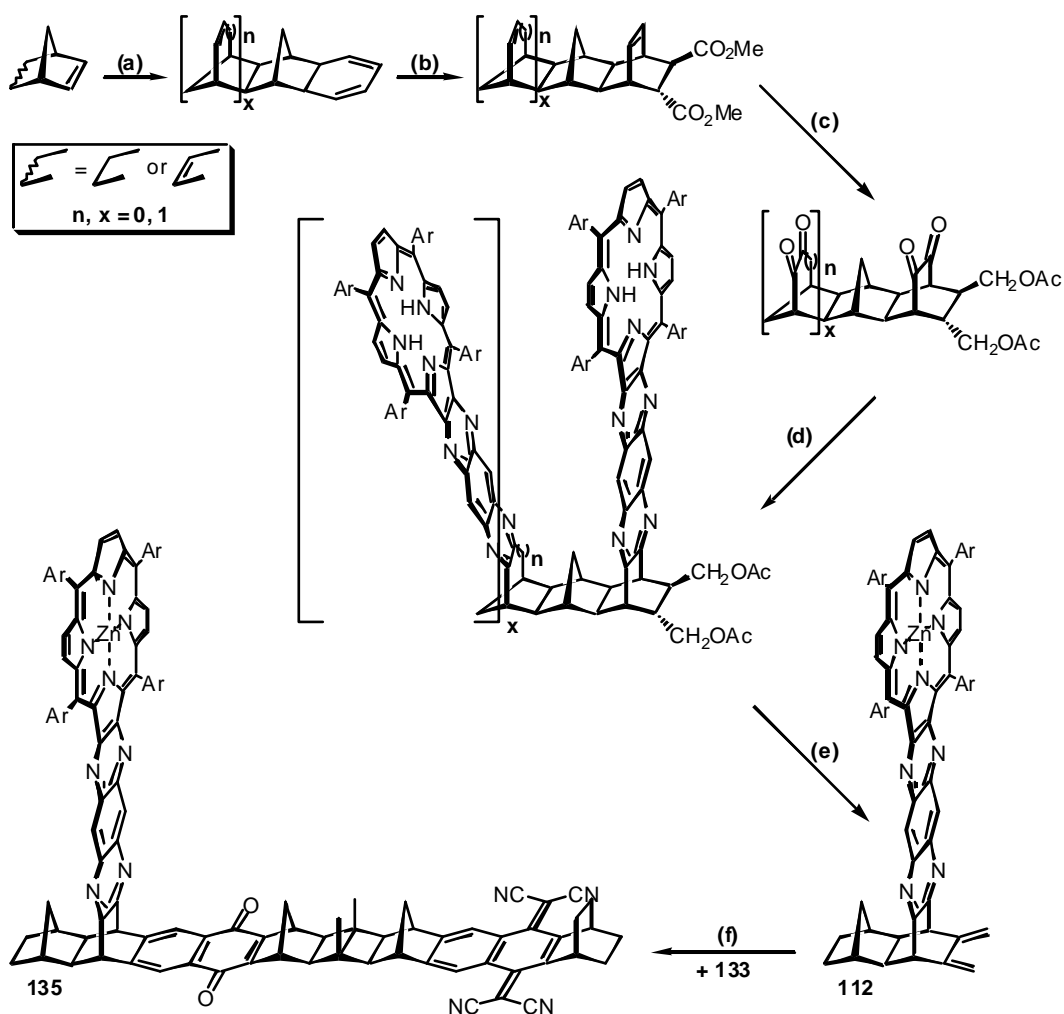
allow the study of interporphyrin (through space) energy, electron, and hole-transfer processes in conjunction with the projected electron transfer to the TCNQ acceptor. The potential of our bichromophoric 'special pair' models is convincing. With the addition of the kinked bis-porphyrin dyads, the targeted series of bichromophores will be completed. Problems experienced with the attachment of a second 'diaminoporphyrin' molecule should be overcome by the application of high pressure as used in the synthesis of the triad donors (**B.3.1.4**, page 97). The according experiment was carried out but a technical fault (the reaction vessel burst!) disabled not just the confirmation of the proposed high-pressure method but also the successful synthesis of the kinked bis-porphyrin dyads to date.



Scheme 63: High pressure to the rescue? Proposed conditions (a) DCM, 15 kbar, 80 °C, 3 d

C.2 THE SERIES OF TRIADS

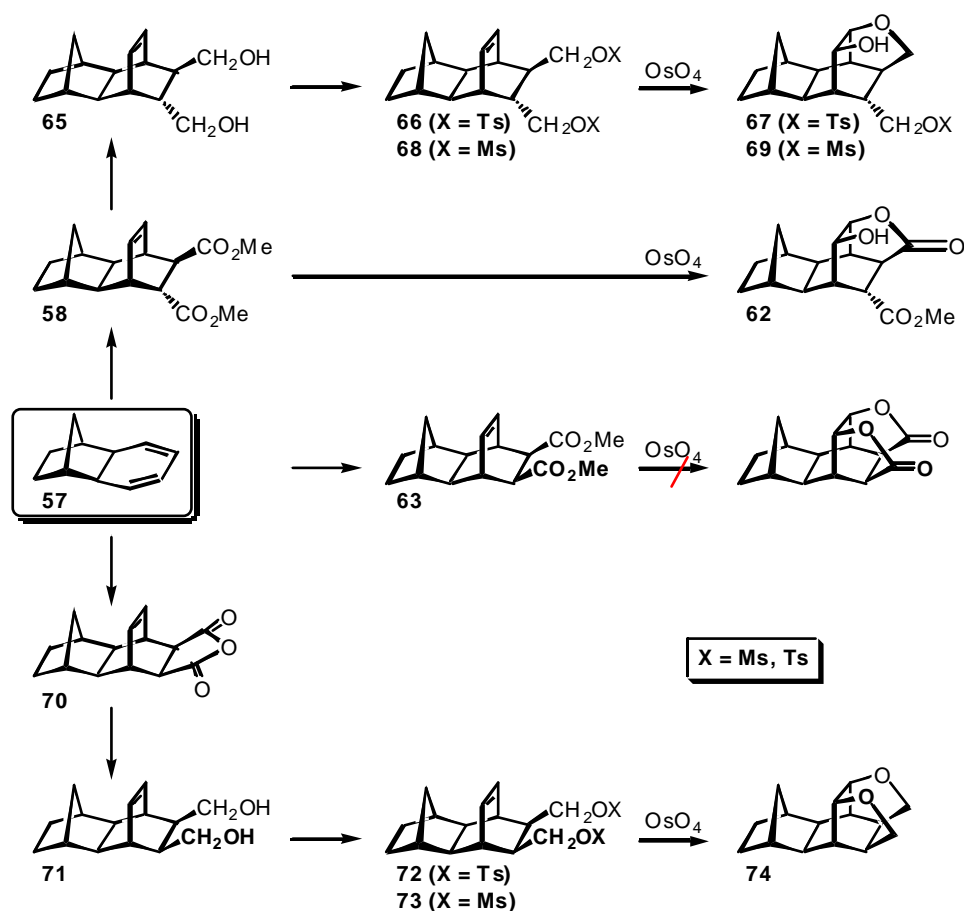
The series of triads comprises an extension to the successful work carried out on the synthesis of the series of dyads. Unfortunately the synthesis of the triads was not as smooth as the synthesis of the bichromophoric systems. A number of synthetic challenges, in particular with the synthesis of the triad donors, had to be met. The challenges were met and added interesting findings, such as the 'bis-ketonisation' under *Sharpless* 'bis-hydroxylation' conditions, to the outcome of this thesis. More importantly all problems faced were finally overcome and allowed at least the successful synthesis of the 2B-porphyrin-NQ-TCNQ trichromophore **131** within the given time limit. After alterations of functional groups and reaction conditions, the strategic plan originally developed proved to be a successful approach towards the synthesis of advanced trichromophoric photosynthetic mimics (**Scheme 64**).



Scheme 64: The triad strategy. (a) building the backbone; (b) Diels-Alder reaction with dimethyl fumarate; (c) introduction of keto-functionalities; (d) attachment of porphyrin moieties; (e) conversion to enophile; (f) assembling the triad

The developed procedures which led to the successful synthesis of the 2B-porphyrin-NQ-TCNQ giant trichromophore **135** are believed to be valid for the synthesis of its 'special pair' analogues as well. Therefore, we are confident that with this thesis a successful method has been developed for synthesising the giant kinked and non-kinked bis-porphyrin-NQ-TCNQ triads in the near future.

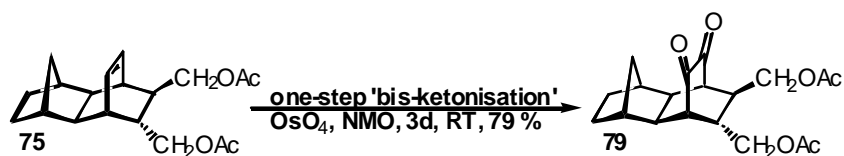
Amongst the problems faced in the synthesis of the series of triads were the number of unfortunate ring-closure reactions under *Sharpless* bis-hydroxylation conditions (**Scheme 65** and **B.3.1.1**, page 82).



Scheme 65: Ring-closure reactions under *Sharpless* bis-hydroxylation conditions

Those lactone and furan formations were circumvented by the introduction of acetoxy groups. No ring-closure was observed for the 2B-ene-*trans*-diacetate **75** exposed to the bis-hydroxylation conditions but further oxidation to the corresponding dione occurred.

This finding was by all means surprising but to an equal extent welcome, as it consequently would save one synthetic step and potentially avoid anticipated solubility problems of the corresponding alcohols, if promoted from a side-reaction to the main reaction pathway. By tuning the *Sharpless* bis-hydroxylation conditions they became 'bis-ketonisation' conditions and the one-step formation of the 2B-dione-*trans*-diacetate **79** from the 2B-ene-*trans*-diacetate **75** was achieved in 79 % yield (**Scheme 66**).



Scheme 66: Optimised 'bis-ketonisation' conditions - 2 % OsO_4 , 6 eq NMO, high concentration in 1,4-dioxane, three days at RT

Even more intriguing was the finding that the 'bis-ketonisation' was not restricted to the diacetate but worked equally well for similar [2.2.2] ring systems (**Table 9**, page 91). In contrast, [2.2.1] and [3.2.1] ring systems did not convincingly undergo further oxidation to the ketones under the 'bis-ketonisation' conditions applied to the [2.2.2] ring-systems (**Scheme 32**, page 91). Both the OsO_4 solution as well as the N-methylmorpholine-N-oxide were found to be essential for the ketonisation to proceed. Different geometries of the intermediate [2.2.1], [2.2.2], or [3.2.1] osmate ester were put forward as an explanation for the promotion or non-promotion of the ketonisation pathway.

Pleasant side effect of this discriminating behaviour was the conceptual possibility of a stepwise introduction of keto functionalities and consequently the (different) porphyrin moieties (**Figure 76**).

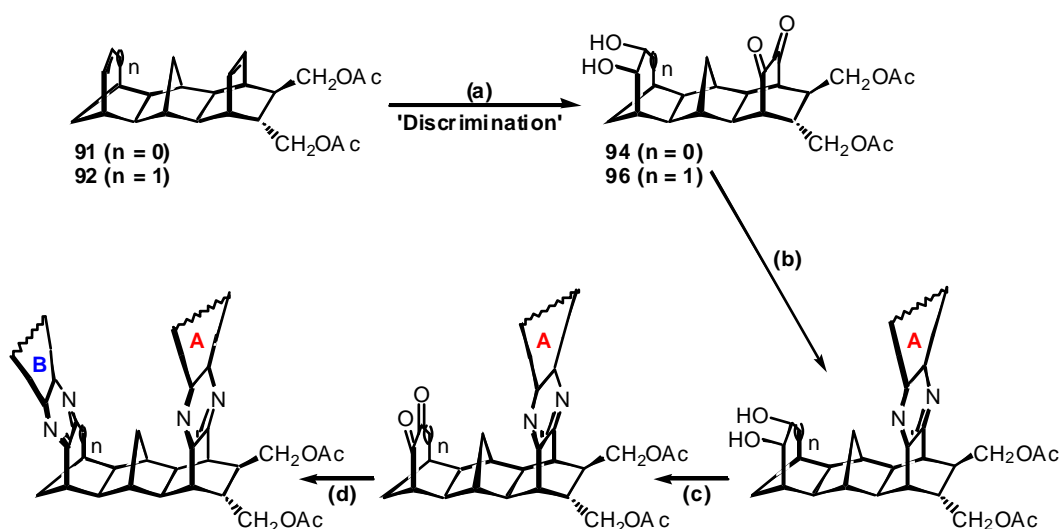
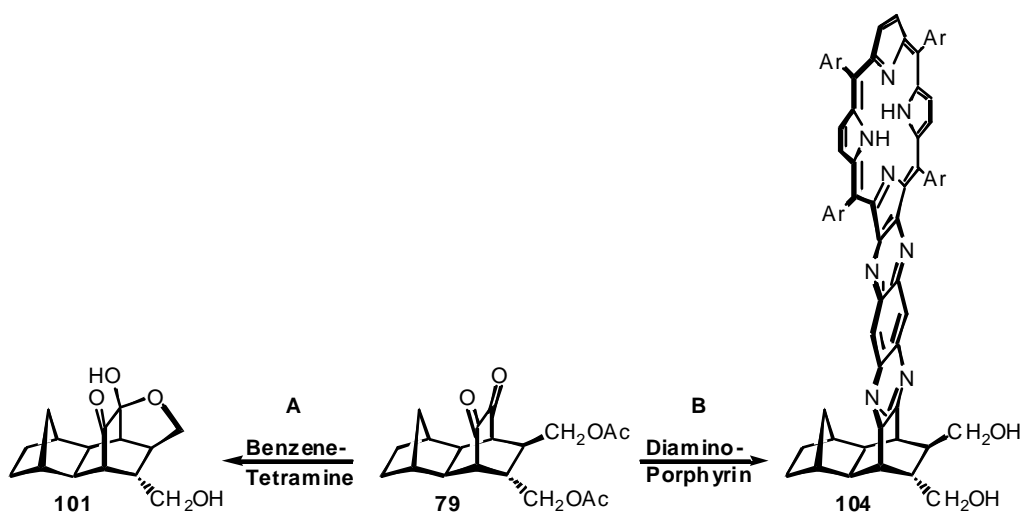


Figure 76: Controlled attachment of two different porphyrin moieties (A and B) through (a) selective 'bis-ketonisation' followed by (b) condensation, (c) TEMPO reaction, and (d) condensation of second porphyrin

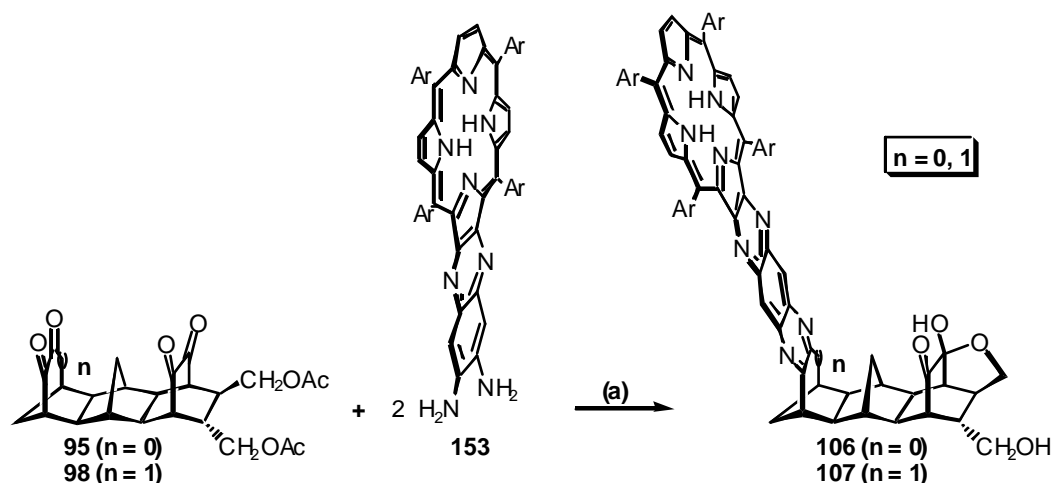
The attachment of the porphyrin moiety, however, comprised another problem faced in the synthesis of the triad donors. The bulky acetoxy groups next to the reacting keto functionalities limited their accessibility to an extent that under 'normal' conditions, namely atmospheric pressure, no condensation occurred. The application of high pressure (15 kbar) led to a conversion of the 2B-dione-*trans*-diacetate **79**, however, the products obtained with benzenetetramine or 'diaminoporphyrin' in pyridine were not the desired ones. The reaction with benzenetetramine gave the hemi-acetal **101** and with 'diaminoporphyrin' the successful condensation was accompanied by the loss of the acetoxy groups (**Scheme 67**).



Scheme 67: High-pressure reactions in anhydrous pyridine

Two different mechanisms were proposed for the loss of the acetoxy groups, depending on the presence or absence of water. In the absence of water, namely a non-proceeding condensation (**Scheme 67 A**), a nucleophilic attack of the strong base benzenetetramine at the carboxyl group rather than the carbonyl group was proposed for the reaction in high pressure (**Scheme 41**, page 103). With the condensation successfully proceeding (**Scheme 67 B**), water is released, which is then causing the hydrolysis of the acetoxy groups in the basic medium pyridine (**Scheme 44**, page 105).

Basic hydrolysis was also put forward as an explanation for the formation of the 6B-porphyrin-hemi-acetals **106** and **107** in pyridine (**Scheme 68**). The condensation was found to proceed at the more accessible 6B-dione first and the water released led to the hemi-acetal formation before the second porphyrin was attached.



Scheme 68: Hemi-acetal formation in pyridine. (a) 15 kbar, 80 °C, 3 d

In dichloromethane the hydrolysis of the acetoxy groups and consequently the hemi-acetal formation was avoided, resulting in the sought after 2B-porphyrin-*trans*-diacetate **103** (**Figure 54**, page 107) and the bis-porphyrin-*trans*-diacetate **100** (**Scheme 46**, page 109).

With the successful attachment of the porphyrin moieties, the major obstacles in the synthesis of the triad donors had been overcome. The conversion into the 2B-porphyrin-dienophile **112** worked well (**Scheme 48**, page 113) and so did the synthetic procedures envisaged for the synthesis of the bridge **123** (**Scheme 49**, page 117), the acceptor precursor **129** (**Scheme 53**, page 120) and the bridge-acceptor component **133** (**Scheme 55**, page 122 and **Scheme 56**, page 122), all depicted in **Figure 77**.

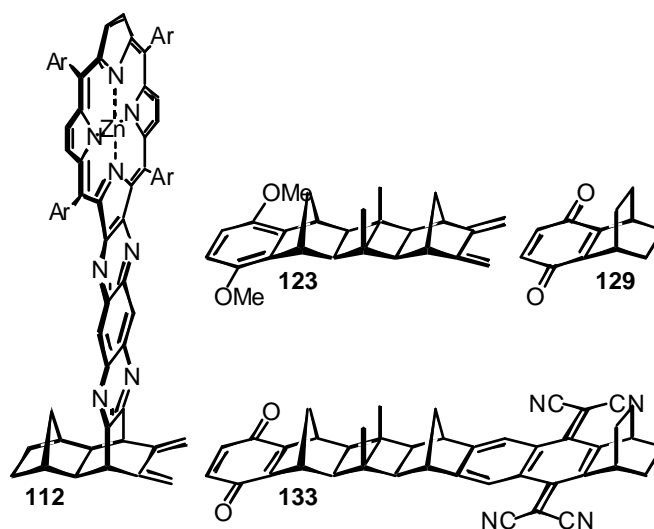


Figure 77: Triad components 2B-porphyrin-2,3-dimethylidene 112, bridge 123, acceptor precursor 129, and the bridge-acceptor component 133

Obstacles on the synthetic pathway re-appeared when the final two steps of the 48-step synthesis of 2B-porphyrin-NQ-TCNQ **135**, a Diels-Alder reaction followed by an aromatisation with 2,3-dichloro-5,6-dicyano-1,4-benzoquinone (DDQ), gave a "wealth" of side-products, making the purification and unmistakable characterisation somewhat difficult. Despite those difficulties evidence was presented that strongly indicate the successful synthesis of the giant trichromophore **135** (**Figure 78**) as the first example of the targeted series of three triads.

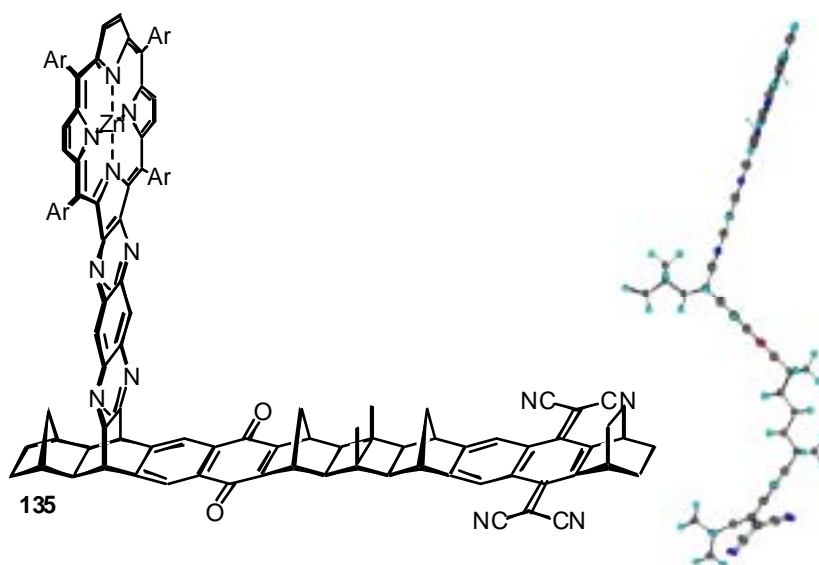


Figure 78: 2B-porphyrin-NQ-TCNQ 135, shown the *syn* isomer (AM1)

With the knowledge gained from **135**'s synthesis, the syntheses of the kinked and non-kinked bis-porphyrinic analogues, two truly advanced 'special pair' photosynthetic mimics, are expected to be straightforward. The interaction between the two 'special pair' porphyrin units is anticipated to be similar to the one found for the bichromophoric systems as AM1 calculations reveal almost identical porphyrin-porphyrin distances. Both electron transfer "hops", from the porphyrin to the naphthoquinone as well as from the naphthoquinone unit to the TCNQ are thermodynamically accessible (**Figure 39**, page 78). Two subsequent electron transfer processes result in a giant charge separated state, which is expected to exhibit a lifetime greater than the one anticipated for the corresponding dyad. Again, time-resolved spectroscopic methods will have to shed light onto the photophysical characteristics of the series of trichromophoric photosynthetic models.

C.3 THE ALL-TRANS RING-EXPANDED DYAD

The final section of chapter **B** 'Syntheses' outlined the successful preparation of the all-*trans* ring-expanded dyad **147** (**Scheme 69**). In the light of the parity rule compound **147**, or more importantly its TCNQ analogue **137** (**Figure 79**, $n = 1$, $m = 0$), will enable an interesting study through comparison with the corresponding non-ring-expanded (**Figure 79**, n , $m = 0$) and double-ring-expanded systems (**Figure 79**, n , $m = 1$), either synthesised previously or suggested for synthesis.

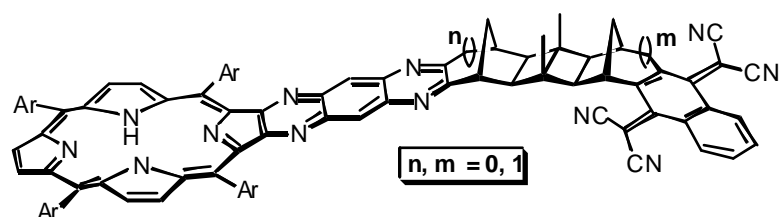
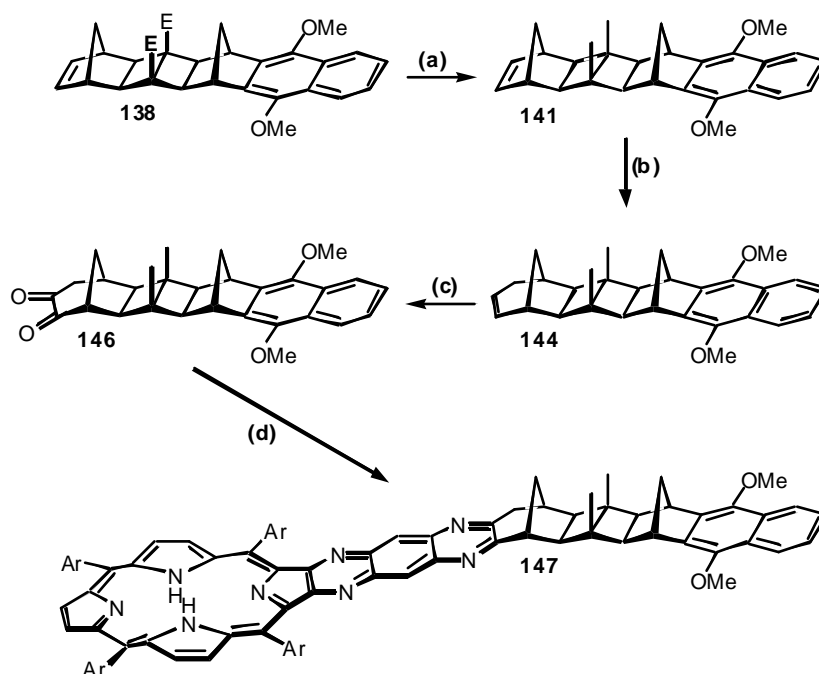


Figure 79: Three all-*trans* ring-expanded 6B-porphyrin-TCNQ systems

The synthesis of the all-*trans* ring-expanded 6B-porphyrin-DMN **147** started with the diester-DMN **138** and proceeded as planned: conversion of ester into methyl groups, ring-expansion, introduction of keto-functionalities, and attachment of 'diaminoporphyrin' **153** (Scheme 69).



Scheme 69: The all-*trans* strategy. (a) Conversion of ester into methyl groups; (b) ring-expansion; (c) introduction of keto-functionalities, and (d) attachment of 'diaminoporphyrin'

The all-*trans* ring-expanded 6B-porphyrin-DMN **147** was characterised by ^1H -NMR spectroscopy and MALDI mass spectrometry. For ^{13}C -NMR spectroscopy the required amount of dyad was not available and the conversion of the DMN unit into the TCNQ acceptor, known from the synthesis of the series of dyads (B.2.4, page 69), was not attempted. Initially designed as a small side project, the synthesis of all-*trans* ring-expanded systems has proven potential to be an accessible and worthwhile project in a larger context.

The description of the synthesis of known 'daminoporphyrin' **153**, outlined in the last section of chapter **B**, completed the picture on the 'Synthesis of Advanced 'Special Pair' Models for the Photosynthetic Reaction Centre'.

In summary, the project has provided the synthetic challenges anticipated. Solutions on how to meet these challenges have been provided and will greatly benefit future work in this area. Research never ends, and so will the investigation of fascinating natural systems, such as the photosynthetic reaction centre continue.

D 'EXPERIMENTAL PART'

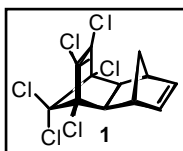


D EXPERIMENTAL PART

Chemicals were purchased from major chemical suppliers and used as received. Solvents were dried, and reagents purified where necessary using literature procedures.²²⁴ AR-grade toluene, 1,4-dioxane and *iso*-propanol were used. Pyridine and tetrahydrofuran was used anhydrous only. Anhydrous 1,4-dioxane and dichloromethane were used where indicated. Dichloromethane and chloroform were distilled prior to use. Celite filter aid R70 was obtained from Ajax Chemicals. Thin-layer chromatography (TLC) was carried out on aluminium sheets precoated with Merck 5735 Kieselgel 60F. Column chromatography was carried out using Merck 9385 Kieselgel 60 (0.040 - 0.063 mm mesh). Melting points were determined with a Melt-Temp (II) apparatus and are uncorrected. Low-resolution mass spectra (MS) were obtained using either electron impact (EI) or matrix-assisted laser desorption ionisation (MALDI) mass spectrometry. The EI mass spectra were recorded on a VG Quattro mass spectrometer with a 70 eV ionising voltage and an ion source temperature of 210 °C. The MALDI linear time-of-flight (TOF) mass spectra were recorded either on a Finnigan Lasermat 2000 spectrometer or a Kompact Maldi III instrument in conjunction with either a 3,5-dihydroxybenzoic acid or 2-cyano-hydroxy-cinnamic acid matrix. ¹H-NMR spectra were obtained on a Bruker AC300F (300 MHz) or a Bruker AM500 (500 MHz) spectrometer. ¹H-NMR data are reported as follows: chemical shift (δ) measured in parts per million down or up field from TMS, proton count, multiplicity and observed coupling constants (or line separations) in Hertz. Multiplicity is reported as singlet (s), broad singlet (bs), doublet (d), doublet of doublets (dd), doublet of triplets (dt), triplet (t), triplet of doublets (td), quartet (quart), quintet (q) or multiplet (m). ¹³C-NMR spectra were obtained on a Bruker AC300F (75.47 MHz) spectrometer. ¹³C-NMR data is reported as follows: chemical shift (δ) measured in parts per million down field from TMS and assignments are given if signals were identifiable. Assignment was determined with the aid of 90° and 135° DEPT experiments. IR spectra were recorded on a Perkin-Elmer Model 21. The UV-Vis absorption spectra were obtained using a CARY 5 spectrophotometer in dual-beam mode. Optically matched quartz cells (Starna) were used throughout. Crystallography data were obtained with an Enraf-Nonius CAD-4 diffractometer in $\theta/2\theta$ scan mode using nickel-filtered copper radiation ($\lambda = 1.5428 \text{ \AA}$).

D.1 SYNTHESIS OF THE DYADS

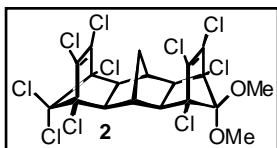
1,2,3,4,10,10-Hexachloro-1,4,4a,5,8,8a-hexahydro-*endo*-1,4-*exo*-5,8-dimethanonaphthalene (**1**)¹⁴⁵⁻¹⁴⁷



Hexachlorocyclopentadiene (119 mL, 202 g, 740 mmol) was added dropwise to refluxing norbornadiene (100 mL, 91 g, 987 mmol) over a period of 90 minutes. The mixture was heated at 120 °C for 5 hours with a white precipitate being formed. The yellow-orange mixture was allowed to cool down to RT and the white precipitate was filtered off, then washed with ice-cold light petroleum and dried under high vacuum. Yield: 188.64 g (516 mmol, 70 %) aldrin **1**. R_f (light petroleum/ethyl acetate 3:1) = 0.62; Melting point: 101-102 °C, m/z : 364.

$^1\text{H-NMR}$ (300 MHz, CDCl_3): δ = 1.33 (1H, d, J = 11.3 Hz), 1.57 (1H, d, J = 11.3), 2.73 (2H, s), 2.89 (2H, bs), 6.32 (2H, bs) ppm; $^{13}\text{C-NMR}$ (75.5 MHz, CDCl_3): δ = 40.8 (CH_2), 40.9 (2CH), 54.6 (2CH), 80.0 (2CCl), 105.4 (CCl_2), 130.7 (2=CCl), 141.1 (2=CH) ppm.

(1 α ,4 α ,4 $\alpha\alpha$,5 α ,8 α ,8 $\alpha\alpha$,9 β ,9 $\alpha\alpha$,10 β ,10 $\alpha\alpha$)-1,2,3,4,5,6,7,8,12,12-Decachloro-4a,8a,9,9a,10,10a-hexahydro-1,4:5,8:9,10-trimethano-13,13-dimethoxyanthracene (**2**)

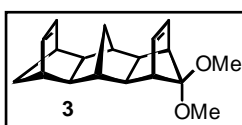


A solution of **1** (139.6 g, 382 mmol) and 5,5-dimethoxy-1,2,3,4-tetrachlorocyclopentadiene (67.2 mL, 100.8 g, 382 mmol) in toluene (130 mL) was heated at reflux in reference to literature procedures^{148,170}

for 46 hours. The mixture was placed in the freezer to form a white precipitate, which was filtered off, washed with ice-cold light petroleum and dried under high vacuum. Yield: 171.74 g (273 mmol, 71.5 %) **2**. Melting point: 241-243 °C.

$^1\text{H-NMR}$ (300 MHz, CDCl_3): δ = 1.20 (2H, bs), 2.46 (2H, s), 2.60 (2H, s), 2.64 (2H, s), 3.51 (3H, s), 3.59 (3H, s) ppm; $^{13}\text{C-NMR}$ (75.5 MHz, CDCl_3): δ = 28.2 (CH_2), 35.5 (2CH), 51.8 (OCH_3), 52.7 (OCH_3), 57.3 (4CH), 80.1 (2CCl), 80.2 (2CCl), 104.4 (CCl_2), 114.1 ($\text{C}(\text{OMe})_2$), 129.0 (2=CCl), 130.6 (2=CCl) ppm.

(1 α ,4 α ,4 $\alpha\alpha$,5 α ,8 α ,8 $\alpha\alpha$,9 β ,9 $\alpha\alpha$,10 β ,10 $\alpha\alpha$)-1,4,4a,5,8,8a,9,9a,10,10a-Decahydro-1,4:5,8:9,10-trimethano-13,13-dimethoxyanthracene (**3**)



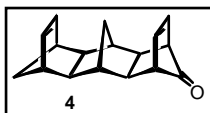
To a refluxing colourless solution of **2** (42.9 g, 68.2 mmol) in a mixture of tetrahydrofuran (250 mL) and *iso*-propanol (200 mL) was added sodium (125 g, 5.4 mol, ~80 eq.) in small pieces over a period of 3 hours.^{148,170}

After two, three and four days more *iso*-propanol (3 x 100 mL) was added to the purple

mixture. After five days the mixture was poured onto ice. The organic phase was extracted with diethyl ether (3 x 400 mL). The combined organic layers were washed with H₂O (2 x 300 mL), half-saturated NaHCO₃ (400 mL) and brine (300 mL) then dried over Na₂SO₄. The solvents were removed under reduced pressure to yield 18 g of a dark yellow/brown oil, which was crystallised from dichloromethane/methanol to give the product as a white solid. The mother liquor was purified by column chromatography (light petroleum/ethyl acetate 4:1) to give further product and 4 g of partly dechlorinated compounds. Yield: 10.45 g (36.6 mmol, 53.6 %) **3**. R_f (light petroleum/ethyl acetate 3:1) = 0.52; Melting point: 104 °C; m/z: 284; elemental analysis for C₁₉H₂₄O₂: C 80.24, H 8.51, found: C 80.12, H 8.47.

¹H-NMR (300 MHz, CDCl₃): δ = 1.18 (1H, d, *J* = 7.7 Hz), 1.27 (1H, dt, *J* = 7.7, 2.0 Hz), 1.57 (1H, d, *J* = 12.3 Hz), 1.65 (1H, d, *J* = 12.3 Hz), 1.90 (2H, bs), 1.98 (4H, q, *J* = 2.0 Hz), 2.80 (2H, q, *J* = 2.0 Hz), 2.85 (q, *J* = 2.2 Hz), 3.06 (3H, s), 3.18 (3H, s), 5.87 (2H, t, *J* = 2.2 Hz), 5.93 (2H, t, *J* = 2.2 Hz) ppm; ¹³C-NMR (75.5 MHz, CDCl₃): δ = 30.6 (CH₂), 39.8 (2CH), 46.6 (2CH), 48.5 (4CH), 49.6 (2CH), 51.3 (OCH₃), 52.0 (OCH₃), 53.7 (CH₂), 132.5 (2=CH), 135.6 (2=CH) ppm.

(1α,4α,4α,5α,8α,8α,9β,9α,10β,10α)-1,4,4a,5,8,8a,9,9a,10,10a-Decahydro-1,4:5,8:9,10-trimethano-anthracen-13-one (4)

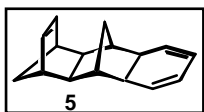


Following literature procedure^{148,170} formic acid (90 %, 50 mL) was added to a solution of **3** (4.7 g, 16.5 mmol) in tetrahydrofuran (50 mL). The colourless solution was stirred at RT for 24 hours. Then Diethyl ether (100 mL) and H₂O (100 mL) were added, and the aqueous phase was extracted with diethyl ether (3 x 100 mL). The combined organic layers were washed with H₂O (100 mL), 1M K₂CO₃ (4 x 50 mL) and H₂O (100 mL) then dried over Na₂SO₄. The solvent was removed under reduced pressure and the crude product was purified by column chromatography (light petroleum/ethyl acetate 4:1). Yield: 2.56g (10.8 mmol, 65 %) **4** as a white solid. Melting point: 103 - 105 °C; m/z: 238, 210 (-CO).

¹H-NMR (300 MHz, CDCl₃): δ = 1.14 (2H, d, *J* = 8.2 Hz), 1.27 (1H, d, *J* = 8.2 Hz), 1.46 (1H, d, *J* = 12.3 Hz), 1.66 (1H, d, *J* = 12.3 Hz), 1.91 (2H, s), 2.00 (2H, s), 2.24 (2H, s), 2.82 (2H, s), 3.06 (2H, d, *J* = 2.1 Hz), 5.88 (2H, s), 6.28 (2H, t, *J* = 2.6 Hz) ppm; ¹³C-NMR (75.5 MHz, CDCl₃): δ = 31.2 (CH₂), 42.1 (2CH), 45.2 (2CH), 46.6 (2CH), 50.9 (2CH), 51.7 (2CH), 53.4 (CH₂), 130.5 (2=CH), 135.6 (2=CH), 199.7 (C=O) ppm.

IR (KBr): 3048, 2940, 2908, 1789, 1767, 1472, 1354, 1081, 844, 747 cm⁻¹.

(1 α ,4 α ,4 α ,8 α ,9 β ,9 α ,10 β ,10 α)-1,4,4a,8a,9,9a,10,10a-Octahydro-1,4:9,10-dimethanoanthracene (5)



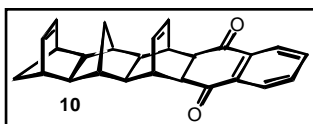
A solution of **4** (2.54 g, 10.66 mmol) in toluene (85 mL) was heated at reflux for 20 minutes. The solution was allowed to cool down to RT and the solvent was removed under reduced pressure. Yield: 2.20 g (10.47 mmol, 97.8 %) **5**

as a white solid. Melting point: 49-51 °C; *m/z*: 210; elemental analysis for C₁₆H₁₈: C 91.37, H 8.63, found: C 91.04, H 8.71.

¹H-NMR (300 MHz, CDCl₃): δ = 1.13 (1H, d, *J* = 7.2 Hz), 1.19 (1H, d, *J* = 10.2 Hz), 1.28 (1H, d, *J* = 7.2 Hz), 1.89 (2H, bs), 2.09 (1H, d, *J* = 10.2 Hz), 2.13 (2H, bs), 2.31 (2H, bs), 2.84 (2H, bs), 5.39 (2H, m), 5.55 (2H, m), 5.95 (2H, s) ppm; ¹³C-NMR (75.5 MHz, CDCl₃): δ = 30.2 (CH₂), 45.4 (2CH), 46.7 (2CH), 47.6 (2CH), 49.5 (2CH), 52.3 (CH₂), 121.5 (2=CH), 128.2 (2=CH), 135.4 (2=CH) ppm.

IR (KBr): 3053, 3024, 2961, 293, 2893, 2866, 1465 cm⁻¹.

(1 α ,4 α ,4a β ,5 α ,5a β ,6 α ,6a β ,12a β ,13 α ,13a β ,14 α ,14a β)-6,13-Etheno-(1,4,4a,5,5a,6,6a,7,12,12a,13,13a,14,14a)-tetradecahydro-1,4:5,14-dimethanopentacene-7,12-dione (10)



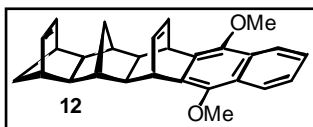
1,4-naphthoquinone (4.40 g, 28.10 mmol) was added to a refluxing solution of **5** (5.89 g, 28.01 mmol) in ethanol (90 mL). After 45 minutes at reflux a white precipitate was filtered off while hot. The

filtrate was heated at reflux for another 2 hours then cooled down to RT and further precipitate was collected. The combined precipitates were washed with ethanol and recrystallised from toluene. Yield: 7.65 g (20.76 mmol, 74.1 %) **10** as a white solid. Melting point: 255-260 °C; *m/z*: 368; elemental analysis for C₂₆H₂₄O₂: C 84.75, H 6.56, found: C 84.85, H 6.63.

¹H-NMR (300 MHz, CDCl₃): δ = 1.14 (1H, d, *J* = 8.2 Hz), 1.27 (1H, d, *J* = 8.2 Hz), 1.48 (1H, d, *J* = 11.3 Hz), 1.61 (1H, d, *J* = 11.3 Hz), 1.76 (2H, s), 1.89 (2H, s), 2.03 (2H, s), 2.82 (2H, bs), 3.14 (2H, s), 3.43 (2H, bs), 5.86 (2H, s), 5.96 (2H, m), 7.65 (2H, m), 7.96 (2H, m) ppm; ¹³C-NMR (75.5 MHz, CDCl₃): δ = 29.3 (CH₂), 40.9 (2CH), 43.4 (2CH), 46.5 (2CH), 50.5 (2CH), 50.9 (2CH), 51.6 (2CH), 53.4 (CH₂), 126.7 (2C_{Ar}H), 133.4 (2=CH), 133.9 (2C_{Ar}H), 135.5 (2=CH), 135.9 (2C_{Ar}), 197.6 (2C=O) ppm.

IR (KBr): 2941, 1673, 1639, 1271 cm⁻¹.

(1 α ,4 α ,4 β ,5 α ,5 β ,6 α ,6 β ,12 α ,13 α ,13 β ,14 α ,14 β)-6,13-Etheno-(1,4,4a,5,5a,6,13,13a,14,14a)-decahydro-1,4:5,14-dimethano-7,12-dimethoxypentacene (12**)**



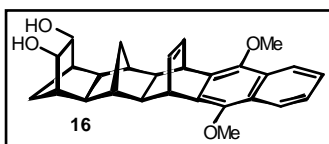
To an ice-cold suspension of **10** (6.72 g, 18.24 mmol) in tetrahydrofuran (120 mL) and HMPA (7.7 mL) was added dropwise a 0.5M solution of potassium bis(trimethylsilyl)amide (108 mL) in toluene (54 mmol). On completion of the addition (30 minutes) the mixture was stirred for another 60 minutes at 0 °C then methyl iodide (51 g, 360 mmol) was added and the mixture was stirred at RT overnight. The solvent was removed under reduced pressure and the residue was dissolved in diethyl ether. The ethereal solution was washed with H₂O (5 x 30 mL) then dried over Na₂SO₄. The solvent was removed under reduced pressure and the residue was recrystallised from acetone/ethanol 7:3. Yield: 5.05 g (12.74 mmol, 69.8 %) 6B-ene-2B-ene-DMN **12** as a white solid. Melting point: 172-174 °C; m/z: 396; elemental analysis for C₂₈H₂₈O₂: C 84.81, H 7.12, found: C 84.41, H 7.13.

¹H-NMR (300 MHz, CDCl₃): δ = 1.09 (1H, d, J = 7.2 Hz), 1.26 (1H, d, J = 7.2 Hz), 1.65 (2H, s), 1.77 (1H, d, J = 11.3 Hz), 1.79 (2H, bs), 1.89 (1H, d, J = 11.3 Hz), 2.19 (2H, s), 2.80 (2H, bs), 3.94 (6H, s), 4.42 (2H, t, J = 4.1 Hz), 5.92 (2H, t, J = 2.0 Hz), 6.41 (2H, m), 7.44 (2H, m), 8.05 (2H, m) ppm; ¹³C-NMR (75.5 MHz, CDCl₃): δ = 29.9 (CH₂), 38.6 (2CH), 42.9 (2CH), 46.5 (2CH), 50.8 (2CH), 52.0 (2CH), 53.6 (CH₂), 62.7 (2OCH₃), 122.2 (2C_{Ar}H), 125.2 (2C_{Ar}H), 127.1 (2C_{Ar}), 134.7 (2C_{Ar}), 135.0 (2=CH), 135.5 (2=CH), 144.9 (2C_{Ar}OMe) ppm. IR (KBr): 3015, 2980, 2949, 2946, 1603, 1456, 1370, 1348, 1281, 1067 cm⁻¹.

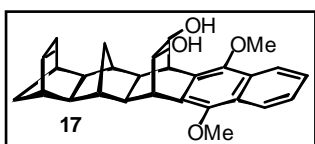
(1 α ,2 α ,3 α ,4 α ,4 α ,5 β ,5 α ,6 β ,13 β ,13 α ,14 β ,14 α)-6,13-Etheno-(1,2,3,4,4a,5,5a,6,13,13a,14,14a)-dodecahydro-2,3-*cis*-dihydroxy-1,4:5,14-dimethano-7,12-dimethoxypentacene (16**) and (1 α ,4 α ,4 α ,5 β ,5 α ,6 β ,13 β ,14 β ,14 α)-6,13-Ethano-(1,4,4a,5,5a,6,13,13a,14,14a)-decahydro-16,17-*cis*-dihydroxy-1,4:5,14-dimethano-7,12-dimethoxypentacene (**17**)**

To a suspension of 6B-ene-2B-ene-DMN **12** (1.74 g, 4.38 mmol) and 4-methyl-N-morpholine-N-oxide (0.51 g, 4.4 mmol) in 1,4-dioxane (20 mL) and H₂O (2.5 mL) was added OsO₄ (45 mg, 4 %) in *t*-butanol (9 mL). The resulting yellow solution was stirred at 45 °C for 8 days, then cooled to RT and filtered. The filtrate was treated with Na₂S₂O₅ (aq.) and stirred for 30 minutes. Layers were separated and the solvent was removed under reduced pressure. The residue was extracted with boiling chloroform. Upon cooling to RT the tetraol-DMN **19** precipitated and was filtered off. The solvent was removed from the filtrate and the crude residue, containing the corresponding diols, was purified by column chromatography

(dichloromethane, then dichloromethane/ethyl acetate 85:15). Yield (**16**): 489 mg (1.14 mmol, 26.0 %) 6B-diol-2B-ene-DMN **16**. Melting point: 130-135 °C (dec.); m/z: 430. Yield (**17**): 140 mg (0.41 mmol, 10.7 %) 6B-ene-2B-diol-DMN **17**. Melting point: 125-128 °C (dec.); m/z: 430.

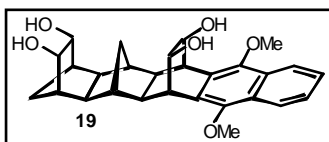


¹H-NMR (300 MHz, CDCl₃, **16**): δ = 0.65 (1H, d, *J* = 12.3 Hz), 1.02 (1H, d, *J* = 10.2 Hz), 1.56 (2H, bs), 1.64 (2H, bs), 1.78 (1H, d, *J* = 10.2 Hz), 2.19 (2H, bs), 2.29 (2H, bs), 2.34 (1H, d, *J* = 12.3 Hz), 3.92 (6H, s), 4.13 (2H, bs), 4.44 (2H, bs), 6.46 (2H, m), 7.44 (2H, m), 8.03 (2H, m) ppm; ¹³C-NMR (75.5 MHz, CDCl₃, **16**): δ = 31.1 (CH₂), 35.5 (CH₂), 38.5 (2CH), 41.2 (2CH), 48.6 (2CH), 50.6 (2CH), 51.0 (2CH), 62.7 (2OCH₃), 70.7 (2CHOH), 122.2 (2C_{Ar}H), 125.3 (2C_{Ar}H), 127.1 (2C_{Ar}), 134.3 (2C_{Ar}), 134.7 (2=CH), 145.0 (2C_{Ar}OMe) ppm. IR (KBr): 3405 (br), 3044, 2943, 2830, 1731, 1603, 1456, 1351, 1281, 1094, 1067, 1044, 969, 772, 751 cm⁻¹.



¹H-NMR (300 MHz, CDCl₃, **17**): δ = 0.87 (1H, d, *J* = 12.3 Hz), 1.08 (1H, d, *J* = 8.2 Hz), 1.30 (1H, d, *J* = 8.2 Hz), 1.48 (2H, bs), 1.83 (2H, bs), 2.22 (2H, bs), 2.29 (3H, m), 2.84 (2H, bs), 3.76 (2H, bs), 3.97 (6H, s), 4.31 (2H, bs), 5.99 (2H, s), 7.47 (2H, m), 8.09 (2H, m) ppm; ¹³C-NMR (75.5 MHz, CDCl₃, **17**): δ = 31.2 (CH₂), 39.8 (2CH), 40.2 (2CH), 46.6 (2CH), 49.4 (2CH), 49.7 (2CH), 53.6 (CH₂), 62.8 (2OCH₃), 65.7 (2CHOH), 122.2 (2C_{Ar}H), 125.4 (2C_{Ar}H), 127.7 (2C_{Ar}), 129.3 (2C_{Ar}), 135.3 (2=CH), 148.3 (2C_{Ar}OMe) ppm. IR (KBr): 3426 (br), 3045, 2950, 2929, 2831, 1739, 1633, 1602, 1456, 1351, 1278, 1068, 1010, 968 cm⁻¹.

(1α,2α,3α,4α,4α,5β,5α,6β,13β,13α,14β,14α)-6,13-Ethano-(1,2,3,4,4a,5,5a,6,13,13a,14,14a)-dodecahydro-2,3,16,17-cis-cis-tetrahydroxy-1,4:5,14-dimethano-7,12-dimethoxy-pentacene (19)



To a suspension of 6B-ene-2B-ene-DMN **12** (3.30 g, 8.32 mmol) and 4-methyl-N-morpholine-N-oxide (1.99 g, 17.0 mmol, ~2 eq.) in 1,4-dioxane (40 mL) and H₂O (5 mL) was added OsO₄ (42 mg, 2 %) in *t*-butanol (8.4 mL). The resulting yellow solution was stirred at 40 °C for 7 days, then a further aliquot of OsO₄ solution was added and the reaction mixture was stirred for a further 7 days. The solution was allowed to cool down to RT and then filtered. The filtrate was treated with Na₂S₂O₅ (aq.) and stirred for 30 minutes. Layers were separated and the solvent

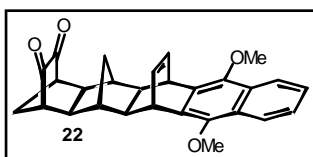
was removed under reduced pressure. The residue was extracted with 100 mL chloroform/*iso*-propanol (3:1). Removal of the solvent mixture yielded an off-white solid, which was combined with the initial precipitate and recrystallised from 1,4-dioxane. Yield: 2.18 g (4.69 mmol, 56.4 %) 6B-diol-2B-diol-DMN **19**. Melting point: >220 °C (dec.); *m/z*: 464.

¹H-NMR (300 MHz, DMSO-*d*₆): δ = 0.86 (1H, d, *J* = 9.5 Hz), 1.14 (1H, d, *J* = 12.4 Hz), 1.30 (2H, bs), 1.37 (1H, d, *J* = 12.4 Hz), 1.52 (2H, bs), 1.69 (1H, d, *J* = 9.5 Hz), 2.04 (2H, bs), 2.34 (2H, s), 3.59 (2H, bs), 3.88 (6H, s), 3.99 (2H, bs), 4.24 (2H, bs), 4.39 (2OH, bs), 4.51 (2OH, bs), 7.46 (2H, m), 7.98 (2H, m) ppm; ¹³C-NMR (75.5 MHz, DMSO-*d*₆): δ = 32.5 (CH₂), 35.3 (CH₂), 38.2 (2CH), 38.5-40.5 (4CH), 48.1 (2CH), 49.8 (2CH), 62.2 (2OCH₃), 64.1 (2CHOH), 69.0 (2CHOH), 121.7 (2C_{Ar}H), 124.9 (2C_{Ar}H), 126.8 (2C_{Ar}), 130.7 (2C_{Ar}), 147.1 (2C_{Ar}OMe) ppm.

IR (KBr): 3453 (br), 2931, 1631, 1604, 1457, 1353, 1068 cm⁻¹.

D.1.1 Synthesis of the 6B-Porphyrin-Dyads

(1α,2α,3α,4α,4α,5β,5α,6β,13β,13α,14β,14α)-6,13-Etheno-(1,4,4a,5a,6,13,13a,14,14a)-decahydro-1,4:5,14-dimethano-7,12-dimethoxypentacene-2,3-dione (**22**)



To a solution of 6B-diol-2B-ene-DMN **16** (392 mg, 0.910 mmol) and *p*-toluenesulfonic acid monohydrate (870 mg, 4.574 mmol, ~5 eq.) in dichloromethane (15 mL) was added dropwise 4-acetamido-TEMPO (986 mg, 4.623 mmol, ~5 eq.) in dichloromethane (25 mL)

at 0 °C in the dark. On completion of the addition (90 minutes) the mixture was stirred for 6 days in the dark at RT. A white precipitate was filtered off and ethanol (10 mL) was added to quench the reaction. The bright yellow solution was washed with H₂O (2 x 30 mL) and brine (30 mL) then dried over Na₂SO₄. The solvents were removed under reduced pressure to give a crude yellow solid (520 mg), which was purified by column chromatography (light petroleum/ethyl acetate 1:2). Yield: 245 mg (0.574 mmol, 63.1 %) 6B-dione-2B-ene-DMN **22** as a bright yellow solid. Melting point: 264-265 °C; *m/z*: 426.

¹H-NMR (300 MHz, CDCl₃): δ = 0.29 (1H, d, *J* = 14.0 Hz), 1.73 (2H, s), 1.83 (1H, d, *J* = 11.4 Hz), 1.96 (1H, d, *J* = 11.4 Hz), 2.19 (2H, s), 2.33 (2H, s), 2.52 (1H, d, *J* = 14.0 Hz), 3.06 (2H, s), 3.92 (6H, s), 4.45 (2H, bs), 6.44 (2H, t, *J* = 4.0 Hz), 7.45 (2H, m), 8.04 (2H, m) ppm;

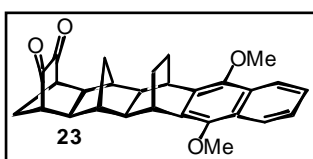
¹³C-NMR (75.5 MHz, CDCl₃): δ = 31.6 (CH₂), 33.4 (CH₂), 38.2 (2CH), 41.6 (2CH), 49.9

(2CH), 53.1 (2CH), 53.8 (2CH), 62.8 (2OCH₃), 122.2 (2C_{Ar}H), 125.5 (2C_{Ar}H), 127.2 (2C_{Ar}), 133.6 (2C_{Ar}), 134.6 (2=CH), 145.2 (2C_{Ar}OMe), 202.9 (2C=O) ppm.

IR(KBr): 2930, 1768, 1747, 1348, 1068, 748 cm⁻¹.

UV-Vis (CH₂Cl₂) λ_{max} (log ε): 462 (1.68), 326 (3.13), 288 (3.82) nm.

(1α,4α,4α,5α,6β,13β,13α,14β,14α)-6,13-Ethano-(1,4,4a,5,5a,6,13,13a,14,14a)-decahydro-1,4:5:14-dimethano-7,12-dimethoxypentacene-2,3-dione (23)



A suspension of 6B-dione-2B-ene-DMN **22** (242 mg, 0.567 mmol) and some 10% Pd/C in ethyl acetate (5 mL) was stirred at RT for 24 hours under a hydrogen atmosphere. The Pd/C was filtered off and the solvent was removed under reduced pressure. The crude yellow

product was purified by column chromatography (light petroleum/ethyl acetate 1:2). Yield: 225 mg (0.525 mmol, 92.6 %) yellow 6B-dione-DMN **23**. Melting point: 230-232 °C; m/z: 428; elemental analysis for C₂₆H₂₄O₂: C 78.48, H 6.59, found: C 77.99, H 6.66.

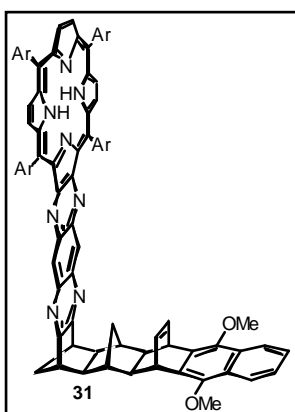
¹H-NMR (500 MHz, CDCl₃): δ = 0.71 (1H, d, *J* = 14.0 Hz), 1.32 (2H, d, *J* = 8.8 Hz), 1.50 (2H, s), 1.88 (1H, d, *J* = 11.4 Hz), 1.93 (2H, d, *J* = 8.8 Hz), 2.00 (1H, d, *J* = 11.4 Hz), 2.09 (1H, d, *J* = 14.0 Hz), 2.26 (2H, s), 2.39 (2H, s), 3.91 (6H, s), 7.48 (2H, m), 8.10 (2H, m) ppm;

¹³C-NMR (75.5 MHz, CDCl₃): δ = 21.3 (2CH₂), 30.9 (2CH), 31.8 (CH₂), 33.7 (CH₂), 39.6 (2CH), 46.3 (2CH), 53.5 (4CH), 62.7 (2 OCH₃), 122.3 (2C_{Ar}H), 125.3 (2C_{Ar}H), 127.5 (2C_{Ar}), 134.5 (2C_{Ar}), 145.6 (2C_{Ar}OMe), 203.3 (2C=O) ppm.

IR(KBr): 2939, 1769, 1746, 1355, 1075 cm⁻¹.

UV-Vis (CH₂Cl₂) λ_{max} (log ε): 458 (1.65), 324 (3.02), 294 (3.78) nm.

6B-Porphyrin-2B-ene-DMN (31)



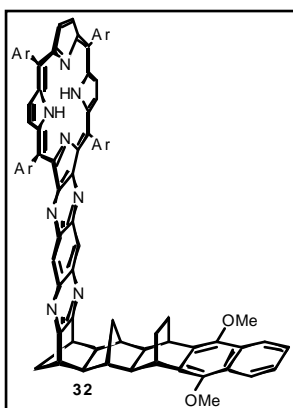
Method 1 (pressure tube): A solution of 6B-dione-2B-ene-DMN **22** (35 mg, 0.082 mmol) and 'diaminoporphyrin' **153** (90 mg, 0.075 mmol) in de-oxygenated pyridine (1 mL) was heated in a dark pressure tube at 125 °C for three days under an argon atmosphere. The solvent was removed under high vacuum and the crude product was purified by column chromatography (chloroform). Yield: 34 mg (0.021 mmol, 28.5 %) 6B-porphyrin-2B-ene-DMN **31**.

Method 2 (high pressure): A solution of 6B-dione-2B-ene-DMN **22** (30 mg, 0.0703 mmol) and 'diaminoporphyrin' **153** (84 mg, 0.0703 mmol) in de-oxygenated

pyridine (2 mL) was reacted for 3 days at 80 °C and 15 kbar. The solvent was removed under an argon stream. The crude product was dried under high vacuum and then purified by column chromatography (chloroform). Yield: 30 mg (0.0189 mmol, 26.9 %) 6B-porphyrin-2B-ene-DMN **31**. Melting point: >300 °C; MH^+ (MALDI): 1586.

1H -NMR (300 MHz, $CDCl_3$): δ = -2.36 (2H, s), -1.08 (1H, d, J = 12.7 Hz), 1.58 (72H), 1.83 (2H, s), 1.94 (1H, d, J = 12.7 Hz), 2.01 (1H, d, J = 8.8 Hz), 2.09 (1H, d, J = 8.8 Hz), 2.40 (4H, s), 3.64 (2H, s), 3.96 (6H, s), 4.45 (2H, s), 6.30 (2H, t, J = 3.9 Hz), 7.48 (2H, quart., J = 3.3 Hz), 7.84 (2H, t, J = 2.0 Hz), 7.98 (2H, t, J = 2.0 Hz), 8.07 (4H, m), 8.08 (2H, m), 8.14 (4H, dd, J = 2.0 Hz, 5.9 Hz), 8.58 (2H, s), 8.81 (2H, s), 9.03 (4H, AB_{quartet}, J = 4.9, 8.8 Hz) ppm; ^{13}C -NMR (75.5 MHz, $CDCl_3$): δ = 30.6 (CH_2), 31.8 ($12CH_3$), 32.0 ($12CH_3$), 35.1 (8C), 38.4 (2CH), 41.8 (2CH), 46.5 (CH_2), 48.1 (2CH), 50.2 (2CH), 52.7 (2CH), 62.9 ($2OCH_3$), 118.0 (2C), 120.7 ($2C_{p-ArH}$), 121.2 ($2C_{p-ArH}$), 122.3 ($2C_{ArH}$), 123.1 (2C), 125.5 ($2C_{ArH}$), 127.2 ($2C_{Ar}$), 128.1 ($2C_{o-ArH}$), 128.4 ($2C_{o-ArH}$), 128.6 ($2C_{o-ArH}$), 128.9 ($2C_{o-ArH}$), 129.3 ($2C_{pyrrolicH}$), 129.6 ($4C_{pyrrolicH}$), 134.1 ($2C_{Ar}$), 134.2 ($2C_{quinoxalineH}$), 134.7 ($2=CH$), 138.1 (2C), 139.6 (2C), 140.0 (4C), 140.8 (2C), 141.1 (2C), 145.1 (2C), 145.6 ($2C_{ArOMe}$), 149.0 ($8C_{Ar(tBu)}$), 153.8 (2C), 155.0 (2C), 164.8 (2C) ppm.

6B-Porphyrin-DMN (**32**)



Method 1: A suspension of 6B-porphyrin-2B-ene-DMN **31** (6 mg, 0.004 mmol) and some 10 % Pd/C in ethyl acetate (1 mL) was stirred under a hydrogen atmosphere for 24 hours. The Pd/C was filtered off and the solvent was removed under reduced pressure. The crude product was purified by column chromatography (chloroform). Yield: 5 mg (0.003 mmol, 78.7 %) 6B-porphyrin-DMN **32**.

Method 2: A solution of **23** (99 mg, 0.231 mmol) and 'diaminoporphyrin' **153** (275 mg, 0.230 mmol) in dichloromethane

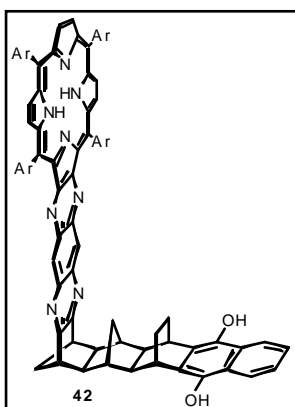
(4 mL) was heated in a dark pressure tube at 125 °C for three days under an argon atmosphere. The solvent was removed under an argon stream and the crude product was purified by column chromatography (chloroform). Yield: 196 mg (0.123 mmol, 53.7 %) 6B-porphyrin-DMN **32**. Melting point: >300 °C.

1H -NMR (600 MHz, $CDCl_3$): δ = -2.39 (2H, s), -0.72 (1H, d, J = 11.8 Hz), 1.18 (2H, d, J = 8.1 Hz), 1.33 (1H, d, J = 11.8 Hz), 1.54 (2H, d, J = 8.1 Hz), 1.51 (18H, s), 1.53 (36H, bs), 1.55 (18H, s), 1.74 (2H, d, J = 7.8 Hz), 2.00 (1H, d, J = 9.8 Hz), 2.09 (1H, d, J = 9.8 Hz), 2.38

(2H, s), 2.43 (2H, s), 3.50 (2H, s), 3.66 (2H, s), 3.91 (6H, s), 7.47 (2H, dd, $J = 6.5, 3.0$ Hz), 7.81 (2H, t, $J = 1.7$ Hz), 7.95 (2H, t, $J = 1.7$ Hz), 8.03 (2H, t, $J = 1.6$ Hz), 8.05 (2H, t, $J = 1.6$ Hz), 8.10 (2H, t, $J = 1.6$ Hz), 8.11 (4H, m), 8.59 (2H, s), 8.77 (2H, s), 8.99 (4H, AB_{quartet}, $J = 15.6, 4.9$ Hz) ppm; ^{13}C -NMR (75.5 MHz, CDCl_3): $\delta = 21.4$ (2CH_2), 29.8 (CH_2), 31.1 (2CH), 31.8 (12CH_3), 32.0 (12CH_3), 35.1 (8C), 39.6 (2CH), 46.5 (CH_2), 47.3 (2CH), 48.4 (2CH), 52.3 (2CH), 62.7 (2OCH_3), 118.1 (2C), 120.7 ($2\text{C}_{\text{p-ArH}}$), 121.2 ($2\text{C}_{\text{p-ArH}}$), 122.3 (2C_{ArH}), 123.1 (2C), 125.3 (2C_{ArH}), 127.5 (2C_{Ar}), 128.1 ($2\text{C}_{\text{o-ArH}}$), 128.5 ($2\text{C}_{\text{o-ArH}}$), 128.7 ($2\text{C}_{\text{o-ArH}}$), 128.9 ($2\text{C}_{\text{o-ArH}}$), 129.4 ($2\text{C}_{\text{pyrrolicH}}$), 129.6 ($4\text{C}_{\text{pyrrolicH}}$), 134.3 ($2\text{C}_{\text{quinoxalineH}}$), 134.9 (2C_{Ar}), 138.2 (2C), 139.6 (2C), 140.0 (2C), 140.1 (2C), 140.9 (2C), 141.1 (2C), 145.1 (2C), 145.5 (2C_{ArOMe}), 148.9 ($4\text{C}_{\text{Ar}}^{\text{tBu}}$), 149.1 ($4\text{C}_{\text{Ar}}^{\text{tBu}}$), 153.8 (2C), 155.0 (2C), 164.9 (2C) ppm.

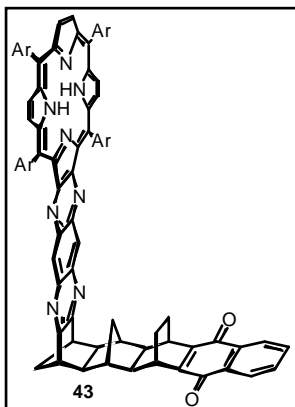
UV-Vis (CH_2Cl_2) λ_{max} (log ϵ): 657 (3.30), 608 (4.09), 537 (4.20), 424 (5.45) nm.

6B-Porphyrin-HNQ (42)



To a solution of 6B-porphyrin-DMN **32** (48 mg, 0.0302 mmol) in anhydrous dichloromethane (2 mL) was added BBr_3 (~0.01 mL) at -30°C . The mixture was allowed to warm up to RT and stirred for 20 hours in the dark under an argon atmosphere. Two drops of methanol were added, the greenish mixture stirred for another 30 minutes and the solvents were removed under reduced pressure to yield the crude product, which was purified by column chromatography (dichloromethane/methanol 99:1) and used without further characterisation. Yield: 45 mg (0.0288 mmol, 95.5 %) 6B-porphyrin-HNQ **42**. Melting point: $>300^\circ\text{C}$.

6B-Porphyrin-NQ (43)

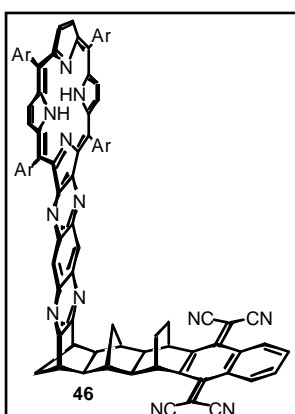


A suspension of 6B-porphyrin-HNQ **42** (45 mg, 0.0288 mmol) and lead dioxide (38 mg, 0.1589 mmol, ~5eq.) in chloroform (6 mL) was stirred at RT for 3 hours. The solvent was evaporated and the crude product was purified by column chromatography (chloroform). Yield: 42 mg (0.0269 mmol, 93.6 %) 6B-porphyrin-NQ **43**. Melting point: $>300^\circ\text{C}$; MH^+ (MALDI): 1558.

^1H -NMR (500 MHz, CDCl_3): $\delta = -2.36$ (2H, s), -0.69 (1H, d, $J = 12.5$ Hz), 1.08 (2H, d, $J = 8.3$ Hz), 1.34 (1H, d, $J = 12.5$ Hz), 1.51

(2H, s), 1.54 (18H, s), 1.56 (18H, s), 1.57 (18H, s), 1.58 (18H, s), 1.66 (2H, d, $J = 8.3$ Hz), 2.06 (1H, d, $J = 9.8$ Hz), 2.13 (1H, d, $J = 9.8$ Hz), 2.35 (2H, s), 2.45 (2H, s), 3.53 (2H, s), 3.69 (2H, s), 7.70 (2H, m), 7.83 (2H, t, $J = 1.8$ Hz), 7.98 (2H, t, $J = 1.8$ Hz), 8.06 (2H, t, $J = 1.7$ Hz), 8.07 (2H, t, $J = 1.7$ Hz), 8.11 (2H, m), 8.12 (2H, t, $J = 1.7$ Hz), 8.14 (2H, t, $J = 1.7$ Hz), 8.61 (2H, s), 8.80 (2H, s), 9.02 (4H, AB_{quartet}, $J = 13.2, 5.0$ Hz) ppm; ^{13}C -NMR (75.5 MHz, CDCl_3): $\delta = 20.5$ (2CH₂), 29.7 (CH₂), 30.7 (2CH), 31.8 (12CH₃), 32.0 (12CH₃), 35.1 (8C), 38.7 (2CH), 46.6 (2CH), 46.7 (CH₂), 48.3 (2CH), 52.2 (2CH), 118.1 (2C), 120.7 (2C_{p-Ar}H), 121.2 (2C_{p-Ar}H), 123.1 (2C), 126.4 (2C_{Ar}H), 128.1 (2C_{o-Ar}H), 128.4 (2C_{o-Ar}H), 128.6 (2C_{o-Ar}H), 128.8 (2C_{o-Ar}H), 129.4 (2C_{pyrrolic}H), 129.6 (4C_{pyrrolic}H), 132.5 (2C_{Ar}), 133.4 (2C_{Ar}H), 134.2 (2C_{quinoxaline}H), 138.2 (2C), 139.6 (2C), 140.0 (4C), 140.8 (2C), 141.1 (2C), 145.6 (2C_{Ar}), 148.9 (4C_{Ar}^tBu), 149.0 (4C_{Ar}^tBu), 152.1 (2C), 153.8 (2C), 155.0 (2C), 164.7 (2C), 181.7 (2C_{Ar}=O) ppm.

6B-Porphyrin-TCNQ (46)



Malononitrile (8 mg, 0.1196 mmol) was added to a solution of 6B-porphyrin-NQ **43** (38 mg, 0.0239 mmol) in anhydrous dichloromethane (5 mL). At 0 °C some drops titanium(IV) chloride (>10 eq.) were added. After 10 minutes β -alanine (12 mg, 0.1347 mmol) and pyridine (0.2 mL) were added and the greenish solution was allowed to warm up to RT. After 2 hours further pyridine (0.2 mL) was added to the now orange-brown solution. After stirring for another 2 hours dichloromethane (5 mL) was added and the

mixture was washed with 0.5M HCl (3 x 10 mL) and sat. NaHCO₃ (10 mL). The organic solution was dried over Na₂SO₄ and the solvents were removed under reduced pressure. The crude product was purified by column chromatography (chloroform). Yield: 23 mg (0.0139 mmol, 58.2 %) 6B-porphyrin-TCNQ **46**. Melting point: >300 °C; MH⁺ (MALDI): 1654.

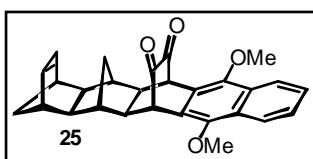
^1H -NMR (500 MHz, CDCl_3): $\delta = -2.37$ (2H, s), -0.71 (1H, d, $J = 12.8$ Hz), 1.28 (1H, dd, $J = 12.8$ Hz), 1.30 (2H, d, $J = 9.2$ Hz), 1.53 (18H, s), 1.55 (18H, s), 1.56 (18H, s), 1.57 (18H, s), 1.62 (2H, s), 1.75 (2H, d, $J = 9.2$ Hz), 2.02 (1H, d, $J = 9.5$ Hz), 2.13 (1H, d, $J = 9.5$ Hz), 2.37 (2H, s), 2.46 (2H, s), 3.69 (2H, s), 3.80 (2H, s), 7.71 (2H, m), 7.83 (2H, t, $J = 1.8$ Hz), 7.98 (2H, t, $J = 1.8$ Hz), 8.03 (2H, bs), 8.06 (2H, bs), 8.12 (4H, t, $J = 2.1$ Hz), 8.30 (2H, m), 8.58 (2H, s), 8.80 (2H, s), 9.02 (4H, AB_{quartet}, $J = 10.8, 5.1$ Hz) ppm; ^{13}C -NMR (75.5 MHz,

CDCl₃): δ = 20.5 (2CH₂), 29.7 (CH₂), 31.8 (12CH₃), 32.0 (12CH₃), 35.1 (8C), 36.5 (2CH), 38.6 (2CH), 46.3 (2CH), 46.6 (CH₂), 48.1 (2CH), 52.0 (2CH), 81.7 (2C(CN)), 113.2 (2CN), 113.7 (2CN), 118.0 (2C), 120.7 (2C_{p-Ar}H), 121.2 (2C_{p-Ar}H), 123.1 (2C), 127.5 (2C_{Ar}H), 128.1 (2C_{o-Ar}H), 128.4 (2C_{o-Ar}H), 128.6 (2C_{o-Ar}H), 128.7 (2C_{o-Ar}H), 129.5 (2C_{pyrrolic}H), 129.6 (4C_{pyrrolic}H), 130.9 (2C), 131.9 (2C_{Ar}H), 134.3 (2C_{quinoxaline}H), 138.2 (2C), 139.6 (2C), 139.9 (2C), 140.0 (2C), 140.8 (2C), 141.1 (2C), 145.6 (2C_{Ar}), 147.9 (2C_{Ar}), 148.9 (4C_{Ar}^tBu), 149.1 (4C_{Ar}^tBu), 153.8 (2C), 155.0 (2C), 156.4 (2C_{Ar}=C(CN)₂), 164.4 (2C) ppm. *m/z* (MALDI)=1654.

UV-Vis (CH₂Cl₂) λ_{\max} (log ϵ): 659 (3.22), 609 (3.98), 537 (4.06), 424 (5.41) nm.

D.1.2 Synthesis of the 2B-Porphyrin-Dyads

(1 α ,4 α ,4 α ,5 β ,5 α ,6 β ,13 β ,13 α ,14 β ,14 α)-6,13-Ethano(1,4,4a,5,5a,6,13,13a,14,14a)-decahydro-1,4:5,14-dimethano-7,12-dimethoxypentacene-16,17-dione (**25**)



To an ice-cold solution of 6B-ene-2B-diol-DMN **17** (506 mg, 1.175 mmol) and *p*-toluenesulfonic acid monohydrate (1153 mg, 6.061 mmol, ~5 eq.) in dichloromethane (20 mL) was added dropwise 4-acetamido-TEMPO (1297 mg, 6.081 mmol, ~5 eq.) in dichloromethane (30 mL) in the dark. On completion of the addition (120 minutes) the mixture was stirred for 5 days in the dark at RT. A white precipitate was filtered off and ethanol (10 mL) was added to quench the reaction. The bright yellow solution was washed with H₂O (2 x 30 mL) and brine (30 mL) then dried over Na₂SO₄. The solvents were removed under reduced pressure to give a crude yellow solid (600 mg), which was purified by column chromatography (light petroleum/ethyl acetate 1:2). Yield: 303 mg (0.710 mmol, 60.5 %) 6B-ene-2B-dione-DMN **25** as a bright yellow solid. Melting point: 264-265 °C; *m/z*: 426.

¹H-NMR (300 MHz, CDCl₃): δ = 0.45 (1H, d, *J* = 12.7 Hz), 1.16 (1H, d, *J* = 8.1 Hz), 1.36 (1H, d, *J* = 8.1 Hz), 2.00 (2H, s), 2.06 (2H, s), 2.31 (2H, s), 2.34 (1H, d, *J* = 12.7 Hz), 2.89 (2H, bs), 3.90 (6H, s), 4.50 (2H, t, *J* = 1.8 Hz), 5.97 (2H, t, *J* = 1.8 Hz), 7.54 (2H, m), 8.09 (2H, m) ppm; ¹³C-NMR (75.5 MHz, CDCl₃): δ = 32.4 (CH₂), 41.9 (2CH), 46.6 (2CH), 48.8 (2CH), 51.6 (2CH), 51.7 (2CH), 53.4 (CH₂), 63.4 (2OCH₃), 122.5 (2C_{Ar}H), 123.4 (2C_{Ar}), 126.8 (2C_{Ar}H), 129.2 (2C_{Ar}), 135.4 (2=CH), 149.2 (2C_{Ar}OMe), 191.8 (2C=O) ppm.

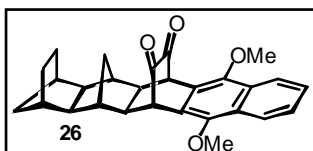
IR(KBr): 3047, 2934, 1743, 1725, 1601, 1455, 1359, 1094, 1089 cm⁻¹.

UV-Vis (CH₂Cl₂) λ_{\max} (log ϵ): 458 (1.59), 322 (3.15), 294 (3.79), 285 (3.77) nm.

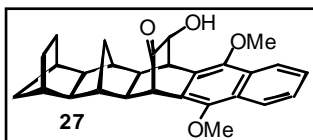
(1 α ,4 α ,4 α ,5 β ,5 α ,6 β ,13 β ,13 α ,14 β ,14 α)-6,13-Ethano(1,2,3,4,4a,5,5a,6,13,13a,14,14a)-dodecahydro-1,4:5,14-dimethano-7,12-dimethoxypentacene-16,17-dione (26) and

(1 α ,4 α ,4 α ,5 β ,5 α ,6 β ,13 β ,13 α ,14 β ,14 α)-6,13-Ethano(1,2,3,4,4a,5,5a,6,13,13a,14,14a)-dodecahydro-17-hydroxy-1,4:5,14-dimethano-7,12-dimethoxypentacene-16-one (27)

A suspension of 6B-ene-2B-dione-DMN **25** (124 mg, 0.291 mmol) and some 10% Pd/C in ethyl acetate (2.5 mL) was stirred at RT for 24 hours under a hydrogen atmosphere. The Pd/C was filtered off and the solvent was removed under reduced pressure. The crude yellow products were purified by column chromatography (light petroleum/ethyl acetate 1:1). Yield (**26**): 48 mg (0.112 mmol, 38.5 %) bright yellow 2B-dione-DMN **26**. Melting point: 257–259 °C; m/z: 428. Yield (**27**): 40 mg (0.093 mmol, 31.9 %) yellow 2B-ketol-DMN **27**.

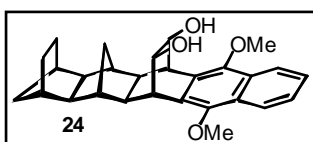


¹H-NMR (300 MHz, CDCl₃, **26**): δ = 0.84 (1H, d, J = 13.8), 1.21 (1H, d, J = 9.2 Hz), 1.27 (1H, d, J = 9.2 Hz), 1.35 (2H, d, J = 8.7 Hz), 1.46 (2H, d, J = 8.7 Hz), 1.69 (2H, s), 1.78 (1H, d, J = 13.8 Hz), 2.05 (2H, d, J = 1.5 Hz), 2.27 (2H, s), 2.36 (2H, s), 3.90 (6H, s), 4.53 (2H, t, J = 1.7 Hz), 7.54 (2H, dd, J = 6.4, 3.4 Hz), 8.09 (2H, dd, J = 6.4, 3.0 Hz) ppm; ¹³C-NMR (75.5 MHz, CDCl₃, **26**): δ = 24.4 (2CH₂), 32.6 (CH₂), 40.3 (2CH), 41.0 (2CH), 42.3 (CH₂), 50.3 (2CH), 50.8 (2CH), 51.9 (2CH), 63.4 (2OCH₃), 122.5 (2C_{Ar}H), 123.4 (2C_{Ar}), 126.7 (2C_{Ar}H), 129.4 (2C_{Ar}), 149.1 (2C_{Ar}OMe), 192.2 (2C=O) ppm.



¹H-NMR (300 MHz, CDCl₃, **27**): δ = 1.19 (2H, d, J = 7.2 Hz), 1.31 (2H, d, J = 7.2 Hz), 1.51 (1H, d, J = 8.2 Hz), 1.55 (2H, s), 1.60 (2H, s), 1.68 (1H, bs), 1.74 (1H, dd, J = 8.2, 3.1 Hz), 1.89 (1H, dd, J = 9.2, 3.1 Hz), 2.21 (1H, s), 2.23 (2H, s), 2.38 (1H, s), 3.10 (1H, s), 3.85 (1H, s), 3.87 (3H, s), 3.96 (3H, s), 4.12 (1H, s), 7.50 (2H, m), 8.07 (2H, m) ppm; ¹³C-NMR (75.5 MHz, CDCl₃, **27**): δ = 24.3 (CH₂), 24.6 (CH₂), 30.6 (CH₂), 39.3 (CH), 39.6 (CH), 40.1 (CH), 41.1 (CH), 41.2 (CH), 42.5 (CH₂), 46.8 (CH), 50.3 (CH), 50.5 (CH), 51.7 (CH), 55.2 (CH), 62.9 (OCH₃), 63.2 (OCH₃), 74.3 (CHOH), 122.3 (C_{Ar}H), 122.5 (C_{Ar}H), 125.4 (C_{Ar}), 126.1 (C_{Ar}H), 126.2 (C_{Ar}H), 128.2 (C_{Ar}), 128.4 (C_{Ar}), 130.7 (C_{Ar}), 146.3 (C_{Ar}OMe), 148.1 (C_{Ar}OMe), 213.0 (C=O) ppm.

(1 α ,4 α ,4 α ,5 β ,5 α ,6 β ,13 β ,13 α ,14 β ,14 α)-6,13-Ethano(1,2,3,4,4a,5,5a,6,13,13a,14,14a)-dodecahydro-16,17-*cis*-dihydroxy-1,4:5,14-dimethano-7,12-dimethoxypentacene (24)

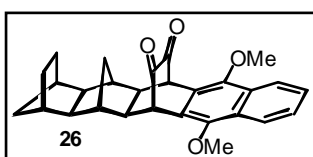


A suspension of 6B-ene-2B-diol-DMN **17** (210 mg, 0.488 mmol) and some 10% Pd/C in ethyl acetate (5 mL) was stirred at RT for 24

hours under a hydrogen atmosphere. The Pd/C was filtered off and the solvent was removed under reduced pressure. Yield: 208 mg (0.481 mmol, 98.5 %) 2B-diol-DMN **24** as a white solid.

$^1\text{H-NMR}$ (300 MHz, CDCl_3): δ = 1.17 (1H), 1.31 (2H), 1.34 (1H), 1.46 (2H, s), 1.51 (2H, bs), 1.54 (1H), 1.67 (1H, d, J = 12.5 Hz), 2.22 (2H, s), 2.24 (2H, s), 2.54 (2H, bs), 3.76 (2H, s), 3.95 (6H, s), 4.41 (2H, s), 7.46 (2H, 6.4, 3.4 Hz), 8.08 (2H, dd, J = 6.4, 3.4 Hz) ppm.

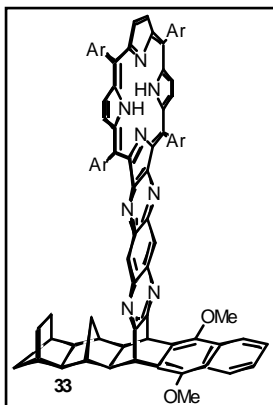
(1 α ,4 α ,4 α ,5 β ,5 α ,6 β ,13 β ,13 α ,14 β ,14 α)-6,13-Ethano(1,2,3,4,4a,5,5a,6,13,13a,14,14a)-dodecahydro-1,4:5,14-dimethano-7,12-dimethoxypentacene-16,17-dione (26**)**



To an ice-cold solution of 2B-diol-DMN **24** (208 mg, 0.481 mmol) and *p*-toluenesulfonic acid monohydrate (462 mg, 2.429 mmol, ~5 eq.) in dichloromethane (10 mL) was added dropwise 4-acetamido-TEMPO (548 mg, 2.569 mmol, ~5 eq.) in

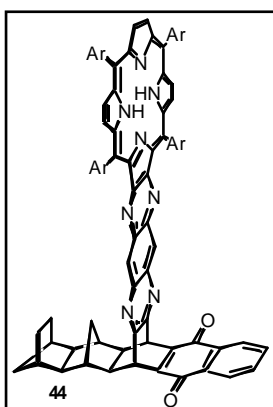
dichloromethane (10 mL) in the dark. On completion of the addition (120 minutes) the mixture was stirred at RT for 5 days in the dark. A white precipitate was filtered off and ethanol (10 mL) was added to the slightly orange solution. The bright yellow solution was washed with H_2O (2 x 15 mL) and brine (15 mL) then dried over Na_2SO_4 . The solvents were removed under reduced pressure and the crude yellow solid was purified by column chromatography (light petroleum/ethyl acetate 1:1). Yield: 187 mg (0.436 mmol, 90.6 %) 2B-dione-DMN **26** as a bright yellow solid. Melting point: 257-259 °C; m/z : 428.

$^1\text{H-NMR}$ (300 MHz, CDCl_3): δ = 0.84 (1H, d, J = 13.8), 1.21 (1H, d, J = 9.2 Hz), 1.27 (1H, d, J = 9.2 Hz), 1.35 (2H, d, J = 8.7 Hz), 1.46 (2H, d, J = 8.7 Hz), 1.69 (2H, s), 1.78 (1H, d, J = 13.8 Hz), 2.05 (2H, d, J = 1.5 Hz), 2.27 (2H, s), 2.36 (2H, s), 3.90 (6H, s), 4.53 (2H, t, J = 1.7 Hz), 7.54 (2H, dd, J = 6.4, 3.4 Hz), 8.09 (2H, dd, J = 6.4, 3.0 Hz) ppm; $^{13}\text{C-NMR}$ (75.5 MHz, CDCl_3): δ = 24.4 (2 CH_2), 32.6 (CH_2), 40.3 (2CH), 41.0 (2CH), 42.3 (CH_2), 50.3 (2CH), 50.8 (2CH), 51.9 (2CH), 63.4 (2 OCH_3), 122.5 (2 C_{ArH}), 123.4 (2 C_{Ar}), 126.7 (2 C_{ArH}), 129.4 (2 C_{Ar}), 149.1 (2 $\text{C}_{\text{Ar}}\text{OMe}$), 192.2 (2 $\text{C}=\text{O}$) ppm.

2B-Porphyrin-DMN (33)

A solution of **26** (42 mg, 0.098 mmol) and 'diaminoporphyrin' **153** (118 mg, 0.099 mmol) in dichloromethane (3 mL) was heated in a dark pressure tube for 4 days at 120 °C under an argon atmosphere. Over the 4 days the solvent was allowed to boil off slowly. The crude product was then purified by column chromatography (chloroform). Yield: 114 mg (0.072 mmol, 73.2 %) 2B-porphyrin-DMN **33**. Melting point: >300 °C.

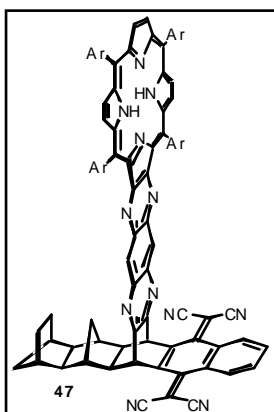
¹H-NMR (300 MHz, CDCl₃): δ = -2.30 (2H, s), -0.16 (1H, d, *J* = 13.2 Hz), 1.24 (1H, d, *J* = 11.3 Hz), 0.8-1.7 (6H), 1.55 (18H, s), 1.60 (18H, s), 1.61 (18H, s), 1.63 (18H, s), 1.77 (2H, s), 2.26 (2H, s), 2.31 (2H, s), 2.47 (2H, s), 4.13 (6H, s), 5.25 (2H, s), 7.53 (2H, m), 7.88 (2H, s), 8.03 (2H, t, *J* = 1.5 Hz), 8.08 (2H, s), 8.1 (2H, s), 8.16 (2H, bs), 8.17 (2H, m), 8.19 (2H, bs), 8.70 (2H, s), 8.85 (2H, s), 9.06 (4H, dd, *J* = 4.9, 6.8 Hz) ppm; ¹³C-NMR (75.5 MHz, CDCl₃): δ = 24.4 (2CH₂), 30.4 (CH₂), 31.8 (12 CH₃), 32.0 (6CH₃), 32.1 (6CH₃), 35.1 (8C), 40.0 (2CH), 41.1 (2CH), 42.4 (CH₂), 45.0 (2CH), 51.0 (2CH), 51.2 (2CH), 63.3 (2OCH₃), 118.0 (2C), 120.7 (2C_{p-Ar}H), 121.2 (2C_{p-Ar}H), 122.4 (2C_{Ar}H), 123.1 (2C), 126.2 (2C_{Ar}H), 128.1 (2C_{o-Ar}H), 128.2 (2C_{Ar}), 128.5 (2C_{o-Ar}H), 128.8 (2C_{o-Ar}H), 128.9 (2C_{o-Ar}H), 129.4 (2C_{pyrrolic}H), 129.6 (4C_{pyrrolic}H), 134.3 (2C_{quinoxaline}H), 138.2 (2C), 139.7 (2C), 140.0 (4C), 140.8 (2C), 141.1 (2C), 145.7 (2C_{Ar}OMe), 147.5 (2C_{Ar}), 148.9 (6C_{Ar}^tBu), 149.0 (2C_{Ar}^tBu), 149.1 (2C), 153.8 (2C), 155.0 (2C), 158.4 (2C) ppm.

2B-Porphyrin-NQ (44)

To a solution of 2B-porphyrin-DMN **33** (80 mg, 0.0504 mmol) in anhydrous dichloromethane (2.5 mL) under an argon atmosphere was added boron tribromide (3 drops) at -45 °C. The red-brown solution was allowed to warm-up to RT and was stirred overnight in the dark. The green mixture was poured onto half-saturated NaHCO₃ (5 mL) and washed with more half-saturated NaHCO₃ (5 mL), Na₂S₂O₅ (5 mL) and brine (5 mL). To the organic phase was added lead dioxide (220 mg) and the mixture was stirred in the dark for 30 minutes, then filtered and solvents were removed under reduced pressure. The crude product was purified by column chromatography (chloroform/light petroleum 10:1). Yield: 75 mg (0.0481 mmol, 95.5 %) 2B-porphyrin-NQ **44**. Melting point: >300 °C.

^1H -NMR (500 MHz, CDCl_3): δ = -2.39 (2H, s), -0.51 (1H, d, J = 11.3 Hz), 0.88 (2H), 1.18 (1H, d, J = 11.3 Hz), 1.27 (4H), 1.50 (18H, s), 1.54 (18H, s), 1.55 (18H, s), 1.56 (18H, s), 1.70 (2H, bs), 2.16 (2H, s), 2.25 (2H, bs), 2.37 (2H, s), 5.19 (2H, bs), 7.71 (2H, m), 7.81 (2H, t, J = 1.5 Hz), 7.96 (2H, t, J = 1.6 Hz), 8.00 (2H, bs), 8.04 (2H, bs), 8.09 (2H, bs), 8.12 (2H, bs), 8.13 (2H, m), 8.64 (2H, s), 8.78 (2H, s), 8.99 (4H, dd, J = 6.8, 5.3 Hz) ppm; ^{13}C -NMR (75.5 MHz, CDCl_3): δ = 24.4 (2CH_2), 30.1 (CH_2), 31.8 (12CH_3), 32.1 (12CH_3), 35.1 (8C), 39.6 (2CH), 41.0 (2CH), 42.7 (CH_2), 44.2 (2CH), 50.8 (2CH), 51.3 (2CH), 118.1 (2C), 120.7 ($2\text{C}_{\text{p-ArH}}$), 121.3 ($2\text{C}_{\text{p-ArH}}$), 123.1 (2C), 126.7 (2C_{ArH}), 128.2 ($2\text{C}_{\text{o-ArH}}$), 128.5 ($2\text{C}_{\text{o-ArH}}$), 128.7 ($2\text{C}_{\text{o-ArH}}$), 128.9 ($2\text{C}_{\text{o-ArH}}$), 129.6 ($4\text{C}_{\text{pyrrolicH}}$), 129.7 ($2\text{C}_{\text{pyrrolicH}}$), 132.2 (2C_{Ar}), 133.9 (2C_{ArH}), 134.3 ($2\text{C}_{\text{quinoxalineH}}$), 138.2 (2C), 139.5 (2C), 139.9 (2C), 140.0 (2C), 140.8 (2C), 141.1 (2C), 145.5 (2C_{Ar}), 148.9 ($4\text{C}_{\text{Ar}}^{\text{tBu}}$), 149.1 ($4\text{C}_{\text{Ar}}^{\text{tBu}}$), 149.4 (2C), 154.0 (2C), 155.1 (2C), 156.3 (2C), 180.9 ($2\text{C}_{\text{Ar=O}}$) ppm.

2B-Porphyrin-TCNQ (47)



To an ice-cold solution of 2B-porphyrin-NQ **44** (75 mg, 0.0481 mmol) in anhydrous dichloromethane (5 mL) was added titanium(IV) chloride (0.015 mL, 26 mg, 0.1368 mmol, ~ 2.5 eq.). The red-brown solution was heated at reflux for 10 minutes, after which malononitrile (16 mg, 0.2407, ~ 5 eq.) in anhydrous dichloromethane (2.5 mL) was added, followed by another 2 hours at reflux. Pyridine (23 mg, 0.2907 mmol, ~ 5 eq.) in anhydrous dichloromethane (1.5 mL) was added dropwise and the mixture stirred at RT for 3 days. The mixture was poured onto

0.5M HCl (10 mL), washed with 0.5M HCl (10 mL) and brine (10 mL). The solvent was removed under reduced pressure and the crude product was purified by column chromatography (chloroform/light petroleum 1.5:1) to yield the product along with 10 mg (0.0064 mmol, 13.3 %) of starting material. Yield: 25 mg (0.0151 mmol, 31.4 %) 2B-porphyrin-TCNQ **47**. Melting point: $>300^\circ\text{C}$; M^+ (MALDI): 1654.

^1H -NMR (500 MHz, CDCl_3): δ = -2.42 (2H, s), -0.68 (1H, d, J = 13.6 Hz), 0.90 (2H), 1.17 (1H, d, J = 13.6 Hz), 1.25 (1H), 1.40 (1H), 1.52 (18H, s), 1.53 (18H, s), 1.54 (36 H), 1.60 (2H), 1.83 (2H, s), 2.29 (2H, s), 2.40 (2H, s), 2.65 (2H, s), 5.44 (2H, s), 7.61 (2H, dd, J = 6.0, 3.4 Hz), 7.80 (2H, t, J = 1.9 Hz), 7.93 (2H, t, J = 1.9 Hz), 7.95 (2H, bs), 8.03 (2H, bs), 8.07 (2H, bs), 8.08 (2H, bs), 8.24 (2H, dd, J = 6.0, 3.4 Hz), 8.56 (2H, s), 8.77 (2H, s), 8.98 (4H, bs) ppm; ^{13}C -NMR (75.5 MHz, CDCl_3): δ = 24.4 (2CH_2), 30.0 (CH_2), 31.8 (12CH_3), 31.9

(6CH₃), 32.0 (6CH₃), 35.1 (8C), 39.5 (2CH), 41.0 (2CH), 42.6 (CH₂), 49.5 (2CH), 50.2 (2CH), 51.0 (2CH), 82.6 (2=C(CN)₂), 113.1 (2CN), 113.3 (2CN), 118.0 (2C), 120.7 (2C_{p-Ar}H), 121.3 (2C_{p-Ar}H), 123.3 (2C), 127.8 (2C_{Ar}H), 128.3 (2C_{o-Ar}H), 128.5 (2C_{o-Ar}H), 128.6 (2C_{o-Ar}H), 128.7 (2C_{o-Ar}H), 129.0 (2C_{Ar}), 129.6 (4C_{pyrrolic}H), 129.8 (2C_{pyrrolic}H), 132.2 (2C_{Ar}H), 134.4 (2C_{quinoxaline}H), 138.3 (2C), 139.3 (2C), 139.9 (2C), 140.1 (2C), 140.7 (2C), 141.0 (2C), 145.1 (2C_{Ar}), 146.5 (2C_{Ar}), 148.9 (8C_{Ar}^tBu), 149.1 (2C), 154.1 (2C), 154.7 (2C), 155.2 (2C), 156.2 (2C_{Ar}=C(CN)₂) ppm.

UV-Vis (CH₂Cl₂) λ_{max} (log ε): 656 (3.47), 615 (3.94), 428 (5.53) nm.

D.1.3 Synthesis of the Bis-Porphyrin-Dyads

(1α,4α,4α,5β,5α,6β,13β,13α,14β,14α)-6,13-Ethano-(1,4,4a,5,5a,6,13,13a,14,14a)-decahydro-1,4:5,14-dimethano-7,12-dimethoxypentacene-2,3,16,17-tetraone (**28**)



To an ice-cold solution of 6B-diol-2B-diol-DMN **19** (1.05 g, 2.2 mmol) and *p*-toluenesulfonic acid monohydrate (4.29 g, 22 mmol, ~10 eq.) in dichloromethane (30 mL) was added dropwise 4-acetamido-TEMPO (4.80 g, 22 mmol, ~10 eq.) in dichloromethane

(30 mL) in the dark. On completion of the addition (30 minutes) the mixture was stirred for 26 hours in the dark at RT. A white precipitate was filtered off and ethanol (3 mL) was added to quench the reaction. The bright yellow solution was washed with H₂O (3 x 30 mL) and brine (30 mL) then dried over Na₂SO₄. The solvents were removed under reduced pressure and the residue was dissolved in boiling chloroform. Upon addition of diethyl ether the tetraone precipitated as a yellow solid. Yield: 560 mg (1.227 mmol, 55.8 %) tetraone-DMN **28**. Melting point: >300 °C; m/z: 456.

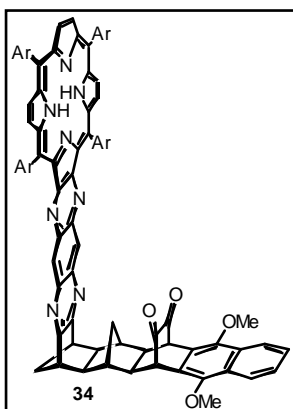
¹H-NMR (300 MHz, CDCl₃): δ = 0.82 (1H, d, *J* = 15.4 Hz), 1.04 (1H, d, *J* = 15.4 Hz), 1.92 (1H, d, *J* = 11.3 Hz), 2.06 (1H, d, *J* = 11.3 Hz), 2.18 (2H, bs), 2.42 (2H, bs), 2.54 (2H, s), 3.17 (2H, bs), 3.89 (6H, s), 4.55 (2H, bs), 7.56 (2H, m), 8.09 (2H, m) ppm; ¹³C-NMR (75.5 MHz, CDCl₃): δ = 31.8 (CH₂), 34.9 (CH₂), 40.8 (2CH), 48.9 (2CH), 51.4 (2CH), 51.8 (2CH), 53.1 (2CH), 63.5 (2OCH₃), 122.5 (2C_{Ar}H), 122.7 (2C_{Ar}), 127.1 (2C_{Ar}H), 129.2 (2C_{Ar}), 149.3 (2C_{Ar}OMe), 191.1 (2C=O), 202.1 (2C=O) ppm.

IR (KBr): 2987, 2932, 1750, 1723, 1603, 1452, 1360 cm⁻¹.

UV-Vis (CH₂Cl₂) λ_{max} (log ε): 458 (2.89), 317 (3.24), 274 (4.25), 252 (4.13) nm.

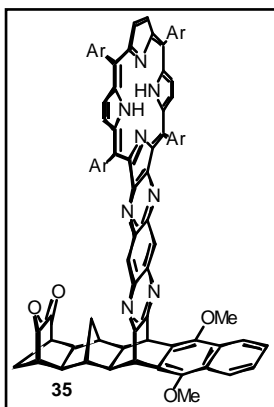
6B-Porphyrin-2B-dione-DMN (34) and 6B-dione-2B-porphyrin-DMN (35)

A solution of tetraone-DMN **28** (95 mg, 0.209 mmol) and 'diaminoporphyrin' **153** (499 mg, 0.417 mmol, ~2 eq.) in de-oxygenated dichloromethane (5 mL) was heated in a dark pressure tube at 125 °C for three days under an argon atmosphere. The solvent was removed under an argon stream and the crude products were purified by column chromatography (chloroform). Yield (**34**): 40 mg (0.0248 mmol, 11.8 %) 6B-porphyrin-2B-dione-DMN **34**. Melting point: >300 °C; MH^+ (MALDI): 1616. Yield (**35**): 103 mg (0.0637 mmol, 30.5%) 6B-dione-2B-porphyrin **35**. Melting point: >300 °C; M^+ (MALDI): 1616.



$^1\text{H-NMR}$ (500 MHz, CDCl_3 , **34**): δ = -2.29 (2H, s), -0.56 (1H, d, J = 14.6 Hz), 0.45 (1H, d, J = 14.6 Hz), 1.60 (18H, s), 1.62 (18H, s), 1.63 (18H, s), 1.66 (18H, s), 2.11 (1H, d, J = 9.0 Hz), 2.21 (1H, d, J = 9.0 Hz), 2.32 (2H, s), 2.62 (2H, s), 2.67 (2H, s), 3.79 (2H, s), 3.95 (6H, s), 4.61 (2H, s), 7.58 (2H, m), 7.90 (2H, t, J = 1.6 Hz), 8.06 (2H, t, J = 1.6 Hz), 8.10 (2H, t, J = 1.6 Hz), 8.16 (2H, m), 8.17 (2H, t, J = 1.6 Hz), 8.21 (4H, t, J = 2.1 Hz), 8.65 (2H, s), 8.88 (2H, s), 9.10 (4H, AB_{quartet}, J = 12.8, 5.1 Hz) ppm; $^{13}\text{C-NMR}$ (75.5 MHz, CDCl_3 , **34**):

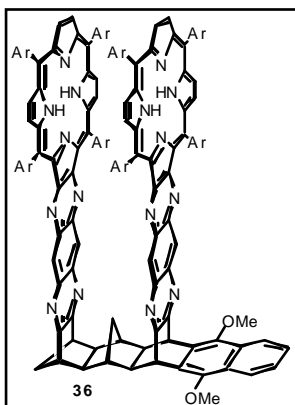
δ = 29.8 (CH_2), 31.9 (24CH_3), 35.2 (8C), 41.1 (2CH), 46.6 (2CH), 46.6 (CH_2), 48.2 (2CH), 50.1 (2CH), 50.9 (2CH), 51.6 (2CH), 63.6 (2OCH_3), 118.2 (2C), 120.8 ($2\text{C}_{\text{p-ArH}}$), 121.3 ($2\text{C}_{\text{p-ArH}}$), 122.6 (2C_{ArH}), 122.9 (2C_{Ar}), 123.1 (2C), 127.0 (2C_{ArH}), 128.2 ($2\text{C}_{\text{o-ArH}}$), 128.6 ($2\text{C}_{\text{o-ArH}}$), 128.7 ($2\text{C}_{\text{o-ArH}}$), 128.8 ($2\text{C}_{\text{o-ArH}}$), 129.3 ($2\text{C}_{\text{pyrrolicH}}$), 129.7 ($4\text{C}_{\text{pyrrolicH}}$), 131.0 (2C_{Ar}), 134.4 ($2\text{C}_{\text{pyrrolicH}}$), 138.3 (2C), 139.8 (2C), 139.9 (2C), 140.0 (2C), 140.9 (2C), 141.2 (2C), 145.7 (2C), 148.9 ($4\text{C}_{\text{Ar}}(\text{tBu})_3$), 149.0 ($4\text{C}_{\text{Ar}}(\text{tBu})_3$), 149.3 (2C_{ArOMe}), 154.0 (2C), 155.1 (2C), 163.6 (2C), 191.4 ($2\text{C}=\text{O}$) ppm.



$^1\text{H-NMR}$ (300 MHz, CDCl_3 , **35**): δ = -2.36 (2H, s), -0.04 (1H, d, J = 14.6 Hz), 0.24 (1H, d, J = 14.6 Hz), 1.58 (18H), 1.59 (36H), 1.61 (18H), 1.88 (1H, d, J = 11.3 Hz), 2.06 (1H, d, J = 11.3 Hz), 2.35 (2H, s), 2.48 (2H, s), 2.61 (2H, s), 3.17 (2H, s), 4.11 (6H, s), 5.25 (2H, s), 7.52 (2H, m), 7.86 (2H, t, J = 1.8 Hz), 8.02 (2H, t, J = 1.6 Hz), 8.04 (2H, bs), 8.10 (2H, bs), 8.13 (4H), 8.14 (2H, m), 8.63 (2H, s), 8.83 (2H, s), 9.04 (4H, AB_{quartet}, J = 10.3, 5.1 Hz) ppm; $^{13}\text{C-NMR}$ (75.5 MHz, CDCl_3 , **35**): δ = 30.6 (CH_2), 31.8 (12CH_3), 31.9 (6CH_3), 32.1 (6CH_3), 33.7 (CH_2), 35.1 (8C), 40.6 (2CH), 44.4 (2CH), 49.2 (2CH), 52.8 (2CH), 53.2 (2CH), 63.5 (2OCH_3), 118.1 (2C), 120.7 ($2\text{C}_{\text{p-ArH}}$), 121.2 ($2\text{C}_{\text{p-ArH}}$), 122.5 (2C_{ArH}), 123.1 (2C), 126.4 (2C_{ArH}), 128.1

(2C_{o-Ar}H), 128.3 (2C_{Ar}), 128.5 (2C_{o-Ar}H), 128.6 (2C_{o-Ar}H), 128.8 (2C_{o-Ar}H), 129.6 (6C_{pyrrolic}H), 134.2 (2C_{quinoxaline}H), 138.2 (2C), 139.8 (4C), 140.0 (2C), 140.8 (2C), 141.1 (2C), 145.6 (2C_{Ar}), 147.6 (2C_{Ar}OMe), 148.9 (8C_{Ar}^tBu), 149.3 (2C), 153.9 (2C), 155.0 (2C), 157.0 (2C), 202.4 (2C=O) ppm.

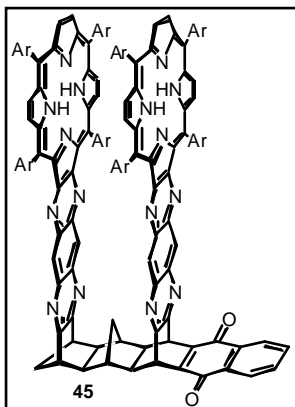
Bis-porphyrin-DMN (36)



A mixture of mono-adducts **34/35** (90 mg, 0.0558 mmol) and 'diaminoporphyrin' **153** (75 mg, 0.0633 mmol) in dichloromethane (2 mL) was heated in a dark pressure tube for 4 days at 120 °C under an argon atmosphere. Over the 4 days the solvent was allowed to evaporate slowly through a tiny leak. The crude product was then purified by column chromatography (chloroform). Yield: 59 mg (0.0212 mmol, 38.0 %) bis-porphyrin-DMN **36**. Melting point: >300 °C, MH⁺ (MALDI): 2777.

¹H-NMR (500 MHz, CDCl₃): δ = -2.62 (2H, s), -2.59 (2H, s), -0.82 (1H, d, *J* = 12.8 Hz), -0.26 (1H, d, *J* = 12.8 Hz), 1.36 (18H, s), 1.38 (18H, s), 1.42 (18H, s), 1.43 (18H, s), 1.436 (18H, s), 1.442 (18H, s), 1.46 (18H, s), 1.47 (18H, s), 2.04 (2H, m), 2.38 (2H, bs), 2.62 (2H, m), 2.63 (2H, bs), 3.68 (2H, s), 4.04 (6H, s), 5.17 (2H, s), 7.49 (2H, dd, *J* = 6.5, 3.3 Hz), 7.72 (2H, t, *J* = 1.9 Hz), 7.73 (2H, t, *J* = 1.9 Hz), 7.78 (2H, t, *J* = 1.7), 7.79 (2H, t, *J* = 1.8 Hz), 7.83 (2H, t, *J* = 1.7 Hz), 7.85 (2H, t, *J* = 1.8 Hz), 7.86 (2H, t, *J* = 1.7 Hz), 7.88 (2H, t, *J* = 1.8 Hz), 7.94 (2H, t, *J* = 1.7 Hz), 7.95 (2H, t, *J* = 1.7 Hz), 7.97 (2H, t, *J* = 1.7 Hz), 7.99 (2H, t, *J* = 1.7 Hz), 8.09 (2H, dd, *J* = 6.5, 3.3 Hz), 8.36 (2H, s), 8.37 (2H, s), 8.642 (2H, s), 8.644 (2H, s), 8.85 (8H, m) ppm; ¹³C-NMR (75.5 MHz, CDCl₃): δ = 27.5 (CH₂), 32.1 (24CH₃), 32.2 (6CH₃), 32.3 (12 CH₃), 32.4 (6CH₃), 35.4 (16C), 41.1 (2CH), 45.0 (2CH), 47.4 (CH₂), 48.6 (2CH), 50.7 (2CH), 52.2 (2CH), 63.7 (2OCH₃), 118.17 (2C), 118.24 (2C), 120.9 (4C_{p-Ar}H), 121.4 (4C_{p-Ar}H), 122.8 (2C_{Ar}H), 123.2 (4C), 126.7 (2C_{Ar}H), 128.3 (4C_{o-Ar}H), 128.6 (4C_{o-Ar}H), 128.9 (8C_{o-Ar}H), 129.6 (4C_{pyrrolic}H), 129.7 (2C_{Ar}), 129.8 (8C_{pyrrolic}H), 134.5 (4C_{quinoxaline}H), 138.3 (4C), 139.8 (4C), 140.1 (8C), 140.9 (2C), 141.0 (2C), 141.3 (4C), 145.8 (2C_{Ar}), 147.9 (2C_{Ar}OMe), 149.1 (16C_{Ar}^tBu), 149.3 (4C), 153.9 (2C), 154.0 (2C), 155.2 (4C), 157.9 (2C), 164.5 (2C) ppm.

UV-Vis (CH₂Cl₂) λ_{max} (log ε): 658 (3.66), 609.5 (4.32), 536 (4.51), 424 (5.79) nm.

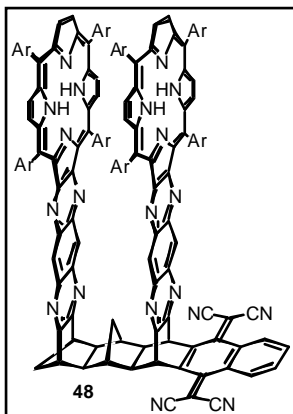
Bis-porphyrin-NQ (45)

To a solution of bis-porphyrin-DMN **36** (28 mg, 0.010 mmol) in anhydrous dichloromethane (2.5 mL) was added boron tribromide (one drop) at $-45\text{ }^{\circ}\text{C}$. The mixture was slowly allowed to warm to RT and was stirred overnight under an argon atmosphere in the dark. The green solution was poured onto half-saturated NaHCO_3 (10 mL) and washed with H_2O (10 mL) and brine (10 mL). Without isolating the hydroquinone lead dioxide (50 mg, 0.209 mmol) was added to the burgundy red solution. The mixture was stirred for 1.5 hours, the

solvent was removed under reduced pressure and the crude product was purified by column chromatography (chloroform). Yield: 23 mg (0.0084 mmol, 83.8 %) bis-porphyrin-NQ **45**.

Melting point: $>300\text{ }^{\circ}\text{C}$; $(\text{M}+2\text{H})^+$ (MALDI): 2748.

^1H -NMR (300 MHz, CDCl_3): δ = -2.60 (4 H, s), -0.84 (1H, d, J = 12.8 Hz), -0.52 (1H, d, J = 12.8 Hz), 1.40 (36H, s), 1.42 (18H, s), 1.439 (18H, s), 1.444 (36H, s), 1.47 (18H, s), 1.48 (18H, s), 2.08 (2H, s), 2.37 (2H, s), 2.62 (2H, s), 2.63 (2H, s), 3.69 (2H, s), 5.20 (2H, s), 7.72 (2H, dd, J = 5.6, 3.4 Hz), 7.74 (4H), 7.80 (2H, s), 7.81 (2H, s), 7.83 (2H, bs), 7.87 (6H), 7.95 (4H, s), 7.99 (4H), 8.14 (2H, dd, J = 5.6, 3.4 Hz), 8.36 (2H, s), 8.41 (2H, s), 8.65 (4H, s), 8.85 (8H, m) ppm; ^{13}C -NMR (75.5 MHz, CDCl_3): δ = 29.7 (CH_2), 31.7 (CH_3), 31.9 (CH_3), 35.0 (16C), 40.3 (2CH), 43.9 (2CH), 48.2 (CH_2), 50.2 (2CH), 52.0 (2CH), 53.4 (2CH), 117.9 (4C), 120.5 ($4\text{C}_{\text{p-ArH}}$), 121.1 ($4\text{C}_{\text{p-ArH}}$), 122.8 (2C), 122.9 (2C), 126.7 (C_{ArH}), 127.9 ($4\text{C}_{\text{o-ArH}}$), 128.3 ($4\text{C}_{\text{o-ArH}}$), 128.6 ($8\text{C}_{\text{o-ArH}}$), 129.3 ($4\text{C}_{\text{pyrrolicH}}$), 129.5 ($8\text{C}_{\text{pyrrolicH}}$), 132.2 (2C_{Ar}), 134.0 (2C_{ArH}), 134.1 ($4\text{C}_{\text{quinoxalineH}}$), 138.0 (4C), 139.1 (2C), 139.5 (2C), 139.7 (8C), 140.5 (2C), 140.6 (2C), 141.0 (4C), 145.2 (2C), 145.4 (2C_{Ar}), 148.7 ($8\text{C}_{\text{Ar}}^{\text{tBu}}$), 148.9 ($4\text{C}_{\text{Ar}}^{\text{tBu}}$), 149.0 ($4\text{C}_{\text{Ar}}^{\text{tBu}}$), 149.7 (2C), 153.5 (2C), 153.7 (2C), 154.9 (4C), 155.4 (2C), 163.9 (2C), 180.8 ($2\text{C}_{\text{Ar}}=\text{O}$) ppm.

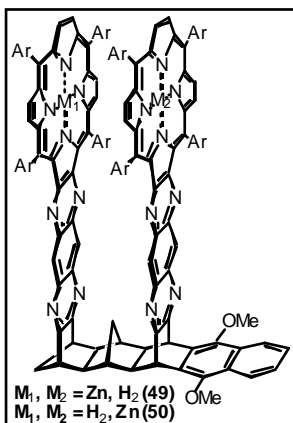
Bis-porphyrin-TCNQ (48)

Malononitrile (7 mg, 0.1060 mmol) was added to a solution of bis-porphyrin-NQ **45** (59 mg, 0.0214 mmol) in anhydrous dichloromethane (5 mL). At 0 °C titanium(IV) chloride (0.02 mL) was added. The mixture was allowed to warm-up to RT and stirred for 9 hours in the dark under an argon atmosphere. Then β -alanine (8 mg, 0.0898 mmol) along with anhydrous pyridine (0.1 mL) was added to the brown solution. After 10 hours further pyridine (0.1 mL) was added. After 2 hours the mixture was poured onto 0.25M HCl (10 mL). The organic layer was washed with 0.25M HCl (2 x 10 mL), 1M HCl (10 mL), NaHCO₃ (sat., 10 mL) and brine (10 mL) then dried over Na₂SO₄. The solvents were removed under reduced pressure and the crude product was purified twice by column chromatography (chloroform, then light petroleum/ethyl acetate 3:1). Yield: 18 mg (0.0063 mmol, 29.6 %) bis-porphyrin-TCNQ **48**. Melting point: >300 °C, (M+2H)⁺ (MALDI): 2845. 14 mg (0.0051, 23.8 %) starting material bis-porphyrin-NQ **45** was recovered.

¹H-NMR (500 MHz, CDCl₃): δ = -2.62 (2 H, s), -2.61 (2H, s), -0.84 (1H, d, J = 12.1 Hz), -0.68 (1H, d, J = 12.1 Hz), 1.37 (18H, s), 1.41 (36H, s), 1.42 (18H, s), 1.44 (36H, s), 1.476 (18H, s), 1.480 (18H, s), 2.06 (1H, d, J = 9.4 Hz), 2.14 (1H, d, J = 9.4 Hz), 2.69 (2H, s), 2.78 (2H, s), 2.88 (2H, s), 3.74 (2H, s), 5.46 (2H, t, J = 1.4 Hz), 7.61 (2H, dd, J = 6.4, 2.9 Hz), 7.739 (2H, t, J = 1.8 Hz), 7.741 (2H, t, J = 1.8 Hz), 7.76 (2H, t, J = 1.7 Hz), 7.816 (2H, t, J = 1.7 Hz), 7.825 (2H, t, J = 1.8 Hz), 7.826 (2H, t, J = 1.8 Hz), 7.85 (2H, t, J = 1.8 Hz), 7.87 (2H, t, J = 1.8 Hz), 7.93 (2H, t, J = 1.7 Hz), 7.94 (2H, t, J = 1.7 Hz), 7.98 (2H, t, J = 1.7 Hz), 7.99 (2H, t, J = 1.7 Hz), 8.24 (2H, dd, J = 6.1, 3.3 Hz), 8.34 (2H, s), 8.35 (2H, s), 8.647 (2H, s), 8.650 (2H, s), 8.85 (8H, m) ppm; ¹³C-NMR (75.5 MHz, CDCl₃): δ = 29.7 (CH₂), 31.7 (24CH₃), 31.9 (12CH₃), 32.0 (12CH₃), 35.0 (16C), 40.2 (2CH), 47.3 (CH₂), 48.1 (2CH), 49.1 (2CH), 49.7 (2CH), 51.8 (2CH), 82.9 (2=C(CN)₂), 113.2 (4CN), 117.8 (4C), 120.47 (2C_{p-Ar}H), 120.52 (2C_{p-Ar}H), 121.05 (2C_{p-Ar}H), 121.11 (2C_{p-Ar}H), 122.8 (2C), 123.0 (2C), 127.8 (C_{Ar}H), 127.9 (2C_{o-Ar}H), 128.0 (2C_{o-Ar}H), 128.26 (2C_{o-Ar}H), 128.3 (2C_{o-Ar}H), 128.4 (2C_{o-Ar}H), 128.5 (4C_{o-Ar}H), 128.6 (2C_{o-Ar}H), 128.8 (2C_{Ar}), 129.2 (2C_{pyrrolic}H), 129.4 (4C_{pyrrolic}H), 129.5 (4C_{pyrrolic}H), 129.7 (2C_{pyrrolic}H), 132.3 (2C_{Ar}H), 134.1 (2C_{quinoxaline}H), 134.2 (2C_{quinoxaline}H), 138.0 (2C), 138.1 (2C), 139.1 (2C), 139.4 (2C), 139.6 (2C), 139.7 (4C), 139.9 (2C), 140.5 (2C), 140.6 (2C), 140.8 (2C), 141.0 (1C), 144.8 (2C), 145.4 (2C_{Ar}), 146.8 (2C), 148.7

(16C_{Ar}^tBu), 153.5 (2C), 153.8 (4C), 154.8 (2C), 155.0 (2C), 156.1 (2C_{Ar}=C(CN)₂), 163.9 (2C) ppm.

6B-[Porphyrinato]zinc-2B-porphyrin-DMN (49) and 6B-porphyrin-2B-[porphyrinato]zinc-DMN (50)



A solution of 6B-dione-2B-porphyrin-DMN **35** (44 mg, 0.0272 mmol) and [diaminoporphyrinato] zinc **149** (40 mg, 0.0318 mmol) in deoxygenated dichloromethane (2.5 mL) was heated in a dark pressure tube at 120 °C for three weeks under an argon atmosphere. The solvent was removed under an argon stream and the crude product was purified by column chromatography (chloroform). Yield: 17 mg (0.0059 mmol, 21.7 %) of a mixture of 6B-[porphyrinato]zinc-2B-porphyrin-DMN **49** and 6B-porphyrin-2B-[porphyrinato]zinc-DMN

50. Melting points: >300 °C.

D.1.4 Synthesis of the Kinked Bis-Porphyrin-Dyads

(1 α ,4 α ,4 $\alpha\alpha$,5 β ,5 $\alpha\alpha$,6 α ,10 α ,10 $\alpha\alpha$,11 β ,11 $\alpha\alpha$)-1,4,4a,5,5a,6,10,10a,11,11a-decahydro-7,8-dichloro-1,4:5,11:6:10-trimethano-12,12-dimethoxy-9H-cyclohepta[*b*]naphthalene (6)



CCl₃CO₂C₂H₅ (16.6 mL, 22.86 g, 119.4 mmol) was added dropwise to an ice-cold suspension of **3** (11.06 g, 38.9 mmol) and sodium methoxide (6.79 g, 95 %, 119.4 mmol) in double-bond and aromatic compounds-free light petroleum (180 mL). On completion of the addition (5 hours) the

mixture was allowed to warm up to RT and stirred for 17 hours. The yellow-brown suspension was poured onto H₂O (500 mL). The aqueous layer was extracted with chloroform (3 x 100 mL), the combined organic layers were washed with H₂O (200 mL) then dried over Na₂SO₄. The solvent was removed under reduced pressure to give the crude product, which was purified by washing with ice-cold ethyl acetate. Yield: 3.85 g (10.5 mmol, 26 %) **6**.

The mother liquor was evaporated to dryness and purified by column chromatography (ethyl acetate/light petroleum 1:5) to give a mixture of product/starting material (7.06 g, 1:3.7), which was reacted again at the above mentioned conditions to give further 3.44 g (9.4 mmol) **6** as colourless crystals. Yield after two runs: 7.56 g (20.6 mmol, 52 %) **6**. Melting point: 174–176 °C; m/z: 366.

^1H -NMR (500 MHz, CDCl_3): δ = 0.93 (1H, d, J = 11.3 Hz), 1.44 (1H, dt, J = 11.8, 3.4), 1.83 (1H, d, J = 11.3), 1.95 (2H, dd, J = 11.3 Hz), 2.04 (4H), 2.11 (1H, s), 2.63 (1H, dd, J = 10.9, 6.8 Hz), 2.82 (1H, t, J = 5.6), 2.87 (1H, bs), 2.90 (1H, bs), 3.06 (3H, s), 3.16 (3H, s), 4.12 (1H, bs), 5.99 (2H, t, J = 1.5 Hz), 6.02 (1H, s) ppm; ^{13}C -NMR (75.5 MHz, CDCl_3): δ = 31.0 (CH_2), 33.8 (CH_2), 36.9 (2CH), 38.8 (CH), 38.9 (CH), 47.6 (CH), 47.7 (CH), 48.5 (CH), 48.6 (CH), 49.6 (OCH_3), 52.1 (OCH_3), 54.7 (CH), 55.6 (CH), 62.6 (CHCl), 121.9 ($\text{C}(\text{OMe})_2$), 132.2 ($=\text{CH}$), 132.56 ($=\text{CCl}$), 132.64 ($=\text{CH}$), 134.3 ($=\text{CH}$) ppm.

(1 α ,4 α ,4 α ,5 β ,5 α ,6 α ,10 α ,10 α ,11 β ,11 α)-1,4,4a,5,5a,6,10,10a,11,11a-decahydro-1,4:5,11:6:10-trimethano-12,12-dimethoxy-9H-cyclohepta[b]naphthalene (7)



Over a period of 45 minutes sodium (9.5 g, 412 mmol) was added in small pieces to a refluxing solution of **6** (7.51 g, 20.4 mmol) in a mixture of anhydrous *iso*-propanol (30 mL) and tetrahydrofuran (100 mL) under an argon atmosphere. After refluxing for 21 hours the mixture was cooled to RT and poured onto H_2O (300 mL). Diethyl ether (100 mL) was added, the layers were separated and the aqueous layer was extracted with diethyl ether (4 x 100 mL). The combined, slightly yellow organic solutions were reduced to 250 mL, washed with H_2O (200 mL) and dried over Na_2SO_4 . The solvents were removed under reduced pressure and the white product was recrystallised from dichloromethane/methanol. Yield: 6.09 g (20.3 mmol, 99 %) **7**. Melting point: 112-114 °C; m/z : 298.

^1H -NMR (300 MHz, CDCl_3): δ = 1.40 (1H, d, J = 10.2 Hz), 1.44 (1H, d, J = 4.5 Hz), 1.47 (1H, bs), 1.82 (2H, m), 1.87 (2H), 1.91 (1H, m), 1.97 (2H, s), 2.02 (1H, dd, J = 7.5, 4.1), 2.20 (1H), 2.29 (1H, m), 2.38 (1H, m), 2.87 (2H, m), 3.07 (3H, s), 3.16 (3H, s), 5.38 (1H, dt, J = 9.4, 3.1 Hz), 5.80 (1H, t, J = 8.1 Hz), 5.98 (2H, t, J = 2.3 Hz) ppm; ^{13}C -NMR (75.5 MHz, CDCl_3): δ = 30.8 (CH_2), 30.9 (CH_2), 36.6 (CH), 37.1 (CH), 37.9 (CH), 38.1 (CH_2), 38.4 (CH), 47.8 (CH), 47.9 (CH), 48.6 (CH), 48.7 (CH), 49.6 (CH_3), 52.0 (CH_3), 56.4 (CH), 57.9 (CH), 122.0 (C), 128.4 ($=\text{CH}$), 132.2 ($=\text{CH}$), 132.5 ($=\text{CH}$), 133.3 ($=\text{CH}$) ppm.

(1 α ,4 α ,4 α ,5 β ,5 α ,6 α ,10 α ,10 α ,11 β ,11 α)-1,4,4a,5,5a,6,10,10a,11,11a-decahydro-1,4:5,11:6:10-trimethano-9H-cyclohepta[b]naphthalene-12-one (8)

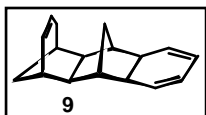


A solution of **7** 3.00 g, 10.0 mmol) in tetrahydrofuran (60 mL) and formic acid (90 %, 60 mL) was stirred overnight at RT. The colourless solution was poured onto H_2O (100 mL). The white precipitate was filtered off, washed

with methanol and dried under high vacuum to give **8** (2.11 g, 8.36 mmol, 83.6 %). The mother-liquor was extracted with diethyl ether (4 x 100 mL) and the combined organic layers were washed with H₂O (2 x 100 mL), 1M K₂CO₃ (until no more gas evolved) and brine (100 mL), then dried over Na₂SO₄. The solvents were evaporated under reduced pressure and the white solid was washed with methanol to give further **8** (0.2 g, 0.793 mmol, 7.9 %). Total yield: 2.31 g (9.15 mmol, 91.5 %) **8**. Melting point: 94 °C; m/z (-CO): 224.

¹H-NMR (500 MHz, CDCl₃): δ = 1.43 (2H, m), 1.55 (1H, dd, *J* = 11.6, 1.3 Hz), 1.60 (1H, s), 1.72 (1H, dt, *J* = 11.6, 1.6 Hz), 1.82 (1H, d, *J* = 9.2 Hz), 1.85 (2H, m), 1.96 (1H, dd, *J* = 8.2, 4.2 Hz), 2.06 (1H, dd, *J* = 8.6, 4.2 Hz), 2.23 (2H, bs), 2.32 (1H, m), 2.40 (1H, m), 3.07 (2H, m), 5.38 (1H, dt, *J* = 9.2, 3.1 Hz), 5.80 (1H, dd, *J* = 9.2, 7.2 Hz), 6.34 (2H, t, *J* = 2.6 Hz) ppm; ¹³C-NMR (75.5 MHz, CDCl₃): δ = 30.8 (CH₂), 31.2 (CH₂), 36.7 (CH), 37.8 (CH₂), 37.9 (CH), 39.6 (CH), 40.8 (CH), 44.6 (CH), 44.7 (CH), 51.8 (CH), 51.9 (CH), 56.1 (CH), 57.5 (CH), 128.5 (=CH), 130.3 (=CH), 130.7 (=CH), 133.1 (=CH), 199.7 (C=O) ppm.

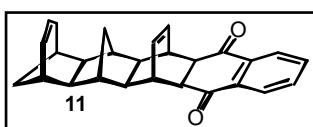
(4α,5β,5α,6α,10α,10α,11β,11α)-4a,5,5a,6,10,10a,11,11a-Octcahydro-5,11:6,10-dimethano-9H-cyclohepta[b]naphthalene (9)



A solution of **8** (2.3 g, 9.114 mmol) in toluene (50 mL) was heated at reflux for 2 hours, followed by stirring at RT overnight. Toluene was removed under reduced pressure to yield **9** as a white solid. Melting point: 91-92 °C.

¹H-NMR (300 MHz, CDCl₃): δ = 1.42 (2H, m), 1.43 (1H, m), 1.92 (1H, s), 1.95 (1H, s), 1.97 (1H, dt), 2.06 (1H, dt, *J* = 10.2, 1.7 Hz), 2.10 (2H, m), 2.23 (1H, d, *J* = 15.5 Hz), 2.31 (2H, m), 2.33 (1H, m), 2.42 (1H, m), 5.42 (1H, m), 5.46 (2H, m), 5.58 (2H, m), 5.84 (1H, m) ppm; ¹³C-NMR (75.5 MHz, CDCl₃): δ = 30.2 (CH₂), 30.6 (CH₂), 37.1 (CH), 37.4 (CH₂), 38.3 (CH), 44.69 (CH), 44.73 (CH), 45.5 (CH), 46.5 (CH), 54.3 (CH), 56.0 (CH), 121.3 (2=CH), 128.43 (=CH), 128.46 (=CH), 128.53 (=CH), 133.0 (=CH) ppm.

(5α,6β,6α,7β,7α,8α,12α,12α,13β,13α,14β,14α)-5a,6,6a,7,7a,8,12,12a,13,13a,14,14a-Dodecahydro-6,14-etheno-7,13:8,12-dimethano-9H-cyclohepta[b]naphthacene-5,15-dione (11)



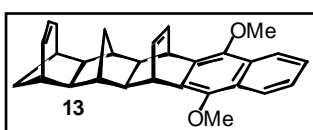
To the refluxing solution of crude **9** in ethanol (30 mL) was added 1,4-naphthoquinone (1.45 g, 9.166 mmol). After one hour a white precipitate was filtered off and the mother liquor was heated at reflux for further three hours. More precipitate was filtered off and combined with the first

precipitate. Yield: 2.93 g (7.660 mmol, 84.0 %) **11**. Melting point: 224-226 °C (dec.); *m/z*: 382.

¹H-NMR (300 MHz, CDCl₃): δ = 1.42 (2H, m), 1.50 (1H, d, *J* = 11.3 Hz), 1.72 (2H, m), 1.83 (4H, m), 2.02 (1H, s), 2.03 (1H, s), 2.19 (1H, d), 2.31 (1H), 2.40 (1H), 3.14 (2H, s), 3.45 (2H, bs), 5.37 (1H, dt, *J* = 9.1, 5.7 Hz), 5.79 (1H, t, *J* = 8.3 Hz), 6.00 (2H, t, *J* = 3.8 Hz), 7.66 (2H, m), 7.98 (2H, m) ppm; ¹³C-NMR (75.5 MHz, CDCl₃): δ = 29.5 (CH₂), 30.8 (CH₂), 36.7 (CH), 37.9 (CH₂), 38.0 (CH), 41.0 (CH), 41.0 (CH), 41.2 (CH), 42.3 (CH), 50.2 (CH), 50.3 (CH), 51.6 (CH), 51.7 (CH), 55.8 (CH), 57.2 (CH), 126.8 (2C_{Ar}H), 128.5 (=CH), 133.0 (=CH), 133.1 (=CH), 133.4 (=CH), 133.9 (2C_{Ar}H), 136.0 (2C_{Ar}), 197.7 (2C=O) ppm.

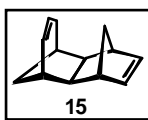
(6β,6α,7β,7α,8α,12α,12α,13β,13α,14β)-6,6a,7,7a,8,12,12a,13,13a,14-Decahydro-6,14-etheno-7,13:8,12-dimethano-5,15-dimethoxy-9H-cyclohepta[*b*]naphthacene (13) and **(1α,4α,4aβ,5α,9α,9aβ)-1,4,4a,5,9,9a-Hexahydro-1,4:5,9-dimethano-6H-cyclohepta[*b*]benzene (15)**

To an ice-cold suspension of **11** (2.75 g, 7.23 mmol) in tetrahydrofuran (50 mL) and hexamethylphosphoramide (3 mL) under an argon atmosphere was added dropwise a solution of potassium bis(trimethylsilyl)amide (4.33 g, 21.70 mmol, ~3 eq.) in toluene (43 mL). On completion of the addition (2 hours), methyl iodide (4.5 mL, 10.26 g, 72.3 mmol, ~20 eq.) was added dropwise to the dark brown solution. The mixture was allowed to warm-up to RT and stirred overnight. The solvents were removed under reduced pressure and the residue was dissolved in diethyl ether (100 mL) and H₂O (100 mL). The organic layer was washed with H₂O (3 x 100 mL) and brine (100 mL), then dried over Na₂SO₄. The solvent was removed under reduced pressure and the crude orange oil was purified by column chromatography (chloroform/light petroleum 1:1). Yield: 1.28 g (3.11 mmol, 43.0 %) ring-expanded 6B-ene-2B-ene-DMN **13** as a colourless solid. The retro-Diels-Alder products 9,10-dimethoxyanthracene (as a yellow solid) and **15** (as a colourless oil) were isolated as side-products.



¹H-NMR (300 MHz, CDCl₃, **13**): δ = 1.44 (2H, t, *J* = 2.3 Hz), 1.65 (2H, m), 1.77 (4H, m), 1.95 (1H, dt, *J* = 17.7, 2.6 Hz), 2.18 (1H, d, *J* = 11.3 Hz), 2.23 (2H, s), 2.31 (1H, bs), 2.39 (1H, bs), 3.96 (6H, s), 4.49 (2H, m, *J* = 2.7 Hz), 5.47 (1H, dt, *J* = 6.7, 2.6 Hz), 5.88 (1H, t, *J* = 8.2 Hz), 6.49 (2H, t, *J* = 4.0 Hz), 7.47 (2H, dd, *J* = 6.4, 3.0 Hz), 8.08 (2H, dd, *J* = 6.4, 3.4 Hz) ppm; ¹³C-NMR (75.5 MHz, CDCl₃, **13**): δ = 30.0 (CH₂), 30.8 (CH₂), 36.6 (CH), 37.9 (CH), 38.0 (CH₂), 38.7

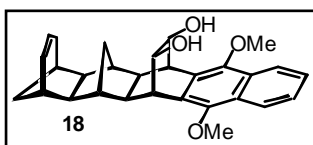
(CH), 38.8 (CH), 40.4 (CH), 41.7 (CH), 51.2 (CH), 51.4 (CH), 55.9 (CH), 57.4 (CH), 62.6 (2OCH₃), 122.2 (2C_{Ar}H), 125.2 (2C_{Ar}H), 127.1 (2C_{Ar}), 128.4 (=CH), 133.1 (=CH), 134.6 (=CH), 134.68 (C_{Ar}), 134.73 (C_{Ar}), 134.9 (=CH), 144.89 (C_{Ar}OMe), 144.94 (C_{Ar}OMe) ppm.



¹H-NMR (300 MHz, CDCl₃, **15**): δ = 1.20 (1H, d, *J* = 8.7), 1.65 (1H, d, *J* = 10.2), 1.80 (1H, m), 1.96 (1H, dd, *J* = 17.7, 2.7 Hz), 2.08 (2H, t, *J* = 7.0 Hz), 2.15 (1H, d, *J* = 9.0 Hz), 2.26 (1H, s), 2.30 (1H), 2.40 (1H, bs), 2.49 (1H, s), 2.55 (1H, s), 5.56 (1H, d, *J* = 9.0 Hz), 5.88 (1H, t, *J* = 7.9 Hz), 6.24 (2H, dd, *J* = 5.6, 3.0), 6.31 (2H, dd, *J* = 5.3, 3.0) ppm; ¹³C-NMR (75.5 MHz, CDCl₃, **15**): δ = 30.5 (CH₂), 34.5 (CH), 36.1 (CH), 40.4 (CH), 41.0 (CH₂), 41.68 (CH), 41.73 (CH₂), 50.1 (CH), 52.1 (CH), 128.8 (=CH), 132.6 (=CH), 141.2 (=CH), 142.3 (=CH) ppm.

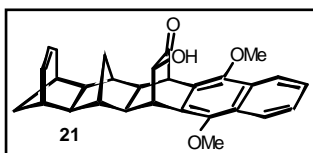
(6β,6α,7β,7α,8α,12α,12α,13β,13α,14β)-6,6a,7,7a,8,12,12a,13,13a,14-Decahydro-6,14-ethano-16,17-cis-dihydroxy-7,13:8,12-dimethano-5,15-dimethoxy-9H-cyclohepta[b]naphthacene (18) and **(6β,6α,7β,7α,8α,12α,12α,13β,13α,14β)-6,6a,7,7a,8,12,12a,13,13a,14-Decahydro-6,14-ethano-16-hydroxy-7,13:8,12-dimethano-5,15-dimethoxy-9H-cyclohepta[b]naphthacene-17-one (21)**

To a colourless suspension of ring-expanded 6B-ene-2B-ene-DMN **13** (800 mg, 1.949 mmol) and 4-methyl-N-morpholine-N-oxide (570 mg, 4.871 mmol, ~2.5 eq.) in 1,4-dioxane (40 mL) was added dropwise OsO₄ (10 mg, 2 %) in *tert*-butanol (2 mL) and H₂O (2 mL). The golden solution was stirred at RT for 7 days, after which further OsO₄ (1 %) in *tert*-butanol (1 mL) and H₂O (2 mL) were added. After 15 days, Na₂S₂O₅ (1 g) in H₂O (10 mL) was added and the mixture stirred for a further 30 minutes, then extracted with dichloromethane (3 x 20 mL). The solvents were removed under reduced pressure and the crude residue was purified by column chromatography (light petroleum/ethyl acetate 3:1). Yield: 175 mg (0.394 mmol, 20.2 %) ring-expanded 6B-ene-2B-diol-DMN **18** as a white solid. Melting point: 136 °C (dec.); *m/z*: 444. As a side product a diastereomeric mixture of the ring-expanded 6B-ene-2B-ketol-DMN **21** was isolated. Yield: 43 mg (0.097 mmol, 5.0 %) **21**.



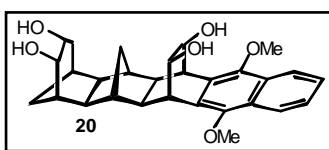
¹H-NMR (500 MHz, CDCl₃, **18**): δ = 1.16 (1H, d, *J* = 12.3 Hz), 1.41 (2H, bs), 1.44 (1H, dd, *J* = 9.9, 2.8 Hz), 1.53 (1H, dd, *J* = 9.9, 2.8 Hz), 1.78 (2H, bs), 1.96 (1H, dt, *J* = 17.0, 2.7 Hz), 2.14 (1H, d, *J* = 12.3 Hz), 2.22 (1H, s), 2.25 (1H, s), 2.30 (1H, bs), 2.40 (1H, bs), 2.46 (2H, t, *J* = 5.2 Hz), 3.77 (2H, dd, *J* = 8.7, 3.0 Hz), 3.93 (1H, dd, *J* = 3.4, 1.9 Hz), 3.960 (3H, s), 3.963 (3H, s), 4.39 (2H, bs), 5.51 (1H, d, *J* = 9.4 Hz), 5.87 (1H, t, *J* = 3.8 Hz), 7.46 (2H, m), 8.08 (2H,

m) ppm; ^{13}C -NMR (75.5 MHz, CDCl_3 , **18**): δ = 30.7 (CH_2), 31.6 (CH_2), 36.6 (CH), 37.79 (CH), 37.85 (CH_2), 37.9 (CH), 39.0 (CH), 39.86 (CH), 39.93 (CH), 48.7 (CH), 48.8 (CH), 55.1 (CH), 56.5 (CH), 62.9 (2OCH_3), 65.66 (CHOH), 65.72 (CHOH), 122.2 (2C_{ArH}), 125.4 (2C_{ArH}), 127.7 (2C_{Ar}), 128.7 ($=\text{CH}$), 129.45 (C_{Ar}), 129.49 (C_{Ar}), 132.9 ($=\text{CH}$), 148.2 (2C_{ArOMe}) ppm.



^1H -NMR (300 MHz, CDCl_3 , **21**): δ = 0.97 (1H, dd, J = 12.8, 6.0 Hz), 1.72 (1H, s), 1.78 (1H, m), 1.80 (1H, bs), 1.84 (2H, bs), 1.95 (1H, m), 2.11 (1H, d, J = 12.8 Hz), 2.20 (1H, s), 2.24 (2H, d, J = 7.5 Hz), 2.33 (1H, d, J = 6.7 Hz), 2.38 (1H, d, J = 3.8 Hz), 2.45 (1H, bs), 2.54 (1H, t, J = 1.7 Hz), 4.42 (1H, d, J = 13.2 Hz), 3.98 (3H, s), 3.89 (3H, s), 4.12 (1H, m), 5.48 (1H, m), 5.85 (1H, dd, J = 16.7, 8.7 Hz), 7.49 (2H, m), 8.08 (2H, m) ppm; ^{13}C -NMR (75.5 MHz, CDCl_3 , **21**): δ = 30.5, 30.8 (CH_2), 31.9, 32.2 (CH_2), 36.5, 36.77 (CH), 37.76, 38.0 (CH), 37.8, 37.9 (CH_2), 38.7, 39.0 (CH), 40.1 (CH), 40.6 (CH), 47.38, 47.42 (CH), 51.1, 51.3 (CH), 52.2 (CH), 53.8, 56.7 (CH), 55.2, 55.3 (CH), 63.1 (OCH_3), 63.2 (OCH_3), 69.89 (CHOH), 69.94 (CHOH), 122.3, 122.4 (2C_{ArH}), 125.8, 126.1 (2C_{ArH}), 128.3, 128.4 (2C_{Ar}), 128.6, 128.9 ($=\text{CH}$), 128.80, 128.82 (2C_{Ar}), 132.7, 132.9 ($=\text{CH}$), 147.8, 148.8 (2C_{ArOMe}), 212.8, 212.9 ($\text{C}=\text{O}$) ppm.

(6 β ,6 α ,7 β ,7 α ,8 α ,12 α ,12 α ,13 β ,13 α ,14 β)-6,6a,7,7a,8,10,11,12,12a,13,13a,14-Dodecahydro-6,14-ethano-10,11,16,17-*cis,cis*-tetrahydroxy-7,13:8,12-dimethano-5,15-dimethoxy-9H-cyclohepta[*b*]naphthacene (20**)**

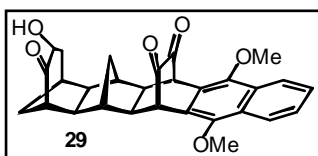


To a solution of ring-expanded 6B-ene-2B-diol-DMN **18** (180 mg, 0.4048 mmol) and 4-methyl-N-morpholine-N-oxide (130 mg, 1.110 mmol, ~2.5 eq.) in 1,4-dioxane (8 mL) was added OsO_4 (2 mg, 2 %) in *tert*-butanol (0.4 mL) and H_2O (0.5 mL). The golden solution was stirred at RT in the dark for eight weeks, after which dichloromethane (5 mL) and $\text{Na}_2\text{S}_2\text{O}_5$ (0.5 g) in H_2O (5 mL) were added. The brown mixture was stirred for 1 hour, the layers were separated and the aqueous phase was extracted with dichloromethane (3 x 10 mL). The combined organic layers were washed with H_2O (2 x 20 mL) and brine (20 mL), then dried over Na_2SO_4 . The solvents were removed under reduced pressure to give a slightly yellow solid, which was recrystallised from ethyl acetate/light petroleum. Yield: 136 mg (0.2841 mmol, 70.2 %) ring-expanded 6B-diol-2B-diol-DMN **20** as a white solid; m/z : 478.

^1H -NMR (300 MHz, CDCl_3): δ = 1.05 (1H, dd, J = 11.7, 3.9 Hz), 1.40 (1H, d, J = 13.2 Hz), 1.68 (1H, m), 1.80 (1H, dd, J = 16.6, 7.1 Hz), 1.90 (2H, m), 2.05 (1H), 2.13 (2H, bs), 2.26 (1H, s), 2.32 (1H, d, J = 7.9 Hz), 2.45 (1H, bs), 2.52 (1H, bs), 2.85 (1H, s), 3.82 (2H, bs), 3.91 (1H, dd, J = 10.6, 2.3 Hz), 3.98 (3H, s), 3.99 (3H, s), 4.38 (1H), 4.41 (2H, bs), 7.50 (2H, dd, J = 6.4, 3.4 Hz), 8.10 (2H, dd, J = 6.4, 3.4 Hz) ppm; ^{13}C -NMR (75.5 MHz, CDCl_3): δ = 30.9 (CH_2), 31.4 (CH_2), 33.3 (CH_2), 34.0 (CH), 38.1 (CH), 38.9 (CH), 39.9 (2CH), 46.1 (CH), 47.9 (2CH), 52.2 (CH), 52.8 (CH), 63.0 (2OCH_3), 63.7 (CHOH), 65.7 (2CHOH), 68.6 (CHOH), 122.3 (2C_{ArH}), 125.7 (2C_{ArH}), 127.9 (2CAr), 129.0 (2C_{Ar}), 148.5 (2C_{ArOMe}) ppm.

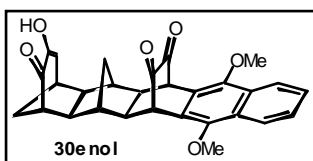
(6 β ,6 α ,7 β ,7 α ,8 α ,12 α ,12 α ,13 β ,13 α ,14 β)-6,6a,7,7a,8,10,12,12a,13,13a,14-Undecahydro-6,14-ethano-10-hydroxy-7,13:8,12-dimethano-5,15-dimethoxy-9H-cyclohepta[*b*]naphthacene-11,16,17-trione (29) and **(6 β ,6 α ,7 β ,7 α ,8 α ,12 α ,12 α ,13 β ,13 α ,14 β)-6,6a,7,7a,8,12,12a,13,13a,14-Decahydro-6,14-ethano-10-hydroxy-7,13:8,12-dimethano-5,15-dimethoxy-cyclohepta[*b*]naphthacene-11,16,17-trione (30enol)**

To an ice-cold solution of ring-expanded 6B-diol-2B-diol-DMN **20** (130 mg, 0.2716 mmol) and *p*-toluenesulfonic acid monohydrate (521 mg, 2.730 mmol, ~10 eq.) in anhydrous dichloromethane (5 mL) was added dropwise 4-acetamido-TEMPO (488 mg, 2.757 mmol, ~10 eq.) in anhydrous dichloromethane (10 mL). On completion of the addition (30 minutes) the mixture was stirred for five days in the dark at RT. A white precipitate was filtered off and ethanol (5 mL) was added to the yellow solution, which was stirred for a further 30 minutes. The bright yellow solution was washed with H_2O (10 mL) and brine (10 mL), then dried over Na_2SO_4 . The solvents were removed under reduced pressure to give a yellow oil (245 mg), which was purified by column chromatography (light petroleum/ethyl acetate 1:4, 1:6). Yield (**29**): 69 mg (0.146 mmol, 53.8 %) of the bright yellow ring-expanded 6B-ketol-2B-dione-DMN **29**. Melting point: 170 °C dec.; m/z : 472. Yield (**30enol**): 37 mg (0.0786 mmol, 28.9 %) ring-expanded 6B-keto-enol-2B-dione-DMN **30enol** as a yellow solid.



^1H -NMR (300 MHz, CDCl_3 , **29**): δ = 0.73 (1H, d, J = 13.9 Hz), 1.05 (1H, d, J = 13.9 Hz), 1.70 (1H, m), 1.95 (2H, s), 2.16 (2H, bs), 2.25 (2H, s), 2.50 (1H, s), 2.54 (1H, s), 2.58 (1H, s), 3.02 (1H, s), 3.32 (1H, s), 3.89 (6H, s), 4.43 (1H, s), 4.57 (1H, s), 4.60 (1H, s), 5.43 (1OH), 7.55 (2H, dd, J = 6.0, 3.0 Hz), 8.10 (2H, bs) ppm; ^{13}C -NMR (75.5 MHz, CDCl_3 , **29**): δ = 32.3 (CH_2), 35.1 (CH_2), 40.3 (CH), 40.7 (CH), 40.8 (CH), 43.3 (CH), 44.8 (CH), 46.2, 46.4 (CH_2), 49.8 (CH), 51.0 (CH), 51.2 (CH), 51.5 (CH), 51.6 (CH), 63.4 (2OCH_3), 72.3

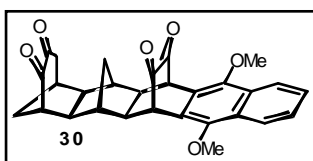
(CHOH), 122.4 ($C_{Ar}H$), 122.5 ($C_{Ar}H$), 122.6 ($2C_{Ar}$), 126.9 ($2C_{Ar}H$), 129.08 (C_{Ar}), 129.13 (C_{Ar}), 149.1 ($C_{Ar}OMe$), 149.2 ($C_{Ar}OMe$), 191.6 ($C=O$), 192.0 ($C=O$), 210.1 ($C=O$) ppm.



1H -NMR (300 MHz, $CDCl_3$, **30enol**): δ = 0.69 (1H, d, J = 14.3 Hz), 1.33 (1H, d, J = 14.3 Hz), 1.92 (2H, d, J = 11.3 Hz), 2.12 (2H, s), 2.30 (2H, m), 2.41 (2H, bs), 3.00 (1H, bs), 3.15 (1H, bs), 3.88 (6H, s), 4.52 (2H, s), 6.11 (1H, d, J = 10.5 Hz), 7.54 (2H, dd, J = 6.4,

3.4 Hz), 8.08 (2H, dd, J = 6.4, 3.4 Hz) ppm; ^{13}C -NMR (75.5 MHz, $CDCl_3$, **30enol**): δ = 33.0 (CH_2), 38.6 (CH), 39.7 (CH), 41.2 (CH), 43.1 (CH_2), 50.4 (CH), 50.5 (CH), 50.9 (CH), 51.3 (CH), 51.5 (CH), 51.6 (CH), 52.7 (CH), 63.4 ($2OCH_3$), 119.5 ($=CH$), 122.45 ($C_{Ar}H$), 122.49 ($C_{Ar}H$), 122.9 (C_{Ar}), 123.0 (C_{Ar}), 126.9 ($C_{Ar}H$), 127.0 ($C_{Ar}H$), 129.1 ($2C_{Ar}$), 149.10 ($C_{Ar}OMe$), 149.15 ($C_{Ar}OMe$), 149.9 ($=COH$), 191.45 ($C=O$), 191.47 ($C=O$), 196.4 ($C=O$) ppm

(6 β ,6 α ,7 β ,7 α ,8 α ,12 α ,12 α ,13 β ,13 α ,14 β)-6,6a,7,7a,8,12,12a,13,13a,14-Decahydro-6,14-ethano-7,13:8,12-dimethano-5,15-dimethoxy-9H-cyclohepta[b]naphthacene-10,11,16,17-tetraone (30**)**



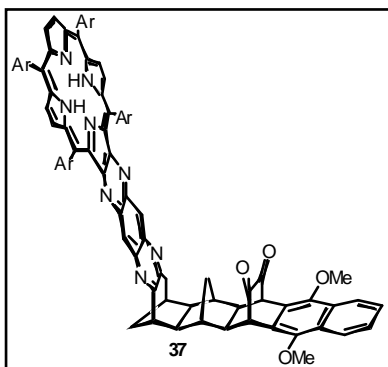
To an ice-cold solution of ring-expanded 6B-ketol-2B-dione-DMN **29** (115 mg, 0.2423 mmol) and *p*-toluenesulfonic acid monohydrate (230 mg, 1.2115 mmol, ~5 eq.) in anhydrous dichloromethane (4 mL) was added portionwise a solution of 4-acetamido-TEMPO

(258 mg, 1.2115 mmol, ~5 eq.) in dichloromethane (6 mL). On completion of the addition (30 minutes) the mixture was allowed to warm-up to RT and was stirred for 20 days in the dark. Ethanol (2 mL) was added to the yellow solution, which was stirred for further 30 minutes. The bright yellow solution was washed with H_2O (10 mL) and brine (10 mL) then dried over Na_2SO_4 . The solvents were removed under reduced pressure to give a yellow solid, which was purified by column chromatography (light petroleum/ethyl acetate 1:4). Yield: 65 mg (0.1381 mmol, 57.0 %) ring-expanded 6B-dione-2B-dione-DMN **30** as a yellow solid.

1H -NMR (300 MHz, $CDCl_3$): δ = 0.32 (1H, d, J = 14.6 Hz), 1.01 (1H, d, J = 14.6 Hz), 1.81 (2H, m), 2.21 (2H, bs), 2.28 (1H, d, J = 13.2 Hz), 2.38 (2H, bs), 2.53 (1H, s), 2.56 (1H, s), 3.19 (2H, bs), 3.86 (1H, bs), 3.90 (6H, s), 4.55 (1H, d, J = 3.0 Hz), 4.58 (1H, d, J = 2.6 Hz), 7.56 (2H, m), 8.10 (2H, m) ppm; ^{13}C -NMR (75.5 MHz, $CDCl_3$): δ = 30.8 (CH_2), 35.9 (CH_2), 39.7 (CH), 40.4 (CH), 40.6 (CH), 41.3 (CH), 46.1 (CH_2), 48.3 (CH), 49.3 (CH), 50.2 (CH), 51.1 (CH), 51.3 (CH), 53.5 (CH), 63.3 ($2OCH_3$), 122.2 ($2C_{Ar}$), 122.3 ($2C_{Ar}H$), 126.8 ($2C_{Ar}H$),

128.9 (C_{Ar}), 129.0 (C_{Ar}), 148.9 ($C_{Ar}OMe$), 149.0 ($2C_{Ar}OMe$), 190.9 ($C=O$), 191.4 ($C=O$), 191.9 ($C=O$), 196.4 ($C=O$) ppm.

Kinked 6B-porphyrin-2B-dione-DMN (**37**)



A solution of ring-expanded 6B-dione-2B-dione-DMN **30** (30 mg, 0.0637 mmol) and 'diaminoporphyrin' (80 mg, 0.0669 mmol) in de-oxygenated dichloromethane (3 mL) was heated for five days in a dark pressure tube at 120 °C. The crude product was purified by column chromatography (chloroform). Yield: 16 mg (0.0098 mmol, 15.4 %) kinked 6B-porphyrin-2B-dione-DMN **37**. Melting point: >300 °C; MH^+

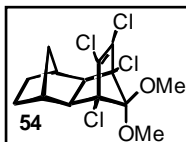
(MALDI): 1631.

1H -NMR (500 MHz, $CDCl_3$): δ = -2.37 (2H, s), 0.48 (1H, d, J = 13.6 Hz), 0.60 (1H, d, J = 13.6 Hz), 1.54 (72H), 1.92 (1H, d, J = 12.1 Hz), 2.08 (1H, bs), 2.24 (1H, d, J = 8.4 Hz), 2.28 (1H, d, J = 7.8 Hz), 2.32 (1H, t, J = 8.3 Hz), 2.48 (1H, s), 2.52 (1H, t, J = 8.3 Hz), 2.59 (1H, s), 2.94 (1H, m), 3.22 (1H, d, J = 18.5 Hz), 3.38 (1H, dd, J = 18.5, 6.2 Hz), 3.74 (1H, m), 3.90 (3H, s), 3.91 (3H, s), 4.52 (1H, d, J = 3.2 Hz), 4.57 (1H, d, J = 3.2 Hz), 7.56 (2H, dd, J = 6.2, 3.1 Hz), 7.83 (2H, dd, J = 2.8, 1.8 Hz), 7.96 (1H, t, J = 0.9 Hz), 8.00 (1H, t, J = 0.9 Hz), 8.02 (1H, bs), 8.05 (2H, d, J = 1.8 Hz), 8.11 (2H, dd, J = 6.2, 3.1 Hz), 8.12 (4H, m), 8.13 (1H, t, J = 1.7 Hz), 8.55 (1H, s), 8.66 (1H, s), 8.79 (2H, s), 9.01 (4H, m) ppm; ^{13}C -NMR (75.5 MHz, $CDCl_3$): δ = 28.9 (CH_2), 31.8 ($18CH_3$), 32.0 ($6CH_3$), 34.0 (CH_2), 35.1 (8C), 35.3 (CH_2), 36.4 (CH), 40.0 (CH), 40.2 (CH), 47.6 (CH), 49.8 (CH), 50.0 (CH), 51.6 (CH), 51.7 (CH), 52.3 (CH), 55.9 (CH), 63.47 (OCH_3), 63.49 (OCH_3), 68.2 (CH_2), 118.0 (2C), 120.6 ($C_{p-Ar}H$), 121.1 ($C_{p-Ar}H$), 122.6 ($2C_{Ar}H$), 123.06 ($2C_{Ar}$), 123.11 (C), 126.9 ($2C_{Ar}H$), 128.1 ($C_{o-Ar}H$), 128.4 ($C_{o-Ar}H$), 128.5 ($C_{o-Ar}H$), 128.7 ($C_{o-Ar}H$), 128.8 ($C_{pyrrolic}H$), 128.9 ($C_{pyrrolic}H$), 129.17 (C_{Ar}), 129.21 (C_{Ar}), 129.3 ($C_{pyrrolic}H$), 129.6 ($C_{pyrrolic}H$), 131.0 (CH), 132.3 (C), 134.2 ($2C_{quinoxaline}H$), 138.06 (C), 138.09 (C), 139.0 (C), 139.85 (2C), 139.92 (C), 139.95 (2C), 140.0 (C), 140.72 (C), 140.75 (C), 141.1 (C), 145.6 (C), 145.7 (C), 148.75 (C_{Ar}^tBu), 148.81 ($2C_{Ar}^tBu$), 148.85 ($4C_{Ar}^tBu$), 148.9 (C_{Ar}^tBu), 149.14 ($C_{Ar}OMe$), 149.18 ($C_{Ar}OMe$), 154.0 (C), 154.91 (C), 154.93 (C), 158.8 (C), 167.76 (C), 167.81 (C), 191.6 ($C=O$), 191.7 ($C=O$) ppm.

D.2 SYNTHESIS OF THE TRIADS

D.2.1 Synthesis of the 2B-Porphyrin Donor

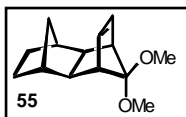
1,2,3,4-Tetrachloro-1,4,4a,5,6,7,8,8a-octahydro-10,10-dimethoxy-*endo*-1,4-*exo*-5,8-dimethanonaphthalene (**54**)¹⁷⁴



A mixture of norbornene (18.11 g, 192 mmol) and 5,5-dimethoxy-1,2,3,4-tetrachlorocyclopentadiene (50.76 g, 192 mmol) [**D.1**, page **153**) dissolved in toluene (15 mL) was heated at reflux for 40 hours. The solvent was removed under reduced pressure to give a brown oil, which crystallised in the fridge. The crystals were washed with ice-cold light petroleum (10 mL) to give a white solid, which was dried under high vacuum. Yield: 35.42 g (98.9 mmol, 51.5 %) acetal **54**. Melting point: 94 - 95 °C (lit.:¹⁷⁴ 95 - 96 °C); *m/z* (-HCl): 321.

¹H-NMR (300 MHz, CDCl₃): δ = 0.92 (1H, d, *J* = 11.3 Hz), 1.14 (2H, m), 1.38 (1H, dt, *J* = 11.3, 1.9 Hz), 1.54 (2H, m), 2.28 (2H, bs), 2.46 (2H, s), 3.51 (3H, s), 3.58 (3H, s) ppm.

10,10-Dimethoxy-1,4,4a,5,6,7,8,8a-octahydro-*endo*-1,4-*exo*-5,8-dimethano-naphthalene (**55**)^{171,174}



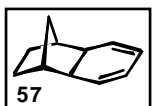
To a refluxing solution of **54** (35.0 g, 98 mmol) in a mixture of *iso*-propanol (900 mL) and tetrahydrofuran (300 mL) was added sodium (91 g, 3.96 mol) in small pieces over a period of 5 hours. On completion of the addition the suspension was stirred at reflux for 16 hours. After cooling to RT H₂O (500 mL) was added and the aqueous layer extracted with ethyl acetate (3 x 100 mL). The combined organic layers were evaporated to dryness to give a brown oil, which was dissolved in dichloromethane. This solution was washed with half-saturated NaHCO₃ (200 mL). The aqueous layer was extracted with dichloromethane (3 x 100 mL) and the combined organic solutions were dried over Na₂SO₄. The solvent was removed under reduced pressure to give crude **55** (28 g), which was used without further purification.

¹H-NMR (300 MHz, CDCl₃): δ = 0.60 (1H, d, *J* = 10.3 Hz), 1.09 (2H, m), 1.40 (2H, m), 2.02 (2H, s), 2.10 (2H, s), 2.17 (1H, dt, *J* = 10.3, 1.8 Hz), 2.87 (2H, bs), 3.08 (3H, s), 3.18 (3H, s), 6.00 (2H, s) ppm.

1,4,4a,5,6,7,8,8a-Octahydro-*endo*-1,4-*exo*-5,8-dimethanonaphthalene-10-one (56)^{171,174}

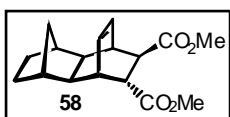
A yellow-milky mixture of crude **55** (28.01 g) in tetrahydrofuran (200 mL) and formic acid (90 %, 250 mL) was stirred at RT overnight, after which diethyl ether (600 mL) and H₂O (400 mL) were added. The colourless aqueous layer was extracted with diethyl ether (2 x 200 mL) and the combined organic solutions were washed with H₂O (2 x 200 mL) and 1M K₂CO₃ (4 x 100 mL), then dried over Na₂SO₄. The solvent was removed under reduced pressure and the resulting orange oil was dried under high vacuum. Yield: 21.6 g crude **56**. Melting point: 42 - 44 °C (lit.:¹⁷⁴ 44 - 45 °C).

¹H-NMR (300 MHz, CDCl₃): δ = 0.73 (1H, d, *J* = 10.2 Hz), 1.15 (2H, m), 1.44 (2H, m), 2.07 (1H, d, *J* = 10.2 Hz), 2.18 (2H, bs), 2.26 (2H, bs), 3.04 (2H, bs), 6.36 (2H, s) ppm.

(1α,4α,4aβ,8aβ)-1,2,3,4,4a,8a-Hexahydro-1,4-methanonaphthalene (57)^{171,174}

A solution of crude **56** (21.6 g) in toluene (150 mL) was heated to reflux for 17 hours. The solvent was removed under reduced pressure to give 24.48 g of **57** as a colourless oil.

¹H-NMR (300 MHz, CDCl₃): δ = 1.25 (1H, d, *J* = 9.2 Hz), 1.35 (2H, m), 1.54 (2H, m), 1.76 (1H, dt, *J* = 9.2, 2.0 Hz), 2.03 (2H, s), 2.48 (2H, s), 5.40 (2H, d, *J* = 11.2 Hz), 5.56 (2H, d, *J* = 11.2 Hz) ppm.

(1α,4α,4aβ,5α,8α,8aβ)-1,2,3,4,4a,5,6,7,8,8a-Decahydro-1,4-etheno-5,8-methanonaphthalene-2,3-*trans*-dicarboxylate (58)¹⁷⁵

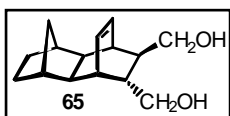
A yellow solution of crude **57** (10.31 g) and dimethyl fumarate (5.13 g, 35.6 mmol) in toluene (80 mL) was heated at reflux for 18 hours. The solution was concentrated under reduced pressure and placed in the freezer.

White crystals (excess dimethyl fumarate) were filtered off and the mother-solution was placed in the freezer again. The product precipitated as white crystals, which were dried under high vacuum. Yield: 6.94 g (24.2 mmol) 2B-ene-*trans*-diester **58**. Melting point: 104-106 °C; *m/z*: 290.

¹H-NMR (500 MHz, CDCl₃): δ = 0.63 (1H, d, *J* = 10.0), 1.05 (2H, m), 1.36 (2H, m), 1.53 (1H, dd, *J* = 8.4, 2.5 Hz), 1.75 (1H, dd, *J* = 8.4, 2.7 Hz), 1.95 (1H, bs), 2.01 (1H, bs), 2.09 (1H, dt, *J* = 10.1, 2.2 Hz), 2.73 (1H, dd, *J* = 5.6, 2.9 Hz), 3.02 (1H, dt, *J* = 6.6, 3.2 Hz), 3.08 (1H, dt, *J* = 6.6, 3.2 Hz), 3.13 (1H, dd, *J* = 5.6, 2.2 Hz), 3.62 (3H, s), 3.73 (3H, s), 6.05 (1H, t, *J* = 7.4), 6.22 (1H, t, *J* = 7.4) ppm; ¹³C-NMR (75.5 MHz, CDCl₃): δ = 31.4 (2CH₂), 34.8

(CH₂), 37.4 (2CH), 41.0 (CH), 41.4 (CH), 43.7 (CH), 46.0 (CH), 47.1 (CH), 48.1 (CH), 52.0 (OCH₃), 52.2 (OCH₃), 131.7 (=CH), 134.0 (=CH), 174.5 (C=O), 176.5 (C=O) ppm.

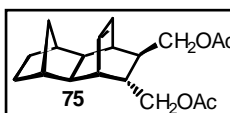
(1 α ,4 α ,4 $\alpha\beta$,5 α ,8 α ,8 $\alpha\beta$)-1,2,3,4,4a,5,6,7,8,8a-Decahydro-1,4-etheno-2,3-*trans*-bis(hydroxymethyl)-5,8-methanonaphthalene (65)



A solution of 2B-ene-*trans*-diester **58** (3.50 g, 12.05 mmol) in tetrahydrofuran (70 mL) was added dropwise to an ice-cold suspension of LiAlH₄ (2.29 g, 60.3 mmol, ~5 eq.) in tetrahydrofuran (70 mL) under an argon atmosphere. On completion of the addition (60 minutes) the mixture was heated at reflux for 20 hours. After cooling the greyish mixture to 0 °C, 1M K₂CO₃ (40 mL) was added dropwise to quench the reaction. The mixture was heated at reflux for 15 minutes then filtered hot through a pad of filter aid, which was extracted with boiling diethyl ether. The organic layer was washed with H₂O (2 x 40 mL) then dried over Na₂SO₄. The solvents were removed under reduced pressure to give a white solid, which was dried under high vacuum. Yield: 2.784 g (11.88 mmol, 98.6 %) 2B-ene-*trans*-diol **65** as colourless needles. Melting point: 103-104 °C; m/z: 234.

¹H-NMR (300 MHz, CDCl₃): δ = 0.63 (1H, d, J = 9.2 Hz), 1.05 (2H, m), 1.17 (1H, m), 1.37 (2H, m), 1.51 (1H, m), 1.63 (2H, bs), 1.92 (1H, s), 1.97 (1H, s), 2.16 (1H, d, J = 9.2 Hz), 2.49 (1H, d, J = 6.2 Hz), 2.55 (1H, d, J = 6.2 Hz), 3.04 (1H, t, J = 9.7 Hz), 3.49 (1H, dd, J = 9.2, 5.1 Hz), 3.58 (2H, bs, OH), 3.65 (2H, m), 5.96 (1H, t, J = 7.2 Hz), 6.20 (1H, t, J = 7.2 Hz) ppm; ¹³C-NMR (75.5 MHz, CDCl₃): δ = 31.6 (CH₂), 31.6 (CH₂), 35.3 (CH₂), 37.1 (CH), 37.4 (CH), 41.1 (CH), 41.6 (CH), 42.9 (CH), 45.9 (CH), 47.9 (CH), 49.6 (CH), 66.1 (-CH₂OH), 67.3 (CH₂OH), 131.1 (=CH), 135.0 (=CH) ppm.

(1 α ,4 α ,4 $\alpha\beta$,5 α ,8 α ,8 $\alpha\beta$)-1,2,3,4,4a,5,6,7,8,8a-Decahydro-2,3-*trans*-bis(acetoxymethyl)-1,4-etheno-5,8-methanonaphthalene (75)

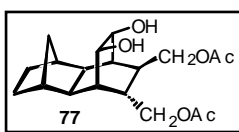


To a solution of 2B-ene-*trans*-diol **65** (436 mg, 1.86 mmol) in anhydrous pyridine (10 mL) was added acetic anhydride (0.53 mL, 570 mg, 5.58 mmol). The colourless solution was stirred overnight then poured onto a mixture of ice (60 g), dichloromethane (20 mL) and 1M HCl (10 mL). The aqueous layer was extracted with dichloromethane (4 x 20 mL). The combined organic layers were washed with 1M HCl (2 x 25 mL) and NaHCO₃ (sat., 2 x 25 mL) then dried over Na₂SO₄. The solvent was removed under reduced pressure to give crude **75** (495 mg) as a slightly

yellow oil, which was purified by column chromatography (light petroleum/ethyl acetate 3:1). Yield: 445 mg (1.40 mmol, 75%) 2B-ene-*trans*-diacetate **75** as a colourless oil that crystallises upon standing.

$^1\text{H-NMR}$ (500 MHz, CDCl_3): δ = 0.64 (1H, d, J = 9.9 Hz), 1.06 (2H, m), 1.13 (1H, m), 1.38 (2H, m), 1.44 (1H, m), 1.56 (1H, dd, J = 8.5, 2.6 Hz), 1.74 (1H, dd, J = 8.5, 2.6 Hz), 1.93 (1H, s), 1.98 (1H, s), 2.03 (3H, s), 2.06 (3H, s), 2.17 (1H, dt, J = 10.0, 1.8 Hz), 2.57 (2H, m), 3.64 (1H, dd, J = 10.7, 9.0 Hz), 3.72 (1H, dd, J = 10.7, 6.2 Hz), 4.04 (1H, dd, J = 11.0, 9.0 Hz), 4.19 (1H, dd, J = 11.0, 6.7 Hz), 6.00 (1H, t, J = 7.3 Hz), 6.21 (1H, t, J = 7.3 Hz) ppm; $^{13}\text{C-NMR}$ (75.5 MHz, CDCl_3): δ = 21.0 (2CH₃), 31.5 (CH₂), 31.6 (CH₂), 35.3 (CH₂), 35.5 (CH), 36.5 (CH), 41.0 (CH), 41.5 (CH), 42.0 (CH), 42.5 (CH), 49.2 (2CH), 66.0 (CH₂-O), 67.5 (CH₂-O), 131.3 (=CH), 134.9 (=CH), 171.07 (OAc), 171.12 (OAc) ppm.

(1 α ,4 α ,4a β ,5 α ,8 α ,8a β)-1,2,3,4,4a,5,6,7,8,8a-Decahydro-2,3-*trans*-bis(acetoxymethyl)-1,4-ethano-10,11-*cis*-dihydroxy-5,8-methanonaphthalene (77**)**

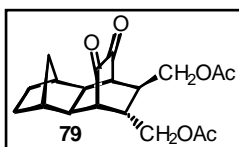


To a solution of 2B-ene-*trans*-diacetate **75** (200 mg, 0.63 mmol) and 4-methyl-N-morpholine-N-oxide (221 mg, 1.89 mmol) in 1,4-dioxane (4 mL) were added OsO₄ (1.6 mg, 1 %) in *tert*-butanol (0.3 mL) and H₂O (2 drops). After stirring at RT for 3 days NaS₂O₅ (1g) in H₂O (10 mL) and dichloromethane (10 mL) were added to the slightly yellow solution. The red mixture was stirred for 30 minutes, the layers were separated and the aqueous layer was extracted with dichloromethane (3 x 10 mL). The combined yellow organic layers were washed with H₂O (10 mL) and brine (10 mL) then dried over Na₂SO₄. The solvents were removed under reduced pressure to give a yellow oil (236 mg), which was purified by column chromatography (light petroleum/ethyl acetate 1.5:1). Yield: 99 mg (0.28 mmol, 44.6 %) 2B-diol-*trans*-diacetate **77** as a colourless oil that crystallises upon standing. Melting point: 132 °C. As a side product the bright yellow 2B-dione-*trans*-diacetate **79** (61 mg, 0.17 mmol, 27.6%) was isolated.

$^1\text{H-NMR}$ (300 MHz, CDCl_3): δ = 1.12 (1H, bs), 1.14 (1H, bs), 1.19 (1H, d, J = 10.0 Hz), 1.28 (1H, d, 11.3 Hz), 1.59 (2H, m), 1.84 (1H, m), 1.88 (1H, d, J = 2.5 Hz), 1.91 (1H, bs), 2.03 (2H, dd, J = 10.0, 4.3), 2.04 (3H, s), 2.09 (3H, s), 2.14 (1H, d, J = 3.7 Hz), 2.24 (1H, m), 2.29 (1H, m), 2.39 (1H, dd, J = 6.2, 3.7 Hz), 2.44 (1H, t, J = 4.3 Hz), 3.62 (1H, dd, J = 11.3, 9.3 Hz), 4.01 (1H, dd, J = 11.3, 5.6 Hz), 4.11 (1H, dd, J = 10.6, 8.1 Hz), 4.19 (1H, m) ppm; $^{13}\text{C-NMR}$ (75.5 MHz, CDCl_3): δ = 21.0 (2CH₃), 29.7 (CH₂), 31.2 (CH), 31.6 (CH₂), 36.6

(CH₂), 37.9 (CH), 39.4 (CH), 39.9 (CH), 40.2 (CH), 41.8 (CH), 49.6 (2CH), 65.7 (CH₂O), 65.9 (CH₂O), 70.4 (2CHOH), 170.7 (OAc) ppm.

(1 α ,4 α ,4 $\alpha\beta$,5 α ,8 α ,8 $\alpha\beta$)-1,2,3,4,4a,5,6,7,8,8a-Decahydro-2,3-*trans*-bis(acetoxymethyl)-1,4-ethano-5,8-methanonaphthalene-10,11-dione (79**)**



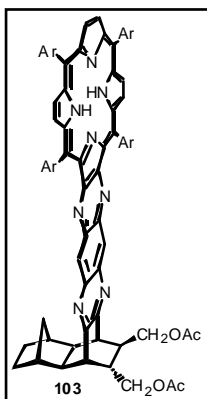
Method 1 (TEMPO reaction): To an ice-cold solution of 2B-diol-*trans*-diacetate **77** (676 mg, 1.92 mmol) and *p*-toluenesulfonic acid monohydrate (1.80 g, 9.5 mmol, 5 eq.) in dichloromethane (25 mL) was added dropwise 4-acetamido-TEMPO (2.03 g, 9.5 mmol, ~5 eq.) in dichloromethane (50 mL). On completion of the addition (120 minutes) the mixture was stirred for 72 hours in the dark at RT. A white precipitate was filtered off and ethanol (50 mL) was added to the orange solution to quench the reaction. The bright yellow solution was washed with H₂O (50 mL) and brine (50 mL) then dried over Na₂SO₄. The solvents were removed under reduced pressure to give an orange oil (2.30 g), which was purified by column chromatography (light petroleum/ethyl acetate 1:1.5). Yield: 511 mg (1.47 mmol, 76.6 %) 2B-diol-*trans*-diacetate **79** as a bright yellow solid.

Method 2 ('bis-ketonisation'): To a suspension of 2B-ene-*trans*-diacetate **75** (60 mg, 0.19 mmol) and 4-methyl-N-morpholine-N-oxide (132 mg, 1.13 mmol, 5 eq.) in 1,4-dioxane (1.5 mL) was added OsO₄ (1 mg, 2 %) in *tert*-butanol (0.2 mL). After stirring the bright yellow solution for 3 days at RT, NaS₂O₅ (0.5 g) in H₂O (5 mL) and dichloromethane (5 mL) were added. The red mixture was stirred for 30 minutes, and the aqueous layer was extracted with dichloromethane (3 x 5 mL). The combined bright yellow organic layers were washed with H₂O (5 mL) and brine (5 mL) then dried over Na₂SO₄. The solvents were removed under reduced pressure to give 115 mg of a bright yellow oil, which was purified by column chromatography (light petroleum/ethyl acetate 1.5:1). Yield: 52 mg (0.15 mmol, 78.5 %) 2B-dione-*trans*-diacetate **79** as a bright yellow solid. Melting point: 124 °C; m/z: 348. 5 mg (0.0014 mmol, 7.5 %) 2B-diol-*trans*-diacetate **77** was isolated as a side product.

¹H-NMR (500 MHz, CDCl₃): δ = 0.95 (1H, dd, *J* = 12.8, 2.2 Hz), 1.13 (1H, dd, *J* = 12.8, 1.5 Hz), 1.26 (2H, m), 1.57 (2H, m), 1.90 (1H, m), 1.95 (3H, s), 2.07 (1H, m), 2.08 (3H, s), 2.11 (1H, dt, *J* = 6.8, 1.9 Hz), 2.15 (1H, m), 2.17 (1H, m), 2.27 (1H, dquart, *J* = 9.4, 1.6 Hz), 2.85 (1H, dd, *J* = 3.4, 2.0 Hz), 2.88 (1H, dd, *J* = 3.0, 2.0), 3.80 (1H, dd, *J* = 11.4, 5.6 Hz), 4.08 (1H, dd, *J* = 11.4, 4.3 Hz), 4.23 (1H, dd, *J* = 11.1, 8.1 Hz), 4.24 (1H, dd, *J* = 1.1, 6.8 Hz) ppm; ¹³C-NMR (75.5 MHz, CDCl₃): δ = 20.4 (CH₃), 20.8 (CH₃), 29.9 (CH₂), 30.0 (CH₂), 35.8

(CH₂), 35.9 (CH), 39.8 (CH), 39.9 (CH), 40.2 (CH), 41.3 (CH), 48.9 (CH), 49.9 (CH), 52.6 (CH), 64.1 (CH₂-O), 65.4 (CH₂-O), 170.5 (OAc), 170.8 (OAc), 197.4 (C=O), 197.5 (C=O) ppm.

2B-Porphyrin-*trans*-diacetate (**103**)



A solution of 2B-dione-*trans*-diacetate **79** (66 mg, 0.1894 mmol) and 'diaminoporphyrin' **153** (230 mg, 0.1923 mmol) in anhydrous and de-oxygenated dichloromethane (5 mL) was heated for 3 days at 80 °C and 15 kbar. The solvent was removed under an argon stream and the crude product was purified by column chromatography (chloroform). Yield: 180 mg (0.119 mmol, 63.0 %) 2B-porphyrin-*trans*-diacetate **103** as a purple solid.

Melting point: >300 °C.

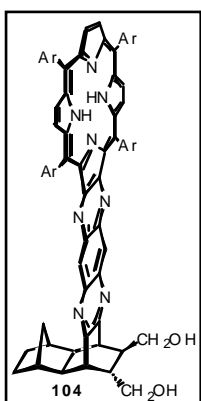
¹H-NMR (500 MHz, CDCl₃): δ = -2.38 (2H, s), -0.51 (1H, d, *J* = 11.3 Hz), 0.54 (1H, d, *J* = 11.3 Hz), 1.30 (2H), 1.50 (2H), 1.516 (9H), 1.526 (9H), 1.528 (9H), 1.535 (18H), 1.540 (27H), 1.60 (1H), 1.68 (1H), 1.78 (3H, s), 1.88 (1H, m), 1.98 (1H, m), 2.18 (3H, s), 2.19 (1H, bs), 2.37 (1H, dd, *J* = 8.8, 2.8 Hz), 3.47 (1H, t, *J* = 5.4 Hz), 3.50 (1H, t, *J* = 5.4 Hz), 3.67 (1H, dd, *J* = 11.5, 7.3 Hz), 3.89 (1H, dd, *J* = 11.5, 5.7 Hz), 4.38 (1H, d, *J* = 2.3 Hz), 4.41 (1H, s), 7.81 (2H, t, *J* = 1.8 Hz), 7.94 (2H, t, *J* = 1.9 Hz), 8.03 (2H, t, *J* = 1.7 Hz), 8.05 (2H, t, *J* = 1.9 Hz), 8.10 (2H, t, *J* = 1.7 Hz), 8.13 (2H, t, *J* = 1.7 Hz), 8.67 (1H, d, *J* = 0.7 Hz), 8.68 (1H, d, *J* = 0.7 Hz), 8.78 (2H, s), 8.98 (4H, d, *J* = 3.0 Hz) ppm; ¹³C-NMR (75.5 MHz, CDCl₃): δ = 20.7 (CH₃), 21.1 (CH₃), 30.6 (CH₂), 30.8 (CH₂), 31.8 (12CH₃), 32.0 (12CH₃), 34.9 (CH₂), 35.1 (8C), 39.6 (CH), 39.9 (CH), 40.4 (CH), 41.1 (CH), 41.7 (CH), 42.4 (CH), 44.5 (CH), 49.5 (CH), 64.7 (CH₂O), 66.3 (CH₂O), 118.0 (2C), 120.6 (2C_{p-Ar}H), 121.2 (2C_{p-Ar}H), 123.1 (2C), 128.1 (2C_{o-Ar}H), 128.5 (2C_{o-Ar}H), 128.7 (2C_{o-Ar}H), 128.9 (2C_{o-Ar}H), 129.6 (6C_{pyrrolic}H), 134.3 (2C_{quinoxaline}H), 138.2 (2C), 139.7 (2C), 140.0 (2C), 140.7 (2C), 140.8 (2C), 141.1 (2C), 145.5 (2C), 148.9 (4C_{Ar}-^tBu), 149.0 (4C_{Ar}-^tBu), 154.0 (2C), 155.0 (2C), 158.2 (C), 159.3 (C), 170.7 (OAc), 171.1 (OAc) ppm.

2B-Porphyrin-*trans*-diol (**104**) and 2B-porphyrin-*trans*-ol-acetate (**105**)

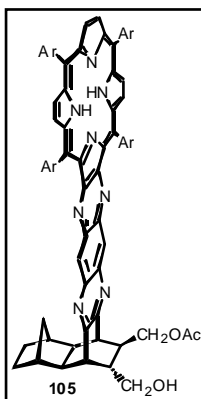
Method 1 (hydrolysis): To a solution of 2B-porphyrin-*trans*-diacetate **103** (180 mg, 0.119 mmol) in tetrahydrofuran (50 mL) was added a solution of K₂CO₃ (5.9 g, 10 mmol) in a 1:1 mixture of H₂O/methanol (100 mL). The red/brown solution was stirred overnight at RT under an argon atmosphere. The layers were separated and the solvent was removed from the

organic phase under reduced pressure. The crude product was purified by column chromatography (dichloromethane/methanol 20:1). Yield: 102 mg (0.0716 mmol, 60.2 %) 2B-porphyrin-*trans*-diol **104**.

Method 2 (high pressure, pyridine): A solution of 2B-dione-*trans*-diacetate **79** (32 mg, 0.0919 mmol) and 'diaminoporphyrin' **153** (100 mg, 0.0836 mmol) in anhydrous and deoxygenated pyridine (1 mL) was heated for 3 days at 80 °C and 15 kbar. The solvent was removed under an argon stream and the crude product was purified by column chromatography (dichloromethane/methanol 20:1). Yield: 59 mg (0.0415 mmol, 49.6 %) 2B-porphyrin-*trans*-diol **104** as a purple solid. Melting point: >300 °C; M^+ (MALDI): 1424. As a side product the 2B-Porphyrin-*trans*-ol-acetate **105** was isolated. Melting point: >300 °C, M^+ (MALDI): 1466.



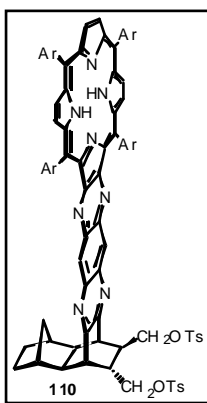
$^1\text{H-NMR}$ (300 MHz, CDCl_3 , **104**): δ = -2.38 (2H, s), -0.43 (1H, d, J = 11.7 Hz), 0.53 (1H, d, J = 11.7 Hz), 1.2-1.7 (3H), 1.53 (72H), 1.99 (2H), 2.08 (1H), 2.19 (3H), 2.32 (1H, d, J = 6.8 Hz), 3.02 (1H, t, J = 9.3 Hz), 3.41 (1H, s), 3.49 (1H), 3.54 (1H, m), 3.98 (2H, m), 7.80 (2H, s), 7.93 (2H), 8.03 (4H), 8.09 (4H, d, J = 2.0 Hz), 8.65 (2H, s), 8.77 (2H, s), 8.97 (4H, d, J = 3.9 Hz) ppm; $^{13}\text{C-NMR}$ (75.5 MHz, CDCl_3 , **104**): δ = 30.6 (CH_2), 30.7 (CH_2), 31.8 (12CH_3), 32.0 (12CH_3), 34.8 (CH_2), 35.1 (8C), 40.0 (CH), 40.4 (CH), 42.4 (CH), 43.5 (CH), 44.0 (CH), 44.3 (CH), 45.3 (CH), 49.2 (CH), 65.3 (CH_2OH), 65.9 (CH_2OH), 117.9 (2C), 120.5 ($\text{C}_{\text{p-ArH}}$), 120.6 ($\text{C}_{\text{p-ArH}}$), 121.2 ($2\text{C}_{\text{p-ArH}}$), 123.1 (2C), 128.1 ($2\text{C}_{\text{o-ArH}}$), 128.4 ($2\text{C}_{\text{o-ArH}}$), 128.6 ($2\text{C}_{\text{o-ArH}}$), 128.8 ($2\text{C}_{\text{o-ArH}}$), 129.4 ($2\text{C}_{\text{pyrrolicH}}$), 129.5 ($4\text{C}_{\text{pyrrolicH}}$), 134.2 ($2\text{C}_{\text{quinoxalineH}}$), 138.1 (2C), 139.6 (2C), 140.0 (2C), 140.5 (C), 140.6 (C), 140.8 (2C), 141.0 (2C), 145.5 (2C), 148.9 ($4\text{C}_{\text{Ar}}^t\text{Bu}$), 149.0 ($4\text{C}_{\text{Ar}}^t\text{Bu}$), 153.9 (2C), 155.0 (2C), 158.6 (C), 159.8 (C) ppm.



$^1\text{H-NMR}$ (300 MHz, CDCl_3 , **105**): δ = -2.37 (2H, s), -0.47 (1H, d, J = 11.3 Hz), 0.54 (1H, d, J = 11.3 Hz), 1.2-1.7 (4H), 1.53 (72H), 1.69 (1H, d, J = 7.8 Hz), 1.75 (1H), 2.03 (1H, m), 1.80, 2.17 (3H, s), 2.20 (2H, bs), 2.37 (1H, d, J = 6.8 Hz), 3.47 (1H, bs), 3.57 (1H, bs), 3.66 (1H, dd, J = 10.7, 7.8 Hz), 3.88 (1H, dd, J = 11.7, 4.9 Hz), 3.98 (2H, d, J = 7.8 Hz), 7.81 (2H, t, J = 1.9 Hz), 7.93 (2H, bs), 8.03 (2H, bs), 8.05 (2H, bs), 8.10 (4H, d, J = 1.9 Hz), 8.66 (1H, s), 8.69 (1H, s), 8.78 (2H, s), 8.98 (4H, d, J = 3.9 Hz) ppm; $^{13}\text{C-NMR}$ (75.5 MHz, CDCl_3 , **105**): δ = 20.7 (CH_3), 30.7

(2CH₂), 31.8 (12CH₃), 32.0 (12CH₃), 34.9 (CH₂), 35.1 (8C), 40.0 (CH), 40.4 (CH), 41.4 (CH), 41.8 (CH), 42.5 (CH), 43.1 (CH), 44.7 (CH), 49.3 (CH), 64.4 (CH₂OH), 66.7 (CH₂O), 117.97 (C), 118.03 (C), 120.56 (C_{p-Ar}H), 120.62 (C_{p-Ar}H), 121.1 (2C_{p-Ar}H), 121.2 (2C_{p-Ar}H), 123.1 (2C), 128.1 (2C_{o-Ar}H), 128.46 (2C_{o-Ar}H), 128.54 (C_{o-Ar}H), 128.65 (C_{o-Ar}H), 128.8 (C_{o-Ar}H), 128.9 (C_{o-Ar}H), 129.6 (6C_{pyrrolic}H), 134.2 (2C_{quinoxaline}H), 138.2 (2C), 139.6 (2C), 140.0 (C), 140.1 (C), 140.6 (C), 140.7 (C), 140.8 (2C), 141.1 (2C), 145.5 (2C), 148.8, 148.9 (4C_{Ar}^tBu), 149.0 (4C_{Ar}^tBu), 154.0 (2C), 155.0 (2C), 158.5 (C), 159.9 (C), 170.8 (OAc) ppm.

2B-Porphyrin-*trans*-ditosylate (**110**)

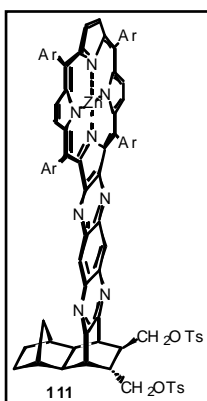


At -20 °C tosylchloride (73 mg, 0.383 mmol, ~5 eq.) was added to a solution of 2B-porphyrin-*trans*-diol **104** (102 mg, 0.0716 mmol) in anhydrous dichloromethane (6 mL) and pyridine (4 mL) under an argon atmosphere. The mixture was placed in the freezer for 7 days then poured onto 1M HCl (15 mL). The dark red organic layer was washed with 1M HCl (2 x 15 mL), NaHCO₃ (sat., 15 mL) and brine (15 mL) and was then dried over Na₂SO₄. The solvent was removed under reduced pressure and the crude product was purified by column chromatography (chloroform). Yield: 123 mg (0.0709 mmol, 99.0 %) 2B-porphyrin-*trans*-ditosylate **110**. Melting point: >300 °C; M⁺ (MALDI): 1732.

¹H-NMR (500 MHz, CDCl₃): δ = -2.38 (2H, s), -0.63 (1H, d, *J* = 10.8 Hz), 0.48 (1H, d, *J* = 10.8 Hz), 1.12 (1H, t, *J* = 4.4 Hz), 1.19 (1H, t, *J* = 4.4 Hz), 1.43 (2H, bs), 1.54 (9H, s), 1.553 (36H, s), 1.554 (9H, s), 1.557 (9H, s), 1.566 (9H, s), 1.70 (1H, dd, *J* = 15.0, 6.4 Hz), 2.01 (1H, dd, *J* = 13.4, 6.7 Hz), 2.05 (1H, 1H, 1H, s), 2.09 (3H, s), 2.14 (1H, s), 2.50 (3H, s), 3.38 (1H, s), 3.43 (1H, s), 3.57 (1H, dd, *J* = 10.4, 6.9 Hz), 3.72 (1H, dd, *J* = 10.4, 6.9 Hz), 4.29 (2H, m), 7.05 (2H, d, *J* = 8.3 Hz), 7.44 (2H, d, 8.3 Hz), 7.56 (2H, d, *J* = 8.3 Hz), 7.83 (2H, t, *J* = 1.8 Hz), 7.93 (2H, d, *J* = 8.3 Hz), 7.968 (1H, t, *J* = 0.9 Hz), 7.974 (1H, t, *J* = 0.9 Hz), 8.04 (1H, t, *J* = 1.8 Hz), 8.05 (2H, dd, *J* = 4.7, 1.8 Hz), 8.09 (1H, t, *J* = 1.8 Hz), 8.11 (4H, bs), 8.61 (1H, s), 8.62 (1H, s), 8.79 (2H, s), 9.00 (4H, d, *J* = 5.2 Hz) ppm; ¹³C-NMR (75.5 MHz, CDCl₃): δ = 21.5 (CH₃), 21.8 (CH₃), 30.47 (CH₂), 30.53 (CH₂), 31.8 (12CH₃), 31.99 (6CH₃), 32.03 (6CH₃), 34.8 (CH₂), 35.1 (8C), 39.5 (CH), 39.8 (CH), 40.2 (CH), 40.7 (CH), 41.3 (CH), 41.7 (CH), 43.6 (CH), 48.8 (CH), 69.4 (CH₂O), 70.8 (CH₂O), 118.0 (2C), 120.7 (2C_{p-Ar}H), 121.2 (2C_{p-Ar}H), 123.2 (C), 127.7 (4C_{Tos}H), 128.2 (4C_{o-Ar}H), 128.5 (C_{o-Ar}H), 128.7 (2C_{o-Ar}H), 128.8 (C_{o-Ar}H), 129.6 (2C_{pyrrolic}H), 129.7 (4C_{pyrrolic}H), 130.2 (4C_{Tos}H), 132.1 (2C_{Tos}), 132.6

(2C_{Tos}), 134.3 (2C_{quinoxaline}H), 138.1 (C), 138.2 (C), 139.56 (C), 139.64 (C), 139.95 (C), 140.00 (C), 140.4 (2C), 140.7 (2C), 140.97 (C), 141.00 (C), 144.9 (C), 145.3 (C), 148.9 (4C_{Ar}^tBu), 148.95 (2C_{Ar}^tBu), 148.98 (2C_{Ar}^tBu), 154.0 (2C), 155.00 (C), 155.03 (C), 157.0 (C), 158.3 (C) ppm.

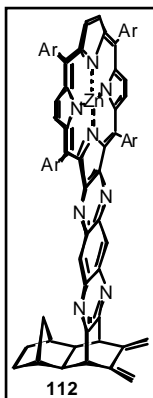
2B-[Porphyrinato]zinc-*trans*-ditosylate (**111**)



To a solution of 2B-porphyrin-*trans*-ditosylate **110** (123 mg, 0.0709 mmol) in dichloromethane (10 mL) was added a solution of Zn(OAc)₂ · 2 H₂O (147 mg, 0.6697 mmol, ~10 eq.) in methanol (10 mL). The mixture was stirred overnight at RT under an argon atmosphere, then washed with H₂O (3 x 15 mL) and brine (15 mL), then dried over Na₂SO₄. The solvent was removed under reduced pressure and the crude product was purified by column chromatography (chloroform). Yield: 118 mg (0.0657 mmol, 92.7 %) 2B-[porphyrinato]zinc-*trans*-ditosylate **111**. Melting point: >300 °C.

¹H-NMR (500 MHz, CDCl₃): δ = -0.66 (1H, d, *J* = 11.3 Hz), 0.46 (1H, d, *J* = 11.3 Hz), 1.20 (2H, m), 1.40 (2H, m), 1.49 (18H), 1.51 (9H), 1.53 (36H), 1.54 (9H), 1.73 (1H), 1.98 (1H, dd, *J* = 12.8, 6.0 Hz), 2.07 (3H, s), 2.12 (1H, bs), 2.49 (3H, s), 3.38 (1H, bs), 3.44 (1H, bs), 3.56 (1H, dd, *J* = 10.2, 6.8 Hz), 3.73 (1H, dd, *J* = 10.2, 6.8 Hz), 4.26 (1H, bs), 4.29 (1H, t, *J* = 1.7 Hz), 7.03 (2H, d, *J* = 8.3 Hz), 7.43 (2H, d, *J* = 8.3 Hz), 7.54 (2H, d, *J* = 8.3 Hz), 7.80 (2H, t, *J* = 1.7 Hz), 7.92 (2H, d, *J* = 8.3 Hz), 7.94 (1H, t, *J* = 1.7 Hz), 8.00 (1H, t, *J* = 1.5 Hz), 8.01 (1H, d, *J* = 1.5), 8.04 (1H, t, *J* = 1.6 Hz), 8.08 (4H, d, *J* = 1.5 Hz), 8.67 (1H, s), 8.68 (1H, s), 8.86 (2H, s), 8.92 (2H, dd, *J* = 6.0, 4.9 Hz), 8.97 (2H, d, *J* = 6.0 Hz) ppm; ¹³C-NMR (75.5 MHz, CDCl₃): δ = 21.4 (CH₃), 21.7 (CH₃), 29.7 (CH₂), 30.6 (CH₂), 31.8 (12CH₃), 32.0 (12CH₃), 34.8 (CH₂), 35.1 (8C), 39.6 (CH), 39.8 (CH), 40.3 (CH), 40.8 (CH), 41.4 (CH), 41.8 (CH), 43.7 (CH), 48.8 (CH), 69.5 (CH₂O-), 70.8 (CH₂O-), 118.8 (C), 120.4 (2C_{p-Ar}H), 121.1 (2C_{p-Ar}H), 125.4 (C), 127.7 (2C_{Ar}H), 128.2 (4C_{o-Ar}H), 128.4 (2C_{o-Ar}H), 128.5 (2C_{o-Ar}H), 128.8 (C), 129.3 (2C_{Ar}H), 129.6 (2C_{pyrrolic}H), 129.7 (2C_{Ar}H), 130.2 (4C_{Ar}H), 131.6 (2C_{pyrrolic}H), 131.7 (2C_{pyrrolic}H), 132.3 (C), 132.6 (2C_{quinoxaline}H), 132.8 (C), 139.7 (C), 139.8 (C), 140.3 (C), 141.3 (C), 141.5 (C), 144.9 (C_{Ar}), 145.3 (C), 148.7 (C), 148.9 (C_{Ar}^tBu), 149.2 (C_{Ar}^tBu), 150.1 (C), 152.3 (C), 153.2 (C), 157.1 (C), 158.4 (C) ppm.

2B-[Porphyrinato]zinc-dimethylidene (**112**)



To a solution of 2B-[porphyrinato]zinc-*trans*-ditosylate **111** (48 mg, 0.0267 mmol) in anhydrous and deoxygenated dimethylformamide (4 mL) was added potassium *tert*-butoxide (10 mg, 0.0891 mmol, ~3.5 eq.) at -20 °C. The mixture was allowed to warm up to RT slowly and the reaction followed by TLC (light petroleum/ethyl acetate 3:1). After 3 hours the mixture was poured onto of ice (20 g). Sodium chloride was added and the aqueous phase was extracted with dichloromethane until it was colourless. The combined organic layers were washed with H₂O (20 mL) and brine (20 mL) then dried over Na₂SO₄. Solvents

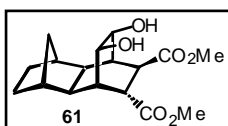
were removed under reduced pressure and the crude product was purified by column chromatography (light petroleum/ethyl acetate 3:1). Yield: 36 mg (0.0248 mmol, 92.9 %) 2B-[porphyrinato]zinc-dimethylidene **112**. Melting point: >300 °C; MH⁺ (MALDI): 1452.2.

¹H-NMR (500 MHz, CDCl₃): δ = -0.39 (1H, d, *J* = 11.3 Hz), 0.57 (1H, d, *J* = 11.3 Hz), 1.26 (2H), 1.48 (2H), 1.50 (18H, s), 1.54 (54H), 2.29 (2H, s), 2.37 (2H, s), 4.11 (2H, s), 5.21 (2H, s), 5.48 (2H, s), 7.79 (2H, t, *J* = 1.8 Hz), 7.92 (2H, t, *J* = 1.8 Hz), 7.98 (2H, t, *J* = 1.8 Hz), 8.02 (2H, t, *J* = 1.6 Hz), 8.08 (4H, bs), 8.72 (2H, s), 8.86 (2H, s), 8.94 (4H, dd, *J* = 13.3 Hz, 4.6 Hz) ppm; ¹³C-NMR (75.5 MHz, CDCl₃): δ = 30.5 (2CH₂), 31.8 (12CH₃), 32.0 (12CH₃), 34.5 (CH₂), 35.1 (8C), 40.0 (2CH), 48.8 (2CH), 53.0 (2CH), 107.8 (2=CH₂), 118.8 (2C), 120.3 (2C_{p-Ar}H), 121.1 (2C_{p-Ar}H), 125.3 (2C), 128.4 (4C_{o-Ar}H), 128.6 (4C_{o-Ar}H), 129.3 (4C_{pyrrolic}H), 129.4 (2C_{pyrrolic}H), 131.6 (2C), 132.5 (2C_{quinoxaline}H), 139.7 (2C), 140.6 (2C), 141.3 (2C), 141.6 (2C), 141.7 (2C), 143.2 (2C=CH₂), 148.7 (4C_{Ar}^tBu), 148.9 (2C_{Ar}^tBu), 149.1 (2C_{Ar}^tBu), 150.1 (2C), 152.1 (2C), 153.2 (2C), 157.6 (2C) ppm.

D.2.2 Model Reactions

D.2.2.1 Neighbourgroup Variations

(1α,4α,4aβ,5α,8α,8aβ)-1,2,3,4,4a,5,6,7,8,8a-Decahydro-1,4-ethano-10,11-*cis*-dihydroxy-5,8-methanonaphthalene-2,3-*trans*-dicarboxylate (**61**)

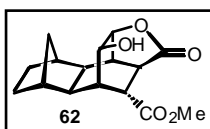


To a solution of 2B-ene-*trans*-diester **58** (500 mg, 1.75 mmol) and 4-methyl-N-morpholine-N-oxide (620 mg, 5.25 mmol, 3 eq.) in 1,4-dioxane (6 mL) were added OsO₄ (4.45 mg, 2 %) in *tert*-butanol (0.9 mL) and H₂O

(3 drops). The yellow solution was stirred for 16 hours after which dichloromethane (10 mL) and Na₂S₂O₅ (1g) in H₂O (10 mL) were added. After stirring for 30 minutes at RT the two layers were separated and the aqueous layer was extracted with dichloromethane (5 x 5 mL). The combined yellow organic layers were washed with brine and H₂O, then dried over Na₂SO₄. The solvents were removed and the crude product was purified by column chromatography (light petroleum/ethyl acetate 1:1). Yield: 260 mg (0.8 mmol, 46.4 %) 2B-diol-*trans*-diester **61** as a colourless oil.

¹H-NMR (300MHz, CDCl₃): δ = 1.10 (2H), 1.14 (2H), 1.35 (1H, d, *J* = 11.3 Hz), 1.52 (2H, m), 1.72 (1H, dd, *J* = 11.3, 3.1 Hz), 2.14 (1H, bs), 2.17 (1H, bs), 2.34 (1H, quart., *J* = 2.1 Hz), 2.57 (1H, quart., *J* = 2.1 Hz), 2.98 (1H, dd, *J* = 7.2, 2.1 Hz), 3.66 (1H, dd, *J* = 7.2, 2.1 Hz), 3.69 (3H, s), 3.73 (3H, s), 4.07 (1H, dd, *J* = 8.2, 3.1 Hz), 4.20 (1H, t, *J* = 8.2, 3.1 Hz) ppm.

(1α,2α,4α,4aβ,5α,8α,8aβ)-1,2,3,4,4a,5,6,7,8,8a-Decahydro-1,4-ethano-[3,11-*b*]furan-10-hydroxy-5,8-methanonaphthalene-2-carboxylate (62**)**



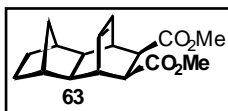
Method 1: To a suspension of 2B-ene-*trans*-diester **58** (50 mg, 0.17 mmol) and 4-methyl-N-morpholine-N-oxide (156 mg, 1.33 mmol, ~8 eq.) in anhydrous 1,4-dioxane (1 mL) was added OsO₄ (0.86 mg, 2 %) in *tert*-butanol (0.17 mL). After stirring at RT for 24 hours Na₂S₂O₅ (0.5 g) in H₂O (5 mL) and dichloromethane (5 mL) were added. The red mixture was stirred for 30 minutes, layers were separated and the aqueous layer was extracted with dichloromethane (4 x 5 mL). The combined yellow organic layers were washed with H₂O (5 mL) and brine (5 mL) then dried over Na₂SO₄. The solvents were removed under reduced pressure to give the crude product (76 mg) which was purified by column chromatography (light petroleum/ethyl acetate 1.5:1). Yield: 28mg (0.10 mmol, 56%) lactone **62** as a yellow solid. *m/z*: 292.

Method 2: Upon dissolving the 2B-diol-*trans*-diester **61** in acetic chloroform-d₁ and deuterium oxide the corresponding lactone **62** was formed. Yield: 100 %.

¹H-NMR (500 MHz, CDCl₃): δ = 1.14 (2H, bs), 1.17 (2H, bs), 1.45 (1H, dd, *J* = 9.9, 4.1 Hz), 1.52 (2H, m), 1.93 (1H, dd, *J* = 9.7, 2.4 Hz), 2.13 (1H, d, *J* = 4.1 Hz), 2.18 (1H, d, *J* = 3.5 Hz), 2.38 (1H, quart., *J* = 2.8 Hz), 2.61 (1H, m), 3.07 (1H, dd, *J* = 3.9, 1.4 Hz), 3.09 (1H, m), 3.72 (3H, s), 4.35 (1H, dd, *J* = 6.9, 2.6 Hz), 4.68 (1H, t, *J* = 5.6 Hz) ppm; ¹³C-NMR (75.5 MHz, CDCl₃): δ = 29.2 (CH₂), 31.3 (CH₂), 36.7 (CH₂), 37.4 (CH), 37.8 (CH), 39.1 (CH), 39.4 (CH), 39.5 (CH), 40.0 (CH), 40.9 (CH), 41.5 (CH), 52.5 (OCH₃), 63.3 (CHOH), 76.6 (HC-O), 173.6 (MeO-C=O), 178.0 (O-C=O) ppm.

IR (CCl₄) ν_{\max} : 3450, 2940, 1770, 1730 cm⁻¹.

(1 α ,2 β ,3 β ,4 α ,4 $\alpha\beta$,5 α ,8 α ,8 $\alpha\beta$)-1,2,3,4,4a,5,6,7,8,8a-Decahydro-1,4-etheno-5,8-methano-naphthalene-2,3-*cis*-dicarboxylate (63**)**



To a solution of (500 mg, 3.4 mmol) **57** in (2 mL) toluene was added (540 mg, 3.7 mmol) dimethylmaleate. The slightly yellow solution was heated at reflux for 4 days, after which the toluene was removed under reduced pressure. The brown residue was purified by column chromatography (light petroleum/ethyl acetate 3:1). Yield: 405 mg (1.4 mmol, 41.2 %) 2B-ene-*cis*-diester **63** as a white solid. Dimethylmaleate (315 mg, 2.2 mmol) was recovered.

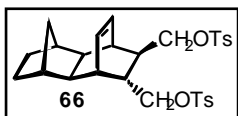
¹H-NMR (300 MHz, CDCl₃): δ = 0.60 (1H, d, J = 10.3 Hz), 1.02 (2H, dd, J = 7.2, 2.0 Hz), 1.35 (2H, d, J = 7.2 Hz), 1.62 (2H, s), 1.97 (2H, s), 2.13 (1H, d, J = 10.3 Hz), 2.91 (2H, s), 2.93 (2H, s), 3.51 (6H, s), 6.14 (2H, dd, J = 5.1, 3.1 Hz) ppm; ¹³C-NMR (75.5 MHz, CDCl₃): δ = 31.3 (2CH₂), 34.4 (CH₂), 37.3 (2CH), 41.1 (2CH), 47.9 (2CH), 48.4 (2CH), 51.3 (2OCH₃), 131.4 (2=CH), 173.0 (2O=C-OMe) ppm.

(1 α ,4 α ,4 $\alpha\beta$,5 α ,8 α ,8 $\alpha\beta$)-1,2,3,4,4a,5,6,7,8,8a-Decahydro-1,4-ethano-5,8-methano-naphthalene-2,10:3,11-dicarbonylactone (64**, attempted)**



To a suspension of 2B-ene-*cis*-diester **63** (170 mg, 0.58 mmol) and 4-methyl-N-morpholine-N-oxide (432 mg, 3.7 mmol, ~6 eq.) in 1,4-dioxane (1 mL) was added OsO₄ (3.5 mg, 2 %) in *tert*-butanol (0.7 mL). After 7 days at RT no reaction occurred. The yellow solution was then stirred at 80 °C for 10 days, after which dichloromethane (5 mL) and Na₂S₂O₅ (0.5 g) in H₂O (5 mL) were added. The aqueous layer was extracted with dichloromethane (5 x 5 mL) and the combined organic layers were washed with 1M HCl (2 x 5 mL) and NaHCO₃ (sat., 5 mL), then dried over Na₂SO₄. The solvents were removed under reduced pressure and the crude mixture was purified by column chromatography (light petroleum / ethyl acetate 1:1). ¹H-NMR showed a mixture of the 2B-ene-*cis*-diester **63** (starting material) and the 2B-ene-*trans*-diester **58** (2:3). No bis(lactone) was found.

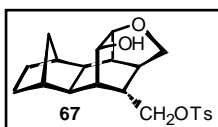
(1 α ,4 α ,4 β ,5 α ,8 α ,8 β)-1,2,3,4,4a,5,6,7,8,8a-Decahydro-1,4-etheno-5,8-methano-2,3-*trans*-bis(tosyloxymethyl)naphthalene (66)



At $-23\text{ }^{\circ}\text{C}$ *p*-toluenesulfonyl chloride (843 mg, 4.42 mmol) in anhydrous pyridine (4 mL) was added dropwise to a solution of 2B-ene-*trans*-diol **65** (200 mg, 0.88 mmol) in anhydrous pyridine (15 mL) under an argon atmosphere. On completion of the addition the flask was stoppered and placed in the freezer for 8 days, after which the slightly blue solution was poured onto ice (20 g). The suspension was extracted with dichloromethane (4 x 15 mL) and the combined slightly yellow organic layers were washed with 1M HCl (3 x 10 mL), NaHCO_3 (sat., 2 x 10 mL) and H_2O (15 mL) then dried over Na_2SO_4 . The solvent was removed under reduced pressure and the residue dried under high vacuum. Yield: 444 mg (0.83 mmol, 94.3 %) 2B-ene-*trans*-ditosylate **66** as slightly yellow crystals. Melting point: $125\text{--}127\text{ }^{\circ}\text{C}$; m/z : 542.

^1H -NMR (500 MHz, CDCl_3): δ = 0.59 (1H, d, J = 10.3 Hz), 0.89 (1H, dt, J = 8.1, 1.8 Hz), 0.94 (1H, td, J = 8.1, 2.5 Hz), 0.99 (1H, m), 1.27 (1H, d), 1.33 (3H), 1.38 (2H, s), 1.79 (1H, s), 1.92 (1H, s), 2.03 (1H, dt, J = 10.3, 1.8 Hz), 2.46 (6H, s), 2.52 (1H, d, J = 7.4 Hz), 2.57 (1H, d, J = 6.6 Hz), 3.52 (1H, s), 3.54 (1H, d, 1.6 Hz), 3.94 (1H, t, J = 9.7 Hz), 4.02 (1H, dd, J = 9.9, 6.4 Hz), 5.80 (1H, t, J = 7.00 Hz), 6.11 (1H, t, J = 7.0 Hz), 7.34 (2H, dd, J = 8.6, 0.6 Hz), 7.36 (2H, dd, J = 8.6, 0.6 Hz), 7.73 (2H, dt, J = 8.4, 2.0 Hz), 7.79 (2H, dt, J = 8.4, 2.0 Hz) ppm; ^{13}C -NMR (75.5 MHz, CDCl_3): δ = 21.7 (2CH_3), 31.3 (CH_2), 31.4 (CH_2), 34.7 (CH), 35.1 (CH), 35.8 (CH_2), 40.8 (2CH), 41.4 (2CH), 41.6 (CH), 42.1 (CH), 70.9 (CH_2O), 72.6 (CH_2O), 127.9 ($2\text{C}_{\text{Ar}}\text{H}$), 128.0 ($2\text{C}_{\text{Ar}}\text{H}$), 129.9 ($2\text{C}_{\text{Ar}}\text{H}$), 130.0 ($2\text{C}_{\text{Ar}}\text{H}$), 131.0 ($=\text{CH}$), 133.0 (2C_{Ar}), 135.0 ($=\text{CH}$), 145.0 (2C_{Ar}) ppm.

(1 α ,2 α ,4 α ,4 β ,5 α ,8 α ,8 β)-1,2,3,4,4a,5,6,7,8,8a-Decahydro-1,4-ethano-[3,11-*b*]-furan-10-hydroxy-5,8-methano-2-tosyloxymethylnaphthalene (67)

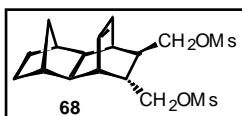


To a solution of 2B-ene-*trans*-ditosylate **66** (420 mg, 0.77 mmol) and 4-methyl-N-morpholine-N-oxide (313 mg, 2.67 mmol) in 1,4-dioxane (4 mL) were added OsO_4 (2 mg, 2%) in *tert*-butanol (0.4 mL) and H_2O (2 drops). The yellow mixture was stirred for 23 hours after which dichloromethane (10 mL) and $\text{Na}_2\text{S}_2\text{O}_5$ (1 g) in H_2O (10 mL) were added. The mixture was stirred for another 30 minutes and the two layers were separated. The yellow aqueous layer was washed with dichloromethane (4 x 10 mL) and the combined organic solutions were washed with H_2O (10 mL) then dried over Na_2SO_4 . The solvents were removed under reduced pressure to give

the crude product, which was purified by column chromatography (light petroleum/ethyl acetate 2:1). Yield: 222 mg (0.55 mmol, 71.4 %) **67** as a white solid. Melting point: 136-137 °C; *m/z*: 405.

¹H-NMR (500 MHz, CDCl₃): δ = 1.08 (3H, m), 1.27 (1H, d, *J* = 10.3 Hz), 1.40 (1H, dd, *J* = 9.6, 4.4 Hz), 1.44 (1H, m), 1.54 (1H, m), 1.70 (1H, d, *J* = 0.7 Hz), 1.83 (2H, m), 2.01 (1H, m), 2.04 (1H, m), 2.07 (2H, bs), 2.46 (3H, s), 3.36 (1H, d, *J* = 7.9 Hz), 3.73 (1H, dd, *J* = 7.9, 4.0 Hz), 3.99 (2H, m), 4.13 (2H, m), 7.35 (2H, dd, *J* = 8.6, 0.7 Hz), 7.79 (2H, dt, *J* = 8.4, 2.0 Hz) ppm; ¹³C-NMR (75.5 MHz, CDCl₃): δ = 21.7 (CH₃), 29.5 (CH₂), 31.6 (CH₂), 35.1 (CH), 36.4 (CH₂), 38.0 (CH), 38.9 (CH), 39.5 (CH), 39.8 (CH), 40.1 (CH), 41.7 (CH), 41.8 (CH), 64.7 (CHOH), 72.6 (CH₂OTs), 73.8 (HC-O), 74.2 (CH₂O), 127.9 (2CH_{Ar}), 129.9 (2CH_{Ar}), 133.1 (C_{Ar}), 145.1 (C_{Ar}) ppm.

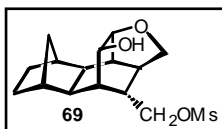
(1α,4α,4aβ,5α,8α,8aβ)-1,2,3,4,4a,5,6,7,8,8a-Decahydro-1,4-etheno-5,8-methano-2,3-trans-bis(mesyloxymethyl)naphthalene (68)



At -23 °C methanesulfonyl chloride (506 mg, 4.42 mmol) was added dropwise to a solution of 2B-ene-*trans*-diol **65** (200 mg, 0.88 mmol) in anhydrous pyridine (15 mL) under an argon atmosphere. On completion of the addition the flask was stoppered and placed in the freezer for 8 days, after which the slightly yellow solution was poured onto ice (20 g). The resulting suspension was extracted with dichloromethane (4 x 15 mL) and the combined organic layers were washed with 1M HCl (3 x 10 mL), NaHCO₃ (sat., 2 x 10 mL) and H₂O (15 mL) then dried over Na₂SO₄. The solvent was removed under reduced pressure and the residue was dried under high vacuum. Yield: 306 mg (0.80 mmol, 90.9 %) 2B-ene-*trans*-dimesylate **68** as slightly yellow crystals. Melting point: 104-106 °C; *m/z*: 390.

¹H-NMR (500 MHz, CDCl₃): δ = 0.68 (1H, d, *J* = 9.9 Hz), 1.08 (2H, m), 1.27 (1H, m), 1.41 (2H, m), 1.60 (1H, dd, *J* = 8.4, 2.6 Hz), 1.61 (1H, m), 1.72 (1H, dd, *J* = 8.4, 2.6 Hz), 1.97 (1H, s), 2.03 (1H, s), 2.13 (1H, dt, *J* = 10.3, 2.0 Hz), 2.70 (2H, bs), 3.00 (3H, s), 3.05 (3H, s), 3.83 (2H, d, *J* = 7.7 Hz), 4.23 (1H, dd, *J* = 9.9, 8.6 Hz), 4.33 (1H, dd, *J* = 9.9, 7.2 Hz), 6.06 (1H, t, *J* = 7.7 Hz), 6.26 (1H, t, 7.7 Hz) ppm; ¹³C-NMR (75.5 MHz, CDCl₃): δ = 31.4 (CH₂), 31.7 (CH₂), 35.2 (CH), 35.3 (CH), 36.0 (CH₂), 37.4 (CH₃), 37.5 (CH₃), 40.9 (CH), 41.3 (CH), 41.5 (CH), 42.0 (CH), 42.9 (CH), 48.8 (CH), 71.0 (CH₂OMs), 72.3 (CH₂OMs), 131.2 (=CH), 135.0 (=CH) ppm.

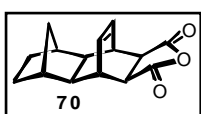
(1 α ,2 α ,4 α ,4 $\alpha\beta$,5 α ,8 α ,8 $\alpha\beta$)-1,2,3,4,4a,5,6,7,8,8a-Decahydro-1,4-ethano-[3,11-*b*]-furan-10-hydroxy-5,8-methano-2-mesyloxymethyl-naphthalene (69)



To a solution of 2B-ene-*trans*-dimesylate **68** (270 mg, 0.69 mmol) and (271 mg, 2.31 mmol) 4-methyl-N-morpholine-N-oxide in (4 mL) 1,4-dioxane was added (2 mg, 2%) OsO₄ in (0.4 mL) *tert*-butanol and H₂O (2 drops). The yellow mixture was stirred for 23 hours at RT, after which dichloromethane (10 mL) and Na₂S₂O₅ (1 g) in H₂O (10 mL) were added. The mixture was stirred for another 30 minutes and the two layers were separated. The yellow aqueous layer was washed with dichloromethane (3 x 10 mL) and the combined organic solutions were washed with H₂O (10 mL) then dried over Na₂SO₄. The solvents were removed under reduced pressure to give the crude product, which was purified by column chromatography (light petroleum/ethyl acetate 1.5:1) to give a colourless oil, which was dried under high vacuum. Yield: 174 mg (0.53 mmol, 76.8 %) **69** as a white solid. Melting point: 111-113 °C; m/z: 328.

¹H-NMR (300 MHz, CDCl₃): δ = 0.8-1.33 (5H), 1.46-1.60 (3H), 1.82 (1H, m), 1.91 (2H), 2.09 (2H, bs), 2.16 (1H), 3.03 (3H, s), 3.44 (1H, d, *J* = 8.2 Hz), 3.79 (1H, dd, *J* = 8.2, 4.1 Hz), 4.06 (1H, dd, *J* = 6.2, 2.1 Hz), 4.15-4.33 (3H, m) ppm; ¹³C-NMR (75.5 MHz, CDCl₃): δ = 29.6 (2CH₂), 31.7 (CH₂), 35.1 (CH), 36.4 (CH₂), 38.2 (CH), 39.0 (CH), 39.6 (CH), 39.8 (CH), 40.2 (CH), 41.7 (CH), 41.9 (CH), 64.7 (CHOH), 71.8 (CH₂-OMs), 73.8 (HC-O), 74.2 (CH₂-O) ppm.

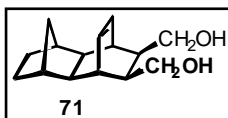
(1 α ,2 β ,3 β ,4 α ,4 $\alpha\beta$,5 α ,8 α ,8 $\alpha\beta$)-3a,4,4a,5,6,7,8,8a,9a-Decahydro-4,9-etheno-5,8-methano-[2,3-*c*]-furan-1,3-dione (70)



Under an argon atmosphere a solution of **57** (500 mg, 3.4 mmol) and maleic anhydride (451 mg, 4.6 mmol) in toluene (6 mL) was heated at reflux for 15 hours. The slightly yellow solution was placed in the freezer and the white precipitate formed was filtered off under an argon atmosphere, washed with (2 mL) ice-cold toluene and dried under high vacuum. Yield: 445 mg (1.8 mmol, 52.9 %) **70**. Melting point: 184-185 °C.

¹H-NMR (300 MHz, CDCl₃): δ = 0.71 (1H, d, *J* = 10.2 Hz), 1.09 (2H, dd, *J* = 7.2, 3.1 Hz), 1.45 (2H, m), 1.72 (2H, s), 2.00 (1H, dt, *J* = 10.2, 2.4 Hz), 2.09 (2H, s), 3.09 (2H, d, *J* = 2.0 Hz), 3.28 (2H, s), 6.20 (2H, t, *J* = 4.1 Hz) ppm; ¹³C-NMR (75.5 MHz, CDCl₃): δ = 31.3 (2CH₂), 34.4 (CH₂), 36.5 (2CH), 41.0 (2CH), 45.6 (2CH), 47.0 (2CH), 132.4 (2=CH), 172.5 (2O-C=O) ppm.

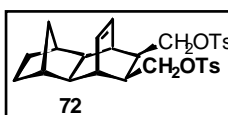
(1 α ,2 α ,3 α ,4 α ,4 β ,5 α ,8 α ,8 β)-1,2,3,4,4a,5,6,7,8,8a-Decahydro-1,4-etheno-5,8-methano-2,3-*cis*-bis(hydroxymethyl)naphthalene (71**)**



To an ice-cold suspension of LiAlH_4 (250 mg, 6.59 mmol) in tetrahydrofuran (20 mL) was added dropwise **70** (410 mg, 1.68 mmol) in tetrahydrofuran (60 mL) under an argon atmosphere. On completion of the addition (45 minutes) the greyish mixture was stirred for 3 hours at RT, then cooled down to 0 °C and 1M K_2CO_3 (10 mL) were added dropwise to quench the reaction. The suspension was heated at reflux for 15 minutes then filtered through a pad of filter aid, which was extracted with boiling diethyl ether. The colourless aqueous layer was extracted with diethyl ether (2 x 50 mL). The combined colourless organic layers were washed with brine (2 x 50 mL) then dried over Na_2SO_4 . The solvents were removed under reduced pressure and the white product was dried under high vacuum. Yield: 370 mg (1.58 mmol, 94.0 %) 2B-ene-*cis*-diol **71**. Melting point: 187-188 °C; m/z : 234.

^1H -NMR (300 MHz, CDCl_3): δ = 0.60 (1H, d, J = 9.2 Hz), 1.08 (2H, d, J = 7.2 Hz), 1.37 (2H, m), 1.72 (2H, s), 1.98 (2H, s), 2.08 (1H, d, J = 9.2 Hz), 2.21 (2H, m), 2.53 (2H, s), 3.53 (4H, m), 6.01 (2H, t, J = 8.2 Hz) ppm; ^{13}C -NMR (75.5 MHz, CDCl_3): δ = 31.5 (2CH_2), 34.7 (CH_2), 39.7 (2CH), 41.5 (2CH), 46.7 (2CH), 49.1 (2CH), 65.0 ($2\text{CH}_2\text{OH}$), 132.3 ($2=\text{CH}$) ppm.

(1 α ,2 α ,3 α ,4 α ,4 β ,5 α ,8 α ,8 β)-1,2,3,4,4a,5,6,7,8,8a-Decahydro-1,4-etheno-5,8-methano-2,3-*cis*-bis(tosyloxymethyl)naphthalene (72**)**

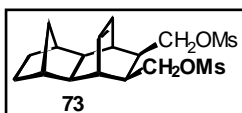


To a solution of 2B-ene-*cis*-diol **71** (200 mg, 0.88 mmol) in anhydrous pyridine (15 mL) was added dropwise *p*-toluenesulfonyl chloride (847 mg, 4.42 mmol, 5 eq.) in anhydrous pyridine (5 mL) at -23 °C under an argon atmosphere. On completion of the addition (15 minutes) the flask was stoppered and placed in the freezer for 6 days. The champagne coloured solution was poured onto ice (20 g) and the mixture was extracted with dichloromethane (3 x 15 mL). The combined organic layers were washed with 1M HCl (3 x 15 mL) and NaHCO_3 (sat., 2 x 15 mL) then dried over Na_2SO_4 . The solvent was removed under reduced pressure and the white solid was dried under high vacuum. Yield: 406 mg (0.75 mmol, 85.0 %) 2B-ene-*cis*-ditosylate **72**. Melting point: 123-125 °C.

^1H -NMR (500 MHz, CDCl_3): δ = 0.59 (1H, d, J = 9.2 Hz), 1.01 (2H, dd, J = 7.2, 2.4 Hz), 1.35 (2H, dt, J = 7.2, 2.3 Hz), 1.56 (2H, s), 1.94 (2H, s), 2.00 (1H, dt, J = 9.2, 2.3 Hz), 2.16 (2H, t), 2.46 (6H, s), 2.64 (2H, t, J = 3.5 Hz), 3.55 (2H, t, J = 9.2 Hz), 3.73 (2H, dd, J = 9.2, 5.8 Hz),

5.90 (2H, t, $J = 3.6$ Hz), 7.35 (4H, d, $J = 8.2$ Hz), 7.74 (4H, d, $J = 8.2$ Hz) ppm; ^{13}C -NMR (75.5 MHz, CDCl_3): $\delta = 31.4$ (2CH_2), 34.6 (CH_2), 37.0 (2CH), 41.3 (2CH), 41.4 (2CH), 48.2 (2CH), 70.0 ($2\text{CH}_2\text{O}$), 127.9 (4C_{ArH}), 130.0 (4C_{ArH}), 132.5 ($2=\text{CH}$), 132.8 (2C_{Ar}), 143.8 (2C_{Ar}) ppm.

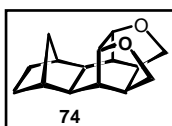
(1 α ,2 α ,3 α ,4 α ,4 $\alpha\beta$,5 α ,8 α ,8 $\alpha\beta$)-1,2,3,4,4a,5,6,7,8,8a-Decahydro-1,4-etheno-5,8-methano-2,3-*cis*-bis(mesyloxymethyl)naphthalene (73**)**



To a solution of 2B-ene-*cis*-diol **71** (143 mg, 0.61 mmol) in anhydrous pyridine (13 mL) was added dropwise methanesulfonyl chloride (0.35 mL, 515 mg, 4.5 mmol) at -23 °C under an argon atmosphere. On completion of the addition (15 minutes) the flask was stoppered and placed in the freezer for 6 days, after which the yellow solution was poured onto ice (20 g). The mixture was extracted with dichloromethane (3 x 15 mL) and the combined organic layers were washed with 1M HCl (3 x 15 mL) and NaHCO_3 (sat., 2 x 15 mL) then dried over Na_2SO_4 . The solvent was removed under reduced pressure and the white solid was dried under high vacuum. Yield: 158 mg (0.41 mmol, 67.0 %) 2B-ene-*cis*-dimesylate **73**. Melting point: 109–111 °C.

^1H -NMR (500 MHz, CDCl_3): $\delta = 0.65$ (1H, d, $J = 10.0$ Hz), 1.08 (2H, dd, $J = 7.2, 2.5$ Hz), 1.39 (2H, m), 1.69 (2H, s), 2.02 (2H, s), 2.07 (1H, dt, $J = 10.0, 2.2$ Hz), 2.34 (2H, t), 2.77 (2H, t, $J = 3.5$ Hz), 3.00 (6H, s), 3.89 (2H, t, $J = 8.7$ Hz), 4.03 (2H, dd, $J = 9.2$ Hz), 6.16 (2H, t, $J = 3.6$ Hz) ppm; ^{13}C -NMR (75.5 MHz, CDCl_3): $\delta = 31.4$ (2CH_2), 34.7 (CH_2), 37.3 (2CH), 37.5 (2CH_3), 41.3 (2CH), 41.9 (2CH), 48.3 (2CH), 69.6 ($2\text{CH}_2\text{O}$), 132.7 ($2=\text{CH}$) ppm.

(1 α ,4 α ,4 $\alpha\beta$,5 α ,8 α ,8 $\alpha\beta$)-1,2,3,4,4a,5,6,7,8,8a-Decahydro-1,4-ethano-5,8-methano-naphthalene-2,10:3,11-difuran (74**)**



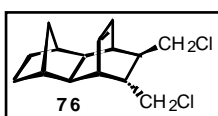
Method 1: To a solution of 2B-ene-*cis*-ditosylate **72** (352 mg, 0.65 mmol) and 4-methyl-N-morpholine-N-oxide (289 mg, 2.47 mmol) in 1,4-dioxane (4 mL) were added OsO_4 (3.30 mg, 2 %) in *tert*-butanol (0.66 mL) and H_2O (2 drops). The slightly yellow mixture was stirred at RT for 6 days then dichloromethane (10 mL) and $\text{Na}_2\text{S}_2\text{O}_5$ (1 g) in H_2O (10 mL) were added. The mixture was stirred for another 30 minutes and the two layers were separated. The yellow aqueous layer was washed with dichloromethane (3 x 10 mL) and the combined organic solutions were washed with H_2O (10 mL) then dried over Na_2SO_4 . The solvents were removed under reduced pressure to give the crude product, which was purified by column chromatography (light petroleum/ethyl

acetate 2:1). Yield: 32 mg (0.14 mmol, 21.2 %) **74** as a white solid. Starting material 2B-ene-*cis*-ditosylate **72** (131 mg, 0.24 mmol, 36.9 %) was recovered.

Method 2: To a solution of 2B-ene-*cis*-dimesylate **73** (142 mg, 0.36 mmol) and 4-methyl-N-morpholine-N-oxide (131 mg, 1.12 mmol) in anhydrous 1,4-dioxane (4 mL) were added OsO₄ (1.8 mg, 2%) in *tert*-butanol (0.36 mL) and H₂O (2 drops). The slightly yellow mixture was stirred for 6 days, after which dichloromethane (10 mL) and Na₂S₂O₅ (1 g) in H₂O (10 mL) were added. The mixture was stirred for another 30 minutes and the two layers were separated. The yellow aqueous layer was extracted with dichloromethane (3 x 10 mL) and the combined organic solutions were washed with H₂O (10 mL) then dried over Na₂SO₄. The solvents were removed under reduced pressure to give the crude product, which was purified by column chromatography (light petroleum/ethyl acetate 1:2). Yield: 20 mg (0.09 mmol, 23.9 %) **74** as a white solid. Starting material 2B-ene-*cis*-dimesylate **73** (71 mg, 0.18 mmol, 50.0 %) was recovered. Melting point: 230-232 °C (dec.), m/z: 232.

¹H-NMR (500 MHz, CDCl₃): δ = 1.09 (1H, d, *J* = 10.6 Hz), 1.20 (3H, m), 1.53 (2H, m), 1.76 (2H, bs), 1.92 (2H, dd, *J* = 3.3, 1.5 Hz), 2.10 (2H, m), 2.31 (2H, d, *J* = 1.0 Hz), 3.45 (1H, t, *J* = 1.8 Hz), 3.46 (1H, dt, *J* = 8.5, 1.7 Hz), 3.94 (2H, d, *J* = 8.5 Hz), 4.15 (2H, t, *J* = 2.1 Hz) ppm; ¹³C-NMR (75.5 MHz, CDCl₃): δ = 30.1 (2CH₂), 34.9 (CH₂), 37.8 (2CH), 39.7 (2CH), 40.7 (2CH), 40.9 (2CH), 67.5 (2CH₂O), 73.7 (2HC-O) ppm;

(1α,4α,4aβ,5α,8α,8aβ)-1,2,3,4,4a,5,6,7,8,8a-Decahydro-2,3-*trans*-bis(chloromethyl)-1,4-etheno-5,8-methanonaphthalene (76)



Following a method reported in literature²²⁵ a solution of 2B-ene-*trans*-diol **65** (240 mg, 1.02 mmol) in anhydrous pyridine (8 mL) was added dropwise to thionyl chloride (0.2 mL, 334 mg, 4.2 mmol) under an argon atmosphere.

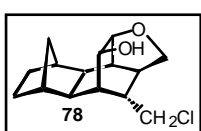
On completion of the addition the greenish yellow mixture was stirred for two hours at 70 °C then cooled down to 0 °C and dichloromethane (10 mL) and H₂O (5 mL) were added to quench the reaction. The organic layer was washed with H₂O (3 x 5 mL) then dried over Na₂SO₄. The solvents were removed under reduced pressure to give a yellow-brown oil, which was purified by column chromatography (light petroleum/ethyl acetate 3:1). Yield: 137 mg (0.51 mmol, 49.5 %) 2B-ene-*trans*-bis(chloromethyl) **76** as a white solid.

¹H-NMR (300 MHz, CDCl₃): δ = 0.67 (1H, d, *J* = 10.3 Hz), 1.09 (2H, m), 1.21 (2H, m), 1.41 (2H, m), 1.57 (1H, dd, *J* = 8.7, 3.1 Hz), 1.71 (1H, dd, *J* = 9.2, 3.1 Hz), 1.97 (1H, s), 2.03 (1H, s), 2.16 (1H, d, *J* = 9.2 Hz), 2.78 (1H, s), 2.80 (1H, s), 3.16 (1H, t, *J* = 9.7 Hz), 3.27 (2H, dd,

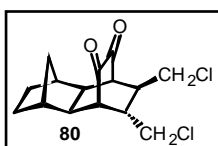
$J = 11.3, 6.2 \text{ Hz}$), 3.55 (1H, t, $J = 10.2 \text{ Hz}$), 3.75 (1H, dd, $J = 10.2, 7.2 \text{ Hz}$), 6.04 (1H, t, $J = 7.2 \text{ Hz}$), 6.25 (1H, t, $J = 7.2 \text{ Hz}$) ppm; ^{13}C -NMR (75.5 MHz, CDCl_3): $\delta = 31.4 (\text{CH}_2)$, 31.8 (CH_2), 35.2 (CH_2), 36.1 (CH), 37.5 (CH), 40.8 (CH), 41.4 (CH), 41.6 (CH), 46.5 (CH), 47.0 (CH_2Cl), 48.1 (CH), 48.7 (CH_2Cl), 49.0 (CH), 131.4 ($=\text{CH}$), 135.0 ($=\text{CH}$) ppm.

(1 α ,2 α ,4 α ,4 $\alpha\beta$,5 α ,8 α ,8 $\alpha\beta$)-1,2,3,4,4a,5,6,7,8,8a-Decahydro-1,4-ethano-[3,11-*b*]-furan-10-hydroxy-5,8-methano-2-chloromethylnaphthalene (78) and (1 α ,4 α ,4 $\alpha\beta$,5 α ,8 α ,8 $\alpha\beta$)-1,2,3,4,4a,5,6,7,8,8a-Decahydro-2,3-*trans*-bis(chloromethyl)-1,4-ethano-5,8-methano-naphthalene-10,11-dione (80)

To a suspension of 2B-ene-*trans*-dimethylchloride **76** (58 mg, 0.21 mmol) and 4-methyl-N-morpholine-N-oxide (178 mg, 1.52 mmol, ~ 7 eq.) in anhydrous 1,4-dioxane (2 mL) was added OsO_4 (0.97 mg, 2 %) in *tert*-butanol (0.19 mL). After stirring the solution for 3 days at RT $\text{Na}_2\text{S}_2\text{O}_5$ (0.5 g) in H_2O (5 mL) and dichloromethane (5 mL) were added. The red mixture was stirred for 30 minutes, layers were separated and the aqueous layer was extracted with dichloromethane (4 x 5 mL). The combined yellow organic layers were washed with H_2O (5 mL) and brine (5 mL) then dried over Na_2SO_4 . The solvents were removed under reduced pressure to give 60 mg of crude product, which was purified by column chromatography (light petroleum/ethyl acetate 1:2). Yield: 35 mg (0.10 mmol, 57%) **78** as a colourless solid and 8 mg (0.025 mmol, 12.5 %) 2B-dione-*trans*-bis(chloromethyl) **80** as a yellow side product.

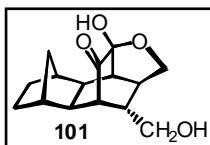


^1H -NMR (300 MHz, CDCl_3 , **78**): $\delta = 1.09$ (1H, d, $J = 7.2 \text{ Hz}$), 1.14 (1H, m), 1.18 (1H, d, $J = 8.2 \text{ Hz}$), 1.31 (1H, d, $J = 11.3 \text{ Hz}$), 1.54 (3H, m), 1.87 (1H, bs), 1.91 (2H, m), 2.10 (4H, m), 3.44 (1H, d, $J = 7.2 \text{ Hz}$), 3.57 (1H, s), 3.60 (1H, s), 3.78 (1H, dd, $J = 7.2, 4.1 \text{ Hz}$), 4.05 (1H, m), 4.1 (1H, t, $J = 5.7 \text{ Hz}$) ppm; ^{13}C -NMR (75.5 MHz, CDCl_3 , **78**): $\delta = 29.6 (\text{CH}_2)$, 31.7 (CH_2), 36.4 (CH_2), 38.9 (CH), 39.1 (CH), 40.2 (CH), 41.6 (2CH), 42.0 (3CH), 48.2 (CH_2Cl), 64.9 (CHOH), 73.9 (HC-O), 74.3 (CH_2O) ppm.



^1H -NMR (300 MHz, CDCl_3 , **80**): $\delta = 0.93$ (1H, dt, $J = 12.3, 2.0 \text{ Hz}$), 1.16 (1H, d, $J = 12.3 \text{ Hz}$), 1.28 (2H, m), 1.59 (2H), 1.62 (2H, m), 2.06 (2H, m), 2.20 (1H, bs), 2.22 (1H, bs), 3.05 (1H, t, $J = 2.6 \text{ Hz}$), 3.12 (1H, t, $J = 2.6 \text{ Hz}$), 3.28 (1H, dd, $J = 11.3, 7.2 \text{ Hz}$), 3.42 (1H, dd, $J = 11.3, 6.2 \text{ Hz}$), 3.69 (1H, dd, $J = 11.3, 8.2 \text{ Hz}$), 3.85 (1H, dd, $J = 11.3, 6.2 \text{ Hz}$) ppm; ^{13}C -NMR (75.5 MHz, CDCl_3 , **80**): $\delta = 29.8 (\text{CH}_2)$, 30.1 (CH_2), 35.9 (CH_2), 39.8 (CH), 40.3 (CH), 40.6 (CH), 40.9 (CH), 41.2 (CH), 44.5 (CH), 45.2 (CH_2Cl), 46.4 (CH_2Cl), 50.5 (CH), 52.6 (CH), 196.6 (2C=O) ppm.

(1 α ,2 β ,4 α ,4 $\alpha\beta$,5 α ,8 α ,8 $\alpha\beta$)-1,2,3,4,4a,5,6,7,8,8a-Decahydro-1,4-ethano-[3,11-*b*]-furan-11-hydroxy-2-hydroxymethyl-5,8-methanonaphthalene-10-one (101**)**



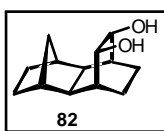
Method 1: To a bright yellow solution of 2B-dione-*trans*-diacetate **79** (300 mg, 0.861 mmol) in (5 mL) tetrahydrofuran was added K₂CO₃ (1.38 g, 10 mmol) in a mixture of H₂O (10 mL) and methanol (7 mL). The yellow solution was stirred at RT for 18 hours, after which the layers were separated and tetrahydrofuran (10 mL) and brine (10 mL) were added to the organic layer. The aqueous layer was extracted with tetrahydrofuran (3 x 10 mL), the combined organic layers were washed with brine (10 mL) then dried over Na₂SO₄. The solvent was removed under reduced pressure to give the crude yellow product, which was purified by column chromatography (light petroleum/ethyl acetate 1:5). Yield: 72 mg (0.272 mmol, 31.6 %) **101**.

Method 2: To a solution of 2B-ene-*trans*-diol **65** (60 mg, 0.26 mmol) and 4-methyl-N-morpholine-N-oxide (152 mg, 1.30 mmol, ~5 eq.) in 1,4-dioxane (1.5 mL) was added OsO₄ (1.3 mg, 2%) in *tert*-butanol (0.3 mL). The solution changed colour from bright yellow to golden after the solution was stirred for 5 days at RT. Na₂S₂O₅ (0.5 g) in H₂O (5 mL) and dichloromethane (10 mL) were added and the dark brown mixture was stirred for a further 30 minutes at RT. The aqueous layer was extracted with dichloromethane (5 x 10 mL) and the combined organic layers were washed with H₂O (5 mL) and brine (5 mL). The solvents were removed under reduced pressure to give the crude product (67 mg), which was purified by column chromatography (light petroleum/ethyl acetate 1:5). Yield: 37 mg (0.14 mmol, 54.6 %) **101**. Melting point: 152-153 °C, m/z: 264.

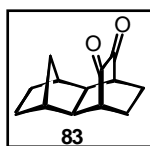
¹H-NMR (300 MHz, CDCl₃): δ = 0.94 (1H, d, *J* = 12.5 Hz), 1.13 (2H, m), 1.50 (2H), 1.54 (1H, d, *J* = 12.5 Hz), 1.91 (1H), 1.94 (2H, m), 1.97 (1H), 2.02 (1H), 2.14 (1H, s), 2.38 (1H, t, *J* = 3.2 Hz), 2.49 (1H, t, *J* = 3.2 Hz), 2.80 (1OH, bs), 3.42 (1H, d, *J* = 7.1 Hz), 3.74 (1H, s), 3.76 (1H, d, *J* = 1.6 Hz), 3.99 (1H, dd, *J* = 2.3, 7.1 Hz), 4.79 (1OH, bs) ppm; ¹³C-NMR (75.5 MHz, CDCl₃): δ = 30.4 (CH₂), 30.8 (CH₂), 34.3 (CH₂), 39.1 (CH), 40.0 (CH), 40.5 (CH), 41.5 (CH), 41.9 (CH), 43.1 (CH), 45.4 (2CH), 63.5 (CH₂OH), 72.9 (CH₂O), 100.8 (C), 210.8 (C=O) ppm.

(1 α ,4 α ,4 α ,5 α ,8 α ,8 α)-1,2,3,4,4a,5,6,7,8,8a-Decahydro-1,4-ethano-10,11-*cis*-dihydroxy-5,8-methanonaphthalene (82) and (1 α ,4 α ,4 α ,5 α ,8 α ,8 α)-1,2,3,4,4a,5,6,7,8,8a-Decahydro-1,4-ethano-5,8-methano-naphthalene-10,11-dione (83)

To a suspension of 2B-ene **81** (54 mg, 0.31 mmol) and 4-methyl-N-morpholine-N-oxide (218 mg, 1.86 mmol, ~6 eq.) in anhydrous 1,4-dioxane (1.4 mL) was added OsO₄ (1.6 mg, 2 %) in *tert*-butanol (0.32 mL). After stirring at RT for 48 hours Na₂S₂O₅ (0.5 g) in H₂O (5 mL) and dichloromethane (5 mL) were added. The red mixture was stirred for 30 minutes, layers were separated and the aqueous layer was extracted with dichloromethane (5 x 5 mL). The bright yellow organic layers were washed with H₂O (5 mL) and brine (5 mL) then dried over Na₂SO₄. The solvents were removed under reduced pressure to give the crude products (62 mg) which were purified by column chromatography (light petroleum/ethyl acetate 3:1). Yield (**82**): 8 mg (0.04 mmol, 12 %) 2B-diol **82** as a colourless solid. Melting point: 155-157 °C; m/z: 208. Yield (**83**): 33 mg (0.16 mmol, 52%) 2B-dione **83** as a bright yellow solid. Melting point: 92-94 °C.



¹H-NMR (300 MHz, CDCl₃, **82**): δ = 1.07 (1H, d, J = 11.2 Hz), 1.16 (4H, m), 1.41 (1H, d, J = 11.2 Hz), 1.51 (2H, m), 1.71 (2H, s), 1.75 (2H, s), 1.90 (2H, d, J = 9.2 Hz), 2.14 (2H, s), 2.58 (2 OH, bs), 4.11 (2H, s) ppm; ¹³C-NMR (75.5 MHz, CDCl₃, **82**): δ = 18.8 (2CH₂), 31.4 (2CH₂), 35.4 (CH₂), 37.0 (2CH), 39.4 (2CH), 47.9 (2CH), 64.9 (2CHOH) ppm.



¹H-NMR (300 MHz, CDCl₃, **83**): δ = 0.88 (1H, d, J = 12.3 Hz), 1.10 (1H, d, J = 13.3 Hz), 1.24 (2H, m), 1.55 (2H, m), 1.85 (2H, dd, J = 8.2, 2.0 Hz), 1.90 (2H, m), 1.97 (2H, m), 2.11 (2H, s), 2.78 (2H, s) ppm; ¹³C-NMR (75.5 MHz, CDCl₃, **83**): δ = 22.4 (2CH₂), 29.9 (2CH₂), 35.6 (CH₂), 40.3 (2CH), 48.3 (2CH), 48.8 (2CH), 199.1 (2C=O) ppm.

D.2.2.2 Sharpless Discrimination

1,2,3,4-Tetrahydro-*cis*-2,3-dihydroxy-1,4-methano-5,8-dimethoxynaphthalene (84)

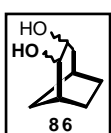


To a suspension of DMB-[2.2.1]-olefin **114**^{186,187,193} (150 mg, 0.74 mmol) and 4-methyl-N-morpholine-N-oxide (695 mg, 5.93 mmol, ~8 eq.) in anhydrous 1,4-dioxane (4 mL) was added OsO₄ (3.8 mg, 2 %) in *tert*-butanol (0.75 mL). After stirring at RT for 3 days Na₂S₂O₅ (1 g) in H₂O (10 mL) and dichloromethane

(10 mL) were added. The red mixture was stirred for 30 minutes, layers were separated and the aqueous layer was extracted with dichloromethane (4 x 5 mL). The combined orange organic layers were washed with H₂O (5 mL) and brine (5 mL) then dried over Na₂SO₄. The solvents were removed under reduced pressure to give the crude product (163 mg) which was purified by column chromatography (light petroleum/ethyl acetate 1:2). Yield: 64 mg (0.27 mmol, 36.6%) DMB-[2.2.1]-diol **84** as a colourless solid. Melting point: 133-134 °C.

¹H-NMR (300 MHz, CDCl₃): δ = 1.81 (1H, d, *J* = 9.2 Hz), 2.16 (1H, d, *J* = 10.3 Hz), 3.36 (2H, s), 3.41 (2H, s), 3.74 (6H, s), 3.76 (1OH, bs), 3.83 (1OH, bs), 6.57 (2H, s) ppm; ¹³C-NMR (75.5 MHz, CDCl₃): δ = 42.4 (CH₂), 46.8 (2CH), 55.9 (2OCH₃), 70.4 (2CHOH), 110.1 (2C_{Ar}H), 134.0 (2C_{Ar}), 148.5 (2C_{Ar}OMe) ppm.

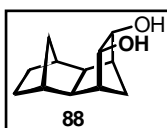
6,7-dihydroxy-1,4-methanocycloheptane (**86**)



To a suspension of the [3.2.1]-olefin **85** (96 mg, 0.89 mmol) and 4-methyl-N-morpholine-N-oxide (662 mg, 5.65 mmol, ~6 eq.) in anhydrous 1,4-dioxane (2 mL) was added OsO₄ (4.7 mg, 2 %) in *tert*-butanol (0.9 mL). After stirring at RT for 3 days Na₂S₂O₅ (1 g) in H₂O (10 mL) and dichloromethane (10 mL) were added to the brown solution. The brown mixture was stirred for 90 minutes, the layers were separated and the aqueous layer was extracted with dichloromethane (4 x 10 mL). The combined colourless organic layers were washed with H₂O (10 mL) and brine (10 mL) then dried over Na₂SO₄. The solvents were removed under reduced pressure to give the crude product, which was dried under high vacuum. Yield: 89 mg (0.63 mmol, 70.3 %) [3.2.1]-diol **86** as a colourless solid.

¹H-NMR (300 MHz, CDCl₃): δ = 1.12 (1H, m), 1.40 (2H, m), 1.65 (2H, m), 1.84 (1H, d, *J* = 11.7 Hz), 2.15 (1H, bs), 2.37 (1H, m), 2.91 (2H, bs), 3.70 (2H, m) ppm.

(1α,2α,3α,4α,4α,5β,8β,8α)-1,2,3,4,4a,5,6,7,8,8a-Decahydro-1,4:5,8-dimethanonaphthalene-*cis*-2,3-diol (**88**)²²⁶



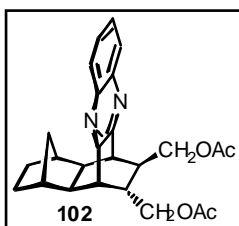
To a suspension of the [2.2.1]-olefin **87** (300 mg, 1.88 mmol) and 4-methyl-N-morpholine-N-oxide (1.28 g, 10.94 mmol, ~6 eq.) in anhydrous 1,4-dioxane (10 mL) was added OsO₄ (9.5 mg, 2 %) in *tert*-butanol (1.9 mL). After stirring at RT for 3 days Na₂S₂O₅ (1 g) in H₂O (10 mL) and dichloromethane (10 mL) were added. The red mixture was stirred for 30 minutes, the layers were separated and the aqueous layer was extracted with dichloromethane (4 x 5 mL). The combined orange organic layers were

washed with H₂O (5 mL) and brine (5 mL) then dried over Na₂SO₄. The solvents were removed under reduced pressure to give (311 mg) the crude product, which was purified by column chromatography (light petroleum, ethyl acetate 1:1). Yield: 166 mg (0.86 mmol, 45.7 %) [2.2.1]-diol **88** as a white solid. Melting point: 132 - 133 °C; m/z: 194.

¹H-NMR (300 MHz, CDCl₃): δ = 0.95-1.09 (3H), 1.10-1.20 (2H), 1.47 (2H, m), 1.78 (3H, m), 2.20 (4H, bs), 2.46 (2H, m), 4.15 (2H, m) ppm; ¹³C-NMR (75.5 MHz, CDCl₃): δ = 31.2 (2CH₂), 35.3 (CH₂), 35.6 (CH₂), 36.5 (2CH), 48.6 (2CH), 48.8 (2CH), 70.8 (2CHOH) ppm.

D.2.2.3 Condensations

(1α,4α,4aβ,5α,8α,8aβ)-1,2,3,4,4a,5,6,7,8,8a-Decahydro-2,3-*trans*-bis(acetoxymethyl)-1,4-ethano-5,8-methano-10,11-quinoxalinonaphthalene (**102**)



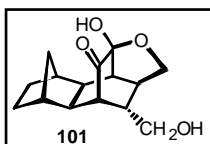
Method 1 (ethanol): Under an argon atmosphere a solution of 2B-dione-*trans*-diacetate **79** (55 mg, 0.16 mmol) and phenylenediamine (22 mg, 0.20 mmol) in absolute ethanol (2 mL) was heated at reflux for 6 days. Dichloromethane (15 mL) was added and the organic solution was washed with H₂O (10 mL). The yellow aqueous layer was extracted with dichloromethane (3 x 10 mL) and the combined orange organic layers were washed with H₂O (10 mL) and brine (10 mL) then dried over Na₂SO₄. The crude product (84 mg) was purified by column chromatography (light petroleum/ethyl acetate 1:2, 1:4).

Method 2 (pyridine): Under an argon atmosphere a solution of 2B-dione-*trans*-diacetate **79** (50 mg, 0.14 mmol) and phenylenediamine (18 mg, 0.16 mmol) in oxygen-free pyridine (1.5 mL) was heated at reflux for 6 days. Dichloromethane (10 mL) was added and the organic solution was washed with 1M HCl (3 x 10 mL) and NaHCO₃ (half sat., 2 x 10 mL) then dried over Na₂SO₄. The crude products (45 mg) were purified by column chromatography (light petroleum/ethyl acetate 1:1).

Method 3 (pyridine, high pressure): A mixture of 2B-dione-*trans*-diacetate **79** (10 mg, 0.030 mmol) and phenylenediamine (5 mg, 0.044 mmol, 1.5 eq.) in pyridine was heated at 40 °C and 15 kbar for 3 days. The pyridine was removed under high vacuum and the crude product was purified by column chromatography (light petroleum/ethyl acetate 1:2). Yield: 9 mg (0.02 mmol, 72.1 %) 2B-quinoxalinonaphthalene-*trans*-diacetate **102**.

^1H -NMR (300 MHz, CDCl_3): δ = -0.82 (1H, d, J = 11.7 Hz), 0.42 (1H, d, J = 11.7 Hz), 1.22 (2H, m), 1.42 (2H, m), 1.64 (2H, m), 1.87 (3H, s), 1.92 (1H, d, J = 6.3 Hz), 2.08 (2H, bs), 2.12 (3H, s), 2.29 (1H, dd, J = 8.6, 2.3 Hz), 3.39 (2H, m), 3.50 (1H, dd, J = 10.9, 7.8 Hz), 3.75 (1H, dd, J = 10.9, 5.4 Hz), 4.34 (2H, m), 7.72 (2H, dd, J = 6.3, 3.9 Hz), 8.06 (2H, m) ppm; ^{13}C -NMR (75.5 MHz, CDCl_3): δ = 20.7 (CH_3), 20.9 (CH_3), 30.6 (CH_2), 30.8 (CH_2), 34.6 (CH_2), 39.9 (2CH), 40.3 (CH), 41.0 (CH), 41.6 (CH), 42.1 (CH), 43.9 (CH), 49.0 (CH), 64.6 (CH_2O), 66.2 (CH_2O), 129.0 (4C_{ArH}), 142.2 (2C_{Ar}), 152.7 (2C_{Ar}), 170.7 (2OAc) ppm.

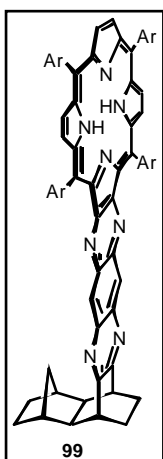
(1 α ,2 β ,4 α ,4 $\alpha\beta$,5 α ,8 α ,8 $\alpha\beta$)-1,2,3,4,4a,5,6,7,8,8a-Decahydro-1,4-ethano-[3,11-*b*]-furan-11-hydroxy-2-hydroxymethyl-5,8-methanonaphthalene-10-one (101**)**



A solution of 2B-dione-*trans*-diacetate **79** (21 mg, 0.060 mmol) and benzenetetramine \cdot 4HCl (17 mg, 0.060 mmol) was reacted at 15 kbar and 100 °C for 2 days. A precipitate was filtered off and the dark purple solution was evaporated to dryness, then taken up in dichloromethane and washed with sat. NaHCO_3 , changing colour to orange-yellow. Layers were separated and the aqueous layer was extracted with dichloromethane. The combined organic layers were dried over Na_2SO_4 and the solvent was removed under reduced pressure to give **101** as a yellow-orange solid. Melting point: 152-153 °C; m/z : 264.

^1H -NMR (500 MHz, CDCl_3): δ = 0.96 (1H, d, J = 11.8 Hz), 1.16 (2H, d, J = 8.8 Hz), 1.53 (2H), 1.54 (1H, d, J = 11.8 Hz), 1.91 (1H), 1.94 (2H, m), 1.97 (1H), 2.02 (1H), 2.17 (1H, s), 2.41 (1H, s), 2.52 (1H, s), 3.45 (1H, d, J = 7.8 Hz), 3.79 (2H, d, J = 7.8 Hz), 4.02 (1H, d, J = 5.9 Hz) ppm; ^{13}C -NMR (75.5 MHz, CDCl_3): δ = 30.5 (CH_2), 30.9 (CH_2), 34.4 (CH_2), 39.1 (CH), 40.0 (CH), 40.6 (CH), 41.7 (CH), 42.1 (CH), 43.3 (CH), 45.2 (2CH), 63.8 (CH_2OH), 72.9 (CH_2O), 100.4 (C), 210.2 (C=O) ppm.

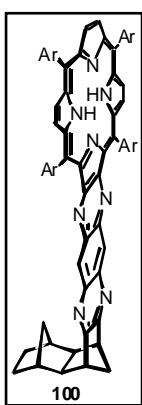
2B-porphyrin (99**)**



A solution of 2B-dione **83** (17 mg, 0.084 mmol) and 'diaminoporphyrin' **153** (100 mg, 0.084 mmol) in oxygen-free pyridine (2 mL) was heated at 110 °C for 11 days under an argon atmosphere in a dark pressure tube. The solvent was removed under reduced pressure to give the crude product, which was purified by column chromatography (chloroform). Yield: 48 mg (0.035 mmol, 42 %) 2B-porphyrin **99**. Melting point: >300 °C.

^1H -NMR (300 MHz, CDCl_3): δ = -2.35 (2H, s), -0.36 (1H, d, J = 10.7 Hz), 0.54 (1H, d, J = 10.7 Hz), 0.8-1.8 (6H), 1.52 (18H, s), 1.56 (54H, s), 2.09 (2H, d, J = 7.8 Hz), 2.19 (2H, s), 2.23 (2H, s), 3.40 (2H, s), 7.82 (2H, bs), 7.95 (2H, bs), 8.04 (2H, bs), 8.07 (2H, bs), 8.12 (4H, t, J = 1.5 Hz), 8.67 (2H, s), 8.79 (2H, s), 8.99 (4H, s) ppm; ^{13}C -NMR (75.5 MHz, CDCl_3): δ = 29.7 (2 CH_2), 30.7 (2 CH_2), 31.8 (12 CH_3), 32.0 (12 CH_3), 35.1 (8C), 28.8 (2CH), 41.3 (2CH), 48.8 (2CH), 118.0 (2C), 120.6 (2 $\text{C}_{\text{p-ArH}}$), 121.2 (2 $\text{C}_{\text{p-ArH}}$), 123.1 (2C), 128.1 (2 $\text{C}_{\text{o-ArH}}$), 128.4 (2 $\text{C}_{\text{o-ArH}}$), 128.8 (2 $\text{C}_{\text{o-ArH}}$), 128.9 (2 $\text{C}_{\text{o-ArH}}$), 129.4 (2 $\text{C}_{\text{pyrrolicH}}$), 129.6 (4 $\text{C}_{\text{pyrrolicH}}$), 134.2 (2 $\text{C}_{\text{quinoxalineH}}$), 138.1 (2C), 139.5 (2C), 140.1 (2C), 140.9 (4C), 141.1 (2C), 145.7 (2C), 148.9 (4 $\text{C}_{\text{Ar-tBu}}$), 149.0 (4 $\text{C}_{\text{Ar-tBu}}$), 153.9 (2C), 155.0 (2C), 160.6 (2C) ppm.

[2.2.1]-porphyrin (100)

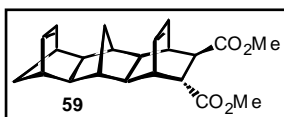


A solution of the [2.2.1]-dione **155**²²⁶ (10 mg, 0.0525 mmol) and 'diaminoporphyrin' **153** (65 mg, 0.0543 mmol) in oxygen-free pyridine (1 mL) was heated at 125 °C under an argon atmosphere for 12 days in a dark pressure tube. The solvent was removed under reduced pressure and the crude product was purified by column chromatography (dichloromethane/light petroleum 5:1). Yield 7 mg (0.0051 mmol, 9.7 %) [2.2.1]-porphyrin **100**. Melting point: >300 °C.

^1H -NMR (300 MHz, CDCl_3): δ = -2.40 (2H, s), -0.87 (1H, d, J = 11.7 Hz), 0.46 (1H, d, J = 11.7 Hz), 1.15 (2H, d, J = 5.9 Hz), 1.3-1.5 (2H), 1.53 (36 H, s), 1.54 (36H, s), 2.06 (2H, dd, J = 16.6, 9.8 Hz), 2.24 (2H, s), 2.54 (2H, s), 3.64 (2H, s), 7.81 (2H, t, J = 2.0 Hz), 7.94 (2H, s), 8.02 (4H, t, J = 2.9 Hz), 8.10 (4H, t, J = 2.4 Hz), 8.56 (2H, s), 8.77 (2H, s), 8.99 (4H, AB_{quartet}, J = 8.8, 5.9 Hz) ppm; ^{13}C -NMR (75.5 MHz, CDCl_3): δ = 29.7 (CH₂), 30.5 (CH₂), 31.8 (12CH₃), 32.0 (12CH₃), 35.1 (8C), 37.0 (2CH), 46.1 (CH₂), 48.5 (2CH), 50.6 (2CH), 118.0 (2C), 120.7 (2 $\text{C}_{\text{p-ArH}}$), 121.2 (2 $\text{C}_{\text{p-ArH}}$), 123.0 (2C), 128.1 (2 $\text{C}_{\text{o-ArH}}$), 128.4 (2 $\text{C}_{\text{o-ArH}}$), 128.6 (2 $\text{C}_{\text{o-ArH}}$), 128.8 (2 $\text{C}_{\text{o-ArH}}$), 129.3 (2 $\text{C}_{\text{pyrrolicH}}$), 129.6 (4 $\text{C}_{\text{pyrrolicH}}$), 134.2 (2 $\text{C}_{\text{quinoxalineH}}$), 138.1 (2C), 139.5 (2C), 139.9 (2C), 140.1 (2C), 140.8 (2C), 141.1 (2C), 148.9 (8 $\text{C}_{\text{Ar-tBu}}$), 149.0 (2C), 153.8 (2C), 155.0 (2C), 164.8 (2C) ppm.

D.2.3 Synthesis of the Bis-Porphyrin Donor

(1 α ,4 α ,4 α ,5 α ,8 α ,8 α ,9 β ,9 α ,10 β ,10 α)-1,4,4a,5,8,8a,9,9a,10,10a-Decahydro-5,8-ethano-1,4:9,10-dimethanoanthracene-12,13-*trans*-dicarboxylate (**59**)



A solution of ketone **4** (2.54 g, 10.6 mmol) [**D.1**, page 153] and dimethyl fumarate (1.68, 11.8 mmol) in toluene (20 mL) was heated at reflux for 87 hours. Half of the toluene was removed under reduced pressure and the slightly yellow solution was placed in the freezer. The white precipitate was filtered off, washed with ice-cold methanol and dried under high vacuum. Yield: 3.09 g (8.73 mmol, 82.4 %) 6B-ene-2B-ene-*trans*-diester **59** as a white solid.

$^1\text{H-NMR}$ (300 MHz, CDCl_3): δ = 1.11 (1H, d, J = 7.7 Hz), 1.24 (1H, dt, J = 7.7, 1.5 Hz), 1.39 (1H, dd, J = 8.7, 2.6 Hz), 1.58 (2H), 1.62 (1H, bs), 1.84 (2H, t, J = 3.1 Hz), 1.90 (1H, s), 1.96 (1H, s), 2.70 (1H, dd, J = 5.1, 3.1 Hz), 2.78 (2H, bs), 3.04 (1H, t, J = 3.1 Hz), 3.08 (1H, m), 3.12 (1H), 3.62 (3H, s), 3.81 (3H, s), 5.85 (2H, t, J = 1.8 Hz), 6.00 (1H, t, J = 7.7 Hz), 6.18 (1H, t, J = 7.7 Hz) ppm; $^{13}\text{C-NMR}$ (75.5 MHz, CDCl_3): δ = 29.6 (CH_2), 37.4 (CH), 37.5 (CH), 42.9 (CH), 43.3 (CH), 46.3 (2CH), 46.4 (CH), 46.5 (CH), 47.6 (2CH), 50.5 (CH), 50.7 (CH), 52.0 (OCH₃), 52.2 (OCH₃), 53.4 (CH_2), 132.0 (=CH), 134.3 (=CH), 135.4 (=CH), 135.5 (=CH), 174.6 (C=O), 176.5 (C=O) ppm.

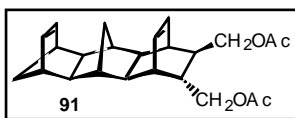
(1 α ,4 α ,4 α ,5 α ,8 α ,8 α ,9 β ,9 α ,10 β ,10 α)-1,4,4a,5,8,8a,9,9a,10,10a-Decahydro-5,8-ethano-12,13-*trans*-bis(hydroxymethyl)-1,4:9,10-dimethanoanthracene (**89**)



To an ice-cold slurry solution of LiAlH_4 (1.21 g, 31.9 mmol, ~4.5 eq.) in tetrahydrofuran (40 mL) was added dropwise 6B-ene-2B-ene-*trans*-diester **59** (2.48 g, 7.0 mmol) in tetrahydrofuran (40 mL) under an argon atmosphere. On completion of the addition the mixture was heated at reflux for 20 hours then cooled down to 0 °C and quenched with 1M K_2CO_3 (15 mL). The mixture was heated at reflux for another 15 minutes then filtered hot through a pad of filter aid, which was extracted with boiling diethyl ether (3 x 30 mL). The organic layer was washed with H_2O (2 x 30 mL), the combined aqueous layers were extracted with diethyl ether (3 x 30 mL) and the combined organic layers were washed with brine (30 mL) and dried over Na_2SO_4 . The solvents were removed under reduced pressure to give the crude product, which was used without further purification. Yield: 1.764 g (5.91 mmol, 84.4 %) 6B-ene-2B-ene-*trans*-diol **89**. Melting point: 131-132 °C; m/z: 298.

$^1\text{H-NMR}$ (300 MHz, CDCl_3): δ = 1.13 (1H, d, J = 7.7 Hz), 1.17 (1H, m), 1.25 (1H, d, J = 7.7 Hz), 1.49 (3H, m), 1.59 (1H, d, J = 11.3 Hz), 1.67 (1H, d, J = 11.3 Hz), 1.84 (2H, 1.87 (1H, s), 1.93 (1H, s), 2.11 (2OH, b), 2.52 (1H, d, J = 7.2 Hz), 2.58 (1H, d, J = 7.2 Hz), 2.78 (2H, s), 3.06 (1H, t, J = 8.7 Hz), 3.49 (1H, dd, J = 9.2, 5.1 Hz), 3.67 (1H, d, J = 3.1), 3.69 (1H, s), 5.86 (2H, t, J = 2.1 Hz), 5.92 (1H, t, J = 7.2 Hz), 6.15 (1H, t, J = 7.2 Hz) ppm.

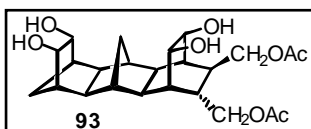
(1 α ,4 α ,4 α ,5 α ,8 α ,8 α ,9 β ,9 α ,10 β ,10 α)-1,4,4a,5,8,8a,9,9a,10,10a-Decahydro-5,8-ethano-12,13-*trans*-bis(acetoxymethyl)-1,4:9,10-dimethanoanthracene (91)



Acetic anhydride (1.00 g, 9.76 mmol, ~3 eq.) was added to a colourless solution of 6B-ene-2B-ene-*trans*-diol **89** (970 mg, 3.25 mmol) in pyridine (20 mL). After stirring at RT for 23 hours the solution was poured onto a mixture of ice (100 g), 1M HCl (50 mL) and dichloromethane (30 mL). The aqueous layer was extracted with dichloromethane (4 x 30 mL). The combined organic layers were washed with 1M HCl (3 x 30 mL) and NaHCO_3 (sat., 30 mL) then dried over Na_2SO_4 . The solvents were removed under reduced pressure to give the crude product (1.6 g), which was purified by column chromatography (light petroleum/ethyl acetate 3:1). Yield: 1.159 g (3.03 mmol, 93.2 %) 6B-ene-2B-ene-*trans*-diacetate **91**.

$^1\text{H-NMR}$ (300 MHz, CDCl_3): δ = 1.13 (1H, d, J = 8.2 Hz), 1.25 (1H, dt, J = 8.2, 2.1 Hz), 1.42 (2H, m), 1.63 (4H, m), 1.8 (2H, m), 1.88 (1H, s), 1.94 (1H, s), 2.04 (3H, s), 2.08 (3H, s), 2.58 (2H, t, J = 6.2 Hz), 2.78 (2H, s), 3.62 (1H, dd, J = 11.3, 9.2), 3.71 (1H, dd, J = 10.3, 6.2 Hz), 4.07 (1H, dd, J = 11.3, 9.2 Hz), 4.19 (1H, dd, J = 10.3, 6.2 Hz), 5.86 (2H, t, J = 2.1 Hz), 5.95 (1H, t, J = 7.7 Hz), 6.16 (1H, t, J = 7.7 Hz) ppm; $^{13}\text{C-NMR}$ (75.5 MHz, CDCl_3): δ = 21.0 (2CH₃), 30.2 (CH₂), 35.4 (CH), 36.4 (CH), 41.4 (CH), 42.9 (CH), 43.0 (CH), 43.5 (CH), 44.7 (CH), 46.6 (2CH), 50.6 (CH), 50.8 (CH), 51.8 (CH), 53.4 (CH₂), 65.8 (CH₂-O), 67.4 (CH₂-O), 131.6 (=CH), 135.2 (=CH), 135.4 (=CH), 135.5 (=CH), 171.07 (OAc), 171.12 (OAc) ppm.

(1 α ,4 α ,4 α ,5 α ,8 α ,8 α ,9 β ,9 α ,10 β ,10 α)-1,2,3,4,4a,5,6,7,8,8a,9,9a,10,10a-Tetradecahydro-12,13-*trans*-bis(acetoxymethyl)-2,3,6,7-*cis*,*cis*-tetrahydroxy-5,8-ethano-1,4:9,10-dimethanoanthracene (93)

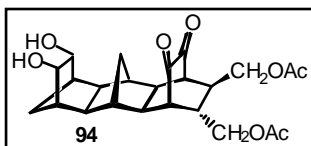


To a suspension of 6B-ene-2B-ene-*trans*-diacetate **91** (292 mg, 0.76 mmol) and 4-methyl-N-morpholine-N-oxide (1098 mg, 9.47 mmol, ~12.5 eq.) in anhydrous 1,4-dioxane (12 mL) was added

OsO₄ (3.9 mg, 2 %) in *tert*-butanol (0.80 mL). After stirring at RT for 18 hours Na₂S₂O₅ (1 g) in H₂O (10 mL) and dichloromethane (10 mL) were added. The red mixture was stirred for 30 minutes, layers were separated and the aqueous layer was extracted with dichloromethane (4 x 5 mL). The combined bright yellow organic layers were washed with H₂O (5 mL) and brine (5 mL) then dried over Na₂SO₄. The solvents were removed under reduced pressure to give a yellow oil (424 mg), which was purified by column chromatography (light petroleum/ethyl acetate 1:5). Yield: 110 mg (0.24 mmol, 32.1%) 6B-diol-2B-diol-*trans*-diacetate **93** as a colourless solid. As a bright yellow side product 89 mg (0.20 mmol, 26.2 %) 6B-diol-2B-dione-*trans*-diacetate **94** were isolated.

¹³C-NMR (75.5 MHz, DMSO): δ = 21.26 (CH₃), 21.31 (CH₃), 24.9 (CH), 31.8 (CH₂), 32.7 (CH), 35.8 (CH₂), 37.0 (CH), 37.7 (CH), 39.1 (CH), 39.4 (CH), 40.3 (CH), 41.1 (CH), 42.4 (CH), 48.6 (CH), 50.6 (CH), 51.1 (CH), 63.3 (CHOH), 64.4 (CHOH), 65.3 (CH₂-O), 69.5 (2CHOH), 69.9 (CH₂-O), 170.8 (2OAc) ppm.

(1α,4α,4α,5α,8α,8α,9β,9α,10β,10α)-1,2,3,4,4a,5,8,8a,9,9a,10,10a-Dodecahydro-12,13-*trans*-bis(acetoxymethyl)-5,8-ethano-2,3-*cis*-dihydroxy-1,4:9,10-dimethano-anthracene-6,7-dione (94)



To a suspension of 6B-ene-2B-ene-*trans*-diacetate **91** (507 mg, 1.33 mmol) and 4-methyl-N-morpholine-N-oxide (1882 mg, 16.06 mmol, ~12 eq.) in anhydrous 1,4-dioxane (20 mL) was added (6.76 mg, 2 %) OsO₄ in (1.35 mL) *tert*-butanol. After stirring at RT for 6 days Na₂S₂O₅ (1 g) in H₂O (10 mL) and dichloromethane (30 mL) were added. The red mixture was stirred for 45 minutes, the layers were separated and the aqueous layer was extracted with dichloromethane (4 x 30 mL). The combined bright yellow organic layers were washed with H₂O (30 mL) and brine (30 mL) then dried over Na₂SO₄. The solvents were removed under reduced pressure to give a bright yellow oil (772 mg), which was purified by column chromatography (light petroleum/ethyl acetate 1:6). Yield: 351 mg (0.80 mmol, 59 %) 6B-diol-2B-dione-*trans*-diacetate **94** as a bright yellow solid. Melting point: 136-138 °C; m/z: 446.

¹H-NMR (300 MHz, CDCl₃): δ = 0.63 (1H, d, *J* = 14.4 Hz), 1.08 (1H, d, *J* = 11.3 Hz), 1.11 (1H, d, *J* = 9.2 Hz), 1.82-1.86 (4H), 1.92 (1H), 1.97 (3H, s), 2.09 (3H, s), 2.13 (2H, m), 2.20 (1H, s), 2.23 (1H, s), 2.26 (2H, bs), 2.89 (1H, t, *J* = 3.1 Hz), 2.91 (1H, t, *J* = 3.1 Hz), 3.79 (1H, dd, *J* = 11.3, 6.2 Hz), 4.05 (2H, s), 4.06 (1H, dd, *J* = 11.3, 4.4 Hz), 4.19 (1H, s), 4.22 (1H, s) ppm; ¹³C-NMR (75.5 MHz, CDCl₃): δ = 20.3 (CH₃), 20.8 (CH₃), 33.0 (CH₂), 35.3

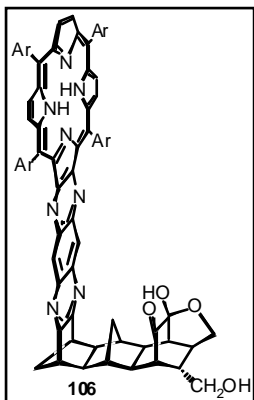
(CH₂), 36.0 (CH), 39.9 (CH), 40.0 (CH), 40.4 (CH), 42.9 (CH), 48.2 (2CH), 49.0 (CH), 49.1 (CH), 49.5 (CH), 50.5 (CH), 52.2 (CH), 63.9 (CH₂-O), 65.2 (CH₂-O), 70.0 (2CHOH), 170.4 (OAc), 170.7 (OAc), 196.9 (C=O), 197.1 (C=O) ppm.

(1 α ,4 α ,4 α ,5 α ,8 α ,8 α ,9 β ,9 α ,10 β ,10 α)-1,2,3,4,4a,5,8,8a,9,9a,10,10a-Dodecahydro-5,8-ethano-12,13-*trans*-bis(acetoxymethyl)-1,4:9,10-dimethanoanthracene-2,3,6,7-tetraone (95)



To an ice-cold bright yellow solution of 6B-diol-2B-dione-*trans*-diacetate **94** (199 mg, 0.446 mmol) and *p*-toluenesulfonic acid monohydrate (424 mg, 2.229 mmol, ~5 eq.) in dichloromethane (10 mL) was added dropwise 4-acetamido-TEMPO (455 mg, 2.086 mmol, ~5 eq.) in dichloromethane (10 mL) in the dark. On completion of the addition the mixture was stirred for 4 days in the dark at RT. A white precipitate was filtered off and ethanol (10 mL) was added to the filtrate to quench the reaction. The bright yellow solution was washed with H₂O (2 x 20 mL) and brine (20 mL) then dried over Na₂SO₄. The solvents were removed under reduced pressure to give a yellow solid (246 mg), which was purified by column chromatography (light petroleum/ethyl acetate 1:4). Yield: 146 mg (0.330 mmol, 74.0 %) 6B-dione-2B-dione-*trans*-diacetate **95** as a yellow solid. Melting point: 225-227 °C; m/z: 442.

¹H-NMR (300 MHz, CDCl₃): δ = 0.62 (1H, d, J = 15.9 Hz), 0.77 (1H, d, J = 15.9 Hz), 1.86 (1H), 1.93 (3H, s), 2.04 (1H, s), 2.08 (3H, s), 2.13 (1H, d, J = 7.1 Hz), 2.22 (1H, s), 2.23 (2H, s), 2.27 (2H, s), 2.45 (2H, m), 2.89 (2H, dd, J = 5.1, 2.3 Hz), 3.13 (2H, d, J = 5.1 Hz), 3.78 (1H, dd, J = 11.3, 5.6 Hz), 4.06 (1H, dd, J = 11.3, 4.1 Hz), 4.18 (1H, s), 4.21 (1H, d, J = 2.0 Hz) ppm; ¹³C-NMR (75.5 MHz, CDCl₃): δ = 20.3 (CH₃), 20.8 (CH₃), 31.6 (CH₂), 34.4 (CH₂), 36.1 (CH), 39.8 (CH), 40.5 (CH), 40.9 (CH), 41.5 (CH), 48.8 (CH), 49.4 (CH), 51.8 (CH), 52.0 (CH), 52.1 (CH), 53.2 (2CH), 63.6 (CH₂-O), 65.0 (CH₂-O), 170.3 (OAc), 170.7 (OAc), 196.1 (C=O), 196.2 (C=O), 202.2 (2C=O) ppm.

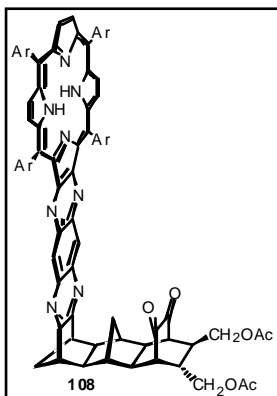
6B-porphyrin-hemi-acetal (106)

A solution of 6B-dione-2B-dione-*trans*-diacetate **95** (20 mg, 0.0452 mmol) and 'diaminoporphyrin' **153** (66 mg, 0.0552 mmol) in de-oxygenated pyridine (1 mL) was reacted for 3 days at 80 °C and 15 kbar. The solvent was blown off with argon and the crude product was dried under high vacuum, then purified by column chromatography (dichloromethane/methanol 20:1). Yield: 15 mg (0.0099 mmol, 21.9 %) 6B-porphyrin-hemi-acetal **106**.

$^1\text{H-NMR}$ (600 MHz, CDCl_3): δ = -2.39 (2H, s), -0.93 (1H, d, J =13.1 Hz), 0.83 (1H, d, J =13.1 Hz), 1.49 (1H), 1.50 (9H), 1.54 (54H), 1.57 (9H), 1.75 (1H, s), 1.94 (2H, bs), 2.02 (1H, d, J =9.6 Hz), 2.05 (1H), 2.08 (1H, d, J =9.6 Hz), 2.10 (1H, bs), 2.25 (1H, s), 2.32 (1H, d, J =8.3 Hz), 2.42 (1H, bs), 2.49 (1H, m), 2.54 (1H, m), 3.38 (1H, d, J =7.6 Hz), 3.65 (2H, s), 3.78 (2H, m), 3.98 (1H, d, J =7.6 Hz), 7.82 (2H, t, J =1.8 Hz), 7.94 (1H, t, J =1.8 Hz), 7.95 (1H, t, J =1.8 Hz), 7.99 (1H, t, J =1.5 Hz), 8.00 (1H, t, J =1.5 Hz), 8.05 (1H, t, J =1.5 Hz), 8.06 (1H, t, J =1.5 Hz), 8.10 (2H, t, J =1.5 Hz), 8.11 (2H, t, J =1.5 Hz), 8.526 (1H, s), 8.528 (1H, s), 8.79 (2H, s), 9.00 (4H, AB_{quartet}, J =14.8, 4.8 Hz) ppm; $^{13}\text{C-NMR}$ (75.5 MHz, CDCl_3): δ = 30.3 (CH_2), 31.8 (12CH_3), 32.0 (12CH_3), 35.1 (8C), 39.8 (CH), 40.8 (CH), 41.6 (CH), 41.7 (CH), 42.2 (CH), 44.4 (CH), 44.7 (CH), 44.9 (CH), 46.4 (CH_2), 48.2 (2CH), 51.5 (CH), 51.8 (CH), 63.6 (CH_2OH), 72.7 (CH_2O), 100.2 (-OCOH), 118.1 (2C), 120.7 ($2\text{C}_{\text{p-ArH}}$), 221.2 ($2\text{C}_{\text{p-ArH}}$), 123.0 (2C), 128.1 ($2\text{C}_{\text{o-ArH}}$), 128.5 ($2\text{C}_{\text{o-ArH}}$), 128.7 ($4\text{C}_{\text{o-ArH}}$), 129.5 ($2\text{C}_{\text{pyrrolicH}}$), 129.6 ($4\text{C}_{\text{pyrrolicH}}$), 134.2 ($2\text{C}_{\text{quinoxalineH}}$), 138.1 (2C), 139.6 (C), 140.0 (3C), 140.8 (2C), 141.1 (2C), 145.7 (2C), 148.9 ($8\text{C}_{\text{Ar}}^t\text{Bu}$), 149.2 (2C), 153.8 (2C), 155.0 (2C), 164.0 (2C), 209.2 (C=O) ppm.

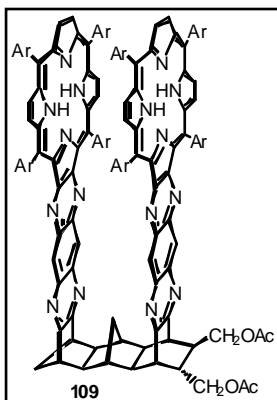
6B-porphyrin-2B-dione-*trans*-diacetate (108) and Bis-porphyrin-*trans*-diacetate (109)

A solution of 6B-dione-2B-dione-*trans*-diacetate **95** (36 mg, 0.0814 mmol) and 'diaminoporphyrin' **153** (200 mg, 0.1673 mmol) in anhydrous and de-oxygenated dichloromethane (4 mL) was heated at 80 °C and 15 kbar for 3 days. The solvent was removed under an argon stream and the crude products were purified by column chromatography (dichloromethane/methanol 50:1). Yield: 46 mg (0.0287 mmol, 35.3 %) 6B-porphyrin-2B-dione-*trans*-diacetate **108** and 20 mg (0.0072 mmol, 8.9 %) bis-porphyrin-*trans*-diacetate **109** as purple solids. Melting points: >300 °C.



$^1\text{H-NMR}$ (300 MHz, CDCl_3 , **108**): δ = -2.34 (2H, s), -0.76 (1H, d, J = 14.4 Hz), 0.16 (1H, d, J = 14.4), 1.54 (18H), 1.58 (54H), 1.77 (1H), 1.87 (1H, m), 1.96 (3H, s), 2.06 (2H), 2.09 (1H), 2.16 (3H, s), 2.18 (1H, s), 2.28 (1H, s), 2.31 (1H, s), 2.61 (1H, dd, J = 8.7, 4.2 Hz), 2.68 (1H, dd, J = 8.7, 4.2 Hz), 2.91 (1H, s), 2.92 (1H, s), 3.73 (2H, bs), 3.77 (1H, dd, J = 11.7, 5.6 Hz), 4.07 (1H, dd, J = 11.3, 4.2 Hz), 4.24 (1H, s), 4.27 (1H, s), 7.85 (2H, t, J = 1.9 Hz), 7.99 (2H, t, J = 1.6 Hz), 8.04 (2H, bs), 8.10 (2H, bs), 8.15 (4H), 8.56 (2H, s), 8.83 (2H, s), 9.05 (4H, AB_{quartet},

J = 10.5, 4.9 Hz) ppm; $^{13}\text{C-NMR}$ (75.5 MHz, CDCl_3 , **108**): δ = 20.4 (CH_3), 20.9 (CH_3), 31.8 (12 CH_3), 31.97 (6 CH_3), 32.04 (6 CH_3), 32.3 (CH_2), 35.1 (8C), 36.1 (CH), 39.9 (CH), 40.6 (CH), 41.0 (CH), 42.5 (CH), 46.3 (CH_2), 48.1 (2CH), 49.4 (CH), 50.0 (CH), 50.7 (CH), 50.9 (CH), 52.1 (CH), 63.8 ($\text{CH}_2\text{-O}$), 65.1 ($\text{CH}_2\text{-O}$), 118.1 (2C), 120.6 ($2\text{C}_{\text{p-ArH}}$), 221.2 ($2\text{C}_{\text{p-ArH}}$), 123.0 (2C), 128.1 ($2\text{C}_{\text{o-ArH}}$), 128.5 ($2\text{C}_{\text{o-ArH}}$), 128.6 ($2\text{C}_{\text{o-ArH}}$), 128.7 ($2\text{C}_{\text{o-ArH}}$), 129.5 ($2\text{C}_{\text{pyrrolicH}}$), 129.6 ($4\text{C}_{\text{pyrrolicH}}$), 134.2 ($2\text{C}_{\text{quinoxalineH}}$), 138.1 (2C), 139.65 (C), 139.70 (C), 139.9 (2C), 140.8 (2C), 141.1 (2C), 145.6 (2C), 148.8 ($4\text{C}_{\text{Ar}}^{\text{tBu}}$), 148.9 ($4\text{C}_{\text{Ar}}^{\text{tBu}}$), 149.17 (C), 149.21 (C), 153.9 (2C), 155.0 (2C), 163.35 (C), 163.39 (C), 170.4 (OAc), 170.8 (OAc), 196.0 (C=O), 196.3 (C=O) ppm.



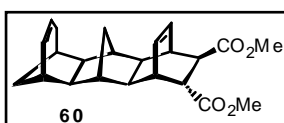
$^1\text{H-NMR}$ (300 MHz, CDCl_3 , **109**): δ = -2.60 (4H, s), -0.96 (1H, d, J = 13.2 Hz), -0.64 (1H, d, J = 13.2 Hz), 1.38 (9H), 1.40 (9H), 1.42 (27H), 1.45 (63H), 1.48 (36H), 1.7 (1H), 1.76 (3H, s), 2.04 (4H, m), 2.23 (3H, s), 2.37 (1H, s), 2.41 (1H, s), 2.43 (1H), 2.70 (2H, m), 3.51 (1H, m), 3.53 (2H, bs), 3.68 (2H, bs), 3.78 (1H, dd, J = 11.3, 5.3 Hz), 4.42 (2H, m), 7.74 (4H, bs), 7.81 (2H, bs), 7.84 (4H, bs), 7.86 (8H, bs), 7.96 (4H, bs), 8.00 (4H, bs), 8.35 (2H, s), 8.45 (1H, s), 8.47 (1H, s), 8.668 (2H, s), 8.672 (2H, s), 8.85 (8H) ppm; $^{13}\text{C-NMR}$ (75.5 MHz, CDCl_3 , **109**):

δ = 20.6 (CH_3), 21.1 (CH_3), 29.7 (CH_2), 31.70 (CH_3), 31.72 (CH_3), 31.8 (CH_3), 31.9 (CH_3), 32.0 (CH_3), 35.0 (16C), 40.0 (CH), 40.7 (CH), 41.2 (CH), 41.5 (CH), 42.0 (CH), 42.9 (CH), 44.0 (CH), 46.9 (CH_2), 48.3 (2CH), 50.4 (CH), 51.7 (CH), 52.0 (CH), 64.5 ($\text{CH}_2\text{-O}$), 65.8 ($\text{CH}_2\text{-O}$), 117.77 (C), 117.82 (C), 120.4 ($2\text{C}_{\text{p-ArH}}$), 120.5 ($2\text{C}_{\text{p-ArH}}$), 121.1 ($4\text{C}_{\text{p-ArH}}$), 122.8 (C), 122.9 (C), 127.9 ($4\text{C}_{\text{o-ArH}}$), 128.27 ($2\text{C}_{\text{o-ArH}}$), 128.30 ($2\text{C}_{\text{o-ArH}}$), 128.56 ($4\text{C}_{\text{o-ArH}}$), 128.62 ($4\text{C}_{\text{o-ArH}}$), 129.2 ($\text{C}_{\text{pyrrolicH}}$), 129.4 ($\text{C}_{\text{pyrrolicH}}$), 129.5 ($\text{C}_{\text{pyrrolicH}}$), 134.1 ($4\text{C}_{\text{quinoxalineH}}$), 137.9 (C), 139.4 (C), 139.46 (C), 139.50 (C), 139.6 (C), 139.68 (C), 139.74 (C), 140.3 (C), 140.4 (C), 140.5 (C), 140.6 (C), 140.9 (C), 145.2 (C), 145.4 (C), 148.7 ($\text{C}_{\text{Ar}}^{\text{tBu}}$), 148.8 ($\text{C}_{\text{Ar}}^{\text{tBu}}$),

153.5 (C), 153.8 (C), 154.77 (C), 154.81 (C), 157.2 (C), 158.5 (C), 164.0 (C), 164.1 (C), 170.6 (OAc), 171.2 (OAc) ppm.

D.2.4 Synthesis of the Kinked Bis-Porphyrin Donor

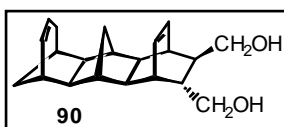
(1 α ,4 α ,4 α ,5 β ,5 α ,6 α ,10 α ,10 α ,11 β ,11 α)-1,4,4a,5,5a,6,10,10a,11,11a-Decahydro-1,4-ethano-5,11:6,10-dimethano-7H-cyclohepta[*b*]naphthalene-12,13-*trans*-dicarboxylate (60)



A solution of ketone **8** (4.05 g, 16.05 mmol) [D.1.4, page 173] and dimethyl fumarate (2.31 g, 16.05 mmol) in toluene (60 mL) was heated at reflux for 18 hours. The solvent was removed under reduced pressure to give the off-white product. Yield: 3.60 g (9.78 mmol, 60.9 %) ring-expanded 6B-ene-2B-ene-*trans*-diester **60**.

$^1\text{H-NMR}$ (300 MHz, CDCl_3): δ = 1.39 (2H, m), 1.43 (1H, m), 1.52 (1H, d, J = 11.3 Hz), 1.54 (1H), 1.62 (1H, m), 1.80 (2H, s), 1.84 (1H, bs), 1.91 (1H, bs), 1.96 (1H, bs), 2.19 (1H, d, J = 18.5 Hz), 2.28 (1H, bs), 2.36 (bs), 2.72 (1H, m), 3.07 (1H, m), 3.11 (2H, d, J = 5.1 Hz), 3.63 (3H, s), 3.73 (3H, s), 5.37 (1H, dt, J = 9.2, 3.1 Hz), 5.78 (1H, m), 6.05 (1H, m), 6.22 (1H, td, J = 14.4, 3.1 Hz) ppm.

(1 α ,4 α ,4 α ,5 β ,5 α ,6 α ,10 α ,10 α ,11 β ,11 α)-1,4,4a,5,5a,6,10,10a,11,11a-Decahydro-12,13-*trans*-bis(hydroxymethyl)-1,4-ethano-5,11:6,10-dimethano-7H-cyclohepta[*b*]naphthalene (90)

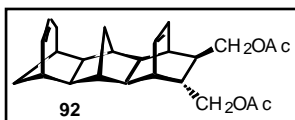


To an ice-cold suspension of LiAlH_4 (1.60 g, 42.5 mmol) in tetrahydrofuran (50 mL) was added dropwise a solution of ring-expanded 6B-ene-2B-ene-*trans*-diester **60** (5.40 g, 14.5 mmol) in tetrahydrofuran (50 mL) under an argon atmosphere. On completion of the addition (1 hour) the greyish mixture was heated at reflux for 24 hours, then cooled down to 0 °C and 1M K_2CO_3 (20 mL) was added dropwise to quench the reaction. The mixture was heated at reflux for further 30 minutes then filtered hot through a pad of filter aid, which was extracted with boiling diethyl ether (3 x 20 mL). The combined organic layers were washed with H_2O (2 x 30 mL). The combined aqueous layers were extracted with diethyl ether (4 x 30 mL) and the combined organic layers were washed with brine (30 mL) then dried over Na_2SO_4 . The

solvents were removed under reduced pressure to give the crude product as a white solid, which was used without further purification. Yield: 4.5 g (14.4 mmol, 99%) ring-expanded 6B-ene-2B-ene-*trans*-diol **90**. Melting point: 169-171 °C; *m/z*: 312.

¹H-NMR (300 MHz, CDCl₃): δ = 1.17 (1H, m), 1.39-1.57 (6H), 1.80 (1H, m), 1.87 (1H, m), 1.93 (1H, m), 2.18 (1H), 2.27 (1H), 2.40 (4H, bs), 2.53 (1H, m), 2.59 (1H, m), 3.06 (1H, td, *J* = 4.7, 2.3 Hz), 3.49 (1H, m), 3.64 (2H, m), 5.37 (1H, dt, *J* = 8.6, 2.8 Hz), 5.78 (1H, t, *J* = 8.2 Hz), 5.95 (1H, m), 6.18 (1H, m) ppm; ¹³C-NMR (75.5 MHz, CDCl₃): δ = 30.3 (CH₂), 30.8 (CH₂), 36.7 (CH), 37.3, 37.4 (CH), 37.5, 37.6 (CH), 37.9 (CH₂), 38.0 (CH), 40.5, 41.0 (CH), 41.8, 42.4 (CH), 44.7, 44.8 (CH), 46.1, 46.2 (CH), 48.3, 48.4 (CH), 51.4, 51.5 (CH), 55.8, 56.0 (CH), 57.3, 57.5 (CH), 66.2 (CH₂OH), 67.3 (CH₂OH), 128.4 (=CH), 131.1, 131.4 (=CH), 133.1 (=CH), 134.8, 135.2 (=CH) ppm.

(1α,4α,4α,5β,5α,6α,10α,10α,11β,11α)-1,4,4a,5,5a,6,10,10a,11,11a-Decahydro-12,13-*trans*-bis(acetoxymethyl)-1,4-ethano-5,11:6,10-dimethano-7H-cyclohepta[*b*]naphthalene (92)



To a solution of ring-expanded 6B-ene-2B-ene-*trans*-diol **90** (4.50 g, 14.4 mmol) in pyridine (75 mL) was added acetic anhydride (4.43, 43.4 mmol, ~3 eq.). The slightly yellow solution was stirred at RT for 17 hours then poured onto a mixture of ice (100 g), 1M HCl (50 mL) and dichloromethane (50 mL). The aqueous layer was extracted with dichloromethane (4 x 50 mL). The combined organic layers were washed with 1 M HCl (3 x 50 mL) and NaHCO₃ (sat., 50ml) then dried over Na₂SO₄. The solvents were removed under reduced pressure and the resulting yellow oil was purified by column chromatography (light petroleum/ethyl acetate 3:1) to give the desired product as a colourless oil. Yield: 5.085 g (12.82 mmol, 89.1 %) ring-expanded 6B-ene-2B-ene-*trans*-diacetate **92**.

¹H-NMR (300 MHz, CDCl₃): δ = 1.12 (1H, m), 1.35-1.44 (4H), 1.47 (1H, bs), 1.53 (1H, d, *J* = 7.2 Hz), 1.65 (1H, d, *J* = 6.2 Hz), 1.81 (2H), 1.88 (2H), 1.93 (2H), 2.03 (3H, s), 2.06 (3H, s), 2.27 (1H), 2.34 (1H), 2.60 (2H), 3.69 (2H, m), 4.05 (1H, m), 4.16 (1H, m), 5.37 (1H, dt, *J* = 9.2, 3.1 Hz), 5.77 (1H, t, *J* = 8.2 Hz), 5.99 (1H, m), 6.20 (1H, m) ppm; ¹³C-NMR (75.5 MHz, CDCl₃): δ = 21.0 (2CH₃), 30.2 (CH₂), 30.8 (CH₂), 35.4, 35.6 (CH), 36.5, 36.6 (CH), 36.7 (CH), 37.9 (CH₂), 38.0 (CH), 40.3, 40.9 (CH), 41.2, 41.3 (CH), 41.7, 42.3 (CH), 42.8, 42.9 (CH), 43.8, 43.9 (CH), 50.9, 51.1 (CH), 55.8, 56.0 (CH), 57.3, 57.5 (CH), 65.8, 65.9

(CH₂O), 67.5 (CH₂O), 128.4 (=CH), 131.2, 131.6 (=CH), 133.1 (=CH), 134.9, 135.3 (=CH), 171.1 (2OAc) ppm.

(1 α ,4 α ,4 α ,5 β ,5 α ,6 α ,10 α ,10 α ,11 β ,11 α)-1,4,4a,5,5a,6,8,9,10,10a,11,11a-Dodecahydro-12,13-*trans*-bis(acetoxymethyl)-1,4-ethano-8,9-*cis*-dihydroxy-5,11:6,10-dimethano-7H-cyclohepta[*b*]naphthalene-2,3-dione (96) and **(1 α ,4 α ,4 α ,5 β ,5 α ,6 α ,10 α ,10 α ,11 β ,11 α)-1,4,4a,5,5a,6,8,10,10a,11,11a-Undecahydro-12,13-*trans*-bis(acetoxymethyl)-1,4-ethano-8-hydroxy-5,11:6,10-dimethano-7H-cyclohepta[*b*]naphthalene-2,3,9-trione (97)**

To a suspension of ring-expanded 6B-ene-2B-ene-*trans*-diacetate **92** (950 mg, 2.396 mmol) and 4-methyl-N-morpholine-N-oxide (2.82 g, 24.072 mmol, ~10 eq.) in 1,4-dioxane (25 mL) was added OsO₄ (12 mg, 2 %) in *tert*-butanol (2.4 mL). The golden-brown solution was stirred at RT for 50 days then Na₂S₂O₅ (1g) in H₂O (10ml) and dichloromethane (10 mL) were added. The mixture was stirred for another 30 minutes, then the layers were separated and the aqueous phase was extracted with dichloromethane (5 x 10 mL). The combined bright yellow organic layers were washed with H₂O (3 x 20 mL) and brine (30 mL) then dried over Na₂SO₄. The solvents were removed under reduced pressure to give the yellow crude residue, which was then partly dissolved in chloroform. The insoluble residue was recrystallised from tetrahydrofuran to give 215 mg (0.467 mmol, 19.5 %) pale yellow ring-expanded 6B-diol-2B-dione-*trans*-diacetate **96**. The soluble products were purified by column chromatography (light petroleum/ethyl acetate 1:4). Yield: 200 mg (0.436 mmol, 18.2 %) ring-expanded 6B-ketol-2B-dione-*trans*-diacetate **97** as a bright yellow solid.



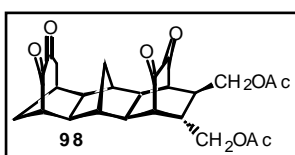
¹³C-NMR (75.5 MHz, CDCl₃, **96**): δ = 20.4 (CH₃), 20.8 (CH₃), 29.9 (CH₂), 31.2 (CH₂), 32.5 (CH₂), 36.0 (CH), 39.2, 39.6 (CH), 39.8 (CH), 40.3, 40.7 (CH), 42.0, 42.2 (CH), 47.9 (CH), 49.5 (CH), 49.8 (CH), 50.8, 50.9 (CH), 51.4, 51.5 (CH), 52.3, 52.4 (CH), 54.8, 55.0 (CH), 58.4 (CHOH), 64.0 (CH₂O), 65.2 (CH₂O), 68.1 (CHOH), 170.5 (OAc), 170.8 (OAc), 196.7 (C=O), 196.9 (C=O) ppm.



¹H-NMR (300 MHz, CDCl₃, **97**): δ = 0.23 (1H, d, *J* = 14.3 Hz), 0.63 (1H, d, *J* = 14.3 Hz), 1.48 (1H, d, *J* = 11.8 Hz), 1.83 (1H, d, *J* = 7.7 Hz), 1.85 (1H), 1.89 (1H, d, *J* = 9.0 Hz), 1.93 (3H, s), 1.96 (1H, d, *J* = 9.1 Hz), 2.05 (1H), 2.07 (3H, s), 2.08-2.18 (4H), 2.18 (1H, d, *J* = 9.2 Hz), 2.24 (1H, d, *J* = 11.8 Hz), 2.52 (1H, bs), 2.82 (1H, bs), 2.87 (2H, m), 3.69 (1H, d, *J* = 7.1 Hz), 3.78 (1H, dd, *J* = 10.9, 4.8 Hz), 4.05 (1H, m), 4.18 (2H, d, *J* = 7.7 Hz) ppm; ¹³C-NMR (75.5 MHz,

CDCl₃, **97**): δ = 20.4 (CH₃), 20.8 (CH₃), 29.3 (CH₂), 31.5 (CH₂), 32.9 (CH₂), 34.0 (CH), 35.9, 36.0 (CH), 39.1, 39.5 (CH), 39.7, 40.1 (CH), 39.8 (CH), 41.2, 41.8 (CH), 48.7, 49.6 (CH), 49.4, 49.5 (CH), 51.0, 51.2 (CH), 51.9 (CH), 52.2, 52.4 (CH), 53.3, 53.4 (CH), 63.8 (CH₂O), 65.2 (CH₂O), 69.9 (CHOH), 170.5 (OAc), 170.8 (OAc), 196.6, 196.7, 196.8, 197.0 (2C=O), 212.46, 212.50 (C=O) ppm.

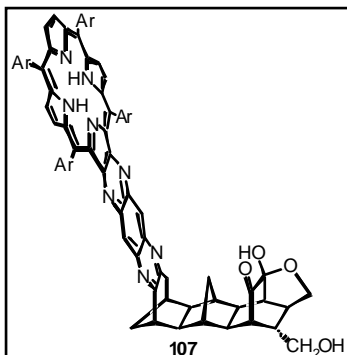
(1 α ,4 α ,4 α ,5 β ,5 α ,6 α ,10 α ,10 α ,11 β ,11 α)-1,4,4a,5,5a,6,10,10a,11,11a-Decahydro-12,13-*trans*-bis(acetoxymethyl)-1,4-ethano-5,11:6,10-dimethano-7H-cyclohepta[b]naphthalene-2,3,8,9-tetraone (98**)**



To an ice-cold solution of ring-expanded 6B-ketol-2B-dione-*trans*-diacetate **97** (160 mg, 0.35 mmol) and *p*-toluenesulfonic acid monohydrate (532 mg, 2.8 mmol, ~8 eq.) in dichloromethane (12 mL) was added portionwise 4-acetamido-TEMPO reagent (597 mg, 2.8 mmol, ~8 eq.) in dichloromethane (25 mL) in the dark. The orange solution was allowed to warm up to RT and stirred for 4 days in the dark. The orange mixture was filtered and ethanol (10 mL) was added to the filtrate to quench the reaction. To the yellow solution H₂O (10 mL) was added and the aqueous layer was extracted with dichloromethane (3 x 8 mL). The combined organic layers were washed with brine (20 mL) then dried over Na₂SO₄. The solvents were removed under reduced pressure to give a yellow solid (375 mg) which was purified by column chromatography (dichloromethane/methanol 20:1). Yield: 91.1 mg (0.200 mmol, 57.0 %) ring-expanded 6B-dione-2B-dione-*trans*-diacetate **98**.

¹H-NMR (300 MHz, CDCl₃): δ = 0.59 (1H, d, *J* = 15.8 Hz), 1.71 (1H, m), 1.83 (1H, bs), 1.87 (1H, bs), 1.92 (3H, s), 1.93 (1H), 2.00 (1H), 2.05 (3H, s), 2.06 (2H, s), 2.09 (1H, bs), 2.13 (1H, bs), 2.27 (1H, m), 2.40 (1H, m), 2.53 (1H, m), 2.87 (2H, bs), 3.09 (1H, dd, *J* = 8.8, 3.5 Hz), 3.77 (1H, m), 4.04 (1H, m), 4.18 (2H, m) ppm; ¹³C-NMR (75.5 MHz, CDCl₃): δ = 20.3 (CH₃), 20.7 (CH₃), 29.7 (CH₂), 32.5 (CH₂), 33.8 (CH₂), 36.0 (CH), 39.8 (CH), 39.9, 40.1 (CH), 40.7, 41.2 (CH), 42.0, 42.2 (CH), 48.7 (CH), 49.4, 49.5 (CH), 50.9 (CH), 51.5 (CH), 52.1, 52.3 (CH), 52.5 (CH), 54.2, 54.3 (CH), 63.7 (CH₂O), 65.1 (CH₂O), 170.4 (OAc), 170.7 (OAc), 196.1 (C=O), 196.3 (C=O), 196.7 (C=O), 203.3 (C=O) ppm

Ring-expanded 6B-porphyrin-hemi-acetal (**107**)



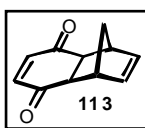
A solution of ring-expanded 6B-dione-2B-dione-*trans*-diacetate **98** and 'diaminoporphyrin' **153** (66 mg, 0.0552 mmol) in deoxygenated pyridine (1 mL) was reacted at 80 °C and 15 kbar for 3 days. The solvent was removed under an argon stream. The crude product was dried under high vacuum and purified by column chromatography (dichloromethane/methanol 20:1). Yield: 21 mg (0.0137 mmol, 24.8 %) ring-expanded 6B-porphyrin-hemi-

acetal **107**. Melting point: >300 °C.

$^1\text{H-NMR}$ (300 MHz, CDCl_3): δ = -2.34 (2H, s), -0.01 (1H, dd, J = 12.1, 7.0 Hz), 1.08 (1H, t, J = 13.0 Hz), 1.53 (18H), 1.55 (36H), 1.56 (9H), 1.58 (9H), 2.01 (2H), 2.14 (2H), 2.27 (2H, d, J = 11.0 Hz), 2.35 (2H, d, J = 11.0 Hz), 2.44 (2H, d, J = 9.0 Hz), 2.59 (2H, d, J = 13.0 Hz), 2.67 (2H, m), 3.40 (1H, d, J = 7.0 Hz), 3.59 (1H, bs), 3.79 (2H, d, J = 5.0 Hz), 4.01 (2H, m), 7.82 (2H, s), 8.00 (6H, m), 8.11 (4H, bs), 8.60 (1H, s), 8.62 (1H, s), 8.78 (2H, s), 9.01 (4H, m) ppm; $^{13}\text{C-NMR}$ (75.5 MHz, CDCl_3): δ = 32.1 (12 CH_3), 32.3 (12 CH_3), 32.7 (CH_2), 32.9 (CH_2), 35.5 (8C), 37.9 (CH_2), 39.5, 40.0 (CH), 40.4, 40.8 (CH), 41.4, 41.9 (CH), 42.0 (CH), 42.3, 42.5 (CH), 44.2, 44.4 (CH), 45.1 (CH), 45.4 (CH), 48.6, 48.7 (CH), 54.3, 54.5 (CH), 55.0, 55.2 (CH), 63.8 (CH_2OH), 73.1 (CH_2O), 100.6 (O-C-OH), 118.5 (2C), 121.0 (2 $\text{C}_{\text{p-ArH}}$), 121.6 (2 $\text{C}_{\text{p-ArH}}$), 123.6 (2C), 128.5 ($\text{C}_{\text{O-ArH}}$), 128.6 ($\text{C}_{\text{O-ArH}}$), 129.0 (4 $\text{C}_{\text{O-ArH}}$), 129.2 (2 $\text{C}_{\text{O-ArH}}$), 129.7 (2 $\text{C}_{\text{pyrrolicH}}$), 129.9 (4 $\text{C}_{\text{pyrrolicH}}$), 133.3 ($\text{C}_{\text{quinoxalineH}}$), 134.7 ($\text{C}_{\text{quinoxalineH}}$), 138.6 (2C), 140.2 (C), 140.4 (2C), 140.5 (C), 140.9 (C), 141.1 (C), 141.3 (2C), 142.1 (C), 145.3 (C), 145.7 (C), 146.5 (C), 149.3 (4 $\text{C}_{\text{Ar}}^{\text{tBu}}$), 149.4 (2 $\text{C}_{\text{Ar}}^{\text{tBu}}$), 149.7 (2 $\text{C}_{\text{Ar}}^{\text{tBu}}$), 154.8 (C), 155.1 (C), 155.5 (2C), 159.7 (2C), 209.4, 210.1 (C=O) ppm.

D.2.5 Synthesis of the Bridge

1,4,4a,8a-tetrahydro-1,4-methanonaphthalene-5,8-dione (**113**)^{184,185,193}

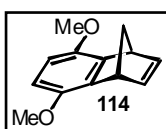


To an ice-cold suspension of benzoquinone (59.0 g, 546 mmol) in absolute ethanol (225 mL) was added freshly cracked cyclopentadiene (45.0 mL, 36.1 g, 546 mmol) over a period of 30 minutes. The orange-yellow solution was stirred at

0 °C for 2 hours. The resulting precipitate was collected by filtration and washed with ice-cold absolute ethanol and dried under high vacuum. Yield: 58.04 g (333 mmol, 61 %) slightly yellow **113**. Melting point: 76-77 °C (lit.:¹⁸⁵ 77-78 °C).

¹H-NMR (300 MHz, CDCl₃): δ = 1.42 (1H, d, J = 8.6 Hz), 1.54 (1H, dt, J = 8.6 Hz, J = 1.8 Hz), 3.21 (2H, t, J = 3.9 Hz), 3.53 (2H, t, J = 3.9 Hz), 6.05 (2H, d, J = 1.8 Hz), 6.56 (2H, s) ppm.

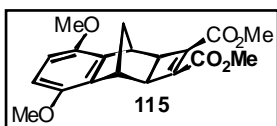
1,4-dihydro-5,8-dimethoxy-1,4-methanonaphthalene (**114**)^{186,187,193}



Over a period of 1 hour a solution of **113** (41.1 g, 237 mmol) in tetrahydrofuran (150 mL) was added dropwise to an ice-cold suspension of NaH (13.6 g, 566 mmol) in tetrahydrofuran (200 mL) under an argon atmosphere. The mixture was stirred for 16 hours at RT then cooled to 0 °C and methyl iodide (71 g, 31.3 mL, 500 mmol) in tetrahydrofuran (30 mL) was added dropwise. The dark brown solution was stirred for a further 18 hours at RT then quenched with H₂O (100 mL). The aqueous phase was extracted with diethyl ether (4 x 100 mL) and the combined organic solutions were washed with H₂O (3 x 100 mL) and brine (100 mL) then dried over Na₂SO₄. The solvents were removed under reduced pressure to give a brown oil, which was crystallised from ethanol. Yield: 24.7 g (122 mmol, 51.5 %) **114**. Melting point: 77-79 °C (lit.:¹⁸⁶ 78.5 - 79 °C).

¹H-NMR (300 MHz, CDCl₃): δ = 2.20 (1H, d, J = 7.2 Hz), 2.22 (1H, d, J = 2.2 Hz), 3.78 (6H, s), 4.16 (2H, s), 6.51 (2H, s), 6.83 (2H, bs) ppm.

Dimethyl (2 α ,3 β ,8 β ,8 α)-2a,3,8,8a-Tetrahydro-3,8-methano-4,7-dimethoxycyclobuta-[b]naphthalene-1,2-dicarboxylate (**115**)^{43,148,183,193}



A solution of **114** (26.1 g, 129 mmol), DMAD (18.3 g, 129 mmol) and RuH₂CO(PPh₃)₃¹⁹¹ (400 mg, 0.43 mmol, ~0.3%) in toluene (100 mL) was heated at reflux for 24 hours under an argon atmosphere. Toluene was removed until the solution became cloudy. Ethanol (120 mL) was added and a white precipitate appeared. After cooling to 0 °C the white precipitate was filtered off, washed with ice-cold ethanol and dried under high vacuum. Yield: 20 g (58 mmol, 45 %) **115**. Melting point: 171-172 °C (lit.:¹⁸³ 172-173 °C); m/z : 344.

¹H-NMR (300 MHz, CDCl₃): δ = 1.71 (1H, d, J = 10.4 Hz), 1.76 (1H, d, J = 10.4 Hz), 2.76 (2H, s), 3.50 (2H, s), 3.79 (6H, s), 3.83 (6H, s), 6.62 (2H, s) ppm.

Dimethyl (1 α ,4 α ,4 $\alpha\beta$,4 $\beta\alpha$,4 $c\beta$,5 α ,10 α ,10 $\alpha\beta$,10 $\beta\alpha$,10 $c\beta$)-1,4,4 α ,4 β ,4 c ,5,10,10 α ,10 β ,10 c -Decahydro-1,4:5,10-dimethano-6,9-dimethoxybenzo[3',4']cyclobuta[1',2':3,4]cyclobuta[1,2-*b*]naphthalene-4 β ,10 β -dicarboxylate (116**)**^{43,148,169,183,193}



A solution of **115** (20 g, 58 mmol) in quadricyclane (10.7 g, 116 mmol) and toluene (20 mL) was heated at reflux for 6 days under an argon atmosphere. The brownish mixture was allowed to cool down to RT.

The white solid formed was filtered off and washed with ice-cold acetone (3 x 20 mL) then dried under high vacuum. Yield: 18.9 g (43.3 mmol, 74.6 %) **116**. Melting point: 195-197 °C (lit.:¹⁸³ 196-197 °C); m/z: 436.

¹H-NMR (300 MHz, CDCl₃): δ = 1.14 (1H, d, J = 9.8 Hz), 1.51 (2H, dt, J = 10.3, 1.8 Hz), 1.88 (1H, d, J = 9.8 Hz), 2.07 (2H, s), 2.29 (2H, s), 2.33 (1H, d, J = 10.3 Hz), 2.85 (2H, t, J = 1.8 Hz), 3.56 (2H, bs), 3.76 (6H, s), 3.78 (6H, s), 6.04 (2H, t, J = 1.8 Hz), 6.60 (2H, s) ppm; ¹³C-NMR (75.5 MHz, CDCl₃): δ = 40.8 (CH₂), 42.07 (2CH), 42.13 (CH₂), 43.9 (2CH), 47.3 (2CH), 49.2 (2CH), 51.1 (2OCH₃), 52.8 (2C), 56.0 (2OCH₃), 110.0 (2C_{Ar}H), 135.8 (2C_{Ar}), 136.3 (2=CH), 148.0 (2C_{Ar}OMe), 170.6 (2MeO-C=O) ppm.

(1 α ,4 α ,4 $\alpha\beta$,4 $\beta\alpha$,4 $c\beta$,5 α ,10 α ,10 $\alpha\beta$,10 $\beta\alpha$,10 $c\beta$)-1,4,4 α ,4 β ,4 c ,5,10,10 α ,10 β ,10 c -Decahydro-1,4:5,10-dimethano-6,9-dimethoxybenzo-4 β ,10 β -bishydroxymethyl[3',4']cyclobuta[1',2':3,4]-cyclobuta[1,2-*b*]naphthalene (117**)**^{43,148,169,183}



A solution of **116** (40.2 g, 92.1 mmol) in tetrahydrofuran (600 mL) was added dropwise to an ice-cold suspension of LiAlH₄ (8.75 g, 230 mmol) in tetrahydrofuran (200 mL) under an argon atmosphere. On

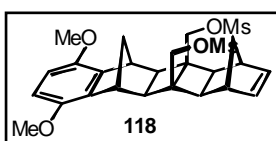
completion of the addition (3 hours) the brownish mixture was heated at reflux for 20 hours then 1M K₂CO₃ (50 mL) was added at 0 °C to quench the reaction. The resulting mixture was heated at reflux for 15 minutes and filtered hot through a pad of filter aid. The filter was extracted with boiling diethyl ether and the combined organic layers were washed with H₂O (300 mL) and brine (300 mL) then dried over Na₂SO₄. The solvents were removed under reduced pressure to give an off-white solid, which was dried under high vacuum. Yield: 30.6 g (80.4 mmol, 87.3 %) **117**. Melting point: 234-235 (dec.).

¹H-NMR (300 MHz, CDCl₃): δ = 1.30 (1H, d, J = 9.4 Hz), 1.47 (1H, d, J = 8.9 Hz), 1.66 (1H, d, J = 9.4 Hz), 1.82 (2H, s), 1.83 (1H, d, J = 8.9 Hz), 2.04 (2H, s), 2.94 (2H, s), 3.69 (2H, s), 3.72 (2H, s), 3.75 (2H, s), 3.77 (6H, s), 6.07 (2H, s), 6.60 (2H, s) ppm; ¹³C-NMR (75.5 MHz, CDCl₃): δ = 40.7 (2CH), 42.3 (2CH), 42.3 (CH₂), 43.4 (CH₂), 44.6 (2CH), 46.0 (2C), 46.7

(2CH), 56.1 (2OCH₃), 57.3 (CH₂OH), 109.3 (2C_{Ar}H), 136.6 (2C_{Ar}), 136.7 (2=CH), 147.9 (2C_{Ar}OMe) ppm.

IR (Nujol) ν_{\max} : 3250 cm⁻¹.

(1 α ,4 α ,4 $\alpha\beta$,4 $\beta\alpha$,4 $c\beta$,5 α ,10 α ,10 $\alpha\beta$,10 $\beta\alpha$,10 $c\beta$)-1,4,4a,4b,4c,5,10,10a,10b,10c-Decahydro-1,4:5,10-dimethano-6,9-dimethoxybenzo-4b,10b-bismesyloxymethyl[3',4']cyclobuta-[1',2':3,4]-cyclobuta[1,2-*b*]naphthalene (118)^{43,148,169,183}

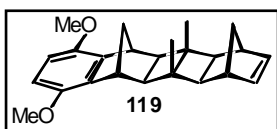


To a solution of **117** (12.1 g, 31.8 mmol) in anhydrous pyridine (100 mL) was added dropwise methanesulfonyl chloride (15 mL, 194 mmol) under an argon atmosphere at -7 °C. On completion of the addition the mixture was stoppered and placed in the freezer for 70 hours, then poured onto ice (200 g). The resulting brown suspension was extracted with dichloromethane (3 x 100 mL) and the combined organic solutions were washed with 1M HCl (3 x 100 mL) and NaHCO₃ (sat., 50 mL) then dried over Na₂SO₄. The solvent was removed under reduced pressure to yield crude **118** (15.1 g) as a brownish solid, which was used without further purification.

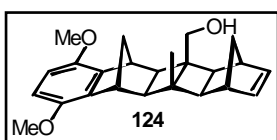
(1 α ,4 α ,4 $\alpha\beta$,4 $\beta\alpha$,4 $c\beta$,5 α ,10 α ,10 $\alpha\beta$,10 $\beta\alpha$,10 $c\beta$)-1,4,4a,4b,4c,5,10,10a,10b,10c-Decahydro-1,4:5,10-dimethano-6,9-dimethoxybenzo-4b,10b-dimethyl[3',4']cyclobuta[1',2':3,4]-cyclobuta[1,2-*b*]naphthalene (119)^{148,169,183} and **(1 α ,4 α ,4 $\alpha\beta$,4 $\beta\alpha$,4 $c\beta$,5 α ,10 α ,10 $\alpha\beta$,10 $\beta\alpha$,10 $c\beta$)-6,9-Dimethoxy-1,4,4a,4c,5,10,10a,10c-octahydro-4b-hydroxymethyl-10b-methyl-1,4:5,10-dimethano-benzo[3',4']cyclobuta-[1',2':3,4]cyclobuta[1,2-*b*]naphthalene (124)**

A solution of crude **118** (14 g, < 26.8 mmol) in tetrahydrofuran (100 mL) was added dropwise to an ice-cold suspension of LiAlH₄ (2.9 g, 76 mmol) in tetrahydrofuran (100 mL) under an argon atmosphere. On completion of the addition the greyish mixture was heated at reflux for 3 days then cooled in an ice bath and 1M K₂CO₃ (50 mL) was added to quench the reaction. The resulting mixture was heated at reflux for 10 minutes and filtered hot through a pad of filter aid. The filter pad was extracted with boiling diethyl ether (3 x 50 mL). The yellow organic solutions were combined, washed with brine (2 x 50 mL) and dried over Na₂SO₄. The solvents were removed under reduced pressure to give a yellow-orange oil/solid, which was crystallised from dichloromethane/methanol. Solvents were removed from the mother-liquor and the residue was purified by column chromatography (light petroleum/ethyl acetate 3:1) to give further pure product. Yield (**119**): 4.9 g (14 mmol, 52.2 %) **119**. Melting point: 174-175

°C (lit.:¹⁸³ 178-179 °C). Yield (**124**): 260 mg (0.710 mmol, 2.7 %) of the corresponding mono-methyl-mono-hydroxymethyl compound **124**.



¹H-NMR (300 MHz, CDCl₃, **119**): δ = 0.90 (6H, s), 1.18 (1H, d, J = 8.8 Hz), 1.38 (1H, d, J = 8.8 Hz), 1.58 (1H, d, J = 9.2 Hz), 1.68 (2H, s), 1.77 (1H, d, J = 9.2 Hz), 1.91 (2H, s), 2.74 (2H, t, J = 1.8 Hz), 3.51 (2H, s), 3.79 (6H, s), 5.98 (2H, t, 1.8 Hz), 6.58 (2H, s) ppm; ¹³C-NMR (75.5 MHz, CDCl₃, **119**): δ = 9.2 (2CH₃), 40.4 (2CH), 41.6 (2C), 41.9 (2CH), 42.5 (CH₂), 43.6 (CH₂), 47.8 (2CH), 50.0 (2CH), 56.2 (2OCH₃), 109.1 (2C_{Ar}H), 136.0 (2=CH), 137.0 (2C_{Ar}), 147.9 (2C_{Ar}) ppm.



¹H-NMR (300 MHz, CDCl₃, **124**): δ = 0.95 (3H, s), 1.26 (1H, d, J = 8.2 Hz), 1.42 (1H, d, J = 9.2 Hz), 1.63 (1H, d, J = 9.2 Hz), 1.71 (1H, d, J = 6.2 Hz), 1.78 (1H, s), 1.81 (1H, d, J = 4.1 Hz), 1.93 (1H, d, J = 6.2 Hz), 2.01 (1H, d, J = 5.1 Hz), 2.78 (1H, bs), 2.92 (1H, bs), 3.55 (1H, s), 3.67 (2H, s), 3.71 (1H, s), 3.77 (3H, s), 3.79 (3H, s), 6.03 (2H, m), 6.59 (2H, s) ppm; ¹³C-NMR (75.5 MHz, CDCl₃, **124**): δ = 9.9 (CH₃), 40.4 (CH), 40.7 (CH), 41.9 (CH), 42.2 (C), 42.2 (CH), 42.4 (CH₂), 43.6 (CH₂), 44.7 (CH), 45.6 (C), 46.8 (CH), 47.5 (CH), 49.6 (CH), 56.1 (2OCH₃), 57.3 (CH₂OH), 109.2 (=CH), 109.3 (2C_{Ar}H), 136.0 (2=CH), 136.7 (2C_{Ar}), 148.0 (2C_{Ar}OMe) ppm.

Dimethyl (1 α ,4 α ,4 α ,4 β ,4 α ,4 β ,5 α ,10 α ,10 α ,10 β ,10 β ,10 β)-6,9-dimethoxy-1,2,3,4,4a,4c,5,10,10a,10c-decahydro-4b,10b-dimethyl-1,4:5,10-dimethano-benzo[3',4']cyclobuta[1',2':3,4]cyclobuta[1,2-b]-naphthalene-2-*exo*,3-*exo*-dicarboxylate (120**)**^{169,193,197}



To a suspension of **119** (2.85 g, 8.2 mmol), anhydrous copper(II) chloride (4.32 g, 32 mmol) and anhydrous sodium acetate (2.64 g, 32 mmol) in anhydrous methanol (270 mL) and tetrahydrofuran (210 mL) was added 10% Pd/C catalyst (30 mg). The flask was flushed with carbon monoxide and two balloons of carbon monoxide were attached to the three neck flask. The mixture was stirred at RT for 97 hours then H₂O (300 mL) and dichloromethane (300 mL) were added and the resulting suspension was filtered through a pad of filter aid. The blue aqueous layer plus H₂O (200 mL) were extracted with dichloromethane (3 x 150 mL). The combined organic solutions were reduced to 250 mL, washed with H₂O (150 mL) and NaHCO₃ (sat., 3 x 200 mL) then dried over Na₂SO₄. The solvent was removed under reduced pressure and the off-white solid was recrystallised from dichloromethane/methanol. Yield:

2.4 g (5.2 mmol, 63.4 %) **120** as a white solid. Melting point: 248-250 °C (lit.:¹⁹⁷ 248-250 °C; m/z: 466.

¹H-NMR (300 MHz, CDCl₃): δ = 0.89 (6H, s), 1.52 (1H, d, *J* = 11.3 Hz), 1.66 (1H, d, *J* = 11.3 Hz), 1.71 (1H, d, *J* = 10.8 Hz), 1.96 (4H, s), 2.09 (1H, d, *J* = 10.8 Hz), 2.48 (2H, s), 2.55 (2H, d, *J* = 2.1 Hz), 3.48 (2H, s), 3.61 (6H, s, MeO-C=O), 3.78 (6H, s, OCH₃), 6.59 (2H, s) ppm; ¹³C-NMR (75.5 MHz, CDCl₃): δ = 9.4 (2CH₃), 32.5 (CH₂), 40.1 (2C), 40.2 (2CH), 43.4 (CH₂), 43.7 (2CH), 49.7 (2CH), 49.8 (2CH), 51.4 (2CH), 51.5 (C(=O)OCH₃), 56.0 (2OCH₃), 109.0 (2C_{Ar}H), 136.5 (2C_{Ar}), 147.7 (2C_{Ar}), 173.5 (2C=O) ppm.

2-exo,3-exo-Di(hydroxymethyl)-(1α,4α,4aβ,4bα,4cβ,5α,10α,10aβ,10bα,10cβ)-1,2,3,4,4a,4c,5,10,10a,10c-decahydro-6,9-dimethoxy-4b,10b-dimethyl-1,4:5,10-dimethanobenzo-[1,2-*b*]-naphthalene (121**)^{169,193}**

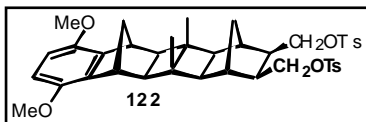


To an ice-cold suspension of LiAlH₄ (590 mg, 15.6 mmol, ~3 eq.) in tetrahydrofuran (60 mL) was added dropwise **120** (2.40 g, 5.1 mmol) in tetrahydrofuran (100 mL) under an argon atmosphere. On completion of the addition (2 hours) the mixture was heated to reflux for 15 hours. The slightly yellow mixture was cooled to 0 °C and 1M K₂CO₃ (80 mL) was added to quench the reaction. After refluxing for 15 minutes the mixture was filtered hot through a pad of filter aid, which was extracted with boiling diethyl ether. The aqueous layer was extracted with diethyl ether (2 x 80 mL) and the combined organic layers were washed with H₂O (80 mL) then dried over Na₂SO₄. The solvents were removed under reduced pressure and the white solid was dried under high vacuum. Yield: 2.02 g (4.98 mmol, 97.6 %) **121**. Melting point: 102-105 °C; m/z: 410.

¹H-NMR (300 MHz, CDCl₃): δ = 0.83 (6 H, s), 1.33 (1H, d, *J* = 11.3 Hz), 1.45 (1H, d, *J* = 11.3 Hz), 1.52 (1H, d, *J* = 9.2), 1.70 (1H, d, *J* = 9.2 Hz), 1.84 (2H, q, *J* = 3.3 Hz), 1.91 (2H, s), 1.97 (2H, s), 2.02 (2H, s), 3.12 (2H, bs, OH), 3.47 (2H, s), 3.65 (2H, dd, *J* = 11.3, 4.1 Hz), 3.74 (1H), 3.77 (1H), 3.79 (6H, s), 6.59 (2H, s) ppm; ¹³C-NMR (75.5 MHz, CDCl₃): δ = 9.3 (2CH₃), 31.7 (CH₂), 40.1 (2CH), 40.6 (2CH), 43.4 (CH₂), 47.6 (2CH), 49.7 (2CH), 52.2 (2CH), 56.1 (2OCH₃), 63.5 (2CH₂O), 109.0 (2C_{Ar}H), 136.6 (2C_{Ar}), 147.8 (2C_{Ar}OMe) ppm.

IR (Nujol) ν_{max}: 3325 cm⁻¹.

2-exo,3-exo-Bis(*p*-tosyloxymethyl)-(1 α ,4 α ,4 β ,4 β ,4 β ,5 α ,10 α ,10 α ,10 β ,10 β ,10 β)-6,9-dimethoxy-4b,10b-dimethyl-1,2,3,4,4a,4c,5,10,10a,10c-decahydro-1,4:5,10-dimethanobenzo[3',4']cyclobuta[1,2-b]-naphthalene (122**)^{169,193}**



At -23 °C *p*-toluenesulfonyl chloride (4.90 g, 24.6 mmol) in anhydrous pyridine (4 mL) was added dropwise to a solution of **121** (2.00 g, 4.92 mmol) in anhydrous pyridine (60 mL) under an argon atmosphere. On completion of the addition the flask was stoppered and placed in the freezer for 6 days, after which the orange solution was poured onto ice (50 g). The resulting suspension was extracted with dichloromethane (4 x 80 mL). The combined organic layers were washed with 1M HCl (3 x 100 mL), NaHCO₃ (sat., 2 x 50 mL) and H₂O (80 mL) then dried over Na₂SO₄. The solvent was removed under reduced pressure and the red oil was purified by column chromatography (light petroleum/ethyl acetate 2:1). Yield: 2.32 g (3.25 mmol, 66.0 %) **122** as a white solid.

¹H-NMR (300 MHz, CDCl₃): δ = 0.77 (6H, s), 1.23 (1H, d, J = 11.3 Hz), 1.39 (1H, d, J = 11.3 Hz), 1.50 (1H, d, J = 9.2 Hz), 1.65 (1H, d, J = 9.2 Hz), 1.73 (2H, bs), 1.82 (2H, s), 1.88 (2H, s), 1.94 (2H, s), 2.46 (6H, s), 3.44 (2H, s), 3.77 (6H, s), 3.82 (2H, m), 3.92 (2H, dd, J = 9.5 Hz), 6.58 (2H, s), 7.35 (4H, d, J = 8.2 Hz), 7.75 (4H, d, J = 8.2 Hz) ppm.

¹³C-NMR (75.5 MHz, CDCl₃): δ = 9.3 (2CH₃), 21.7 (2CH₃), 30.3 (CH₂), 39.5 (2CH), 40.1 (2CH), 43.2 (2C), 43.3 (2CH), 43.5 (CH₂), 49.7 (2CH), 51.6 (2CH), 56.1 (2OCH₃), 69.5 (2CH₂), 109.1 (2C_{Ar}H), 127.9 (2C_{tos}H), 130.0 (2C_{tos}H), 131.6 (2C_{tos}), 136.5 (2C_{Ar}), 145.0 (2C_{tos}), 147.8 (2C_{Ar}) ppm.

2,3-Dimethyliden-(1 α ,4 α ,4 β ,4 β ,4 β ,5 α ,10 α ,10 α ,10 β ,10 β ,10 β)-6,9-dimethoxy-4b,10b-dimethyl-1,2,3,4,4a,4c,5,10,10a,10c-decahydro-1,4:5,10-dimethano-benzo[3',4']cyclobuta[1,2-*b*]-naphthalene (123**)^{169,193}**

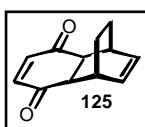


To a colourless solution of **122** (2.32 g, 3.23 mmol) in anhydrous DMF (150 mL) was added potassium *tert*-butoxide (1.08 g, 9.6 mmol) in small portions at -5 to -10 °C under an argon atmosphere. On completion of the addition the green solution was stirred at RT for 18 hours, after which the then orange solution was poured onto ice (400 g) to form a yellow suspension, which was extracted with diethyl ether (5 x 200 mL). The combined organic layers were washed with H₂O (4 x 150 mL) and brine (150 mL), then dried over Na₂SO₄. The solvents were removed under reduced pressure to result in a slightly yellow solid, which was purified by column chromatography (light petroleum/ethyl acetate 4:1). Yield: 1.09 g (2.91 mmol, 90.1 %) **123** as a white solid. Melting point: 159-161 °C (lit.:¹⁹³ 160-162 °C).

¹H-NMR (300 MHz, CDCl₃): δ = 0.90 (6H, s), 1.44 (1H, d, J = 9.4 Hz), 1.53 (1H, d, J = 9.4 Hz), 1.73 (2H, d, J = 10.2 Hz), 1.98 (2H, s), 2.07 (2H, s), 2.72 (2H, s), 3.49 (2H, s), 3.78 (6H, s), 4.73 (2H, s), 5.06 (2H, s), 6.58 (2H, s) ppm; ¹³C-NMR (75.5 MHz, CDCl₃): δ = 9.3 (2CH₃), 35.0 (CH₂), 40.2 (2CH), 43.5 (2CH), 43.8 (CH₂), 43.8 (2C), 45.5 (2CH), 49.7 (2CH), 50.7 (2CH), 56.0 (2OCH₃), 99.9 (2=CH₂), 109.0 (2C_{Ar}H), 136.6 (2C_{Ar}), 147.8 (2C_{Ar}), 151.5 (2=C) ppm.

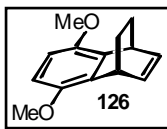
D.2.6 Synthesis of the Acceptor Precursor

1,4,4a,8a-Tetrahydro-1,4-ethanonaphthalene-5,8-dione (125**)^{184,193}**



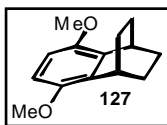
To a suspension of benzoquinone (30.0 g, 278 mmol) in absolute ethanol (125 mL) was added dropwise 1,3-cyclohexadiene (26.5 mL, 278 mmol) in absolute ethanol (10 mL) at 60 °C. On completion of the addition (1 hour) the orange solution was heated at 60 °C for further 90 minutes then cooled down to 0 °C. The slightly yellow precipitate was filtered off, washed with ice-cold absolute ethanol and dried under high vacuum. Yield: 30.0 g (159 mmol, 57%) **125** as a white solid. Melting point: 97-98 °C (lit.:¹⁸⁴ 98 °C).

¹H-NMR (300 MHz, CDCl₃): δ = 1.37 (2H, d, J = 7.2 Hz), 1.71 (2H, d, J = 7.2), 2.98 (2H, s), 3.21 (2H, bs), 6.21 (2H, t, J = 3.4 Hz), 6.63 (2H, s) ppm.

1,4-Dihydro-5,8-dimethoxy-1,4-ethanonaphthalene (126)¹⁹³

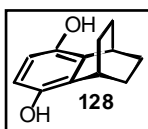
A solution of **125** (19.2 g, 102 mmol) in tetrahydrofuran (80 mL) was added dropwise to an ice-cold suspension of NaH (13 g, 542 mmol) in tetrahydrofuran (100 mL) under an argon atmosphere. On completion of the addition (2.5 hours) the mixture was allowed to warm up to RT and stirred for 15 hours. The brownish suspension was cooled to 0 °C again and methyl iodide (30 mL, 68.1 g, 480 mmol) was added dropwise. The mixture was stirred at RT for 64 hours, then H₂O (60 mL) was added to quench the reaction. The resulting yellow-orange solution was extracted with diethyl ether (3 x 100 mL) and the combined organic solutions were washed with H₂O (2 x 80 mL) and brine (80 mL) then dried over Na₂SO₄. The solvents were removed under reduced pressure to yield a yellow-orange oil. Yield: 14.2 g (64.8 mmol, 63.5 %) **126**.

¹H-NMR (300 MHz, CDCl₃): δ = 1.41 (2H, d, *J* = 7.2 Hz), 1.53 (2H, d, *J* = 7.2 Hz), 3.80 (6H, s), 4.43 (2H, bs), 6.51 (2H, t, *J* = 3.6 Hz), 6.61 (2H, s) ppm.

1,2,3,4-Tetrahydro-5,8-dimethoxy-1,4-ethanonaphthalene (127)¹⁹³

A suspension of **126** (14.02 g, 64.8 mmol) and 10 % Pd/C catalyst (0.3 g) in ethyl acetate (150 mL) was stirred vigorously under an hydrogen atmosphere for 10 hours. The mixture was filtered through a pad of filter aid and the solvent was removed from the filtrate under reduced pressure to give an orange oil. Yield: 13.40 g (61.3 mmol, 94.6 %) **127**.

¹H-NMR (300 MHz, CDCl₃): δ = 1.33 (4H, d, *J* = 7.2 Hz), 1.74 (4H, d, *J* = 7.2 Hz), 3.46 (2H, bs), 3.80 (6H, s), 6.69 (2H, s) ppm.

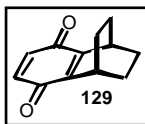
1,2,3,4-Tetrahydro-5,8-dihydroxy-1,4-ethanonaphthalene (128)^{193,201}

To an ice-cold solution of **127** (13.40 g, 61.3 mmol) in anhydrous dichloromethane (80 mL) was added dropwise boron tribromide (20 mL, 52.8 g, 210 mmol) in anhydrous dichloromethane (150 mL) under an argon atmosphere.

On completion of the addition (2 hours) the brown mixture was stirred at RT for 20 hours. At 0 °C H₂O (100 mL) was added dropwise to quench the reaction. The suspension was heated at reflux for 30 minutes then cooled to 0 °C and filtered. The slightly brown precipitate was washed with ice-cold dichloromethane and dried under high vacuum. Yield: 8.85 g (46.5 mmol, 88 %) **128** as a white solid. Melting point: 204-207 °C (lit.:²⁰¹ 204-206 °C).

$^1\text{H-NMR}$ (300 MHz, CDCl_3): δ = 1.25 (4H, d, J = 7.2 Hz), 1.71 (4H, d, J = 7.2 Hz), 3.40 (2H, bs), 5.74 (2OH, b), 6.50 (2H, s) ppm.

1,2,3,4-Tetrahydro-1,4-ethanonaphthalene-5,8-dione (**129**)^{193,200}



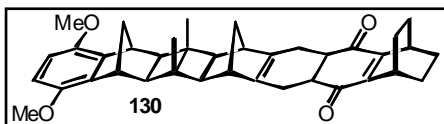
To a suspension of **128** (2.23 g, 11.7 mmol) in diethyl ether (100 mL) were added $\text{MgSO}_4 \cdot 3 \text{H}_2\text{O}$ (15.88 g, 91 mmol) and silver(I) oxide (11.31 g, 49 mmol).

The mixture was stirred at RT for 3.5 hours in the dark under an argon atmosphere and then filtered through a pad of filter aid. The solvent was removed under reduced pressure to give a bright yellow solid. Yield: 1.75 g (9.3 mmol, 79 %) **129**. Melting point: 85-87 °C (lit.:²⁰⁰ 85.7-87 °C).

$^1\text{H-NMR}$ (300 MHz, CDCl_3): δ = 1.29 (4H, d, J = 7.2 Hz), 1.73 (4H, d, J = 7.2 Hz), 3.32 (2H, bs), 6.68 (2H, s) ppm.

D.2.7 Assembling the Triads

(1 α ,4 α ,7 α ,7 $\alpha\beta$,7 $\beta\alpha$,7 $\beta\beta$,8 α ,13 α ,13 $\alpha\beta$,13 $\beta\beta$,14 α)-1,2,3,4,6,7,7 α ,7 β ,8,13,13 α ,13 β ,14,15-Octadecahydro-1,4-ethano-7,14:8,15-dimethano-9,12-dimethoxy-7 β ,13 β -dimethylnaphtho[2'',3'':3',4']cyclobuta[1',2':3,4]cyclobuta[1,2-*b*]naphthacene-5,16-dione (**130**)^{169,193}

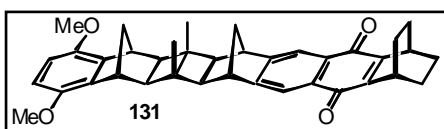


Method 1: A gold coloured solution of **123** (196 mg, 0.52 mmol) and **129** (112 mg, 0.59 mmol) in toluene (5 mL) was heated at reflux for 53 hours. The solvent was removed and the crude product was purified by column chromatography (light petroleum/ethyl acetate 4:1). Yield 144 mg (0.26 mmol, 50%) **130**.

Method 2:²⁰⁶ A solution of **123** (1.62 g, 4.33 mmol) and **129** (825 mg, 4.38 mmol) in anhydrous 5M ethereal LiClO_4 (50 mL) was stirred for 3 days in the dark at RT under an argon atmosphere. The yellow solution was poured onto ice (100 mL) and extracted with dichloromethane (5 x 75 mL). The combined organic extracts were washed with H_2O (5 x 75 mL) and dried over Na_2SO_4 . The solvents were removed under reduced pressure to give the crude product as an orange/yellow solid, which was purified by column chromatography (light petroleum/ethyl acetate 4:1). Yield: 4.42 g (4.3 mmol, 98 %) **130**.

^1H -NMR (300 MHz, CDCl_3): δ = 0.87 (6H, s), 1.25 (4H, d, J = 7.2 Hz), 1.36 (1H, d, J = 9.2 Hz), 1.56 (4H, s), 1.73 (6H), 1.92 (2H, s), 2.03 (2H, dd, J = 15.4, 7.2 Hz), 2.52 (1H, d, J = 5.1 Hz), 2.56 (2H, s), 3.01 (2H, t, J = 5.1 Hz), 3.25 (2H, s), 3.51 (2H, s), 3.78 (6H, s), 6.58 (2H, s) ppm; ^{13}C -NMR (75.5 MHz, CDCl_3): δ = 9.3 (2 CH_3), 23.9 (2 CH_2), 25.1 (2 CH_2), 25.2 (2 CH_2), 27.0 (2CH), 40.4 (2CH), 40.7 (CH_2), 42.7 (2C), 43.4 (CH_2), 45.3 (2CH), 47.9 (2CH), 50.1 (2CH), 50.2 (2CH), 56.2 (2 OCH_3), 109.1 (2 C_{ArH}), 136.9 (2 C_{Ar}), 137.7 (2=C), 147.9 (2 C_{ArOMe}), 151.0 (2=C), 197.3 (2C=O) ppm.

(1 α ,4 α ,7 α ,7 $\alpha\beta$,7 $\beta\alpha$,7 $\beta\beta$,8 α ,13 α ,13 $\alpha\beta$,13 $\beta\beta$,14 α)-1,2,3,4,7,7a,7c,8,13,13a,13c,14-Hexadecahydro-1,4-ethano-7,14:8,15-dimethano-9,12-dimethoxy-7b,13b-dimethyl-naphtho[2'',3'':3',4']cyclobuta[1',2':3,4]cyclobuta[1,2-*b*]naphthacene-5,16-dione (**131**)^{169,193}



To a colourless solution of **130** (500 mg, 0.89 mmol) in 1,4-dioxane (15 mL) and chloroform (7 mL) was added 2,3-dichloro-5,6-dicyano-1,4-benzoquinone (DDQ,

500 mg, 2.20 mmol). The dark brown solution was heated at reflux for 48 hours. A white precipitate was formed and the solution turned orange-brown. The precipitate was filtered off and extracted with chloroform. The solvents were removed under reduced pressure to give a dark solid (990 mg) which was purified by column chromatography (light petroleum/ethyl acetate 3:1). Yield: 326 mg (0.58 mmol, 66%) yellow **131**. Melting point: 284-286 °C (lit.:¹⁹³ 284-285 °C).

^1H -NMR (300 MHz, CDCl_3): δ = 1.02 (6H, s), 1.33 (4H), 1.56 (1H, d, J = 7.2 Hz), 1.62 (1H, d, J = 7.2 Hz), 1.73 (2H, s), 1.76 (2H, bs), 1.79 (1H, d, J = 7.2 Hz), 1.89 (2H, s), 1.90 (2H, s), 1.91 (1H, d, J = 7.2 Hz), 3.40 (2H, s), 3.50 (2H, s), 3.54 (2H, s), 3.77 (6H, s), 6.57 (2H, s), 7.83 (2H, s) ppm; ^{13}C -NMR (75.5 MHz, CDCl_3): δ = 9.4 (2 CH_3), 25.3 (2 CH_2), 26.7 (2CH), 26.9 (2 CH_2), 40.3 (2CH), 42.6 (2C), 43.5 (CH_2), 43.6 (CH_2), 44.0 (2CH), 49.4 (2CH), 49.7 (2CH), 56.0 (2 OCH_3), 109.0 (2 C_{ArH}), 118.3 (2 C_{ArH}), 131.2 (C_{nq}), 136.5 (2 C_{Ar}), 147.8 (2 C_{ArOMe}), 149.9 (2 C_{nq}), 153.6 (2 C_{nq}), 182.4 (2 $\text{C}_{\text{nq}}=\text{O}$) ppm.

IR (Nujol) ν_{max} : 1675, 1610 cm^{-1} .

(1 α ,4 α ,7 α ,7 β ,7 $\beta\alpha$,7 $\beta\beta$,8 α ,13 α ,13 β ,13 $\beta\alpha$,13 $\beta\beta$,14 α)-1,2,3,4,7,7a,7c,8,13,13a,13c,14-Dodecahydro-5,16-bis(dicyanomethylidene)-7,14:8,13-dimethano-7b,13b-dimethyl-9,12-dimethoxy-1,4-ethano-naphtho[2'',3'':3',4']cyclobuta[1',2':3,4]cyclobuta[1,2-b]naphthacene (**132**)¹⁶⁹



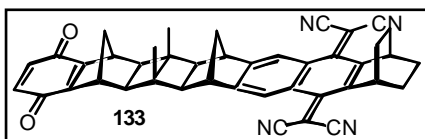
To a solution of **131** (320 mg, 0.57 mmol) in anhydrous dichloromethane (20 mL) under an argon atmosphere was added malononitrile (189 mg, 2.86 mmol, ~5 eq.) in anhydrous dichloromethane (6 mL). After 5 minutes pyridine (230 mg, 0.24 mL, ~5 eq.) in anhydrous dichloromethane (6 mL) was added and the resulting yellow solution was heated at reflux. To the refluxing solution titanium(IV) chloride (280 mg, 0.16 mL, 1.43 mmol, ~2.5 eq.) was added in two portions. The solution turned dark immediately. The reaction was followed by TLC and after 15 minutes the mixture was allowed to cool down to RT and H₂O (20 mL) was added dropwise to quench the reaction. The aqueous layer was extracted with dichloromethane (4 x 40 mL). The combined red organic extracts were washed with 1M HCl (3 x 50 mL) and NaHCO₃ (sat., 2 x 50 mL) then dried over Na₂SO₄. The solvent was removed under reduced pressure to give a red-brown solid (434 mg), which was purified by column chromatography (light petroleum/ethyl acetate 2:1). Yield: 328 mg (0.50 mmol, 87.9 %) yellow-orange **132**. Melting point: >300 °C.

¹H-NMR (300 MHz, CDCl₃): δ = 1.02 (6H, s), 1.47 (2H, d, J = 7.2 Hz), 1.55 (2H), 1.60 (1H), 1.76 (2H), 1.82 (2H), 1.86 (2H), 1.88 (2H, s), 1.89 (2H, s), 1.95 (1H, d, J = 10.3), 3.45 (2H, s), 3.54 (2H, s), 3.76 (6H, s), 3.77 (2H, s), 6.55 (2H, s), 7.99 (2H, s) ppm.; ¹³C-NMR (75.5 MHz, CDCl₃): δ = 9.3 (2CH₃), 25.0 (2CH₂), 25.1 (2CH₂), 32.5 (2CH), 40.3 (2CH), 42.5 (2C), 43.2 (CH₂), 43.3 (CH₂), 44.2 (2CH), 49.5 (2CH), 49.9 (2CH), 56.2 (2OCH₃), 80.3 (2C(CN₂)), 109.2 (2C_{Ar}H), 113.5 (2CN), 114.1 (2CN), 120.0 (2C_{tcnq}H), 127.5 (2C_{tcnq}), 136.4 (2C_{Ar}), 146.0 (2C_{tcnq}), 147.8 (2C_{Ar}OMe), 152.3 (2C_{tcnq}), 158.0 (2C_{tcnq}=C(CN)₂) ppm.

IR (Nujol) ν_{\max} : 2225 cm⁻¹.

UV-Vis (CH₃CN) λ_{\max} (log ϵ): 388 (4.21), 296 (3.99), 208 (4.52) nm.

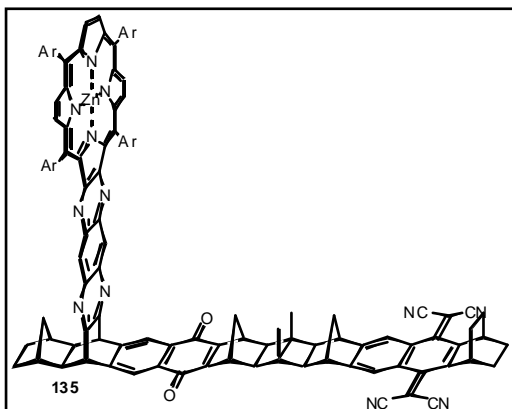
(1 α ,4 α ,7 α ,7 β ,7 $\beta\alpha$,7 β ,8 α ,13 α ,13 β ,13 $\beta\alpha$,13 β ,14 α)-1,2,3,4,7,7a,7c,8,13,13a,13c,14-Dodecahydro-5,16-bis(dicyanomethylidene)-1,4-ethano-7,14:8,13-dimethano-7b,13b-dimethyl-9,12-naphthoquino[2'',3'':3',4']cyclobuta[1',2':3,4]cyclobuta[1,2-b]naphthacene (**133**)¹⁶⁹



A suspension of **132** (70 mg, 0.107 mmol) and freshly made Ag₂O (250 mg, 1.07 mmol, ~10 eq.) in tetrahydrofuran (5 mL) was strongly stirred under an argon atmosphere. Over a period of 15 minutes 6M HNO₃ (5 mL) was added in the dark. The yellow solution was filtered through a pad of filter aid, which was extracted with dichloromethane (2 x 5 mL). To the filtrate H₂O (5 mL) was added, layers were separated and the yellow organic solution was washed with NaHCO₃ (sat., 2 x 20 mL) then dried over Na₂SO₄. Solvents were removed under reduced pressure to yield an orange oil (122 mg), which was purified by column chromatography (light petroleum/ethyl acetate 2:1). Yield: 46 mg (0.074 mmol, 68.8 %) yellow **133**. Melting point: >175 °C (dec.).

¹H-NMR (300 MHz, CDCl₃): δ = 1.00 (6H, s), 1.42 (2H, d, J = 4.6 Hz), 1.52 (2H, d, J = 9.7 Hz), 1.59 (2H, d, J = 7.9 Hz), 1.66 (2H, d, J = 9.7 Hz), 1.82 (4H), 1.89 (2H, s), 1.92 (2H, s), 3.46 (2H, s), 3.49 (2H, s), 3.78 (2H, s), 6.53 (2H, s), 8.01 (2H, s) ppm; ¹³C-NMR (75.5 MHz, CDCl₃): δ = 9.2 (2CH₃), 25.0 (2CH₂), 25.1 (2CH₂), 32.5 (2CH), 41.1 (2CH), 41.4 (CH₂), 42.7 (2C), 43.0 (CH₂), 44.2 (2CH), 48.6 (2CH), 49.5 (2CH), 80.5 (2C(CN)₂), 113.5 (2CN), 114.0 (2CN), 120.1 (2C_{tenq}H), 127.7 (2C_{tenq}), 136.1 (2C_{Ar}H), 146.7 (2C_{tenq}), 151.5 (2C_{Ar}), 151.9 (2C_{tenq}), 157.9 (2C_{tenq}=C(CN)₂), 183.8 (2C_{Ar}=O) ppm.

2B-Porphyrin-NQ-TCNQ (**135**)



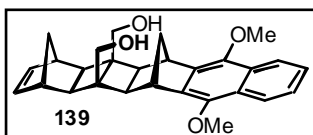
A solution of **112** (36 mg, 0.025 mmol) and **133** (20 mg, 0.032 mmol) in deoxygenated toluene (0.5 mL) was heated at 80 °C for three days in the dark under an argon atmosphere. The solvent was removed under reduced pressure and the dark, slightly greyish residue was dried under high vacuum. Without further purification the residue containing **134** was dissolved in dichloromethane (1 mL) and 1,4-dioxane (0.2 mL) and 2,3-dichloro-5,6-dicyano-1,4-benzoquinone (DDQ) (12 mg, 0.056 mmol, ~2 eq.) was added. After stirring for 5 hours at RT in the dark and

under an inert atmosphere the solvents were removed and the crude products were purified by column chromatography (chloroform). Yield: 13 mg (0.006 mmol, 25.1 %) **135-syn** and **135-anti** of unsatisfying purity. Further column chromatography and size-exclusion chromatography was applied in an attempt to separate the *syn* from the *anti*-isomer as well as the mixture of both from other unknown impurities.

^1H -NMR (300 MHz, CDCl_3 , in parts): δ = -0.45 (1H, d, J = 11.7 Hz), 0.53 (1H, d, J = 9.4 Hz), 1.01 (6H, s),... 1.54 (72H),... 1.92 (2H, s), 1.95 (2H, s),... 3.42 (2H, s), 3.49 (2H, s),... 3.78 (2H, s), 7.78 (2H, bs), 7.89 (2H, bs), 7.97 (2H, bs), 8.00 (2H, bs), 8.02 (1H, s), 8.03 (1H, s), 8.07 (4H, bs), 8.62 (2H, s), 8.86 (2H, s), 8.94 (4H, dd, J = 14.3 Hz, 4.8 Hz) ppm; ^{13}C -NMR (75.5 MHz, CDCl_3): δ = 9.2 (2 CH_3), 25.1 (4 CH_2), 30.4 (2 CH_2), 34.6 (CH_2), 31.8 (18 CH_3), 32.0 (6 CH_3), 32.6 (2CH), 35.1 (8C), 39.1 (2CH), 41.2 (2CH), 41.4 (CH_2), 42.7 (2C), 43.2 (CH_2), 44.2 (2CH), 49.0 (2CH), 49.5 (4CH), 51.0 (2CH), 80.5 (2 $\text{C}(\text{CN})_2$), 113.5 (2CN), 114.1 (2CN), 118.8 (2C), 120.1 (2 $\text{C}_{\text{tcnq}}\text{H}$), 120.2 (2 $\text{C}_{\text{NQ}}\text{H}$), 120.3 (2 $\text{C}_{\text{p-Ar}}\text{H}$), 121.0 (2 $\text{C}_{\text{p-Ar}}\text{H}$), 125.2 (2C), 127.7 (2 C_{tcnq}), 128.4 (4 $\text{C}_{\text{o-Ar}}\text{H}$), 128.6 (4 $\text{C}_{\text{o-Ar}}\text{H}$), 129.3 (6 $\text{C}_{\text{pyrrolic}}\text{H}$), 131.6 (2C), 131.6 (2 C_{NQ}), 132.5 (2 $\text{C}_{\text{quinoxaline}}\text{H}$), 139.3(2C), 139.8 (2C), 141.4 (2C), 141.6 (2C), 141.7 (2C), 146.1 (2 C_{tcnq}), 148.7 (4 $\text{C}_{\text{Ar}}^{\text{tBu}}$), 148.8 (2 $\text{C}_{\text{Ar}}^{\text{tBu}}$), 149.1 (2 $\text{C}_{\text{Ar}}^{\text{tBu}}$), 150.0 (2C), 151.3 (2 C_{NQ}), 151.9 (2 C_{tcnq}), 152.0 (2 C_{NQ}), 152.1 (2C), 153.1 (2C), 157.8 (2C), 157.9 (2 $\text{C}_{\text{tcnq}}=\text{C}(\text{CN})_2$) ppm.

D.3 SYNTHESIS OF THE ALL-*TRANS* RING-EXPANDED DYAD

(1 α ,4 α ,4a β ,4b α ,4c β ,5 α ,12 α ,12a β ,12b α ,12c β)-1,4,4a,4c,5,12,12a,12c-octahydro-4b,12b-bis(hydroxymethyl)-1,4:5,12-dimethano-6,11-dimethoxybenzo[3',4']cyclobuta[1',2':3,4]cyclobuta[1,2-*b*]anthracene (139)^{43,118,148,170,183,192,193}

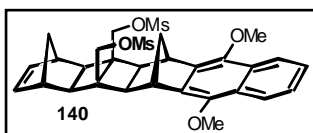


To an ice-cold slurry solution of LiAlH₄ (1.72 g, 45.3 mmol, ~2.2 eq.) in tetrahydrofuran (250 mL) was added dropwise **138** (10.0 g, 20.55 mmol) in tetrahydrofuran (150 mL) under an argon

atmosphere. On completion of the addition the grey/brownish mixture was heated at reflux overnight, then cooled to 0 °C, after which 1M K₂CO₃ (50 mL) was added to quench the reaction. The mixture was heated at reflux for 15 minutes then filtered hot through a pad of filter aid, which was extracted with boiling diethyl ether (3 x 50 mL). The organic layer was washed with H₂O (3 x 100 mL), the combined aqueous layers were extracted with diethyl ether (150 mL). The combined organic layers were washed with brine (2 x 100 mL), dried over Na₂SO₄ and the solvents were removed under reduced pressure to yield the crude product as an off-white solid, which was further dried under high vacuum. Yield: 8.66 g (20.1 mmol, 97.9 %) **139**. Melting point: 222-224 °C (dec.).

¹H-NMR (300 MHz, CDCl₃): δ = 1.32 (1H, d, J = 9.2 Hz), 1.47 (1H, d, J = 9.2 Hz), 1.81 (1H, d, J = 10.3 Hz), 1.87 (2H, s), 2.06 (1H, d, J = 10.3 Hz), 2.27 (2H, s), 2.95 (2H, s), 3.77 (4H, quart., J = 9.9 Hz), 3.91 (2H, s), 4.00 (6H, s), 6.08 (2H, s), 7.44 (2H, dd, J = 6.2, 3.1 Hz), 8.08 (2H, dd, J = 6.2, 3.1 Hz) ppm.

(1 α ,4 α ,4a β ,4b α ,4c β ,5 α ,12 α ,12a β ,12b α ,12c β)-1,4,4a,4c,5,12,12a,12c-octahydro-4b,12b-bis(mesyloxymethyl)-1,4:5,12-dimethano-6,11-dimethoxybenzo[3',4']cyclobuta[1',2':3,4]cyclobuta[1,2-*b*]anthracene (140)^{43,118,148,170,183,192,193}



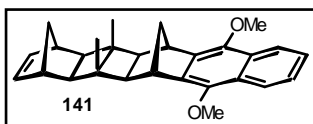
To a solution of **139** (8.40 g, 19.5 mmol) in pyridine (60 mL) was added dropwise methanesulfonyl chloride (6.70 g, 58.5 mmol, ~3 eq.) at -10 °C under an argon atmosphere. On completion of the

addition the mixture was stoppered and placed in the freezer for 3 days, after which it was poured onto ice (150 g). The mixture was extracted with dichloromethane (4 x 100 mL) and the combined organic layers were washed with 1M HCl (3 x 150 mL), NaHCO₃ (sat., 150 mL) and brine (200 mL). The brown/yellow solution was dried over Na₂SO₄ and solvents were removed under reduced pressure. The white, slightly brownish crude product was dried under

high vacuum and used without further purification in the next step. Yield: 8.66 g (14.76 mmol, 75.7 %) crude **140**. Melting point: 90 °C (dec.).

$^1\text{H-NMR}$ (300 MHz, CDCl_3): δ = 1.38 (1H, d, J = 6.2 Hz), 1.84 (1H, d, J = 5.2 Hz), 1.87 (2H, s), 1.94 (1H, d, J = 6.2 Hz), 2.27 (2H, s), 2.33 (1H, d, J = 5.2 Hz), 3.06 (2H, s), 3.13 (6H, s), 3.69 (4H, quart., J = 10.6 Hz), 4.01 (2H, s), 4.03 (6H, s), 6.11 (2H, s), 7.45 (2H, dd, J = 6.2, 3.1 Hz), 8.10 (2H, dd, J = 6.2, 3.1 Hz) ppm.

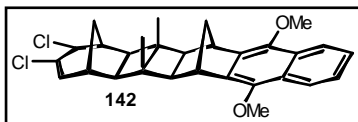
(1 α ,4 α ,4 $\alpha\beta$,4 $\beta\alpha$,4 $\alpha\beta$,5 α ,12 α ,12 $\alpha\beta$,12 $\beta\alpha$,12 $\alpha\beta$)-1,4,4a,4c,5,12,12a,12c-octahydro-1,4:5,12-dimethano-6,11-dimethoxybenzo-4b,12b-dimethyl[3',4']cyclobuta[1',2':3,4]cyclobuta[1,2-*b*]anthracene (141**)**^{43,118,148,170,183,192,193}



To an ice-cold slurry solution of LiAlH_4 (2.60 g, 68.5 mmol, ~ 4.6 eq.) in tetrahydrofuran (100 mL) was added dropwise crude **140** (8.60 g, 14.7 mmol) in tetrahydrofuran (50 mL) under an argon atmosphere. On completion of the addition the grey/brownish mixture was heated at reflux for 2 days, then cooled to 0 °C, after which 1M K_2CO_3 (30 mL) was added to quench the reaction. The mixture was heated at reflux for 15 minutes then filtered hot through a pad of filter aid, which was extracted with boiling diethyl ether (3 x 50 mL). The organic layer was washed with H_2O (2 x 100 mL), the combined aqueous layers were extracted with diethyl ether (2 x 100 mL). The combined organic layers were washed with brine (2 x 100 mL), dried over Na_2SO_4 and the solvents were removed under reduced pressure to yield the crude product as a brown oil which was purified by column chromatography (light petroleum/ethyl acetate 4:1) and recrystallised from dichloromethane/methanol. Yield: 3.0 g (7.53 mmol, 51.2 %) **141** as a white solid. Melting point: 157-159 °C (lit.:¹¹⁸ 158-159 °C).

$^1\text{H-NMR}$ (300 MHz, CDCl_3): δ = 0.97 (6H, s), 1.21 (1H, d, J = 8.8 Hz), 1.41 (1H, d, J = 8.8 Hz), 1.72 (1H, d, J = 9.7 Hz), 1.73 (2H, s), 1.96 (1H, d, J = 9.7 Hz), 2.13 (2H, s), 2.79 (2H, s), 3.70 (2H, s), 3.99 (6H, s), 5.99 (2H, s), 7.43 (2H, dd, J = 7.0, 3.5 Hz), 8.07 (2H, dd, J = 6.2, 3.5 Hz) ppm; $^{13}\text{C-NMR}$ (75.5 MHz, CDCl_3): δ = 9.5 (2 CH_3), 40.7 (2CH), 42.0 (2CH), 42.1 (CH_2), 42.4 (CH_2), 42.8 (2C), 48.0 (2CH), 50.8 (2CH), 61.8 (2 OCH_3), 122.0 (2 C_{ArH}), 125.0 (2 C_{ArH}), 127.8 (2 C_{Ar}), 135.4 (2 C_{Ar}), 136.0 (2=CH), 144.3 (2 $\text{C}_{\text{Ar-OMe}}$) ppm.

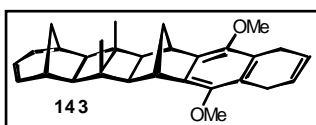
(1 α ,5 α ,5 β ,5 β ,5 β ,6 α ,13 α ,13 β ,13 β ,13 β)-1,5,5a,5c,6,13,13a,13c-octahydro-3,4-dichloro-1,5:6,13-dimethano-7,12-dimethoxybenzo-5b,13b-dimethyl[3',4']cyclobuta[1',2':3,4]cyclobuta[1,2-*b*]-4H-cyclohepta[*b*]naphthalene (142)



To an ice-cold suspension of **141** (980 mg, 2.46 mmol) and NaOMe (516 mg, 9.55 mmol, ~4 eq.) in double-bond (15 mL) and aromatics-free light petroleum was added dropwise Cl₃CCO₂Et (1.4 mL, 1.883 g, 9.84 mmol, ~4 eq.) under an argon atmosphere. On completion of the addition (4 hours) the off-white suspension was stirred for 3 days at RT. The suspension was then poured onto H₂O (75 mL) and extracted with chloroform (3 x 75 mL). The combined organic layers were washed with H₂O (100 mL) and brine (100 mL) then dried over Na₂SO₄. The solvents were removed under reduced pressure to give the brownish crude product, which was purified by column chromatography (light petroleum/ethyl acetate 6:1). Yield: 385 mg (0.80 mmol, 32.5 % (76.1 % based on recovered starting material)) **142** as a white solid. Starting material **141** (562 mg, 1.41 mmol, 57.3 %) was recovered.

¹H-NMR (300 MHz, CDCl₃): δ = 0.93 (3H, s), 0.94 (3H, s), 1.72 (1H), 1.73 (1H, d, J = 10.6 Hz), 1.97 (1H, d, J = 10.8 Hz), 2.09 (1H, d, J = 12.3 Hz), 2.18 (1H, d, J = 5.3 Hz), 2.24 (1H, d, J = 6.2 Hz), 2.28 (1H, d, J = 5.3 Hz), 2.45 (1H, d, J = 6.2 Hz), 2.58 (1H, quart., J = 1.2 Hz), 2.65 (1H, bs), 3.66 (1H, s), 3.69 (1H, s), 3.98 (3H, s), 3.99 (3H, s), 4.24 (1H, d, J = 2.6 Hz), 6.14 (1H, d, J = 7.9 Hz), 7.45 (2H, m), 8.09 (2H, m) ppm; ¹³C-NMR (75.5 MHz, CDCl₃): δ = 9.1 (CH₃), 9.3 (CH₃), 28.3 (CH₂), 37.0 (CH), 40.3 (CH), 40.5 (CH), 42.7 (CH₂), 42.8 (C), 43.6 (C), 44.9 (CH), 50.7 (CH), 50.8 (CH), 51.2 (CH), 55.5 (CH), 61.8 (2OCH₃), 65.7 (CH), 73.3 (CHCl), 122.0 (2C_{Ar}H), 125.1 (2C_{Ar}H), 127.8 (2C_{Ar}), 130.3 (=CCl), 134.8 (C_{Ar}), 134.9 (C_{Ar}), 135.5 (=CH), 144.3 (2C_{Ar}OMe) ppm.

(1 α ,5 α ,5 β ,5 β ,5 β ,6 α ,13 α ,13 β ,13 β ,13 β)-1,5,5a,5c,6,8,11,13,13a,13c-decahydro-1,5:6,13-dimethano-7,12-dimethoxybenzo-5b,13b-dimethyl[3',4']cyclobuta[1',2':3,4]cyclobuta[1,2-*b*]-4H-cyclohepta[*b*]naphthalene (143)

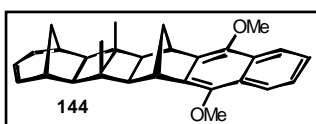


To a refluxing solution of **142** (80 mg, 0.1661 mmol) in tetrahydrofuran (5 mL) and *iso*-propanol (5 mL) was added sodium (90 mg, 3.9 mmol, ~22 eq.) in small pieces under an argon atmosphere. After 24 hours the brownish mixture was poured onto H₂O (25 mL) and extracted with diethyl ether (3 x 25 mL). The combined organic solutions were washed with H₂O (2 x 25 mL), 1M NaHCO₃ (25 mL) and brine (25 mL) then dried over Na₂SO₄. The solvent was

removed under reduced pressure to yield a brown oil, which was purified by column chromatography (light petroleum/ethyl acetate 6:1). Yield: 37 mg (0.0892 mmol, 53.7 %) **143**.

^1H -NMR (300 MHz, CDCl_3): δ = 0.84 (3H, s), 0.86 (3H, s), 1.59 (1H), 1.72 (4H), 1.84 (1H, m), 2.10 (1H, m), 2.24 (2H, m), 2.30 (1H, m), 2.46 (1H, d, J = 17.6 Hz), 2.53 (2H, d, J = 5.3 Hz), 2.73 (1H, m), 3.31 (2H, s), 3.46 (2H, t, J = 4.8 Hz), 3.79 (3H, s), 3.80 (3H, s), 5.31 (1H, d, J = 8.8 Hz), 5.88 (2H, 1H, bs) ppm; ^{13}C -NMR (75.5 MHz, CDCl_3): δ = 9.1 (CH_3), 9.3 (CH_3), 24.6 (2CH_2), 33.1 (CH_2), 35.1 (CH), 35.9 (CH), 36.6 (CH_2), 40.7 (CH), 40.8 (CH), 42.9 (C), 43.4 (CH_2), 43.6 (C), 50.74 (CH), 56.04 (CH), 59.1 (CH), 60.7 (OCH_3), 123.9 ($2=\text{CH}$), 124.6 ($=\text{CH}$), 125.1 (2C_{Ar}), 134.8 ($=\text{CH}$), 137.0 (2C_{Ar}), 147.1 ($2\text{C}_{\text{Ar}}\text{OMe}$) ppm.

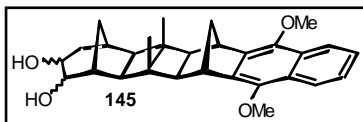
(1 α ,5 α ,5 $\alpha\beta$,5 $\beta\alpha$,5 $\text{c}\beta$,6 α ,13 α ,13 $\alpha\beta$,13 $\beta\alpha$,13 $\text{c}\beta$)-1,5,5 α ,5 c ,6,13,13 α ,13 c -octahydro-1,5:6,13-dimethano-7,12-dimethoxybenzo-5b,13b-dimethyl[3',4']cyclobuta[1',2':3,4]cyclobuta[1,2-*b*]-4H-cyclohepta[*b*]naphthalene (144**)**



To a solution of **143** (35 mg, 0.089 mmol) in dichloromethane (2 mL) was added 2,3-dichloro-5,6-dicyano-1,4-benzoquinone (DDQ) (44 mg, 0.194 mmol, ~2.2 eq.). The solution turns dark brown immediately and was stirred for 22 hours at RT. The brown solution was filtered and H_2O (20 mL) and dichloromethane (20 mL) were added to the filtrate. The aqueous layer was extracted with dichloromethane (3 x 15 mL), the combined organic layers were washed with H_2O (3 x 20 mL) and brine (20 mL) then dried over Na_2SO_4 . The solvent was removed under reduced pressure to give a dark brown solid, which was purified by column chromatography (light petroleum/ethyl acetate 6:1). Yield: 30 mg (0.073 mol, 81.7 %) yellow **144**.

^1H -NMR (300 MHz, CDCl_3): δ = 0.89 (3H, s), 0.91 (3H, s), 1.70 (1H, d, 9.6 Hz), 1.74 (2H, m), 1.82 (1H, d, J = 17.6 Hz), 1.99 (1H, d, J = 9.6 Hz), 2.22 (3H, m), 2.28 (1H, d, J = 6.2 Hz), 2.33 (1H, quart., J = 3.5 Hz), 2.47 (dq, J = 17.6, 2.2 Hz), 2.56 (1H, d, J = 5.3 Hz), 3.64 (1H, s), 3.66 (1H, s), 3.986 (3H, s), 3.992 (3H, s), 5.31 (1H, dt, J = 9.6, 3.1 Hz), 5.87 (1H, dd, J = 8.8, 6.1 Hz), 7.44 (2H, m), 8.08 (2H, m) ppm; ^{13}C -NMR (75.5 MHz, CDCl_3): δ = 9.2 (CH_3), 9.4 (CH_3), 33.2 (CH_2), 35.1 (CH), 35.9 (CH), 36.6 (CH_2), 40.4 (CH), 40.5 (CH), 42.9 (CH_2), 43.3 (C), 44.0 (C), 50.8 (CH), 50.9 (CH), 56.1 (CH), 59.2 (CH), 61.8 (2OCH_3), 122.0 ($2\text{C}_{\text{Ar}}\text{H}$), 124.6 ($=\text{CH}$), 124.9 ($2\text{C}_{\text{Ar}}\text{H}$), 127.8 (2C_{Ar}), 134.8 ($=\text{CH}$), 135.4 (2C_{Ar}), 144.2 ($2\text{C}_{\text{Ar}}\text{OMe}$) ppm.

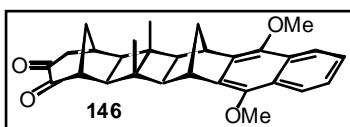
(1 α ,5 α ,5 β ,5 β ,5 β ,6 α ,13 α ,13 α ,13 β ,13 β ,13 β)-1,2,3,5,5a,5c,6,13,13a,13c-decahydro-2,3-dihydroxy-1,5:6,13-dimethano-7,12-dimethoxybenzo-5b,13b-dimethyl[3',4']cyclobuta[1',2':3,4]cyclobuta[1,2-*b*]-4H-cyclohepta[*b*]naphthalene (145)



To a slightly yellow solution of **144** (30 mg, 0.0727 mmol) and 4-methyl-N-morpholine-N-oxide (10 mg, 0.0853 mmol) in 1,4-dioxane (1 mL) was added OsO₄ (0.5 mg, ~2.5 %) in *tert*-butanol (0.1 mL). The yellow solution was stirred for 2 days at RT, after which dichloromethane (4 mL) and Na₂S₂O₅ (2.2 g) in H₂O (4 mL) were added. The mixture was stirred for 30 minutes than the aqueous layer was extracted with dichloromethane (3 x 10 mL). The combined organic layers were washed with H₂O (15 mL) and brine (15 mL) then dried over Na₂SO₄. The solvents were removed under reduced pressure to yield a yellow liquid, which was purified by column chromatography (light petroleum/ethyl acetate 1:2). Yield: 18 mg (0.0403 mol, 55.4 %) diol **145**.

¹H-NMR (300 MHz, CDCl₃): δ = 0.88 (6H, s), 1.44 (1H, m), 1.52 (1H, dd, *J* = 11.4, 2.6 Hz), 1.71 (2H, d, *J* = 9.7 Hz), 1.91 (1H, d, *J* = 12.3 Hz), 1.99 (1H, d, *J* = 9.7 Hz), 2.12 (1H, bs), 2.15 (1H, d, *J* = 5.3 Hz), 2.22 (1H, d, *J* = 5.3 Hz), 2.23 (2H, s), 2.37 (1H, t, *J* = 4.0 Hz), 3.49 (1H, m), 3.66 (2H, s), 3.71 (1H, t, *J* = 4.4 Hz), 3.99 (6H, s), 7.44 (2H, dd, *J* = 6.2, 3.5 Hz), 8.08 (2H, dd, *J* = 6.2, 3.5 Hz) ppm; ¹³C-NMR (75.5 MHz, CDCl₃): δ = 9.09 (CH₃), 9.31 (CH₃), 28.7 (CH₂), 34.2 (CH), 37.8 (CH₂), 40.5 (2CH), 41.7 (CH), 42.5 (C), 42.8 (CH₂), 42.9 (C), 49.7 (CH), 51.1 (2CH), 51.4 (CH), 61.9 (2OCH₃), 67.0 (CHOH), 72.5 (CHOH), 12.0 (2C_{Ar}H), 125.0 (2C_{Ar}H), 127.9 (2C_{Ar}), 135.2 (2C_{Ar}), 144.3 (2C_{Ar}OMe) ppm.

(1 α ,5 α ,5 β ,5 β ,5 β ,6 α ,13 α ,13 α ,13 β ,13 β ,13 β)-1,5,5a,5c,6,13,13a,13c-octahydro-1,5:6,13-dimethano-7,12-dimethoxybenzo-5b,13b-dimethyl[3',4']cyclobuta[1',2':3,4]cyclobuta[1,2-*b*]-4H-cyclohepta[*b*]naphthalene-2,3-dione (146)

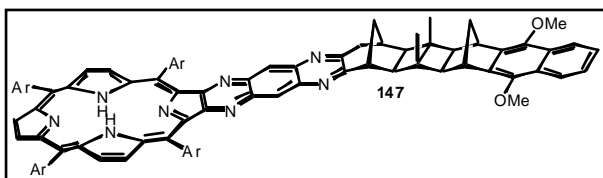


To an ice-cold solution of diol **145** (17 mg, 0.038 mmol) and *p*-toluenesulfonic acid monohydrate (36 mg, 0.19 mmol, ~5 eq.) in dichloromethane (1 mL) was added dropwise a solution of 4-acetamido TEMPO (40 mg, 0.19 mmol, ~5 eq.) in dichloromethane (1 mL) in the dark. On completion of the addition the orange solution was stirred at RT for 3 days, after which the yellow mixture was filtered through a pad of filter aid. Ethanol (5 mL) was added to the filtrate, followed by the addition of H₂O (10 mL). The aqueous layer was extracted with chloroform (3 x 10 mL) and the combined organic layers were washed with H₂O (20 mL) and

brine (20 mL) then dried over Na_2SO_4 . The solvents were removed under reduced pressure to yield an orange oil, which was purified by column chromatography (light petroleum/ethyl acetate 1:2). Yield: 7 mg (0.0158 mmol, 41.6 %) yellow dione **146**.

^1H -NMR (300 MHz, CDCl_3): δ = 0.96 (6H, s), 1.76 (2H, d, J = 9.7 Hz), 1.92 (1H, d, J = 12.3 Hz), 1.99 (1H, d, J = 9.7 Hz), 2.20 (1H, d, J = 12.3 Hz), 2.21 (2H, s), 2.26 (1H, d, J = 8.8 Hz), 2.43 (1H, d, J = 5.3 Hz), 2.55 (1H, s), 2.87 (1H, dd, J = 7.0, 4.3 Hz), 3.09 (1H, d, J = 4.3 Hz), 3.70 (2H, s), 3.97 (3H, s), 3.98 (3H, s), 7.44 (2H, dd, J = 6.2, 3.5 Hz), 8.07 (2H, m) ppm.

7,7a,7c,8,34,34a,34c,35-octahydro-7,35:8,34-dimethano-1,6-dimethoxybenzo-7b,34b-dimethyl-8b,32b-(pyrazino[2',3':6,7]quinoxalino[2,3-b](13,18,23,28-tetrakis-(3,5-di-*tert*-butylphenyl)porphyrino))-[3',4']cyclobuta[1',2':3,4]cyclobuta-[1,2-b]-4H-cyclohepta[b]naphthalene (147)



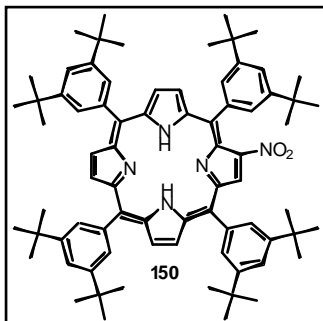
A solution of **145** (7 mg, 0.0158 mmol) and 'diaminoporphyrin' **153** (22 mg, 0.018 mmol) in de-oxygenated pyridine (1 mL) was reacted for 1 day at 80 °C and 5 kbar. The solvent

was removed under an argon stream and the crude product was dried under high vacuum, then purified by column chromatography (chloroform). Yield: 3 mg (0.0019 mmol, 11.6 %) all-*trans* ring-expanded 6B-porphyrin-DMN **147**. Melting point: >300 °C; M^+ (MALDI): 1602.

^1H -NMR (300 MHz, CDCl_3): δ = -2.38 (2H, s), 1.08 (3H, s), 1.18 (3H, s), 1.47, 1.51, 1.52, 1.53 (72H), 1.69 (1H, m), 1.76 (1H, d, J = 10.7 Hz), 2.07 (1H, d, J = 9.8 Hz), 2.14 (1H, d, J = 11.7 Hz), 2.27 (2H, s), 2.36 (1H, m), 2.54 (1H, d, J = 5.9 Hz), 2.70 (1H, d, J = 5.4 Hz), 2.78 (1H, bs), 3.48 (1H, dd, J = 18.6, 5.7 Hz), 3.62 (1H, d, J = 3.5 Hz), 3.72 (2H, s), 3.96 (3H, s), 3.99 (3H, s), 7.41 (2H, m), 7.79 (2H, bs), 7.90 (2H, quart., J = 2.6 Hz), 7.99 (2H, bs), 8.03 (2H, bs), 8.06 (2H, m), 8.09 (4H, quart., J = 2.6 Hz), 8.52 (1H, s), 8.58 (1H, s), 8.76 (2H, s), 8.95 (4H, bs) ppm.

D.4 SYNTHESIS OF THE 'DIAMINOPORPHYRIN'

2-Nitro-5,10,15,20-tetrakis-(3,5-di-*tert*-butylphenyl)porphyrin (**150**)^{215,217}



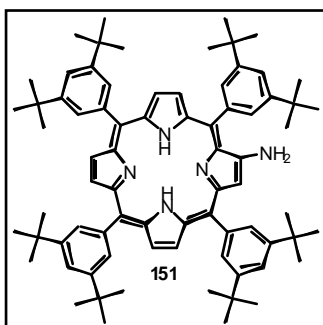
To a stirring solution of [5,10,15,20-tetrakis-(3,5-di-*tert*-butylphenyl)porphyrinato]copper(II) **148** (12.7 g, 11.29 mmol) in dichloromethane (400 mL) was added dropwise a solution of NO₂ in light petroleum (1 g in 375 mL). The reaction was monitored by TLC. On completion of the addition, argon was bubbled through the solution for 15 minutes, followed by washing with H₂O (300 mL).

The solvents were removed under reduced pressure to give crude [2-Nitro-5,10,15,20-tetrakis-(3,5-di-*tert*-butylphenyl)porphyrinato]copper(II) **149** as a blue/purple solid which was dissolved in dichloromethane (500 mL) before sulfuric acid (conc., 100 mL) was added with strong stirring. Again, the reaction was followed by TLC. After 6 minutes the green mixture was poured onto ice. The organic layer was subsequently washed with H₂O, NaHCO₃ (sat.), H₂O and brine. The crude product was purified by column chromatography (light petroleum/dichloromethane 3:1). Yield: 9.7 g (8.77 mmol, 77.7 %)

150. Melting point: >300 °C.

¹H-NMR (300 MHz, CDCl₃): δ = -2.52 (2H, s), 1.56 (72H, s), 7.80 (1H), 7.83 (2H), 7.85 (1H), 8.09 (6H, bs), 8.11 (2H, t, *J* = 2.3 Hz), 8.80 (2H, bs), 8.98 (3H, bs), 9.08 (1H), 9.10 (1H, d, *J* = 2.6 Hz) ppm; ¹³C-NMR (75.5 MHz, CDCl₃): δ = 31.6 (6CH₃), 31.8 (18CH₃), 35.0 (2C), 35.1 (6C), 121.2 (C), 121.3 (2C_{p-Ar}H), 121.7 (C), 121.8 (2C_{p-Ar}H), 121.9 (C), 123.9 (C), 128.4 (CH), 129.0 (CH), 129.6 (CH), 129.7 (6C_{o-Ar}H), 130.0 (CH), 130.7 (2C_{o-Ar}H), 132.0 (CH), 135.1 (CH), 135.2 (CH), 138.2 (C), 139.5 (2C), 140.3 (C), 140.5 (2C), 140.7 (2C), 140.9 (2C), 142.5 (C), 148.95 (4C_{Ar}^tBu), 149.00 (2C_{Ar}^tBu), 149.03 (2C_{Ar}^tBu), 153.3 (C), 156.5 (C) ppm.

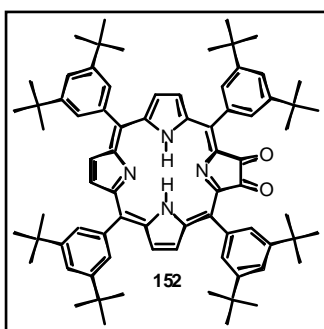
2-Amino-5,10,15,20-tetrakis-(3,5-di-*tert*-butylphenyl)porphyrin (**151**)²¹⁷



To a solution of **150** (9.5 g, 8.57 mmol) in dichloromethane (250 mL) was added SnCl₂ · 2 H₂O (8.0 g, 35.46 mmol) in HCl (conc., 100 mL). The mixture was stirred for 2 days at RT in the dark. The two layers were separated and the green organic phase was washed with H₂O, NaHCO₃ (sat.) [solution turns brown], H₂O and brine. The solvent was removed under reduced pressure to give

the crude purple product, which was purified by column chromatography (light petroleum/ethyl acetate 1:1). Yield: 7.0 g (6.49 mmol, 75.8 %) **151**. Melting point: >300 °C.

^1H -NMR (300 MHz, CDCl_3): δ = -2.60 (2H, bs), 1.49 (18H), 1.51 (18H), 1.53 (36H), 4.48 (2H, NH_2), 7.75 (2H), 7.86 (1H, t, J = 1.7 Hz), 8.01 (2H, d, J = 1.9 Hz), 8.02 (1H, bs), 8.04 (2H, d, J = 1.5 Hz), 8.09 (4H, t, J = 1.3 Hz), 8.57 (1H, d, J = 4.9 Hz), 8.64 (1H, bs), 8.71 (1H, d, J = 4.9 Hz), 8.84 (4H, m) ppm; ^{13}C -NMR (75.5 MHz, CDCl_3): δ = 31.71 (6 CH_3), 31.74 (6 CH_3), 31.78 (12 CH_3), 35.1 (8C), 117.7 (2C), 118.5 (2C), 120.4 (2C), 120.7 ($\text{C}_{\text{p-ArH}}$), 120.8 ($\text{C}_{\text{p-ArH}}$), 120.9 ($\text{C}_{\text{p-ArH}}$), 121.8 ($\text{C}_{\text{p-ArH}}$), 127.3 (2 $\text{C}_{\text{o-ArH}}$), 127.4 (4 $\text{C}_{\text{o-ArH}}$), 127.5 (2 $\text{C}_{\text{o-ArH}}$), 129.1 (2 $\text{C}_{\text{pyrrolicH}}$), 129.3 ($\text{C}_{\text{pyrrolicH}}$), 129.6 (2 $\text{C}_{\text{pyrrolicH}}$), 129.7 (2 $\text{C}_{\text{pyrrolicH}}$), 140.2 (2C), 141.4 (2C), 141.6 (2C), 142.3 (2C), 148.5 (2 $\text{C}_{\text{Ar}^t\text{Bu}}$), 148.6 (2 $\text{C}_{\text{Ar}^t\text{Bu}}$), 148.7 (2 $\text{C}_{\text{Ar}^t\text{Bu}}$), 149.0 ($\text{C}_{\text{Ar}^t\text{Bu}}$), 149.1 ($\text{C}_{\text{Ar}^t\text{Bu}}$), 150.4 (2C), 155.5 (C) ppm.



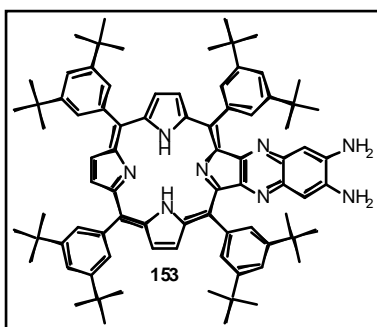
5,10,15,20-tetrakis-(3,5-di-*tert*-butylphenyl)porphyrin-2,3-dione (152**)²¹⁶**

A dark solution of **151** (600 mg, 0.556 mmol) in dichloromethane (200 mL) was stirred at RT in an open conical flask. After 6 days 3M sulfuric acid (5 mL) was added and the mixture was stirred for a further 2 hours, after which it was washed with H_2O (3 x 100 mL) and brine (150 mL). The organic layer was dried over Na_2SO_4 and

the solvent was removed under reduced pressure. The crude product was purified by column chromatography (light petroleum/dichloromethane 2:1). Yield: 520 mg (0.475 mmol, 85.5 %) 'porphyrindione' **152**. Melting point: >300 °C.

^1H -NMR (300 MHz, CDCl_3): δ = -1.70 (2H, s), 1.66 (36 H, s), 1.68 (36 H, s), 7.93 (6H, bs), 7.95 (2H, bs), 8.82 (4H, bs), 8.98 (2H) ppm; ^{13}C -NMR (75.5 MHz, CDCl_3): δ = 31.8 (12 CH_3), 31.9 (12 CH_3), 35.1 (4C), 35.2 (4C), 115.1 (2C), 121.4 (2 $\text{C}_{\text{p-ArH}}$), 121.6 (2 $\text{C}_{\text{p-ArH}}$), 125.3 (2C), 127.7 (4CH), 128.5 (2CH), 128.6 (2CH), 129.3 (4CH), 134.6 (2CH), 138.4 (2C), 138.6 (2C), 140.2 (2C), 140.6 (2C), 141.0 (2C), 149.15 (4 $\text{C}_{\text{Ar}^t\text{Bu}}$), 149.18 (4 $\text{C}_{\text{Ar}^t\text{Bu}}$), 155.6 (2C), 188.1 (2 $\text{C}=\text{O}$) ppm.

5,10,15,20-tetrakis-(3,5-di-*tert*-butylphenyl)-2³-2⁴-di-aminoquinoxalino[2,3-*b*]porphyrin (153)¹⁴²

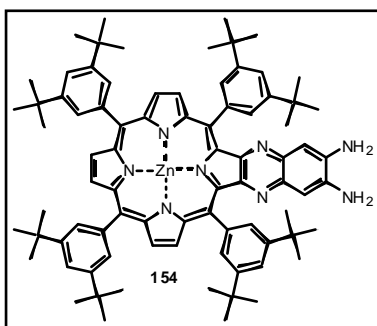


A solution of 'porphyrindione' **152** (402 mg, 0.3676 mmol) and benzenetetramine · 4HCl (164 mg, 0.5774 mmol, ~1.5 eq.) in deoxygenated pyridine (50 mL) was stirred at RT in the dark under an argon atmosphere for 20 hours. Dichloromethane (50 mL) and 1M HCl (30 mL) were added, and the organic layer was washed with 1M HCl (3 x 30 mL). The combined aqueous layers were extracted with dichloromethane (3 x

20 mL) and the combined organic layers were dried over Na₂SO₄. The solvent was removed under reduced pressure to give a dark redish crude residue, which was purified by column chromatography (dichloromethane). Yield: 437 mg (0.3654 mmol, 99.4 %) 'diaminoporphyrin' **153**. Melting point: >300 °C.

¹H-NMR (300 MHz, CDCl₃): δ = -2.41 (2H, s), 1.55 (36H, s), 1.59 (36H, s), 3.96 (4H, bs), 7.00 (2H, s), 7.85 (2H, t, *J* = 2.0 Hz), 7.95 (2H, t, *J* = 2 Hz), 8.04 (4H, d, *J* = 1 Hz), 8.17 (4H, d, *J* = 1 Hz), 8.84 (2H, s), 9.05 (4H, AB_{quartet}, *J* = 15.6, 4.9 Hz) ppm; ¹³C-NMR (75.5 MHz, CDCl₃): δ = 31.8 (12CH₃), 32.0 (12CH₃), 38.8 (8C), 117.9 (2C), 120.5 (2C_{p-Ar}H), 121.0 (2C_{p-Ar}H), 122.4 (2C), 127.8 (2C_{o-Ar}H), 128.0 (2C_{o-Ar}H), 128.7 (2C_{o-Ar}H), 128.9 (2C_{o-Ar}H), 129.6 (6C_{pyrrolic}H), 130.9 (2C), 133.9 (2C_{quinoxaline}H), 137.9 (2C), 138.4 (2C), 139.7 (2C), 139.9 (2C), 141.3 (C), 141.4 (C), 147.1 (2C), 148.7 (4C_{Ar}^tBu), 148.8 (4C_{Ar}^tBu), 151.1 (2C), 154.5 (2C) ppm.

[5,10,15,20-tetrakis-(3,5-di-*tert*-butylphenyl)-2³-2⁴-di-aminoquinoxalino[2,3-*b*]porphyrinato]zinc(II) (154 'diamino[porphyrinato]zinc(II)')



To a solution of 'diaminoporphyrin' **153** (105 mg, 0.0878 mmol) in dichloromethane (5 mL) was added Zn(OAc)₂ · 2 H₂O (210 mg, 0.957 mmol, ~10 eq.) in methanol (5 mL). The mixture was heated at reflux for 3 hours under an argon atmosphere in the dark, then left overnight at RT. The green solution was washed with H₂O (2 x 10 mL) then dried over Na₂SO₄. The solvents were removed under reduced pressure to

give the pure product. Yield: 110 mg (0.0874 mmol, 99.5 %) **154**. Melting point: >300 °C.

^1H -NMR (300 MHz, CDCl_3): δ = 1.48 (24H), 1.52 (48H), 3.93 (4H, bs), 6.98 (2H, s), 7.78 (2H, t, J = 1.7 Hz), 7.88 (2H, t, J = 1.7 Hz), 7.95 (4H, d, J = 1.9 Hz), 8.09 (4H, d, J = 1.9 Hz), 8.89 (2H, s), 8.98 (4H, AB_{quartet}, J = 6.4, 4.5 Hz) ppm; ^{13}C -NMR (75.5 MHz, CDCl_3): δ = 31.8 (12CH₃), 31.9 (12CH₃), 34.9 (4C), 35.1 (4C), 111.4 (2C_{quinoxaline}H), 118.4 (2C), 120.2 (2C_{p-Ar}H), 120.8 (2C_{p-Ar}H), 124.2 (2C), 128.4 (4C_{o-Ar}H), 129.4 (4C_{o-Ar}H), 131.4 (4C_{pyrrolic}H), 132.2 (2C_{pyrrolic}H), 138.6 (2C), 139.0 (2C), 141.8 (2C), 141.9 (2C), 142.8 (2C), 148.48 (4C_{Ar}^tBu), 148.53 (4C_{Ar}^tBu), 148.8 (2C), 149.0 (2C), 149.7 (2C), 152.6 (2C) ppm.

E 'APPENDIX'



E APPENDIX

E.1 ABBREVIATIONS

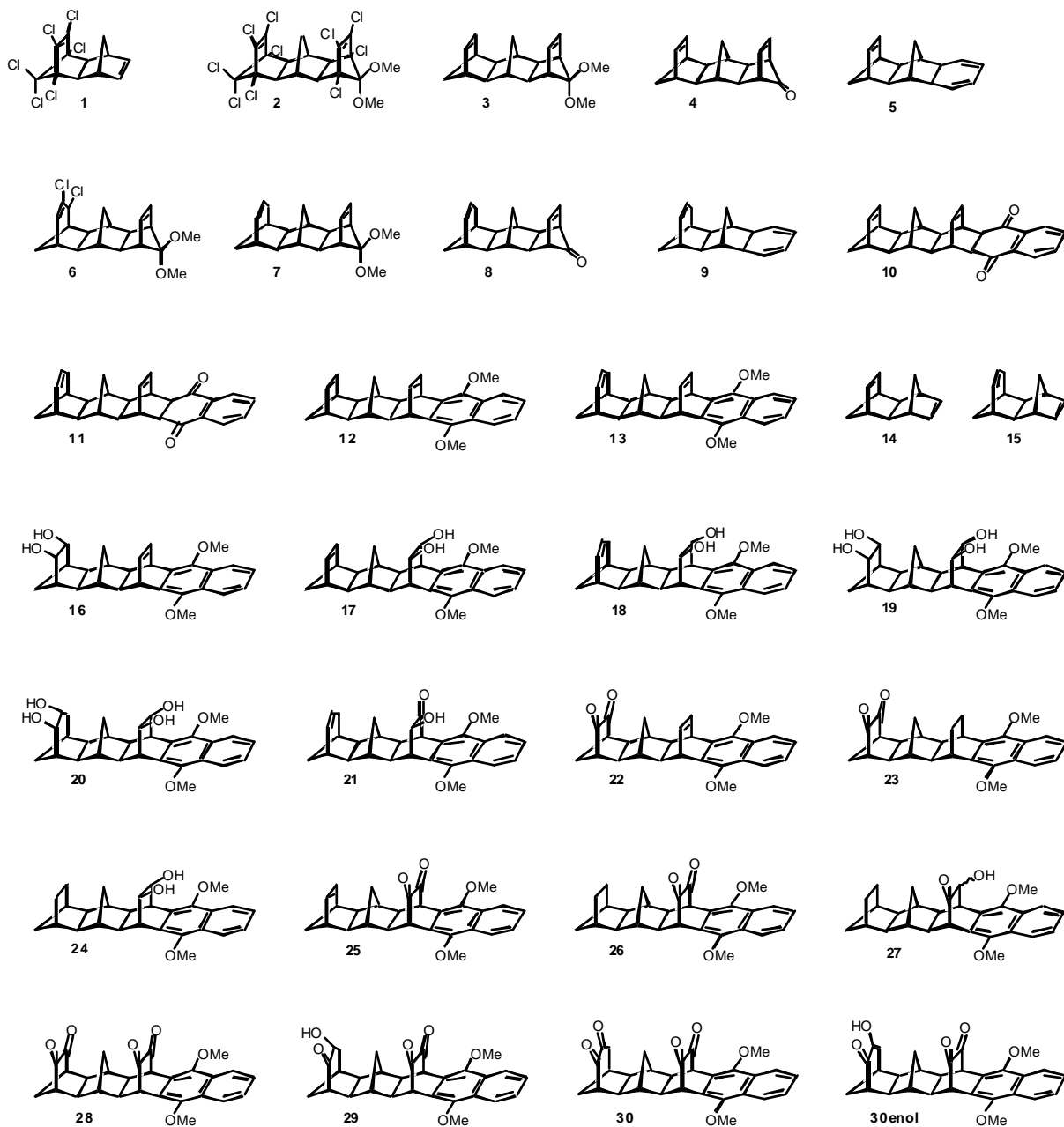
2B	two σ -bonds
4B	four σ -bonds
6B	six σ -bonds
A	acceptor
Ar	aryl
B	bridge
b.p.	boiling point
BQ	benzoquinone
C	carotenoid
°C	degrees Celsius
conc.	concentrated
CR	charge recombination
CS	charge separated
d	days
D	donor
δ	chemical shift in ppm relative to TMS
DCM	dichloromethane
DCV	dicyanovinyl
2,3-dichloro-5,6-dicyano-1,4-benzoquinone (DDQ)	2,3-dichloro-5,6-dicyano-1,4-benzoquinone
dec.	decomposition
DEPT	distorsionless enhancement by polarisation transfer
'diaminoporphyrin'	5,10,15,20-tetrakis-(3,5-di- <i>tert</i> -butylphenyl)-2 ³ -2 ⁴ -di-aminoquinoxalino[2,3- <i>b</i>]porphyrin
DMAD	dimethoxyacetylenedicarboxylate
DMB	dimethoxybenzene
DMF	dimethylformamide

DMN	dimethoxynaphthalene
ethyl acetate	ethyl acetate
EnT	energy transfer
eq.	equivalents
ET	electron transfer
Et ₂ O	diethyl ether
EtOH	ethanol
g	gram
h	hours
HMPA	hexamethylphosphoramide
HNQ	hydronaphthoquinone
IR	infrared
MALDI	matrix assisted laser desorption ionisation
mg	milligram
min.	minutes
mL	millilitre
m.p.	melting point
MS	mass spectroscopy
MTHF	2-methyl tetrahydrofuran
NMR	nuclear magnetic resonance
NQ	naphthoquinone
P	porphyrin
Ph	phenyl
'porphrindione'	5,10,15,20-tetrakis-(3,5-di- <i>tert</i> -butyl-phenyl)porphyrin-2,3-dione
PRC	photosynthetic reaction centre
PSI	photosystem I
PSII	photosystem II
Q	quinone
RT	room temperature
sat.	saturated
s.m.	starting material
T	temperature

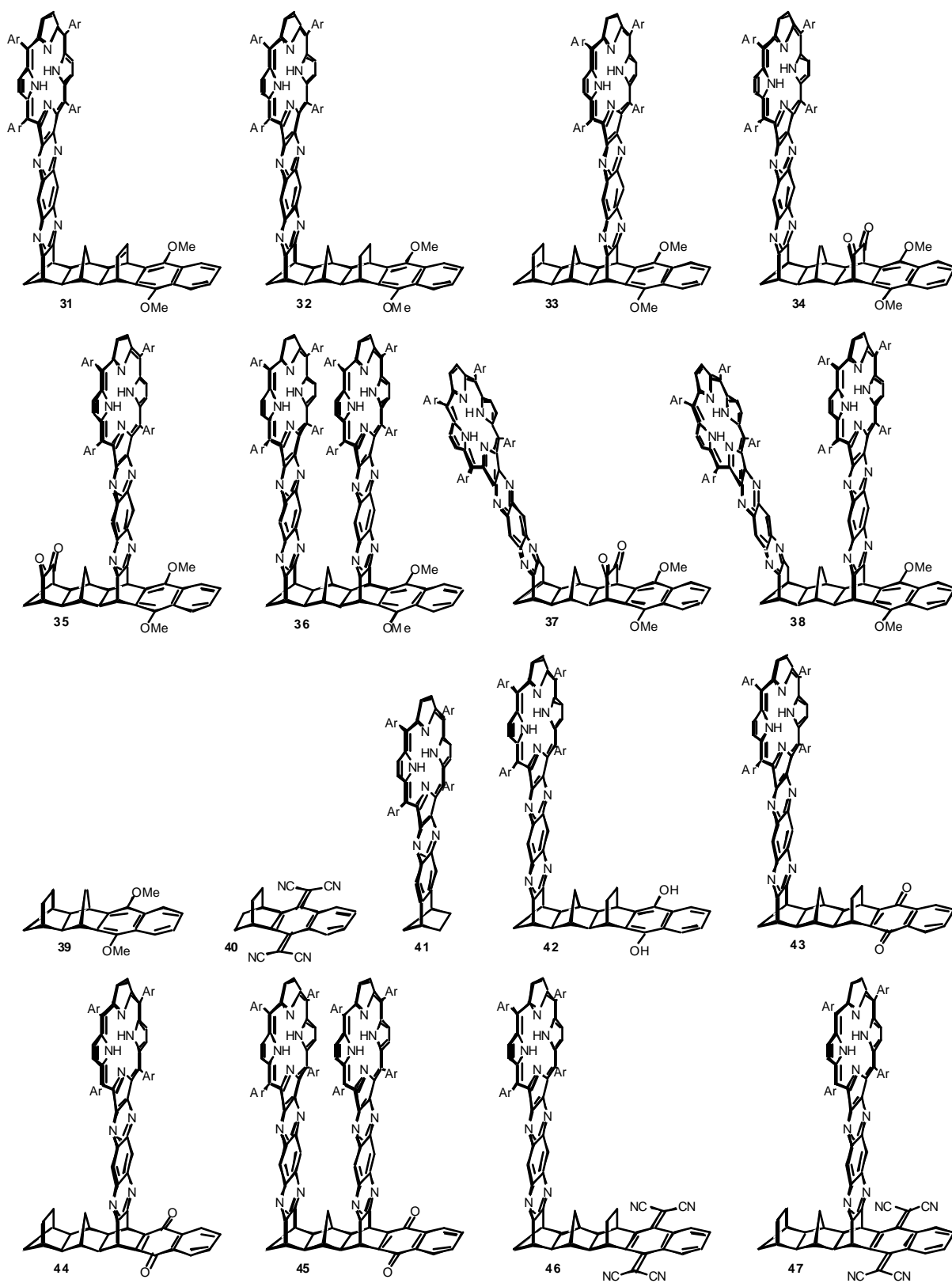
TB	through bond
TCNQ	tetracyanonaphthoquinodimethane
TEMPO	2,2,6,6-tetramethylpiperidin-1-oxyl
THF	tetrahydrofuran
TLC	thin layer chromatography
TMS	tetramethylsilane
TS	through space
TsCl	<i>p</i> -toluenesulfonyl chloride
UV	ultra violet
Vis	visible

E.2 COMPOUNDS IN NUMERICAL ORDER

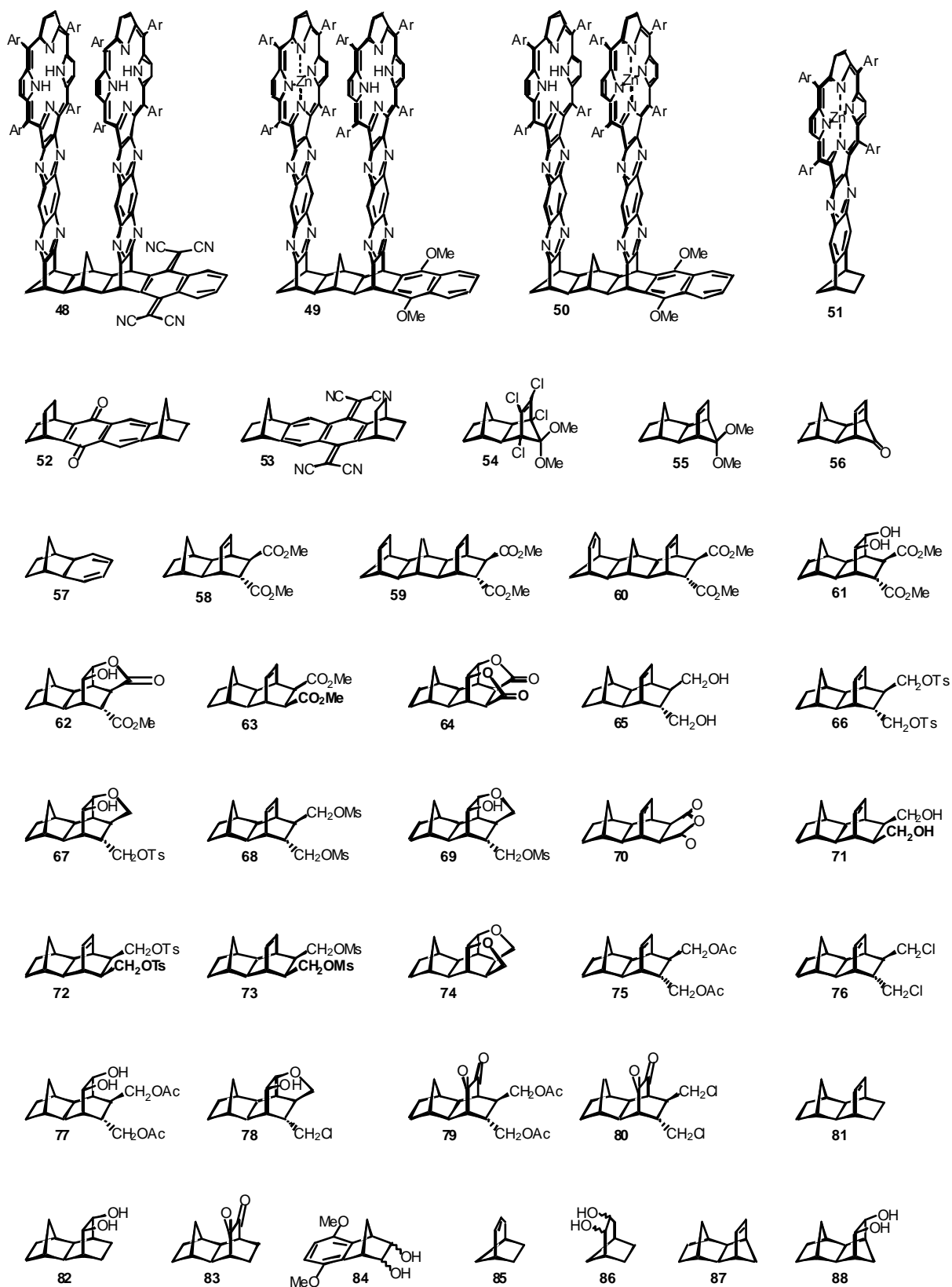
E.2.1 Compounds 1 to 30

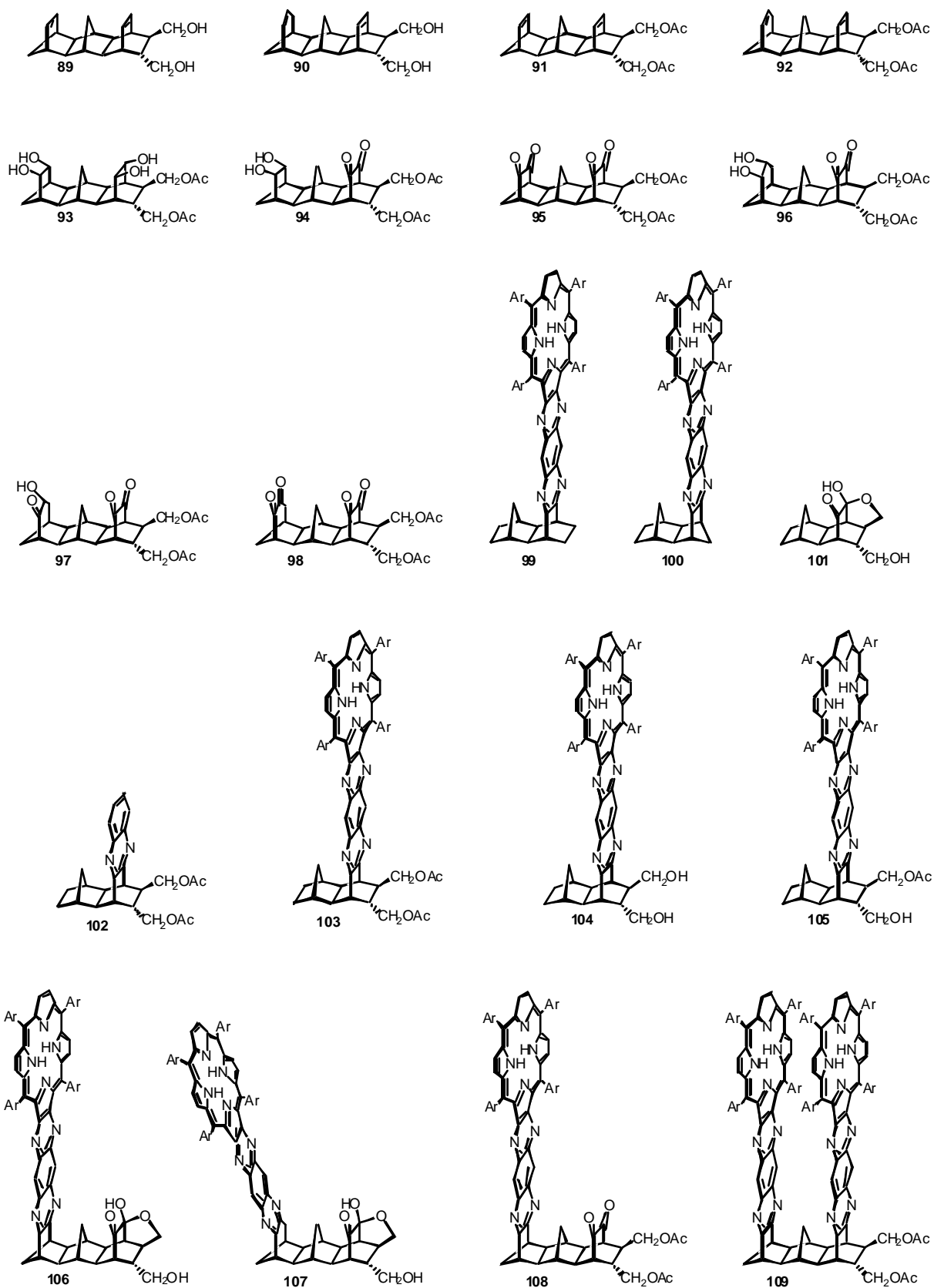


E.2.2 Compounds 31 to 47

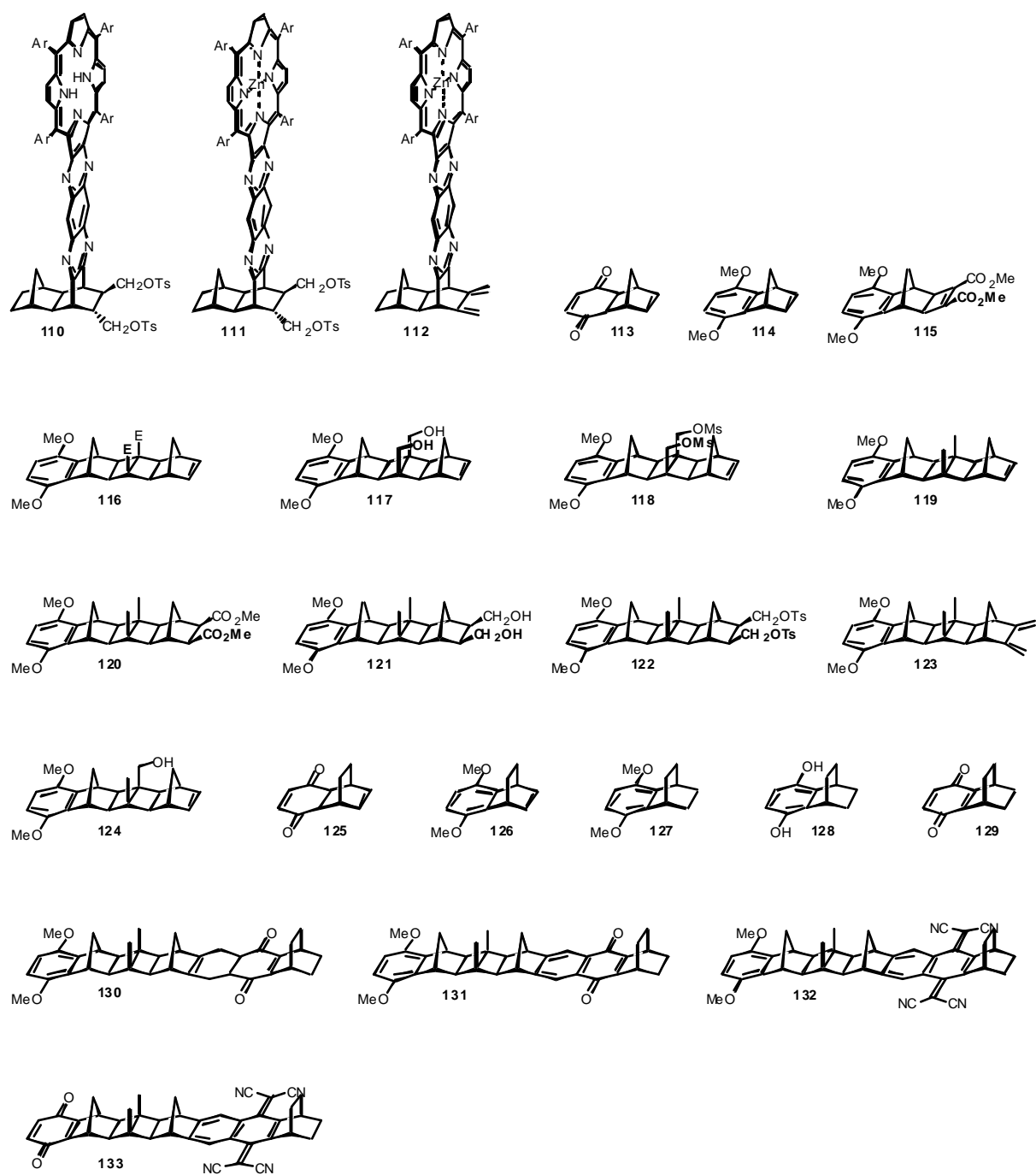


E.2.3 Compounds 48 to 88

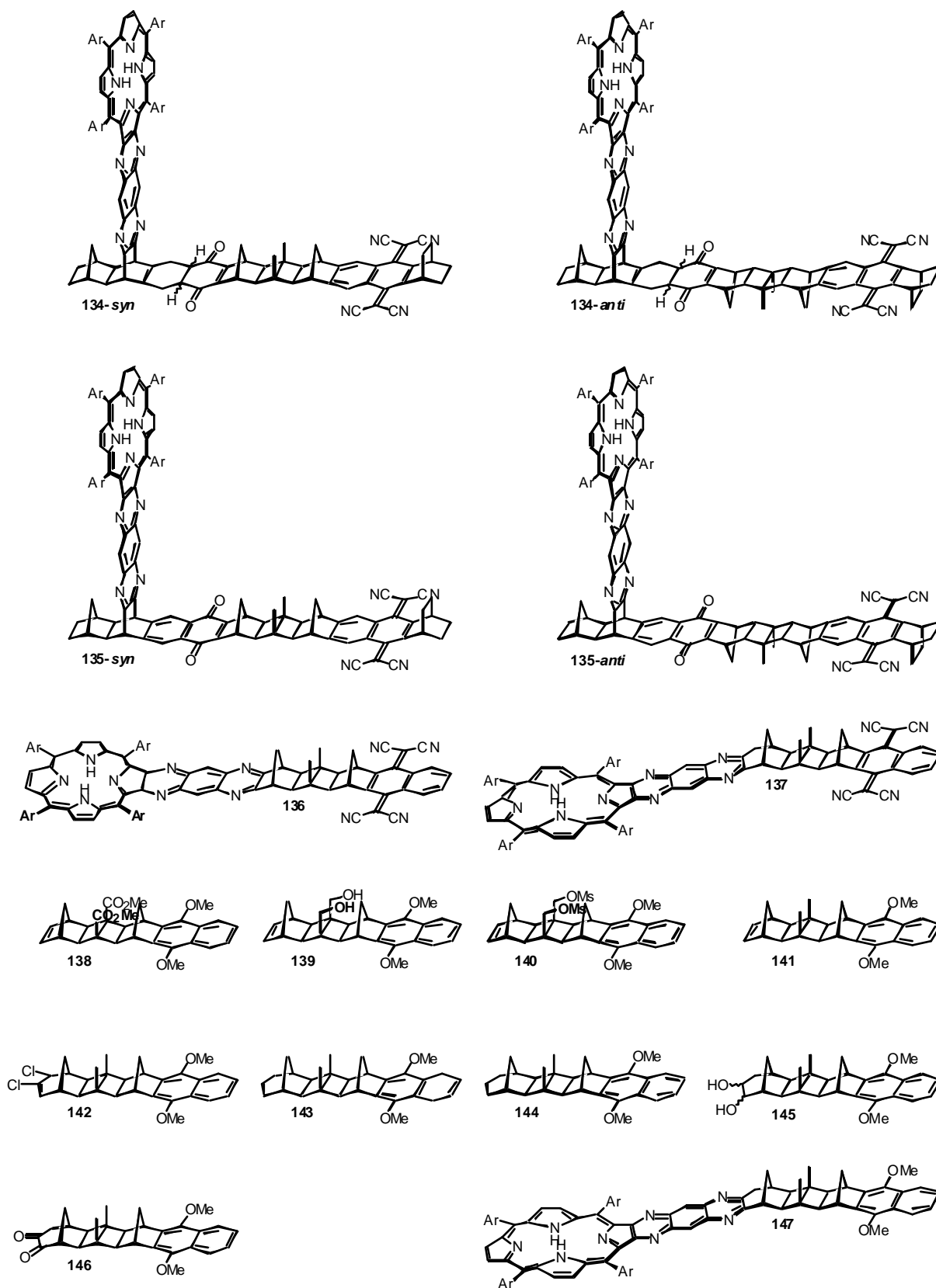


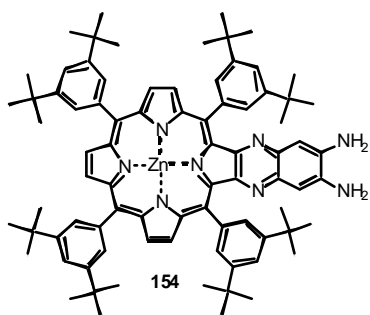
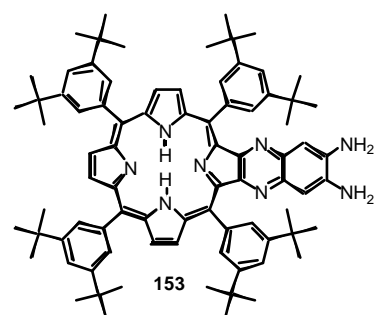
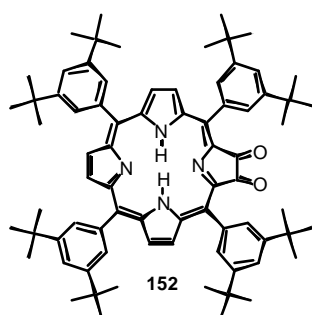
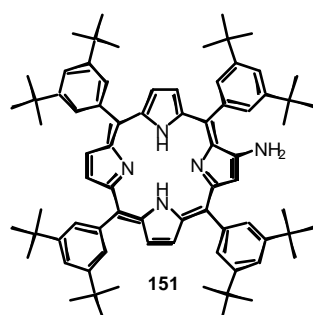
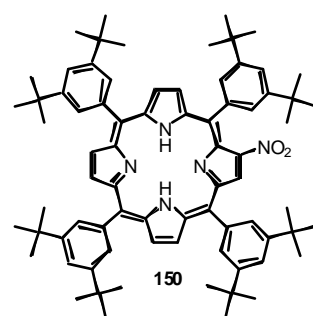
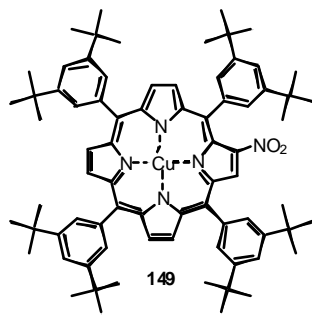
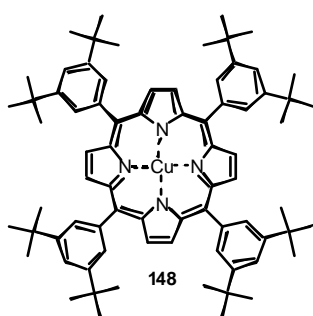
E.2.4 Compounds 89 to 109

E.2.5 Compounds 110 to 133



E.2.6 Compounds 134 to 147



E.2.7 Compounds 148 to 155

E.3 CHEMICALS IN ALPHABETICAL ORDER

The following list contains hazardous chemicals used for the synthesis of compounds described in this thesis.

Chemical	Hazards
4-Acetamido-TEMPO FW: 213.30, m.p.: 144 °C	irritating R: 36/37/38 S:
Acetic anhydride FW: 102.09, b.p.: 140 °C, d: 1.08	corrosive R: 10-34 S: 26-45
Acetone FW: 58.08, b.p.: 56 °C, d: 0.79	highly flammable R: 11 S: 9-16-23.2-33
1,4-Benzoquinone FW: 108.10	toxic R: 23/25-36/37/38 S: 26-28.1-45
Boron tribromide FW: 250.54, b.p.: 90 °C, d: 2.64	very toxic, corrosive R: 14-26/28-35 S: 9-26-28.6-36/37/39-45
Bromomethane FW: 94.94, b.p.: 4 °C	toxic R: 23-36/37/38 S: 15-27-36/37/3/-38-45
Carbon monoxide FW: 28.01, b.p.: -191 °C	extremely flammable, toxic R: 12-23 S: 7-16-45

Chemical	Hazards
Carbon tetrachloride FW: 153.82, b.p.: 76 °C, d: 1.59	toxic, environmentally unfriendly R: 23/24/25-40-48/23-59 S: 23.2-36/37-45-59-61
Chloroform FW: 119.38, b.p.: 61 °C, d: 1.49	harmful R: 22-38-40-48/20/22 S: 36/37
Copper(II) chloride FW: 134.45	toxic R: 25-36/37/38 S: 37-45
1,3-Cyclohexadiene FW: 80.13, b.p.: 80 °C, d: 0.841	highly flammable R: 11 S: 16
Cyclopentadiene FW: 66.10, b.p.: 40 °C, d: 0.80	highly flammable R: 11 S: 16-29-33
2,3-Dichloro-5,6-dicyano-1,4-benzoquinone FW: 227.01, m.p.: 213-216 °C	toxic R: 25-29 S: 45
Dichloromethane FW: 84.93, b.p.: 40 °C, d: 1.32	harmful R: 40 S: 23.2-24/25-36/37
Dicyclopentadiene FW: 132.21, b.p.: 170 °C, d: 0.986	toxic, highly flammable R: 10-22-23-36/38-52/53 S: 37-45

Chemical	Hazards
Diethyl ether FW: 72.11, b.p.: 34 °C, d: 0.71	highly flammable, irritating R: 12-19 S: 9-16-29-33
Dimethyl acetylenedicarboxylate FW: 142.11, b.p.: 95 (25 hPa), d: 1.16	irritating R: 36/37/38 S: -
N,N-Dimethylformamide FW: 73.10, b.p.: 153 °C, d: 0.95	toxic, mutagenic R: 61-E20/21-36 S: 53-45
Dimethyl fumarate FW: 144.13, b.p. 192 °C	harmful R: 21-36/37/38 S: 36/37/39
Dimethylmaleate FW: 172.18, b.p. 225 °C, d: 1.064	harmful, flammable R: - S: -
1,4-Dioxane FW: 88.11, b.p.: 101 °C, d: 1.03	highly flammable, harmful R: 11-19-36/37-40 S: 16-36/37
Ethanol MW: 46.07, b.p. 78°C, d: 0.79	highly flammable R: 11 S: 7-16
Ethyl acetate FW: 88.10, b.p. 77 °C, d: 0.90	highly flammable R: 11 S: 16-23.2-29-33

Chemical	Hazards
Ethyl trichloroacetate FW: 191.44, b.p.: 168 °C, d: 1.378	corrosive, irritant R: 36/37/38 S: 26-28
Formaldehyde FW: 30.03, b.p. 96-98 °C, d: 1.09	toxic R: 23/24/25-3440-43 S: 26-36/37/39-45-51
Formic acid FW: 46.03, b.p. 100 °C, d: 1.22	corrosive R: 35 S: 23.2-26-45
Hexachlorocyclopentadiene FW: 272.77, m.p.: -10 °C, d: 1.702	very toxic R: 23/24/25-36 S: 26-27-28-44
Hexane FW: 86.18, b.p.: 68°C, d: 0.66	highly flammable, harmful R: 11-19-36/37 S: 9-16-24/25-29-51
Hydrochloric acid FW: 36.46	corrosive R: 34-37 S: 26-36/37/39-45
Hydrogen FW: 2.02, m.p.: -259°C, b.p.: -253 °C	extremely flammable R: 12 S: 9-16-33
Lithium aluminium hydride FW: 37.95, m.p.: 150 °C	highly flammable R: 15 S: 7/8-24/25-43.6

Chemical	Hazards
Lithium perchlorate trihydrate FW: 160.44, m.p.: 95 °C	oxidizing, harmful R: 9-22-36/37/38 S: -
Malononitrile FW: 66.06, b.p.: 218 °C	toxic R: 23/24/25 S: 23.2-27-45
Methanesulfonyl chloride FW: 114.55, b.p.: 164 °C, d: 1.47	corrosive R: 21/22-35 S: 23.2-26-36/37/39-45
Methanol FW: 32.04, b.p. 65 °C, d: 0.79	highly flammable, toxic R: 11-23/25 S: 7-16-24-45
Methyliodide FW: 141.94, b.p. 41-43 °C, d: 2.27	very toxic, cancer R: 21-23/25-37/38-40 S: 36/37-38-45
4-Methylmorpholine N-oxide FW: 117.15	irritating R: - S: 22-24/25
1,4-Naphthoquinone FW: 158.16	very toxic R: 25-26-36/37/38-43 S: 26-28.1-36/37-45
Norbornadiene FW: 92.14, b.p.: 89 °C, d: 0.91	highly flammable, harmful R: 11-22 S: 16-29-33

Chemical	Hazards
Norbornene FW: 94.16, b.p. 96 °C	highly flammable R: 11 S: 9-16
Osmiumtetroxide FW: 254.20	toxic R: 26/27/28-34 S: 7/9-26-45
1,2-Phenylenediamine FW: 108.14, m.p.: 99 °C, b.p.: 258 °C	toxic R: 23/24/25-430 S: 28.1-45
Potassium hydroxide FW: 56.11, m.p.: 360 °C	corrosive R: 35 S: 26-37/39-45
Potassium <i>tert</i> .-butylate FW: 112.22, m.p.: 256-258 °C	highly flammable, corrosive R: 11-14-22-36 S: 7/8-16-26-36/37/39-43-45
iso-Propanol FW: 60.10, b.p.: 82 °C, d: 0.78	highly flammable R: 11 S: 7-16
Pyridine FW: 79.10, b.p.: 115 °C, d: 0.98	highly flammable, harmful R: 11-20/21/22 S: 26-28.1
Quadricyclane FW: 92.14, d: 1.702	highly flammable R: S:

Chemical	Hazards
Silver nitrate FW: 169.87, m.p.: 212 °C	corrosive R: 35 S: 26-45
Silver(I) oxide FW: 231.74	irritating, oxidizing R: 8-41-44 S: 26-39
Sodium FW: 22.99, m.p.: 97 °C	highly flammable, corrosive R: 14/15-34 S: 5.3-8-43.7-45
Sodium borohydride FW: 37.83, m.p.: 500 °C	highly flammable, toxic R: 15-25-34 S: 14.2-26-36/37/39-43.6-45
Sodium hydride FW: 24.00	highly flammable, corrosive R: 15-34 S: 7/8-26-36/37/39-43.6-45
Sodium hydroxide FW: 40.00, m.p.: 324 °C	corrosive R: 35 S: 26-36/37/39-45
Sodium methoxide FW: 54.02	corrosive, highly flammable R: 11-14-34 S: 8-16-26-43.6-45
Sulfuric acid FW: 98.08, b.p.: 330 °C, d: 1.84	corrosive R: 35 S: 26-30-45

Chemical	Hazards
Sulfuryl chloride FW: 134.97, b.p. 69 °C, d:1.67	corrosive R: 14-34-37 S: 26-45
Tetrahydrofuran FW: 72.11, b.p.: 66 °C, d: 0.89	highly flammable, irritating R: 11-19-36/37 S 16-29-33
Thionyl chloride FW: 118.97, b.p.: 76 °C, d: 1.64	corrosive R: 14-34-37 S: 26-45
Tin(II) chloride dihydrate FW: 225.65, m.p.: 38 °C	harmful R: 22-36/37/38 S: 26
Titanium(IV) chloride FW: 189.71, b.p.: 136 °C, d: 1.73	corrosive R: 14-34-36/37 S: 7/8-26-45
Toluene FW: 92.14, b.p.: 111 °C, d: 0.87	highly flammable, harmful R: 47-11-20 S: 53-16-25-29-33
p-Toluenesulfonyl chloride FW: 190.65, b.p.: 135 °C	irritating R: 36/37/38 S: 7/8
Triphenylphosphine FW: 262.29, m.p.: 78-81 °C	harmful, dangerous to the environment R:43-48/20/22-50-53 S: 22-24-37

E.4 X-RAY DATA

X-ray data for **79** and **69** are given below.²²⁷⁻²³⁰

E.4.1 2B-dione-*trans*-diacetate **79**

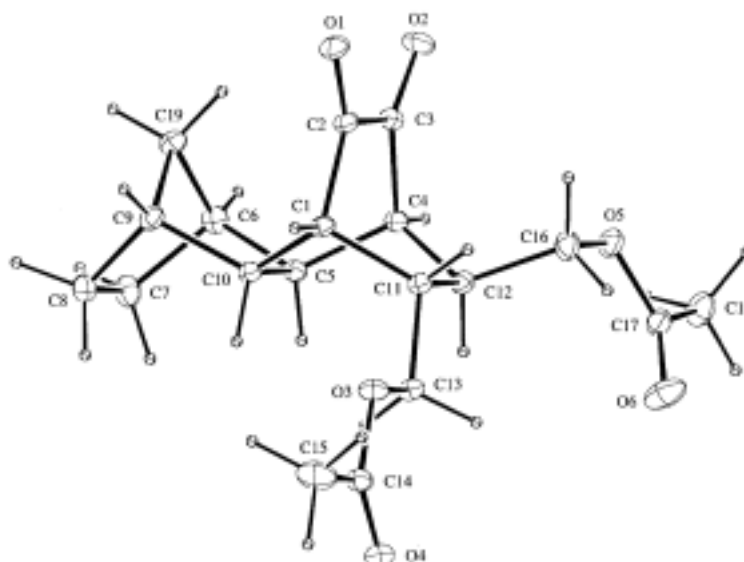


Figure 80: ORTEP plot of 2B-dione-*trans*-diacetate **79**

E.4.1.1 Chemical Data

chemical formula moiety	'C ₁₉ H ₂₄ O ₆ '
chemical formula sum	'C ₁₉ H ₂₄ O ₆ '
chemical formula weight	348.4

E.4.1.2 Crystal Data

symmetry cell setting	triclinic
symmetry space group name H-M	'P-1'
cell length a	6.876(2)
cell length b	10.561(4)
cell length c	13.324(4)
cell angle alpha	106.10(2)
cell angle beta	104.31(2)
cell angle gamma	96.91(2)
cell volume	882.0(6)
cell formula units Z	2
cell measurement reflns used	10
cell measurement theta minutes	20
cell measurement theta max	25
cell measurement temperature	294

exptl crystal description	plate
exptl crystal colour	yellow
exptl crystal size max	0.25
exptl crystal size mid	0.19
exptl crystal size minutes	0.10
exptl crystal density diffrn	1.31
exptl crystal F 000	372.0
exptl absorpt coefficient mu	0.765
exptl absorpt correction type	analytical
exptl absorpt correction T-minutes	0.83
exptl absorpt correction T-max	0.90

E.4.1.3 Experimental Data

diffrn radiation type	'CuK α '
diffrn radiation wavelength	1.54184
diffrn measurement device type	'NoniusCAD-4'
diffrn measurement method	ω -- 2θ
diffrn reflns number	3341
diffrn reflns theta max	70
diffrn reflns h minutes	-8
diffrn reflns h max	8
diffrn reflns k minutes	-12
diffrn reflns k max	12
diffrn reflns l minutes	-16
diffrn reflns l max	16
diffrn standards number	1
diffrn standards interval time	30min
diffrn standards decay %	0

E.4.1.4 Refinement Data

reflns number total	3341
reflns number gt	2386
reflns threshold expression	$I > 3\sigma(I)$
refine ls structure factor coef	F
refine ls R factor gt	0.047
refine ls wR factor ref	0.073
refine ls hydrogen treatment	noref
refine ls number reflns	2386
refine ls number parameters	226
refine ls goodness of fit ref	1.81
refine ls weighting scheme	calc
refine ls weighting details	' $w=1/[\sigma^2(F)+0.0016F^2]$ '
refine ls shift/su max	0.003
refine diff density max	0.26
refine diff density minutes	-0.27
refine ls extinction method	none
refine ls extinction coef	?

E.4.1.5 Atomic Coordinates and Displacement Parameters

A: atom site label

B: atom site fract x

C: atom site fract y

D: atom site fract z

E: atom site U iso or equiv

F: atom site adp type

G: atom site type symbol

A	B	C	D	E	F	G
O1	-0.0320(2)	0.1663(2)	0.6869(1)	0.0601(5)	Uani	O
O2	-0.1143(2)	0.3960(2)	0.6273(2)	0.0703(5)	Uani	O
O3	0.7061(2)	0.2768(2)	0.8781(1)	0.0541(4)	Uani	O
O4	1.0412(2)	0.3593(2)	0.9203(1)	0.0681(5)	Uani	O
O5	0.2680(3)	0.7123(2)	0.8174(1)	0.0630(5)	Uani	O
O6	0.5810(3)	0.8247(2)	0.9125(2)	0.0982(8)	Uani	O
C1	0.3270(3)	0.2456(2)	0.7074(2)	0.0421(5)	Uani	C
C2	0.1014(3)	0.2475(2)	0.6819(2)	0.0447(5)	Uani	C
C3	0.0549(3)	0.3717(2)	0.6478(2)	0.0467(5)	Uani	C
C4	0.2469(3)	0.4563(2)	0.6467(2)	0.0424(5)	Uani	C
C5	0.3546(3)	0.3713(2)	0.5716(2)	0.0413(5)	Uani	C
C6	0.2327(4)	0.3093(2)	0.4499(2)	0.0542(6)	Uani	C
C7	0.3825(4)	0.2544(3)	0.3882(2)	0.0649(7)	Uani	C
C8	0.4171(4)	0.1277(2)	0.4218(2)	0.0600(6)	Uani	C
C9	0.2882(3)	0.1271(2)	0.5001(2)	0.0473(5)	Uani	C
C10	0.3977(3)	0.2450(2)	0.6059(2)	0.0404(5)	Uani	C
C11	0.4362(3)	0.3779(2)	0.8013(2)	0.0433(5)	Uani	C
C12	0.3928(3)	0.5023(2)	0.7647(2)	0.0456(5)	Uani	C
C13	0.6671(3)	0.3906(2)	0.8418(2)	0.0493(5)	Uani	C
C14	0.9054(3)	0.2726(3)	0.9147(2)	0.0551(6)	Uani	C
C15	0.9337(4)	0.1496(4)	0.9450(3)	0.089(1)	Uani	C
C16	0.3113(4)	0.5948(2)	0.8478(2)	0.0614(6)	Uani	C
C17	0.4168(4)	0.8223(2)	0.8571(2)	0.0563(6)	Uani	C
C18	0.3517(5)	0.9354(3)	0.8214(2)	0.0760(8)	Uani	C
C19	0.1041(3)	0.1768(2)	0.4450(2)	0.0555(6)	Uani	C
HC1	0.3559	0.1657	0.7304	0.042	Uani	H
HC4	0.2151	0.5357	0.6236	0.042	Uani	H
HC5	0.4878	0.4275	0.5782	0.041	Uani	H
HC6	0.1519	0.3693	0.4188	0.054	Uani	H
H1C7	0.5140	0.3215	0.4117	0.065	Uani	H
H2C7	0.3206	0.2300	0.3074	0.065	Uani	H
H1C8	0.5652	0.1352	0.4593	0.060	Uani	H
H2C8	0.3684	0.0445	0.3567	0.060	Uani	H
HC9	0.2537	0.0383	0.5113	0.047	Uani	H
HC10	0.5484	0.2473	0.6242	0.040	Uani	H
HC11	0.3796	0.3801	0.8639	0.043	Uani	H
HC12	0.5258	0.5529	0.7652	0.046	Uani	H
H1C13	0.7287	0.4761	0.9040	0.049	Uani	H

A	B	C	D	E	F	G
H2C13	0.7283	0.3911	0.7812	0.049	Uani	H
H1C15	1.0834	0.1507	0.9716	0.089	Uani	H
H2C15	0.8694	0.1469	1.0042	0.089	Uani	H
H3C15	0.8672	0.0682	0.8796	0.089	Uani	H
H1C16	0.4163	0.6246	0.9211	0.061	Uani	H
H2C16	0.1823	0.5439	0.8517	0.061	Uani	H
H1C18	0.4677	1.0153	0.8531	0.076	Uani	H
H2C18	0.3114	0.9083	0.7399	0.076	Uani	H
H3C18	0.2320	0.9589	0.8473	0.076	Uani	H
H1C19	0.0310	0.1172	0.3686	0.056	Uani	H
H2C19	0.0037	0.1909	0.4880	0.056	Uani	H

A atom site aniso label

B atom site aniso U 11

C atom site aniso U 22

D atom site aniso U 33

E atom site aniso U 12

F atom site aniso U 13

G atom site aniso U 23

A	B	C	D	E	F	G
O1	0.0484(9)	0.0550(9)	0.070(1)	-0.0115(7)	0.0198(8)	0.0163(8)
O2	0.0368(8)	0.079(1)	0.103(2)	0.0200(8)	0.0223(9)	0.037(1)
O3	0.0351(7)	0.065(1)	0.063(1)	0.0082(7)	0.0081(6)	0.0290(8)
O4	0.0408(8)	0.073(1)	0.075(1)	0.0014(8)	0.0108(8)	0.0101(9)
O5	0.061(1)	0.0433(8)	0.071(1)	0.0112(7)	0.0094(8)	0.0048(7)
O6	0.067(1)	0.075(1)	0.126(2)	-0.001(1)	-0.022(1)	0.042(1)
C1	0.035(1)	0.037(1)	0.052(1)	0.0022(8)	0.0067(8)	0.0186(9)
C2	0.036(1)	0.044(1)	0.048(1)	-0.0027(8)	0.0117(9)	0.0113(9)
C3	0.034(1)	0.050(1)	0.056(1)	0.0088(8)	0.0141(9)	0.015(1)
C4	0.038(1)	0.036(1)	0.057(1)	0.0100(8)	0.0141(9)	0.0181(9)
C5	0.037(1)	0.036(1)	0.056(1)	0.0081(8)	0.0159(9)	0.0191(9)
C6	0.060(1)	0.054(1)	0.054(1)	0.020(1)	0.015(1)	0.023(1)
C7	0.084(2)	0.056(1)	0.065(2)	0.018(1)	0.035(1)	0.021(1)
C8	0.064(2)	0.051(1)	0.064(2)	0.015(1)	0.023(1)	0.011(1)
C9	0.049(1)	0.036(1)	0.052(1)	0.0041(9)	0.0098(9)	0.0117(9)
C10	0.0323(9)	0.0346(9)	0.052(1)	0.0052(8)	0.0074(8)	0.0147(8)
C11	0.036(1)	0.041(1)	0.049(1)	0.0019(8)	0.0081(8)	0.0150(9)
C12	0.042(1)	0.037(1)	0.054(1)	0.0027(8)	0.0126(9)	0.0115(9)
C13	0.037(1)	0.050(1)	0.054(1)	0.0001(9)	0.0052(9)	0.017(1)
C14	0.037(1)	0.070(2)	0.052(1)	0.010(1)	0.0095(9)	0.013(1)
C15	0.057(2)	0.103(2)	0.122(3)	0.030(2)	0.020(2)	0.062(2)
C16	0.076(2)	0.040(1)	0.068(2)	0.011(1)	0.029(1)	0.011(1)
C17	0.055(1)	0.046(1)	0.057(1)	0.009(1)	0.008(1)	0.007(1)
C18	0.087(2)	0.051(1)	0.077(2)	0.020(1)	0.005(2)	0.014(1)
C19	0.046(1)	0.060(1)	0.048(1)	0.004(1)	0.0026(9)	0.011(1)

E.4.1.6 Molecular Geometry**A** geom bond atom site label 1**B** geom bond atom site label 2**C** geom bond distance

A	B	B
O1	C2	1.206(2)
O2	C3	1.203(2)
O3	C13	1.444(3)
O3	C14	1.347(2)
O4	C14	1.199(3)
O5	C16	1.450(3)
O5	C17	1.334(3)
O6	C17	1.180(3)
C1	C2	1.507(3)
C1	C10	1.546(3)
C1	C11	1.547(3)
C2	C3	1.545(3)
C3	C4	1.508(3)
C4	C5	1.544(3)
C4	C12	1.547(3)
C5	C6	1.538(3)
C5	C10	1.563(3)
C6	C7	1.540(3)
C6	C19	1.538(3)
C7	C8	1.550(3)
C8	C9	1.528(3)
C9	C10	1.543(3)
C9	C19	1.527(3)
C11	C12	1.559(3)
C11	C13	1.521(3)
C12	C16	1.527(3)
C14	C15	1.483(4)
C17	C18	1.480(3)

A geom angle atom site label 1**B** geom angle atom site label 2**C** geom angle atom site label 3**D** geom angle

A	B	C	D
C13	O3	C14	115.2(2)
C16	O5	C17	117.8(2)
C2	C1	C10	109.2(2)
C2	C1	C11	105.8(2)
C10	C1	C11	109.3(2)
O1	C2	C1	126.9(2)

A	B	C	D
O1	C2	C3	121.7(2)
C1	C2	C3	111.4(2)
O2	C3	C2	122.8(2)
O2	C3	C4	125.9(2)
C2	C3	C4	111.3(2)
C3	C4	C5	110.8(2)
C3	C4	C12	106.3(2)
C5	C4	C12	107.4(2)
C4	C5	C6	116.6(2)
C4	C5	C10	110.5(2)
C6	C5	C10	102.7(2)
C5	C6	C7	107.3(2)
C5	C6	C19	103.3(2)
C7	C6	C19	100.4(2)
C6	C7	C8	103.0(2)
C7	C8	C9	103.3(2)
C8	C9	C10	106.9(2)
C8	C9	C19	100.4(2)
C10	C9	C19	103.9(2)
C1	C10	C5	110.4(2)
C1	C10	C9	116.7(2)
C5	C10	C9	103.0(2)
C1	C11	C12	110.6(2)
C1	C11	C13	113.3(2)
C12	C11	C13	108.6(2)
C4	C12	C11	110.3(2)
C4	C12	C16	113.4(2)
C11	C12	C16	109.1(2)
O3	C13	C11	108.2(2)
O3	C14	O4	122.5(2)
O3	C14	C15	112.3(2)
O4	C14	C15	125.2(2)
O5	C16	C12	111.2(2)
O5	C17	O6	122.2(2)
O5	C17	C18	112.3(2)
O6	C17	C18	125.5(2)
C6	C19	C9	94.4(2)

A geom torsion atom site label 1

B geom torsion atom site label 2

C geom torsion atom site label 3

D geom torsion atom site label 4

E geom torsion

A	B	C	D	E
C14	O3	C13	C11	178.8(2)
C13	O3	C14	O4	2.4(3)

A	B	C	D	E
C13	O3	C14	C15	-177.0(2)
C17	O5	C16	C12	-91.8(2)
C16	O5	C17	O6	2.2(4)
C16	O5	C17	C18	-179.0(2)
C10	C1	C2	O1	122.2(2)
C10	C1	C2	C3	-58.5(2)
C11	C1	C2	O1	-120.3(2)
C11	C1	C2	C3	59.1(2)
C2	C1	C10	C5	58.5(2)
C2	C1	C10	C9	-58.6(2)
C11	C1	C10	C5	-56.9(2)
C11	C1	C10	C9	-174.0(2)
C2	C1	C11	C12	-60.5(2)
C2	C1	C11	C13	177.4(2)
C10	C1	C11	C12	57.0(2)
C10	C1	C11	C13	-65.2(2)
O1	C2	C3	O2	2.0(3)
O1	C2	C3	C4	-179.3(2)
C1	C2	C3	O2	-177.4(2)
C1	C2	C3	C4	1.3(2)
O2	C3	C4	C5	-125.4(2)
O2	C3	C4	C12	118.2(2)
C2	C3	C4	C5	56.0(2)
C2	C3	C4	C12	-60.4(2)
C3	C4	C5	C6	61.8(2)
C3	C4	C5	C10	-54.9(2)
C12	C4	C5	C6	177.5(2)
C12	C4	C5	C10	60.7(2)
C3	C4	C12	C11	58.0(2)
C3	C4	C12	C16	-64.7(2)
C5	C4	C12	C11	-60.7(2)
C5	C4	C12	C16	176.7(2)
C4	C5	C6	C7	168.9(2)
C4	C5	C6	C19	-85.6(2)
C10	C5	C6	C7	-70.2(2)
C10	C5	C6	C19	35.3(2)
C4	C5	C10	C1	-2.1(2)
C4	C5	C10	C9	123.1(2)
C6	C5	C10	C1	-127.1(2)
C6	C5	C10	C9	-1.9(2)
C5	C6	C7	C8	72.8(2)
C19	C6	C7	C8	-34.8(2)
C5	C6	C19	C9	-53.8(2)
C7	C6	C19	C9	56.9(2)
C6	C7	C8	C9	-1.3(2)
C7	C8	C9	C10	-70.9(2)
C7	C8	C9	C19	37.2(2)

A	B	C	D	E
C8	C9	C10	C1	-165.8(2)
C8	C9	C10	C5	73.1(2)
C19	C9	C10	C1	88.5(2)
C19	C9	C10	C5	-32.5(2)
C8	C9	C19	C6	-57.9(2)
C10	C9	C19	C6	52.6(2)
C1	C11	C12	C4	2.0(2)
C1	C11	C12	C16	127.2(2)
C13	C11	C12	C4	126.9(2)
C13	C11	C12	C16	-108.0(2)
C1	C11	C13	O3	-58.1(2)
C12	C11	C13	O3	178.6(2)
C4	C12	C16	O5	-56.5(2)
C11	C12	C16	O5	-179.9(2)

E.4.2 Mono-ring closed Mesylate 69

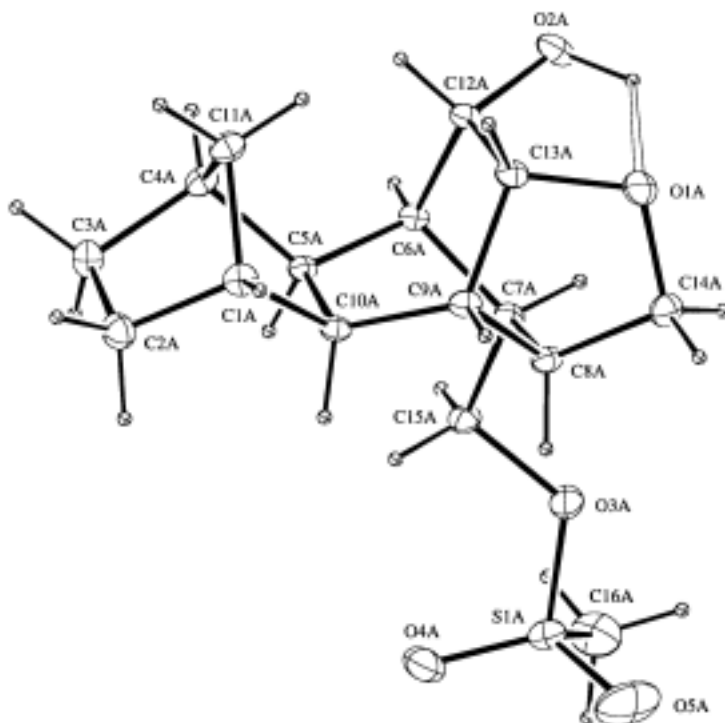


Figure 81: ORTEP plot of mono-ring closed mesylate 69

E.4.2.1 Chemical Data

chemical formula moiety	'C ₁₆ H ₂₃ O ₅ '
chemical formula sum	'C ₁₆ H ₂₃ O ₅ '
chemical formula weight	327.4

E.4.2.2 Crystal Data

symmetry cell setting	triclinic
symmetry space group name H-M	'P-1'
cell length a	7.066(1)
cell length b	11.065(2)
cell length c	20.449(4)
cell angle alpha	99.08(1)
cell angle beta	93.29(1)
cell angle gamma	91.46(1)
cell volume	1575.2(5)
cell formula units Z	4
cell measurement reflns used	10
cell measurement theta min	20
cell measurement theta max	22
cell measurement temperature	294

exptl crystal description	irregular
exptl crystal colour	colourless
exptl crystal size rad	0.10
exptl crystal density diffrn	1.38
exptl crystal density method	'not measured'
exptl crystal F 000	700.0
exptl absorpt coefficient mu	1.968
exptl absorpt correction type	none

E.4.2.3 Experimental Data

diffn radiation type	'CuK α '
diffn radiation wavelength	1.54184
diffn measurement device type	'NoniusCAD-4'
diffn measurement method	ω -- 2θ
diffn reflns number	5993
diffn reflns theta max	70
diffn reflns h minutes	-8
diffn reflns h max	8
diffn reflns k minutes	-13
diffn reflns k max	13
diffn reflns l minutes	0
diffn reflns l max	24
diffn standards number	1
diffn standards interval time	30min
diffn standards decay %	7

E.4.2.4 Refinement Data

reflns number total	5993
reflns number gt	4015
reflns threshold expression	$I > 3\sigma(I)$
refine ls structure factor coef	F
refine ls R factor gt	0.056
refine ls wR factor ref	0.082
refine ls hydrogen treatment	noref
refine ls number reflns	4015
refine ls number parameters	397
refine ls goodness of fit ref	1.69
refine ls weighting scheme	calc
refine ls weighting details	' $w=1/[\sigma^2(F)+0.0016F^2]$ '
refine ls shift/su max	0.005
refine diff density max	0.45
refine diff density minutes	-0.45
refine ls extinction method	none

E.4.2.5 Atomic Coordinates and Displacement Parameters**A** atom site label**B** atom site fract x**C** atom site fract y**D** atom site fract z**E** atom site U iso or equiv**F** atom site adp type**G** atom site type symbol

A	B	C	D	E	F	G
S1A	-0.2475(1)	0.07020(9)	0.56980(5)	0.0615(3)	Uani	S
O1A	0.4654(3)	-0.0765(2)	0.7312(1)	0.0611(6)	Uani	O
O2A	0.5693(3)	0.1549(2)	0.7599(1)	0.0670(7)	Uani	O
O3A	-0.0481(4)	0.0794(3)	0.6059(1)	0.0756(8)	Uani	O
O4A	-0.3867(4)	0.1196(4)	0.6127(2)	0.118(1)	Uani	O
O5A	-0.2710(7)	-0.0473(3)	0.5341(3)	0.158(2)	Uani	O
C1A	0.0281(5)	0.0183(3)	0.8938(2)	0.0542(8)	Uani	C
C2A	-0.1429(6)	0.0892(4)	0.9215(2)	0.067(1)	Uani	C
C3A	-0.0787(6)	0.2257(4)	0.9241(2)	0.064(1)	Uani	C
C4A	0.1152(5)	0.2152(3)	0.8930(2)	0.0524(8)	Uani	C
C5A	0.0742(4)	0.1637(2)	0.8187(1)	0.0388(6)	Uani	C
C6A	0.2282(4)	0.1776(2)	0.7705(2)	0.0392(6)	Uani	C
C7A	0.1676(4)	0.1047(3)	0.7014(2)	0.0412(7)	Uani	C
C8A	0.1502(4)	-0.0340(3)	0.7059(2)	0.0466(7)	Uani	C
C9A	0.1708(4)	-0.0514(3)	0.7785(2)	0.0438(7)	Uani	C
C10A	0.0287(4)	0.0256(3)	0.8194(2)	0.0413(7)	Uani	C
C11A	0.1935(5)	0.1066(3)	0.9241(2)	0.0580(9)	Uani	C
C12A	0.4136(4)	0.1248(3)	0.7946(2)	0.0441(7)	Uani	C
C13A	0.3826(4)	-0.0158(3)	0.7903(2)	0.0466(7)	Uani	C
C14A	0.3167(5)	-0.1034(3)	0.6790(2)	0.0601(9)	Uani	C
C15A	-0.0147(5)	0.1517(3)	0.6730(2)	0.0513(8)	Uani	C
C16A	-0.2210(8)	0.1663(6)	0.5126(3)	0.106(2)	Uani	C
S1B	0.76080(1)	0.54292(8)	0.43420(4)	0.0521(2)	Uani	S
O1B	-0.0038(3)	0.3493(2)	0.2696(1)	0.0624(7)	Uani	O
O2B	-0.0124(3)	0.5660(2)	0.2389(2)	0.0732(8)	Uani	O
O3B	0.5685(3)	0.5301(3)	0.3936(1)	0.0809(9)	Uani	O
O4B	0.9079(3)	0.5826(3)	0.3964(1)	0.0678(7)	Uani	O
O5B	0.7842(5)	0.4342(3)	0.4593(2)	0.126(1)	Uani	O
C1B	0.4275(5)	0.2712(3)	0.1057(2)	0.0573(9)	Uani	C
C2B	0.6205(6)	0.2881(4)	0.0766(2)	0.070(1)	Uani	C
C3B	0.6341(6)	0.4283(4)	0.0755(2)	0.067(1)	Uani	C
C4B	0.4481(5)	0.4746(3)	0.1043(2)	0.0532(8)	Uani	C
C5B	0.4671(4)	0.4674(3)	0.1792(2)	0.0422(7)	Uani	C
C6B	0.3254(4)	0.5344(2)	0.2257(2)	0.0421(7)	Uani	C
C7B	0.3621(4)	0.5037(3)	0.2958(2)	0.0433(7)	Uani	C
C8B	0.3242(4)	0.3641(3)	0.2947(2)	0.0464(7)	Uani	C
C9B	0.2865(4)	0.3007(3)	0.2229(2)	0.0460(7)	Uani	C
C10B	0.4468(4)	0.3274(3)	0.1800(2)	0.0430(7)	Uani	C

A	B	C	D	E	F	G
C11B	0.3130(5)	0.3650(4)	0.0745(2)	0.063(1)	Uani	C
C12B	0.1221(4)	0.4931(3)	0.2026(2)	0.0480(8)	Uani	C
C13B	0.0929(4)	0.3556(3)	0.2101(2)	0.0504(8)	Uani	C
C14B	0.1367(5)	0.3390(3)	0.3228(2)	0.0605(9)	Uani	C
C15B	0.5598(5)	0.5469(4)	0.3242(2)	0.0580(9)	Uani	C
C16B	0.7178(7)	0.6572(5)	0.4980(2)	0.108(2)	Uani	C
HO2A	0.5926	0.0784	0.7287	0.067	Uani	H
HC1A	0.0367	-0.0665	0.9047	0.054	Uani	H
H1C2A	-0.1676	0.0716	0.9668	0.067	Uani	H
H2C2A	-0.2596	0.0680	0.8914	0.067	Uani	H
H1C3A	-0.0654	0.2698	0.9708	0.064	Uani	H
H2C3A	-0.1701	0.2689	0.8974	0.064	Uani	H
HC4A	0.1974	0.2916	0.9022	0.052	Uani	H
HC5A	-0.0434	0.2014	0.8027	0.039	Uani	H
HC6A	0.2495	0.2660	0.7672	0.039	Uani	H
HC7A	0.2700	0.1165	0.6710	0.041	Uani	H
HC8A	0.0277	-0.0714	0.6839	0.047	Uani	H
HC9A	0.1502	-0.1399	0.7820	0.044	Uani	H
HC10A	-0.1019	0.0044	0.7986	0.041	Uani	H
H1C11A	0.3194	0.0803	0.9080	0.058	Uani	H
H2C11A	0.2011	0.1220	0.9737	0.058	Uani	H
HC12A	0.4403	0.1605	0.8424	0.044	Uani	H
HC13A	0.4381	-0.0445	0.8310	0.047	Uani	H
H1C14A	0.2851	-0.1933	0.6693	0.060	Uani	H
H2C14A	0.3557	-0.0746	0.6376	0.060	Uani	H
H1C15A	0.0003	0.2409	0.6703	0.051	Uani	H
H2C15A	-0.1224	0.1385	0.7010	0.051	Uani	H
H1C16A	-0.3432	0.1681	0.4856	0.106	Uani	H
H2C16A	-0.1852	0.2508	0.5360	0.106	Uani	H
H3C16A	-0.1192	0.1361	0.4827	0.106	Uani	H
HO2B	-0.0405	0.5059	0.2692	0.073	Uani	H
HC1B	0.3721	0.1857	0.0962	0.057	Uani	H
H1C2B	0.6230	0.2405	0.0308	0.070	Uani	H
H2C2B	0.7260	0.2624	0.1055	0.070	Uani	H
H1C3B	0.6425	0.4454	0.0291	0.067	Uani	H
H2C3B	0.7465	0.4672	0.1036	0.067	Uani	H
HC4B	0.4091	0.5557	0.0933	0.053	Uani	H
HC5B	0.5985	0.4959	0.1965	0.042	Uani	H
HC6B	0.3414	0.6248	0.2269	0.042	Uani	H
HC7B	0.2690	0.5487	0.3248	0.043	Uani	H
HC8B	0.4312	0.3268	0.3176	0.046	Uani	H
HC9B	0.2702	0.2103	0.2216	0.046	Uani	H
HC10B	0.5678	0.3000	0.1999	0.043	Uani	H
H1C11B	0.1819	0.3731	0.0904	0.063	Uani	H
H2C11B	0.3061	0.3490	0.0249	0.063	Uani	H
HC12B	0.1018	0.5005	0.1546	0.048	Uani	H
HC13B	0.0214	0.3081	0.1702	0.050	Uani	H

A	B	C	D	E	F	G
H1C14B	0.1314	0.2549	0.3349	0.060	Uani	H
H2C14B	0.1164	0.4007	0.3629	0.060	Uani	H
H1C15B	0.5821	0.6352	0.3208	0.058	Uani	H
H2C15B	0.6572	0.4970	0.2998	0.058	Uani	H
H1C16B	0.8342	0.6747	0.5286	0.108	Uani	H
H2C16B	0.6835	0.7329	0.4797	0.108	Uani	H
H3C16B	0.6107	0.6307	0.5230	0.108	Uani	H

A atom site aniso label

B atom site aniso U 11

C atom site aniso U 22

D atom site aniso U 33

E atom site aniso U 12

F atom site aniso U 13

G atom site aniso U 23

A	B	C	D	E	F	G
S1A	0.0626(6)	0.0647(6)	0.0552(5)	-0.0080(4)	-0.0131(4)	0.0111(4)
O1A	0.053(1)	0.051(1)	0.079(2)	0.019(1)	0.003(1)	0.006(1)
O2A	0.040(1)	0.058(2)	0.105(2)	-0.003(1)	0.006(1)	0.017(1)
O3A	0.062(2)	0.111(2)	0.050(1)	0.023(2)	-0.013(1)	0.001(1)
O4A	0.054(2)	0.220(4)	0.076(2)	-0.004(2)	0.000(2)	0.015(2)
O5A	0.172(4)	0.066(2)	0.215(5)	-0.013(2)	-0.068(3)	-0.015(3)
C1A	0.060(2)	0.050(2)	0.056(2)	-0.001(2)	0.000(2)	0.019(2)
C2A	0.064(2)	0.078(3)	0.060(2)	0.004(2)	0.012(2)	0.016(2)
C3A	0.069(2)	0.064(2)	0.060(2)	0.010(2)	0.014(2)	0.004(2)
C4A	0.061(2)	0.044(2)	0.050(2)	-0.003(1)	-0.006(2)	0.004(1)
C5A	0.037(1)	0.032(1)	0.046(2)	0.003(1)	-0.006(1)	0.006(1)
C6A	0.038(1)	0.029(1)	0.052(2)	0.001(1)	-0.005(1)	0.012(1)
C7A	0.038(2)	0.038(2)	0.049(2)	0.004(1)	0.000(1)	0.011(1)
C8A	0.047(2)	0.039(2)	0.052(2)	0.000(1)	-0.008(1)	0.004(1)
C9A	0.044(2)	0.029(1)	0.058(2)	-0.001(1)	-0.005(1)	0.009(1)
C10A	0.038(2)	0.036(2)	0.051(2)	-0.003(1)	-0.003(1)	0.010(1)
C11A	0.064(2)	0.062(2)	0.048(2)	0.001(2)	-0.012(2)	0.012(2)
C12A	0.031(1)	0.041(2)	0.060(2)	0.000(1)	-0.004(1)	0.011(1)
C13A	0.043(2)	0.039(2)	0.059(2)	0.007(1)	-0.007(1)	0.013(1)
C14A	0.065(2)	0.046(2)	0.066(2)	0.013(2)	-0.003(2)	-0.001(2)
C15A	0.050(2)	0.058(2)	0.046(2)	0.010(2)	-0.010(1)	0.010(2)
C16A	0.106(4)	0.129(5)	0.093(4)	0.009(3)	-0.015(3)	0.059(4)
S1B	0.0516(5)	0.0514(5)	0.0518(5)	-0.0036(3)	-0.0080(4)	0.0087(3)
O1B	0.043(1)	0.055(1)	0.089(2)	-0.008(1)	0.004(1)	0.012(1)
O2B	0.053(1)	0.056(2)	0.113(2)	0.024(1)	0.006(1)	0.018(2)
O3B	0.048(1)	0.147(3)	0.045(1)	-0.023(2)	-0.007(1)	0.015(2)
O4B	0.046(1)	0.091(2)	0.066(2)	-0.006(1)	-0.001(1)	0.013(1)
O5B	0.107(3)	0.091(3)	0.195(4)	-0.001(2)	-0.015(3)	0.081(3)
C1B	0.065(2)	0.045(2)	0.057(2)	0.006(2)	-0.008(2)	-0.003(2)
C2B	0.075(3)	0.079(3)	0.055(2)	0.024(2)	0.007(2)	0.001(2)

A	B	C	D	E	F	G
C3B	0.067(2)	0.085(3)	0.051(2)	0.006(2)	0.004(2)	0.013(2)
C4B	0.058(2)	0.053(2)	0.049(2)	0.006(2)	-0.008(2)	0.011(2)
C5B	0.039(2)	0.040(2)	0.046(2)	0.001(1)	-0.010(1)	0.008(1)
C6B	0.044(2)	0.029(1)	0.052(2)	0.000(1)	-0.007(1)	0.007(1)
C7B	0.038(2)	0.037(2)	0.051(2)	-0.003(1)	-0.004(1)	0.002(1)
C8B	0.045(2)	0.039(2)	0.057(2)	0.005(1)	-0.002(1)	0.013(1)
C9B	0.047(2)	0.029(1)	0.061(2)	0.004(1)	-0.006(1)	0.008(1)
C10B	0.041(2)	0.036(2)	0.050(2)	0.010(1)	-0.008(1)	0.005(1)
C11B	0.067(2)	0.064(2)	0.052(2)	0.005(2)	-0.022(2)	0.002(2)
C12B	0.039(2)	0.040(2)	0.063(2)	0.008(1)	-0.010(1)	0.005(1)
C13B	0.041(2)	0.039(2)	0.068(2)	-0.006(1)	-0.012(2)	0.003(1)
C14B	0.060(2)	0.049(2)	0.075(3)	-0.011(2)	0.008(2)	0.016(2)
C15B	0.049(2)	0.078(3)	0.044(2)	-0.019(2)	-0.007(1)	0.005(2)
C16B	0.101(4)	0.113(4)	0.092(4)	-0.034(3)	0.028(3)	-0.043(3)

E.4.2.6 Molecular Geometry

A geom bond atom site label 1

B geom bond atom site label 2

C geom bond distance

A	B	C
S1A	O3A	1.546(2)
S1A	O4A	1.419(3)
S1A	O5A	1.388(4)
S1A	C16A	1.715(5)
O1A	C13A	1.449(4)
O1A	C14A	1.445(4)
O2A	C12A	1.404(4)
O3A	C15A	1.477(4)
C1A	C2A	1.544(5)
C1A	C10A	1.536(4)
C1A	C11A	1.540(5)
C2A	C3A	1.558(6)
C3A	C4A	1.542(5)
C4A	C5A	1.546(4)
C4A	C11A	1.545(5)
C5A	C6A	1.530(4)
C5A	C10A	1.557(4)
C6A	C7A	1.543(4)
C6A	C12A	1.535(4)
C7A	C8A	1.554(4)
C7A	C15A	1.521(4)
C8A	C9A	1.527(4)
C8A	C14A	1.504(4)
C9A	C10A	1.532(4)

A	B	C
C9A	C13A	1.533(4)
C12A	C13A	1.553(4)
S1B	O3B	1.542(2)
S1B	O4B	1.430(3)
S1B	O5B	1.390(3)
S1B	C16B	1.714(4)
O1B	C13B	1.440(4)
O1B	C14B	1.451(4)
O2B	C12B	1.427(4)
O3B	C15B	1.459(4)
C1B	C2B	1.537(5)
C1B	C10B	1.546(4)
C1B	C11B	1.527(5)
C2B	C3B	1.556(6)
C3B	C4B	1.538(5)
C4B	C5B	1.544(4)
C4B	C11B	1.548(5)
C5B	C6B	1.543(4)
C5B	C10B	1.554(4)
C6B	C7B	1.534(4)
C6B	C12B	1.522(4)
C7B	C8B	1.557(4)
C7B	C15B	1.517(4)
C8B	C9B	1.529(4)
C8B	C14B	1.511(4)
C9B	C10B	1.522(4)
C9B	C13B	1.536(4)
C12B	C13B	1.563(4)

A geom angle atom site label 1

B geom angle atom site label 2

C geom angle atom site label 3

D geom angle

A	B	C	D
O3A	S1A	O4A	111.6(2)
O3A	S1A	O5A	107.1(2)
O3A	S1A	C16A	101.9(2)
O4A	S1A	O5A	120.8(3)
O4A	S1A	C16A	107.4(3)
O5A	S1A	C16A	106.3(3)
C13A	O1A	C14A	108.3(2)
S1A	O3A	C15A	120.5(2)
C2A	C1A	C10A	107.8(3)
C2A	C1A	C11A	100.8(3)
C10A	C1A	C11A	103.0(3)
C1A	C2A	C3A	103.2(3)

A	B	C	D
C2A	C3A	C4A	102.6(3)
C3A	C4A	C5A	106.5(3)
C3A	C4A	C11A	99.7(3)
C5A	C4A	C11A	104.9(3)
C4A	C5A	C6A	118.8(2)
C4A	C5A	C10A	102.7(2)
C6A	C5A	C10A	109.9(2)
C5A	C6A	C7A	109.8(2)
C5A	C6A	C12A	110.0(2)
C7A	C6A	C12A	107.6(2)
C6A	C7A	C8A	109.6(2)
C6A	C7A	C15A	111.4(2)
C8A	C7A	C15A	112.0(2)
C7A	C8A	C9A	109.4(2)
C7A	C8A	C14A	112.5(3)
C9A	C8A	C14A	100.6(2)
C8A	C9A	C10A	110.7(2)
C8A	C9A	C13A	97.2(2)
C10A	C9A	C13A	118.7(2)
C1A	C10A	C5A	103.1(2)
C1A	C10A	C9A	117.8(2)
C5A	C10A	C9A	109.2(2)
C1A	C11A	C4A	93.7(2)
O2A	C12A	C6A	112.7(2)
O2A	C12A	C13A	112.3(2)
C6A	C12A	C13A	108.4(2)
O1A	C13A	C9A	103.9(2)
O1A	C13A	C12A	108.8(3)
C9A	C13A	C12A	110.3(2)
O1A	C14A	C8A	104.6(3)
O3A	C15A	C7A	105.3(2)
O3B	S1B	O4B	110.8(1)
O3B	S1B	O5B	106.8(2)
O3B	S1B	C16B	101.4(2)
O4B	S1B	O5B	117.8(2)
O4B	S1B	C16B	109.7(2)
O5B	S1B	C16B	109.0(3)
C13B	O1B	C14B	108.4(2)
S1B	O3B	C15B	119.9(2)
C2B	C1B	C10B	107.8(3)
C2B	C1B	C11B	100.4(3)
C10B	C1B	C11B	103.1(3)
C1B	C2B	C3B	102.8(3)
C2B	C3B	C4B	103.5(3)
C3B	C4B	C5B	106.6(3)
C3B	C4B	C11B	99.5(3)
C5B	C4B	C11B	104.3(3)

A	B	C	D
C4B	C5B	C6B	119.4(2)
C4B	C5B	C10B	102.6(2)
C6B	C5B	C10B	109.2(2)
C5B	C6B	C7B	109.5(2)
C5B	C6B	C12B	111.0(2)
C7B	C6B	C12B	107.5(2)
C6B	C7B	C8B	109.6(2)
C6B	C7B	C15B	111.2(3)
C8B	C7B	C15B	112.7(3)
C7B	C8B	C9B	109.4(2)
C7B	C8B	C14B	111.5(3)
C9B	C8B	C14B	100.6(3)
C8B	C9B	C10B	111.5(2)
C8B	C9B	C13B	97.2(2)
C10B	C9B	C13B	118.2(3)
C1B	C10B	C5B	103.7(2)
C1B	C10B	C9B	117.6(3)
C5B	C10B	C9B	110.0(2)
C1B	C11B	C4B	94.4(3)
O2B	C12B	C6B	112.0(3)
O2B	C12B	C13B	110.3(3)
C6B	C12B	C13B	108.8(2)
O1B	C13B	C9B	104.4(3)
O1B	C13B	C12B	108.7(3)
C9B	C13B	C12B	109.5(2)
O1B	C14B	C8B	104.4(3)
O3B	C15B	C7B	106.3(3)

A geom torsion atom site label 1

B geom torsion atom site label 2

C geom torsion atom site label

D geom torsion atom site label 4

E geom torsion

A	B	C	D	E
O4A	S1A	O3A	C15A	-9.8(4)
O5A	S1A	O3A	C15A	-144.1(4)
C16A	S1A	O3A	C15A	104.5(3)
C14A	O1A	C13A	C9A	20.9(3)
C14A	O1A	C13A	C12A	-96.6(3)
C13A	O1A	C14A	C8A	10.8(3)
S1A	O3A	C15A	C7A	160.6(2)
C10A	C1A	C2A	C3A	-74.0(3)
C11A	C1A	C2A	C3A	33.6(3)
C2A	C1A	C10A	C5A	67.2(3)
C2A	C1A	C10A	C9A	-172.5(3)
C11A	C1A	C10A	C5A	-38.9(3)

A	B	C	D	E
C11A	C1A	C10A	C9A	81.4(3)
C2A	C1A	C11A	C4A	-57.0(3)
C10A	C1A	C11A	C4A	54.4(3)
C1A	C2A	C3A	C4A	3.7(3)
C2A	C3A	C4A	C5A	69.3(3)
C2A	C3A	C4A	C11A	-39.5(3)
C3A	C4A	C5A	C6A	162.2(2)
C3A	C4A	C5A	C10A	-76.2(3)
C11A	C4A	C5A	C6A	-92.6(3)
C11A	C4A	C5A	C10A	28.9(3)
C3A	C4A	C11A	C1A	59.3(3)
C5A	C4A	C11A	C1A	-50.8(3)
C4A	C5A	C6A	C7A	172.2(2)
C4A	C5A	C6A	C12A	54.1(3)
C10A	C5A	C6A	C7A	54.4(3)
C10A	C5A	C6A	C12A	-63.8(3)
C4A	C5A	C10A	C1A	5.9(3)
C4A	C5A	C10A	C9A	-120.2(3)
C6A	C5A	C10A	C1A	133.3(2)
C6A	C5A	C10A	C9A	7.2(3)
C5A	C6A	C7A	C8A	-63.6(3)
C5A	C6A	C7A	C15A	61.0(3)
C12A	C6A	C7A	C8A	56.1(3)
C12A	C6A	C7A	C15A	-179.4(2)
C5A	C6A	C12A	O2A	-168.7(2)
C5A	C6A	C12A	C13A	66.4(3)
C7A	C6A	C12A	O2A	71.7(3)
C7A	C6A	C12A	C13A	-53.1(3)
C6A	C7A	C8A	C9A	8.0(3)
C6A	C7A	C8A	C14A	-102.9(3)
C15A	C7A	C8A	C9A	-116.2(3)
C15A	C7A	C8A	C14A	132.9(3)
C6A	C7A	C15A	O3A	176.6(2)
C8A	C7A	C15A	O3A	-60.3(3)
C7A	C8A	C9A	C10A	54.4(3)
C7A	C8A	C9A	C13A	-70.1(3)
C14A	C8A	C9A	C10A	173.0(2)
C14A	C8A	C9A	C13A	48.5(3)
C7A	C8A	C14A	O1A	78.3(3)
C9A	C8A	C14A	O1A	-38.0(3)
C8A	C9A	C10A	C1A	179.4(2)
C8A	C9A	C10A	C5A	-63.5(3)
C13A	C9A	C10A	C1A	-69.5(3)
C13A	C9A	C10A	C5A	47.5(3)
C8A	C9A	C13A	O1A	-42.9(3)
C8A	C9A	C13A	C12A	73.5(3)
C10A	C9A	C13A	O1A	-161.3(2)

A	B	C	D	E
C10A	C9A	C13A	C12A	-44.9(4)
O2A	C12A	C13A	O1A	-24.1(3)
O2A	C12A	C13A	C9A	-137.5(3)
C6A	C12A	C13A	O1A	101.1(3)
C6A	C12A	C13A	C9A	-12.3(4)
O4B	S1B	O3B	C15B	5.5(4)
O5B	S1B	O3B	C15B	-124.0(4)
C16B	S1B	O3B	C15B	122.0(3)
C14B	O1B	C13B	C9B	20.7(3)
C14B	O1B	C13B	C12B	-96.0(3)
C13B	O1B	C14B	C8B	10.6(3)
S1B	O3B	C15B	C7B	168.9(2)
C10B	C1B	C2B	C3B	-71.1(3)
C11B	C1B	C2B	C3B	36.4(3)
C2B	C1B	C10B	C5B	69.8(3)
C2B	C1B	C10B	C9B	-168.5(3)
C11B	C1B	C10B	C5B	-35.8(3)
C11B	C1B	C10B	C9B	85.8(3)
C2B	C1B	C11B	C4B	-58.1(3)
C10B	C1B	C11B	C4B	53.1(3)
C1B	C2B	C3B	C4B	0.3(3)
C2B	C3B	C4B	C5B	71.9(3)
C2B	C3B	C4B	C11B	-36.2(3)
C3B	C4B	C5B	C6B	166.0(3)
C3B	C4B	C5B	C10B	-73.2(3)
C11B	C4B	C5B	C6B	-89.4(3)
C11B	C4B	C5B	C10B	31.4(3)
C3B	C4B	C11B	C1B	57.9(3)
C5B	C4B	C11B	C1B	-52.0(3)
C4B	C5B	C6B	C7B	174.8(3)
C4B	C5B	C6B	C12B	56.3(3)
C10B	C5B	C6B	C7B	57.3(3)
C10B	C5B	C6B	C12B	-61.1(3)
C4B	C5B	C10B	C1B	2.4(3)
C4B	C5B	C10B	C9B	-124.2(3)
C6B	C5B	C10B	C1B	130.0(3)
C6B	C5B	C10B	C9B	3.4(3)
C5B	C6B	C7B	C8B	-63.4(3)
C5B	C6B	C7B	C15B	61.8(3)
C12B	C6B	C7B	C8B	57.2(3)
C12B	C6B	C7B	C15B	-177.5(3)
C5B	C6B	C12B	O2B	-171.6(2)
C5B	C6B	C12B	C13B	66.3(3)
C7B	C6B	C12B	O2B	68.7(3)
C7B	C6B	C12B	C13B	-53.4(3)
C6B	C7B	C8B	C9B	6.9(3)
C6B	C7B	C8B	C14B	-103.6(3)

A	B	C	D	E
C15B	C7B	C8B	C9B	-117.5(3)
C15B	C7B	C8B	C14B	132.1(3)
C6B	C7B	C15B	O3B	171.6(3)
C8B	C7B	C15B	O3B	-65.0(4)
C7B	C8B	C9B	C10B	54.6(3)
C7B	C8B	C9B	C13B	-69.6(3)
C14B	C8B	C9B	C10B	172.1(2)
C14B	C8B	C9B	C13B	48.0(3)
C7B	C8B	C14B	O1B	78.3(3)
C9B	C8B	C14B	O1B	-37.6(3)
C8B	C9B	C10B	C1B	-179.0(2)
C8B	C9B	C10B	C5B	-60.7(3)
C13B	C9B	C10B	C1B	-67.7(3)
C13B	C9B	C10B	C5B	50.7(3)
C8B	C9B	C13B	O1B	-42.6(3)
C8B	C9B	C13B	C12B	73.6(3)
C10B	C9B	C13B	O1B	-161.8(2)
C10B	C9B	C13B	C12B	-45.6(4)
O2B	C12B	C13B	O1B	-22.4(3)
O2B	C12B	C13B	C9B	-135.8(3)
C6B	C12B	C13B	O1B	100.8(3)
C6B	C12B	C13B	C9B	-12.6(4)

E.5 REPRESENTATIVE PROTON NMR DATA

This section provides selected expansions of the 500 MHz ^1H -NMR spectrum of the bis-porphyrin-TCNQ target **48**. The spectrum of **48** features aspects characteristic for the series of porphyrin adducts synthesised throughout this thesis and it can be seen as a representative example of its kind. Whereas mostly 300 MHz spectra are depicted above, the spectroscopic data given in the Experimental Part are often based on 500 MHz spectra, which allow the determination of the small coupling constants given. COSY experiments were carried out for the assignment of most proton signals.

The 300 MHz ^1H -NMR spectrum of bis-porphyrin-TCNQ **48** is given in **Figure 28** on page 65. The expansion of the 500 MHz spectrum given here (**Figure 82**) reveals the slightly different chemical shifts for the two pairs of β -pyrrolic protons at 8.648 ppm and 8.650 ppm, respectively. Slightly different chemical shifts can also be expected for the remaining eight lateral β -pyrrolic protons, which results in the pattern depicted in the spectrum below rather than in an often observed AB quartet (**31**, **32**, **34**, **35**, **43**, **46**, **100**, **106**, **108**, **153**, **154**). The COSY experiment revealed the coupling between the inner porphyrin protons (with a chemical shift of -2.61 ppm and -2.62 ppm, respectively) and the β -pyrrolic protons.

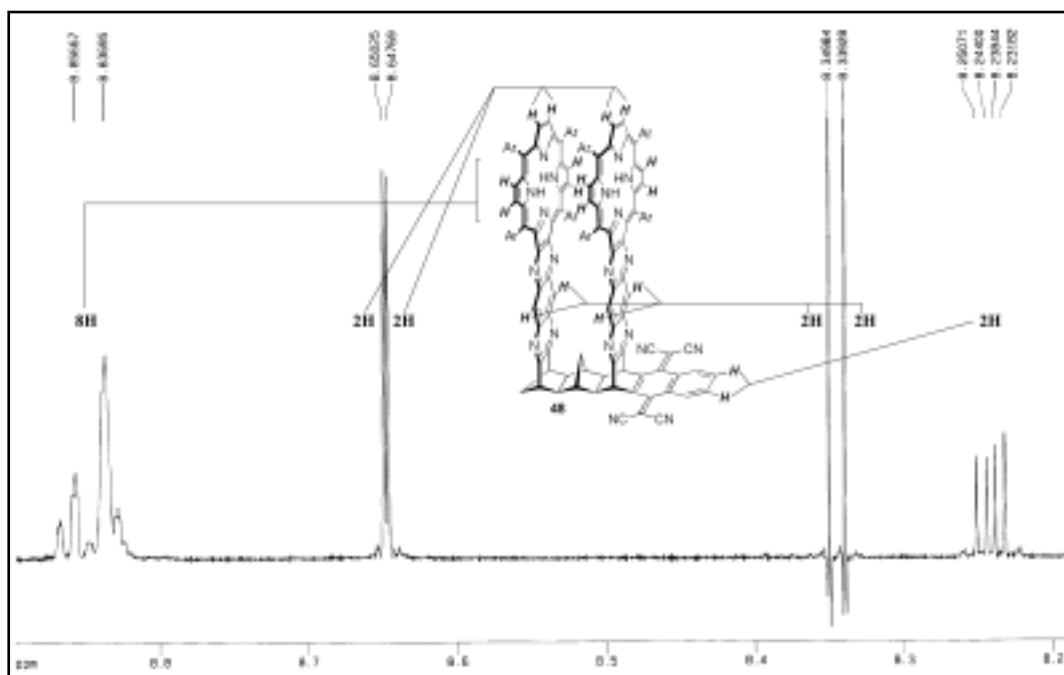
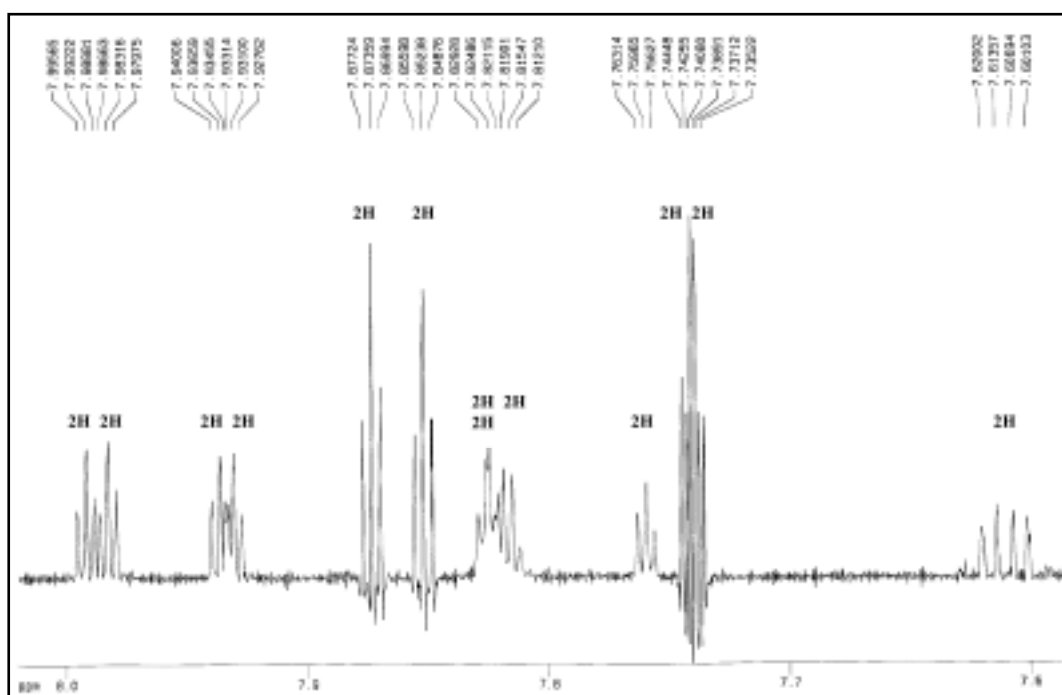


Figure 82: ^1H -NMR expansion (500 MHz, 8.2 ppm to 9.0 ppm) of bis-porphyrin-TCNQ **48**

The four quinoxaline protons of the two donor moieties give two singlets at 8.34 ppm and 8.35 ppm, respectively. The four aromatic protons of the TCNQ acceptor show as doublets of doublets at 8.24 ppm (**Figure 82**) and 7.61 ppm (**Figure 83**), respectively. Coupling constants for these protons typically range between 5.6 to 6.4 ppm and 2.9 to 3.4 ppm, depending on the type of acceptor (DMN, NQ, TCNQ). The triplets observed for the 24 aromatic protons of the eight 3,5-di-*tert*-butylphenyl groups show small coupling constants of 1.7 Hz and 1.8 Hz, respectively, and chemical shifts between 7.7 and 8.0 ppm (**Figure 83**).



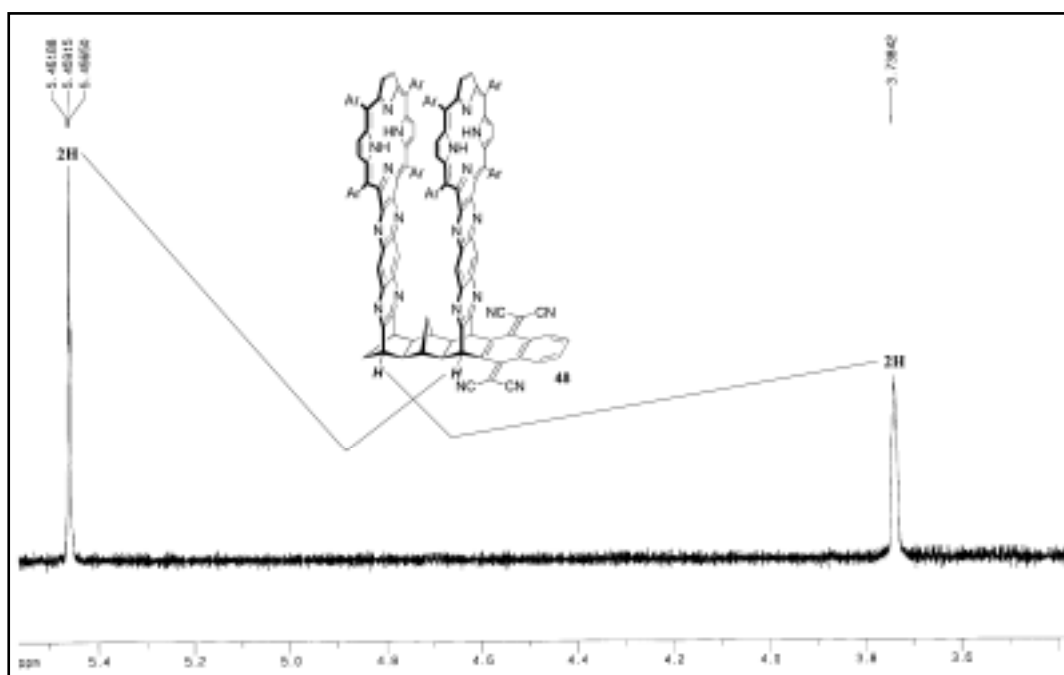


Figure 84: ^1H -NMR expansion (500 MHz, 3.5 ppm to 5.5 ppm) of bis-porphyrin-TCNQ 48

The proton signals for the carbon backbone can be assigned as depicted in **Figure 85**. The methylene bridge protons appear as doublets at 2.06 ppm and 2.14 ppm ($J = 9.4$ Hz), and at -0.84 ppm and -0.68 ppm for the methylene bridge protons between the two aromatic systems. The strong up-field shift has been discussed in **B.2.3 Condensations** (page 60) and the observed coupling constant ($J = 12.1$ Hz) is within the usually observed range.

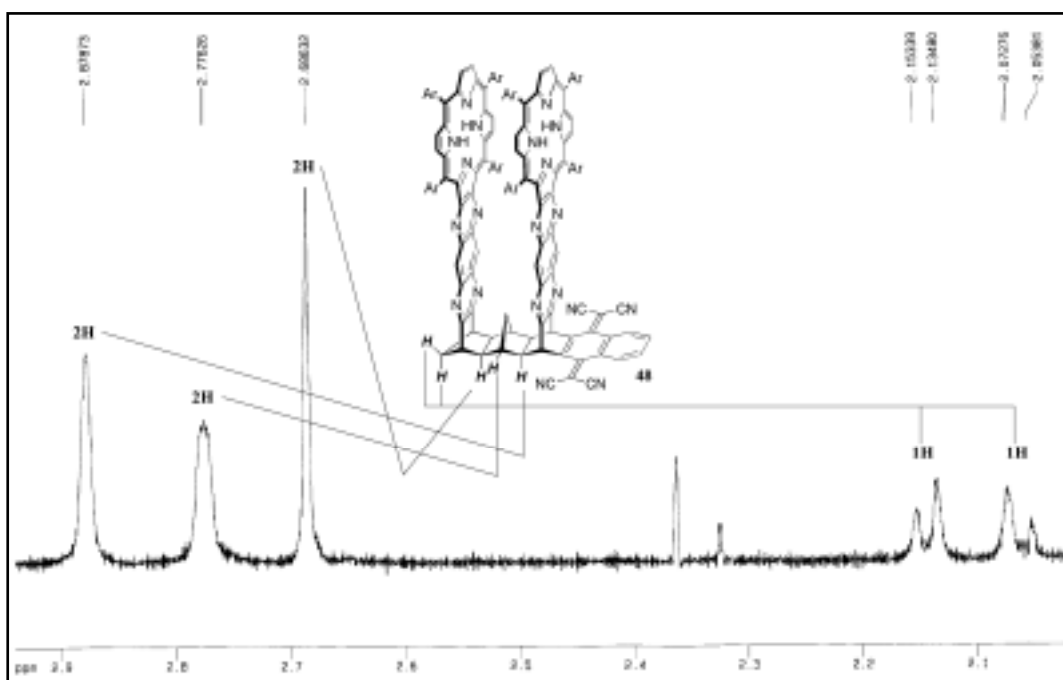


Figure 85: ^1H -NMR expansion (500 MHz, 2.0 ppm to 2.9 ppm) of bis-porphyrin-TCNQ **48**

The 500 MHz ^1H -NMR spectrum shows four distinct singlets integrating to 18 protons each and two singlets counting for 36 protons each (**Figure 86**). For some compounds (e.g. the DMN equivalent **36**) eight singlets can be observed.

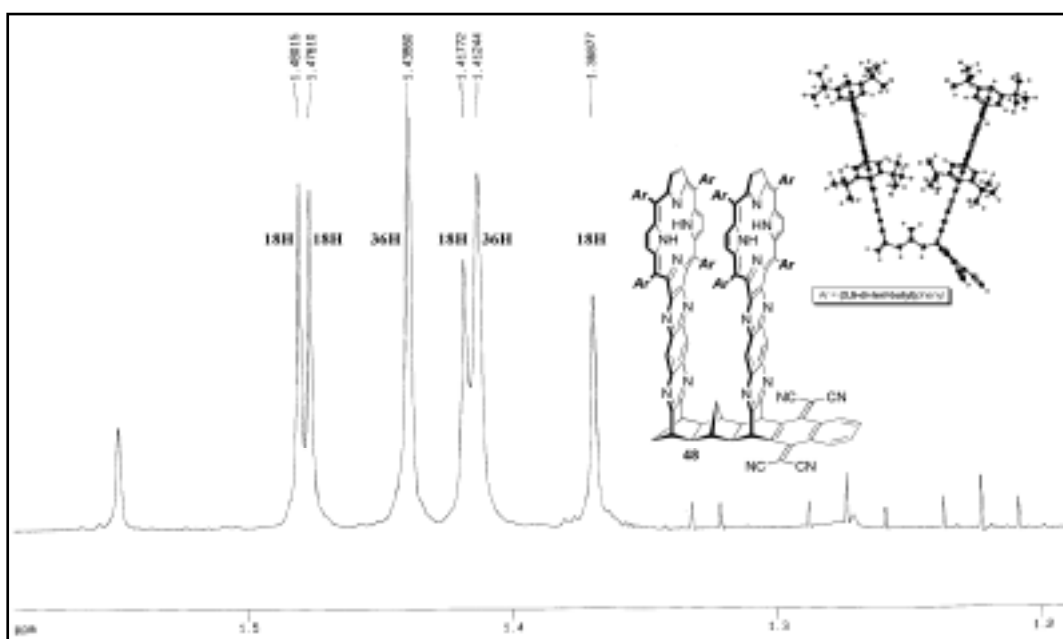


Figure 86: ^1H -NMR expansion (500 MHz, 1.2 ppm to 1.6 ppm) of bis-porphyrin-TCNQ **48**

The inner protons of the porphyrin systems show as two singlets (here hardly resolved) at -2.61 ppm and -2.62 ppm, respectively (**Figure 87**).

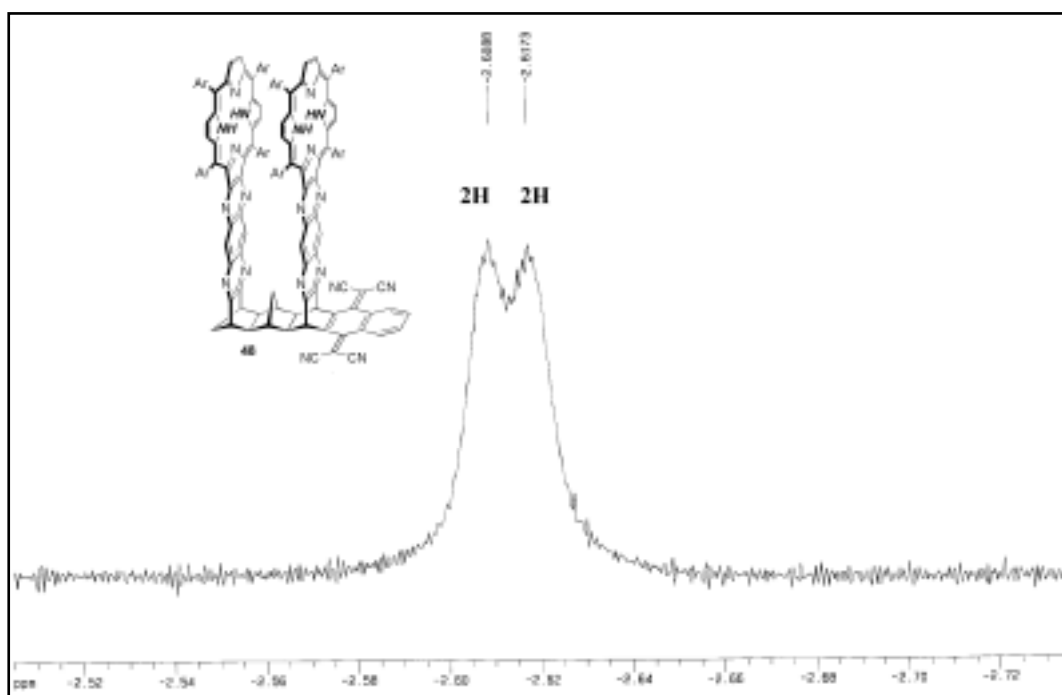


Figure 87: ¹H-NMR expansion (500 MHz, -2.7 ppm to -2.5 ppm) of bis-porphyrin-TCNQ 48

E.6 CAPTIONS

E.6.1 List of Equations

Equation 1: Definition of the electronic coupling element H_{rp}	4
Equation 2: Fermi's golden rule	5
Equation 3: Gibbs free energy of activation.....	7
Equation 4: First order rate constant in classical transition-state theory.....	7
Equation 5: Classical Marcus equation	7
Equation 6: Outer component of the total reorganisation energy	7
Equation 7: High-temperature limit of the semiclassical Marcus expressions	9
Equation 8: Classic equivalent	9
Equation 9: Rehm-Weller equation for infinite $[D^+]-[A^-]$ separation	10
Equation 10: Rehm-Weller equation for finite $[D^+]-[A^-]$ separation.....	10
Equation 11: Coulombic attraction energy	11
Equation 12: Exponential dependence of H_{rp} on distance.....	13
Equation 13: Rate constant - distance relation	14
Equation 14: Rehm-Weller equation for large donor-acceptor separation. E_{00} is the zero-zero electronic excitation energy to the first excited singlet state (D^*); $E_{ox}(D)$ and $E_{red}(A)$ are the oxidation and reduction potentials of donor and acceptor, respectively	69
Equation 15: Gibbs free energy of activation (Equation 3, page 7)	75
Equation 16: ΔV^* : activation volume; V^* : molar volume of transition state; ΣV : sum of partial molar volumes of reactants.....	100
Equation 17: Reaction volume - pressure - rate constant.....	100

E.6.2 List of Examples

Example 1: First intramolecular ET models by Miller <i>et al.</i> to establish experimentally the existence of the Marcus inverted region	11
Example 2: Intramolecular photoinduced ET models by Wasielewski <i>et al.</i> Proof for the existence of the Marcus inverted region	12
Example 3: Series of DMN-DCV dyads by the Paddon-Row group	14
Example 4: Bis-porphyrin dyads by Therien <i>et al.</i> (1995)	16

Example 5: Porphyrin-quinone dyads by Sakata <i>et al.</i> (1994)	17
Example 6: Porphyrin-quinone dyad by Schmidt <i>et al.</i> (1985)	18
Example 7: Chlorophyll-pyromellitimide-naphthalenediimide (Chl-PI-NI) triad by Wiederrecht <i>et al.</i> (1996)	19
Example 8: Porphyrin-quinone dyad by Tabushi <i>et al.</i> (1979).....	28
Example 9: Porphyrin-quinone dyads by Joran <i>et al.</i> (1985)	29
Example 10: Rigid porphyrin-quinone dyad by Antolovich <i>et al.</i> (1991).....	29
Example 11: Non-covalent porphyrin-quinone dyad by Sessler <i>et al.</i> (1993).....	31
Example 12: Capped porphyrin-ubiquinone dyads linked <i>via</i> multiple hydrogen bonds by Hayashi and Ogoshi (1994)	31
Example 13: Capped porphyrin-quinone dyad linked covalently by Staab <i>et al.</i> (1984).....	32
Example 14: Carotenoid-porphyrin-quinone [C-P-Q] triad by Moore, Gust and Moore (1987).....	33
Example 15: Carotenoid-porphyrin-naphthoquinone-benzoquinone tetrad by Moore, Gust and Moore (1988).....	34
Example 16: Carotenoid - porphyrin _{Zn} - porphyrin - naphthoquinone -benzoquinone pentad by Moore, Gust and Moore (1990).....	34
Example 17: Carotene-porphyrin-quinone dyad by Moore, Gust and Moore implanted into a lipid bilayer (1995)	36
Example 18: Bis-porphyrin arrays by Osuka <i>et al.</i> (1997).....	39
Example 19: Bis-porphyrin rotaxane by Harriman and Sauvage (1996).....	40
Example 20: Mono metallated bis-porphyrin quinone triads by Sessler <i>et al.</i> (1989)	41
Example 21: First bis-porphyrins covalently linked through the β -pyrrolic positions by Crossley <i>et al.</i> (1987).....	60

E.6.3 List of Figures

Figure 1: Photo-excitation followed by an electron-transfer step resulting in a high- energy charge-separated species.....	1
Figure 2: Electron transfer vs. electron transport	3
Figure 3: Schematic representations showing (a) thermal ET, (b) optical ET, and (c) photoinduced ET.....	3
Figure 4: (1) adiabatic and (2) nonadiabatic Gibbs free energy surfaces	5

Figure 5: Representation of the Gibbs free energy surfaces according to Marcus theory	6
Figure 6: Marcus "normal", "optimal" and "inverted" region	8
Figure 7: Schematic representation of the change in free energy (ΔG^0) for a photoinduced electron transfer reaction. E_{00} is the zero-zero electronic excitation energy to the first excited singlet state (D^*); $E_{ox}(D)$ and $E_{red}(A)$ are the oxidation and reduction potentials of D and A, respectively	10
Figure 8: Rate constant for the Wasielewski series Example 2 (a) - (e) vs. driving force $-\Delta G$	13
Figure 9: Energy diagram illustrating pathways available in a photoinduced electron-transfer event within a dyad [D-A].....	21
Figure 10: Energy diagram for multichromophoric concept	22
Figure 11: Proposed scheme for the evolution of photosynthetic reaction centres (after Nitschke and Rutherford, 1991, and Blankenship, 1992).....	24
Figure 12: Chromophores in the photosynthetic reaction centre (PRC) (this one of <i>Rhodopseudomonas viridis</i>).....	25
Figure 13: Downhill ET in PRC from a photo-excited 'special pair'	27
Figure 14: Transient states for Example 16 by Moore, Gust and Moore.....	35
Figure 15: Photoelectrochemical cycle of the 'proton pump' generating a pH gradient across a liposome bilayer	37
Figure 16: Diagram of a liposome-based artificial photosynthetic membrane by Moore, Gust and Moore (1998).....	38
Figure 17: Sought after rigid model of the photosynthetic reaction centre (PRC). SP: 'special pair', A1: primary acceptor, A2: secondary acceptor.....	42
Figure 18: Comparison with the L-branch of the photosynthetic reaction centre of <i>Rhodopseudomonas viridis</i> determined the synthetic goal. Interchromophoric separations are given in Å.....	43
Figure 19: The kinked model of the photosynthetic reaction centre. Only two pyrrole rings are staggered above each other	44
Figure 20: Series of targets derived from comparison with PRC's.....	44
Figure 21: <i>Syn</i> - and <i>anti</i> -isomers result in four different shapes: y, w, s, and u.....	45
Figure 22: Series of bichromophoric targets closely related to triads	46
Figure 23: (A) Representation of selected chemical shifts (proton and carbon); (B) The '2B' and '6B' numbering concept used throughout this thesis.....	49
Figure 24: Four target molecules per acceptor group (DMN or TCNQ).....	49

Figure 25: Retrosynthetic approach for chromophore attachment	50
Figure 26: Retrosynthetic approach for dione/tetraone synthesis.....	51
Figure 27: Selected ^{13}C -NMR chemical shifts (75.5 MHz) for the isolated ring-expanded systems 6B-ene-2B-ene-DMN (13), 6B-ene-2B-diol-DMN (18), and 6B-diol-2B-diol-DMN (20).....	55
Figure 28: ^1H -NMR spectrum (300 MHz) of bis-porphyrin-DMN 36.....	65
Figure 29: Detail of COSY spectrum (500 MHz) of bis-porphyrin-DMN 36.....	65
Figure 30: UV-Vis spectra of bis-porphyrin-DMN 36 and 6B-porphyrin-DMN 32 in dichloromethane	66
Figure 31: Absorption and emission spectrum of bis-porphyrin-DMN 36.....	67
Figure 32: Redox potentials of related acceptor and donor chromophores	69
Figure 33: ^1H -NMR spectrum (300 MHz) of bis-porphyrin-TCNQ 48.....	72
Figure 34: ^{13}C -NMR spectrum (75.5 MHz) of bis-porphyrin-TCNQ 48.....	73
Figure 35: Up field shift of inner-proton resonance in bis-porphyrin systems compared to the 6B- and 2B-mono-porphyrin dyads.....	74
Figure 36: Fluorescence spectra of 6B-porphyrin-DMN 32 and 6B-porphyrin-TCNQ; 94 % quenching	76
Figure 37: Two-times three targets in the triad synthesis (w/u- and y/s-shaped) and the AM1 calculated structures of <i>anti</i> and <i>syn</i> bis-porphyrin-NQ-TCNQ	77
Figure 38: Envisaged sequence of ET processes for the series of triads	78
Figure 39: Redox potentials of relevant donor and acceptor chromophores ^{113,164,169}	78
Figure 40: Retrosynthetic approach for the triad synthesis	79
Figure 41: Stereoisomeric forms of the ring-expanded <i>trans</i> -diester 60.....	81
Figure 42: AM1-optimised structures for the 2B-ene- <i>trans</i> -diester 58 and 2B-ene- <i>cis</i> -diester 63.....	84
Figure 43: ^1H -NMR spectrum (300 MHz) of a mixture (2:3) of 2B-ene- <i>cis</i> -diester 63 and 2B-ene- <i>trans</i> -diester 58 as found after attempted OsO_4 -reaction at 80 °C.....	85
Figure 44: X-ray structure of mono-ring-closed mesyl derivative 69	87
Figure 45: Carbon chemical shifts for the mono and double cyclic ethers.....	88
Figure 46: Selected ^1H -NMR and ^{13}C -NMR chemical shifts of the 2B-diones 79 and 80 formed under <i>Sharpless</i> bis-hydroxylation conditions	89
Figure 47: X-ray structure for the 2B-dione- <i>trans</i> -diacetate 79	90

Figure 48: Controlled attachment of two different porphyrin moieties (A and B) through (a) selective 'bis-ketonisation' followed by (b) condensation, (c) TEMPO reaction, and (d) condensation of second porphyrin.....	93
Figure 49: ^1H -NMR spectrum (300 MHz) of 95	96
Figure 50: ^{13}C -NMR spectrum (75.5 MHz) of 6B-dione-2B-dione- <i>trans</i> -diacetate 95	96
Figure 51: Comparison of carbonyl group accessibility in dyad 28 (left) and triad donor systems 79 (right)	97
Figure 52: High pressure apparatus at Griffith University, Queensland	101
Figure 53: ^{13}C -NMR spectrum (75.5 MHz) of the mono-hydrolysed 2B-porphyrin- <i>trans</i> -ol-acetate 105	106
Figure 54: ^1H -NMR chemical shifts of the methylene-bridge protons for the 2B-porphyrin- <i>trans</i> -diacetate 103 and the 2B-porphyrin- <i>trans</i> -diol 104.....	107
Figure 55: Selected ^{13}C -NMR chemical shifts for the 6B-porphyrin-hemi-acetals 106 and 107 formed in pyridine.....	108
Figure 56: ^1H -NMR spectrum (300 MHz) of bis-porphyrin- <i>trans</i> -diacetate 109	110
Figure 57: MALDI mass spectra of 6B-porphyrin-2B-dione- <i>trans</i> -diacetate 108 and bis-porphyrin- <i>trans</i> -diacetate 109	111
Figure 58: ^1H -NMR spectrum (300 MHz) of 2B-porphyrin-dimethylidene 112	114
Figure 59: Vicinal and long-range (W-type) couplings to assist assignment of signals hidden under the giant <i>tert</i> -butyl signals of 2B-porphyrin-dimethylidene 112.....	115
Figure 60: ^{13}C -NMR spectrum (75.5 Hz) of the 2B-porphyrin-dimethylidene 112.....	116
Figure 61: Norbornylogous bridge designed for the attachment of donor and acceptor moieties <i>via</i> Diels-Alder methodology	117
Figure 62: ^{13}C chemical shifts of the mono-hydroxymethyl-mono-methyl side product 124	118
Figure 63: W-type coupling of <i>endo</i> -protons with one methylene bridge proton in 120.....	119
Figure 64: MALDI mass spectra obtained for the proposed 2B-porphyrin-NQ-TCNQ triad 135.....	124
Figure 65: Anticipated ^1H -NMR shifts of the proposed 2B-porphyrin-NQ-TCNQ triad 135 (pictured: 135- <i>syn</i>).....	125
Figure 66: ^{13}C -NMR spectrum (75.5 MHz) of the proposed 2B-porphyrin-NQ-TCNQ triad 135.....	126
Figure 67: Selected ^{13}C -NMR chemical shifts of the proposed 2B-porphyrin-NQ-TCNQ triad 135 (pictured: 135- <i>syn</i>).....	126

Figure 68: 6B-porphyrin-TCNQ 46 and the comparable all- <i>trans</i> -analogues	128
Figure 69: Electron transfer pathways for the non-ring-expanded (left) and ring-expanded norbornylogous bridge	129
Figure 70: Constructive interference to a large extent: a 'superbridge'!	130
Figure 71: Selected ¹ H-NMR data of the all- <i>trans</i> ring-expanded 6B-ene-DMN 144.....	132
Figure 72: ¹³ C-NMR spectrum (75.5 MHz) of the all- <i>trans</i> ring-expanded 6B-ene-DMN 144.....	132
Figure 73: ¹ H-NMR spectrum (300 MHz) of the ring-expanded all- <i>trans</i> -6B-porphyrin-DMN 147.....	133
Figure 74: MALDI mass spectrum of the all- <i>trans</i> ring-expanded 6B-porphyrin-DMN 147	134
Figure 75: Interaction despite 12 Å separation (AM 1).....	140
Figure 76: Controlled attachment of two different porphyrin moieties (A and B) through (a) selective 'bis-ketonisation' followed by (b) condensation, (c) TEMPO reaction, and (d) condensation of second porphyrin.....	144
Figure 77: Triad components 2B-porphyrin-2,3-dimethylidene 112, bridge 123, acceptor precursor 129, and the bridge-acceptor component 133.....	147
Figure 78: 2B-porphyrin-NQ-TCNQ 135, shown the <i>syn</i> isomer (AM 1).....	148
Figure 79: Three all- <i>trans</i> ring-expanded 6B-porphyrin-TCNQ systems	149
Figure 80: ORTEP plot of 2B-dione- <i>trans</i> -diacetate 79.....	260
Figure 81: ORTEP plot of mono-ringlosed mesylate 69	268
Figure 82: ¹ H-NMR expansion (500 MHz, 8.2 ppm to 9.0 ppm) of bis-porphyrin-TCNQ 48.....	280
Figure 83: ¹ H-NMR expansion (500 MHz, 7.6 ppm to 8.0 ppm) of bis-porphyrin-TCNQ 48.....	281
Figure 84: ¹ H-NMR expansion (500 MHz, 3.5 ppm to 5.5 ppm) of bis-porphyrin-TCNQ 48.....	282
Figure 85: ¹ H-NMR expansion (500 MHz, 2.0 ppm to 2.9 ppm) of bis-porphyrin-TCNQ 48.....	283
Figure 86: ¹ H-NMR expansion (500 MHz, 1.2 ppm to 1.6 ppm) of bis-porphyrin-TCNQ 48.....	283
Figure 87: ¹ H-NMR expansion (500 MHz, -2.7 ppm to -2.5 ppm) of bis-porphyrin-TCNQ 48.....	284

E.6.4 List of Schemes

Scheme 1: Building the dyad carbon backbone. (a) 1,2,3,4,5,5-Hexachlorocyclopentadiene, reflux, 6h, 70 %; (b) 5,5-dimethoxy-1,2,3,4-tetrachlorocyclopentadiene toluene, reflux, 46 h, 72 %; (c) Na, THF/ <i>i</i> -PrOH, reflux, 4 d, 54 %; (d) NaOMe, CCl ₃ CO ₂ C ₂ H ₅ , light petroleum, RT, 22 h, 52 %; (e) Na, THF/ <i>i</i> -PrOH, reflux, 21 h, 99 %; (f) HCOOH, THF, RT, 92 %; (g) toluene, reflux, 2 h.....	51
Scheme 2: Formation of two enantiomeric dimethyl acetals 6 after ring-expansion with <i>in-situ</i> generated dichlorocarbene.....	52
Scheme 3: Diels-Alder reaction with 1,4-naphthoquinone. (a) Ethanol, reflux, 4 h, 74 % (10), 84 % (11).....	52
Scheme 4: Aromatisation / methylation. (a) HMPA, THF, KN(SiMe ₃) ₂ , toluene, 0 °C, followed by MeI, RT, 18 h, 43 %.....	53
Scheme 5: Retro-Diels-Alder reaction	53
Scheme 6: <i>Sharpless</i> bis-hydroxylation with catalytic amounts of OsO ₄ and NMO as oxidant, shown is a concerted [3+2] mechanism.....	54
Scheme 7: <i>Sharpless</i> bis-hydroxylation. (a) OsO ₄ , 1 eq. NMO, 45 °C, 8 d, 31 %; (b, n = 0) OsO ₄ , 1 eq. NMO, 45 °C, 8 d, 9 %; (b, n = 1) OsO ₄ , 2.5 eq. NMO, RT, 15 d, 20 %; (c, n = 0) OsO ₄ , 2 eq. NMO, 40 °C, 14 d, 56 %; (c, n = 1) OsO ₄ , 2.5 eq. NMO, RT, 56 d, 70 %.....	54
Scheme 8: Oxidation to α-ketols 21 under <i>Sharpless</i> bis-hydroxylation conditions. (a) OsO ₄ , 2.5 eq. NMO, RT, 15 d, 5 %.....	56
Scheme 9: TEMPO reaction followed by hydrogenation. (a) TEMPO reagent, <i>p</i> -toluenesulfonic acid, DCM, 0 °C/RT, 6 d, 63%; (b) Pd/C-H ₂ , ethyl acetate, RT, 24 h, 93 %.....	56
Scheme 10: Hydrogenation then TEMPO or TEMPO then Hydrogenation? (a) and (d) Pd/C-H ₂ , ethyl acetate, RT, 24 h; (b) and (c) TEMPO reagent, <i>p</i> -toluenesulfonic acid, DCM, 0 °C/RT, 5 d.....	57
Scheme 11: TEMPO reaction of the non-ring-expanded tetraol. (a) TEMPO reagent, <i>p</i> -toluenesulfonic acid, DCM, 0 °C/RT, 26 h, 56 %.....	57
Scheme 12: TEMPO reaction on ring-expanded tetraol. (a) TEMPO reagent, <i>p</i> -toluenesulfonic acid, DCM, 0 °C/RT, 5 d, 29 % (tetraone) / 54 % (trione-ol); (b) TEMPO reagent, <i>p</i> -toluenesulfonic acid, DCM, 0 °C/RT, 20 d, 57 %.....	59
Scheme 13: Mechanism of keto-enol tautomerism for a ring-expanded dione.....	59

Scheme 14: Two condensation sequences. Path A: 'porphyrindione' followed by diones/tetraones; Path B: diones/tetraones followed by porphyrindione	61
Scheme 15: Synthesis of 6B-porphyrin-DMN. (a) Pd/C-H ₂ , ethyl acetate, RT, 24 h, 93 %; (b) 'diaminoporphyrin', pyridine, 125 °C, pressure tube, 3d, 29 %; (c) 'diaminoporphyrin', DCM, 125 °C, pressure tube, 3d, 54 %; (d) Pd/C, H ₂ , ethyl acetate, RT, 24 h, 79 %.....	62
Scheme 16: Synthesis of 2B-porphyrin-DMN 33. (a) DCM, 125 °C, pressure tube, 4d, 73 %.....	63
Scheme 17: Condensation of the non-ring-expanded tetraone. (a) 'diaminoporphyrin', DCM, 125 °C, pressure tube, 3 d, 12 % (34), 31 % (35); (b) 'diaminoporphyrin', DCM, 120 °C, pressure tube, 4 d, 38 %.....	64
Scheme 18: Condensation of the ring-expanded tetraone 30. (a) 2 eq. 'diaminoporphyrin', DCM, 120 °C, pressure tube, 5 d, 15 % (b) not successful to date.....	68
Scheme 19: From DMN to TCNQ. (a) BBr ₃ , DCM, -45 °C / RT, over night; (b) PbO ₂ , DCM, RT, 30 min; (c) malononitrile, TiCl ₄ , DCM, β-alanine, pyridine.....	70
Scheme 20: Attempted synthesis of a 6B-[porphyrinato]zinc(II)-2B-porphyrin-DMN 49. (a) de-oxygenated DCM, dark pressure tube, 120 °C, 21 d.....	75
Scheme 21: Synthesis of the triad carbon backbones. (a) 0, toluene, reflux, 40 h, 52 %; (b) Na, THF / <i>i</i> -PrOH, reflux, 16 h; (c) HCOOH, THF, RT, 16 h; (d) toluene, reflux, 2 h; (e) dimethyl fumarate, toluene, reflux, 18 h; (f) dimethyl fumarate, toluene, reflux, 87 h, 82 % (n = 0); 18 h, 61 % (n = 1).....	80
Scheme 22: Proposed synthetic pathway for mono-dione. (a) <i>Sharpless</i> bis-hydroxylation; (b) TEMPO reaction; (c) condensations; (d) reduction; (e) tosylation; (f) de-tosylation	81
Scheme 23: Products of the <i>Sharpless</i> bis-hydroxylation and selected ¹³ C chemical shifts. (a) OsO ₄ (2 %), NMO (3 eq.), H ₂ O, 1,4-dioxane, RT, 16 h, 50 %	82
Scheme 24: Proposed mechanism of the acid-catalysed lactone formation.....	83
Scheme 25: Attempted synthesis of a double lactone. (a) Dimethyl maleate, toluene, reflux, 4 d, 41 %; (b) OsO ₄ , NMO, 1,4-dioxane, 80 °C, 10 d	83
Scheme 26: Conversion of ester groups into tosylates. (a) LiAlH ₄ , THF, reflux, 20 h, 99 %; (b) TsCl, pyridine, -23 °C, 8 d, 94 %.....	85
Scheme 27: Proposed mechanism of the base-catalysed cyclic ether formation. (a) OsO ₄ (2 %), NMO (3 eq.), 1,4-dioxane, RT, 23 h, 71 %	86

Scheme 28: Cyclic ether formation with a mesyl functionality acting as leaving group.	
(a) OsO ₄ (2 %), NMO (3 eq.), 1,4-dioxane, RT, 23 h, 77 %.....	86
Scheme 29: (a) Toluene, reflux, 15 h, 53 %; (b) LiAlH ₄ , THF, RT, 3 h, 94 %; (c) TsCl (X = Ts) or MsCl (X = Ms), pyridine, -18 °C, 6 d, 85 % (X = Ts) or 67 % (X = Ms); (d) OsO ₄ , NMO, RT, 6 d, 21 % (X = Ts) or 24 % (X = Ms).....	87
Scheme 30: (a) Acetic anhydride, pyridine, RT, 18 h, 75 %; (b) OsO ₄ , NMO, 1,4-dioxane, RT, 3 d, 45 % (c) thionyl chloride, pyridine, 70 °C, 2 h, 50 %; (d) OsO ₄ , NMO, 1,4-dioxane, RT, 3 d, 57 %.....	88
Scheme 31: Formation of diones 79 and 80 under <i>Sharpless</i> bis-hydroxylation conditions.....	89
Scheme 32: Application of the optimised 'bis-ketonisation' conditions to [2.2.1] and [3.2.1] ring systems. (a) OsO ₄ (2 %), NMO (6 eq.), 1,4-dioxane (minimum amount), RT, 3d	91
Scheme 33: What is the oxidising species in the 'bis-ketonisation'?.....	92
Scheme 34: Synthesis of tetraones (a) LiAlH ₄ , THF, reflux, 20 / 24 h, 84 % (n = 0) / 99 % (n = 1); (b) acetic anhydride, RT, 23 / 17 h, 93 % (n = 0) / 89 % (n = 1); (c) OsO ₄ , NMO, RT, 18 h - 6 d (n = 0) / 50 d (n = 1); (d) TEMPO reagent, p-toluenesulfonic acid, DCM, RT, 4 d, 74 % (n = 0) / 57 % (n = 1)	94
Scheme 35: 'Neighbour group-free' condensation reactions. (a) 'diaminoporphyrin', pyridine, 110 °C, pressure tube, 11 d, 42 %; (b) 'diaminoporphyrin', pyridine, 125 °C, pressure tube, 12 d, 10 %.....	98
Scheme 36: Mild transesterification and subsequent hemi-acetal formation. (a) K ₂ CO ₃ , MeOH, H ₂ O, 18 h, RT, 32 %.....	99
Scheme 37: 'Bis-ketonisation' and subsequent hemi-acetal formation. (a) OsO ₄ (2 %), NMO (5 eq.), 1,4-dioxane, RT, 5d, 55 %	99
Scheme 38: Formation of the initial tetrahedral adduct and subsequent loss of two water molecules	100
Scheme 39: Condensation successful under high pressure. (a) phenylenediamine, pyridine, 40 °C, 15 kbar, 3 d, 72 %	101
Scheme 40: Nucleophilic attack on acetoxy, not ketone group in pyridine at 15 kbar and high temperatures.....	102
Scheme 41: Proposed mechanism for loss of acetoxy groups under high pressure in anhydrous pyridine	103

Scheme 42: Envisaged reaction of the 2B-dione- <i>trans</i> -diacetate 79 with the weaker base 'diaminoporphyrin' 153	104
Scheme 43: Loss of acetoxy groups in pyridine. (a) 'Diaminoporphyrin', pyridine, 15 kbar, 80 °C, 3d, 50 %.....	105
Scheme 44: Hydrolysis of 2B-porphyrin- <i>trans</i> -diacetate 95 in pyridine. Double hydrolysis results in the formation of the main product 2B-porphyrin- <i>trans</i> -diol 96	105
Scheme 45: 6B-mono-condensations only between 'diaminoporphyrin' 153 and tetraones 95 and 98 in pyridine. (a) 80 °C, 15 kbar, 3 d, 22 % (106), 25 % (107).....	108
Scheme 46: Condensation between the non-ring-expanded tetraone 89 and 'diaminoporphyrin' in dichloromethane. (a) 'Diaminoporphyrin', 80 °C, 15 kbar, 3 d, 35 % (108), 9 % (109)	109
Scheme 47: Summary of high-pressure findings	112
Scheme 48: From acetate to diene. (a) K ₂ CO ₃ , MeOH, THF, H ₂ O, RT, 18 h, 60 %; (b) TsCl, pyridine, DCM, freezer, 7 d, 99 %; (c) ZnOAc, MeOH, DCM, RT, 18h, 93 %; (d) KO ^t Bu, DMF, RT, 3 h, 93 %.....	113
Scheme 49: Synthesis of the bridge component. (a) EtOH, 0 °C, 2 h, 61 %; (b) 1) NaH, 2) MeI, THF, RT, 18 h, 52 %; (c) DMAD, RuH ₂ CO(PPh ₃) ₃ ¹⁸⁸ , toluene, reflux, 24 h, 45 %; (d) quadricyclane, toluene, reflux, 6 d, 75 %; (e) LiAlH ₄ , THF, reflux, 20 h, 87 %; (f) Mesyl chloride, pyridine, freezer, 70 h; (g) LiAlH ₄ , THF, reflux, 3 d, 52 %; (h) - (k) see Scheme 50, page 118	117
Scheme 50: Synthesis of the bridge component, part 2. (a) CuCl ₂ , NaOAc, CO, Pd/C, MeOH, THF, RT, 97 h, 63 %; (b) LiAlH ₄ , THF, reflux, 15 h, 98 %; (c) tosyl chloride, pyridine, freezer, 6 d, 66 %; (d) KO ^t Bu, DMF, RT, 18 h, 91 %.....	118
Scheme 51: Proposed mechanism for Pd-catalysed bismethoxy carbonylation	119
Scheme 52: (a) Tosyl chloride, pyridine, freezer, 6 d, 66 %; (b) KO ^t Bu, DMF, RT, 18h, 91 %.....	120
Scheme 53: Synthesis of acceptor precursor. (a) benzoquinone, 1,3-cyclohexadiene, EtOH, 60 °C, 2.5 h, 57 %; (b) NaH, THF, MeI, RT, 64 h, 64 %; (c) Pd/C, H ₂ , EA, RT, 10 h, 95 %; (d) BBr ₃ , DCM, 0 °C / RT, 20 h, 88 %; (e) Ag ₂ O, MgSO ₄ , Et ₂ O, RT, 3.5 h, 79 %.....	120
Scheme 54: Assembling the triads using Diels-Alder methodology	121

Scheme 55: Fusing bridge and acceptor. (a) 5M etheral LiClO ₄ , RT, 3 d, 98 %; (b) DDQ, 1,4-dioxane, reflux, 48 h, 66 %; (c) malononitrile, pyridine, TiCl ₄ , DCM, reflux, 15 minutes, 88 %	122
Scheme 56: Deprotection of dimethoxybenzene. (a) AgO, 6M HNO ₃ , THF, RT, 15 min, 69 %.....	122
Scheme 57: Final two steps of 2B-porphyrin-NQ-TCNQ triad 135	123
Scheme 58: Synthesis of the all- <i>trans</i> ring-expanded 6B-porphyrin-DMN 147. (a) LiAlH ₄ , THF, reflux, 18 h, 98 %; (b) MsCl, pyridine, -18 °C, 3 d, 76 %; (c) LiAlH ₄ , THF, reflux, 2 d, 51 %; (d) Cl ₃ CCO ₂ Et, NaOMe, PE, RT, 3 d, 33 %; (e) Na, <i>i</i> -PrOH, THF, reflux, 1 day, 54 %; (f) DDQ, DCM, RT, 22 h,.....	131
Scheme 59: Synthesis of porphyrindione. (g) NO ₂ , light petroleum, RT; (h) H ₂ SO ₄ , RT, 78 %; (i) SnCl ₂ , HCl, DCM, RT, 2d, 76 %; (j) O ₂ , hv, RT, 6d, H ₂ SO ₄ (3M), 2 hr, 86 %.....	135
Scheme 60: Mechanism of photo-oxidation followed by hydrolysis.....	136
Scheme 61: Synthesis of 5,10,15,20-tetrakis-(3,5-di- <i>tert</i> -butylphenyl)-2 ³ -2 ⁴ -diaminoquinoxalino[2,3- <i>b</i>]porphyrin 153 ('diaminoporphyrin')	137
Scheme 62: The dyad strategy. (a) building the backbone; (b) Diels-Alder reaction with naphthoquinone; (c) introduction of keto functionalities; (d) attachment of porphyrin moieties; (e) increase of the acceptor strength	139
Scheme 63: High pressure to the rescue? Proposed conditions (a) DCM, 15 kbar, 80 °C, 3 d	141
Scheme 64: The triad strategy. (a) building the backbone; (b) Diels-Alder reaction with dimethyl fumarate; (c) introduction of keto-functionalities; (d) attachment of porphyrin moieties; (e) conversion to enophile; (f) assembling the triad	142
Scheme 65: Ring-closure reactions under <i>Sharpless</i> bis-hydroxylation conditions	143
Scheme 66: Optimised 'bis-ketonisation' conditions - 2 % OsO ₄ , 6 eq. NMO, high concentration in 1,4-dioxane, three days at RT.....	144
Scheme 67: High-pressure reactions in anhydrous pyridine.....	145
Scheme 68: Hemi-acetal formation in pyridine. (a) 15 kbar, 80 °C, 3 d.....	146
Scheme 69: The all- <i>trans</i> strategy. (a) Conversion of ester in methyl groups; (b) ring-expansion; (c) introduction of keto-functionalities, and (d) attachment of 'diaminoporphyrin'	149

E.6.5 List of Tables

Table 1: First experimental proof for the Marcus inverted region by Miller <i>et al.</i> (1984)	12
Table 2: Electron transfer rates and lifetimes of the charge-separated state for DMN-DCV dyads by the Paddon-Row group	15
Table 3: β -values for different media, $k_{ET} \propto \exp(-\beta r)$	15
Table 4: Distance, driving force, and electron-transfer rates for bis-porphyrin dyads by Therien <i>et al.</i>	17
Table 5: Edge-to-edge distance, driving force, ET-, and CR-rates for porphyrin-quinone dyads by Sakata <i>et al.</i> (1994).....	18
Table 6: ^{13}C -NMR shifts for non-ring-expanded TEMPO-reaction products in ppm relative to TMS.....	58
Table 7: ^{13}C -NMR shifts for ring-expanded TEMPO-reaction products in ppm relative to TMS.....	60
Table 8: Yields from DMN to TCNQ.....	71
Table 9: OsO ₄ -reaction under optimised 'bis-ketonisation' conditions	91
Table 10: ^{13}C -NMR shifts for OsO ₄ and TEMPO reaction products in ppm relative to TMS.....	95
Table 11: Summary for condensations between the 2B-dione- <i>trans</i> -diacetate 79 and phenylenediamine (X = H) or benzenetetramine (X = NH ₂).....	103
Table 12: Summary for condensations between 2B-dione- <i>trans</i> -diacetate 79 and 'diaminoporphyrin'.....	104

E.7 LITERATURE

- (1) Press, A. In *The Australian*, **1998**.
- (2) Ward, M. In *New Scientist*, **1998**.
- (3) Greenbaum, E.; Tevault, J. W.; Blankinship, S. L.; Mets, L. J. "New Photosynthesis or old? Reply", *Nature* **1996**, 379, 305-305.
- (4) Greenbaum, E.; Lee, J. W.; Tevault, C. V.; Blankenship, S. L.; Mets, L. J. "CO₂ Fixation and Photoevolution of H₂ and O₂ in a Mutant of *Chlamydomonas* lacking Photosystem-I", *Nature* **1995**, 376, 438-441.
- (5) *Molecular Electronics*; 1 ed.; Jortner, J.; Ratner, M. A., Eds.; Blackwell Science: Oxford, **1997**.
- (6) Marcus, R. A. "Electron Transfer Reactions in Chemistry: Theory and Experiment (Nobel Lecture)", *Angew. Chem. Int. Ed. Engl.* **1993**, 32, 1111-1121.
- (7) Davies, W. B.; Wasielewski, M. R.; Ratner, M. A.; Mujica, V.; Nitzan, A. "Electron Transfer Rates in Bridged Molecular Systems: A Phenomenological Approach to Relaxation", *J. Phys. Chem. A* **1997**, 101, 6158-6164.
- (8) Davies, W. B.; Svec, W. A.; Ratner, M. A.; Wasielewski, M. R. "Molecular-wire behaviour in p-phenylenevinylene oligomers", *Nature* **1998**, 396, 60-63.
- (9) Bolton, J. R.; Archer, M. D. In *Electron Transfer in Inorganic, Organic, and Biological Systems*; 228 ed.; Bolton, J. R., Mataga, N., McLendon, G., Eds.; American Chemical Society: Washington, **1991**.
- (10) Jordan, K. D.; Paddon-Row, M. N. In *Modern Models of Bonding and Delocalization*; Liebmann, J. F., Greenberg, A., Eds.; VCH Publishers: New York, **1988**; Vol. 6.
- (11) Jordan, K. D.; Paddon-Row, M. N. "Analysis of the Interactions Responsible for Long-Range Through-Bond-Mediated Electronic Coupling between Remote Chromophores Attached to Rigid Polynorbornyl Bridges", *Chem. Rev.* **1992**, 92, 395-410.
- (12) Connolly, J. S.; Bolton, J. R. In *Photoinduced Electron Transfer Reactions: Inorganic Substrates and Applications*; Fox, M. A., Chanon, M., Eds.; Elsevier: Amsterdam, **1988**; Vol. Part D.
- (13) Marcus, R. A.; Sutin, N. "Electron transfers in chemistry and biology", *Biochim. Biophys. Acta* **1985**, 811, 265-322.

- (14) Miller, J. R.; Calceterra, L. T.; Closs, G. L. "Intramolecular Long-Distance Electron Transfer in Radical Anions. The Effects of Free Energy and Solvent on the Reaction Rates", *J. Am. Chem. Soc.* **1984**, *106*, 3047-3049.
- (15) Penfield, K. W.; Miller, J. R.; Paddon-Row, M. N.; Cotsaris, E.; Oliver, A. M.; Hush, N. S. "Optical and Thermal Electron Transfer in Rigid Difunctional Molecules of Fixed Distance and Orientation", *J. Am. Chem. Soc.* **1987**, *109*, 5061-5065.
- (16) Wasielewski, M. R.; Gaines, G. L.; O'Neil, M. P.; Svec, W. A.; Niemczyk, M. P.; Prodi, L.; Gosztola, D. In *Dynamics and Mechanisms of Photoinduced Transfer and Related Phenomena*; Mataga, N., Okada, T., Masuhara, H., Eds.; Elsevier: Amsterdam, **1992**.
- (17) Closs, G. L.; Calceterra, L. T.; Green, N. J.; Penfield, K. W.; Miller, J. R. "Distance, Stereoelectronic Effects, and the Marcus Inverted Region in Intramolecular Electron Transfer in Organic Radical Anions", *J. Phys. Chem.* **1986**, *90*, 3673-3683.
- (18) Miller, J. R.; Beitz, J. V.; Huddleston, R. K. "Effect of Free Energy on Rates of Electron Transfer between Molecules", *J. Am. Chem. Soc.* **1984**, *106*, 5057-5068.
- (19) Rehm, D.; Weller, A. "Kinetik und Mechanismus der Elektronenuebertragung bei der Fluoreszenzloeschung in Acetonitril", *Ber. Bunsenges. Phys. Chem.* **1969**, *73*, 834-839.
- (20) Weller, A. "Photoinduced Electron Transfer in Solution: Exciplex and Radical Ion Pair Formation Free Enthalpies and their Solvent Dependence", *Z. Phys. Chem., Neue Folge* **1982**, *133*, 93-98.
- (21) Kavarnos, G. J. In *Photoinduced Electron Transfer I*; Springer-Verlag, **1989**; Vol. 156.
- (22) Wasielewski, M. R.; Niemczyk, M. P.; Svec, W. A.; Pewitt, E. B. "High-Quantum-Yield Long-Lived Charge Separation in a Photosynthetic Reaction Centre Model", *J. Am. Chem. Soc.* **1985**, *107*, 5562-5563.
- (23) Wasielewski, M. R.; Niemczyk, M. P. "Photoinduced Electron Transfer in *meso*-Triphenyltriptycenyloporphyrin-Quinones. Restricting Donor-Acceptor Distances and Orientations.", *J. Am. Chem. Soc.* **1984**, *106*, 5043-5045.
- (24) Wasielewski, M. R.; Johnson, D. G.; Svec, W. A.; Kersey, K. M.; Minsek, D. W. "Achieving High Quantum Yield Charge Separation in Porphyrin-Containing Donor-Acceptor Molecules at 10 K", *J. Am. Chem. Soc.* **1988**, *110*, 7219-7221.

- (25) Gaines, G. L.; O'Neil, M. P.; Svec, W. A.; Niemczyk, M. P.; Wasielewski, M. R. "Photoinduced Electron Transfer in the Solid State: Rate vs Free Energy Dependence in Fixed-Distance Porphyrin-Acceptor Molecules", *J. Am. Chem. Soc.* **1991**, *113*, 719-721.
- (26) Wasielewski, M. R.; Niemczyk, M. P.; Johnson, D. G.; Svec, W. A.; Minsek, D. W. "Ultrafast Photoinduced Electron Transfer in Rigid Donor-Spacer-Acceptor Molecules: Modification of Spacer as a Probe for Superexchange", *Tetrahedron* **1989**, *45*, 4785-4806.
- (27) Beitz, J. V.; Miller, J. R. "Exothermic rate restrictions on electron transfer in a rigid medium", *J. Chem. Phys.* **1979**, *71*, 4579-4595.
- (28) Miller, J. R.; Beitz, J. V. "Long range transfer of positive charge between dopant molecules in rigid glasses", *J. Chem. Phys.* **1981**, *74*, 6746-6756.
- (29) Miller, J. R.; Hartman, K. W.; Abrash, S. "Long-Distance (25 Å) Electron Transfer by Triplet Excited States in Rigid Media", *J. Am. Chem. Soc.* **1982**, *104*, 4296-4298.
- (30) Kira, A.; Nosaka, Y.; Imamura, M.; Ichikawa, T. "Pulse Radiolysis Experiment on Solute Deuteration Effects on the Electron Transfer Rate in Organic Glasses at 77K", *J. Phys. Chem.* **1982**, *86*, 1866-1868.
- (31) Kira, A.; Imamura, M.; Tagawa, S.; Tabata, Y. "Pulse Radiolysis Study of Positive-Charge Transfer in Freon-Mixture Matrix at 77 K", *Bull. Chem. Soc. Jpn.* **1986**, *59*, 593-597.
- (32) Finklea, H. O.; Hanshew, D. D. "Electron-Transfer Kinetics in Organized Thiol Monolayers with Attached Pentaamine(pyridine)ruthenium Redox Centers", *J. Am. Chem. Soc.* **1992**, *114*, 3173-3181.
- (33) Kuhn, H. "Electron Transfer in Monolayer Assemblies", *Pure Appl. Chem.* **1979**, *51*, 341-352.
- (34) Moebius, D. "Designed Monolayer Assemblies", *Ber. Bunsenges. Phys. Chem.* **1978**, *82*, 848-858.
- (35) Ogawa, M. Y.; Moreira, I.; Wishart, J. F.; Isied, S. S. "Long range electron transfer in helical polyproline II oligopeptides", *Chem. Phys.* **1993**, *176*, 589-600.
- (36) Ogawa, M. Y.; Wishart, J. F.; Young, Z.; Miller, J. R.; Isied, S. S. "Distance Dependence of Intramolecular Electron Transfer across Oligoproline in $[(bpy)_2Ru^{II}L^*-(Pro)_n-Co^{III}(NH_3)_5]^{3+}$, $n = 1-6$: Different Effects for Helical and Nonhelical Polyproline II Structures", *J. Phys. Chem.* **1993**, *97*, 11456-11463.

- (37) Isied, S. S. In *Electron Transfer Reactions: Inorganic, Organometallic, and Biological Applications*; Isied, S. S., Ed.; American Chemical Society: Washington, **1997**.
- (38) Tamiaki, H.; Nomura, K.; Maruyama, K. "Energy and Electron Transfer in Synthetic Oligoproline-Bridged Porphyrin Donor-Acceptor Molecules", *Bull. Chem. Soc. Jpn.* **1994**, *67*, 1863-1871.
- (39) Lewis, F. D.; Wu, T.; Zhang, Y.; Letsinger, R. L.; Greenfield, S. R.; Wasielewski, M. R. "Distance-Dependent Electron Transfer in DNA Hairpins", *Science* **1997**, *277*, 673-676.
- (40) Meggers, E.; Kusch, D.; Spichty, M.; Wille, U.; Giese, B. "Electron Transfer through DNA in the Course of Radical-Induced Strand Cleavage", *Angew. Chem. Int. Ed. Engl.* **1998**, *37*, 460-462.
- (41) Warman, J. M.; Haas, M. P. d.; Paddon-Row, M. N.; Cotsaris, E.; Hush, N. S.; Oevering, H.; Verhoeven, J. W. "Light-induced giant dipoles in simple model compounds for photosynthesis", *Nature* **1986**, *320*, 615-616.
- (42) Oevering, H.; Verhoeven, J. W.; Paddon-Row, M. N.; Warman, J. M. "Charge-Transfer Absorption and Emission Resulting from Long-Range Through-Bond Interaction; Exploring the Relation Between Electronic Coupling and Electron-Transfer in Bridged Donor-Acceptor Systems", *Tetrahedron* **1989**, *45*, 4751-4766.
- (43) Lawson, J. M.; Craig, D. C.; Oliver, A. M.; Paddon-Row, M. N. "Synthesis and Structural Characterisation of a Novel Pair of Rigid Diastereomeric Triads", *Tetrahedron* **1995**, *51*, 3841-3864.
- (44) Lawson, J. M.; Craig, D. C.; Paddon-Row, M.; Kroon, J.; Verhoeven, J. W. "Trough-bond modulation of intramolecular electron transfer in rigidly linked donor-acceptor systems", *Chem. Phys. Lett.* **1989**, *164*, 120-125.
- (45) Lawson, J. M.; Paddon-Row, M. N.; Schuddeboom; Warman; Clayton, A. H. A.; Ghiggino, K. P. *J. Phys. Chem.* **1993**, *97*, 13099.
- (46) Paddon-Row, M. N. "Investigating Long-Range Electron-Transfer Processes with Rigid, Covalently Linked Donor-(Norbornylogous Bridge)-Acceptor Systems", *Acc. Chem. Res.* **1994**, *27*, 18-25.
- (47) Warman, J. M.; Smit, K. J.; Jonker, S. A.; Verhoeven, J. W.; Oevering, H.; Kroon, J.; Paddon-Row, M. N.; Oliver, A. M. "Intramolecular charge separation and recombination in non-polar environments via long-distance electron transfer through saturated hydrocarbon barriers", *Chem. Phys.* **1993**, *170*, 359-380.

- (48) Paddon-Row, M. N.; Oliver, A. M.; Warman, J. M.; Smith, K. J.; deHaas, M. P.; Oevering, H.; Verhoeven, J. W. "Factors Affecting Charge Separation and Recombination in Photoexcited Rigid Donor-Insulator-Acceptor Compounds", *J. Phys. Chem.* **1988**, *92*, 6958-6962.
- (49) Williams, R. M.; Koeberg, M.; Lawson, J. M.; An, Y.-Z.; Rubin, Y.; Paddon-Row, M. N.; Verhoeven, J. W. "Photoinduced Electron Transfer to C₆₀ across Extended 3- and 11-Bond hydrocarbon Bridges: Creation of a Long-Lived Charge-Separated State", *J. Org. Chem.* **1996**, *61*, 5055-5062.
- (50) Langen, e. a. *J. Biol. Inorg. Chem.* **1996**, *1*, 221.
- (51) Brun, A. M.; Harriman, A. "Dynamics of Electron Transfer between Intercalated Polycyclic Molecules: Effect of Interspersed Bases", *J. Am. Chem. Soc.* **1992**, *114*, 3656-3660.
- (52) Michel-Beyerle, M. E.; Meggers, E.; Giese, B. *J. Am. Chem. Soc.* **1998**, *120*, 12950.
- (53) Bixon, M.; Giese, B.; Wessely, S.; Langenbacher, T.; Beyerle-Michele, M. E.; Jortner, J. *Proc. Natl. Acad. Sci. USA* **1999**, *96*, 11713.
- (54) Giese, B.; Wessely, S.; Sporman, M.; Lindemann, U.; Meggers, E.; Michel-Beyerle, M. E. *Angew. Chem. Int. Ed. Engl.* **1999**, *38*, 996.
- (55) Murphy, C. J.; Arkin, M. R.; Jenkins, Y.; Ghatlia, N. D.; Bossmann, S. H.; Turro, N. J.; Barton, J. K. "Long-Range Photoinduced Electron Transfer Through a DNA Helix", *Science* **1993**, *262*, 1025-1029.
- (56) Isied, S. S. In *Electron Transfer in Inorganic, Organic, and Biological Systems*; 228 ed.; Bolton, J. R., Mataga, N., McLendon, G., Eds.; American Chemical Society: Washington, **1991**.
- (57) Heiler, D.; McLendon, G.; Rogalsky, P. "Synthesis and Electron-Transfer Rates of Coplanar Diporphyrins: Models for (Heme) Protein-Protein Electron Transfer Reactions", *J. Am. Chem. Soc.* **1987**, *109*, 604-606.
- (58) Holmlin, R. E.; Stemp, E. D. A.; Barton, J. K. "Os(phen)₂dppz²⁺ in Photoinduced DNA-Mediated Electron Transfer Reactions", *J. Am. Chem. Soc.* **1996**, *118*, 5236-5244.
- (59) Holmlin, R. E.; Dandliker, P. J.; Barton, J. K. "Charge Transfer through the DNA Base Stack", *Angew. Chem. Int. Ed. Engl.* **1997**, *36*, 2714-2730.

- (60) Hartshorn, R. M.; Barton, J. K. "Novel Dipyridophenazine Complexes of Ruthenium(II): Exploring Luminescent Reporters to DNA", *J. Am. Chem. Soc.* **1992**, *114*, 5919-5925.
- (61) Harriman, A.; Sauvage, J.-P. "A Strategy for Constructing Photosynthetic Models: Porphyrin-containing Modules Assembled Around Transition Metals", *Chem. Soc. Rev.* **1996**, 41-47.
- (62) Hayashi, T.; Miyahara, T.; Koide, N.; Kato, Y.; Masuda, H.; Ogoshi, H. "Molecular Recognition of Ubiquinone Analogues. Specific Interaction between Quinone and Functional Porphyrin via Multiple Hydrogen Bonding", *J. Am. Chem. Soc.* **1997**, *119*, 7281-7290.
- (63) Osuka, A.; Yoneshima, R.; Shiratori, H.; Okada, T.; Taniguchi, S.; Mataga, N. "Electron transfer in a hydrogen-bonded assembly consisting of porphyrin-diimide", *Chem. Comm.* **1998**, 1567-1568.
- (64) Harriman, A.; Kubo, Y.; Sessler, J. L. "Molecular Recognition via Base Pairing: Photoinduced Electron Transfer in Hydrogen-Bonded Zinc Porphyrin-Benzoquinone Conjugates", *J. Am. Chem. Soc.* **1992**, *114*, 388-390.
- (65) Rege, P. J. F. d.; Williams, S. A.; Therien, M. J. "Direct Evaluation of Electronic Coupling Mediated by Hydrogen Bonds: Implications for Biological Electron Transfer", *Science* **1995**, *269*, 1409-1413.
- (66) Cave, R. J.; Siders, P.; Marcus, R. A. "Mutual Orientation Effects on Electron Transfer between Porphyrins", *J. Phys. Chem.* **1986**, *90*, 1436-1444.
- (67) Helms, A.; Heiler, D.; McLendon, G. "Dependence of Electron Transfer Rates on Donor-Acceptor Angle in Bis-Porphyrin Adducts", *J. Am. Chem. Soc.* **1991**, *113*, 4325-4327.
- (68) Lendzian, F.; Schluepmann, J.; Gersdorff, J. v.; Moebius, K.; Kurreck, H. "Investigation of the Light-Induced Charge Transfer between Covalently Linked Porphyrin and Quinone Units by Time-Resolved EPR Spectroscopy", *Angew. Chem. Int. Ed. Engl.* **1991**, *30*, 1461-1463.
- (69) Sakata, Y.; Tsue, H.; O'Neil, M. P.; Wiederrecht, G. P.; Wasielewski, M. R. "Effect of Donor-Acceptor Orientation on Ultrafast Photoinduced Electron Transfer and Dark Charge Recombination in Porphyrin-Quinone Molecules", *J. Am. Chem. Soc.* **1994**, *116*, 6904-6909.

- (70) Sakata, Y.; Tsue, H.; Goto, Y.; Misumi, S.; Asahi, T.; Nishikawa, S.; Okada, T.; Mataga, N. "Observation of Large Orientation Effect on Photoinduced Electron Transfer in Rigid Porphyrin-Quinone Compounds", *Chem. Lett.* **1991**, 1307-1310.
- (71) Sakata, Y.; Nakashima, S.; Goto, Y.; Tatemitsu, H.; Misumi, S.; Asahi, T.; Hagihara, M.; Nishikawa, S.; Okada, T.; Mataga, N. "Synthesis of Completely Fixed Porphyrin-Quinone Compounds and the Mutual Orientation Effect on Electron Transfer", *J. Am. Chem. Soc.* **1989**, *111*, 8979-8982.
- (72) Schmidt, J. A.; Liu, J.-Y.; Bolton, J. R.; Archer, M. D.; Gadzekpo, V. P. Y. "Intramolecular Photochemical Electron Transfer", *J. Chem. Soc., Faraday Trans. 1* **1989**, *85*, 1027-1041.
- (73) Liu, J.-Y.; Bolton, J. R. "Intramolecular Photochemical Electron Transfer. 7. Temperature Dependence of Electron-Transfer Rates in Covalently Linked Porphyrin-Amide-Quinone Molecules", *J. Phys. Chem.* **1992**, *96*, 1718-1725.
- (74) Bolton, J. R.; Schmidt, J. A.; Ho, T.-F.; Liu, J.-y.; Roach, K. J.; Weedon, A. C.; Archer, M. D.; Wilford, J. H.; Gadzekpo, V. P. Y. In *Electron Transfer in Inorganic, Organic, and Biological Systems*; 228 ed.; Bolton, J. R., Mataga, N., McLendon, G., Eds.; American Chemical Society: Washington, **1991**.
- (75) Schmidt, J. A.; Siemiarz, A.; Weedon, A. C.; Bolton, J. R. "Intramolecular Photochemical Electron Transfer. 3. Solvent Dependence of Fluorescence Quenching and Electron Transfer Rates in a Porphyrin-Amide-Quinone Molecule", *J. Am. Chem. Soc.* **1985**, *107*, 6112-614.
- (76) Zusman, L. D. "Outer-Sphere Electron Transfer in Polar Solvents", *Chem. Phys.* **1980**, *49*, 295-304.
- (77) Wiederrecht, G. P.; Niemczyk, M. P.; Svec, W. A.; Wasielewski, M. R. "Ultrafast Photoinduced Electron Transfer in a Chlorophyll-Based Triad: Vibrationally Hot Ion Pair Intermediates", *J. Am. Chem. Soc.* **1996**, *118*, 81-88.
- (78) Harrison, R. J.; Pearce, B.; Beddard, G. S.; Cowan, J. A.; Sanders, J. K. M. "Photoinduced Electron Transfer in Pyromellitimide-Bridged Porphyrins", *Chem. Phys.* **1987**, *116*, 429-448.
- (79) Heitele, H.; Finckh, P.; Weeren, S.; Poellinger, F.; Michel-Beyerle, M. E. "Solvent Polarity Effects on Intramolecular Electron Transfer. 1. Energetic Aspects", *J. Phys. Chem.* **1989**, *93*, 5173-5179.

- (80) Heitele, H.; Poellinger, F.; Haeberle, T.; Michel-Beyerle, M. E.; Staab, H. A. "Energy Gap and Temperature Dependence of Photoinduced Electron Transfer in Porphyrin-Quinone Cyclophanes", *J. Phys. Chem.* **1994**, 98, 7402-7410.
- (81) Kroon, J.; Oevering, H.; Verhoeven, J. W.; Warman, J. M.; Oliver, A. M.; Paddon-Row, M. N. "Temperature Effects on Intramolecular Electron Transfer Kinetics under "Normal", "Inverted", and "Nearly Optimal" Conditions", *J. Phys. Chem.* **1993**, 97, 5065-5069.
- (82) Bixon, M.; Jortner, J. "Non-Arrhenius Temperature Dependence of Electron-Transfer Rates", *J. Phys. Chem.* **1991**, 95, 1941-1944.
- (83) Miller, J. R. In *Electron Transfer in Inorganic, Organic, and Biological Systems*; 228 ed.; Bolton, J. R., Mataga, N., McLendon, G., Eds.; American Chemical Society: Washington, **1991**.
- (84) Balzani, V.; Scandola, F. *Supramolecular Photochemistry - Photochemical Molecular Devices*; Ellis Horwood Limited: Chichester, **1991**.
- (85) Gust, D.; Moore, T. A.; Moore, A. L. "Molecular Mimicry of Photosynthetic Energy and Electron Transfer", *Acc. Chem. Res.* **1993**, 198-205.
- (86) Clayton, R. K. *Photosynthesis: Physical Mechanisms and Chemical Patterns*; Cambridge University Press: London, **1980**.
- (87) Gorkom, H. J. v. In *Photosynthesis*; Ames, J., Ed.; Elsevier Science Publishers B.V.: Amsterdam, **1987**; Vol. 15.
- (88) Hall, D. O.; Rao, K. K. *Photosynthesis*; 5 ed.; Cambridge University Press: Cambridge, **1995**.
- (89) Chang, C.-H.; Tiede, D.; Tang, J.; Smith, U.; Norris, J.; Schiffer, M. "Structure of *Rhodospseudomonas sphaeroides* R-26 reaction center", *FEBS Lett.* **1986**, 205, 82-86.
- (90) Deisenhofer, J.; Epp, O.; Miki, K.; Huber, R.; Michel, H. "Structure of the protein subunits in the photosynthetic reaction centre of *Rhodospseudomonas viridis* at 3 Å resolution", *Nature* **1985**, 318, 618-624.
- (91) El-Kabbani, O.; Chang, C.-H.; Tiede, D.; Norris, J.; Schiffer, M. "Comparison of Reaction Centers from *Rhodobacter sphaeroides* and *Rhodospseudomonas viridis*: Overall Architecture and Protein-Pigment Interactions", *Biochemistry* **1991**, 30, 5361-5369.
- (92) Deisenhofer, J.; Michel, H. "The Photosynthetic Reaction Center from the Purple Bacterium *Rhodospseudomonas viridis* (Nobel Lecture)", *Angew. Chem. Int. Ed. Engl.* **1989**, 28, 829-847.

- (93) Huber, R. "A Structural Basis of Light Energy and Electron Transfer in Biology (Nobel Lecture)", *Angew. Chem. Int. Ed. Engl.* **1989**, 28, 848-869.
- (94) Treutlein, H.; Schulten, K.; Bruenger, A. T.; Karplus, M.; Deisenhofer, J.; Michel, H. "Chromophore-protein interactions and the function of the photosynthetic reaction center: A molecular dynamics study", *Proc. Natl. Acad. Sci. USA* **1992**, 89, 75-79.
- (95) Steffen, M. A.; Lao, K.; Boxer, S. G. "Dielectric Asymmetry in the Photosynthetic Reaction Center", *Science* **1994**, 264, 810-816.
- (96) Heller, B. A.; Holten, D.; Kirmaier, C. "Control of Electron Transfer Between the L- and the M-Sides of Photosynthetic Reaction Centers", *Science* **1995**, 269, 940-945.
- (97) Cogdell, R. J. In *Antennas and Reaction Centers of Photosynthetic Bacteria*; Michel-Beyerle, M. E., Ed.; Springer Verlag: Heidelberg **1985**; Vol. 42.
- (98) Martin, J.-L.; Breton, J.; Hoff, A. J.; Migus, A.; A. Antonetti "Femtosecond spectroscopy of electron transfer in the reaction center of the photosynthetic bacterium *Rhodopseudomonas viridis* R-26: Direct electron transfer from the dimeric bacteriochlorophyll primary donor to the bacteriopheophytin acceptor with a time constant of 2.8 +/- 0.2 psec", *Proc. Natl. Acad. Sci. USA* **1986**, 83, 957-961.
- (99) Breton, J.; Martin, J.-L.; Migus, A.; Antonetti, A.; A. Orszag "Femtosecond spectroscopy of excitation energy transfer and initial charge separation in the reaction center of the photosynthetic bacterium *Rhodopseudomonas viridis*", *Proc. Natl. Acad. Sci. USA* **1986**, 83, 5121-5125.
- (100) Wasielewski, M. R.; M. Tiede, D. "Sub-picosecond measurements of primary electron transfer in *Rhodopseudomonas viridis* reaction centers using near-infrared excitation", *FEBS Lett.* **1986**, 204, 368-372.
- (101) Woodbury, N. M.; Becker, M.; Middendorf, D.; Parson, W. W. "Picosecond Kinetics of the Initial Photochemical Electron-Transfer Reaction in Bacterial Photosynthetic Reaction Centers", *Biochemistry* **1985**, 24, 7516-7521.
- (102) Fleming, G. R.; Martin, J.-L.; Breton, J. "Rates of primary electron transfer in photosynthetic reaction centers and their mechanistic implications", *Nature* **1988**, 333, 190-192.
- (103) Arlt, T.; Schmidt, S.; Kaiser, W.; Lauterwasser, C.; Meyer, M.; Scheer, H.; Zinth, W. "The accessory bacteriochlorophyll: A real electron carrier in primary photosynthesis", *Proc. Natl. Acad. Sci. USA* **1993**, 90, 11757-11761.
- (104) Parson, W. W. *Ann. Rev. Biophys. Bioeng.* **1992**, 11, 57.

- (105) Wasielewski, M. R. "Photoinduced Electron Transfer in Supramolecular Systems for Artificial Photosynthesis", *Chem. Rev.* **1992**, 435-461.
- (106) Paddock, M. L.; Rongey, S. H.; Abresch, E. C.; Feher, G.; Okamura, M. Y. "Reaction centers from three herbicide-resistant mutants of *Rhodobacter sphaeroides* 2.4.1: sequence analysis and preliminary characterization", *Photosynth. Res.* **1988**, 17, 75-96.
- (107) Graige, M. S.; Paddock, M. L.; Bruce, J. M.; Feher, G.; Okamura, M. Y. "Mechanism of Proton-Coupled Electron Transfer for Quinone (Q_B) Reduction in Reaction Centres of *Rb. Sphaeroides*", *J. Am. Chem. Soc.* **1996**, 118, 9005-9016.
- (108) Tabushi, I.; Koga, N.; Yanagita, M. "Efficient Intramolecular Quenching and Electron Transfer in Tetraphenylporphyrin attached with benzoquinone or Hydroquinone as a Photosystem Model", *Tetrahedron Lett.* **1979**, 257-260.
- (109) Joran, A. D.; Leland, B. A.; Geller, G. G.; Hopfield, J. J.; Dervan, P. B. "Models for Photochemical Electron Transfer at Fixed Distances. Porphyrin-Bicyclo[2.2.2]octane-Quinone and Porphyrin-Bibicyclo[2.2.2]octane-Quinone", *J. Am. Chem. Soc.* **1984**, 106, 6090-6092.
- (110) Leland, B. A.; Joran, A. D.; Felker, P. M.; Hopfield, J. J.; Zewail, A. H.; Dervan, P. B. "Picosecond Fluorescence Studies on Intramolecular Photochemical Electron Transfer in Porphyrins Linked to Quinones at Two Different Fixed Distances", *J. Phys. Chem.* **1985**, 89, 5571-5573.
- (111) Joran, A. D.; Leland, B. A.; Felker, P. M.; Zewail, A. H.; Hopfield, J. J.; Dervan, P. B. "Effect of exothermicity on electron transfer rates in photosynthetic molecular models", *Nature* **1987**, 327, 508-511.
- (112) Bolton, J. R.; Ho, T.-F.; Liauw, S.; Siemiarz, A.; Wan, C. S. K.; Weedon, A. "Light-induced Intramolecular Electron Transfer from a Porphyrin linked to a p-Benzoquinone by a Rigid Spacer Group", *J. Chem. Soc., Chem. Commun.* **1985**, 559-560.
- (113) Antolovich, M.; Keyte, P. J.; Oliver, A. M.; Paddon-Row, M. N.; Kroon, J.; Verhoeven, J. W.; Jonker, S. A.; Warman, J. M. "Modelling Long-range Photosynthetic Electron Transfer in Rigidly Bridged Porphyrin-Quinone Systems", *J. Phys. Chem.* **1991**, 95, 1933-1941.
- (114) Paddon-Row, M. N.; Patney, H. K.; Peel, J. B.; Willett, G. D. "The Observation of Long-range Benzene-Benzene Interactions", *J. Chem. Soc., Chem. Commun.* **1984**, 564-566.

- (115) Paddon-Row, M. N. "Some Aspects of Orbital Interactions through Bonds: Physical and Chemical Consequences", *Acc. Chem. Res.* **1982**, *15*, 245-251.
- (116) Paddon-Row, M. N.; Patney, H. K.; Brown, R. S.; Houk, K. N. "Observation of a Very Large Orbital Interaction through Four Bonds. An Alternative Model of Orbital Interactions through Bonds", *J. Am. Chem. Soc.* **1981**, *103*, 5575-5577.
- (117) Joergensen, F. S.; Paddon-Row, M. N.; Patney, H. K. "Photoelectron Spectra of Some Decahydrotrimethanoanthracenes: Observation of Large π Orbital Interactions through Six Bonds and an Apparent Violation of the *trans* Rule", *J. Chem. Soc., Chem. Commun.* **1983**, 573-575.
- (118) Paddon-Row, M. N.; Cotsaris, E.; Patney, H. K. "The Synthesis of Rigid Norbornylogs for the Purpose of Studying Orbital Interactions Through Bonds", *Tetrahedron* **1986**, *42*, 1779-1788.
- (119) Balaji, V.; Ng L.; Jordan, K. D.; Paddon-Row, M. N.; Patney, H. K. "A Study of Long-Range p^*,p^* Interactions in Rigid Molecules Using Electron Transmission Spectroscopy", *J. Am. Chem. Soc.* **1987**, *109*, 6957-6969.
- (120) Paddon-Row, M. N.; Wong, S. S. "A Correlation between the Rates of Photoinduced Long-Range Intramolecular Electron Transfer in Rigidly Linked Donor-Acceptor Systems and Computed π,π and π^*,π^* Splitting Energies in Structurally Related Dienes", *Chem. Phys. Lett.* **1990**, *167*, 432-437.
- (121) Sessler, J. L.; Wang, B.; Harriman, A. "Long-Range Photoinduced Electron Transfer in an Associated but Noncovalently Linked Photosynthetic Model System", *J. Am. Chem. Soc.* **1993**, *115*, 10418-10419.
- (122) Hayashi, T.; Miyahara, T.; Aoyama, Y.; Nonoguchi, M.; Ogoshi, H. "Preparation and Binding Affinity of New Porphyrin Host Molecule for Ubiquinone Analogues", *Chem. Lett.* **1994**, 1749-1752.
- (123) Hayashi, T.; Miyahara, T.; Kumazaki, S.; Ogoshi, H.; Yoshihara, K. "Photoinduzierter Elektronentransfer zwischen multifunktionellen, ueber mehrere H-Bruecken verknuepfter Porphyrin und Ubichinon-Analoga", *Angew. Chem.* **1996**, *108*, 2096-2098.
- (124) Staab, H. A.; Weiser, J.; Baumann, E. "Quinone-Porphyrin-Quinone and Quinone-Porphyrin-Donor Cyclophanes: Syntheses, Structures and Electron-Transfer-Related Properties", *Chem. Ber.* **1992**, *125*, 2275-2283.
- (125) Mauzerall, D.; Weiser, J.; Staab, H. "Electron Transfer in Photoexcited Porphyrin Quinone Cyclophanes", *Tetrahedron* **1989**, *45*, 4807-4814.

- (126) Seta, P.; Bienvenue, E.; Moore, A. L.; Mathis, P.; Bensasson, R. V.; Liddell, P. A.; Pessiki, P. J.; Joy, A.; Moore, T. A.; Gust, D. "Photodriven transmembrane charge separation and electron transfer by a carotenoporphyrin-quinone triad", *Nature* **1985**, *316*, 653-655.
- (127) Gust, D.; Mathis, P.; Moore, A. L.; Liddell, P. A.; Nemeth, G. A.; Lehman, W. R.; Moore, T. A.; Bensasson, R. V.; Land, E. J.; Chachaty, C. *Photochem. Photobiol.* **1983**, *37S*, S46.
- (128) Moore, T. A.; Gust, D.; Mathis, P.; Moore, A. L.; Liddell, P. A.; Nemeth, G. A.; Lehman, W. R.; Bensasson, R. V.; Land, E. J.; Chachaty, C.; Sybesma, C., Ed.; Nijhoff/Junk: The Hague, **1984**.
- (129) Moore, T. A.; Gust, D.; Mathis, P.; Mialocq, J.-C.; Chachaty, C.; Bensasson, R. V.; Land, E. J.; Diozi, D.; Liddell, P. A.; Lehman, W. R.; Nemeth, G. A.; Moore, A. L. "Photodriven charge separation in a carotenoporphyrin-quinone dyad", *Nature* **1984**, *307*, 630-632.
- (130) Gust, D.; Moore, T. A.; Liddell, P. A.; Nemeth, G. A.; Makings, L. R.; Moore, A. L.; Barrett, D.; Pessiki, P. J.; Bensasson, R. V.; Rougee, M.; Chachaty, C.; Schruyver, F. C. D.; Auweraer, M. v. d.; Holzwarth, A. R.; Connolly, J. S. "Charge Separation in Carotenoporphyrin-Quinone Triads: Synthetic, Conformational, and Fluorescence Lifetime Studies", *J. Am. Chem. Soc.* **1987**, *109*, 846-856.
- (131) Hung, S.-C.; Macpjherson, A. N.; Lin, S.; Liddell, P. A.; R.Seely, G.; Moore, A. L.; Moore, T. A.; Gust, D. "Coordinated Photoinduced Electron and Proton Transfer in a Molecular Triad", *J. Am. Chem. Soc.* **1995**, *117*, 1657-1658.
- (132) Gust, D.; Moore, T. A.; Moore, A. L.; Barrett, D.; Harding, L. O.; Makings, L. R.; Liddell, P. A.; Schruyver, F. C. D.; Auweraer, M. v. d.; Bensasson, R. V.; Rougee, M. "Photoinitiated Charge Separation in a Carotenoid-Porphyrin-Diquinone Tetrad: Enhanced Quantum Yields via Multistep Electron Transfer", *J. Am. Chem. Soc.* **1988**, *110*, 321-323.
- (133) Gust, D.; Moore, T. A.; Moore, A. L.; Makings, L. R.; Seely, G. R.; Ma, X. C.; Trier, T. T.; Gao, F. "A Carotenoid-Diporphyrin-Quinone Model for Photosynthetic Multistep Electron and Energy Transfer", *J. Am. Chem. Soc.* **1988**, *110*, 7567-7569.
- (134) Gust, D.; Moore, T. A.; Moore, A. L.; Seely, G.; Liddell, P.; Barrett, D.; Harding, L. O.; Ma, X. C.; Lee, S.-J.; Gao, F. "A Carotenoid-Porphyrin-Diquinone Tetrad: Synthesis, Electrochemistry and Photoinitiated Electron Transfer", *Tetrahedron* **1989**, *45*, 4867-4891.

- (135) Gust, D.; Moore, T. A.; Moore, A. L.; Lee, S.-J.; Bittersmann, E.; Lutrull, D. K.; Rehms, A. A.; Graziano, J. M.; Ma, X. C.; Gao, F.; Belford, R. E.; Trier, T. T. "Efficient Multistep Photoinitiated Electron Transfer in a Molecular Pentad", *Science* **1990**, 248, 199-201.
- (136) Steinberg-Yfrach, G.; Liddell, P. A.; Hung, S.-C.; Moore, A. L.; Gust, D.; Moore, T. A. "Conversion of light energy to proton potential in liposomes by artificial photosynthetic reaction centres", *Nature* **1997**, 385, 239-241.
- (137) Steinberg-Yfrach, G.; Rigaud, J.-L.; Durantini, E. N.; Moore, A. L.; Gust, D.; Moore, T. A. "Light-driven production of ATP catalysed by F0F1-ATP synthase in an artificial photosynthetic membrane", *Nature* **1998**, 392, 479-482.
- (138) Kawabata, S.; Yamazaki, I.; Nishimura, Y.; Osuka, A. "Singlet energy transfer in bis(phenylethynyl)phenylene-bridged zinc-free base hybrid diporphyrins", *J. Chem. Soc., Perk. Trans. 2* **1997**, 479-484.
- (139) Linke, M.; Chambron, J.-C.; Heitz, V.; Sauvage, J.-P. "Electron Transfer between Mechanically Linked Porphyrins in a [2]Rotaxane", *J. Am. Chem. Soc.* **1997**, 119, 11329-11330.
- (140) Sessler, J. L.; Johnson, M. R.; Lin, T.-Y. "Absorption and Static Emission Properties of Monometalated Quinone-Substituted Porphyrin Dimers: Evidence for "Superexchange" Mediated Electron Transfer in Multicomponent Photosynthetic Model Systems", *Tetrahedron* **1989**, 45, 4767-4784.
- (141) Crossley, M. J.; Burn, P. L. "An Approach to Porphyrin-based Molecular Wires: Synthesis of a Bis(porphyrin)tetraone and its Conversion to a Linearly Conjugated Tetrakisporphyrin System", *J. Chem. Soc., Chem. Commun.* **1991**, 1569-1571.
- (142) Crossley, M. J.; Burn, P. L. "Rigid, Laterally-bridged Bis-porphyrin Systems", *J. Chem. Soc., Chem. Commun.* **1987**, 39-40.
- (143) Crossley, M. J.; Burn, P. L.; Langford, S. J.; Prashar, J. K. "Porphyrins with Appended Phenanthroline Units: a Means by which Porphyrin π -Systems can be connected to an External Redox Centre", *J. Chem. Soc., Chem. Commun.* **1995**, 1921-1923.
- (144) Crossley, M. J.; Govenlock, L. J.; Prashar, J. K. "Synthesis of Porphyrin-2,3,12,13- and 2,3,7,8-tetraones: Building Blocks for the Synthesis of Extended Porphyrin Arrays", *J. Chem. Soc., Chem. Commun.* **1995**, 2379-2380.
- (145) Byrne, L. T.; Rye, A. R.; Wege, D. "Diels-Alder Additions of Hexachlorocyclopentadiene to Some 7-Substituted Norbornadienes", *Aust. J. Chem.* **1974**, 27, 1961-1969.

- (146) DeLacy, T. P.; Kennard, C. H. L. "Insecticides. Part III. Crystal Structure of Endrin (1,2,3,4,10,10-Hexachloro-6,7-epoxy-1,4,4a,5,6,7,8,8a-octahydro-*endo*-1,4-*endo*-5,8-dimethanonaphthalene) and Aldrin (1,2,3,4,10,10-Hexachloro-1,4,4a,5,8,8a-hexahydro-*endo*-1,4-*exo*-5,8-dimethanonaphthalen)", *J. Chem. Soc., Perk. Trans. 2* **1972**, 2153-2158.
- (147) Lidov, R. *J. Am. Chem. Soc.* **1954**, 48, 2769.
- (148) Lawson, J. M.; Oliver, A. M.; Rothenfluh, D. F.; An, Y.-Z.; Ellis, G. A.; Ranasinghe, M. G.; Khan, S. I.; Franz, A. G.; Ganapathi, P. S.; Shephard, M. J.; Paddon-Row, M. N.; Rubin, Y. "Synthesis of a Variety of Bichromophoric "Ball-and-Chain" Systems Based on Buckminsterfullerene (C₆₀) for the Study of Intramolecular Electron and Energy Transfer Processes", *J. Org. Chem.* **1996**, 61, 5032-5054.
- (149) McBee, E. T.; Crain, D. L.; Crain, R. D.; Belohlav, L. R.; Braendlin, H. P. "Nucleophilic Displacement Reactions of Polyhalogenated Cyclopentadienes and Cyclopentenes", *J. Am. Chem. Soc.* **1962**, 84, 3557-3561.
- (150) Kolb, H. C.; VanNieuwenhze, M. S.; Sharpless, K. B. "Catalytic Asymmetric Dihydroxylation", *Chem. Rev.* **1994**, 94, 2483-2547.
- (151) Lohray, B. B. "Recent Advances in the Asymmetric Dihydroxylation of Alkenes", *Tetrahedron: Asym.* **1992**, 3, 1317-1349.
- (152) Criegee, R.; Marchand, B.; Wannowias, H. "Zur Kenntnis der organischen Osmium-Verbindungen", *Justus Liebigs Ann. Chem.* **1942**, 550, 99-133.
- (153) Criegee, R. "Osmiumsaeure-ester als Zwischenproducte der Oxydationen", *Justus Liebigs Ann. Chem.* **1936**, 522, 75-96.
- (154) Jacobsen, E. N.; Marko, I.; Mungall, W. S.; Schroeder, G.; Sharpless, K. B. "Assymmetric Dihydroxylation via Ligand-Accelerated Catalysis", *J. Am. Chem. Soc.* **1988**, 110, 1968-1970.
- (155) VanRheenen, V.; Kelly, R. C.; Cha, P. Y. "An Improved Catalytic OsO₄ Oxidation of Olefins to *cis*-1,2-Glycols using Tertiary Amine Oxides as the Oxidant", *Tetrahedron Lett.* **1976**, 23, 1973-1976.
- (156) Kolb, H. C.; Andersson, P. G.; Sharpless, K. B. "Toward an Understanding of the High Enantioselectivity in the Osmium-Catalyzed Asymmetric Dihydroxylation (AD). 1. Kinetics", *J. Am. Chem. Soc.* **1994**, 116, 1278-1291.
- (157) Norrby, P.-O.; Kolb, H. C.; Sharpless, K. B. "Toward an Understanding of the High Enantioselectivity in the Osmium-Catalyzed Asymmetric Dihydroxylation (AD). 2. A

- Qualitative Molecular Mechanics Approach", *J. Am. Chem. Soc.* **1994**, *116*, 8470-8478.
- (158) Norrby, P.-O.; Becker, H.; Sharpless, K. B. "Toward an Understanding of the High Enantioselectivity in the Osmium-Catalyzed Asymmetric Dihydroxylation (AD). 3. New Insights into Isomeric Forms of the Putative Osmaoxetane Intermediate", *J. Am. Chem. Soc.* **1996**, *118*, 35-42.
- (159) Nelson, D. W.; Gypser, A.; Ho, P. T.; Kolb, H. C.; Kondo, T.; Kwong, H.-L.; McGrath, D. V.; Rubin, A. E.; Norrby, P.-O.; Gable, K. P.; Sharpless, K. B. "Toward an Understanding of the High Enantioselectivity in the Osmium-Catalyzed Asymmetric Dihydroxylation (AD). 4. Electronic Effects in Amine-Accelerated Osmylations", *J. Am. Chem. Soc.* **1997**, *119*, 1840-1858.
- (160) Veldkamp, A.; Frenking, G. "Mechanism of the Enantioselective Dihydroxylation of Olefins by OsO₄ in the Presence of Chiral Bases", *J. Am. Chem. Soc.* **1994**, *116*, 4937-4946.
- (161) Torrent, M.; Deng, L.; Duran, M.; Sola, M.; Ziegler, T. "Density Functional Study of the [2+2]- and [2+3]-Cycloaddition for the Osmium-Catalyzed Dihydroxylation of Olefins", *Organomet.* **1997**, *16*, 13-19.
- (162) Banwell, M. G.; Bridges, V. S.; Dupuche, J. R.; Richards, S. L.; Walter, J. M. "Oxidation of vic-Diols to α -Dicarbonyl Compounds Using the Oxoammonium Salt derived from 4-Acetamido-TEMPO and p-toluenesulfonic acid", *J. Org. Chem.* **1994**, *59*, 6338-6343.
- (163) Nooy, A. E. J.; Besemer, A. C.; Bekkum, H. v. "On the Use of Stable Organic Nitroxyl Radicals for the Oxidation of Primary and Secondary Alcohols", *Synthesis* **1996**, 1153-1174.
- (164) Rothenfluh, D. F.; Oliver, A. M.; Paddon-Row, M. N. "Synthesis, electrochemistry and *ab initio* molecular orbital calculations on some norbornana- and bicyclo[2.2.2]octane-fused 5,12-bis(dicyanomethylidene)naphthalene systems", *J. Chem. Soc., Perk. Trans. 2* **1996**, 639-648.
- (165) Oevering, H.; Paddon-Row, M. N.; Heppener, M.; Oliver, A. M.; Cotsaris, E.; Verhoeven, J. W.; Hush, N. S. "Long-Range Photoinduced Through-Bond Electron Transfer and Radiative Recombination via Rigid Nonconjugated Bridges: Distance and Solvent Dependence", *J. Am. Chem. Soc.* **1987**, *109*, 3258-3269.
- (166) McOmie, J. F. W.; Watts, M. L.; West, D. E. "Demethylation of aryl methyl ethers by boron tribromide", *Tetrahedron* **1968**, *24*, 2289-2292.

- (167) Grieco, P. A.; Nizhizawa, M.; Oguri, T.; Burke, S. D.; Marinovic, N. "Sesquiterpene Lactones: Total Synthesis of (+)-Vernolepin and (+)-Vernomenin", *J. Am. Chem. Soc.* **1977**, 99, 5773-5780.
- (168) DeJonge, C. R. M. I.; vonDort, H. M.; Vollbracht, L. "The oxidation of phenols with leaddioxide", *Tetrahedron Lett.* **1970**, 22, 1881-1884.
- (169) Rothenfluh, D. F. PhD, University of New South Wales, **1998**.
- (170) Lawson, J. M.; Paddon-Row, M. N. "A Synthetic Strategy for the Construction of a Novel Series of Rigid Supramolecular Triads", *J. Chem. Soc., Chem. Commun.* **1993**, 1641-1643.
- (171) Craig, D. C.; Oliver, A. M.; Paddon-Row, M. N. "Synthesis of rigidly linked donor-acceptor systems designed to test the effect of orbital symmetry on the dynamics of intramolecular electron transfer processes", *J. Chem. Soc., Perk. Trans. 1* **1993**, 2, 197-203.
- (172) Mackenzie, K. *J. Chem. Soc. (C)* **1960**, 473.
- (173) Binks, R.; Mackenzie, K.; Williams-Smith, D. L. "Electron-impact Fragmentation of Polychlorinated Bridged-ring Systems", *J. Chem. Soc. (C)* **1969**, 1528-1533.
- (174) McCulloch, R. K.; Rye, A. R.; Wege, D. "Preparation and Thermal Decarbonylation of Some Sterically Compressed 5,6-endo-Disubstituted Norborn-2-en-7-ones", *Aust. J. Chem.* **1974**, 27, 1929-1941.
- (175) Suzuki, H.; Hashiba, I. In *Jpn. Kokai Tokkyo Koho*; Nissan Chemical Industries, Ltd., Japan: Japan, **1999**.
- (176) Gabioud, R.; Vogel, P. "The 7,8-epoxy-2,3,5,6-tetrakis(methylene)bicyclo[2.2.2]octane; synthesis and Diels-Alder reactivity", *Tetrahedron* **1980**, 36, 149-154.
- (177) Butler, D. N.; Snow, R. A. "Chemistry of Proximal p-Bond Systems. Part I. Synthesis of Vicinal Exocyclic Dimethylene Hydrocarbons", *Can. J. Chem.* **1972**, 50, 795-802.
- (178) Oberender, F. G.; Dixon, J. A. *J. Org. Chem.* **1959**, 24, 1226.
- (179) Cook, J. W.; Schoental, R. *J. Chem. Soc. (C)* **1950**, 47.
- (180) Sharpless, K. B.; Akashi, K. "Osmium Catalyzed Vicinal Hydroxylation of Olefins by *tert*-Butyl Hydroperoxide under Alkaline Conditions", *J. Am. Chem. Soc.* **1976**, 98, 1986-1987.
- (181) Schroeder, M. "Osmium Tetroxide Cis Hydroxylation of Unsaturated Substrates", *Chem. Rev.* **1980**, 80, 187-213.
- (182) Carpenter, B. K., personal communication.

- (183) Antolovich, M.; Oliver, A. M.; Paddon-Row, M. N. "The Synthesis of Bichromophoric Rigid Norbornylogous Systems Containing the Porphyrin Group as One of the Chromophores", *J. Chem. Soc., Perk. Trans. 2* **1989**, 783-789.
- (184) Diels, O.; Alder, K. "Synthesen in der hydro-aromatischen Reihe, VI. Mitteilung. Kurt Alder und Gerhard Stein: Ueber partiell hydrierte Naphtho- und Anthrachinone mit Wasserstoff in γ - bzw. δ -Stellung", *Chem. Ber.* **1929**, 62, 2337-2373.
- (185) Albrecht, W. *Justus Liebigs Ann. Chem.* **1906**, 348, 34.
- (186) Meinwald, J.; Wiley, G. A. "The Synthesis and Rearrangement of Some Benzonorbornenes", *J. Am. Chem. Soc.* **1958**, 80, 3667-3671.
- (187) Chang, D. S. C.; Filipescu, N. "Unusually Weak Electronic Interaction between Two Aromatic Chromophores Less Than 10 Å Apart in a Rigid Model Molecule", *J. Am. Chem. Soc.* **1972**, 94, 4170-4175.
- (188) Smith, C. D. "Cycloaddition Reactions of "Quadricyclanes"", *J. Am. Chem. Soc.* **1966**, 88, 4273-4274.
- (189) Mitsudo, T.-a.; Kokuryo, K.; Shinsugi, T.; Nakagawa, Y.; Watanabe, Y.; Takegami, Y. "Ruthenium-Catalyzed [2+2] Cross-Addition of Norbornene Derivatives and Dimethyl Acetylenedicarboxylate", *J. Org. Chem.* **1979**, 44, 4492-4496.
- (190) Mitsudo, T.-A.; Kokuryo, K.; Takegami, Y. "Ruthenium-catalysed [2+2] Cross-addition of Norbornene Derivatives and Dimethyl Acetylenedicarboxylate. A Novel Route to the *exo*-Tricyclo[4.2.1.0^{2,5}]nonene System", *J. Chem. Soc., Chem. Commun.* **1976**, 722-723.
- (191) Ahmad, N.; Levison, J. J.; Robinson, S. D.; Uttley, M. F. *Inorg. Synth.* **1974**, 15, 45.
- (192) Craig, D. C.; Ghiggino, K. P.; Joliffe, K. A.; Langford, S. J.; Paddon-Row, M. N. "Synthesis, Structure and Photophysical Studies of a Pair of Novel Rigid Bichromophoric Systems Bearing a Methyl Viologen Acceptor Unit", *J. Org. Chem.* **1997**, 62, 2381-2386.
- (193) Joliffe, K. A. PhD, The University of New South Wales, **1996**.
- (194) Stille, J. K.; Divakaruni, R. "Palladium(II)-Catalyzed Carboxylation Reactions of Olefins: Scope and Utility", *J. Org. Chem.* **1979**, 44, 3474-3482.
- (195) James, D. E.; Stille, J. K. "The Palladium(II) Catalyzes Olefin Carbonylation Reaction. Mechanisms and Synthetic Utility", *J. Am. Chem. Soc.* **1976**, 98, 1810-1823.

- (196) Joliffe, K. A.; Langford, S. J.; Ranasinghe, M. G.; Shephard, M. J.; Paddon-Row, M. N. "Design and Synthesis of Two (Pseudo)symmetric Giant Trichromophoric Systems containing the C₆₀ Chromophore", *J. Org. Chem.* **1999**, *64*, 1238-1246.
- (197) Joliffe, K.; Paddon-Row, M. N. "A Study of the Scope of the Bismethoxycarbonylation of Norbornene Systems", *Tetrahedron* **1995**, *51*, 2689-2698.
- (198) Mahaim, C.; Carrupt, P.-A.; Hagenbuch, J. P.; Florey, A.; Vogel, P. "An Efficient Synthesis of 2,3,5,6-Tetramethylidene-7-oxanorbornane", *Helv. Chim. Acta* **1980**, *63*, 1149-1157.
- (199) Yamada, M.; Kasuma, M.; Matsumoto, T.; Kurosaki, T. "Synthesis of Bicyclo[2.2.1]heptane-2,3,5,6-tetracarboxylic-2,3:5,6-Dianhydrides", *J. Org. Chem.* **1992**, *57*, 6075-6076.
- (200) Kitaguchi, N. "Effects of Substituents and Solvents on the Electronic Spectra of 9,10-Dihydro-9,10-o-benzenoanthracene-1,4-diones: Intramolecular Charge Transfer", *Bull. Chem. Soc. Jpn.* **1989**, *62*, 800-807.
- (201) Russell, G. A.; Holland, G. W.; Chang, K.-Y. "Semidiones. VI. Bicyclo[2.2.2]octane-2,3-semidione and Derivatives", *J. Am. Chem. Soc.* **1967**, *89*, 6629-6635.
- (202) Smith, L. I.; Hac, L. R. "Tetramethyl-o-benzoquinone", *J. Am. Chem. Soc.* **1934**, *56*, 477-478.
- (203) Kaupp, G.; Prinzbach, H. "Bis-homo-dien-Additionen mit Quadricyclanen", *Chem. Ber.* **1971**, *104*, 182-204.
- (204) Jurd, L. "Quinone and Quinone-Methides -I; Cyclization and dimerisation of crystalline ortho-quinone methides from phenol oxidation reactions", *Tetrahedron* **1977**, *33*, 163-168.
- (205) Moser, R. E.; Cassidy, H. G. "Electron-Transfer Polymers. XXVI. Synthesis of Oligomeric Hydroquinones and p-Benzoquinones", *J. Org. Chem.* **1965**, *30*, 2602-2606.
- (206) Grieco, P. A.; Nunes, J. J.; Gaul, M. D. "Dramatic Rate Accelerations of Diels-Alder Reactions in 5 M Lithium Perchlorate-Diethyl Ether: The Cantharidin Problem Reexamined", *J. Am. Chem. Soc.* **1990**, *112*, 4595-4596.
- (207) Lehnert, W. "Knoevenagel-Kondensationen mit TiCl₄/Base - V. 3-Alkyliden- und 3-Aryliden-2,4-pentadione aus Aldehyden und Acetylaceton", *Synthesis* **1974**, 667-669.

- (208) Lehnert, W. "Verbesserte Variante der Knoevenagel-Kondensation mit TiCl_4 /THF/Pyridin (I). Alkyliden- und Arylidenmalonester bei 0 - 25 °C", *Tetrahedron Lett.* **1970**, 54, 4723-4724.
- (209) Snyder, C. D.; Rapoport, H. "Oxidative Cleavage of Hydroquinone Ethers with Argentic Oxide", *J. Am. Chem. Soc.* **1972**, 94, 227-231.
- (210) Joliffe, K. A.; Bell, T. D. M.; Ghiggino, K. P.; Langford, S. J.; Paddon-Row, M. N. "Ein effizienter photoinduzierter Elektronentransfer in einer starren, U-förmigen Tetrade mit endständigen Porphyrin- und Viologen-Einheiten", *Angew. Chem.* **1998**, 110, 960-964.
- (211) Hoffmann, R. "Interaction of Orbitals through Space and through Bonds", *Acc. Chem. Res.* **1971**, 4, 1-9.
- (212) Oliver, A. M.; Craig, D. C.; Paddon-Row, M. N.; Kroon, J.; Verhoeven, J. W. "Strong Effects on the Bridge Configuration on Photoinduced Charge Separation in Rigidly Linked Donor-Acceptor Systems", *Chem. Phys. Lett.* **1989**, 150, 366-373.
- (213) Shephard, M. J.; Paddon-Row, M. N. "Application of the Parity Rule of Through-Bond Coupling to the Design of "Superbridges" That Exhibit Greatly Enhanced Electronic Coupling", *J. Phys. Chem.* **1995**, 99, 17497-17500.
- (214) Paddon-Row, M. N.; Shephard, M. J. "Through-Bond Orbital Coupling, the Parity Rule and the Design of "Superbridges" Which Exhibit Greatly Enhanced Electronic Coupling: A Natural Bond Orbital Analysis", *J. Am. Chem. Soc.* **1997**, 119, 5355-5365.
- (215) Catalano, M. M.; Crossley, M. J.; Harding, M. M.; King, L. G. "Control of Reactivity at the Porphyrin Periphery by Metal Ion Co-ordination: a General Method for Specific Nitration at the β -Pyrrolic Position of 5,10,15,20-Tetra-arylporphyrins", *J. Chem. Soc., Chem. Commun.* **1984**, 1535-1536.
- (216) Crossley, M. J.; King, L. G. "Novel Heterocyclic Systems from Selective Oxidation at the β -Pyrrolic Position of Porphyrins", *J. Chem. Soc., Chem. Commun.* **1984**, 920-922.
- (217) Baldwin, J. E.; Crossley, M. J.; DeBernadis, J. "Efficient Peripheral Functionalization of Porphyrins", *Tetrahedron* **1982**, 38, 685-692.
- (218) King, L. G.; Crossley, M. J. *J. Chem. Soc., Chem. Commun.* **1984**, 921.
- (219) Cook, A. G. *Enamines*; Dekker: New York, **1988**.
- (220) Hopf, F. R.; Witten, D. G. In *Porphyrins and Metalloporphyrins*; Smith, K., Ed.; Elsevier: Amsterdam, **1975**.

- (221) Martin, N. H.; Jefford, C. W. "75. Synthesis and Photo-oxygenation of Some Substituted 1-Benzyl-3,4-dihydroisoquinolines. Mechanism of Enamine Photo-oxygenation", *Helv. Chim. Acta* **1982**, 65, 762-774.
- (222) Martin, N. H.; Jefford, C. W. "Evidence for a charge-transfer mechanism in the photo-oxygenation of an enamine", *Tetrahedron Lett.* **1981**, 22, 3949-3952.
- (223) Burn, P. L. PhD, The University of Sydney, **1989**.
- (224) Perrin, D. D.; Armarego, W. L. *Purification of Laboratory Chemicals*; 3rd ed.; Pergamon Press: New York, **1988**.
- (225) Ashton, P. R.; Brown, G. R.; Isaacs, N. S.; Giuffrida, D.; Kohnke, F. H.; Mathias, J. P.; Slawin, A. M. Z.; Smith, D. R.; Stoddart, J. F.; Williams, D. J. "Molecular LEGO. Substrate-Directed Synthesis via Stereoregular Diels-Alder Oligomerizations", *J. Am. Chem. Soc.* **1992**, 114, 6330-6353.
- (226) Gulyas, P. T.; Langford, S. J.; Lokan, N. R.; Ranasinghe, M. G.; Paddon-Row, M. N. "Convenient Synthetic Route to Rigid Donor-{Bridge}-Acceptor Systems Involving Porphyrin and Phenanthroline Annulation of Norbornyllogous Bridges via 2,3-Norbornanediones", *J. Org. Chem.* **1997**, 62, 3038-3039.
- (227) Altomare, A.; Burla, M. C.; Camalli, M.; Cascarano, G.; Giacovazzo, C.; Guagliardi, A.; Polidori, G. *J. Appl. Cryst.* **1994**, 27, 435.
- (228) DeMeulenaer, J.; Tompa, H. *Acta Cryst.* **1965**, 19, 1014.
- (229) Ibers, J. A.; Hamilton, W. C. *International Tables for X-Ray Crystallography*; Kynoch Press: Birmingham, **1974**.
- (230) Rae, A. D. ; RAELS University of New South Wales: Kensington, **1989**.



NOTES